

**Identification of Novel Glucose-Dependent Alterations
Responsible for Vascular Dysfunction in Type 2 Diabetes
Mellitus (T2DM)**

Olapeju Israel Bolanle,

B.Pharm., Pharm.D., MSc., Pg.Dipl. in Res., AFHEA

A thesis submitted for the degree of PhD

The University of Hull and The University of York

Hull York Medical School

September 2023

Abstract

Despite the plethora of drugs currently available for managing coronary artery disease (CAD) patients with or without type 2 diabetes mellitus (T2DM), yet CAD frequently progresses, necessitating a coronary artery bypass graft (CABG) procedure using human saphenous vein (HSV). However, over 70 % of the procedures fail after 10 years in T2DM patients. We propose that this is due in part to glucose-dependent alterations in the function of HSV smooth muscle cell (HSVSMC), a key cell type involved in vascular dysfunction. Therefore, in this project, we examined T2DM-dependent alterations, including protein *O*-GlcNAcylation, a dynamic and reversible post-translational modification, in the metabolic profile and function of HSVSMC from T2DM patients versus non-diabetic control. Under NHRA ethics approval (NHS REC:15/NE/0138), HSVSMCs were explanted from surplus HSV tissues from T2DM and non-diabetic patients undergoing CABG. Expression levels of *O*-GlcNAcase (OGA), *O*-GlcNAc transferase (OGT), and Glutamine-fructose-6P amidotransferase (GFAT) were determined in lysates of HSVSMCs from T2DM versus non-diabetic patients by SDS-PAGE and immunoblotting using specific antibodies. This experiment was repeated using lysates of HSVSMCs treated with high glucose (HG) concentrations (10 mM and 25 mM) for 48 hours. Our results showed that their expression levels were not significantly different in T2DM patients versus non-diabetic controls, and after treatment with HG concentrations. Furthermore, we used the Seahorse XFP analyzer to determine real-time mitochondrial function of HSVSMCs by measuring the oxygen consumption rate (OCR) and extracellular acidification rate (ECAR) after sequential addition of modulators of respiration; oligomycin, carbonyl cyanide p-(trifluoromethoxy) phenylhydrazone (FCCP), and rotenone and antimycin A. Results revealed that versus unstimulated cells, IL-6/sIL-6R α and PDGF-BB caused an increase in OCR (102.5% and 93.9% in maximal respiration, respectively) and ECAR (basal glycolysis 101.6%; glycolytic reserve 76.3%; maximal glycolysis 117.1%; glycolytic reserve 99.3%, for PDGF-BB) in HSVSMCs from T2DM patients but not in those from non-diabetic control. However, this observed increase was abolished by ruxolitinib. Similarly, versus unstimulated cells, thrombin but not Ang II caused a significant increase in OCR (85.2% in maximal respiration) of HSVSMCs from T2DM patients, and this was abolished by trametinib. Furthermore, flow cytometry assay showed that both ruxolitinib and trametinib versus unstimulated cells significantly reduced mitochondrial reactive oxygen species' production in HSVSMCs from both T2DM (133.2% and 154.8% respectively) and non-diabetic (114.8% and 107.4% respectively) patients. These findings suggest a JAK/STAT- and MAPK/ERK-mediated regulation of mitochondrial function of HSVSMCs, hence, potential targets for regulation of the function of HSVSMCs which can be explored for drug development to limit SV graft failure.

Table of Contents

Abstract	i
Table of Contents	ii
List of Figures	viii
List of Tables	xiii
Abbreviations	xiv
Thesis outputs	xx
Dedication and Acknowledgement	xxi
Author's declaration	xxii
Chapter 1: Introduction	1
1.1 Diabetes Mellitus	1
1.1.1 Pathophysiology of T2DM	3
1.1.1.1 Defective insulin secretion by pancreatic β -cell	3
1.1.1.2 Insulin Resistance	4
1.1.2 Overview of the management of T2DM	8
1.1.2.1 Non-pharmacological management of T2DM	8
1.1.2.2 Pharmacological management of T2DM	10
1.1.3 Role of T2DM in the development of atherosclerosis	13
1.2 Coronary artery disease (CAD)	16
1.2.1 Overview of current management of CAD	18
1.2.2 Coronary artery bypass graft (CABG)	19
1.2.3 Coronary artery bypass graft failure (CABGF)	21
1.2.3.1 Pathophysiology of CABGF	21
1.2.3.1.1 Vasculature	21
1.2.3.1.2 Neointimal hyperplasia (NIH)	22
1.2.3.2 Surgery-related factors predisposing to SVG failure	23
1.3 Protein O-GlcNAcylation	27
1.3.1 Involvement of Protein O-GlcNAcylation in Vascular dysfunction and VGF	31
1.4 Cellular Metabolism	34
1.4.1 Glycolysis	34

1.4.2	TCA Cycle	36
1.4.3	Oxidative phosphorylation	36
1.4.4	Inhibitors of oxidative phosphorylation	39
1.4.5	The mitochondria and its operation	41
1.4.5.1	OCR	42
1.4.5.2	ECAR	44
1.5	Reactive oxygen species (ROS)	45
1.5.1	ROS signalling	46
1.5.1.1	JAK/STAT	46
1.5.2.2	MAPK/ERK	47
1.5.3	Mitochondria oxidative stress	49
1.5.4	ROS and vascular dysfunction	50
1.6	VSMC Signalling	52
1.7	Rationale and justification for study	60
1.8	Hypothesis	63
1.9	Aim and objectives	65
Chapter 2: Materials and Methods		66
2.1	Materials	66
2.2	Methods	72
2.2.1	Cell culture	72
2.2.2	Isolation and characterisation of HSVSMCs	73
2.2.3	Protein assay and immunoblotting	77
2.2.4	Optimisation of <i>O</i> -GlcNAc capture	81
2.2.4.1	Synthesis and purification <i>O</i> -GlcNAc traps	81
2.2.4.2	Small scale protein pulldown	82
2.2.4.3	Digestion and solubilization of HSV tissue	82
2.2.5	RNA Assay	83
2.2.5.1	Preparation of Plasmids	83
2.2.5.2	DNA extraction, purification, and quantification	83
2.2.5.3	Transfection of HEK 293T with plasmid DNA	84
2.2.5.4	Agarose gel electrophoresis	85

2.2.5.5 Polymerase chain reaction	85
2.2.5.6 Real-time quantitative PCR	85
2.2.6 Mitochondria stress analysis to determine the OCR and ECAR of HSVSMCs	87
2.2.7 Flow cytometry (FACS)	88
2.2.8 Sample summary	99
2.2.9 Statistical analysis	99

Chapter 3: Characterisation of HSVSMC and expression of regulatory enzymes of *O*-GlcNAcylation in HSVSMCs from control and T2DM patients **90**

3.1 Introduction	90
3.2. Results	92
3.2.1 Characterisation of HSVSMC by immunofluorescence microscopy	92
3.2.2 Expression of recombinant modulating enzymes of <i>O</i> -GlcNAcylation in HEK 293	97
3.2.3. Effect of passage on the expression of the regulating enzymes of <i>O</i> -GlcNAcylation in HSVSMC	99
3.2.4 Comparison of OGA, OGT, and GFAT expression levels in HSVSMCs from T2DM versus control patients	103
3.2.5 Effect of glucose concentrations on OGT, OGA, and GFAT expression level in HSVSMCs	107
3.2.6 Validation of synthesised <i>O</i> -GlcNAc trap for affinity capture of <i>O</i> -GlcNAcylated proteins in HSVSMCs	111
3.3 Discussion	113

Chapter 4: JAK/STAT-mediated modulation of the metabolic homeostasis of HSVSMC **118**

4.1 Introduction	118
4.2. Results	120
4.2.1 Downstream inhibition of IL-6/sIL-6R α -stimulated activation of STAT3 with Ruxolitinib	120
4.2.1.1 Effect of JAK inhibition on IL-6/sIL-6R α -mediated changes in OCR and ECAR in HSVSMCs	122
4.2.1.1.1 Effect of ruxolitinib on IL-6/sIL-6R α -mediated changes in OCR in HSVSMCs from T2DM and non-diabetic patients.	122

4.2.1.1.2 Effect of JAK inhibition on IL-6/sIL-6R α -mediated change in ECAR of HSVSMCs from T2DM and non-diabetic patients.	126
4.2.1.2 Effect of JAK inhibition on PDGF-BB-mediated changes in OCR and ECAR of HSVSMCs from T2DM and non-diabetic patients.	130
4.2.1.2.1 Effect of JAK inhibition on PDGF-BB-mediated changes in OCR of HSVSMCs from T2DM and non-diabetic patients.	130
4.2.1.2.2 Effect of JAK inhibition on PDGF-BB-mediated changes in ECAR of HSVSMCs from T2DM and non-diabetic patients.	134
4.2.3 Alterations in metabolic homeostasis are not associated with any significant levels of IL-6/sIL-6R α and PDGF-BB-induced phosphorylation STAT3.	138
4.2.4. mtDNA copy number in HSVSMCs from T2DM and non-diabetic patients after treatments with IL-6/sIL-6R α and PDGF-BB +/-ruxolitinib	141
4.3 Discussion	144

Chapter 5: MAPK/ERK-mediated modulation of metabolic homeostasis of

HSVSMC	151
5.1 Introduction	151
5.2 Results	153
5.2.1 Downstream inhibition of MAPK/ERK activation with trametinib	153
5.2.2. Effect of Ang II +/- MEK inhibitor on OCR and ECAR of HSVSMCs from T2DM and non-diabetic patients.	155
5.2.2.1. Effect of Ang II +/- trametinib on ECAR of HSVSMCs from T2DM and non-diabetic patients.	159
5.2.2.2 Effect of thrombin +/- MEK inhibitor on OCR and ECAR of HSVSMCs from T2DM and non-diabetic patients.	163
5.2.2.2.1 Effect of thrombin +/- trametinib on OCR of HSVSMCs from T2DM and non-diabetic patients.	163
5.2.2.2.2 Effect of thrombin +/- trametinib on ECAR of HSVSMCs from T2DM and non-diabetic patients.	167
5.2.3 Alterations in metabolic homeostasis are not associated with any significant levels of agonists' induced phosphorylation of ERK	171
5.2.3.2 Ang II- and thrombin- induced phosphorylation of ERK of HSVSMCs from T2DM versus non-diabetic patients	171

5.2.4. mtDNA copy number in HSVSMCs from T2DM and non-diabetic patients after treatments with Ang II and thrombin +/-trametininb	174
5.3 Discussion	177
Chapter 6: JAK/STAT- and MAPK/ERK- mediated production of mROS in HSVSMCs.	184
6.1 Introduction	184
6.2 Results	187
6.2.1 Effects of JAK inhibition on mROS production in HSVSMCs from T2DM and non-diabetic patients	187
6.2.1.1 Effect of IL-6/sIL-6R α and ruxolitinib on production of mROS in HSVSMCs from T2DM and non-diabetic patients	188
6.2.1.2 Effect of PDGF-BB and ruxolitinib on mROS production in HSVSMCs from T2DM and non-diabetic patients	192
6.2.2 Effects of MEK inhibition on mROS production in HSVSMCs from T2DM and non-diabetic patients	196
6.2.2.1 Effect of Ang II and trametinib mROS production in HSVSMCs from T2DM and non-diabetic patients	197
6.2.2.2 Effect of thrombin and trametinib on mROS production in HSVSMCs from T2DM and non-diabetic patients	201
6.3 Discussion	205
Chapter 7: General discussion	212
7.1 T2DM or hyperglycaemia did not alter the expression of the key enzymes of cellular O-GlcNAcylation in HSVSMCs	213
7.2 Ruxolitinib attenuated JAK-mediated increase in OCR and ECAR in HSVSMCs from T2DM patients	216
7.3 Trametinib attenuated MEK-mediated increase in OCR in HSVSMCs from T2DM patients	219
7.4 ROS production is attenuated in HSVSMCs by inhibiting JAK/STAT and MAPK/ERK signalling	222
7.5 Strengths and limitations of this study	223

CHAPTER 8:	Perspectives and future experiments	225
8.1	Optimisation and isolation of <i>O</i> -GlcNAcylated protein from HSVSMC extracts	226
8.2	Identification of <i>O</i> -GlcNAcylated target proteins in HSVSMCs from T2DM patients	226
8.3	Validation and functional characterisation of <i>O</i> -GlcNAcylated proteins in HSVSMC targets	226
8.4	Assessing these alterations in HSVECs and evaluating the effect of other post-translational modifications	227
8.5	Assessing the impact of phosphorylation and <i>O</i> -GlcNAcylation crosstalk on vascular function	228
8.6	Assessment of the relationship between altered metabolic profile of the HSVSMC and defined functional readouts of vascular dysfunction	228
9.	References	229
10.	Appendix	283

List of Figures

Figure 1.1	Overview of the current management of coronary artery disease.....	18
Figure 1.2	Saphenous vein bypass graft.....	20
Figure 1.3	Patterns of composite grafting with sequential bypass.....	25
Figure 1.4	Hexosamine Biosynthetic Pathway.....	28
Figure 1.5	Mitochondrion respiratory chain complexes.....	40
Figure 1.6	Schematic of real time measurement of mitochondrial oxygen consumption rate (OCR).....	43
Figure 1.7	Schematic of real time measurement of mitochondrial extracellular acidification rate.....	44
Figure 1.8	A proposed schematic of ROS mediated vascular dysfunction in T2DM.....	51
Figure 1.9	A schematic of the domain structure of human IL-6.....	53
Figure 1.10	Hypothesised glucose-dependent alterations responsible for VSMCs' dysfunction in T2DM.....	64
Figure 2.1	Isolation of HSVSMCs from HSV tissue.....	75
Figure 2.2	Representative BCA assay result and standard curve as exported from the BMG FluroStar plate reader.....	78
Figure 3.1	Verification of the identity of HSVSMCs from non-diabetic patients by immunofluorescence microscopy using anti- α SMA.....	94
Figure 3.2	Verification of the identity of HSVSMCs from non-diabetic patients by immunofluorescence microscopy using anti-SMMHC.....	95
Figure 3.3	Excluding the presence of endothelial cell contamination in HSVSMCs from non-diabetic patients	96
Figure 3.4	Expression of recombinant modulating enzymes of <i>O</i> -GlcNAcylation in HEK 293 cells.....	98
Figure 3.5	Expression of OGA across passages (1-4) of HSVSMC samples from non-diabetic patients using OGA-transfected HEK 293 cells as control.....	100
Figure 3.6	Expression of OGT across passages (1-4) of HSVSMC samples from non-diabetic patients using OGT-transfected HEK 293 cells as control.....	101

Figure 3.7	Expression of GFAT across passages (1-4) of HSVSMC samples from non-diabetic patients	102
Figure 3.8	Comparison of OGA expression in HSVSMCs from T2DM and non-diabetic patients using OGA-transfected HEK 293 cells as positive control.....	104
Figure 3.9	Comparison of OGA expression in HSVSMCs from T2DM and non-diabetic patients using OGA-transfected HEK 293 cells as positive control.....	105
Figure 3.10	Comparison of GFAT expression in HSVSMCs from T2DM and non-diabetic patients.....	106
Figure 3.11	Expression of OGA by HSVSMCs from non-diabetic patients treated with normal (5 mM) and high (10 mM and 25 mM) glucose concentrations using OGA-transfected HEK 293 cells as positive control.....	108
Figure 3.12	Expression of OGT by HSVSMCs from non-diabetic patients treated with normal (5 mM) and high (10 mM and 25 mM) glucose concentrations using OGT-transfected HEK 293 cells as positive control.....	109
Figure 3.13	Expression of GFAT by HSVSMCs from non-diabetic patients treated with normal (5 mM) and high (10 mM and 25 mM) glucose concentrations.....	110
Figure 3.14	Validation of the integrity of synthesised <i>O</i> -GlcNAc trap.....	112
Figure 4.1	Downstream activation and inhibition of the JAK/STAT signalling pathway.....	121
Figure 4.2	Mitochondria stress analysis to determine the OCR of HSVSMCs from T2DM patients after stimulation with IL-6/sIL-6R α +/- ruxolitinib.....	123
Figure 4.3	Mitochondria stress analysis to determine the OCR of HSVSMCs from non-diabetic patients after stimulation with IL-6/sIL-6R α +/- ruxolitinib.....	124
Figure 4.4	Comparison of the OCR of HSVSMCs from T2DM and non-diabetic patients after stimulation with IL-6/sIL-6R α +/- ruxolitinib.....	125

Figure 4.5	Mitochondria stress analysis to determine the ECAR of HSVSMCs from T2DM patients after stimulation with IL-6/sIL-6R α ruxolitinib.....	127
Figure 4.6	Mitochondria stress analysis to determine the ECAR of HSVSMCs from non-diabetic patients after stimulation with IL-6/sIL-6R α ruxolitinib.....	128
Figure 4.7	Comparison of the ECAR of HSVSMCs from T2DM and non-diabetic patients after stimulation with IL-6/sIL-6R α +/- ruxolitinib.....	129
Figure 4.8	Mitochondria stress analysis to determine the OCR of HSVSMCs from T2DM patients after stimulation with PDGF-BB +/- ruxolitinib..	131
Figure 4.9	Mitochondria stress analysis to determine the OCR of HSVSMCs from non-diabetic patients after stimulation with PDGF-BB +/- ruxolitinib.....	132
Figure 4.10	Comparison of the OCR of HSVSMCs from T2DM and non-diabetic patients after stimulating with PDGF-BB +/- ruxolitinib.....	133
Figure 4.11	Mitochondria stress analysis to determine the ECAR of HSVSMCs from T2DM patients after stimulating with PDGF-BB +/- ruxolitinib..	135
Figure 4.12	Mitochondria stress analysis to determine the ECAR of HSVSMCs from non-diabetic patients using PDGF-BB +/- ruxolitinib.....	136
Figure 4.13	Comparison of the ECAR of HSVSMCs from T2DM and non-diabetic patients after stimulating with PDGF-BB +/- ruxolitinib.....	137
Figure 4.14	IL-6/sIL-6R α -stimulated phosphorylation of STAT3 on Tyr705 in HSVSMCs from T2DM and non-diabetic patients.....	139
Figure 4.15	PDGF-BB-stimulated phosphorylation of STAT3 on Tyr705 in HSVSMCs from T2DM and non-diabetic patients.....	140
Figure 4.16	mtDNA copy number of HSVSMCs from T2DM and non-diabetic patients after treatment with IL-6/sIL-6R α +/- ruxolitinib	142
Figure 4.17	mtDNA copy number of HSVSMCs from T2DM and non-diabetic patients after treatment with PDGF-BB+/-ruxolitinib	143
Figure 5.1	Downstream activation and inhibition of the MAPK/ERK signalling pathway.....	154
Figure 5.2	Mitochondria stress analysis to determine the OCR of HSVSMCs from T2DM patients after stimulation with Ang II +/- trametinib.....	156

Figure 5.3	Mitochondria stress analysis to determine the OCR of HSVSMCs from non-diabetic patients after stimulation with Ang II +/- trametinib.	157
Figure 5.4	Comparison of the OCR of HSVSMCs from T2DM and non-diabetic patients after stimulation with Ang II +/- trametinib.....	158
Figure 5.5	Mitochondria stress analysis to determine the ECAR of HSVSMCs from T2DM patients after stimulation with Ang II +/- trametinib.....	160
Figure 5.6	Mitochondria stress analysis to determine the ECAR of HSVSMCs from non-diabetic patients after stimulation with Ang II +/- trametinib.	161
Figure 5.7	Comparison of the ECAR of HSVSMCs from T2DM and non-diabetic patients after stimulation with Ang II +/- trametinib.....	162
Figure 5.8	Mitochondria stress analysis to determine the OCR of HSVSMCs from T2DM patients after stimulation with thrombin +/- trametinib.....	164
Figure 5.9	Mitochondria stress analysis to determine the OCR of HSVSMCs from non-diabetic patients after stimulation with thrombin +/- trametinib.....	165
Figure 5.10	Comparison of the OCR of HSVSMCs from T2DM and non-diabetic patients after stimulation with thrombin +/- trametinib.....	166
Figure 5.11	Mitochondria stress analysis to determine the ECAR of HSVSMCs from T2DM patients after stimulation with thrombin +/- trametinib.....	168
Figure 5.12	Mitochondria stress analysis to determine the ECAR of HSVSMCs from non-diabetic patients after stimulation with thrombin +/- trametinib.....	169
Figure 5.13	Comparison of the ECAR of HSVSMCs from T2DM and non-diabetic patients after stimulation with thrombin +/- trametinib.....	170
Figure 5.14	Ang II-stimulated phosphorylation of ERK in HSVSMCs from T2DM and non-diabetic patients.....	172
Figure 5.15	Thrombin-stimulated phosphorylation of ERK in HSVSMCs from T2DM and non-diabetic patients.....	173
Figure 5.16	mtDNA copy number of HSVSMCs from T2DM and non-diabetic patients after treatment with Ang II +/- trametinib.....	175
Figure 5.17	mtDNA copy number of HSVSMCs from T2DM and non-diabetic patients after treatment with thrombin +/- trametinib.....	176

Figure 6.1	Flow cytometry analysis of mROS production in HSVSMCs from T2DM patients after treatment with IL-6/sIL-6R α +/- ruxolitinib.....	189
Figure 6.2	Flow cytometry analysis of mROS production in HSVSMCs from non-diabetic patients after treatment with IL-6/sIL-6R α +/- ruxolitinib.....	190
Figure 6.3	Comparison of the mROS production in HSVSMCs from T2DM and non-diabetic patients after treatment with IL-6/sIL-6R α +/- ruxolitinib.	191
Figure 6.4	Flow cytometry analysis of mROS production in HSVSMCs from T2DM patients after treatment with PDGF-BB +/- ruxolitinib.....	193
Figure 6.5	Flow cytometry analysis of mROS production in HSVSMCs from non-diabetic patients after treatment with PDGF-BB +/- ruxolitinib....	194
Figure 6.6	Comparison of the mROS production in HSVSMCs from T2DM and non-diabetic patients after treatment with PDGF +/- ruxolitinib.....	195
Figure 6.7	Flow cytometry analysis of mROS production in HSVSMCs from T2DM patients after treatment with Ang II +/- trametinib.....	198
Figure 6.8	Flow cytometry analysis of mROS production in HSVSMCs from non-diabetic patients after treatment with Ang II +/- trametinib.....	199
Figure 6.9	Comparison of the mROS production in HSVSMCs from T2DM and non-diabetic patients after treatment with Ang II +/- trametinib.....	200
Figure 6.10	Flow cytometry analysis of mROS production in HSVSMCs from T2DM patients after treatment with thrombin +/- trametinib.....	202
Figure 6.11	Flow cytometry analysis of mROS production in HSVSMCs from non-diabetic patients after treatment with thrombin +/- trametinib.....	203
Figure 6.12	Comparison of the mROS production in HSVSMCs from T2DM and non-diabetic patients after treatment with thrombin +/- trametinib.....	204
Figure 7.1	Proposed model highlighting how JAK regulates metabolic profile in HSVSMC.....	218
Figure 7.2	Proposed model highlighting how MEK regulates metabolic profile in HSVSMC.....	221

List of Tables

Table 1.1	Non-pharmacological approaches to managing T2DM.....	8
Table 1.2A	Management of T2DM with insulin.....	10
Table 1.2B	Oral drugs used to manage T2DM.....	11
Table 2.1	Materials.....	66
Table 2.2	Primary and secondary antibodies used for immunoblotting and characterization of HSVSMCs.....	80
Table 2.3	PCR primer sequence.....	86
Table 2.4	Patient information for HSV samples.....	89

List of Abbreviations

ACEI	Angiotensin converting enzyme inhibitor
ADP	Adenosine diphosphate
AMPK	Adenosine monophosphate-activated protein kinase
Ang II	Angiotensin II
ANT	Adenine nucleotide translocase
APS	Ammonium Persulphate
ARB	Angiotensin receptor blocker
ASK1	Apoptosis signal-regulated kinase 1
ATP	Adenosine triphosphate
BB	Beta blocker
BCA	Bicinchoninic acid
BCT	Beckman's centrifuge tube
BMI	Body mass index
BSA	Bovine serum albumin
CABG	Coronary artery bypass graft
CABGF	Coronary artery bypass graft failure
CAD	Coronary artery disease
Camp	Cyclic adenosine monophosphate
CCB	Calcium channel blocker
CVD	Cardiovascular disease
DALY	Disability-adjusted life-year
DM	Diabetes mellitus
DMEM	Dulbecco's Modified Eagle Medium

DMSO	Dimethyl sulfoxide
DNA	Deoxyribonucleic acid
DPBS	Dulbecco's phosphate buffered saline
DPP-4	Dipeptidyl peptidase-4
ECAR	Extracellular acidification rate
ECM	Extracellular matrix
EDTA	Ethylenediaminetetraacetic acid
EE	Early endosomes
EGFR	Endothelial growth factor receptor
ER	Endoplasmic reticulum
ERC	Endosomal recycling chambers
ERK	Extracellular signal-regulated kinase
ETC	Electron transport chain
F6P	Fructose 6-phosphate
FBP	Fructose- 1,6-bisphosphate
FCCP	Carbonyl cyanide-4 (trifluoromethoxy) phenylhydrazone
FFA	Free fatty acid
FMN	Flavin mononucleotide
FOXO	Forkhead box O
G6P	Glucosamine-6-phosphate
G6Pase	Glucose-6-phosphatase
GAP	Glyceraldehyde 3-phosphate
GAPDH	Glyceraldehyde-3-phosphate dehydrogenase
GEA	Gastroepiploic artery

GFAT	Glutamine-fructose-6P amidotransferase
GFP	Green fluorescent protein
GlcN-6-P	Glucosamine-6-phosphate
GlcNAc-6P	N-acetylglucosamine-6-phosphate
GLP-1	Glucagon-like peptide-1
GLUT2	Glucose transporter 2
GSV	Great saphenous vein
H ₂ O ₂	Hydrogen peroxide
HDL	High-density lipoprotein
HEK	Human embryonic kidney
HG	High glucose
HIF	Hypoxia-inducible factor
HSVSMC	Human saphenous vein smooth muscle cell
HUVEC	Human umbilical vein endothelial cell
IAAP	Islet amyloid polypeptides
IDF	International Diabetes Federation
IGF	Insulin-like growth factor
IL	Interleukin
IMA	Internal mammary artery
IMM	Inner mitochondrial membrane
IMS	Intermembrane space
INSR	Insulin receptor
IPTG	Isopropyl-beta-D-thiogalactoside
IRE	Insulin response element

IRS	Insulin receptor substrates
JAK	Janus kinase
JNK	c-Jun N-terminal kinases
LAD	Left anterior descending artery
LB	Luria-Bertani
LDL	Low-density lipoprotein
LITA	Left internal thoracic artery
MAPKs	Mitogen-activated protein kinase
MCP	Monocyte chemoattractant protein
MMP	Matrix metalloproteinases
NADH	Nicotinamide adenine dinucleotide
NADPH	Nicotinamide adenine dinucleotide phosphate
NF-K β	Nuclear factor kappa-light-chain-enhancer of activated B cells
NIH	Neointimal hyperplasia
NLRP3	Nucleotide-binding oligomerization domain-like receptor 3
NOS	Nitric oxide synthase
OCR	Oxygen consumption rate
OGA	<i>O</i> -GlcNAcase
OGT	<i>O</i> -GlcNAc transferase
OMM	Outer membrane of the mitochondria
PBS	Phosphate-buffered saline
PBST	Phosphate-buffered saline with Tween® detergent
PCI	Percutaneous coronary intervention
PCR	Polymerase chain reaction

PDGF	Platelet derived growth factor
PKD1	Phosphoinositide-dependent kinase 1
PECAM	Platelet endothelial cell adhesion molecule
PEP	Phosphoenolpyruvic
PEPCK	Phosphoenolpyruvate carboxykinase
PI3K	Phosphoinositide 3-kinase
PIP2	Phosphatidylinositol 4,5-bisphosphate
PK	Protein kinase
PLC	Phospholipase C
PP5	Protein phosphatase 5
PPAR- γ	Peroxisome proliferator- activated receptor gamma
PTP1B	Protein-tyrosine phosphatase 1B
PVAT	Perivascular adipose tissue
qPCR	Quantitative polymerase chain reaction
RA	Radial artery
RITA	Right internal thoracic artery
RNA	Ribonucleic acid
ROS	Reactive oxygen species
RR	Relative risk
RY	Ryanodine
S.E.M	Standard error of mean
sdLDL	Small dense lipoprotein
SDS-PAGE	Sodium dodecyl-sulfate polyacrylamide gel electrophoresis
SERCA	Sarco/endoplasmic reticulum Ca ²⁺ -ATPase

SGLT2	Sodium glucose cotransporter 2
SMA	Smooth muscle actin
SMMHC	Smooth muscle-myosin heavy chain
SOD	Superoxide dismutase
STAT	Signal transducer and activator of transcription
SVG	Saphenous vein grafts
T2DM	Type 2 diabetes mellitus
TCA	Tricarboxylic acid
TEMED	Tetramethylethylenediamine
TGA	Triglyceride
TGN	Trans-Golgi network
TNF	Tissue necrotic factor
UAP/AGX1	UDP-N-acetylhexosamine pyrophosphorylase
UDP-GlcNAc	UDP-N acetylglucosamine
VEC	Vascular endothelial cell
VEGF	Vascular endothelial growth factor
VGF	Vein graft failure
VLDL	Very-low-density lipoprotein
VSMC	Vascular smooth muscle cell
WHO	World Health Organization

Thesis Outputs

Some aspects of this thesis have been published as research or review articles and abstracts. Additionally, I have presented some of the findings in this thesis as either an oral presentation or a poster at conferences and seminars. The list below includes a few chosen outputs.

Journal Publications

1. Rotchell JM, Jenner LC, Chapman E, Bennett RT, **Bolanle IO**, Loubani M, Sadofsky L, Palmer TM. Detection of microplastics in human saphenous vein tissue using μ FTIR: A pilot study. *Plos one*. 2023 Feb 1;18(2):e0280594.
2. Saldanha PA, **Bolanle IO**, Palmer TM, Nikitenko LL, Rivero F. (2022) Complex Transcriptional Profiles of the *PPP1R12A* Gene in Cells of the Circulatory System as Revealed by In Silico Analysis and Reverse Transcription PCR. *Cells*.11(15):2315. <https://doi.org/10.3390/cells11152315>
3. **Bolanle IO**, Palmer TM, Sturmey RG, *et al*: (2022). BS5 Jak-mediated IL-6 and PDGF induced alteration of the metabolic homeostasis of human saphenous vein smooth muscle cells of type 2 diabetic and non-diabetic patients. *Heart*;108:A145-A146. <https://doi.org/10.1136/heartjnl-2022-BCS.185>
4. **Bolanle IO**, & Palmer TM. (2022). Targeting Protein *O*-GlcNAcylation, a Link between Type 2 Diabetes Mellitus and Inflammatory Disease. *Cells*, 11(4), 705. <https://doi.org/10.3390/cells11040705>
5. **Bolanle IO**, Riches-Suman K, Loubani M, Williamson R, Palmer TM. (2021). Revascularisation of Type 2 diabetics with coronary artery disease: insights and therapeutic targeting of *O*-GlcNAcylation. *Nutr Metab Cardiovasc Dis*. 31, 1349-1356. <https://doi.org/10.1016/j.numecd.2021.01.017>
6. **Bolanle IO**, Riches-Suman K, Williamson R, Palmer TM. (2021). Emerging roles of protein *O*-GlcNAcylation in cardiovascular diseases: insights and novel therapeutic targets. *Pharmacol. Res*. 165: 105467. <https://doi.org/10.1016/j.phrs.2021.105467>

Selected Conference Presentations

- 1.** Poster presentation at the North of England Cell Biology Forum Conference on the 23rd September 2022
- 2.** Poster presentation at the centenary conference of the British Cardiovascular Society hosted in Manchester on the 7th June 2022.
- 3.** Oral presentation at the Northern Cardiovascular Research Group Meeting 2022 hosted by University of Bradford on the 24th May 2022.
- 4.** Oral presentation at the Northern Vascular Biology Forum 2021 on 14th December 2021.
- 5.** Oral presentation at the Hull York Medical School Postgraduate Research conference 2021 On 9th July 2021.
- 6.** Poster presentation at the 28th Northern Cardiovascular Research Group Meeting 2021 on 26th May 2021.
- 7.** Poster presentation at the University of Hull/HYMS/HUTH research celebration on the 8th April 2021
- 8.** Oral presentation at the 2020 edition of the HYMS Postgraduate Research Conference on 11th September 2020.

Dedication

I dedicate this thesis to the glory of God Almighty who granted me the grace and strength to start and complete my PhD programme. May His name be exalted. Also, I dedicate this to the memory of my late parents Chief and Princess A.G. Bolanle, may their souls continue to rest in perfect peace. I love you Dad and Mum.

Acknowledgment

I would like to thank Prof. Timothy M. Palmer, my supervisor, for his guidance, mentorship, and support throughout this project and my PhD programme. I also like to thank my co-supervisor, Prof. Roger Sturmey, for his expertise, guidance, and support. I want to express my gratitude to Dr. Gillian A. Durham for the technical assistance and training. Special thanks to my Thesis Advisory Panel members, Dr Francisco Rivero, the Chairman, and Dr Laura Sadofsky, the Independent Assessor, for their advice and criticism throughout this research.

Special acknowledgement to Tertiary Education Trust Fund (TETFund), Nigeria for awarding me a scholarship to pursue this programme. Also, my deep appreciation to Hull York Medical School, University of Hull for the grant to support the funding of this programme.

I would like to express my deep gratitude to Prof. E.K.I. Omogbai, for all the fatherly support and encouragement before and during this programme. I would also like to extend my gratitude to Prof. R.I. Ozolua, Prof. A. Falodun, Mummy Omogbai, Dr P. Omogbai and family, and members of the Department of Pharmacology & Toxicology, University of Benin, Nigeria.

Also, I would like to convey my deep appreciation to my family, particularly to my elder sisters, Jumoke, Danni, and Yemi, and elder brothers, Lanre and Deji, for their immense support. Lastly, I want to thank my wife, Dr. Modupe O. Bolanle, for all her support and encouragement. Sincerely, I count myself fortunate to have all of you in my life.

Author's Declaration

'I confirm that this work is original and that if any passage(s) or diagram(s) have been copied from academic papers, books, the internet, or any other sources, these are clearly identified by the use of quotation marks and the reference(s) is fully cited. I certify that, other than where indicated, this is my own work and does not breach the regulations of HYMS, the University of Hull or the University of York regarding plagiarism or academic conduct in examinations. I have read the HYMS Code of Practice on Academic Misconduct, and state that this piece of work is my own and does not contain any unacknowledged work from any other sources. I confirm that any patient information obtained to produce this piece of work has been appropriately anonymised'.

Olapeju I. Bolanle

September 2023

Chapter one: Introduction

1.1 Diabetes Mellitus

Diabetes mellitus (DM), a spectrum of diseases characterised by disorders in protein, lipid, and carbohydrate metabolism, is a global burden and its prevalence is increasing as people are now living longer (Vargas and Carillo, 2019; Martín-Timón et al., 2014). Around one million islets of Langerhans are found scattered throughout the adult pancreatic gland, including the α , β , δ , ϵ , and pancreatic polypeptide cells (Maitra, 2012). Of these cells, the β cells produce insulin, a crucial hormone for maintaining glucose homeostasis (Maitra, 2012). Insulin binds to specific cell surface insulin receptors on cells in target tissues including liver, muscle, and adipose to cause a cascade of effects that are essential in metabolic processes like glycolysis, glycogenesis, lipolysis, and protein synthesis. DM is the most prevalent resulting condition where these cells are dysregulated (Vargas and Carillo, 2019; Maitra, 2012). Furthermore, the extensive destruction of pancreatic islets by conditions such as chronic pancreatitis, Cushing's disease, acromegaly, haemachromatosis, hormonal tumours (such as pheochromocytoma and pituitary tumours), genetic disorders (such as lipodystrophy), pancreatectomy, or pregnancy (gestational diabetes mellitus) can also result in the development of DM (Maitra, 2012).

The prevalence of DM is increasing with the current figure of adults living with DM now estimated to be 537 million (IDF, 2022) compared with 108 million in 1980 (WHO, 2016), and 422 million in 2014 (WHO, 2016). The prediction that this number will increase to 700 million by 2045 (IDF, 2019) is unsettling, and ageing of the populace, urbanisation and westernization are responsible for this rising incidence (Hu, 2011). As global life expectancy is now on the rise, these statistics make DM a major global healthcare problem. DM is poised to affect the developing countries of the world much more than their developed counterparts (Ogbera and Ekpebegh, 2014). Also, there is significant variation across the age groups affected with DM, with middle aged groups (45-64 years) being more predominant in developing countries, while, in developed countries, the elderly (≥ 65 years) account for most cases (Wild et al., 2004).

Furthermore, it has been suggested that ethnicity may play a part in the development of DM given that the prevalence of the disease is six times greater in South Asian and three times higher in African populations (Diabetes UK, 2019). Although the reason for this is not entirely known, however, genetics is suggested to be one possible cause, and it is known that a poor economy and lifestyle can result in harmful eating habits (Diabetes UK, 2019). It has been

further suggested that genetic and environmental factors both have an impact on the epidemiology type 2 diabetes mellitus (T2DM) (Galicia-Garcia et al., 2020). Following exposure to an environment characterised by sedentary behaviour and high calorie intake, genetic variables begin to manifest. Genome-wide association studies have shown common glycaemic genetic variations for T2DM, however these only account for 10% of the variance in all traits, indicating that uncommon variants are significant (Grarup et al., 2014). People with diverse phenotypes may be more predisposed to certain clusters of cardiovascular diseases (CVD) risk factors such as hypertension, insulin resistance, and dyslipidaemia (Wong et al., 2016).

T2DM which is the fifth leading cause of mortality for persons between the ages of 50 and 74 accounts for more than 90% of all DM cases (GBD RF, 2020). On the other hand, type 1 DM only accounts for about 8% of the overall incidence, with the remainder instances being caused by other types of DM such as gestational DM (GBD RF, 2020). T2DM affected 462 million people in 2017, representing 6.28% of the world's population (15% of people in the 50–69 age range and 22% of people in the 70–plus age range) (Khan et al., 2020). Even though T2DM affects adults frequently, it is now known to affect children and adolescents significantly, and girls are more likely than boys to develop T2DM when they are young (Candler et al., 2018; Divers et al., 2020). Epidemiological studies have also revealed that there is a similar rise in the incidence and prevalence of T2DM among adults in the population where the incidence and prevalence of the disease are high among youths. In addition, girls are more likely than boys to develop T2DM when they are young (Candler et al., 2018; Divers et al., 2020).

The burden of T2DM is rising globally, and it poses one of the largest global public health concerns, impacting adversely on global socioeconomic growth and public health (Lin et al., 2020). Increased mortality from infections, CVD, stroke, chronic renal disease, chronic liver disease, and cancer are all linked to diabetes (Bragg et al., 2017; Policardo et al., 2011). In 2019, DM accounts for estimated 4.2 million deaths globally, and \$720 billion in health expenditure (IDF, 2019). Additionally, T2DM is the second-largest factor limiting global health-adjusted life expectancy globally, despite advances in population health promotion and life expectancy extension (Chen et al., 2019). T2DM had a global incidence of 22.9 million cases, a prevalence of 476.0 million cases, a death rate of 1.37 million cases, and a disability-adjusted life-year (DALY) of 67.9 million cases in 2017 (Lin et al., 2020). By 2025, these numbers are expected to rise to 26.6 million cases, 570.9 million cases, 1.59 million cases, and

79.3 million cases, respectively (Lin et al., 2020). As 1 in 3 diabetics equivalent to 232 million people, are undiagnosed, the true disease burden of T2DM is likely underrepresented (Galicia-Garcia et al., 2020).

1.1.1 Pathophysiology of T2DM

T2DM results from the confluence of two main factors: defective insulin secretion by pancreatic β -cell and insulin resistance in insulin-sensitive tissues (Galicia-Garcia et al., 2020). The synthesis, release, and uptake of insulin are tightly regulated because they are essential for maintaining glucose homeostasis, and the development of T2DM has been attributed to defects in any of these processes (Galicia-Garcia et al., 2020).

1.1.1.1 Defective insulin secretion by pancreatic β -cell

Insulin is produced by β -cells in form of pre-proinsulin. Pre-proinsulin then undergoes a conformational alteration throughout the maturation process that is assisted by many proteins in the endoplasmic reticulum (ER) to produce proinsulin (Fu et al., 2013; Halban, 1994). Proinsulin is then moved from the ER to the Golgi apparatus (GA), where it enters immature secretory vesicles and is differentiated into C-peptide and insulin (Fu et al., 2013; Halban, 1994). Once it has reached maturity, insulin is kept in granule form until it is required for release. Insulin secretion needs to be tightly controlled to maintain metabolic homeostasis. For β -cells to respond to metabolic demands, adequate islet integrity must be preserved. However, in pathologic circumstances, there is disruption of islet integrity/organization, affecting ideal cell-to-cell communication within pancreatic islets, causing poor regulation of insulin and glucagon production, and finally aggravating hyperglycaemia. Insulin secretory dysfunction, the major cause of T2DM, can also be a consequence of errors in the synthesis of any insulin precursors or insulin itself, as well as from disruption of the secretion process. For instance, proinsulin folding failure is frequently associated with inadequate insulin synthesis and diabetes (Liu et al., 2018) and decreased expression in the GLUT2 glucose transporter would impact the subsequent downstream signalling cascade that enhances insulin release (Hoang and Thorn, 2015).

Traditionally, malfunction in β -cells has been linked to β -cell death (Christensen and Gannon, 2019). Recent data, however, points to a more intricate network of interactions between the environment and many biochemical pathways involved in cell biology as the potential cause

of the dysfunction of β -cells in T2DM (Halban et al., 2014). Hyperglycaemia and hyperlipidaemia are relatively common in an overeating condition, similar to that in obesity, which favours chronic inflammation and insulin resistance (Christensen and Gannon, 2019). Due to variations in their genetic vulnerability, β -cells are exposed to toxic stresses in these conditions, including inflammation, inflammatory stress, ER stress, metabolic/oxidative stress, and amyloid stress, which have the potential to eventually result in the loss of islet integrity (Christensen and Gannon, 2019). Additionally, by activating the apoptotic unfolded protein response (UPR) pathways and causing ER stress, hyperglycaemia causes β -cell malfunction (Yamamoto et al., 2019).

Additionally, obesity-related lipotoxicity, glucotoxicity, and glucolipotoxicity cause metabolic and oxidative stress, which destroys β -cells (Halban et al., 2014). High levels of saturated free fatty acids (FFAs) can cause stress that activates the UPR pathway by a number of mechanisms, including suppressing the SERCA enzyme that is necessary for ER Ca^{2+} mobilisation, activating IP3 receptors, or directly affecting ER homeostasis. Additionally, proinsulin biosynthesis and islet amyloid polypeptides (IAAP) are increased in β -cells by sustained hyperglycaemia, which causes an accumulation of misfolded insulin and IAAP as well as an increase in the production of oxidative protein folding-mediated reactive oxygen species (ROS) (Yamamoto et al., 2019). These actions change physiological ER Ca^{2+} mobilisation, favour proapoptotic signals, promote the degradation of proinsulin mRNA, and trigger the release of interleukin (IL)-1, which draws in macrophages and intensifies local islet inflammation (Yamamoto et al., 2019).

1.1.1.2 Insulin Resistance

In general, there are three types of insulin-deficient or resistant conditions: reduced insulin secretion by β -cells; insulin antagonists in the plasma, either as a result of counter-regulatory hormones or non-hormonal substances that affect insulin receptors or signalling; and reduced insulin responsiveness in target tissues (Pearson et al., 2016). The interaction of molecules such as growth hormone and IGF-1 in the fed state has an impact on how insulin functions, and to avoid insulin-induced hypoglycaemia during fasting, glucagon, glucocorticoids, and catecholamines reduce the insulin response (Czech, 2017; Pearson et al., 2016). The insulin/glucagon ratio is crucial to this regulation due to the fact that it influences the relative level of phosphorylation of downstream enzymes in the regulatory signalling pathways. In

contrast to glucocorticoids, which stimulate muscle catabolism, gluconeogenesis, and lipolysis, catecholamines only promote lipolysis and glycogenolysis. Consequently, the over secretion of these hormones promotes the development of insulin resistance (Wilcox, 2005; Nussey and Whitehead, 2001). The liver, adipose tissue, and skeletal muscle are the three main extra-pancreatic insulin-sensitive organs that are crucial for the uptake and utilisation of released insulin. Prior to the development of systemic insulin resistance, which eventually results in T2DM, insulin uptake and function is distorted in these organs (Wilcox, 2005; Nussey and Whitehead, 2001).

1.1.1.2.1 Skeletal Muscle

Insulin resistance in skeletal muscle is regarded as the most significant extra-pancreatic component in the onset of T2DM (Petersen and Shulman, 2002). Under physiological circumstances, insulin promotes glucose uptake from plasma, which in turn induces the production of muscle glycogen. Glycogen synthase, hexokinase, and the glucose transporter GLUT4 are the three main rate-limiting enzymes associated in glucose uptake and glycogen formation (Petersen and Shulman, 2002). When insulin binds to the insulin receptor (INSR) in muscle cells, GLUT4 moves from intracellular locations such as the trans-Golgi network (TGN), early endosomes (EE), and endosomal recycling chambers (ERC) to the plasma membrane. This procedure facilitates glucose uptake and lowers blood glucose levels (Sato, 2014). However, hyperglycaemia would occur from mutations that decrease the expression of the insulin receptor or GLUT4, as well as from any abnormality in the upstream or downstream signalling pathway (Czech, 2017). Furthermore, insulin action on the muscle is also compromised by mutations in important proteins of the downstream signalling cascade including Insulin receptor substrates (IRS)-1 and IRS-2 or phosphoinositide 3-kinase (PI3K).

Additionally, the effect of insulin on glucose metabolism depends on the activation of INSR tyrosine kinase activity. Insulin-mediated signalling is made possible by the β -subunit of the INSR being phosphorylated on many tyrosine residues as a result of insulin binding to the INSR. Therefore, changes to any of the major phosphorylation sites can reduce the activity of INSR tyrosine kinase, which in turn reduces the ability of insulin to act on skeletal muscle (Abdul-Ghani and DeFronzo, 2010). Environmental and lifestyle influence have a significant impact on the uptake of glucose by muscle, in addition to mutations or ineffective epigenetic regulation. For instance, exercise improves glucose consumption by increasing blood supply

to skeletal muscle cells (Venkatasamy et al., 2013). Also, more evidence point to the connection between obesity-related skeletal muscle inflammation and enhanced immune cell infiltration and proinflammatory chemical release in intermyocellular and perimuscular adipose tissue. Through paracrine actions, this ultimately causes myocyte inflammation, impairs myocyte metabolism, and increases insulin resistance (Wu and Ballantyne, 2017).

1.1.1.2.2 Adipose Tissue

Adipose tissue is a metabolically active tissue with the ability to produce a variety of physiologically active substances that control metabolic homeostasis at the systemic level (Coelho et al., 2013). In fact, adipose tissue plays a role in a variety of biological functions, including those related to immunology, coagulation, angiogenesis, fibrinolysis, reproduction, control of vascular tone, hunger management, maintenance of body weight homeostasis, and glucose and lipid metabolism (Rosen and Spiegelman, 2006). Insulin has two separate effects on adipose tissue: (1) promoting glucose absorption and triglyceride synthesis; and (2) inhibiting triglyceride hydrolysis and causing the uptake of FFA and glycerol from circulation (Gastaldelli et al., 2017). In the fed state, GLUT4 mediates the intake of glucose into adipocytes from the circulation, activating glycolysis and causing the production of glycerol-3-phosphate (glycerol-3-P), which is then integrated into lipogenic pathways. Triacylglycerol (TGA), which is kept in lipid droplets, is synthesised when glycerol-3-P and the fatty acids from VLDLs are esterified. TGA droplets in the adipocyte are depleted during metabolic stress in order to provide FFA for utilisation as an energy source in other tissues.

Furthermore, adipose-insulin resistance, even in the presence of high insulin levels, can result in decreased suppression of lipolysis, reduced glucose uptake, and increased FFA release into plasma (Czech, 2020). One of the signalling components impacted by adipose-insulin resistance is faulty AKT activation, which inhibits GLUT4 translocation to the membrane and encourages the activation of lipolytic enzymes that exacerbate hyperglycaemia (Czech, 2017). More so, adipose-insulin resistance is linked to impaired glucose tolerance and increased plasma levels of FFA, which build up in other tissues like the liver or muscle. FFA build up in the liver causes poor insulin signalling, which in turn encourages hepatic gluconeogenesis and impedes the insulin response to glucose, leading to the onset of T2DM.

1.1.1.2.3 Liver

In the liver, insulin controls lipid metabolism more extensively in addition to controlling the generation and consumption of glucose. Insulin binding to liver INSR causes the receptor to become autophosphorylated when circulating glucose levels rise and insulin is produced by pancreatic β -cells. IRSs are then bound and phosphorylated. Phosphorylation of phosphatidylinositol (4,5)-bisphosphate (PIP₂) by PI3K, which is activated by IRSs, results in the production of phosphatidylinositol (3,4,5)-triphosphate (PIP₃). PIP₃ then causes PDK1 to become active, phosphorylating AKT. Additionally, mTORC2 phosphorylates AKT, and once AKT has reached full activation, it takes part in a number of downstream pathways that control a number of metabolic processes, including glycogen production, gluconeogenesis, glycolysis, and lipid synthesis (Titchenell et al., 2017). In physiological conditions, glucagon and insulin working in concert allow for precise control of hepatic glucose production. While insulin serves as a powerful inhibitor of glucose production when its concentration in the blood is increased, glucagon acts as an inducer of hepatic glucose production (Cherrington et al., 2007). Both direct and indirect processes contribute to insulin's impact on the liver's ability to produce glucose. But it is still unknown how important each of these mechanisms is in relation to the others (Edgerton et al., 2006).

1.1.2 Overview of the management of T2DM

1.1.2.1 Non-pharmacological management of T2DM

Table 1.1: Non-pharmacological approaches to managing T2DM

No	Approach	Benefit
1	Exercise	Studies have demonstrated that losing weight and increasing daily energy expenditure improves glucose tolerance and reduces insulin resistance (Staffers et al., 1997; Vighnesh et al., 2013; Way et al., 2016). Studies have also shown that regular physical activity was linked to a lower incidence of the disease at long-term follow-up (4 and 5 years, respectively) in both men and women of different age groups (Way et al., 2016; Reyna et al., 2013). Also, it has been established that increased physical activity has protective effects against the development of T2DM. A T2DM patient's long-term mortality reduction is 50–60% lower in those with moderate or high aerobic fitness than in those with low cardio-respiratory fitness (Helmrich et al., 1991; Manson et al., 1992; Ross et al., 2000).
2	Dietary modification	Dietary changes are crucial for managing T2DM. The majority of T2DM patients are overweight and have insulin resistance syndrome and other metabolic diseases. As a result, the goal of dietary modification in T2DM is to lose weight, enhance glycaemic control, and lower the risk of CAD, which is responsible for 70–80% of these patients' deaths (McMillan-Price et al., 2006). Expert dietary counselling is required for patients with T2DM at the time of diagnosis, and reviews and treatment modifications must be done while paying close attention to the patient's lifestyle, age, and CAD risk (Batsaki, 2005).
3	Reduced alcohol consumption	When compared to abstinence, moderate alcohol consumption has consistently been linked to a lower risk of T2DM (Koppes et al., 2005). Mild to moderate alcohol use lowers the incidence of coronary artery disease in both DM patients and the general population, according to studies (Baliunas et al., 2009). One of the main dangers of alcohol usage is increased risk of hypoglycaemia due to diminished awareness of the condition, especially in people who use sulphonylureas. However, when

		moderate alcohol is consumed with meals, no changes in glucose homeostasis are seen in numerous clinical trials (Burge et al., 1999).
4	Smoking cessation	Smoking significantly raises the risk of CAD in people with diabetes. It has been shown that the RR for CAD was 1.21 for former smokers, 1.66 for current smokers who smoke 1–14 cigarettes per day, and 2.68 for current smokers who smoke more than 15 cigarettes per day (Al-Delaimy et al., 2002). Women who had been smoke-free for more than 10 years had RRs that were comparable to those of women who had never smoked (Al-Delaimy et al., 2002). It has been demonstrated that quitting smoking significantly lowers the risk of CAD in diabetic individuals (Pyorala et al., 1997).

T2DM: Type 2 diabetes mellitus; CAD: Coronary artery disease; RR: Relative risk

1.1.2.2 Pharmacological management of T2DM

Table 1.2A: Management of T2DM with insulin

No	Class with example (s)	Onset (hours)	Peak (hours)	Duration (Hours)	References
1.	Rapid-acting: Insulin analogues e.g. Lyspro and Aspart	<0.5	0.5-2.5	3-5	(Pearson and McCrimmon, 2014)
2.	Short-acting: Soluble insulin	0.5-1	1-4	4-8	(Pearson and McCrimmon, 2014)
3.	Intermediate-acting Isophane and lente	1-3	3-8	7-14	(Pearson and McCrimmon, 2014)
4.	Long-acting: Bovine ultra Lente, Glargine	2-4	6-12	12-24	(Pearson and McCrimmon, 2014)

Table 1.2B: Oral drugs used to manage T2DM

No	Class with examples	Mechanism of Action	Side effects	References
1.	Biguanides: Metformin Phenformin	Activates AMP-kinase. It increases peripheral uptake of glucose.	Nausea, agitation, dizziness, decrease intestinal absorption of Vitamin B ₁₂ and folate	(Bastaki, 2005; Schäfer, 1983; Bailey, 1992; Periello et al., 1994; Wilding, 2014; Cheng and Kahyap, 2011)
2.	Sulfonylureas: Glibenclamide, Glimpiride, Gliclazide, Glyburide	Closes K _{ATP} channels on β -cell plasma membranes. As a result, voltage-gated calcium channels are opened, allowing influx of calcium ions causing release of preformed insulin granules	Hypoglycaemia, physiological antagonism of CCBs	(Bastaki, 2005; Paice et al., 1985; Campbell and Howlett, 1995; Bolanle et al., 2018)
3.	GLP-1 receptor agonist: Exanetide, Lixisenatide Liraglutide, Albiglutide	Activates GLP-1 receptors.	Indigestion, heartburn, a sour or acidic stomach, belching, nausea, and vomiting. Dizziness, headaches, and jitteriness.	(Triplitt, and Reasner, 2011; Drucker and Nauck, 2006, Meloni et al., 2013; Degn et al., 2004)
4.	SGLT2 inhibitors: Canagliflozin, Dapagliflozin, Empagliflozin	Inhibits SGLT2 in the proximal nephron. Since glucose is eliminated, plasma glycaemic level reduces.	Urogenital infection, loss of body weight.	(Abdul, 2013; Lee et al, 2010)

5.	DPP-4 inhibitors: Sitagliptin, Saxagliptin, Vidagliptin	Inhibits DPP-4 activity, increasing postprandial incretin (GLP-1, GIP) concentrations	Hypoglycaemia	(Herman et al., 2006; Gadsby, 2009)
6.	Thiazolidinedione: Pioglitazone, Rosiglitazone	Activates the nuclear transcription factor PPAR- γ	Weight gain, haematuria, impotence, insomnia, vertigo, proteinuria, and fluid retention that occasional cause heart failure	(Papoushek, 2003; Kahn et al., 2000; Miyazaki et al., 2007)
7.	Alpha Glucosidase Inhibitors: Acarbose, Miglitol, Voglibose.	Inhibits alpha glucosidase enzyme causing delays in the absorption of carbohydrates, reducing both the postprandial rise in plasma glucose in healthy individuals and in individuals with diabetes.	Flatulence, diarrhea, abdominal pain and bloating.	(Bastaki, 2005)
8.	Meglitinides: Repaglinide, Nateglinide	Binds sulfonylurea receptor subunit and closing the K_{ATP} channel	Hypoglycaemia and hypersensitivity reaction (pruritus, rashes, and urticarial).	(Landgraf, 2000; Bastaki, 2005)

AMP: Adenosine monophosphate; K_{ATP} : ATP-sensitive potassium channel; GLP-1: Glucagon-like peptide-1; CCBs: Calcium channel blockers; SGLT2: Sodium glucose cotransporter 2; DPP-4: Dipeptidyl peptidase-4; PPAR- γ : Peroxisome proliferator- activated receptor gamma.

1.1.3 Role of T2DM in the development of atherosclerosis

That T2DM is a risk factor to cardiovascular diseases (CVD) is a known phenomenon (Martín-Timón et al., 2014). T2DM increases adult mortality rates from heart disease and stroke by a factor of two to four and is linked to both microvascular and macrovascular complications (Martín-Timón et al., 2014). The latter of which includes accelerated atherosclerosis that causes severe peripheral vascular disease, premature coronary artery disease (CAD), and an increased risk of cerebrovascular diseases (Haffner et al., 1998; Beckman et al., 2002; Nesto, 2004). Furthermore, a body of findings has demonstrated the involvement of T2DM in multiple cardiac pathologies including atherosclerosis, vascular dysfunction, oxidative stress, hypertension, macrophage accumulation, and inflammation (Reaven, 2012; Bornfeldt and Tabas, 2011; Davidson and Parkin, 2009; Laakso and Kuusisto, 2014).

Vascular damage caused by hyperglycaemia, oxidative stress, inflammation, and disrupted hemodynamic balance may lead to the development of atherosclerosis and the production of arterial thrombus (Bakker et al., 2009). Circulating LDL binds to matrix proteoglycans in the early stages of atherosclerosis, where their oxidation is promoted, producing highly pro-inflammatory particles that encourage endothelial cells to express several adhesion markers (Giannini et al., 2011; Libby, 2012). This encourages the recruitment and activation of circulating monocytes that develop into macrophages, as well as the selective binding of leukocytes and subsequent transmigration into the vascular wall. A non-regulated method used by macrophages to eliminate the excess oxidised LDL results in the production of foam cells and the beginning of fatty streaks. Also, inflammatory cytokines like IL-1 and IL-6 are released by mononuclear cells, which aid in the attraction of more inflammatory cells. As a result, smooth muscle cells multiply and migrate into the intima, where they create and secrete extracellular matrix, promoting the development of fibroatheromas (Giannini et al., 2011). As the process continues, if a fissure or ulceration of the plaque takes place, highly thrombogenic chemicals are exposed, causing platelets to stick together and aggregate, which encourages the creation of thrombi (Badimon et al., 2012). Additionally, platelets have the ability to release growth factors and pro-inflammatory cytokines that encourage monocyte recruitment to atherosclerotic plaques. This promotes the proliferation of fibroblasts and smooth muscle cells, hastening the atherosclerotic process (Badimon et al., 2012).

In addition, metaflammation, a chronic low-grade inflammatory condition is characteristic of T2DM (Hotamisligil, 2006). This chronic condition, which has been proposed as an underlying factor in the development of atherosclerosis in T2DM, involves the same cellular and molecular actors as acute inflammatory responses. In T2DM, hyperglycaemia can raise the levels of circulating cytokines, which can result in chronic inflammation (Hotamisligil, 2006). It has been shown that T2DM patients had higher levels of cytokines such as IL-1b, IL-6, IL-8, and MCP-1 in both monocytes and macrophages (Johnson et al., 2012). The fundamental mechanisms underlying this process include ROS-mediated activation of p38 and other proinflammatory kinases, oxidative stress, increase in NF-kB induction, and activation of the advanced glycation end product-RAGE pathway, a cascade that has been characterised to mediate several diabetic complications such diabetic neuropathy, nephropathy, and foot syndrome (Johnson et al., 2012; Kay et al., 2016). Additionally, exposure to high glucose levels affects macrophages' ability to carry out their phagocytic functions, which explains why T2DM patients are more likely to develop persistent infections (Lecube et al., 2011). T2DM is linked to higher levels of IL-1 and IL-18 as well as enhanced inflammasome activity and nucleotide-binding oligomerization domain-like receptor 3 (NLRP3) (Lee et al., 2013; Meng et al., 2014; Koenen et al., 2011). These occurrences cause neutrophil extracellular trap activation, also known as NETosis, which is a typical macrophage cell death that results in persistent inflammation (Zeadin et al., 2013). Patients with T2DM have been discovered to have high levels of these markers, which are amplified in hyperglycaemic circumstances (Menegazzo et al., 2015).

Furthermore, T2DM patients have higher levels of hepatic TG, which increases their hepatic production of VLDL and TG rich in small dense lipoprotein (sdLDLs) (Verges, 2015; Ginsberg, 1991). The increased permeability of sdLDL into the subendothelial region accelerates atherosclerosis (Lathief and Inzucchi, 2016; Ference et al., 2017). Due to the high oxidation susceptibility of these sdLDL particles, activated macrophages in the subendothelial region actively scavenge them, resulting in formation of foam cells (Chait et al., 1993). Additionally, sdLDL particles have a longer half-life, higher arterial retention, and facilitated penetration into the artery wall as well as increased proteoglycan binding (Hoogeveen et al., 2014). Also, sdLDL particles are more likely to be glycosylated, more durable, and more vulnerable to free radical oxidation (Witztum et al., 1982). Furthermore, the gene for apoA-I, the main apolipoprotein found in HDL particles, contains an insulin response element (Bays et al., 2013; Mooradian et al., 2004). As the liver develops more insulin resistance, less apoA-I is produced,

and less HDL biogenesis takes place. Insulin resistance decreases adipocytes' capacity to make HDL by downregulating the expression of ABCA1 on their surface, which is a membrane transport protein A1 that binds to ATP (Chung et al., 2011; McGillicuddy et al., 2011; Zhang et al., 2010). Additionally, HDL particle concentrations are not only quantitatively reduced in T2DM but are typically malfunctioning and unable to perform their critical functions, such as reversing cholesterol transport and regulating oxidative and inflammatory processes (Farbstein and Levy; 2012).

These T2DM-driven events strongly promote the formation of atherosclerotic plaques (Bolanle et al., 2021; Galicia-Garcia et al., 2020). Atherosclerosis is progressive and is characterised by persistent low-grade inflammation and cholesterol build-up at vulnerable areas on the coronary artery wall, ultimately resulting in CAD (Bolanle et al., 2021; Galicia-Garcia et al., 2020). Following the formation of atherosclerotic plaques, the endothelium's dysfunctional responses to hemodynamic stress and changes in blood flow result in increased expression of proteins like superoxide dismutase (SOD). SOD activates several intracellular signalling pathways to maintain a prothrombotic and proinflammatory phenotype, which are a contributing factor in plaque formation (Linton et al., 2019; Gimbrone and Garcia-Cardena, 2013). These atherosclerotic plaques can cause angina or, in the event of plaque rupture and thrombosis, myocardial infarction and a risk of death, by narrowing the arteries and decreasing blood flow to the heart muscle formation (Linton et al., 2019; Gimbrone and Garcia-Cardena, 2013).

1.2 Coronary artery disease (CAD)

Over 65,000 people per year in the UK alone die from CAD, which occurs when the coronary artery vasculature is unable to deliver enough oxygen- and nutrient-rich blood to the heart (BHF, 2019). It significantly affects people's quality of life, potential employment, and interpersonal relationships, as well as raising the danger of dying too soon (BHF, 2019). The fact that symptoms are not noticeable until afflicted coronary artery branches are severely dysfunctional is a significant issue limiting successful management of CAD (Bolanle et al., 2021; BHF, 2019). Angina, shortness of breath, exhaustion, weakness, and general feeling of unwell are classical symptoms (BHF, 2020). CAD can cause several complications, some of which, like abnormal heart rhythm or arrhythmia, heart failure, and blood clots in the artery due to ruptured plaque(s), can be managed without hospitalisation; however, myocardial infarction, which is the primary cause of mortality in CAD patients, would require immediate hospitalisation and intervention (BHF, 2020).

The economic burden of CAD is huge as hospitalizations, therapies, revascularization procedures, clinic visits, emergency room visits, and prescribed medication treatments all contribute to its financial burden (Khan et al., 2020). The World Heart Federation estimates that the global cost of CVD in 2010 was roughly US\$863 billion, and that cost will likely surpass US\$1 trillion by 2030. The cost of CAD in nations like the United States is close to 1%-1.5% of the gross domestic product (GDP), with CAD episodes costing more than \$5,000 each (Khan et al., 2020). In the UK, it is estimated that CAD cost the healthcare system about £9 billion and cost the entire economy estimated £19 billion (BHF 2020). Notably, the median total cost of CAD care in low and middle-income countries is 10% of all healthcare spending per capita (Griffiths et al., 2018).

DM patients, especially those with T2DM, are more likely to develop CAD (BHF, 2020). Globally, 50–80% of T2DM patients also have CAD (Landsberg and Molitch, 2004). T2DM is a risk factor for CAD, and when these two disease states coexist in an individual, the prognosis is frequently worse than when they do so separately (Landsberg and Molitch, 2004; Gress et al., 2000). The risk factor of obesity, chronic inflammation, oxidative stress, and insulin resistance are pathways that are conserved in the pathophysiology of CAD and T2DM (Cheung and Li, 2012). CAD is worsened by unhealthy lifestyle such as smoking, high cholesterol, obesity, hypertension, and a lack of regular exercise. Although the related

consequences are much less severe in patients who have well-controlled blood sugar levels, however, the management goals for a CAD patient with or without T2DM remain the same (Cheung and Li, 2012).

1.2.1 Overview of current management of CAD

The aims of management are to improve blood supply to the heart muscle and minimize the risk of long-term microvascular and macrovascular complications as detailed in Figure 1.1.

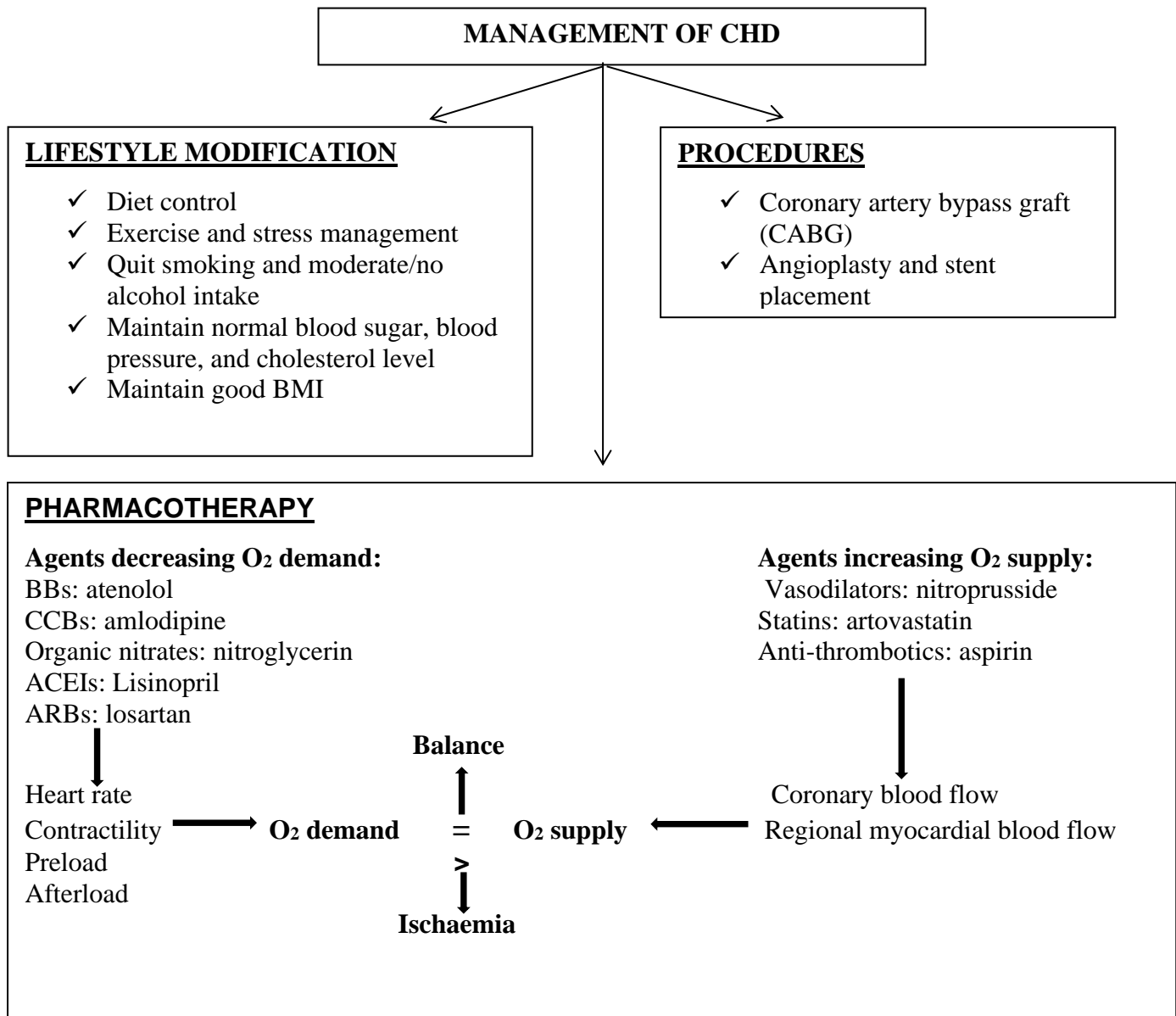


Figure 1.1: Overview of the current management of coronary artery disease. BMI:Body mass index; BBs:Beta blockers; CCBs:Calcium channel blockers; ACEIs:Angiotensin converting enzyme inhibitors; ARBs:Angiotensin receptor blockers.

Despite the documented effectiveness of pharmacological interventions such as statins and anti-platelet medications that decrease atherosclerosis and thrombosis, respectively, and non-pharmacological management, there is a good chance that CAD may worsen to the point where surgical intervention becomes necessary (Goldman et al. 1988). A coronary artery bypass graft (CABG) might be required in such a situation. For instance, when high-grade blockages exist in any of the major coronary arteries or percutaneous coronary intervention (PCI) has failed to remove the blockages, CABG is typically advised (Barbato et al., 2016; Hillis et al., 2011). Specifically, clinical indication for CABG include, one or more significant stenoses greater than 70% in a patient with significant angina symptoms despite receiving the most effective medical treatment; one or more significant stenoses greater than 70% in a patient with left main disease greater than 50%; three-vessel coronary artery disease greater than 70% with or without proximal left anterior descending artery (LAD) involvement; two-vessel disease: LAD plus one other major artery; and one vessel disease greater than 70% in a survivor of sudden cardiac death with ischemia-related ventricular tachycardia (Alexander and Smith, 2016; Hillis et al., 2011).

1.2.2 Coronary artery bypass graft (CABG)

CABG remains a gold standard in the management of patients with CAD and around 20,000 CABG procedures are performed in England each year (NHS, 2020). It uses blood vessels from different regions of the body, including the radial artery (RA) from the arm, the great saphenous vein (GSV) from the leg, and the internal mammary artery (IMA) from the chest (NHS, 2020). These blood vessels are attached to the coronary artery below the area of atherosclerotic narrowing, thereby “bypassing” the affected vessel (Banning et al., 2010). However, CABG failure is a known phenomenon that puts patients at risk for recurrent angina and necessitates repeated coronary revascularization in order to lower the risk of myocardial infarction. The failure rates of saphenous vein grafts (SVG) at one year after surgery, however, have been reported to range between 10% and 25% (McKavanagh et al., 2017; Alexander et al., 2005). From 1 to 5 years, a further 5% to 10% SVGs will occlude, and from years 6 to 10 an additional 20-25% will fail (McKavanagh et al., 2017; Campeau et al., 1979). After 10 years, SVG patency rates are about 50%, with only half of these free of vessel atheroma (McKavanagh et al., 2017; Alexander et al., 2005; Bourassa et al., 1985). On the other hand, the use of IMA has been shown to improve patency results; vascular patency was found to be 85–91% ten years after surgery (Banning et al., 2010). However, despite the higher chance of SVG failure compared to arterial grafts, it is still the preferred approach for CABG because complete

revascularization with arterial grafts is not always attainable and in instance where multiple anastomoses is desired, SV offers a convenient option (McKavanagh et al., 2017).

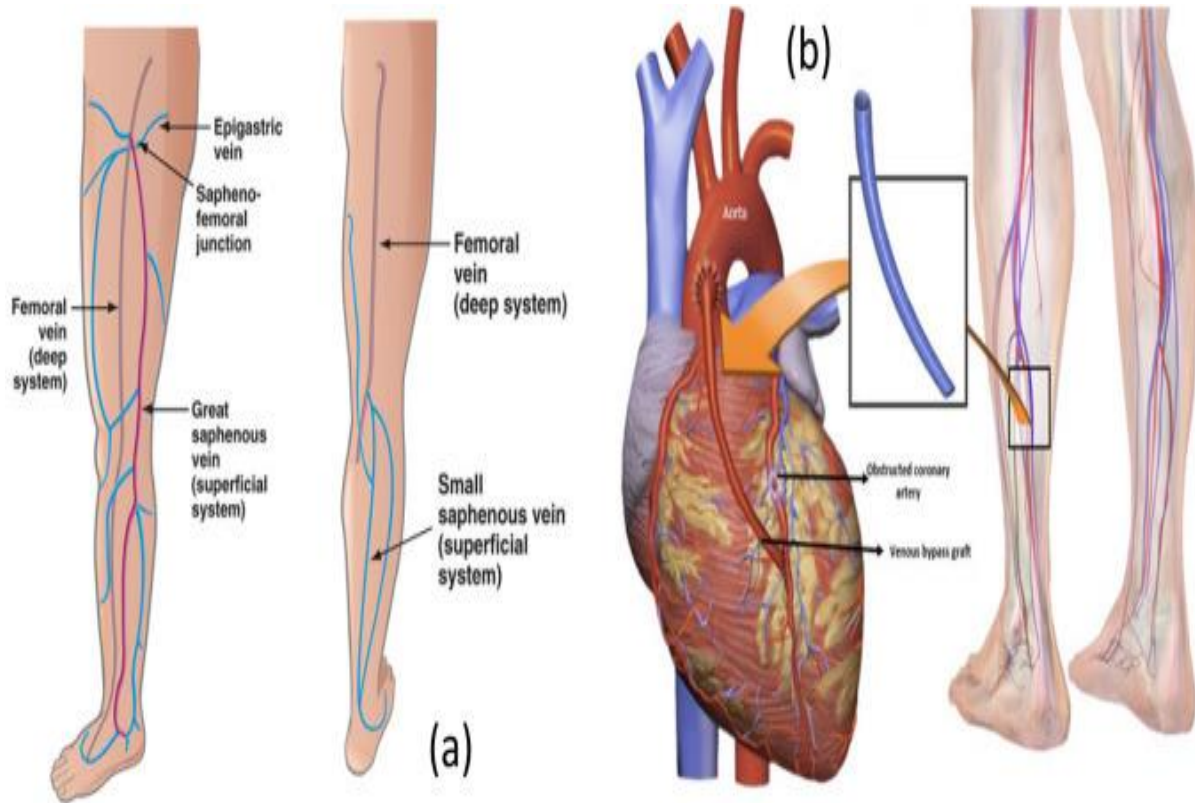


Figure 1.2: Saphenous vein bypass graft. (a) Great and small saphenous veins are shown in this leg section, and (b) a grafted vein been used to bypass a blocked coronary artery. The image in (a) was originally from (<http://www.surgery.usc.edu/vascular/varicoseveinsandvenousdisease.html>), and the image in (b) was taken from (<https://atlasofscience.org/a-novel-treatment-for-saphenous-venous-graft-thrombosis/>). Images adapted from (Li, 2018).

1.2.3 Coronary artery bypass graft failure (CABGF)

SVG failure is suspected to be caused by a number of variables. The majority of effort has been paid to graft-, patient-, and surgery-related variables, while cellular and molecular causes of SVG failure have received relatively less attention. The type of artery or vein that was transplanted and the coronary flow should be taken into account for the graft-related factor. Similar to this, the size of the distal perfusion bed, the presence of focal stenosis, and the graft diameter influence the required perfusion after CABG, while lower flow has been linked to increased neointimal proliferation in SVGs (Faulkner et al., 1975). SVGs to the major right coronary artery are least likely to have long-term patency, followed by those to diagonals, circumflex branches, and the posterior descending artery. SVGs to the left anterior descending artery have the best patency (Sabik and Blackstone, 2008). CABG failure may also be brought on by patient-related variables like age, gender, and other underlying morbid disorders like T2DM, left ventricular hypertrophy, and renal insufficiency (Yanagawa et al., 2014). A better knowledge of these elements has contributed to increased CABG patency.

1.2.3.1 Pathophysiology of CABGF

Significant occurrences in CABGF include thrombosis, NIH, and atherosclerosis (Southerland et al. 2013). Thrombosis is the root cause of early CABGF, which manifests one month after surgery and accounts for 12% of all vein graft occlusions (Mitra et al. 2006). Atherosclerosis and NIH together account for 50% of late CABGF rates over the course of ten years (Goldman et al. 2004). Poor surgical technique, anastomotic issues, graft infection, and mechanical compression of the vein are additional causes of CABGF (Mitra et al. 2006).

1.2.3.1.1 Vasculature

The natural HSV wall is composed of three layers: tunica- intima, media, and adventitia (Cox et al. 1991). The intima, the innermost layer, has a continuous monolayer of vascular endothelial cells (VECs) on a basement membrane (Cox et al. 1991). VECs regulate platelet adhesion, macrophage infiltration from the lumen, cellular proliferation, and inflammatory responses under normal physiological circumstances (Esper et al. 2006). The medial layer consists of the extracellular matrix (ECM) and layers of vascular smooth muscle cells (VSMCs), which make up most of the cell type. They are held in place by internal and external elastic lamina. The primary function of VSMCs is to regulate vascular tone (contraction and

relaxation). By preventing VSMC migration and multiplication, the ECM keeps VSMC differentiated and dormant (Uzui et al. 2000; Johnson and Galis 2004). VSMCs are therefore in a contractile phenotype, quiescent, and with little turnover under physiological conditions. However, VSMCs can quickly and irreversibly switch between contractile and synthetic states in response to environmental disturbances like injury or illness. The loose network of fibroblasts, neurons, and collagen bundles makes up the outermost adventitial layer. They are pervaded by the vasa vasorum (a network of small blood vessels that provide blood supply to the vein wall). Both veins and arteries have three different layers (intima, media and adventitia), which makes them similar. However, arteries have thicker arterial walls because they have more VSMCs and elastic fibres (Cox et al. 1991). Veins typically experience low blood pressure and flow, in contrast to arteries. Therefore, after being grafted into an arterial circulatory bed, veins significantly adapt and change (Cox et al. 1991; Johnson et al. 2001).

1.2.3.1.2 Neointimal hyperplasia (NIH)

NIH is a pathological vascular remodelling that appears post-interventional surgery and is caused by VSMC proliferation and migration into the intima, which results in blood vessel thickening and eventual narrowing (loss of patency), which may impair blood flow and lead to angina (Zain et al. 2020). Additionally, throughout the adaptation phase, HSV grafts in the arterial circulation are exposed to arterial pressure, wall tension, shear stress, and pulsatile blood flow. These changes in vascular hemodynamics act as mechanical stimuli to cause VSC proliferation and migration (Davies et al. 1993; LaMack et al. 2010; Shukla and Jeremy 2012). There is also accumulating evidence that several cytokines such as IL-6, growth factors, and other vasoactive mediators, such as angiotensin II and thrombin, localise to wounded tissue promote NIH (Sukovich et al. 1998; Suzuki et al. 2000; Dronadula et al. 2005; Chava et al. 2009; Xiang et al. 2014).

Endothelium denudation and vascular injury often occur as a result of the surgical preparation (harvesting and implantation) of HSVs for CABG surgery. IL-6, PDGF, and other vasoactive mediators, including thrombin, are released by platelets and leukocytes after extravasation at the vascular injury site. Increased levels of IL-6, PDGF, thrombin, and angiotensin II cause a change in the VSMC's phenotype from contractile to synthetic and the induction of pro-survival genes (cyclin D1), MCP-1, matrix metalloproteinases (MMP)-2 and MMP-9 through activation of the Janus kinase (JAK)/signal transducer and activator of transcription (STAT). All these

phenomena lead to chronic localised VEC inflammation, increased VSMC proliferation, and migration from media to intima, which results in vascular remodelling and lumen constriction known as NIH.

1.2.3.2 Surgery-related factors predisposing to SVG failure

Complications following CABG can occur for a variety of reasons, including variations in size between the graft and the artery, kinking of the graft, inadequate distal washout, and small target arterial diameter (McKavanagh et al., 2017). Studies throughout the years have demonstrated that surgical method variance affects SVG patency and results (McKavanagh et al., 2017). Below are some of these variances.

1.2.3.2.1 Variation in on-pump and off-pump surgery

In on-pump CABG, the cardiopulmonary bypass machine (known as the heart-lung machine or the pump) is used to provide blood supply to the rest of the body while immobilising the heart using cardioplegia solution. In this instance, the operating circumstances are better suited to achieving excellent vascular anastomoses. Off-pump CABG, which is thought to be a more recent technique, seeks to accomplish the same result without the use of a heart-lung machine or cardioplegia medication. Special equipment is utilised throughout the process to mechanically stabilise the affected area of the heart while it is still beating so that suturing can be done on a platform that is reasonably stationary (Shekar, 2006, Detter et al., 2002). In comparison to on-pump CABG, large, randomised studies and meta-analyses have demonstrated that off-pump surgeries result in worse 1-year composite outcomes and graft patency (Hattler et al., 2012, Takagi et al., 2010). These variations might result from the relative hypercoagulability observed with off-pump treatments as opposed to on-pump procedures (McKavanagh et al., 2017). Also, cardiopulmonary bypass during on-pump surgery results in platelet dysfunction and coagulopathy, both of which are advantageous for promoting SVG patency (McKavanagh et al., 2017, Mannacio et al., 2012).

The choice of procedure typically relies on how comfortable the surgeon is performing the procedure, however, of the two procedures, on-pump CABG is the more widely utilised one (Shekar, 2006). Although peri- and post-CABG problems like stroke, kidney or liver failure, a decline in cognitive function, and bleeding are more frequently related with the on-pump technique. These issues are less common with the off-pump procedure, especially in high-risk patients (Shekar, 2006).

1.2.3.2.2 Sequential and composite grafting

Sequential and composite SVG grafting are typically used in situations where there are insufficient conduits. Sequential and composite grafting uses more than one distal anastomosis for every proximal anastomosis in order to achieve complete revascularization, in contrast to the single graft, which uses a single distal anastomosis for every proximal anastomosis (Figure 1.3). In comparison to a single graft, the sequential anastomosis may enable a larger combined perfusion bed, reducing vascular resistance and increasing flow velocity (Sewell and Sewell, 1976). Because the limited SVG conduit is used more effectively, the full revascularization accomplished with sequential and composite grafting is better for patients with multi-vessel CAD (Flemma et al., 1971).

When the graft anastomoses are properly done, early evidence revealed that the clinical outcomes from multiple distal target SVGs were either comparable to or better than those from single distal target SVGs (Grondin and Limet, 1977). Five years after CABG, larger, more recent studies, however, indicate that people who have many distal target SVGs are more likely to experience graft failure and are at a higher risk of dying, having a heart attack, or undergoing repeat revascularization (Mehta et al., 2011). The end-to-side and side-to-side anastomosis may insert into a target vessel of low quality in diabetes patients (Oz et al., 2006). Composite grafts are typically used for arterial conduits when two IMAs or an IMA and radial artery are involved in surgery.

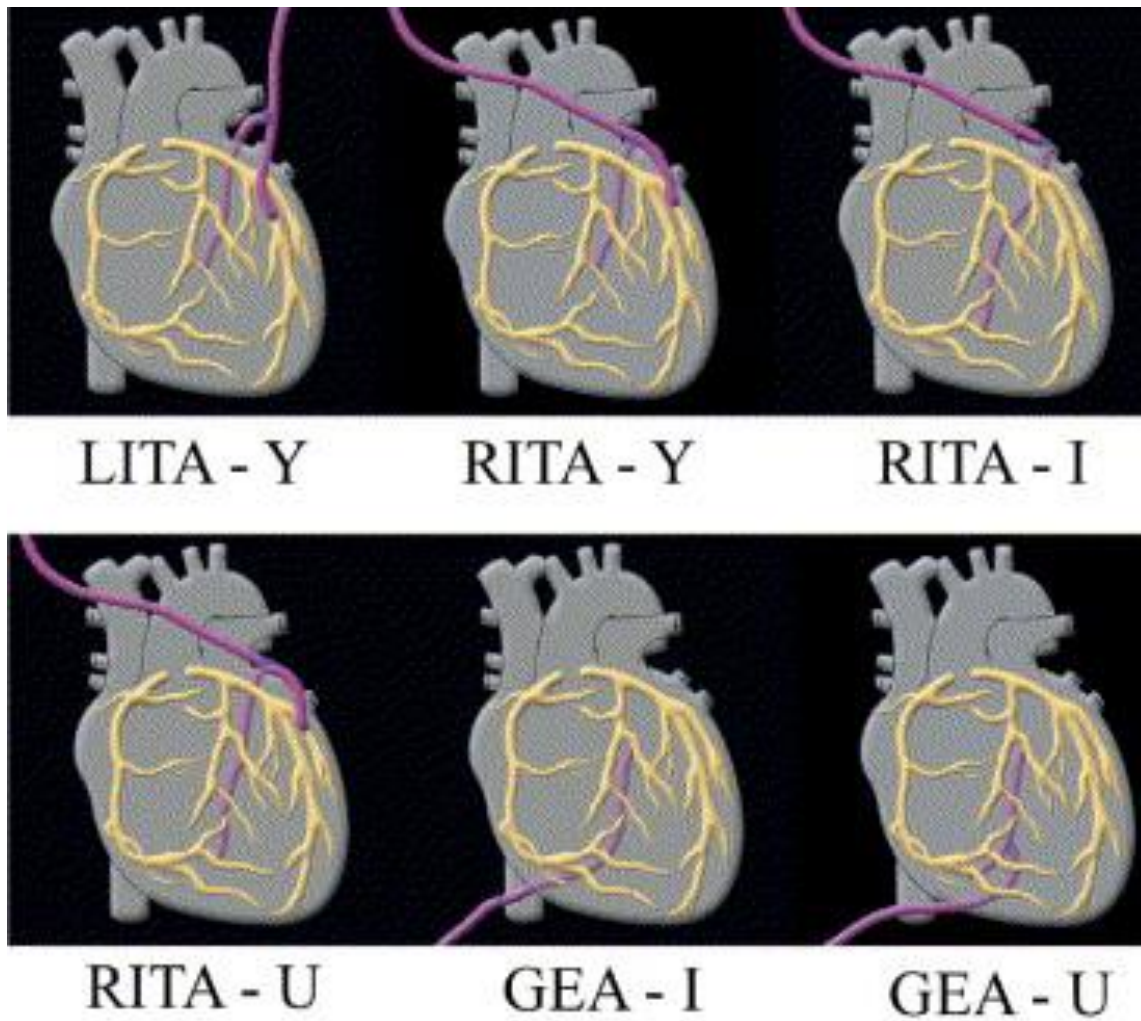


Figure 1.3: Patterns of composite grafting with sequential bypass. (Left to right, top row) left internal thoracic artery (LITA), Right internal thoracic artery (RITA), and I-composite grafted right internal thoracic artery. (Left to right, bottom row) RITA with a U-composite graft, gastroepiploic artery (GEA) with an I-composite graft, and GEA with a U-composite graft. Images adapted from (Fukui et al., 2005).

1.2.3.2.3 No-touch technique

Before "no-touch" SVG harvesting was invented by Souza et al. in 1996 (McKavanagh et al., 2017), a significant post-SVG difficulty was the development of thrombi within grafts as a result of intra-operative manual disruption of the endothelium and hydrostatic dilation (LoGerfo et al., 1977). With no-touch SVG harvesting, the perivascular tissue around the pedicled SVG can be preserved. Compared to the traditional harvesting method, this method offers better graft patency (Souza et al., 2006). More recent information from randomised studies has further revealed that no-touch harvesting reduces the likelihood of neointimal hyperplasia, which is the main cause of long-term CABG failure, by activating the VSMC less during the harvesting process than standard harvesting does (Verma et al., 2014).

1.2.3.2.4 Compression therapy

HSV typically have luminal widths bigger than those of coronary arteries, which may result in aberrant blood currents within transplanted veins that could harm the vessel and raise the risk of thrombus development. Additionally, as veins lack the strong muscle walls present in arteries, the higher flow rates present in arterial circulation have the potential to harm SVG and cause an adaptive thickening of the vessel wall that results in the development of NIH (McKavanagh et al., 2017, Moodley et al., 2013). To reduce this variation, a method utilising external compression via a support device inserted after surgery has been developed. External compression of SVGs promotes downsizing and avoids dilatation, which has been shown to improve arterial-like healing and lessen the occurrence of neointimal hyperplasia (McKavanagh et al., 2017, Moodley et al., 2013).

Although improvements in surgical methods over time have improved patency results, the proportion of VGF is still alarmingly high. This raises the possibility that additional molecular pathways, unrelated to surgical methods, may have an impact and play a role in VGF. For instance, it is well-known that NIH characterised by defective proliferation and migration of vascular ECs and SMCs is a significant contributor to VGF (Bolanle et al., 2021). VGF has also been linked to other molecular pathways, including protein *O*-GlcNAcylation, ROS-induced vascular dysfunction, and altered metabolic balance of vascular ECs and SMCs (Bolanle et al., 2021). However, despite a substantial amount of research findings linking these processes to VGF, not so much has been done on targeting them to develop therapeutic agents that improve patency and treatment outcome.

1.3 Protein O-GlcNAcylation

Protein *O*-GlcNAcylation is a post-translational modification (PTM) that occurs on target proteins that are found in the nucleus, mitochondria, and cytoplasm in response to nutrients and stress changes by attaching a single sugar, β -*N*-acetylglucosamine (*O*-GlcNAc) to the serine or threonine residues (Yang and Qian, 2017; Hart et al., 2007; Hart et al., 1989). According to the rates of glycolysis and UDP-GlcNAc production in ex vivo mouse hearts, glucose metabolism through the hexosamine biosynthetic pathway (HBP) is ~0.006% of glycolytic efflux (Olson et al., 2020), which is substantially lower than the 2-3% suggested by Marshall et al (Marshall et al., 1991). The rate-limiting enzyme L-glutamine-D-fructose 6-phosphate amidotransferase stimulates the activation of the HBP, which promotes the conversion of glucose to UDP-N acetylglucosamine (UDP-GlcNAc), which is utilised for glycosylation (Yang and Qian, 2017).

O-GlcNAc transferase (OGT) and *O*-GlcNAcase (OGA), a single enzyme pair, catalyse the attachment and removal of this monosaccharide to target proteins respectively (Figure 1.4). As shown in Figure 1.4, glucose enters the cell and is converted to fructose-6P (fructose-6-phosphate). Next, the rate-limiting enzyme in the HBP, glutamine-fructose-6P amidotransferase 1 (GFAT), transfers an amino group from glutamine to fructose-6-phosphate to form glucosamine-6-phosphate (GlcN-6-P). Glucosamine-phosphate N-acetyltransferase (GNPNAT, EMeg32) quickly acetylates GlcN-6P to form N-acetylglucosamine-6-phosphate (GlcNAc-6P) (Moremen et al. 2012), which is then isomerized by glucosamine-phosphate phosphomutase (PGM3/AGM1) to produce N- acetylglucosamine-1-phosphate (GlcNAc-1P) (Holt and Hart, 1986). The amino sugar substrate, UDP-GlcNAc, is produced by UDP-N-acetylhexosamine pyrophosphorylase 1 (UAP/AGX1) after the nucleoside has been added to the sugar. Then, in the ER and Golgi, UDP-GlcNAc serves as a substrate for N- and O-linked glycosylation processes, as well as for OGT's *O*-GlcNAc modification of nuclear and cytoplasmic proteins. By adding GlcNAc back to the HBP pool for recycling through the salvage route, OGA catalyses the elimination of *O*-GlcNAc. The generation of the amino sugar substrate UDP-GlcNAc for protein glycosylation is increased by persistent and unresolved hyperglycaemia, which also promotes glycolytic efflux and the activation of HBP (Chang et al., 2020; Wellen et al., 2010; Swamy et al., 2016; Taylor et al., 2009; Weigert et al., 2003).

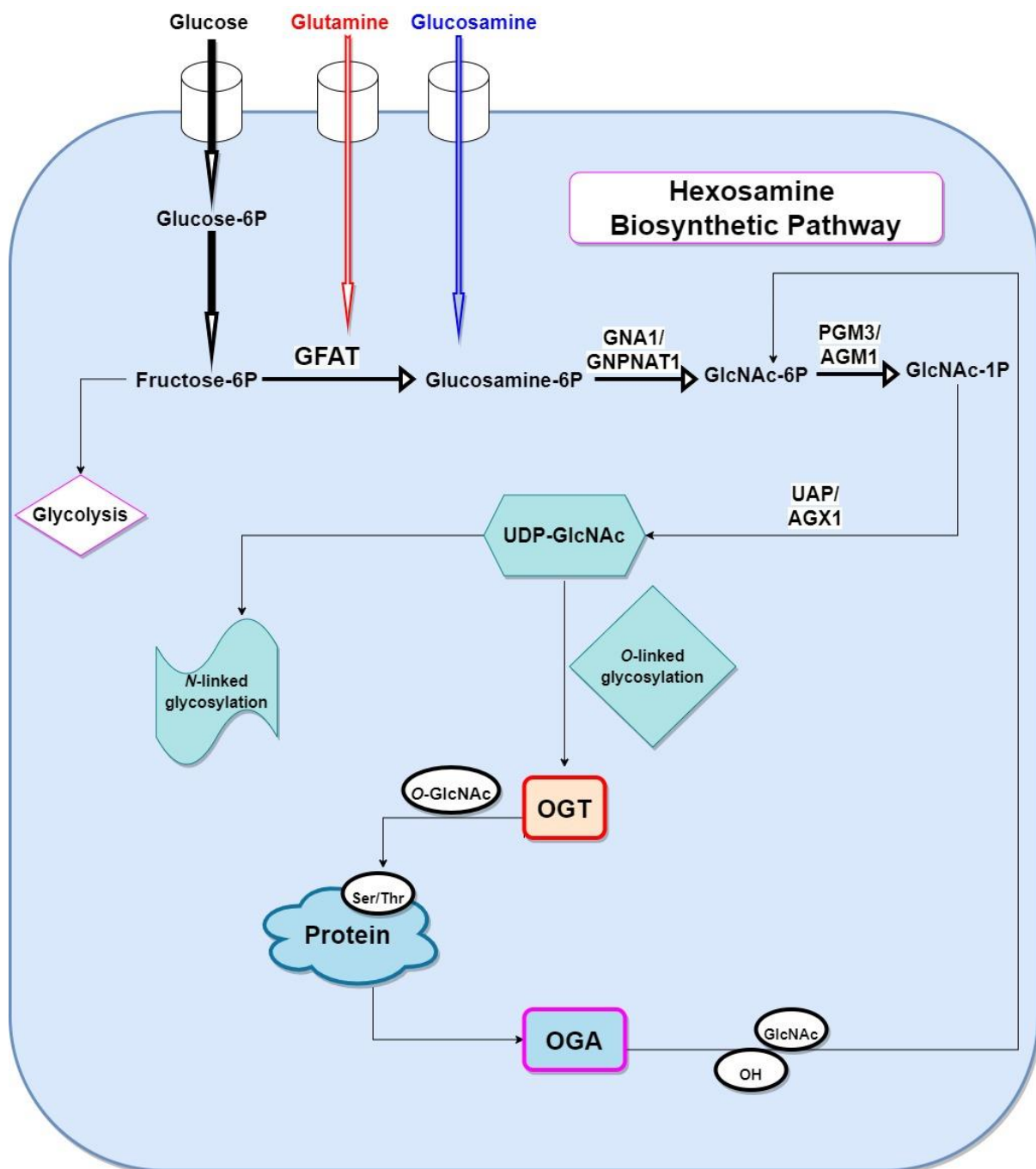


Figure 1.4: Hexosamine Biosynthetic Pathway. Fructose-6P (fructose-6-phosphate), glucosamine-6P (glucosamine-6-phosphate), GFAT (glutamine:fructose-6-phosphate amidotransferase), OGT (O-GlcNAc transferase), OGA (O-GlcNAcase), GNA1/GNPAT1 (glucosamine-6-phosphate N-acetyltransferase (UDP-N-acetylhexosamine pyrophosphorylase), PGM3/AGM1 (phosphoglucomutase), UDP-GlcNAc (uridine diphosphate-N-acetylglucosamine), GlcNAc-6P (N-acetylglucosamine-6-Phosphate), and GlcNAc-1P (N-acetylglucosamine-1-Phosphate), UAP/AGX1 (UDP-N-acetylhexosamine pyrophosphorylase).

In target proteins, the OGT enzyme, which is encoded by the OGT gene, catalyses the addition of a GlcNAc moiety via an O-glycosidic linkage to the free hydroxyl group on either serine or threonine residues (Yang and Qian, 2017; Lazarus et al., 2016). The OGT gene produces the three human OGT isoforms (ncOGT, mOGT, and sOGT). The longest isoform has been found to be ncOGT, which is located in both the nucleus and cytoplasm. It starts with a distinctive N-terminal sequence and is then followed by 12 TPR motifs, a linker region, and the catalytic domain. mOGT, the second isoform contains a different N-terminal sequence, which also encodes a mitochondrial targeting sequence. The N-terminal sequence is then followed by 9 TPR motifs, a linker region, and the catalytic domain. The smallest isoform of OGT, sOGT, is universally expressed in cells. Only two TPR motifs, a linker region, and the catalytic domain make up this structure. The CD I domain and the CD II domain are the only two domains present in the catalytic region of all three isoforms (Lazarus et al., 2016). On the other hand, OGA reverses this O-GlcNAc modification by hydrolysing the O-GlcNAc from protein targets (Yang and Qian, 2017). Numerous proteins, including nuclear pore proteins, RNA polymerase II, related transcription factors, cytoskeletal proteins, proteasomes, synapsins, oncogenic proteins, and tumour suppressor proteins, are modified with the O-GlcNAc molecule (Lazarus et al., 2016).

O-GlcNAcylation has been linked to a number of cellular processes, such as the temporal control of insulin signalling, gene transcription, epigenetic changes, and cell signalling dynamics (Yang et al., 2017; Wells et al., 2001; Yi et al., 2012). Although the mechanisms governing the temporal regulation of O-GlcNAc signalling are extremely dynamic and frequently transient, they remain poorly understood (Wells et al., 2001; Slawson and Hart, 2011; Ruan et al., 2013). The abundance of the donor substrate UDP-GlcNAc, as well as the expression levels of OGT, OGA, and their corresponding adaptor proteins and substrates, are regulated by nutrient availability, which also controls the amounts of cellular O-GlcNAcylation (Wells et al., 2001; Zhu et al., 2014; Bond and Hanover et al., 2013). For instance, hormones like insulin, glucagon, and ghrelin, which are released in response to changes in the body's metabolism, alter O-GlcNAc signalling in particular cell types and organs like the liver, pancreas, and beta cells to control vital pathways that keep metabolic equilibrium (Wells et al., 2001; Bond and Hanover et al., 2015; Levine et al., 2016). While the mutual control of OGT and OGA maintains cellular O-GlcNAcylation levels, persistent hyperglycaemia can shift the balance in favour of OGT-mediated O-GlcNAcylation (Wells et al., 2001; Lazarus et al., 2011). OGT is also a target for post-translational modification by serine/threonine-directed kinases

like AMP-activated protein kinase (AMPK), which phosphorylates OGT on Thr444 to control OGT subcellular localization and substrate specificity, and tyrosine kinases like the insulin receptor, which phosphorylates and boosts OGT activity (Zhu and Hart, 2020). In order for cells to perform at their best, *O*-GlcNAc homeostasis must be maintained; as a result, disruption of this process may play a role in the pathogenesis of disorders like T2DM, which have a clear-cut metabolic component (Wells et al., 2001; Yuzwa et al., 2012).

Additionally, according to recent studies, *O*-GlcNAcylation may directly contribute to the emergence of T2DM, though these findings are preliminary, and the underlying mechanism is not fully understood (McClain et al., 2002; Kruszynska and Olefsky, 1996). In addition to Akt, several significant proteins in the insulin signalling pathway, such as the IRS proteins IRS1 and IRS2, phosphoinositide-dependent kinase 1 (PDK1), and PI3K, have been demonstrated to be *O*-GlcNAcylated (Teo et al., 2010). *O*-GlcNAcylation of IRS1 in insulin-resistant adipocytes was observed in a study using immunoprecipitation and immunoblotting (Voseller et al., 2002). Mass spectrometry study later verified this, identifying Ser1036 as the primary *O*-GlcNAcylation site on IRS1 (Ball et al., 2016). Due to the fact that *O*-GlcNAcylation of IRS1 has been linked to conditions that promote insulin resistance in adipocytes (Voseller et al., 2002), endothelial cells in vitro (Foderici et al., 2002), and skeletal muscle in vivo (Foderici et al., 2002), this site identification has increased our understanding of the molecular interaction and effect of *O*-GlcNAcylation on IRS (Patti et al., 2002). It is significant to note that T2DM patients suffer from reduced IR/IRS/PI3K activation due to insulin resistance (Cusi et al., 2000; Sesti et al., 2001). Additionally, a recent investigation revealed that increasing *O*-GlcNAcylation in 3T3-L1 mice adipocytes prevented Tyr608 phosphorylation of IRS1, which decreased Akt activation and facilitated insulin resistance (Whelan et al., 2010). Together, these data suggest that metabolic regulation of insulin signalling, which is implicated in the development of T2DM, is regulated by *O*-GlcNAc alteration of critical signalling intermediates. However, treatment of 3T3-L1 adipocytes with OGA inhibitor 6-acetamido-6-deoxy-castanospermine was not sufficient to produce insulin resistance (Macauley et al., 2010), suggesting a more complex involvement of *O*-GlcNAcylation in the regulation of insulin resistance.

1.3.1 Involvement of Protein O-GlcNAcylation in Vascular dysfunction and VGF

O-GlcNAcylation alters almost every functional class of proteins, including those with important roles in vascular function, such as eNOS, SERCA, PLC, PKC, and PI3K, as well as those involved in cytoskeleton control and microtubule assembly (Lima et al., 2011; Hart et al., 2007; Zachara, 2009; Holt and Hart, 1986; Zachara and Hart, 2006; Dong and Hart, 1994). Increased responsiveness to vasoconstrictor stimuli, decreased endothelium-dependent vasodilation, and inhibition of eNOS are all associated with higher levels of protein *O*-GlcNAcylation in the vasculature (Zachara, 2009; Marshall, 1996; Voseller et al., 2002; Lima et al., 2009). *O*-GlcNAcylation was recently demonstrated to mediate the impairment of eNOS activation brought on by glucose in endothelial cells from T2DM patients, leading to altered endothelial cell phenotype (Masaki et al., 2020). Venous endothelial cells obtained from T2DM patients and non-diabetic controls were studied in this study. In T2DM patients compared to non-diabetic controls, endothelial *O*-GlcNAcylated protein levels were 1.8-fold greater. In endothelial cells from T2DM patients, normal glucose concentrations (5 mmol/L) decreased *O*-GlcNAc levels and restored insulin-mediated activation of eNOS, but increased glucose concentration (30 mmol/L) maintained both *O*-GlcNAcylated protein levels and impaired insulin action (Masaki et al., 2020). OGA inhibitor, Thiamet G treatment of endothelial cells elevated *O*-GlcNAc levels and inhibited the enhancement of insulin-mediated eNOS phosphorylation by glucose normalisation. These results strongly imply that *O*-GlcNAc is a key player in the endothelial dysfunction seen in T2DM.

O-GlcNAc alteration has also been associated to decreased activation of the insulin receptor/IRS/PI3K/Akt/eNOS pathway (Voseller et al., 2002, Zhang et al., 2013; McClain et al., 2002). Due to insulin's role in maintaining chronic vasodilation through the eNOS-mediated production of nitric oxide, this affects endothelial dysfunction (Fulton et al., 1999; Montagnani et al., 2001; Zhang et al., 2009; Gélinas et al., 2002). Biochemical investigations have also revealed that excessive *O*-GlcNAc modification can inhibit nitric oxide synthesis in the endothelium at many loci within the insulin receptor/IRS/PI3K/Akt/eNOS pathway (Fulop et al., 2007; Federeci et al., 2002; D'Alessandris et al., 2004). Additionally, the HBP activation and hyperglycaemia that promote *O*-GlcNAcylation reduce eNOS activation and phosphorylation through the Akt pathway (Federeci et al., 2002; Michell et al., 1999; Du et al., 2001). All of these findings point to *O*-GlcNAcylation as a key player in the aetiology of numerous cardiovascular disorders and a prominent modulator of vascular dysfunction. *O*-GlcNAcylation, however, has also been demonstrated to be able to suppress endoluminal artery

injury-induced acute inflammatory and neointimal responses, indicating that it may potentially have anti-inflammatory actions that are protective in injured arterial beds (Xing et al., 2008). This study reveals that *O*-GlcNAcylation effects are not always harmful, and it is important to keep this in mind when exploring this pathway for development of new therapy.

In a related study, (Da Costa et al. 2018) found that the anti-contractile qualities of perivascular adipose tissue (PVAT) in metabolic syndrome are compromised by elevated *O*-GlcNAcylation of eNOS. According to Ferrández-Alfonso et al. (2013) and Xia and Li (2017), the PVAT is a highly active endocrine organ that releases vasoactive substances such as adiponectin, hydrogen peroxide, leptin, and nitric oxide that are crucial for maintaining vascular function. This study, however, suggested that the anti-contractile effect was downregulated in PVAT isolated from Wistar rats fed a high-sugar diet that showed features of metabolic syndrome, increased protein *O*-GlcNAcylation, reduced eNOS expression, and increased eNOS *O*-GlcNAcylation at Ser1177, while a related study also showed increased *O*-GlcNAcylation of adenosine monophosphate-activated protein kinase (AMPK), a serine/threonine-directed protein kinase which positively regulates eNOS activity (Ma et al., 2010). Overall, these modifications resulted in a severe deterioration of PVAT's vasoactive characteristics, which favoured vasoconstrictors produced from PVAT and activated the signalling pathways connected to them in nearby vasculature (da Costa et al., 2018; da Costa et al., 2017).

Furthermore, it has been demonstrated that high glucose (HG) induced OGT expression in human aortic endothelial cells and that elevated OGT expression and protein *O*-GlcNAcylation is implicated in endothelial inflammation, as HG induced ICAM-1, VCAM-1, and E-selectin mRNA expression as well as ICAM-1 expression (Lo et al. 2018). It was also demonstrated that THP-1 monocyte adhesion was decreased after OGT depletion by siRNA (Lo et al 2018). In a chronic hyperglycaemic condition characteristic of poorly controlled T2DM, *O*-GlcNAcylation-induced endothelium inflammation is chronically increased (Lo et al 2018). This would maintain the pro-inflammatory environment necessary for the development of a neointima in HSVECs, leading to a progressive loss of patency that might culminate in VGF. On the other hand, when HSV is grafted into the coronary circulation, it must adapt to the higher force of arterial blood flow, which it accomplishes by increasing VSMC proliferation resulting in remodelling and thickening of the vascular wall. These findings point to a critical role for increased protein *O*-GlcNAcylation in the aetiology of vascular dysfunction and VGF in T2DM. I believe that targeting protein *O*-GlcNAcylation in VGF can be further investigated

given that it has recently produced effective treatment alternatives in diseases including cancer and neurological illnesses (Yang and Qian, 2017).

1.4 Cellular Metabolism

The process of cellular metabolism involves intricate networks of managed biochemical processes or metabolic pathways that enable organisms to develop and reproduce, keep up their structural integrity, and adapt to environmental changes (Cooper, 2000). Glycolysis, the tricarboxylic acid (TCA) pathway, and oxidative phosphorylation are the three primary cellular metabolic processes required for energy generation that drive cellular activities (Cooper, 2000). While the TCA cycle, oxidative phosphorylation, and β -oxidation all take place inside the mitochondrion, glycolysis occurs in the cytoplasm of the cell (Cooper, 2000). The mitochondrial matrix is the home of β -oxidation and the TCA cycle, while the inner mitochondrial membrane contains the enzymes of the electron transport chain (ETC) (Cooper, 2000). Mitochondria are dispersed throughout cells close to high-demand regions and can be relocated as needed by following cytoskeletal elements (Frederick & Shaw, 2007). In order for cells to respond to energy demands and function in a tissue-dependent manner, cellular metabolism is closely regulated. Although every cell has the same metabolic machinery, different approaches can be used to produce varied energy situations. The availability of nutrients, external cues, and cellular signalling pathways will all change depending on the microenvironment, as will the method in which different cell types or lines of cells utilise the same metabolic pathways. The many metabolic pathways are allosterically regulated by substrates and products, showing a dependence on one another for cellular metabolism (Metallo & Heiden, 2013).

1.4.1 Glycolysis

Glycolysis is an enzyme-catalyzed mechanism that transforms glucose into two molecules of pyruvate in the presence of oxygen or two molecules of lactate in the absence of oxygen (Harris and Harper, 2015). Anaerobic glycolysis, the latter pathway, is thought to be the ATP-producing mechanism to have arisen naturally (Harris and Harper, 2015). In the majority of cells, glycolysis turns glucose into pyruvate, which is then oxidised by mitochondrial enzymes into carbon dioxide and water. However, because mitochondria are absent in some cells, most notably mature red blood cells, glycolysis is the sole way to produce ATP in these cells. Cells can only produce ATP from glucose by glycolysis in an anaerobic condition (Harris and Harper, 2015). Meanwhile, in the presence of oxygen, glycolysis serves as the initial stage of cellular respiration and enables ATP synthesis to take place (Harris and Harper, 2015). During glycolysis, the six-carbon carbohydrate glucose is broken down into two molecules of three-carbon pyruvate, which results in the creation of two more molecules of ATP. Two NADH

molecules are furthermore created; these serve as electron donors during oxidative phosphorylation (Harris and Harper, 2015). Two protein families, GLUT, which is engaged in facilitated diffusion, and SGLT, active transport mediated by sodium flow, are primarily responsible for the entry of glucose into cells (Deng et al., 2016). Under aerobic condition, the pyruvate produced by glycolysis is converted to acetyl CoA and then further oxidised through the TCA cycle, producing reducing equivalents for oxidative phosphorylation (Chaudhry & Varocallo, 2018). Meanwhile, under anaerobic condition, pyruvate is fermented. The continuation of glycolytic activity is made possible by this fermentation, which results in the recycling of NADH back into NAD⁺ resulting in the conversion of pyruvate into two molecules of lactate (Chaudhry & Varocallo, 2018).

Describing the glycolytic pathway in brief, hexokinase, an enzyme that catalyses the phosphorylation of glucose into ATP, is the first-rate limiting step in the glycolytic pathway. Hexokinase catalyses the conversion of D-glucose into glucose-6-phosphate (G6P). Following this, glucose phosphate isomerase converts G6P to fructose 6-phosphate (F6P), which is then converted to fructose- 1,6-*bis*phosphate (FBP) by phosphofructokinase. After this, fructose 1, 6-*bis*phosphate is broken down by the enzyme Aldolase into two isomers, namely glyceraldehyde 3-phosphate (GAP) and dihydroxyacetone phosphate (DHAP). These isomers, DHAP and GAP, are quickly interconverted by the enzyme triosephosphate isomerase. Glyceraldehyde-3-phosphate dehydrogenase (GAPDH) converts GAP into 1,3-*bis*phosphoglycerate via two quick steps: 1) The coenzyme nicotinamide adenine dinucleotide (NAD) oxidises glyceraldehyde-3-phosphate; and 2) the molecule is phosphorylated by the addition of a free phosphate group. Then, to create ATP and 3-phosphoglycerate, phosphoglycerate kinase moves a phosphate group from 1,3-*bis*phosphoglycerate to ADP. After this, the phospho from 3-phosphoglycerate is moved from the third carbon to the second carbon by the enzyme phosphoglycerate mutase to create 2-phosphoglycerate. The enzyme enolase then removes a molecule of water from 2-phosphoglycerate to form phosphoenolpyruvic acid (PEP) which is then converted to pyruvic acid and ATP by pyruvate kinase (Harris and Harper, 2015).

1.4.2 The tricarboxylic acid (TCA) Cycle

The TCA cycle, also referred to as the Krebs's cycle or the citric acid cycle, is an important metabolic system in cells. In addition to providing most of the energy required by complex organisms, TCA cycle also generates molecules that can serve as the building blocks for a variety of critical processes, such as the production of fatty acids, steroids, cholesterol, amino acids for the synthesis of proteins, and the purines and pyrimidines required for the synthesis of DNA (Frizell and Stillwa, 2018). Lipids and carbohydrates, which are sources of acetyl-CoA, serve as the TCA cycle's fuel. Pyruvate dehydrogenase utilises pyruvate from glycolysis to make acetyl-CoA. Also, through the process of β -oxidation, fatty acids are transformed into acetyl-CoA. Following metabolic modifications, amino acids can enter the TCA as pyruvate, acetyl-CoA, or TCA cycle intermediates (Frizell and Stillwa, 2018). Six-carbon citrate is then created when acetyl-CoA and four-carbon oxaloacetic acid are combined. Then, citrate enters the circular pathway where it is subjected to a series of enzyme-mediated events that produce H^+ , carbon dioxide, FADH₂, NADH, and GTP. The route is both catabolic and anabolic since it produces precursors for biosynthesis when proteins, lipids, and carbohydrates are broken down (Akram, 2013). Several sites in the TCA cycle are regulated. The cycle is regulated by the enzymes citrate synthase, isocitrate dehydrogenase, and beta-ketoglutarate. The enzyme that converts pyruvate into Acetyl CoA, which feeds into the TCA cycle, pyruvate dehydrogenase, also has regulatory functions. Typically, all of these enzymes are up-regulated by substrates and inhibited by the by-products of the processes they catalyse (Berg et al., 2002). By generating the electron donors NADH and FADH₂ needed for the electron transport chain (ETC), TCA forms a direct link to oxidative phosphorylation.

1.4.3 Oxidative phosphorylation

Oxidative phosphorylation has two parts: the ETC and chemiosmosis. The ETC is made up of a group of proteins that are affixed to the inner mitochondrial membrane and organic molecules that allow electrons to pass through and release energy through a series of redox processes. The protein ATP-synthase uses the energy released to create a proton gradient, which is then utilised in chemiosmosis to produce a significant amount of ATP (Guerra et al., 2006; Brand and Nicholas, 2011). Cellularly, the electrons in the ETC pass through a chain of proteins that raises its reduction potential and results in an energy release. A proton gradient is produced by pumping hydrogen ions (H^+) from the mitochondrial matrix to the intermembrane space with the majority of this energy being lost as heat (Guerra et al., 2006). This gradient generates an

electrical difference with a positive charge outside and a negative charge inside, increasing the acidity in the intermembrane gap (Guerra et al., 2006). The ETC is composed of several (I, II, Coenzyme Q, III, IV, and V) protein complexes that work together to phosphorylate ADP to ATP (Figure 1.5).

1.4.3.1 Complex I

Eight iron-sulfur (Fe-S) clusters, flavin mononucleotide (FMN), and NADH dehydrogenase make up Complex I, commonly known as ubiquinone oxidoreductase. Here, the citric acid cycle oxidises the NADH provided by glycolysis, converting two electrons from NADH to FMN. After that, they move on to the Fe-S clusters, and lastly from Fe-S, they move on to coenzyme Q. The electrochemical gradient is aided by the passage of 4 hydrogen ions from the mitochondrial matrix to the intermembrane gap. Complex I might be crucial in triggering apoptosis in cases of planned cell death (Lencina et al., 2018; Hirst, 2009; Sazanov and Hinchliffe, 2006; Hirst, 2005).

1.4.3.2 Complex II

Also referred to as succinate dehydrogenase, absorbs electrons from succinate (a citric acid cycle intermediate) and functions as a second ETC entry point. When succinate oxidises to fumarate, complex II's FAD accepts two electrons. Similar to complex I, FAD transmits them to Fe-S clusters and finally to coenzyme Q. However, complex II does not transport protons across the membrane; as a result, this pathway produces less ATP (Yankovskaya et al., 2003; Horsefield et al., 2004).

1.4.3.3 Coenzyme Q

Also known as ubiquinone is composed of a hydrophobic tail and quinone. Its job is to act as an electron transporter and move electrons to complex III. Through the Q cycle, coenzyme Q is reduced to semiquinone (partially reduced, radical form CoQH[•]), and ubiquinol (completely reduced CoQH₂) (Ahmad et al., 2022).

1.4.3.4 Complex III

Also known as cytochrome c reductase consists of the proteins cytochrome b, Rieske subunits (which have two Fe-S clusters), and cytochrome c. Cytochromes are heme-containing proteins that take part in electron transfer. During the electron transfer, the heme groups switch between

the ferrous (Fe^{2+}) and ferric (Fe^{3+}) states. Contrary to the one-step complex I and II routes, this activity takes place in two steps (the Q cycle) because cytochrome c can only accept one electron at a time. At the conclusion of a full Q cycle, Complex III also discharges 4 protons into the intermembrane gap, adding to the gradient. The electrons are subsequently transferred to complex IV by cytochrome c one at a time (Sun et al., 2018; Iwata et al., 1998; Trumpower, 1990).

1.4.3.5 Complex IV

Also known as cytochrome c oxidase oxidises cytochrome c and transfers the electrons to oxygen, the final electron carrier in aerobic cellular respiration. The complex IV heme and copper groups, along with the cytochrome proteins a and a₃, supply electrons to the attached dioxygen species, causing it to change into water molecules. Four protons enter the intermembrane gap as a result of the electron transfer's free energy, which increases the proton gradient. The following reaction results in oxygen reduction (Calhoun et al., 1994; Schmidt-Rohr, 2020)

1.4.3.6 Complex V

Also called ATP synthase utilises the proton gradient created by the ETC to produce ATP across the inner mitochondrial membrane. The F₀ and F₁ subunits of ATP-synthase function as a rotational motor system. The inner mitochondrial membrane contains hydrophobic F₀. As H^+ ions go down the gradient from intermembrane space to matrix, they repeatedly protonate and deprotonate a proton corridor within the structure. Rotation caused by the alternating ionisation of F₀ changes the orientation of the F₁ subunits. F₁ faces the mitochondrial matrix and is hydrophilic. ADP and P_i are converted to ATP via conformational changes in F₁ subunits. In order to make 1 ATP, 4 H^+ ions are needed. As shown in some bacteria, ATP-synthase can also be made to work in reverse, using ATP to create a hydrogen gradient (Lovero et al., 2018; Okuno et al., 2011; Junge and Nelson, 2015).

1.4.4 Inhibitors of oxidative phosphorylation

Inhibitors of oxidative phosphorylation have now found profound use investigating mitochondria function and metabolic homeostasis (Leese et al. 2016). Some of these inhibitors that were utilised in this project are highlighted below (Figure 1.5).

1.4.4.1 Oligomycin

It is macrolide antibiotics synthesised by *Streptomyces* species. Oligomycin inhibits ATP-synthase (complex V) by inhibiting the F₀ subunit of ATP-synthase, preventing ATP production (Lovero et al., 2018; Leese et al. 2016).

1.4.4.2 Carbonyl cyanide-4 (trifluoromethoxy) phenylhydrazone (FCCP)

This is an uncoupler that collapses the proton gradient and interfere with the potential of the mitochondrial membrane. As a result, complex IV utilises the most oxygen possible and electron transport through the ETC is unrestricted. The difference between maximal respiration and baseline respiration, as determined by the FCCP-stimulated OCR, can subsequently be utilised to determine spare respiratory capacity. The ability of the cell to react to an increase in energy demand or under stress is measured by the cell's spare respiratory capacity (Leese et al. 2016).

1.4.4.3 Rotenone

It is a widely used pesticide, although is most frequently employed as a piscicide in the US. Rotenone inhibits complex I from transporting electrons to ubiquinone from the Fe-S clusters. Although it is poorly absorbed via the skin, poisoning rarely results in death because it can be removed through vomiting, however, deliberate intake may be lethal (Leese et al. 2016).

1.4.4.4 Antimycin A

It inhibits complex III. It is a piscicide that binds to the Q_i binding site of cytochrome c reductase. This action stops ubiquinone from attaching to and receiving an electron, preventing the Q cycle from recycling ubiquinol (CoQH₂) (Leese et al. 2016).

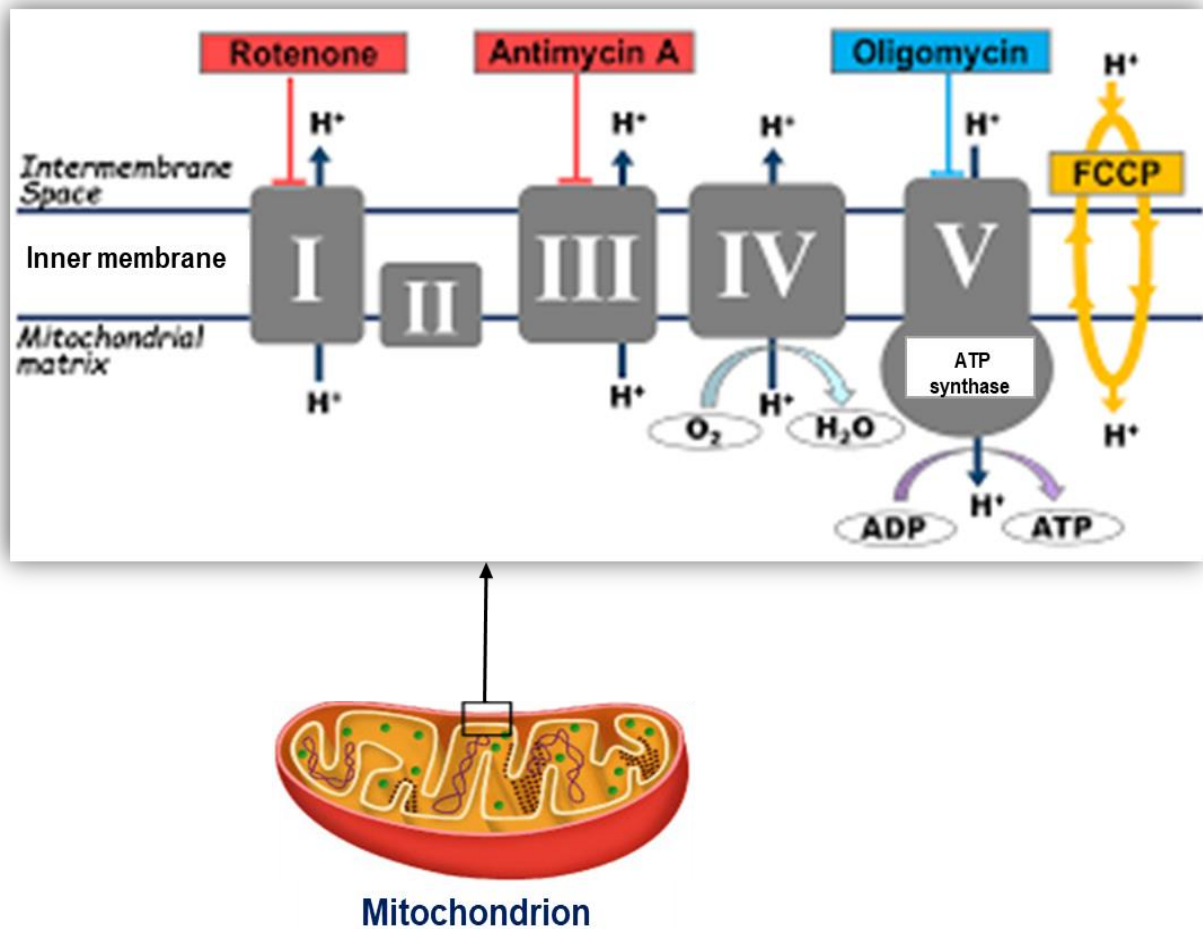


Figure 1.5: Mitochondrion respiratory chain complexes. Protons (H⁺) are pumped from the matrix into the intermembrane space through complexes I, III, and IV as electrons move through the electron transport chain. After that, protons return to the matrix via complex V to generate ATP. Complexes I, III, and IV are inhibited by rotenone, antimycin A, and oligomycin respectively. FCCP on the other hand, collapses the proton gradient allowing uninhibited flow of electron through the electron transport chain.

1.4.5 The mitochondria and its operation

Mitochondria are unique compartments (organelles) in human cells recognised for acting as energy producers by breaking food molecules and producing ATP, a fuel for the remainder of the cell. The mitochondrion has two membranes: an inner membrane that is firmly sealed and features indentations known as cristae, and an outside membrane that is porous for most molecules. Mitochondria can combine, divide, and create vast, dynamic networks within a cell, and can adapt to variations in energy demand in this way (Ernster & Schatz, 1981). The fact that mitochondria have their own genetic material, known as mitochondrial DNA, which is inherited from the mother, is another distinctive quality of mitochondria. The absence or malfunction of mitochondrial proteins can result from mutations in the mitochondrial genome or the genomic DNA in the cell's nucleus (Gray, 2012). In turn, this might result in primary mitochondrial disorders, which have a wide range of symptoms and effects on various body organs. Since mitochondria are so integral to cellular processes, their dysfunction has also been linked to the emergence of extremely complicated secondary diseases like cancer, neurological diseases, CVDs, and stroke (Ernster & Schatz, 1981).

The quantity, size, and location of mitochondria vary depending on the needs of the cell. Since they are constantly undergoing fission and fusion processes, mitochondria are extremely active organelles. Due to the endosymbiotic nature of mitochondrial evolution, they have the distinctive property of carrying their own genetic material. 37 highly conserved genes are encoded by the small circular genome known as mtDNA, which is found in all mammalian species (Taanman, 1999). The ability of mitochondria to function is determined by a mix of their own genetic material and nuclear deoxyribonucleic acid (nDNA), which operate in a strictly controlled process (Chinnery & Hudson, 2013). Up until recently, it was believed that sperm mitochondria were ubiquitinated when they entered the egg, and that all mtDNA is inherited through the maternal line. However, a recent seminal work showed that three unrelated families received paternal mtDNA transmission (Luo et al., 2018). This is an unexpected but crucial discovery for our knowledge of mitochondria and the spread of mitochondrial associated disorders.

Due to their biogenesis, mitochondria are able to adapt to changes in energy requirements brought on by physiological processes such as exercise, hormone response, temperature changes in fat cells, and electrical stimulation (Brown et al., 2010). Up until recently, it was believed that sperm mitochondria were ubiquitinated when they entered the egg, and that all

mtDNA is inherited through the maternal line. However, a recent seminal work showed that three unrelated families received paternal mtDNA transmission (Luo et al., 2018). This is an unexpected but crucial discovery for our knowledge of mitochondria and the spread of mitochondrial illness. The differentiation, proliferation, and migration of vascular cells are all dependent on mitochondrial metabolism (Davidson and Dunchen, 2007; Dranka et al., 2010). More so, a measure of mitochondria respiration has been described as a gold standard in the determination of the metabolic homeostasis of cells such as ECs, SMCs, and platelets (Al-Mehdi et al., 2012; Coutelle et al., 2014; Aibibula et al., 2018). Furthermore, determination of platelet mitochondria oxygen consumption rate (OCR) and extracellular acidification rate (ECAR) were measured as markers of oxidative phosphorylation and glycolysis, respectively (Aibibula et al., 2018). For this reason, mitochondria OCR and ECAR are now appreciated as key metabolic tool in predicting altered metabolic homeostasis in multiple pathologic conditions.

1.4.5.1 OCR

Positive feedback has been given to OCR as reliable markers of metabolic capacity; in fact, (Leese et al. 2016) refers to OCR as the "best marker of metabolic capacity". Since the majority of the increase in cellular ATP demand during implantation development is accounted for by oxidative phosphorylation, as measured by OCR (Brinster, 1973; Sturme and Leese, 2003), the activity of this pathway is a better predictor of metabolic function. It is important that detailed information on the bioenergetic profile of the mitochondria can be obtained using OCR in conjunction with the application of certain inhibitors. Inhibitors that target the various complexes in the ETC can identify the aspects of oxygen consumption that are connected to ATP synthesis. The quantity lost by passive or active proton leakage across the inner mitochondrial membrane, the difference between peak oxygen consumption and basal (spare capacity), and non-mitochondrial oxygen consumption are some of these factors. These assays provide a detailed view of mitochondrial activity as well as dysfunction.

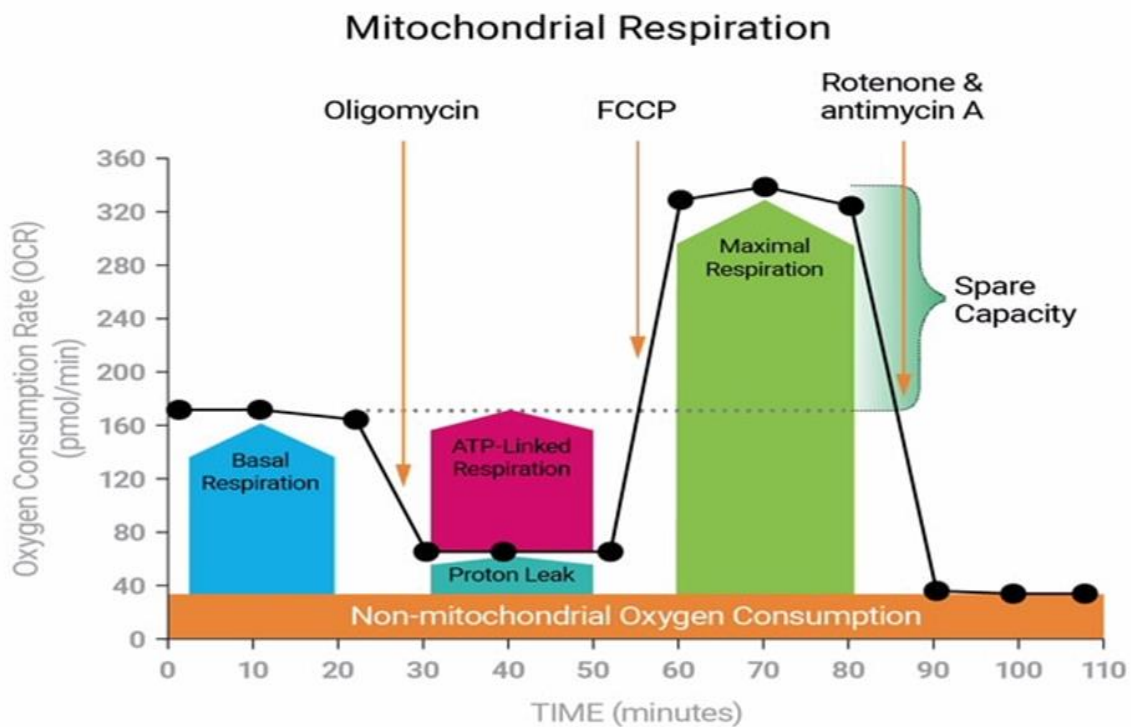


Figure 1.6: Schematic of real time measurement of mitochondrial oxygen consumption rate (OCR).

Basal respiration: measures the oxygen consumption required to meet normal cellular ATP generation. This demonstrates the cell's energy requirements in ideal circumstances; ATP-Linked respiration: shows the portion of basal respiration that was being used to drive ATP generation typified by the decrease in OCR following injection of the ATP synthase inhibitor oligomycin

H⁺ (Proton) leak: shows OCR that is not connected to synthesis of ATP during basal respiration

Maximal respiration: measures the maximum OCR reached after collapsing the proton gradient allowing electron flow through the ETC unhindered. It demonstrates the cell's maximal rate of respiration.

Spare respiratory capacity: shows the cell's ability to meet an energy requirement and how close it is to reaching its maximum possible rate of respiration. The cell's capacity to respond to demand may be a sign of its flexibility or health.

Non-mitochondrial respiration: shows the oxygen consumption that persists as a result of a subset of cellular enzymes that do so even after rotenone and antimycin A have been added. To accurately assess mitochondrial respiration, this is crucial.

FCCP: carbonyl cyanide p-(trifluoromethoxy) phenylhydrazone

1.4.5.2 ECAR

ECAR measures the amounts of lactic acid produced when glucose is converted to lactate during glycolysis (Yetkin-Arik et al., 2019). The flow through catabolic pathways necessary to produce ATP is connected to a cell's ECAR. Also, ECARs are linked to ATP turnover because the rates of ATP synthesis and consumption are equal in steady state (Ferrick et al., 2008). Even though it is technically difficult to quantify ATP turnover, it may be demonstrated that fluctuations in extracellular fluxes are correlated with changes in ATP turnover rates (Ferrick et al., 2008).

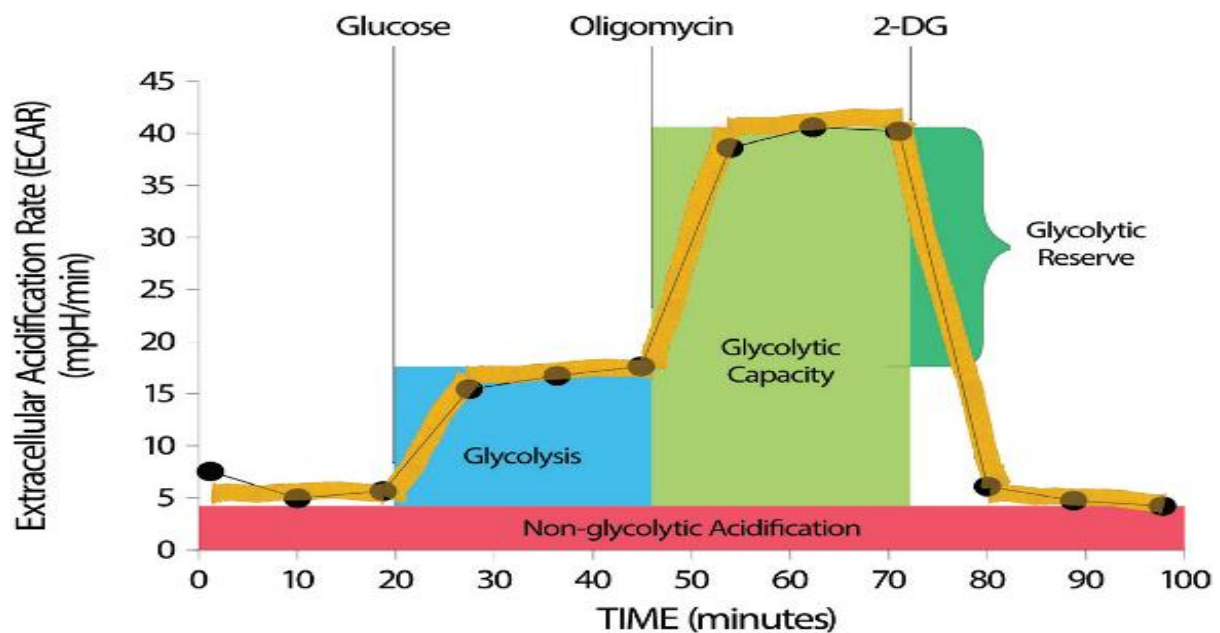


Figure 1.7: Schematic of real time measurement of mitochondrial extracellular acidification rate (ECAR).

Glycolysis: measures the glycolytic rate following the saturation of the glucose concentration caused by the injection of glucose.

Glycolytic capacity: measures the cellular maximum glycolytic capability. When oligomycin is injected, it inhibits oxidative ATP synthesis and switches the energy production to glycolysis causing an increase in ECAR.

Glycolytic reserve: is a measure of the difference between glycolytic capacity and glycolysis rate. The inhibition of glycolysis by the last injection of 2-deoxyl-glucose (2-DG) and the consequent drop in ECAR provide evidence that the ECAR generated during the experiment was generated by glycolysis.

Non-glycolytic acidification: measures ECAR prior to glucose injection or after 2-DG injection, is referred to as non-glycolytic acidification.

1.5 Reactive oxygen species (ROS)

In recent years, more compelling evidence linking ROS to vascular dysfunction have emerged (Chen et al., 2018; Sena et al., 2018). ROS is an umbrella term for a number of molecular oxygen derivatives that are produced naturally during aerobic life (Sies and Jones, 2020). In addition to being produced during cellular reactions to xenobiotics, cytokines, and bacterial invasion, ROS are also produced during mitochondrial oxidative metabolism (Ray et al., 2012). Oxidative stress, a term used to describe molecular damage caused by increased production of various ROS, is characterised by an imbalance between the capacity of the cell to mount an efficient antioxidant response to excess ROS cellularly produced (Ray et al., 2012). Macromolecular damage brought on by oxidative stress is linked to several disease states, including atherosclerosis, diabetes, cancer, neurodegeneration, and ageing (Ray et al., 2012; Trachootham et al., 2009; Andersen, 2004; Paravicini and Touyz, 2006; Haigis and Yankner, 2010). Conversely, emerging research findings show that ROS play a crucial role in cell growth and survival as signalling molecules (Sies and Jones, 2020). More so, clinical experiments in the past have shown that non-specific ROS removal using low molecular mass antioxidant molecules did not successfully halt the onset and progression of ageing and diseases such as neurodegenerative disorder and cancer (Sies and Jones, 2020). However, manipulating ROS-mediated signalling pathways through selective targeting offers hope for a more advanced redox-driven drug development. This involves the control of enzymatic defence mechanisms by the stress-response transcription factors NRF2 and nuclear factor-B, the function of trace elements like selenium, the use of redox medications, and the modification of environmental influences collectively known as the exposome (Sies and Jones, 2020).

More than 40 enzymes, most notably NADPH oxidases and the mitochondrial electron transport chain, produce two species that are essential redox signalling agents: hydrogen peroxide (H_2O_2) and the superoxide anion radical (O_2^-) (Sies and Jones, 2020). These compounds are produced under the control of growth factors and cytokines. H_2O_2 is the main agent signalling through specific protein targets at the low physiological levels in the nanomolar range, which engage in metabolic regulation and stress responses to enable cellular adaptation to a changing environment and stress. Other reactive species, like nitric oxide, hydrogen sulphide, and oxidised lipids, are also implicated in redox signalling (Sies and Jones, 2020). The evaluation of molecular interactions between certain ROS molecules and particular targets in redox signalling pathways is now possible due to methodological advances. As a result, significant progress has been made in our understanding of how these oxidants affect

physiology and disease, including the neurological, cardiovascular, and immunological systems, skeletal muscle, metabolic control, ageing, and cancer (Sies and Jones, 2020; Ray et al., 2012; Trachootham et al., 2009; Andersen, 2004; Paravicini and Touyz, 2006; Haigis and Yankner, 2010).

1.5.1 ROS signalling

Redox signalling affects protein function, leading to changes in signalling outputs, enzyme activity, gene transcription, and membrane and genome integrity (Marinho et al., 2014). Mechanisms that underpin how ROS alter protein function continue to emerge (Marinho et al., 2014). One of these mechanisms is the fact that oxidative interface consists mainly of the redox regulation of redox-reactive cysteine (Cys) residues on proteins by ROS (Ray et al., 2012). Oxidation of these residues forms reactive sulfenic acid ($-SOH$) that can form disulfide bonds with nearby cysteines ($-S-S-$) or undergo further oxidation to sulfinic ($-SO_2H$) or sulfonic ($-SO_3H$) acid; if nearby nitrogen is available sulfenic acid may also form a sulfenamide (Ray et al., 2012). These oxidative modifications result in changes in structure and/or function of the protein. These redox changes can be reversed by reducing systems like thioredoxin and peroxiredoxin, with the exception of sulfonic acid and, to a lesser extent, sulfinic acid. Cysteines in many proteins, including cytoskeletal components, heat shock proteins, scaffold proteins like 14-3-3, and numerous ribonucleoproteins, are extremely sensitive to oxidation, indicating the existence of functional protein networks regulated by redox (Go et al., 2013). When growth factors are stimulated, changes in protein structure can make cryptic cysteines in proteins accessible, as was seen for EGF (Behring et al., 2020).

1.5.1.1 JAK/STAT

The knowledge of the relationship between ROS and the JAK/STAT pathway is thin but continues to expand, and this knowledge may be useful in the development of drugs that can be used to treat a variety of diseases, such as cancer, autoimmune disorders, vascular dysfunction, and CVDs with an inflammatory component (O'Shea et al., 2015; Banerjee et al., 2017; Villarino et al., 2017; Ivashkiv and Donlin, 2014). The JAK/STAT pathway is a quick membrane-to-nucleus signalling pathway that triggers the production of many important inflammatory mediators which comprise proteins, cytokines, nitric oxide, peptides, glycoproteins, oxygen free radicals, and arachidonic acid metabolites (prostaglandins and leukotrienes) (Seif et al., 2017; Juhn et al., 2008). There is strong evidence linking the deregulation of the JAK/STAT pathway to a number of autoimmune and inflammatory

illnesses (Seif et al., 2017; Darnell, 1997). The JAK/STAT signalling system has been linked to more than 50 cytokines and growth factors, including hormones, interferons (IFN), interleukins (ILs), and colony-stimulating factors (Seif et al., 2017; Darnell, 1997). Haematopoiesis, immunological function, tissue repair, inflammation, apoptosis, and adipogenesis are a few examples of the diverse downstream activities mediated by JAK/STAT (Owen et al., 2019). Numerous human disorders are correlated with the loss or mutation of JAK/STAT components. JAKs mediate tyrosine phosphorylation of receptors, recruit one or more STAT proteins, and are noncovalently linked with cytokine receptors. Tyrosine-phosphorylated STATs form dimers, which are then transported across the nuclear membrane into the nucleus to regulate particular genes. Different STATs have nonredundant biological effects even if they might be activated by cytokines that partially overlap (Aittomäki & Pesu, 2014).

In models of diabetic retinopathy, activation of NADPH oxidase has been shown to cause the generation of ROS, which has been shown to cause signalling through STAT3 to enhance VEGF expression. More studies have revealed that NADPH oxidase-derived ROS are crucial for VEGF-induced angiogenesis (Ushio-Fukai et al., 2002), neovascularization in response to hindlimb ischemia (Tojo et al., 2005), hypoxia-induced VEGF production and angiogenesis in a model of ischemic retinopathy (Al-Shabrawey et al., 2005). Additionally, it has been shown that there was a trend toward an increase in oxidative chemicals with an increase in the number of oxygen fluctuations (Saito et al., 2007). More so, it has been discovered that VEGF plays a critical role in the development of pathologic intravitreal neovascularization. Oxidative stress can signal angiogenic processes through molecules such as VEGF (Werdich and Penn, 2006; Geisen et al., 2008). All of these findings point to STAT3 activation as a potential cause of the observed effects because inhibition of STAT3 reversed these effects (Ushio-Fukai et al., 2002; Tojo et al., 2005; Al-Shabrawey et al., 2005).

1.5.1.2 MAPK/ERK

The four main mitogen-activated protein kinase (MAPKs) that make up the MAPK cascades are the large MAP kinase 1 (BMK1/Erk5), the c-Jun N-terminal kinases (JNK), the p38 kinase, and the extracellular signal-related kinases (Erk1/2), JNK, and JNK. These kinases, which are evolutionarily conserved in eukaryotes, are crucial for cellular reactions to a wide range of signals produced by hormones, cytokines, growth factors, and other stressors like genotoxic

and oxidative stress (Ichijo et al., 1997). Apoptosis signal-regulated kinase 1 (ASK1), one of the participants in the MAPK cascades, controls the JNK and p38 MAPK pathways that result in apoptosis by phosphorylating the MAPKKs MKK4, MKK3, and MKK6 (Ichijo et al., 1997). ASK1 is activated under numerous stressful circumstances, such as oxidative stress. When phosphorylated in the activation loop of the human ASK1 kinase domain, a conserved threonine residue (Human: Thr-838, Mouse: Thr-845) causes ASK1 to homo-oligomerize by both C- and N-terminal coiled-coil domain contact (Tobiume et al., 2001).

The direct inhibition of MAPK phosphatases by ROS also triggers MAPK pathways. The reversible oxidation of a catalytic-site cysteine to sulfenic acid by ROS produced by NADPH oxidases or in mitochondria has been demonstrated to block JNK-inactivating phosphatases (Kamata et al., 2005), maintaining JNK activation. Furthermore, it was found that ROS produced by commensal bacteria inactivated dual-specific phosphatase 3 (DUSP3) by oxidising Cys-124, which led to ERK activation (Wentworth et al., 2011). More so, inhibition of phosphatases by ROS has previously been shown to modulate p38 signalling (Robinson et al., 1999; Liu et al., 2010). Additionally, protein tyrosine phosphatases (PTPs) like protein tyrosine phosphatase 1B (PTP1B) and SH2-domain containing PTP (SHP2) are inactivated by ROS in a manner similar to the cysteine redox mechanism (I/V-H-C-X-X-G-X-X-R-S/T) that, in turn, potentiates MAPK and growth factor signalling pathways that are initiated (Meng et al., 2002; Denu et al., 1998; Lee and Esselman, 2002). As with disulfide linkages and sulfenamides, the oxidation of the catalytic site cysteine in PTPs to sulfenic acid (SOH) is reversible. However, additional oxidation to the typically irreversible sulfinic acid (SO₂H) or sulfonic acid (SO₃H) can also happen. In order to reduce sulfenic acid residues and reverse the oxidative inactivation of PTPs, thioredoxin or glutathione appear to be necessary (Lee et al., 1998). The ligand-binding transmembrane receptor-like PTPs (RPTPs), which include RPTP, are members of the classical PTP family. When a ligand binds to RPTP, RPTP dimerizes and enters the catalytically inactive state (Tonks, 2006). More so, human RPTP tyrosine phosphatase activity has been shown to be inhibited by ROS through preferential oxidation of Cys-723 in the second catalytic domain of RPTP rather than oxidation of Cys-433 in the first catalytic domain (Persson et al., 2004). This results in the formation of intermolecular Cys-Cys disulfide bonds and a reversible cyclic sulfen (Blanchetot et al., 2002). Also, production of ROS is commonly linked to growth factor signalling processes (Sunderesan et al., 1995). One of the molecular processes by which growth factor-induced ROS generation is necessary for

converting and maintaining growth factor signals appears to be the oxidation and inhibition of PTPs by ROS (Sunderesan et al., 1995).

1.5.3 Mitochondria oxidative stress

Most mammalian cells contain mitochondria, which are a significant source of ROS (Muller, 2000; Turrens, 2003; Adam-Vizi and Chinopoulos, 2006). This ROS generation is crucial for redox transmission from the organelle to the rest of the cell and contributes to mitochondrial-mediated damage to cells in a variety of diseases (Balaban et al., 2005). Findings have shown that, p66Shc, a proapoptotic protein, contributes to mitochondrial ROS generation, which causes mitochondrial damage and apoptosis when exposed to oxidative or genotoxic stressors such H₂O₂ or UV radiation (Pacini et al., 2004; Favetta et al., 2004; Migliaccio et al., 2006; Gertz and Steegborn, 2010). Although the molecular mechanism by which stress signals increase p66Shc expression is still largely unknown, it has been demonstrated that the Rac1 GTPase, which produces ROS by activating NADPH oxidase (Bokoch and Diebold, 2002), prevents p66Shc from being ubiquitinated and degraded by phosphorylating it on Ser-54 and Thr-386 in a p38-dependent manner (Khanday et al., 2006). Additionally, p66Shc is phosphorylated by oxidative stress-activated PKC- at Ser-36. This causes p66Shc to engage with the prolyl isomerase Pin1 and could cause an isomerization of a p66Shc phospho-Ser36-Pro37 link, which leads to the translocation of p66Shc into mitochondria (Pinto et al., 2007).

Additionally, it was shown that p66Shc is pro-apoptotic in mitochondria after forming two disulfide bonds via Cys-59 in the N-terminus CH2 domain, which results in copper-dependent ROS production and the start of apoptosis (Gertz et al., 2008). By reversibly reducing the active oxidised form of p66Shc with glutathione or thioredoxin, inactivation results (Gertz et al., 2008). Stress-activated p66Shc causes apoptosis, but the exact mechanism by which it does so is yet unclear (Sies and Jones, 2020). However, it has been demonstrated that stress-activated p66Shc functions as a redox protein that generates H₂O₂ in mitochondria through interaction and electron transfer between p66Shc and cytochrome c (Giorgio et al., 2005). This was demonstrated when mutations in the redox centre of p66Shc (E132-E133 to Q132-Q133 in the CB domain), impaired opening of the mitochondrial permeability transition pore (Pelicci et al., 1992). It appears that p66shc promotes apoptosis via producing ROS, while ROS may also activate p66shc. Also, ageing is linked to a decline in mitochondrial function, including decreased oxidative phosphorylation, which increases ROS production (Seo et al., 2010). It is

intriguing to consider if elevated ROS in this situation might cause p66shc to release further ROS, leading to apoptosis and maintaining the continuous ageing process.

1.5.4 ROS and vascular dysfunction

As we continue to learn more about the role ROS play in vascular dysfunction, current research has suggested that ROS alter the activities of the miR-200 family of microRNAs (Magenta et al., 2011). Members of the miR-200 family are particularly sensitive to ROS and play a crucial role in modulating the post-transcriptional regulation of the endothelium oxidative response (Lo et al., 2018; Marin et al., 2013). H₂O₂ specifically increased the miR-200c and miR-141 shared promoters, demonstrating that it regulates the miR-200c at the transcriptional level (Magenta et al., 2011). Furthermore, diabetes-related endothelial dysfunction and inflammation have also been linked to miR-200 overexpression (Lo et al., 2018). Additionally, ROS promote protein kinase C (PKC) activity in cultured aortic SMCs and ECs, which increases the synthesis of vascular endothelial growth factor (VEGF) and activates nuclear factor- κ B (NF- κ B), a transcription factor that promotes inflammation (Inoguchi et al., 2003). When these occur, ECs become activated and release a variety of inflammatory cytokines, including tumour necrosis factor alpha (TNF) and interleukin 1 (IL-1) (Ramji and Davies, 2015). A rise in the expression of adhesion proteins on the surface of ECs also promotes the attraction and invasion of immune cells like monocytes (Ramji and Davies, 2015). Increased pattern recognition receptor expression on the surface of the monocytes occurs along with their differentiation into macrophages, which helps to promote inflammation and the uptake of modified LDL, ultimately resulting in the production of foam cells that are lipid-rich (Figure 1.8). Apoptosis of foam cells results in lipid deposition and an intensification of the inflammatory response due to the continued accumulation of modified LDL and impaired cellular lipid balance (Ramji and Davies, 2015). Also, VSMCs go from the media to the intima where they multiply, take up modified lipoproteins, and release ECM proteins that keep the plaques stable (Cahill and Redmond, 2016). Such plaques are destabilised by ongoing inflammation induced by cytokines through decreased formation of ECM proteins, increased production of MMPs that break down the ECM, and decreased expression of these enzymes' inhibitors (Ramji and Davies, 2015). The accumulated lipid-filled foam cells finally burst in the tunica intima. This promotes atheroma development in grafted veins which can cause SVG failure (Ramji and Davies, 2015; Cahill and Redmond, 2016).

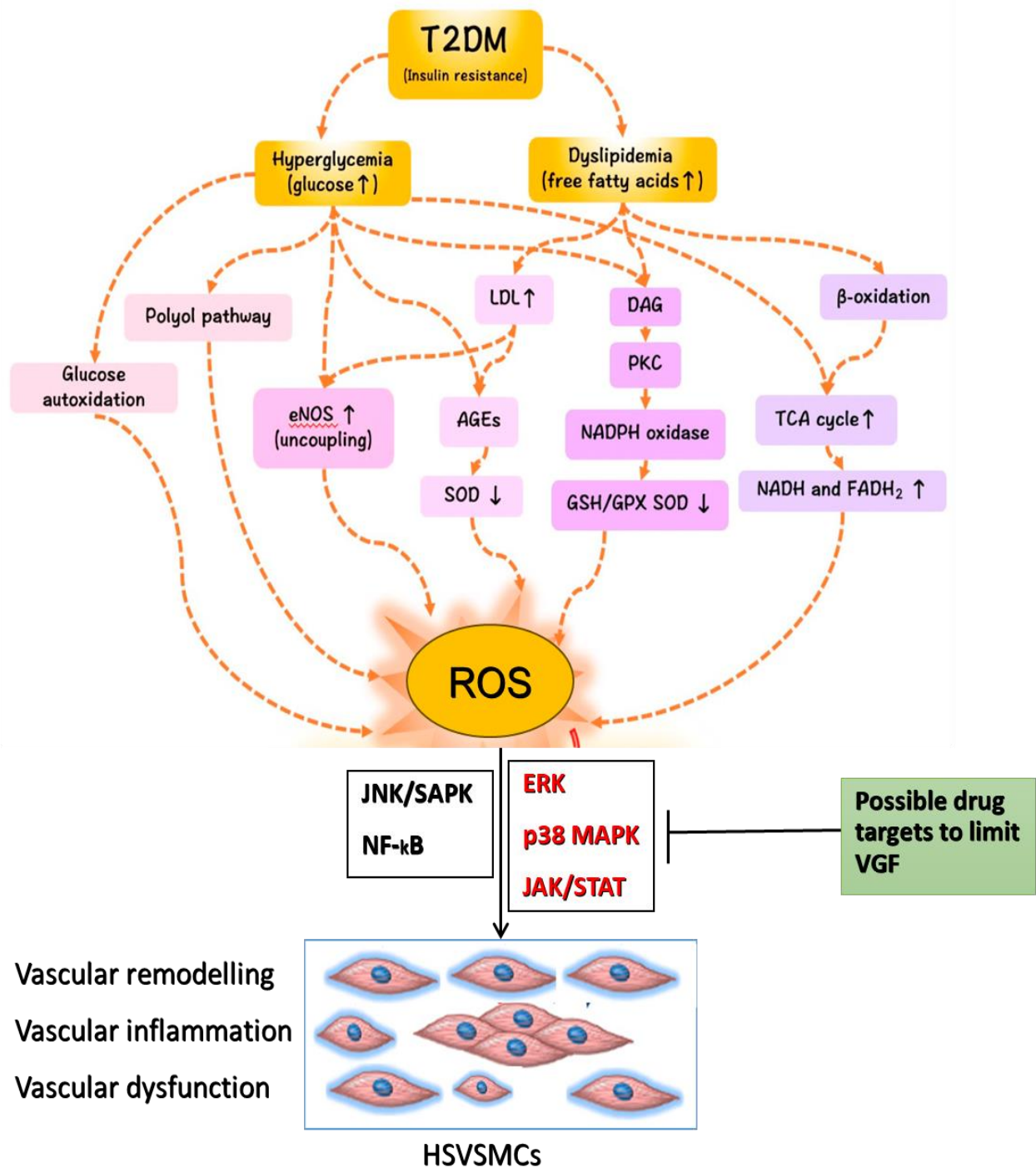


Figure 1.8: A proposed schematic of ROS mediated vascular dysfunction in T2DM. It shows various pathways through which T2DM promotes ROS production and how ROS possibly go on to mediate vascular remodelling, inflammation, and dysfunction by possibly promoting SMC (HSVSMCs) proliferation and migration.

1.6 VSMC Signalling

A growing body of research findings has connected altered vascular integrity and homeostasis, as well as VSMC differentiation, proliferation, and migration, to the activators of both JAK/STAT and MAPK/ERK signalling pathways (Graf et al. 1997; Nelson et al. 1998; Seki et al. 2000; Madamanchi et al. 2001; Xiang et al. 2013; Xiang et al. 2014; Yan et al. 2017). These cellular signalling interactions have been demonstrated to be important contributors to vascular restenosis and the pathogenesis of NIH that are implicated in VGF (Graf et al. 1997; Nelson et al. 1998; Seki et al. 2000; Madamanchi et al. 2001; Xiang et al. 2013; Xiang et al. 2014; Yan et al. 2017). More so, the activities of pro-inflammatory cytokines such as IL-6 and growth factor such PDGF, known activating stimuli of JAK/STAT signalling pathway, have been described to be upregulated in T2DM patients (Akbar and Hassan-Zadeh, 2018; Johnson et al., 2013; Liu et al., 2018; Masamune et al., 2005). Similarly, vasoactive mediators such Ang II and thrombin, known activators of the MAPK/ERK pathway, have been demonstrated to promote VSMC migration, which is crucial for plaque instability and vascular remodelling that are implicated in VGF (Tian et al., 2021; Shapiro et al., 1996; Chen et al., 2009; Yoshizumi et al., 2019). With a focus on their activation of the JAK/STAT and MAPK/ERK signalling pathways, this subsection describes these highlighted mediators of VGF.

1.6.1 IL-6

IL-6 is a member of the IL-6 family of cytokines that include IL-11, cardiotrophin-1, oncostatin M (OSM), leukaemia inhibitory factor, cardiotrophin-1, and ciliary neurotrophic factor (Heinrich et al., 1998; Boulay et al., 2003; Ernst and Jenkins, 2004). In order to generate a "up, up, down, down" configuration, the four straight α -helices (A, B, C, and D) in IL-6 family cytokines are connected by four loops (two big and two smaller) (Somers et al., 1997; Bravo and Heath, 2000). Mature IL-6 glycoprotein has an average molecular weight of 21–28 kDa and 184 amino acids (Boulay et al., 2003). As a homodimer (IL-6 and IL-11) or heterodimer (OSM, leukaemia inhibitory factor-1 and ciliary neurotrophic factor), glycoprotein 130 (gp130), also known as CD130, is used by all of them as a common receptor subunit for signal transduction (Boulay et al., 2003). The cytokine surface has specific "sites" that allow IL-6 to attach to the receptor complex (Figure 1.9). The cytokine binding molecule (CBM) of the α -receptor unit attaches to Site I, which is located within the C-terminal of the AB-loop. Meanwhile, the first signal transducing receptor (gp130) connects with Site II, which is centrally created between Helices A and C. Then, the second signal transducing receptor

(gp130, LIFR, or OSMR) recognises Site III and is then recruited to the complex via its IgG-like domain (Savino et al., 1994; Clackson and Wells 1995; Paonessa et al., 1995; Heinrich et al., 1998). IL-6 binds to a receptor complex made up of the IL-6R receptor subunit and the gp130 homodimer signal transducing subunit (Murakami et al., 1993).

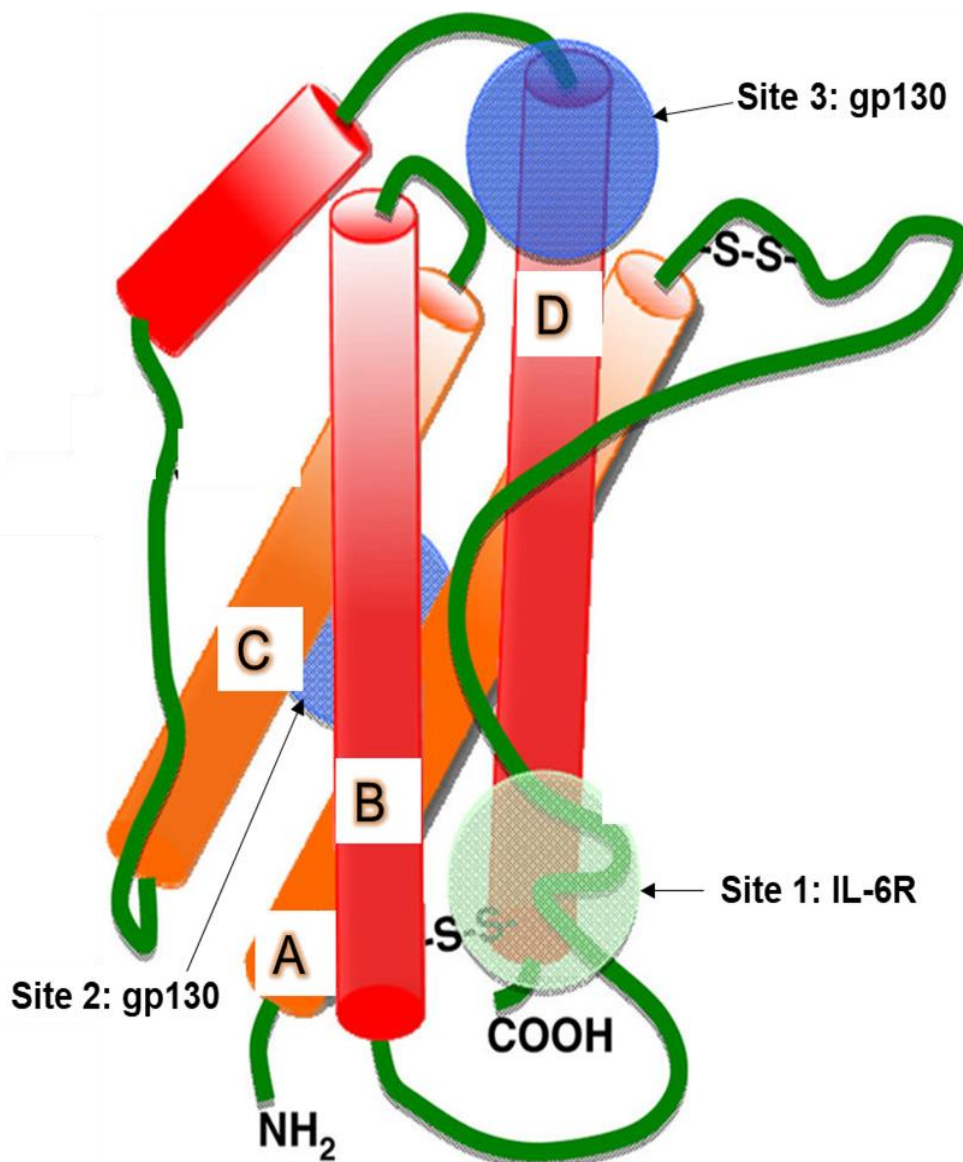


Figure 1.9: A schematic of the domain structure of human IL-6. It shows the four long (A-D) α -helices and the three connecting polypeptide loop that make up the human IL-6. IL-6 can be bound via three receptor binding sites. Site 1 on the C-terminus of helix D binds to IL-6R. Site 2, found on helices A and C binds a molecule of glycoprotein 130 (gp130). Site 3 located on the N-terminal of helix D interacts with another gp130.

1.6.1.1 IL-6 receptor (IL-6R α)

IL-6R α is made up of an N-terminal IgG-like domain, two fibronectin (FN) III-like domains, a membrane-proximal WSXWS motif, four cysteine residues, and then a CBM (Bazan 1990). Four cysteine residues and a membrane-proximal WSXWS motif make up the hinge region of FNIII-like domains, where the CBM is found in loops (Bazan, 1990). Meanwhile, the CBM helps in ligand recognition (Yawata et al., 1993). Except for a short cytoplasmic tail of 82 amino acids residing within the cell, all of the functional domains of IL-6R α are located extracellularly (Heinrich et al., 2003). The typical method of IL-6 signalling is through membrane-bound (mb)IL-6R α ; however, IL-6 trans-signalling via a soluble form of the IL-6R α (sIL-6R α) also takes place. Most cells do not express mbIL-6R α , with the exception of certain leucocytes and hepatocytes (Hirata et al. 1989; Wang and Fuller, 1994; Rojkind et al., 1995). IL-6 trans-signalling can therefore occur in cells like vascular cells that do not express mbIL-6R due to the presence of sIL-6R α (Tamura et al. 2018). It has been demonstrated that a disintegrin and metalloprotease (ADAM)-10, ADAM-17, and the metalloproteases soluble meprin and membrane-bound meprin all cause the receptor's ectodomain to shed in vitro (Mullberg et al., 1993; Schumacher et al., 2015; Riethmueller et al. 2016; Arnold et al. 2017). mbIL-6R is mostly cleaved by proteases to generate sIL-6R α (Chalaris et al., 2011). Additionally, IL-6R α mRNA can also undergo alternative splicing to form sIL-6R (Holub et al. 1999), but this process has a relatively small impact on the production of sIL-6R α (Lust et al., 1992; Rose-John, 2012). Before attaching to ubiquitously expressed membrane-bound gp130 dimers, the sIL-6R α /IL-6 complex is formed in the extracellular environment. Additionally, a short stalk region that is located close to the plasma membrane in mbIL-6R α and in the COOH-terminal of sIL-6R α has been identified. This area controls how ADAM proteins break down IL-6 and allows the sIL-6R α /IL-6 combination to bind to gp130 (Baran et al., 2013).

1.6.2 PDGF

The PDGF family of growth factors consists of four distinct polypeptide chains, each expressed by a different distinct genes PDGF-A, B, C, and D, that are joined together to form five distinct dimers (Fredriksson and Eriksson, 2004). These isoforms, PDGF-AA, PDGF-AB, PDGF-BB, PDGF-CC, and PDGF-DD, act through the PDGF receptors alpha and beta, and two receptor tyrosine kinases (Fredriksson and Eriksson, 2004). Kinases refer to transmembrane receptors

or receptor-activated enzyme proteins. At least 500 protein kinases have been found in the human genome, and they function primarily by transferring a phosphate from ATP to the target protein at Tyr, Thr, and Ser motifs (Kabir and Kazi 2011). About 90 human tyrosine kinases are classified as either non-RTKs, such as JAKs, or RTKs, such as the PDGF receptor (PDGFR), EGFR, and insulin receptor (Kabir and Kazi, 2011). With 60 members, RTKs are the biggest tyrosine kinase family (Lemmon and Schlessinger 2010). While the novel PDGFs, PDGF-C and PDGF-D, are released as latent factors that need activation by extracellular proteases, the traditional PDGFs, PDGF-A and PDGF-B, receive intracellular activation during transit in the exocytic pathway for subsequent secretion. A number of physiological and pathological processes are regulated by the classical PDGF polypeptide chains, PDGF-A and PDGF-B, which primarily target cells with mesenchymal or neuroectodermal origin. It is now known that PDGFR mediates a variety of human diseases, such as graft stenosis (Li et al., 2011).

1.6.2.1 PDGF receptor

The identification of two more ligands for the two PDGF receptors implies that cellular signalling controlled by PDGF is more intricate than previously thought. However, dimeric PDGF isoforms, which can be homodimers (PDGF-AA and PDGF-BB) or heterodimers (PDGF-AB), drive cell responses by attaching to PDGFR- and PDGFR-A, two RTKs that are expressed on the surface of target cells (Manning et al., 2002). PDGFR has a transmembrane domain, an intracellular kinase domain, and a five immunoglobulin (Ig) domain that binds external ligands (Manning et al., 2002). Only PDGFR-AA has a high affinity for the protein, while PDGF-BB binds PDGFR-AA, PDGFR-AA, and PDGFR-AA, and PDGF-AB binds PDGFR-AA homodimers and heterodimers. When PDGF dimer isoforms bind to both PDGFRs at once, they cause the tyrosine kinase domain of PDGFR to homo- or heterodimerize and to become autophosphorylated (Manning et al., 2002). Thus, SH2-domain-containing signalling proteins can now attach at that location.

1.6.3 IL-6- and PDGF- JAK/STAT signalling

IL-6 can transmit signals via two separate receptors. First is the classical signalling, here, IL-6 signals via full-length $mIL-6R\alpha$, although this is restricted to certain cell types, including monocytes, neutrophils, hepatocytes, and B and T cells (Schaper and Rose-John, 2015).

Secondly, IL-6 can also signal by interacting with sIL-6R α , which is produced by immune cells like human neutrophils during inflammation (Chalaris et al., 2007; Schumacher et al., 2015; Yan et al., 2016). Therefore, for cells like VSMCs and ECs that do not express mIL6R, IL-6 can bind circulating sIL-6R α and bind with widely expressed gp130, expanding the range of IL-6 sensitive cells. This process is known as trans-signaling (Romano et al. 1997; Zhuang et al. 2015; Maston et al. 2018; Zegeye et al., 2018; Kurozumi et al., 2019). Normal physiological processes include acquired immunity and other anti-inflammatory processes including intestinal epithelium renewal and metabolic regulation in the liver are linked to IL-6 classical signalling (Scheller et al., 2011). Conversely, trans-signaling facilitates a variety of pathogenic pro-inflammatory functions (Jones et al., 2005; Rose-John, 2012; Schuett et al., 2012), and as a result, it is a target for therapeutic intervention in inflammation-driven illnesses. The IL-6 signal activates the JAK/STAT signalling pathway through the formation of extracellular complex of IL-6 and sIL-6R α first, before they connect to membrane-bound gp130. Local JAK molecules are then activated, resulting in the phosphorylation of the cytoplasmic tail of gp130. STAT3 interacts with phosphorylated gp130 tail residues, which causes STAT3 to become phosphorylated. STAT3 is subsequently transported to the nucleus and begins the transcription of its target genes (Heinrich et al., 2003). The IL-6 signal via JAK/STAT3 can also activate other signalling pathways, including the ERK1/2 and phosphatidylinositol-3 kinase (PI3K)/Akt pathways, which are activated by JAK but independent of STAT (Heinrich et al., 2003).

On the other hand, different signalling cascades, including STATs, are activated by PDGF (Li et al., 2011). Furthermore, there is proof that STAT1, STAT3, and STAT5 bind PDGFR- $\beta\beta$ with high affinities and binds PDGFR- $\alpha\alpha$ to a lesser extent (Yamamoto et al. 1996; Valgeirsdóttir et al. 1998). It is unclear if PDGF activates JAKs linked to receptors. However, PDGF has been shown to activate JAK1 (Valgeirsdóttir et al. 1998). Additionally, there is proof that PDGFR activates SRC family kinases in NIH3T3 mouse embryonic fibroblasts (MEFs), which activate STAT1 and STAT3 (Cirri et al., 1997; Cacalano et al., 2001). However, it is not entirely clear how PDGF activates STAT3 and what its functional importance is.

1.6.4 Ang II

Ang II is the active peptide and the primary mediator of the physiological actions of the renin-angiotensin system (RAS). It raises blood pressure, promotes the renal tubuli to retain sodium and water, and prompts the adrenal gland to secrete aldosterone. Along with its proliferative,

pro-inflammatory, and pro-fibrotic effects, Ang II is a powerful vasoconstrictor (Benigni et al., 2010). In juxtaglomerular cells, proteolytic cleavage of prorenin results in the production of catalytically active renin, which is then released into the systemic circulation (Forrester et al., 2018). Then, the active renin cleaves angiotensinogen, which is produced by the liver, to form Ang I, which is then released into circulation. The vascular endothelium's angiotensin converting enzyme (ACE) then converts Ang I into Ang II, which is then released into the bloodstream. However, all of the RAS components have been found in tissues (de Lannoy et al., 1998; Campbell et al., 1991; Kim et al., 1992), indicating the possibility of a locally operating RAS in the tissues in addition to the RAS in the systemic circulation.

1.6.4.1 Ang II receptors

The identification of the angiotensin II receptor subtypes, AT1, AT2, AT3, and AT4, was made possible by the creation of highly selective angiotensin II receptor ligands. The AT1 receptor is largely responsible for the actions of angiotensin II that are now recognised (e.g. vasoconstriction, aldosterone and vasopressin release and proliferative effects on vascular smooth muscle and other cells) (Unger et al., 1996; De Gasparo et al., 2000; Forrester et al., 2018). The AT1 receptor interacts with G-proteins and activates traditional intracellular second messenger systems, such as phospholipase C activation or adenylate cyclase inhibition (Unger et al., 1996). The AT2 receptor, which only shares a 32–34% homology with the AT1 receptor, has yet to be thoroughly characterised in terms of its function and signal transduction pathways. It has been shown that the AT2 receptor couples to phosphatases, inhibits AT1 receptor- and growth factor-mediated proliferation in endothelium and other cells, and induces neuronal outgrowth in PC12w cells. Also, the AT2 receptor has been linked to cell differentiation and regeneration because of its extensive distribution in foetal tissues, including the central nervous system, and its brief reappearance in the adult body under pathological circumstances (for example, after myocardial infarction) (Unger et al., 1996; De Gasparo et al., 2000).

1.6.5 Thrombin

Thrombin is produced in the prothrombinase complex by proteolytic cleavage of prothrombin. To attain this proteolytic cleavage, factors V and X, calcium, and membrane phospholipids are essential (Bogatcheva et al., 2002). To produce human thrombin, the A chain (49 amino acid residues) and catalytic B chain (259 amino acid residues), which are joined by a disulfide bond, are combined. On its surface, the thrombin globule creates an anion-binding exosite that aids

in thrombin's ability to bind to substrates (Bogatcheva et al., 2002). Being both a procoagulant and an anticoagulant, thrombin is a special kind of molecule whose cellular functions are not fully understood (Narayan, 1999). More so, atherosclerosis, VSMC proliferation, ECM degradation, and vascular inflammatory response have now all been linked to thrombin (Goldsack et al. 1998). Also, it was discovered that thrombin significantly increased the activation of the Raf/ERK1/2 pathway and cell proliferation in rat aortic SMCs (Molloy et al. 1996).

1.6.5.1 Thrombin receptor

Thrombin elicits its activities by activating the proteinase-activated receptor (PAR). PAR is structurally comparable to G-protein-coupled receptors, as it has also seven transmembrane domains (Vu et al., 1991). The 41-amino-acid residue N-terminal exodomain of PAR is proteolyzed as a result of thrombin activation, and the newly generated amino acid sequence functions as a binding ligand by itself (Bogatcheva et al., 2002; Vu et al., 1991). There are now four different forms of PARs, three of which are thrombin-activated and the last one is trypsin-activated (Vu et al., 1991). Thrombin-activated PAR-1 and trypsin-activated PAR-2 have been described in EC (Brass and Molino, 1997). It is thought that tryptases released by mastocytes activate the latter in vivo (Brass and Molino, 1997). It has been demonstrated that animals lacking the PAR-1 gene totally lack some of the effects of thrombin, including an increase in capillary permeability coefficient, an increase in pulmonary artery pressure, and an increase in lung weight due to developing oedema (Vogel et al., 2000).

1.6.6 Ang II- and thrombin- MAPK/ERK signalling

Ang II have been described to upregulate ERK1/2 in human umbilical artery SMCs (HUASMCs), an effect which was abolished by telmisartan, an antagonist of the AT1R, and PD98059, an inhibitor of ERK1/2 (Zhong et al., 2011). Furthermore, stimulation with Ang II caused increased proliferation of HUASMCs which was linked with upregulation of ERK1/2 (Song et al., 2013). These studies suggest that Ang II can mediate its cellular activities through the ERK1/2 signalling pathway whose activation has been implicated in the pathogenesis of NIH VGF (Chen et al., 2009; Yoshizumi et al., 2019).

On the other hand, it has been described that thrombin stimulates VSMC migration, which is essential for plaque instability and vascular remodelling (Tian et al., 2021; Shapiro et al., 1996),

and numerous signalling mechanisms, including thrombin-stimulated MAPK activation, have been described to contribute to the migration of VSMCs (Tian et al., 2021; Shapiro et al., 1996). Thrombin also encourages VSMC migration via P38-MAPK signalling (Wang et al., 2004).

1.7 Rationale and justification for this study

Despite the plethora of drugs currently available for managing CAD patients with or without T2DM, yet CAD could worsen in victims necessitating a CABG (Goldman et al. 1988). The burden of CABG can be huge when the cost and rigor involved are considered. Unfortunately, 50 % of patients that undergo this procedure might require another one after 10 years (Veith et al., 1986; Fitzgibbon et al., 1996; Motwani and Topol, 1998). As worse as this statistic might look, it is even worse in T2DM sufferers as 70% are vulnerable to VGF (Motwani and Topol, 1998). Over the last three decades, there have been advances in surgical techniques employed in CABG, as well as emergence of newer drugs and combination regimens to help limit atherosclerotic plaque formation and deposit in blood conduits (Bolanle et al., 2021). However, the knowledge of how T2DM initiates CABGF is thin. Therefore, assessing how T2DM status alter some HSVSMCs' metabolic responses and signalling would offer promising therapeutic target for drug development.

As previously described in 1.2, VSMCs are integral for the formation of NIH and arterialisation of saphenous vein, which is the preferred blood conduit by surgeons for CABG (Bolanle et al., 2021), however, it is unclear to what extent T2DM alters the metabolic homeostasis of SMCs from T2DM patients compared to non-diabetic controls. As already highlighted in 1.2, the pharmacological and non-pharmacological focus in the management of CVDs is on limiting predisposing factors and preventing micro- and macro-vascular complications. However, little attention has been given to the molecular modifications driven by T2DM. One of such mechanisms which has been extensively described in 1.3 is Protein O-GlcNAcylation. Therefore, targeting protein O-GlcNAcylation in VGF can be promising given that it has recently been validated as a potential target based on pharmacological studies on a range of cancer cell lines in vitro (Yang and Qian, 2017; Ferrer et al., 2014; Lee et al., 2019; Walter et al., 2020; Sodi et al., 2015) and neurodegenerative disorders (Yang and Qian, 2017; Levine et al., 2019; Zhang et al., 2017). Our understanding of this dynamic cellular process has been aided by the discovery of OGT and OGA, the essential enzymes that control protein O-GlcNAcylation and its reversal, respectively, recent advances in affinity purification techniques, creation of an O-GlcNAc-specific antibody, and advances in mass spectrometric technique to identify O-GlcNAcylated targets. Hence, further study of the effect(s) of this dynamic reversible PTM on cell types such as HSVSMCs and involvement in disease pathologies could provide viable target(s) to develop new therapeutic medicines.

Additionally, T2DM is known to trigger changes in mitochondrial function and SVSMCs from T2DM patients have distinct functional properties, more so, it has been demonstrated that VSMCs from T2DM subjects are more migratory than those from non-diabetic controls (Riches et al., 2014; Madi et al., 2009). It remains yet to be studied if increase ATP required to drive this migratory process will translate to increase oxidative phosphorylation measured by OCR or anaerobic glycolysis measured by ECAR. Interestingly, the determination of the mitochondrial OCR and ECAR have been described as gold standards in assessing mitochondrial function (Leese et al. 2016). In fact, OCR has been referred to as the "best marker of metabolic capacity" (Leese et al. 2016), hence will be a useful to evaluate this link. Additionally, the activities of proinflammatory cytokines such as IL-6, vasoactive agonists such as Ang II and thrombin, and growth factors such as PDGF-BB have been suggested to be upregulated in T2DM (Moshepa et al., 2019; García-Olivas et al., 2007; Yaghini et al., 2010; Seasholtz et al., 1999). It is noteworthy that these increased activities have been connected to VSMC proliferation and migration, which is mediated by the activation of a number of downstream signalling pathways, including the JAK/STAT and MAPK/ERK pathways (Graf et al. 1997; Nelson et al. 1998; Seki et al. 2000; Madamanchi et al. 2001; Xiang et al. 2013; Xiang et al. 2014; Yan et al. 2017). Since inhibitors of these downstream signalling pathways have been described, investigated, and explored clinically in treating disease conditions like cancer (Lim et al., 2018; Hoffner and Benchich, 2018), therefore, evaluating the involvement of these pathways could provide insights into possible therapeutic target(s) for drug development to limit VGF.

Lastly, it has been suggested that T2DM triggers increase oxidative stress and vascular reactivity in pre-clinical models (Kaneto et al., 2010; Burgos-Morón et al., 2019; Moshepa et al., 2019; García-Olivas et al., 2007). The mechanisms responsible for this are still being discovered. One of the proposed mechanisms is that increased production of ROS and oxidative stress result from excess glucose and oxidative phosphorylation in mitochondria (Burgos-Morón et al., 2019). Furthermore, pancreatic beta-cells are particularly vulnerable to oxidative stress and mitochondrial malfunction due to the role mitochondria play in insulin release and their susceptibility to hyperglycaemia (Burgos-Morón et al., 2019). Also, chronic hyperglycaemia, which is common in T2DM has been shown to cause deterioration of beta cells by promoting generation of ROS through activation of NADPH oxidase (Kaneto et al., 2010; Mukai et al., 2022). These crosstalks have also been implicated in atherosclerosis, a major factor in VGF (Kaneto et al., 2010; Mukai et al., 2022; Burgos-Morón et al., 2019).

However, the effect of T2DM and these pro-inflammatory and mitogenic stimuli on the generation of ROS in HSVSMC and the signalling mechanisms responsible, are not fully understood. Revealing these mechanisms may inform identification of targets able to reverse mitochondrial dysfunction and ROS formation in T2DM and prevent VGF.

1.8 Hypotheses

Taking into account the findings presented in this introduction, and further summarised in the justification/rationale for the study, we hypothesise the following.

1. That protein *O*-GlcNAcylation, a glucose-dependent modification that links diabetes with protein function, alters HSVSMCs function through post-translational modification of key proteins.
2. That HSVSMCs from T2DM exhibit mitochondrial dysfunction mediated via the JAK/STAT and MAPK/ERK pathways.

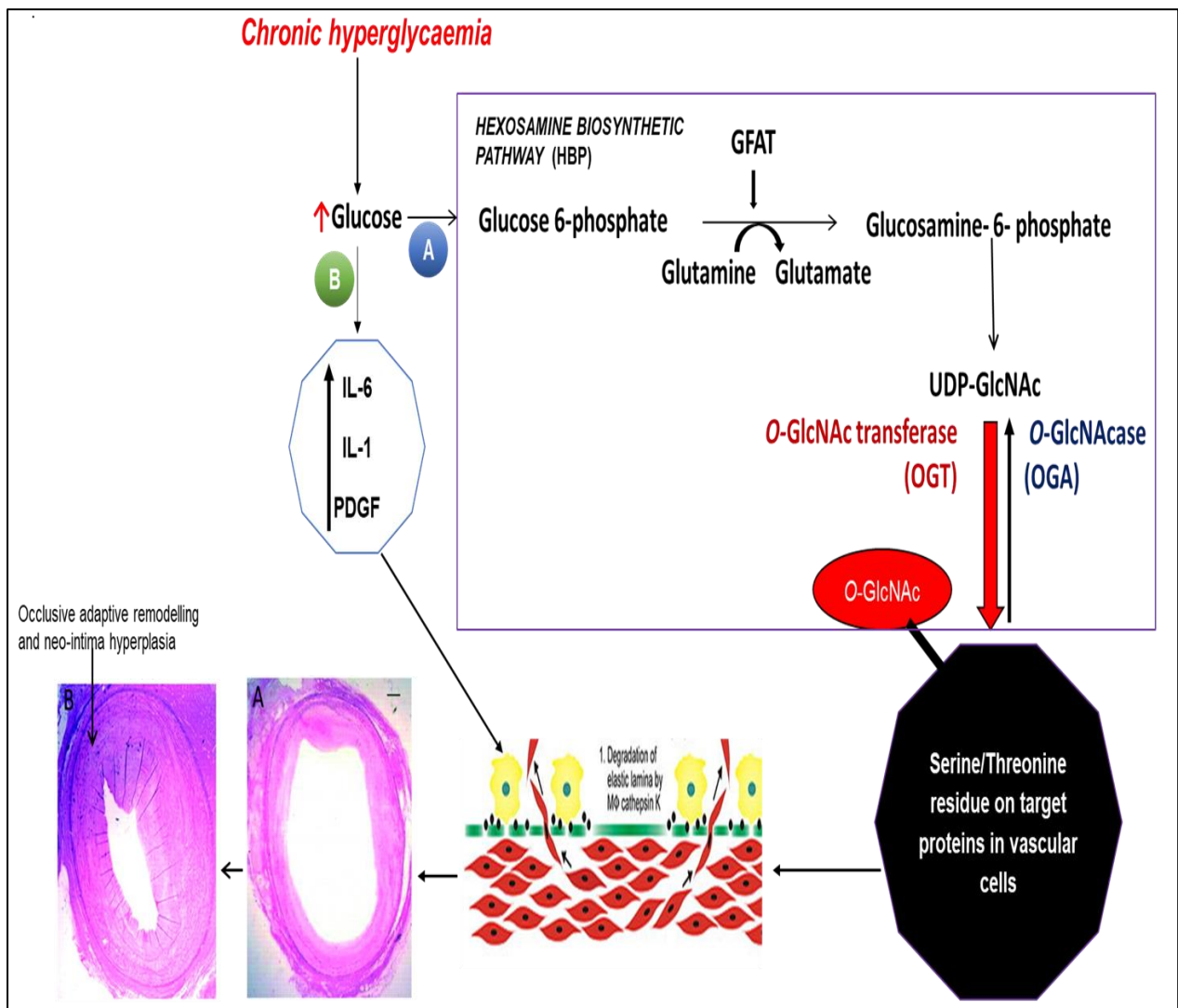


Figure 1.10: Hypothesised glucose-dependent alterations responsible for VSMCs' dysfunction in T2DM.

(A) In chronic hyperglycaemia, more glucose enters the hexosamine biosynthetic pathway which alters the normal *O*-GlcNAc homeostasis in favour of OGT-mediated increase in protein *O*-GlcNAcylation that has been fully described in 1.3. We propose that upregulated protein *O*-GlcNAcylation initiates VSMC proliferation and migration, hence promoting formation of NIH and vascular restenosis implicated in vein graft failure in T2DM.

(B) Also, in sustained hyperglycaemia, which is characteristic of T2DM, the activities of proinflammatory cytokines such as IL-6 and growth factors such as PDGF are upregulated. These further promote increase in ROS production. We therefore propose that these glucose-driven changes alter VSMC integrity including its metabolic homeostasis that we believe further promote vascular dysfunction that contribute to vein graft failure in T2DM.

GFAT: Glutamine:fructose-6-phosphate amidotransferase; IL-6: Interleukin-6; IL-1: Interleukin-1; PDGF: Platelet derived growth factor; ROS: Reactive oxygen species.

1.9 Aim and objectives

Considering the hypotheses stated above, the aim of this project is to investigate and identify T2DM-driven alterations in the functions of HSVSMC, a key cell type involved in vascular dysfunction responsible for saphenous vein graft failure observed in T2DM patients.

The objectives are to:

1. Evaluate how T2DM and hyperglycaemia affect the expression of regulatory enzymes that control cellular *O*-GlcNAcylation status in HSVSMCs *in vitro*.
2. Optimise *O*-GlcNAc capture in HSVSMCs.
3. Evaluate the effects of pro-inflammatory cytokine IL-6/sIL-6R α on the metabolic profiles (OCR and ECAR) of HSVSMC from T2DM patients and non-diabetic control via the JAK/STAT signalling pathway.
4. Evaluate the effects of the mitogenic growth factor PDGF-BB on the metabolic profiles (OCR and ECAR) of HSVSMC from T2DM patients and non-diabetic control via the JAK/STAT signalling pathway.
5. Evaluate the effects of Ang II on the metabolic profiles (OCR and ECAR) of HSVSMC from T2DM patients and non-diabetic controls via the MAPK/ERK signalling pathway.
6. Evaluate the effects of thrombin on the metabolic profiles (OCR and ECAR) of HSVSMC from T2DM patients and non-diabetic controls via the MAPK/ERK signalling mechanism.
7. Evaluate the effects of the activation and inhibition of JAK/STAT pathway on the generation of mROS in HSVSMC from T2DM patients and non-diabetic control.
8. Evaluate the effects of the activation and inhibition of JAK/STAT pathway on the generation of mROS in HSVSMC from T2DM patients and non-diabetic control.

Chapter 2: Materials and Methods

Table 2.1 Materials

Company/Supplier	Catalogue number
Abcam, Cambridge, UK	
Anti- glyceraldehyde-3-phosphate dehydrogenase (GAPDH) antibody [6C5] - Loading Control	ab8245
Anti-O-Linked N-Acetylglucosamine antibody [RL2]	ab2739
Anti-MGEA5/OGA antibody	ab105217
Thiamet G	ab146193
Ruxolitinib	ab141356
Oligomycin	ab141829
Carbonyl cyanide p-(trifluoromethoxy) phenylhydrazone (FCCP)	ab120081
Rotenone	ab143145
Antimycin A	ab141904
Rabbit monoclonal [EPR8965] to non-muscle Myosin IIA	ab 138498
Rabbit monoclonal [SP171] to alpha smooth muscle Actin	ab150301
Donkey Anti-Mouse igg H&L (Alexa Fluor® 488)	ab150105
DHE (dihydroethidium) assay kit - reactive oxygen species	ab236206
Anti-STAT3 antibody (EPR787Y)	ab68153
Agilent Technologies Incorporated, Santa Clara, USA	
Seahorse XF FluxPaks	103022-100
XF DMEM Medium, pH 7.4, 500ml, with 5 mm HEPES, without phenol red, sodium bicarbonate, glucose, sodium pyruvate, L-glutamine	103575-100
BD Bioscience, Berkshire, UK	
BD facsflow™, Sheath Fluid	342003
Facs clean solution	340345
Detergent solution concentrate	660585

Facsuite tm CS&T Research beads	650621
Bio-Rad Laboratories Ltd, Hertfordshire, UK	
Precision Plus Protein Dual Color Stds 500	1610374
Precision Plus Protein TM Kaleidoscope TM prestained protein standards	161-0375
Cell Signalling Technology, Massachusetts, USA	
Phospho-Stat3 (Tyr705) antibody	9131
Phospho-p44/42 MAPK (Erk1/2) (Thr202/Tyr204) (E10) mouse antibody	9106L
Anti- <i>O</i> -GlcNAc (CTD110.6) Mouse mab	9875S
p44/42 MAPK (Erk1/2) antibody	9102L
Gibco laboratories, Maryland, USA	
Dulbecco's phosphate-buffered saline (DPBS)	14190-094
Dulbecco's modified eagle media (DMEM)	11500596
Phosphate buffer solution	14190-094
L-glutamine	25030024
Penicillin/streptomycin/fungizone (PSF)	15240062
Trypsin-EDTA (0.25%), phenol red	25200072
Opti-mem	51985
Insight Biotechnology Limited, Wembley, UK	
(Mgea5) as transfection-ready DNA, 10ug	MG211167
Invitrogen, California, USA	
Hoechst 33342	H3570
F(ab') ₂ -Goat anti-Mouse igg (H+L) Cross-Adsorbed Secondary Antibody, Alexa Fluor 488	A11017
F(ab') ₂ -Goat anti-Rabbit igg (H+L) Secondary Antibody, Alexa Fluor 568	A21069
SYBR Safe DNA Gel Stain	S33102

Wheat Germ Agglutinin, Alexa Fluor™ 594 Conjugate	W11262
Lonza Ltd, Basal, Switzerland	
Lonza DPBS 0.0095M (PO4) without Ca and Mg	LZBE17-512F
Origene Technologies Incorporated, Rockville, USA	
Mgea5 (Myc-DDK-tagged) - Mouse meningioma expressed antigen 5 (hyaluronidase) (Mgea5), (10ug)	MR211167
Promega Corporation, Wisconsin, USA	
Blue/Orange 6x Loading Dye	G190A
Sgfl restriction enzyme	R7103
Mlul restriction enzyme	R6381
Magne(TM) halotag(R) Beads, 20% Slurry, 1ml	G7281
Anti-halotag(R) Monoclonal Antibody	G9211
Magne(TM) halotag(R) Beads, 20% Slurry, 5 X 1ml	G7282
Wizard Plus SV Minipreps DNA Purification Systems	A1330
PromoCell GmbH, Heidelberg, Germany	
Smooth muscle cell growth medium 2 kit	C-22162
R&D systems, Minnesota, USA	
Recombinant human IL-6 protein	206-IL
Recombinant human IL-6 R alpha protein	227-SR-025
Roche Applied Science, West Sussex, UK	
Complete, EDTA-free protease inhibitor cocktail tablets	11836170001
Santa Cruz Biotechnology, Texas, USA	
Anti-GFAT1 antibody (d-9)	Sc-377479

Sarstedt, Nümbrecht, Germany	
Tissue culture flaks, vented caps, 25 cm ²	83.3910.002
Tissue culture flaks, vented caps, 75 cm ²	83.3911.002
Serological Pipette 5ml Individually Wrapped Sterile Non Pyrogenic	86.1253.001
Serological Pipette 10ml Individually Wrapped Sterile Non Pyrogenic	86.1254.001
Serological Pipette 25ml Individually Wrapped Sterile Non Pyrogenic	86.1685.001
Scientific Laboratory Supplies, Nottingham, UK	
Wiva bin 50 L	Saf7362
Ph Electrode Storage Solution 500ml	F151677
Severn Biotech Ltd, Worcestershire, UK	
30% Acrylamide (w/v) Ratio 37.5:1 bis acrylamide	20-2100-10
Sigma-Aldrich (Merck), Dorset, UK	
Ammonium persulfate (APS)	A3678
Anti- <i>O</i> -GlcNAc Transferase (DM-17) antibody produced in rabbit	O6264
Hepes	H3375
Fetal bovine serum	F7524
Dulbecco's Modified Eagles Medium with high glucose	D1145
L-glutamine solution bioextra, 200 mm, so	G7513
Penicillin-streptomycin sterile-filtered	P0781
Medium 199, with hanks' salts and sodium	M7653
N, N", N"-tetramethylethylenediamine b	T9281
Dimethyl sulfoxide hybri-max sterilefilt	D2650
Acrylamide/bis-acrylamide 30% solution 37	A3699
IGEPAL ca-630 molecular biology grad	I8896
Dithiothreitol molecular biology*reagent	D9779-250mg
Dulbecco's modified eagle's medium - low glucose	D6046-6x500ml
D-(+)-Glucose solution 45% in H ₂ O, sterile-filtered, bioextra, suitable for cell culture	G8769-100ML

Sodium azide, reagent plus tm, >= 99.5%	S2002-100g
Angiotensin II human	A9525-5mg
Thrombin from bovine plasma	T4648-1ku
Sino-Biological Incorporated, Beijing, China	
Human GFPT1 Gene ORF cDNA clone expression plasmid, N-Myc tag	HG11071-NM
Human OGT/O-Linked n-acetylglucosamine Transferase Gene ORF cDNA clone expression plasmid, N-Myc tag	HG17892-NM
Starlab UK Limited	
Starguard Protect Nitrile Glove, Violet-Blue, 250mm Long, Medium	SG-P-M
Chemgene hld4l concentrate, clear unfragranced, 5 litre	Xtm309-c
60 x 15 mm cytoone® Dish (Sterile), TC-Treated	CC7682-3359
Cytoone® Plate, 6-Well, Flat Bottom, Non-Treated, Clear (Sterile)	CC7672-7506
Tubeone® Microcentrifuge Tube, 1.5 ml Natural	S1615-5500
Tipone® Filter Tip, 20 µl, Bevelled, Natural, Rack (Sterile)	S1120-1810
Tipone Filter Tip, 200 µl, Graduated, Natural, Rack, (Sterile)	S1120-8810
Tipone® Filter Tip, 1000 µl XL, Graduated, Natural, Rack (Sterile)	S1122-1830
PCR Plate, 96-Well, Skirted, 200 µl, Low Profile, Natural / 10	E1403-5200
Self-Adhesive Plate Seal for PCR, Polypropylene, Clear	E2796-0793
PCR work rack, double sided, hinged lid, polypropylene, mixed	E2396-0599
Stratech, Cambridgeshire, UK	
Trametinib	GSK1120212
Thermo Scientific, Massachusetts, USA	
Poly-D-lysine	A3890401
Dulbecco's modified eagle's medium - low glucose	11885084
Labtek X16 4well N Removable Chamber cvglass, CC Treated, 0.51ml,1.7cm2, 1.0 bglass, Sterile, w/PS lid	16250671
Hoechst 33342, trihydrochide	11534886
16% formaldehyde (w/v), methanolfree	11586711

10ml	
Mitox red mitochondrial supe 50µg	11579096
Rec hu pdgf bb. Recombinant human pdgfb.	10531285
OSMI-1	Sml1621-5mg
Round bottomtest Tube, PS, 5ml, No Cap, Nons	10186360
VWR chemicals, Leicestershire, UK	
Sodium dodecyl sulphate (SDS)	442444H
Centrefeed roll, 1 ply	115-2204

2.2 Methods

2.2.1 Cell culture

Cell culture was carried out in the laminar flow hood designated in the cell culture room. Cells were cultured at 37°C, in 5% (v/v) CO₂ in a humidified atmosphere using a cell culture incubator. Cells were allowed to be 80-90% confluent before subculturing.

2.2.1.1 Cell passage

Tissue culture flasks containing cultivated cells had their growth media removed, and the cells were then given two washes with pre-warmed 5 ml of Dulbecco's PBS. For human umbilical vein endothelial cells (HUVECs) and HSVSMCs, cells were treated for 30 to 60 seconds at 37°C with 2 ml of pre-warmed Trypsin-EDTA (0.25%); for HEK293T, the incubation time was extended (5-10 minutes). Then, tissue culture flasks were tapped to enable total cell detachment, which was verified by visualising under an inverted stage light microscope. Trypsin was neutralised using 8 ml of DMEM supplemented with 10% (v/v) FBS, 100 IU/ml of penicillin, 100 g/ml of streptomycin, and 2 mM L-glutamine. Cells were centrifuged at 500 g for 5 minutes at room temperature to pellet the cells. The supernatant was then discarded, and 10 µl of the cell suspension was counted with a haemocytometer to determine the total number of cells. After that, the desired number of cells were seeded in the tissue flasks, and fresh growth media was added to create total volumes of 10 ml, 3 ml, or 2 ml in T75, 6 cm dish, and 6-well plates, respectively.

2.2.1.2 Freezing down and thawing of cells

Cell pellets were re-suspended in foetal bovine serum (FBS) supplemented with 10% (v/v) DMSO. Before being moved to liquid nitrogen, cells were frozen at -80°C overnight. To thaw frozen cells, cell stocks were rapidly defrosted at 37°C in a water/bead bath and transferred to 8-10 ml a DMEM media. Cells were centrifuged at 500 g for 5 minutes at room temperature to pellet the cells. The supernatant was then discarded, and cells were resuspended in 10 ml of the appropriate growth media and transferred to a sterile T75 tissue culture flask.

2.2.1.3 Maintenance of HSVSMCs

Freshly explanted HSVSMCs from vein preparation or those brought up from storage (-80°C or liquid nitrogen) were seeded in T75 culture flask using 10 ml SmGM₂. For all experiments, early passage (1-4) of HSVSMCs were used.

2.2.1.4 Maintenance of Human embryonic kidney 293T (HEK293T)

Poly-D-lysine was used to coat plates to ensure that HEK293T cells firmly attach to tissue culture plates. The plastic (tissue culture plate) is given a general positive charge by poly-D-lysine, increasing the electrostatic interaction with negatively charged phospholipids at the cell membrane (Harnett et al. 2007). In brief, 12 ml, 2 ml, and 500 µl of 0.01% (w/v) poly-D-lysine solution were pipetted into T75 flask, each well of a 6 well plate, and each well of Lab Tek 4-chambered coverglass, respectively. Poly-D-lysine was allowed to stay in the respective containers for one hour. After that, the poly-D-lysine was taken out, and the dish was thoroughly rinsed with sterile distilled water and allowed to air dry in the laminar flow hood for two hours before seeding cells. High glucose (25 mmol/l) DMEM supplemented with 10% (v/v) FBS, 100 IU/ml penicillin, 100 g/ml streptomycin, and 2 mM L-glutamine was used to culture HEK293T cells.

2.2.1.5 Maintenance of Human umbilical vein endothelial cells (HUVECs)

Endothelial Cell Growth Medium (EGM-2) was used to maintain HUVECs. It was purchased as a bullet kit that included Endothelial Basal Medium (EBM-2) and EGM-2 Single Quot Kit Supplement & Growth Factors and was prepared according to the supplier's instructions. HUVECs were maintained in T75 tissue culture flasks and medium was changed every 48 hours.

2.2.2 Isolation and characterisation of HSVSMCs

2.2.2.1 Isolation of HSVSMCs

Surplus HSV tissues were obtained from T2DM and non-diabetic patients undergoing coronary artery bypass graft (CABG) surgery at the Cardiothoracic Surgery Department, Castle Hill Hospital, Cottingham, UK under NHRA ethical approval (NHS REC:15/NE/0138). HSV tissues (length=0.5 cm to 4 cm) were stored at 4°C (not more than 48 hours before use) in DMEM supplemented with 100 IU/ml penicillin, 100 g/ml streptomycin, and 0.25 g/ml

fungizone. Explant technique as previously described (Mughal et al. 2010; Riches et al. 2014b) was used to extract VSMCs from HSV. Briefly, HSV tissue was placed in a 10 cm dish with enough medium to cover it, and sterile blade was used to remove the perivascular fat, vein branches, connective tissue, and adventitia. The vein was then dissected longitudinally, and the endothelial and tunica intima layers were gently removed. Then, HSV tissue was chopped into small pieces (0.5 cm) and each piece was further dissected into small fragments (~1 mm³). These small fragments were transferred into 25 cm² tissue culture flask with 2 ml of SmGM2 supplemented with 5% (v/v) foetal bovine serum, 0.5 ng/mL epidermal growth factor, 2 ng/mL basic fibroblast growth factor, and 5 g/mL insulin (Promocell, Heidelberg, Germany, Cat. No: C-22162) and maintained in a cell culture in the incubator at 37°C, 5% (v/v) CO₂ in humidified atmosphere. Twice weekly, the growth medium was topped up with 0.5 ml fresh SmGM2. After two weeks, VSMCs were found to have migrated from the explant tissue in most cases. Addition of 0.5 ml fresh SmGM2 continued until a total of 5 ml of growth medium have been added, then, 2.5 ml of growth medium was removed and replenished with fresh 2.5 ml SmGM2 until SMCs become 90% confluent. Thereafter, SMCs were transferred to a 75 cm² tissue culture flask and were fed with 10 ml of SmGM2 which was replaced twice weekly until cells reached 90% confluency.

HSVSMC ISOLATION

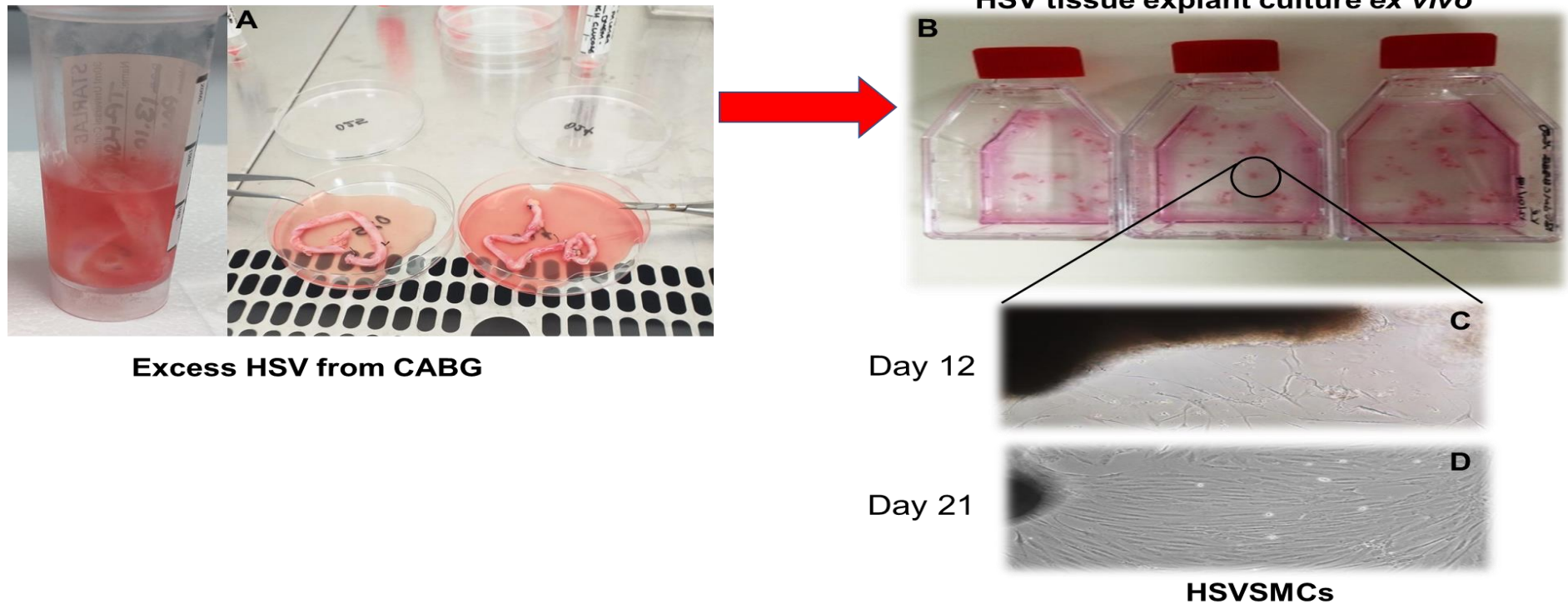


Figure 2.1: Isolation of HSVSMCs from HSV tissue. (A) Excess human saphenous vein (HSV) tissues from patients undergoing coronary artery bypass graft (CABG) (B) Diced small fragments ($\sim 1 \text{ mm}^3$) of HSV tissue seeded in 25 cm^2 tissue culture flask with 2 ml of SMGM2 at day 0 (C) Microscopy images of HSVSMCs beginning to migrate from diced HSV tissue after day 12 (D) Microscopy images of more confluent HSVSMCs after day 21. Magnification $\times 100$, scale bar $100 \mu\text{m}$.

2.2.2.2 Characterisation of HSVSMCs

To validate the integrity of isolated HSVSMCs, they were examined for SMC markers, such as α -smooth muscle actin (α -SMA) and smooth muscle-myosin heavy chain (SMMHC) using confocal immunofluorescence microscopy (Peters et al. 2005; Madi et al.2009). Also, isolated HSVSMCs were examined for EC marker (anti-PECAM (CD31)) to rule out EC contamination. HUVECs were employed as the control in this set of experiments. Lab-Tek 4 chambered coverglasses were pre-coated with poly-D-lysine as described in Section 2.2.1.4. Following this, passages 1 and 4 of the explanted HSVSMCs were seeded in the Lab-Tek 4 chamber coverglass at 10,000 cells/well and allowed to grow until cells reached 40% confluency. Cells were washed three times (for 5-10 sec) with 500 μ l ice cold PBS and fixed with 500 μ l of 4% (w/v) paraformaldehyde in PBS for 10 minutes at room temperature. Then, fixative was removed, and fixed cells were washed three times with 500 μ l PBS on each occasion. Cell membranes of cells were permeabilised by treating with 500 μ l of 0.1% (v/v) Triton X-100 in PBS for 30 minutes at room temperature. Following this, cells were washed three times and blocked with 500 μ l of 5% (w/v) BSA, 0.1% (v/v) Tween 20 in PBS. After this, cells were labelled and incubated with either anti-SMMHC (1:400) or anti- α -SMA (1:200) (primary antibody) in 1% BSA in PBST at 4°C overnight in a humidified chamber. Following this, cells were washed three times with 500 μ l of 5% (w/v) BSA, 0.1% (v/v) Tween 20 in PBS to remove unbound primary antibody. Bound antibody was detected by incubation of cells with 200 μ l/well goat antirabbit IgG. (Alexa 568 1:500) in 1% BSA for 1hr-4hrs at RT in the dark. Then, secondary AB was decanted and washed three times with 500 μ l of 0.1 % (v/v) Tween 20 in PBS followed by three washes with 500 μ l PBS (5min/wash) in the dark. Also, to identify the nuclei, permeabilised cells were stained with 500 μ l of 5 μ g/m Hoechst. Furthermore, to exclude endothelial cell contamination, HSVSMCs and HUVECs from passages 1 and 4 were seeded in the Lab-Tek 4 chamber cover glass. Mouse anti-PECAM (CD31) antibody was used to label fixed and permeabilised HSVSMCs and HUVECs, which was followed by incubation with goat anti-mouse IgG. (Alexa 488 1:500). Also, 500 μ l of 5 μ g/m Hoechst was used to stain the nuclei for identification. The Lab-Tek 4 chambered coverglass was covered with aluminium foil to shield the samples from light until imaging. Images were captured at x200 magnification using a Zeiss laser scanning confocal microscope and images were processed using image J software.

2.2.3 Protein assay and immunoblotting

2.2.3.1 Obtaining cell lysates

Cells within 70-90% confluency in 6 well plates or 6 cm dishes were transferred to an ice bath and the growth media was withdrawn and discarded. The cell monolayer was rinsed twice with 2 to 5 ml of ice-cold PBS, and any leftover PBS was removed using a pipette. Cells were then scrapped into 500 μ l and 1 ml of ice-cold PBS for 6-well dishes and 6 cm dishes respectively. Following this, cell suspension was centrifuged at 500 g for 5 minutes at 4°C. After this, supernatant was gently removed without distorting the pellets and cells were lysed with 70 μ l - 200 μ l of RIPA+ (50 mM HEPES pH 7.4, 150 mM sodium chloride, 1% (v/v) Triton x100, 0.5% (v/v) sodium deoxycholate, 0.1% (w/v) SDS, 10 mM sodium fluoride, 5 mM EDTA, 10 mM sodium phosphate, 0.1 mM PMSF, 10 μ g/ml benzamidine, 10 μ g/ml soybean trypsin inhibitor, 2% (w/v) EDTA-free complete protease inhibitor cocktail (1 tablet per 10 ml extraction)). Samples were allowed to incubate on a rotating wheel at 4°C for 45 minutes and cell lysate was centrifuged at 13,500 g for 15 minutes at 4°C. Then, the supernatant was gently withdrawn without distorting the pellets into a fresh labelled 1.5 ml microcentrifuge tubes. Cell lysates were stored at -80°C and retrieved when required for studies.

2.2.3.2 Determination of protein concentration using BCA assay

The relevant wells on a 96-well plate were filled with 2 to 5 μ l of the supernatant, which was then mixed with RIPA+ buffer to make a total amount of 10 μ l (Figure 2.2). The correct amounts of 2 mg/ml BSA produced in RIPA+ buffer to a total volume of 10 μ l were used to create a standard curve of protein concentrations (0 - 2 mg/ml). Then 200 μ l of BCA reagents was added to each assay well. Composition of the BCA reagent is 49 parts BCA reagent A (1% (w/v) 4,4-dicarboxy-2,2-biquinoline disodium salt, 2% (w/v) anhydrous sodium carbonate, 0.16% (w/v) sodium potassium tartrate, 0.4% (w/v) sodium hydroxide, and 0.95% (w/v)) added to 1 part BCA reagent B (4% (w/v) copper (II) sulphate). Duplicates of assays were performed. The assay was monitored for colour change and the absorbance was determined at 560 nm using the BMG FluroStar plate reader. The A_{560} values of the standard dilutions were used to derive the equation of the best fit straight line, which was then used to determine the protein concentrations.

(A)

Wavelength:	560 nm											
Absorbance	A560 nm											
	Raw Data											
	1	2	3	4	5	6	7	8	9	10	11	12
A	0.092	0.208	0.216	0.249	0.291	0.323	0.356	0.377	0.446	0.464	0.475	
B	0.091	0.176	0.218	0.247	0.299	0.329	0.382	0.382	0.421	0.476	0.487	
C	0.437	0.391	0.356									
D	0.409	0.364	0.36									

(B)

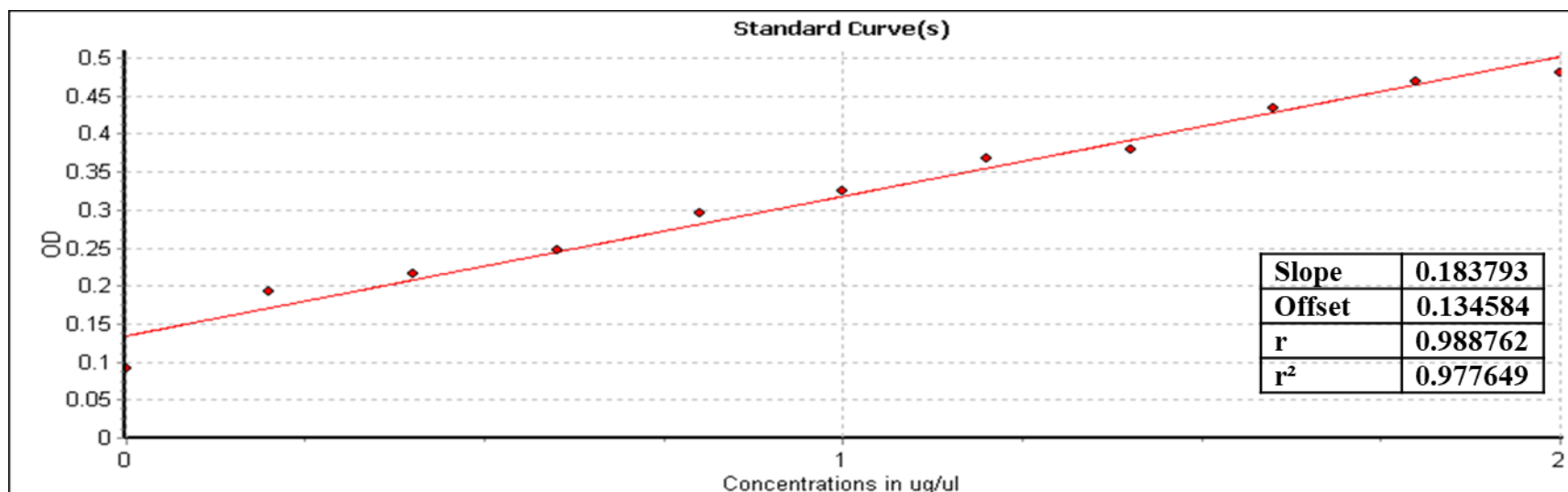


Figure 2.2: Representative BCA assay result and standard curve as exported from the BMG FluroStar plate reader. (A) Protein concentrations of standard preparation in duplicate (corresponding rolls A and B) and samples 1-3 (corresponding rolls C and D) **(B)** Standard curve with the slope and correlation coefficient.

2.2.3.3 SDS-PAGE and protein transfer

Following the BCA assay results, samples were equalised for protein content (10–40 µg) by adding the necessary amount of RIPA+ buffer to make up to 30 µl. Cellular proteins were denatured by adding SDS-loading buffer (50 mM Tris pH 6.8 at room temperature, 10% (v/v) glycerol, 12% (w/v) SDS, 100 mM dithiothreitol, 0.2% (w/v) bromophenol blue). Samples were heated at 70°C for 2 minutes and centrifuged on a bench top centrifuge 13,000 g at room temperature for 30 seconds to recover any condensation. Depending on the size of protein of interest, 8%, 10% or 13% (w/v) acrylamide resolving gels (Appendix 3) was prepared. Precision Plus Protein™ Kaleidoscope™ prestained protein standards and samples were loaded into each well and separated via electrophoresis at 100-180 V in Tris-Glycine-SDS buffer (24.7 mM Tris, 0.19 M glycine). Voltage was first maintained at 100 V, then increased to 180 V when samples entered into the resolving gel until the bromophenol blue tracking dye reached the base of the gel. Separated bands were then transferred from the gel to an Amersham™ Protran® 2µm pore nitrocellulose membrane using the semi-dry Thermofisher transfer device for 1 hr.

2.2.3.4 Immunoblotting

For phospho-specific antibodies, membranes were incubated for 1 hour at room temperature with 5% (w/v) BSA blocking solution diluted in Tris buffered saline-Tween 20 (TBST) (10 mM Tris pH 7.6, 150 mM NaCl, 0.1% (v/v) Tween-20), while for all other antibodies, membranes were incubated in 5% (w/v) dried skimmed milk in TBST. The membrane was then incubated overnight with specific primary antibody (as shown in Table 2.2 prepared in the appropriate blocking buffer) at 4°C on a rotating wheel. Three TBST washes (5 minutes per wash) at room temperature were used to remove unbound primary antibody. Following this, appropriate IRDye-conjugated secondary antibodies (Table 2.2) diluted in 5% (w/v) dried skimmed milk in TBST was used to incubate the membrane at room temperature for 1 hr. The unbound secondary antibody was then removed by washing three times with TBST (5 minutes per wash) at room temperature and once more for 5 minutes using a high detergent buffer (0.5% (w/v) milk powder, 1% (v/v) Triton X-100, and 0.1% (w/v) SDS in PBS). Immunoreactive bands were detected by imaging with a Licor Odyssey DLx.

Table 2.2 Primary and secondary antibodies used for immunoblotting and characterization of HSVSMCs

Primary antibodies			
Antibody	Specie	Dilution	Size (kDa)
pSTAT3 (Tyr 705)	Rabbit	1:500	98
STAT3	Rabbit	1:500	98
GAPDH	Mouse	1:15000	37
ERK	Mouse	1:500	42,44
pERK (Thr202/Tyr204)	Rabbit	1:500	42,44
OGA	Rabbit	1:5000	130
OGT	Rabbit	1:1000	110
GFAT	Mouse	1:500	77
HaloTag	Mouse	1:1000	130
O-GlcNAc	Mouse	1:500	Multiple
SMMHC	Rabbit	1:400	
α-SMA	Mouse	1:200	
PECAM-1 (CD31)	Mouse	1:100	
	Secondary antibodies		
IRDye 680RD	Mouse	1:20000	
IRDye 800CW	Rabbit	1:20000	
Alexa 488	Mouse	1:500	
Alexa 568	Rabbit	1:500	

2.2.4 Optimisation of *O*-GlcNAc capture

2.2.4.1 Synthesis and purification *O*-GlcNAc traps

First, 25 g of the LB broth (Tryptone-10 g, Yeast Extract -10 g and NaCl- 10 g) was weighed and dissolved in 800 ml of distilled water. The suspension was stirred until a solution was attained and made up to 1L volume with distilled water. Following this, the LB broth was autoclaved for 90 minutes and allowed to cool on the bench. 10 ml of LB+KAN was measured into a sample bottle and inoculated with the glycerol stock of the transformed bacteria comprising of the genes of interest (*CpOGA*^{WT} and *CpOGA*^{D298N}). Sample bottle was incubated at 37⁰C in a shaking incubator over the night. The following day, 1 ml of kanamycin was added to the prepared 1 L LB broth and the culture was added to this kanamycin+LB broth mixture to attain a final concentration of 50 µg/ml Kanamycin (LB+Kan). This mixture was then allowed to incubate at 37⁰C in a shaking incubator for 3 hours. The optical density was intermittently determined using a mass spectrophotometry until the desired range is attained (desired range is 0.6-0.8). Once this is attained, the sample was retrieved and allowed to cool at room temperature. Following this, 100 µl of 1M IPTG was added, and the sample was transferred to the shaking incubator and allowed to incubate over the night at 37⁰C.

The sample was removed from the shaking incubator the next day, and 400 g equivalent of the cultured bacterial suspension was weighed using a weighing scale into a Beckman's centrifuge tube (BCT). Then, the BCT containing the suspension was centrifuged at 3500 rpm for 30 minutes at temperature 2-4⁰C. Following this, the supernatant was discarded, and the BT tube was drained inverted on a tissue roll to get rid of left supernatant. The BCT containing the pellet was preserved to -20⁰C until use. On the day of use, pellets were resuspended in 40 ml lysis buffer (50 mM Tris, 250 mM NaCl at pH 7.5) supplemented with protease inhibitors (1 mM benzamidine, 0.2 mM PMSF and 5 µM leupeptin), DNase and lysozyme prior to lysis. The bacterial cell wall was further broken by sonication. Lysate was then centrifuged at 20,000 rpm for 30 minutes at 4⁰C. Following this, the supernatant was loaded onto a HisTrap HP column (GE Healthcare Life Sciences) that had been pre-equilibrated with lysis buffer and charged with NiSO₄. The column was washed with 10 column volumes of lysis buffer. Proteins were eluted with a linear gradient of imidazole (0-500 mM) over 20 column volumes. Then, the eluted protein was further concentrated by centrifuging at 8000 rpm for 5-10 minutes at 4⁰C to concentrate the protein to at most 5 ml. Late elution fractions were pooled and dialysed into 1 x TBS and snap frozen with a final concentration of 20% glycerol and stored at -80 °C

until use. 13% acrylamide gel stained with Coomassie dye (Appendix 10.5) was used to confirm the size and integrity of the purified fusion proteins.

2.2.4.2 Small scale protein pulldown

To do this, 20 μ l of packed volume of MagneTMHaloTag[®] Beads (Promega) (100 μ l of the 20% v/v bead suspension) was measured into an Eppendorf tube and allowed to settle. Settled beads were placed in a magnetic stand for 30 seconds. Following this, the supernatant was gently withdrawn and discarded. Settled beads were equilibrated with 100 μ l equilibration buffer (50 mM Tris pH 7.5, 150 mM NaCl) on a rotating wheel for 5 minutes at room temperature. After which it was placed in the magnetic stand for 30 seconds, and the supernatant was withdrawn and discarded. Washing was repeated for a total of 4 washes. After the final (4th) wash, the required calculated amount of purified Halo-cpOGA was added and made up to 500 μ l with binding buffer (50 mM Tris, 150 mM NaCl, 0.05% Tween 20). This was allowed to thoroughly mix at room temperature for 1 hour or 4-5 hours at 4^oC on a rotating wheel. Following this, the mixture was placed in a magnetic stand for 30 seconds and supernatant was gently removed and discarded (50 μ l of supernatant was retained to check for binding efficiency of beads). As earlier described, a total of three washes was done with equilibration buffer. After the final wash, 1 ml volume of desired concentration of tissue lysate in binding buffer was added to the coupled bead and allowed to mix on a rotating wheel for 90 minutes at 4^oC. Following this, the mixture was kept on a magnetic stand for 30 seconds and a total of four washes as described above with binding buffer was done. After the final wash, to elute the *O*-GlcNAcylated proteins, 4x Laemmli buffer was added directly to the coupled beads and heated at 70^oC for 5 mins. For 20 μ l settled beads, 40 μ l 4x Laemmli buffer was used.

2.2.4.3 Digestion and solubilization of HSV tissue

HSV previously stored in -80^oC was retrieved and snap frozen in liquid nitrogen (LN). Frozen HSV was then pulverized with a mortar and pestle. LN was injected sporadically during the HSV tissue pulverisation to maintain the tissue's stability until it was entirely reduced to a powder. Following this, powdered HSV tissue was weighed and solubilised with a SDS solubilisation buffer (50 mM sodium HEPES, pH 7.5, 150 mM sodium chloride, 10 mM sodium fluoride, 10 mM sodium phosphate, 5 mM EDTA, 2% (w/v) SDS).

2.2.5 RNA Assay

2.2.5.1 Preparation of Plasmids

The DNA plasmid was purchased as lyophilized powder and reconstituted in sterile water before being stored at -20°C . Plasmids were amplified by transformation in competent XL1-Blue E. coli. This entailed incubating 50 μl of thawed competent cells with 500 ng of DNA on ice for 30 minutes, followed by 90 seconds of incubation at 42°C in a water bath and 2 minutes of incubation back on ice. The cells were then mixed with 500 μl of LB media (1% (w/v) bacto-tryptone, 0.5% (w/v) yeast extract, and 1% (w/v) NaCl), and the suspension was incubated at 37°C in a shaker for 45 minutes. Following a 5-minute centrifugation of the cells at 1000 g, the medium volume was adjusted to the necessary level (1 ml/glycerol stock plus 100 μl /LB-agar plate), and after this, the cells were re-suspended. Glycerol stocks were prepared by mixing 1 ml of the LB media with 400 μl of autoclaved sterile 50% (v/v) glycerol and storing the mixture at -80°C . 100 μl of the remaining LB medium was poured aseptically to LB-agar plates that also contained ampicillin (50 $\mu\text{g}/\text{ml}$) and incubated at 37°C overnight. Plates were then kept at 4°C until needed, but not for more than six weeks. A starter culture was made by selecting one colony from the agar plate and inoculating 5 ml of LB media with the appropriate antibiotic (Ampicillin (50 g/ml)) in a 37°C shaker overnight. A stab of glycerol stock was injected into 5 ml of LB media mixed with the appropriate antibiotic for a culture from glycerol stocks, and the mixture was then incubated overnight in a 37°C shaker.

2.2.5.2 DNA extraction, purification, and quantification

Plasmid DNA was isolated using the Promega Wizard Plus Miniprep DNA Purification System in accordance with the manual provided by the manufacturer. In summary, the overnight culture was centrifuged at 10,000 g for 5 minutes to produce a pellet. The supernatant was discarded, and the tube was inverted on a paper towel to remove excess media. Following this, pellet was completely resuspended in 250 μl of Cell Resuspension solution by vortexing and pipetting, and cell suspension was transferred to sterile 1.5ml microcentrifuge tube. 250 μl of Cell Lysis Solution was added to the cell suspension and mixed by inverting the tube 4 times. This was allowed to incubate at room temperature till cell suspension clears (3-5 minutes). Then, 10 μl of Alkaline Protease Solution was added and mixed by inverting the tube 4 times. This was allowed to incubate at room temperature for 5 minutes. Addition of the Alkaline protease helps to inactivate endonucleases and other proteins released during the lysis of the

bacterial cells that can adversely affect the quality of the isolated DNA. Then, 350 µl of Neutralizing Solution was added to cease the reaction. Following this, the lysate was centrifuged at maximum speed (14, 000 x g) for 10 minutes at room temperature.

The cleared lysate was carefully transferred into a spin column without distorting the white precipitate. In any instance that the white precipitate is accidentally transferred with the cleared lysate, the lysate was transferred back to the microcentrifuge tube and lysate was centrifuged for another 5-10 minutes. The supernatant in the spin column was then centrifuged at maximum speed at room temperature for 1 minute and the flow through was discarded. Wash solution was prepared by adding 35 ml 95% ethanol to the Column Wash Solution. The spin column was then filled with 750 µl of Wash Solution before being centrifuged at maximum speed for 1 minute at room temperature. Then, the procedure was repeated using 250 µl of Wash Solution. The spin column was then centrifuged at maximum speed for two minutes at room temperature while still being kept in a collection tube to remove excess Wash Solution. The spin column was then placed in a sterile 1.5 ml centrifuge tube and 100 µl of nuclease-free water was added. This was centrifuged for 1 minute at maximum speed at room temperature. Using a Thermo Scientific™ NanoDrop Lite Spectrophotometer, with UV absorbance at 260nm/280nm (A₂₆₀/A₂₈₀), the concentration of the resultant DNA was determined. A₂₆₀/A₂₈₀ levels over 1.8 were deemed appropriate for analysis. Plasmid DNA was then stored at -80°C.

2.2.5.3 Transfection of HEK 293T with plasmid DNA

A day before transfection, a poly-D lysine pre-coated 6-well plate was seeded with HEK 293T cells at a density of 5-6.25 x 10⁵ cells/well and allowed to be 50–80% confluent. On the day of transfection, growth media was withdrawn and replaced with fresh medium. Then, 2 µg of DNA was dissolved in 500 µl of Opti-MEM I without serum and 5 µl of Lipofectamine LTX reagent was added to the Opti-MEM-DNA solution. This was mixed gently and allowed to incubate for 30 minutes at room temperature to form DNA- Lipofectamine LTX Reagent complexes. Following this, 100 µl of the DNA- Lipofectamine LTX Reagent complex was added to each well directly and incubated at 37°C in a CO₂ incubator for 18–48 hours before visualising with the fluorescence microscope or assaying for transgene expression.

2.2.5.4 Agarose gel electrophoresis

To do this, 1% (w/v) agarose gel was prepared using 1X TAE buffer (40 mM Tris, 20 mM acetate, 1 mM EDTA, pH 8.6 at room temperature). To facilitate the visualisation of nucleic acids under UV light, SYBR safe was added to the agarose gel at a final concentration of 1X in accordance with the manufacturer's recommendations. Then, 2 µl Promega Blue/Orange 6x Loading Dye was added to 10 µl PCR product before being mixed and loaded onto the gel. Following that, samples were separated by electrophoresis at 100 V in 1 X TAE buffer. DNA fractionation was visualised using a Biorad ChemiDoc MP Imaging System.

2.2.5.5 Polymerase chain reaction

To make a total volume of 20 µl PCR mixture, 1 ng of cDNA was added to 14.4 µl of nuclease-free water, 1 µl of primer (25 pmol/l) (Table 2.3), and 2.6 µl of OneTaq® Quick-Load® 2X Master Mix with Standard Buffer. PCR was then performed in an AB 2720 thermal cycler with the following optimised PCR conditions: initial denaturation was at 95°C for 10min for 1 cycle, followed by 35 cycles of denaturing at 95°C for 30 sec, annealing at 57°C for 30 sec, extension at 72°C for 30 sec, and final extension at 72°C for 5min, and then maintained at 4°C until sample collection. PCR product was kept at -20°C for long-term storage or 4°C for short-term use.

2.2.5.6 Real-time quantitative PCR

A total volume of 20 µl PCR mixture, comprising of 1 ng of cDNA, 10 µl of SYBR Green Master Mix, 1 µl of the appropriate primer, and 7.4 µl of RNase-free H₂O, was added to each well of a 96-well PCR plate. The 96-well plate was then installed in the StepOne machine after being sealed with optical adhesive film. StepOne software was used to perform the real-time quantitative PCR (qPCR) in accordance with the manufacturer's recommendations. The cycle conditions for real-time qPCR were optimised and set at 95°C for 10 minutes, followed by 35 cycles of 95°C for 30 seconds, 57°C for 30 seconds, and 72°C for 30 seconds. Every assay was carried out twice and the average was determined. Water devoid of RNase served as the negative control. Each sample's average CT values were computed and normalised to 18S and protein B-actin which were used as loading controls.

Table 2.3 PCR primer sequence

Gene	Primer sequence (5'-3')
MT-COI	Forward- CCT ACT CCT GCT CGC ATC TG Reverse- AGA GGG GCG TTT GGT ATT GG
18S	Forward- GTA ACC CGT TGA ACC CCA TT Reverse- CCA TCC AAT CGG TAG TAG CG
B-actin	Forward- CCT CGC CTT TGC CGA Reverse- TGG TGC CTG GGG CG

2.2.6 Mitochondria stress analysis to determine the OCR and ECAR of HSVSMCs

HSVSMCs were seeded in seahorse XFp 8 well plates at a density of 10,000 cells per well and were allowed to grow over 24 hrs. Following this, cells were treated with the respective inhibitors of the downstream signalling pathways. For JAK/STAT signalling pathway, cells were treated with 0.1 μM ruxolitinib for 90 min after which 1:1000 IL-6 (5 ng/ml) and sIL-6R α (25 ng/ml) (IL-6/sIL-6R α) or 10 ng/ μL PDGF-BB was appropriately used to treat cells over 24 hrs. On the other hand, for MAPK/ERK signalling pathway, cells were treated with 10 nM trametinib for 90 min after which 100 nM Ang II or 1 U/ml thrombin was appropriately used to treat cells over 24 hrs. Treated cells were maintained in a CO₂ incubator at 37°C. Also, the probed of the XFp 8 well plate were hydrated overnight by adding 200 μl of seahorse calibrant into each well and 400 μl into the ridges of the plate to prevent evaporation. A non-CO₂ humidified incubator was used to incubate this hydrated sensor containing XFp 8 well plates overnight at 37°C.

On the day of the assay, modulators of mitochondria respiration; 20 μl oligomycin (1.5 μM), 22 μl carbonyl cyanide p-(trifluoromethoxy) phenylhydrazone (FCCP) (5 μM), and 25 μl rotenone (5 μM) and antimycin A (5 μM) complex were added to pots a, b, and c of the pre-hydrated seahorse XFp 8 well plate respectively. The seahorse XFp 8 well plate was kept in the non-CO₂ incubator for 30 minutes to allow the drugs equilibrate. Following this, plates were mounted in the Agilent Seahorse analyzing machine and allowed to calibrate. While calibrating, the growth media on the pre-treated cells were withdrawn and 180 μl of the XF DMEM medium was added to each well. Following calibration, the cells were mounted in the Agilent Seahorse analyzing machine and real time OCR and ECAR of the pre-treated cells were determined using the seahorse analyzer. After assay, treated cells were lysed and the protein concentrations were determined using BCA assay. There were four (n=4) biological replicates of this experiment using samples from different patients. Determined OCR and ECAR were normalised to determined protein concentration.

2.2.7 Flow cytometry (FACS)

2.2.7.1 Preparation of cell samples for FACS

HSVSMCs from T2DM and non-diabetic patients were cultured in 10 mm dish until 70-90% confluent. Following this, cells were treated with 0.1 μ M ruxolitinib for 90 min to inhibit the JAK/STAT signalling pathway, and then 1:1000 IL-6 (5 ng/ml) and sIL-6R α (25 ng/ml) (IL-6/sIL-6R α) or 10 ng/L PDGF-BB was used to treat the cells over the course of 24 hours. On the other hand, cells were treated with 10 nM trametinib for 90 min to inhibit the MAPK/ERK signalling pathway, followed by treatment with 100 nM Ang II or 1 U/ml thrombin over the course of 24 hrs. On the day of FACS assay, untreated (control) and treated HSVSMCs were transferred into 1.5 ml centrifuge tubes and spun at 654 x g (~1000rpm) at 4°C for 5 minutes. Pelleted cells were washed thrice with 1 ml of 1% (w/v) BSA in PBS. Using a haemocytometer, 5×10^5 cells were resuspended in 100 μ l 1% (w/v) BSA in PBS. Resuspended cells were incubated with 5 μ M MitoSOX for 20 min at 37°C, in a CO₂ incubator. After this, cells were pelleted at 500 x g for 5 minutes at 4°C, and the supernatant was discarded. Pelleted cells were washed twice with 1% (w/v) BSA in PBS at 500 x g for 5 minutes at 4°C. Samples were kept on ice until flow cytometry analysis.

2.2.7.2 FACS analysis with Fortessa Flow cytometer

The FACS Fortessa Flow cytometer was cleaned appropriately and calibrated using a rainbow bead according to manufacturer's specification. The expression of MitoSOX was quantified in the flow cytometer via the PE Channel. In brief, a window with FSC as horizontal axis and SSC as vertical axis was created and a loose gate that excludes debris found at the left corner of the FSC/SSC plots was created. This gate labelled P1 helps exclude dead cells from preparation process and debris from assay. Another gate (P2) that includes mitoSOX-positive cells but excludes mitoSOX-negative cells was drawn from the P1 population. The percentage of cells within P1 that shifted into P2 was determined and acquired as %PE. This procedure was adopted for all treatment conditions. Six (n=6) biological replicates were done and used for statistical analysis.

2.2.8 Sample summary

In this study, HSVSMCs were cultured from a total of 55 patients comprising of 38 non-diabetic and 17 T2DM patients (Table 2.4). For each set of experiments, cells from a minimum of 4 and a maximum of 6 patients were utilised. Samples were randomly selected and their diabetic status were determined based on receiving (or not) diabetes therapies.

Table 2.4 Patient information for HSV samples

Description	T2DM	Non-diabetic
Number of samples	17	38
Age range	56-80	48-84
Sex	Male- 15 Female- 2	Male- 37 Female- 1
Ethnicity	White British- 17	White British- 37 Asian- 1
Reason for surgery	CAD	CAD

CAD: coronary artery disease; T2DM: type 2 diabetes mellitus. HSV samples were collected between January 2020 and May 2022 from patients undergoing elective coronary artery bypass graft procedure.

2.2.9 Statistical analysis

Statistical analysis was carried out using Graphpad Prism® 6, San Diego, USA. Data are presented as mean \pm standard error of mean (S.E.M) and were analysed using independent t-test and one-way analysis of variance followed by Dunnett's post-hoc test to determine significant difference between means where $p < 0.05$ was considered statistically significant.

Chapter 3: Characterisation of HSVSMC and expression of regulatory enzymes of *O*-GlcNAcylation in HSVSMCs from control and T2DM patients

3.1 Introduction

As described in 2.2.2, the multi-step method involved in isolating SMCs from HSV leaves it open to contamination at various steps, which may affect the reliability of the experimental data. Also, the primary culture (HSVSMC culture) used in this experiment is susceptible to typical cell culture contaminants including fibroblasts (Ravi et al., 2021; Payushina et al., 2013; Linge et al., 1989). As a result, it is critical to validate the integrity of primary cell preparations in order to ensure reliable interpretation of results. Additionally, it is crucial to exclude EC contamination due to the proximity of ECs to SMCs in blood vessels. To achieve this, well-known SMC identification markers like SMMHC and α -SMA were used (Riches-Suman and Hussain 2022, Owens et al. 2004). Platelet endothelial cell adhesion molecule-1 (PECAM-1, also known as CD31) was utilised to test for the presence of ECs in order to rule against EC contamination (Woodfin et al., 2007).

Furthermore, the enzymes that modulate protein *O*-GlcNAcylation (OGA, OGT, and GFAT) have been extensively characterised in many cell types and systems (Bolanle et al., 2021, Yang and Qian, 2017). However, our understanding of the factors that influence their expression and functions is still expanding. One of such factors which is of critical interest in this project is hyperglycaemia, a hallmark feature of unresolved or poorly controlled T2DM. The relationship between *O*-GlcNAcylation and prolonged hyperglycaemia has been demonstrated in several studies which have shown that this relationship is causally related (Masaki et al., 2020, Vasconcelos-Dos-Santos et al., 2018, Bond and Hanover, 2015). However, nothing is known about how hyperglycaemia or T2DM regulates the expressions of these regulating enzymes of *O*-GlcNAcylation in HSVSMCs, a key cell type involved in the vascular dysfunction responsible for saphenous VGF observed in T2DM patients. Therefore, in this chapter, HSVSMCs samples obtained from T2DM and non-diabetic patients were probed for variation of the expressions of these key enzymes that control *O*-GlcNAcylation status. To further substantiate this finding, cultured HSVSMCs were incubated with high glucose concentrations (10 mM and 25 mM) for 48 hours to assess any effect of high glucose levels on expression of these enzymes.

Furthermore, protein *O*-GlcNAcylation already described in 1.3, is a key focus of this study as its upregulation has been suggested to alter protein function in VSMC and VEC (Yang and

Qian, 2017). We hypothesise that this dynamic PTM is linked to VGF that is observed in T2DM patients. Therefore, identifying target proteins that are differentially or significantly more *O*-GlcNAcylated could offer novel insights for therapeutic targeting. However, for effective proteomic studies to be done, sufficient *O*-GlcNAcylated protein needs to be affinity captured to allow downstream detection of peptides by mass spectrometry. This can be achieved by trapping *O*-GlcNAc sites with bacterially expressed and purified Halo-tagged CpOGAD298N. Therefore, I optimised affinity capture of *O*-GlcNAcylated proteins in HSVSMCs using purified *O*-GlcNAc trap described in 2.2.4.1.

Putting these together, therefore, the objectives of this chapter were:-

1. To characterise and verify the integrity of the isolated HSVSMCs.
2. Evaluate how early passaging, T2DM, and hyperglycaemia affect the expression of regulatory enzymes that control cellular *O*-GlcNAcylation status in HSVSMCs *in vitro*.
3. Optimise affinity capture of *O*-GlcNAcylated proteins in HSVSMCs.

3.2. Results

3.2.1 Characterisation of HSVSMC by immunofluorescence microscopy

SMC contractile proteins such as SMMHC and α -SMA, contraction regulators such as smoothelin and smooth muscle 22- α (SM22- α), and cytoskeletal proteins such as desmin and vimentin are well-known markers used to identify SMC (Riches-Suman and Hussain 2022, Owens et al. 2004). Of these SMC markers, the most distinct and specific is SMMHC because SMCs express it from development through maturation (Miano et al. 1994). Despite the specificity of SMMHC as a marker of SMCs, it has also been detected in other cell types such as follicular dendritic cells (Ioannidis and Laurini, 2019). There is, therefore, a need for an additional complementary marker such as α -SMA. α -SMA is a highly abundant protein that accounts for 40% of the overall protein composition of SMCs, although like SMMHC it is not exclusive to the SMC lineage (Riches et al., 2009). As the SMCs under investigation are vascular with proximity to the endothelial bed, there is, therefore, a possibility of endothelial cell contamination. Unlike SMCs, ECs in the vascular compartment express platelet endothelial cell adhesion molecule-1 (PECAM-1, also known as CD31) and its expression is primarily concentrated at junctions between adjacent cells (Woodfin et al., 2007). Hence, PECAM-1 was employed as a reliable marker to exclude EC contamination in SMC preparations. To determine the expression of these markers (α -SMA and SMMHC), confocal immunofluorescence microscopy was employed as described in 2.2.2.2. SMCs were isolated from HSVs using an explant method as described in 2.2.2.1 (Mughal et al. 2010; Riches et al. 2014b).

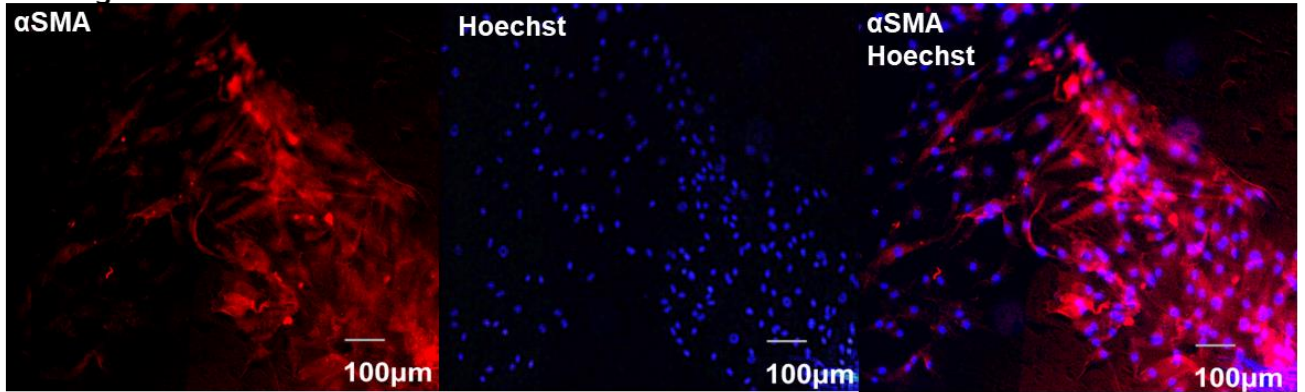
Briefly (detailed protocol is described in 2.2.2.2), the Lab-Tek 4 chamber slides were seeded with passages 1 and 4 of HSVSMCs from non-diabetic patients at a density of 10,000 cells per well. HSVSMCs were fixed with 4% PFA and permeabilized with 0.1% (v/v) Triton X-100 in PBS before being labelled with rabbit anti- α -SMA (Cat No: ab150301, 1:200) and rabbit anti-SMMHC (Cat No: ab 138498, 1:400) primary antibodies and goat anti-rabbit IgG. (Alexa 568, Cat No: A21069, 1:500). To exclude endothelial cell contamination, fixed and permeabilised HSVSMCs (passages 1 and 4) and HUVECs were labelled with rabbit anti-PECAM-1 (Cat No: BD 555444, 1:100) primary antibody and (Alexa 488 Cat No: A11017, 1:500). Hoechst was used to stain the nuclei.

Results revealed that these SMCs (passages 1 and 4) isolated from HSV are exclusively SMCs as they positively reacted to both anti- α -SMA (Figure 3.1-Top and middle panels) and anti-

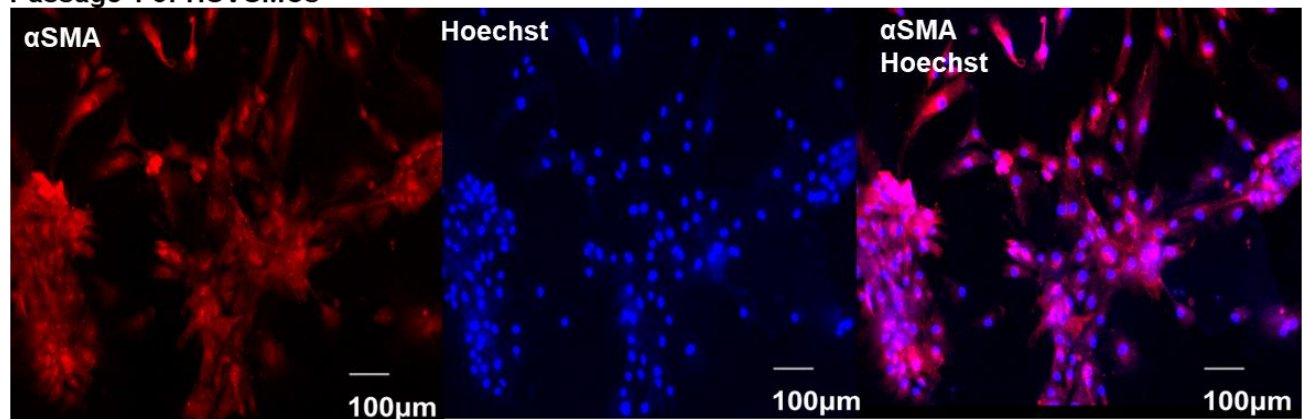
SMMHC (Figure 3.2-Top and middle panels) antibodies which are characteristic of SMCs. Also, as shown in Figure 3.3-Top and middle panels, the isolated SMCs (passages 1 and 4) did not react with anti-PECAM-1, the marker for ECs, hence exclude EC contamination. Additionally, HUVEC was used as negative control and positive control for SMC and EC characterisation respectively. As revealed, HUVECs were negative to both anti- α -SMA and anti-SMMHC (Figures 3.1 and 2- Bottom panels), however, reacted positively with anti-PECAM-1 (Figure 3.3-Bottom panel).

Figure 3.1

Passage 1 of HSVSMCs



Passage 4 of HSVSMCs



HUVECs

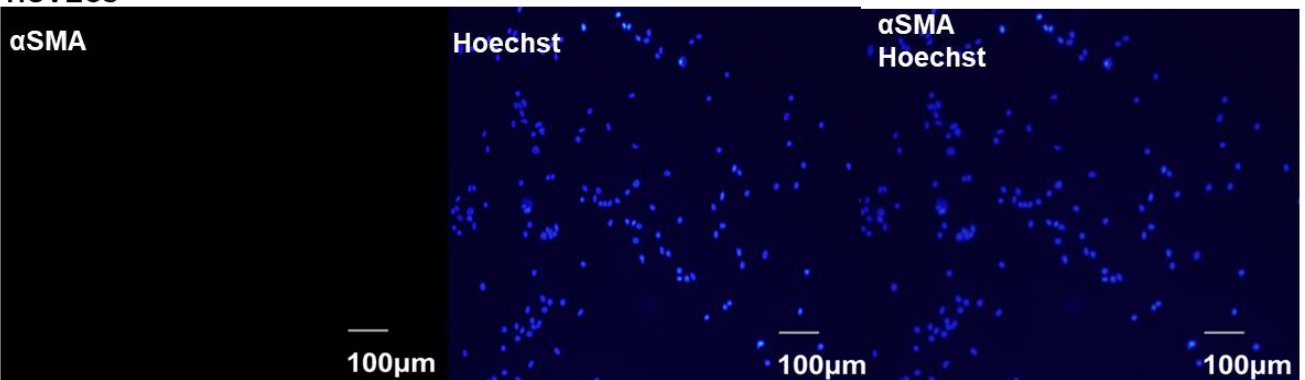


Figure 3.1: Verification of the identity of HSVSMCs from non-diabetic patients by immunofluorescence microscopy using anti- α SMA. Images reveal expression of SMC-specific marker α -SMA (red) and nuclei Hoechst stain (blue). Scale bar 100 μ m, magnification x 200, n=3.

Top panel: Passage 1 of HSVSMCs

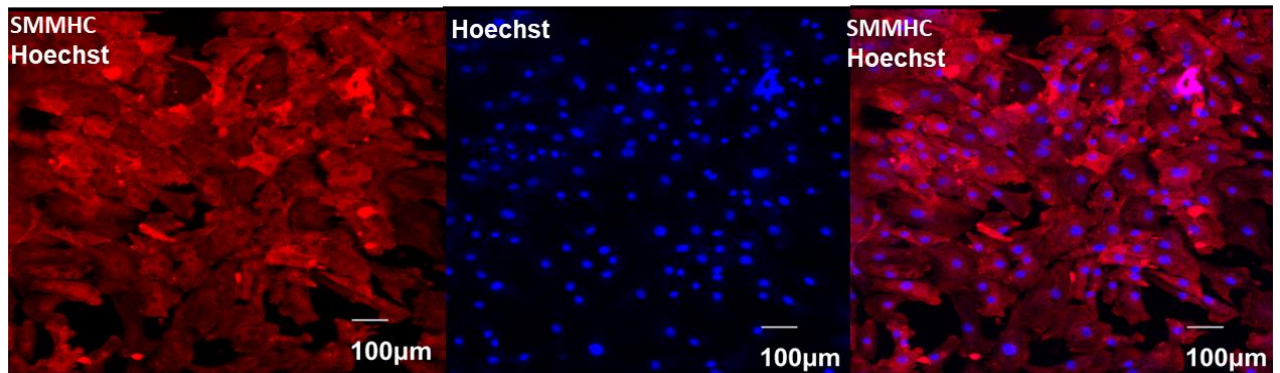
Middle Panel: Passage 4 HSVSMCs

Bottom panel: HUVECs

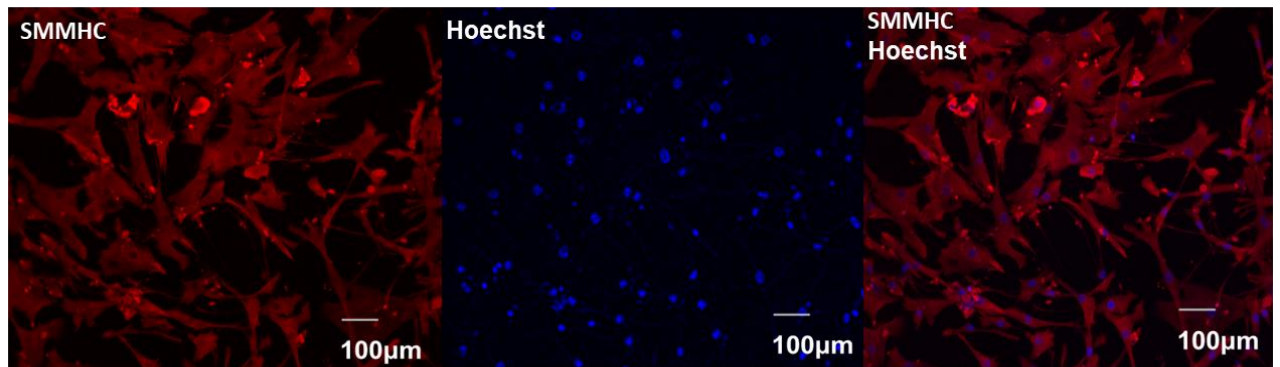
SMA: Smooth muscle actin; HSVSMC: Human saphenous vein smooth muscle cell; HUVEC: Human umbilical vascular endothelial cell.

Figure 3.2

Passage 1 of HSVSMC



Passage 4 of HSVSMC



HUVECs

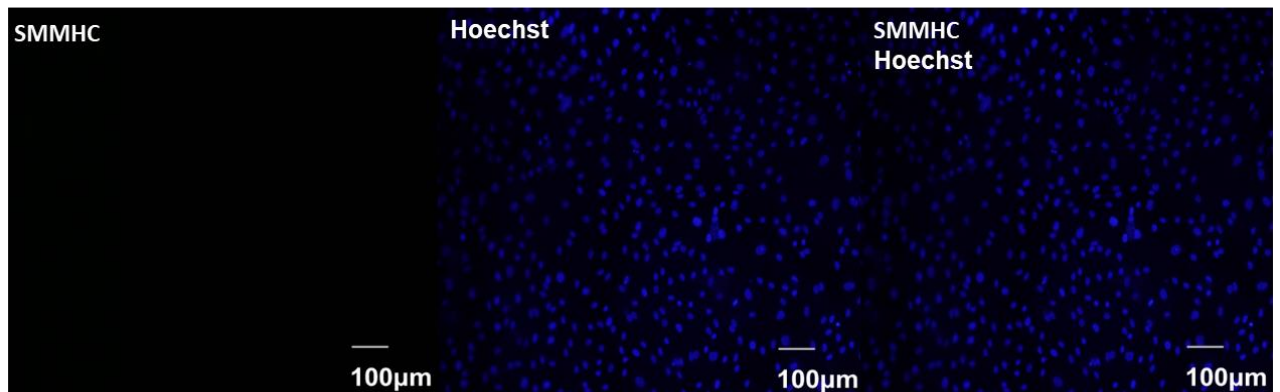


Figure 3.2: Verification of the identity of HSVSMCs from non-diabetic patients by immunofluorescence microscopy using anti-SMMHC. Images reveal expression of SMC-specific marker SMMHC (red) and nuclei Hoechst stain (blue). Scale bar 100µm, magnification x 200, n=3.

Top panel: Passage 1 of HSVSMCs

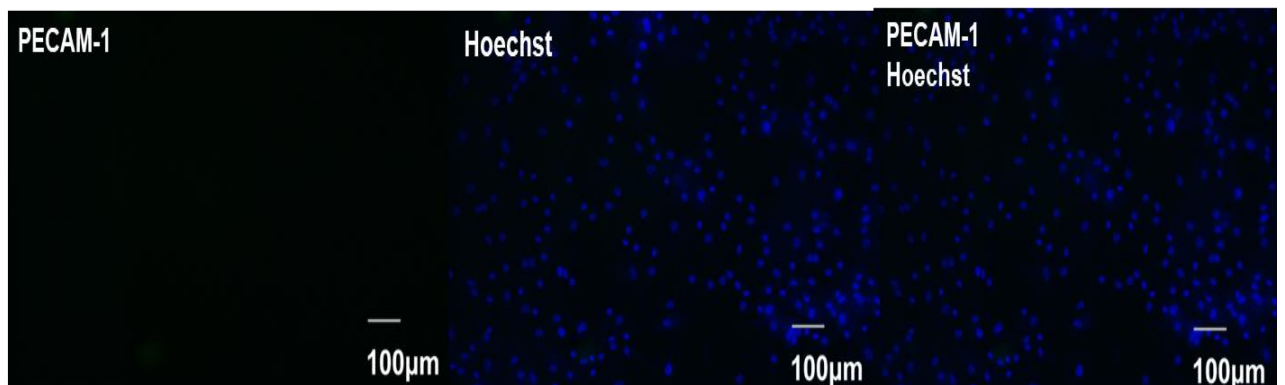
Middle Panel: Passage 4 HSVSMCs

Bottom panel: HUVECs

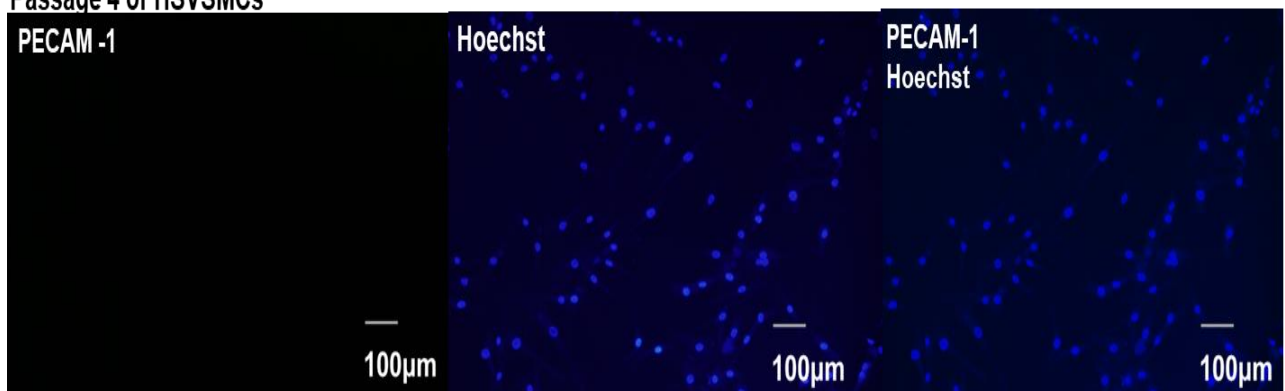
SMMHC: Non-muscle myosin II; HSVSMC: Human saphenous vein smooth muscle cell; HUVEC: Human umbilical vascular endothelial cell

Figure 3.3

Passage 1 of HSVSMCs



Passage 4 of HSVSMCs



HUVECs

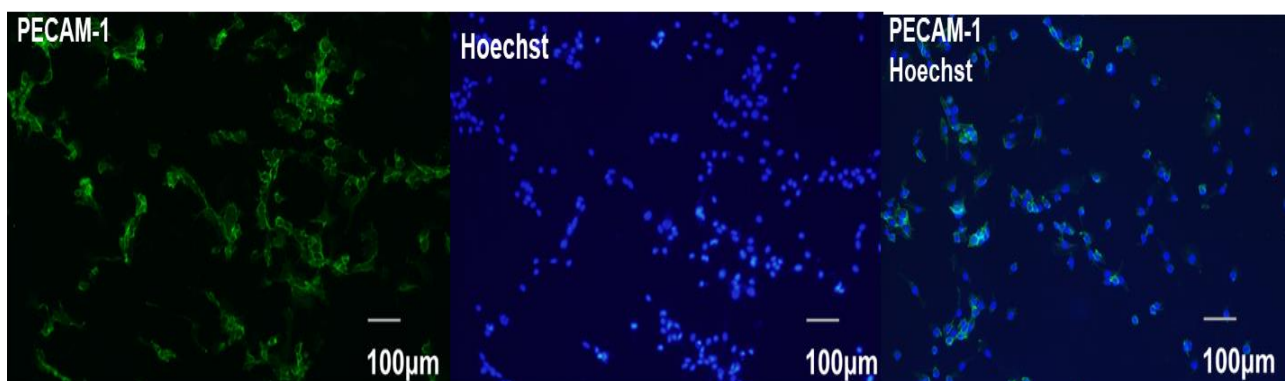


Figure 3.3: Excluding the presence of endothelial cell contamination in HSVSMCs from non-diabetic patients. Images reveal expression of EC-specific marker anti-PECAM (CD31) (green) and nuclei Hoechst stain (blue). Scale bar 100µm, magnification x 200, n=3.

Top panel: Passage 1 of HSVSMCs

Middle Panel: Passage 4 HSVSMCs

Bottom panel: HUVECs

PECAM: Platelet endothelial cell adhesion molecule; HSVSMC: Human saphenous vein smooth muscle cell; HUVEC: Human umbilical vascular endothelial cell

3.2.2 Expression of recombinant modulating enzymes of *O*-GlcNAcylation in HEK 293

Recombinant DNA technology has advanced research in recent years, including the characterisation and validation of proteins (Khan et al., 2016). In this project, constructs of the regulatory enzymes of *O*-GlcNAcylation were synthesised and purified as described in 2.2.5.1. The constructs were transfected in immortalized human embryonic kidney (HEK) 293 cells. HEK 293 cell was used because they are widely used as a target cell type for transfections due to their ability to efficiently express recombinant proteins from transfected mammalian expression constructs (Ooi et al., 2016; Devenish et al., 2019). Also, GFP, a protein that emits bright green fluoresces when exposed to light, was used as a label to track efficiency of transfection (Zimmer, 2002; Prendergast and Mann, 1978). HEK 293 cells were transfected with a total of 2 µg OGA and OGT +/- GFP cDNA constructs. Cells were lysed after 48 hrs and protein contents of cell lysates were determined by BCA assay. Lysates from non-transfected and GFP-labelled HEK 293 cells were used as reference. Following this, protein contents were equalised and resolved by SDS-PAGE for immunoblotting with antibody versus OGA, (Cat No: ab105217; 1:5000) and OGT, (Cat No: O6264; 1:1000) to determine expression of OGA and OGT in transfected cells. Protein expressions were normalised to total STAT3 (Cat No: ab68153; 1:500). Detailed protocol is described in 2.2.3 and 2.2.5.

Lysates from the transfected HEK 293 cells were utilised as positive controls in every instance when probing for the expression of endogenous OGA and OGT proteins in HSVSMCs. Immunoblotting revealed increased expressions of OGA and OGT in OGA and OGT-transfected HEK293 cells compared with non-transfected cells or of those transfected with reduced concentration of the cDNA (Figure 3.4).

Figure 3.4

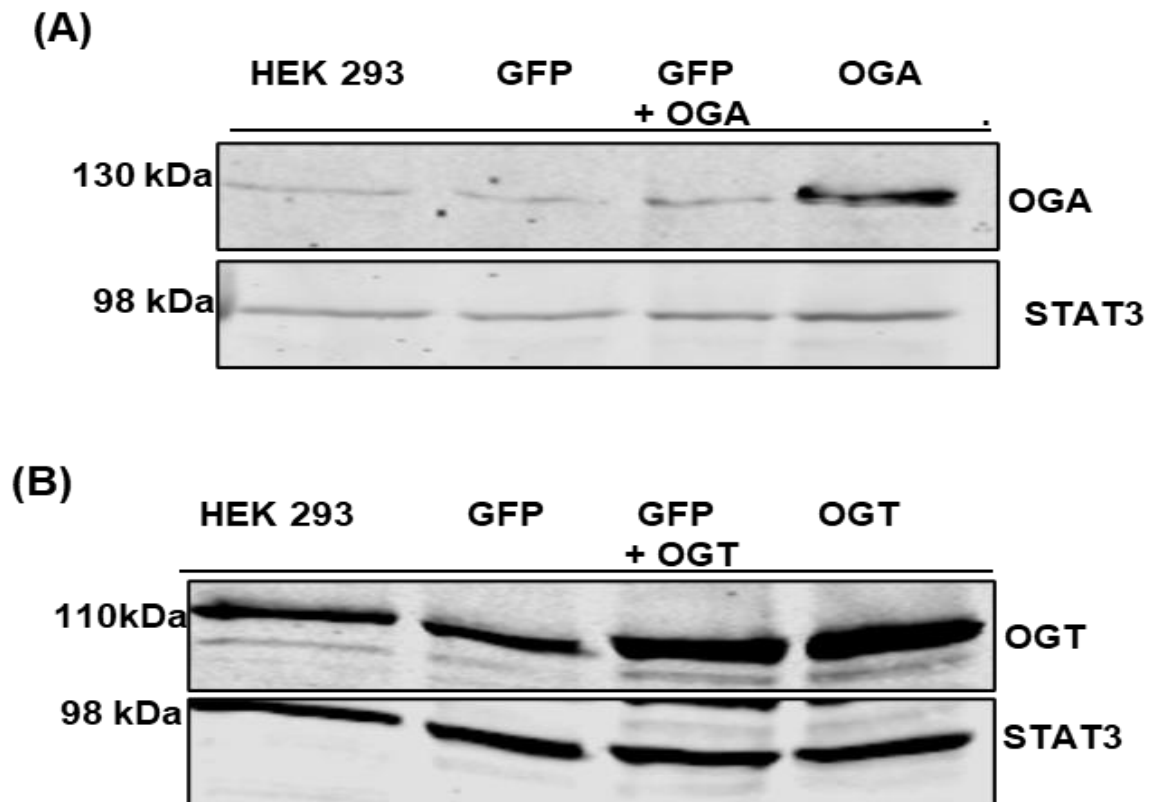


Figure 3.4: Expression of recombinant modulating enzymes of O-GlcNAcylation in HEK 293 cells.

(A) Upper panel: representative western blot for OGA (130kDa) in transfected HEK293. Lower panel: STAT3 expression (98kDa).

(B) Upper panel: representative western blot for OGT (110kDa) in transfected HEK293. Lower panel: STAT3 expression (98kDa).

Protein expressions were normalised to total STAT3

OGA: *O*-GlcNAcase; OGT: *O*-GlcNAc transferase; GFP: Green florescent protein; HEK: Human embryonic kidney cells; STAT3: Signal transducer and activator of transcription 3

3.2.3. Effect of passage on the expression of the regulating enzymes of *O*-GlcNAcylation in HSVSMC

Successive passaging of primary cells can significantly alter gene expression profiles (Mouriaux et al. 2016, Neumann et al. 2010). Since this is thought to vary with cell types, it is unclear exactly when the molecular features that are identical to the primary cells begin to significantly change as the number of passages grows. Studies have shown that early passages have a better likelihood of preserving these molecular characteristics in human SMCs (Frid et al., 1992; Gimona et al., 1990). Hence, in this project, only early passages (1-4) of the HSVSMCs were utilised in all experiments. To further assess if the passage numbers (1-4) utilised in this project alter the expression of these enzymes (OGA, OGT, and GFAT) of interest, SDS-PAGE and immunoblotting as described in 2.2.3 was used to determine their expressions across passages 1-4 of HSVSMCs from same sample in the non-diabetic cohort. A repeat of this experiment was done for four biological replicates using samples from different patients.

Briefly, protein contents of cell lysates from passages 1-4 of HSVSMCs from non-diabetic patients were determined by BCA assay. Following this, protein contents were equalised and resolved by SDS-PAGE for immunoblotting with antibody versus OGA (Cat No: ab105217; 1:5000), OGT (Cat No: O6264; 1:1000), and GFAT (Cat No: Sc-377479; 1:500) to determine expressions of OGA, OGT, and GFAT across passages 1-4 of HSVSMCs. OGA and OGT expression levels were normalised to total STAT3 (Cat No: ab68153; 1:500), and GFAT was normalised to GAPDH (Cat No: ab8245; 1:15000). Detailed protocol is described in 2.2.3.

Following immunoblotting and as shown in figures 3.5, 3.6, and 3.7, for OGA, OGT, and GFAT respectively, the expressions of these enzymes of interest were not significantly altered (n= 4 biological replicates using P1 as reference for P2-4 for comparison) across passages 1-4.

Figure 3.5

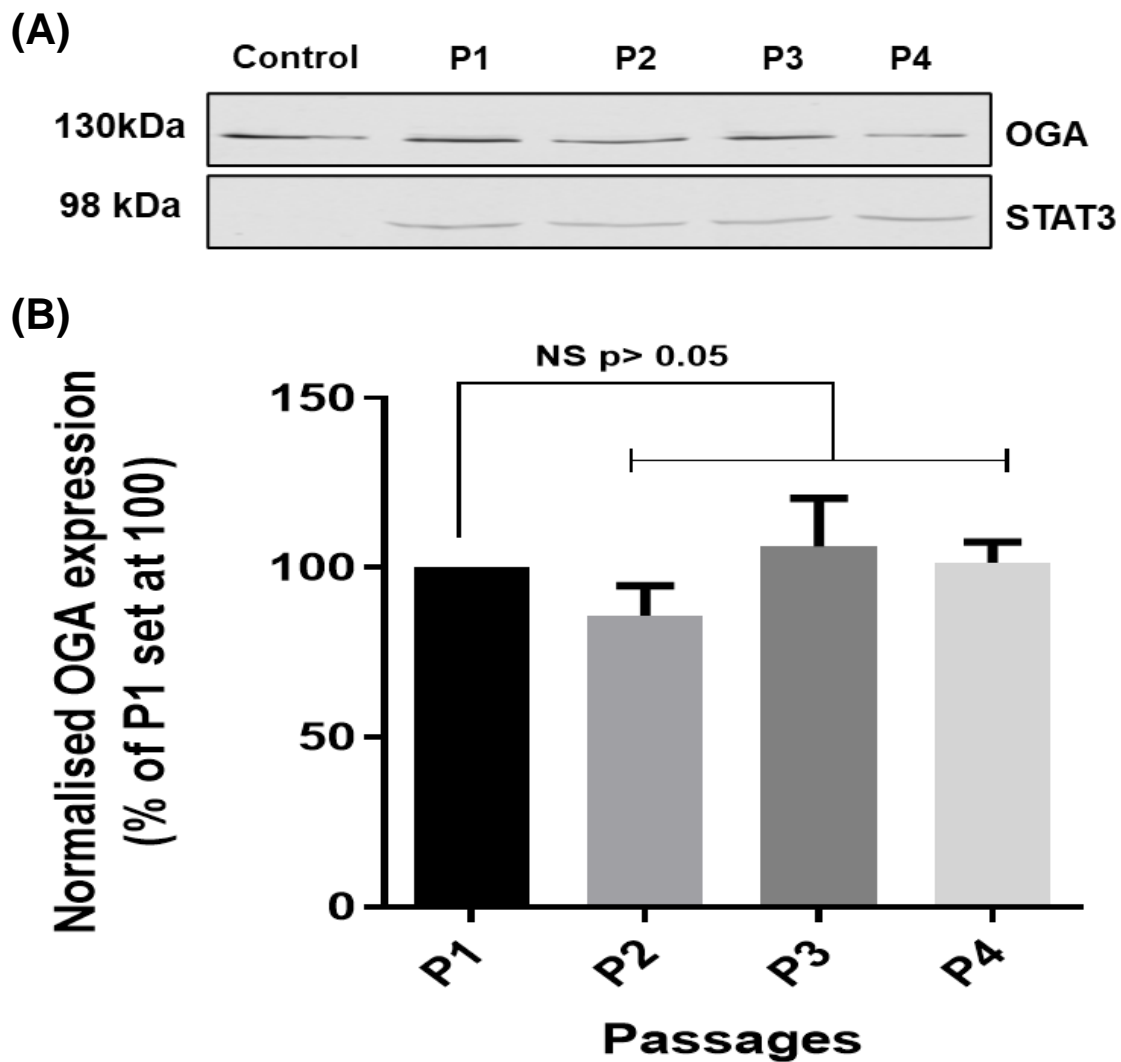


Figure 3.5: Expression of OGA across passages (1-4) of HSVSMC samples from non-diabetic patients using OGA-transfected HEK 293 cells as positive control.

(A) Upper panel: representative western blot for OGA (130kDa) in HEK293 cells (positive control) and in serially passaged HSVSMC (p1-p4) from non-diabetic patients.

Lower panel: STAT3 expression (98kDa).

(B) Densitometric analysis of OGA, normalised to STAT3 and expressed as a percentage of HSVSMC P1 (100%). Normalised data are expressed as mean \pm SEM from n=4 biological replicates using samples from different patients. Data from P2-4 were compared to P1 for statistical difference at $p < 0.05$; NS: not significant.

OGA: *O*-GlcNAcase; STAT3: Signal transducer and activator of transcription 3; P1-4: Passage 1-4; NS: Not significant

Figure 3.6

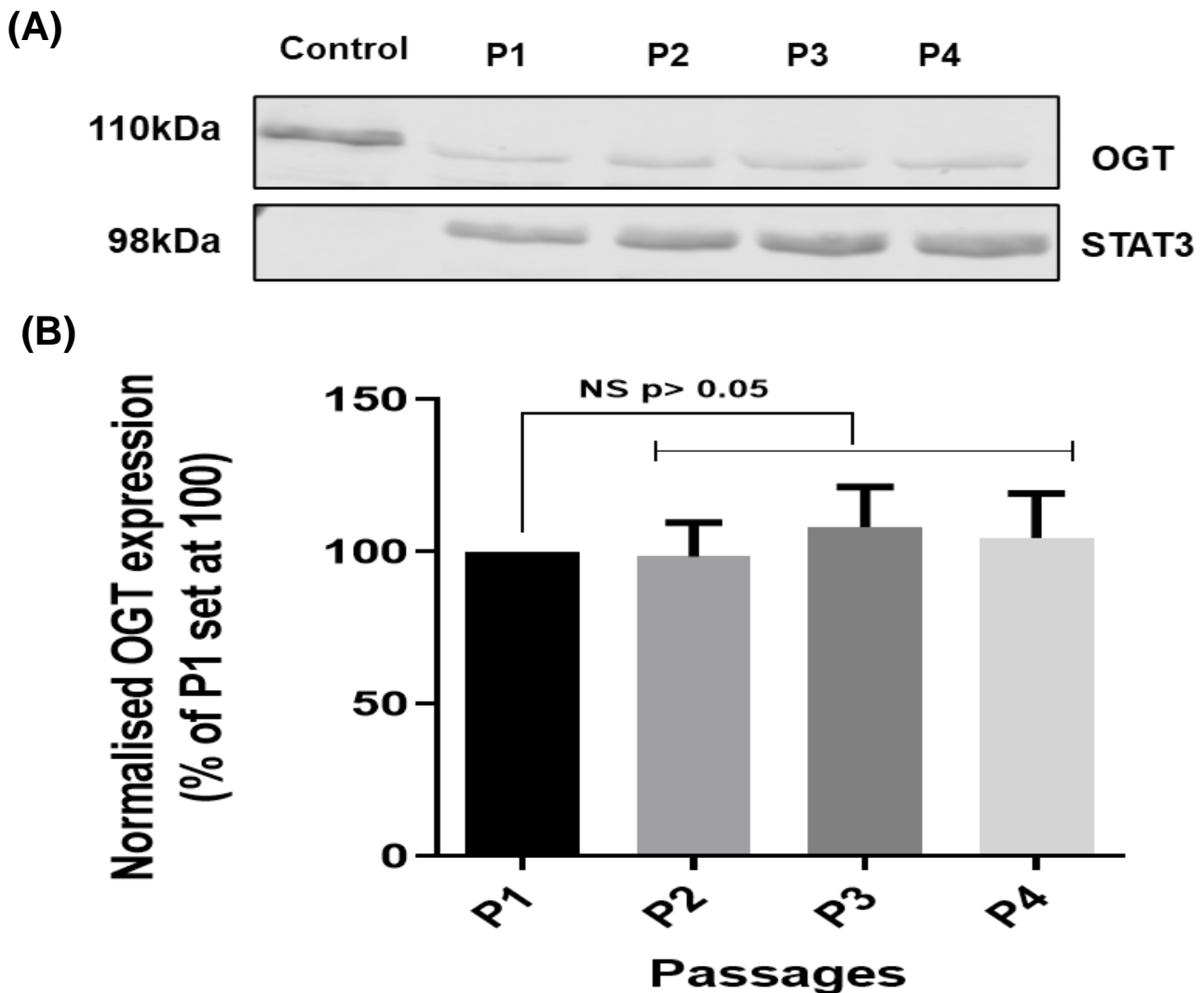


Figure 3.6: Expression of OGT across passages (1-4) of HSVSMC samples from non-diabetic patients using OGT-transfected HEK 293 cells as positive control.

(A) Upper panel: representative western blot for OGT (110kDa) in HEK293 cells (positive control) and in serially passaged HSVSMC (p1-p4) from non-diabetic patients.

Lower panel: STAT3 expression (98kDa).

(B) Densitometric analysis of OGA, normalised to STAT3 and expressed as a percentage of HSVSMC P1 (100%). Normalised data are expressed as mean \pm SEM from n=4 biological replicates using samples from different patients. Data from P2-4 were compared to P1 for statistical difference at $p < 0.05$; NS: not significant.

OGT: *O*-GlcNAc transferase; STAT3: Signal transducer and activator of transcription 3;

P1-4: Passage 1-4

Figure 3.7

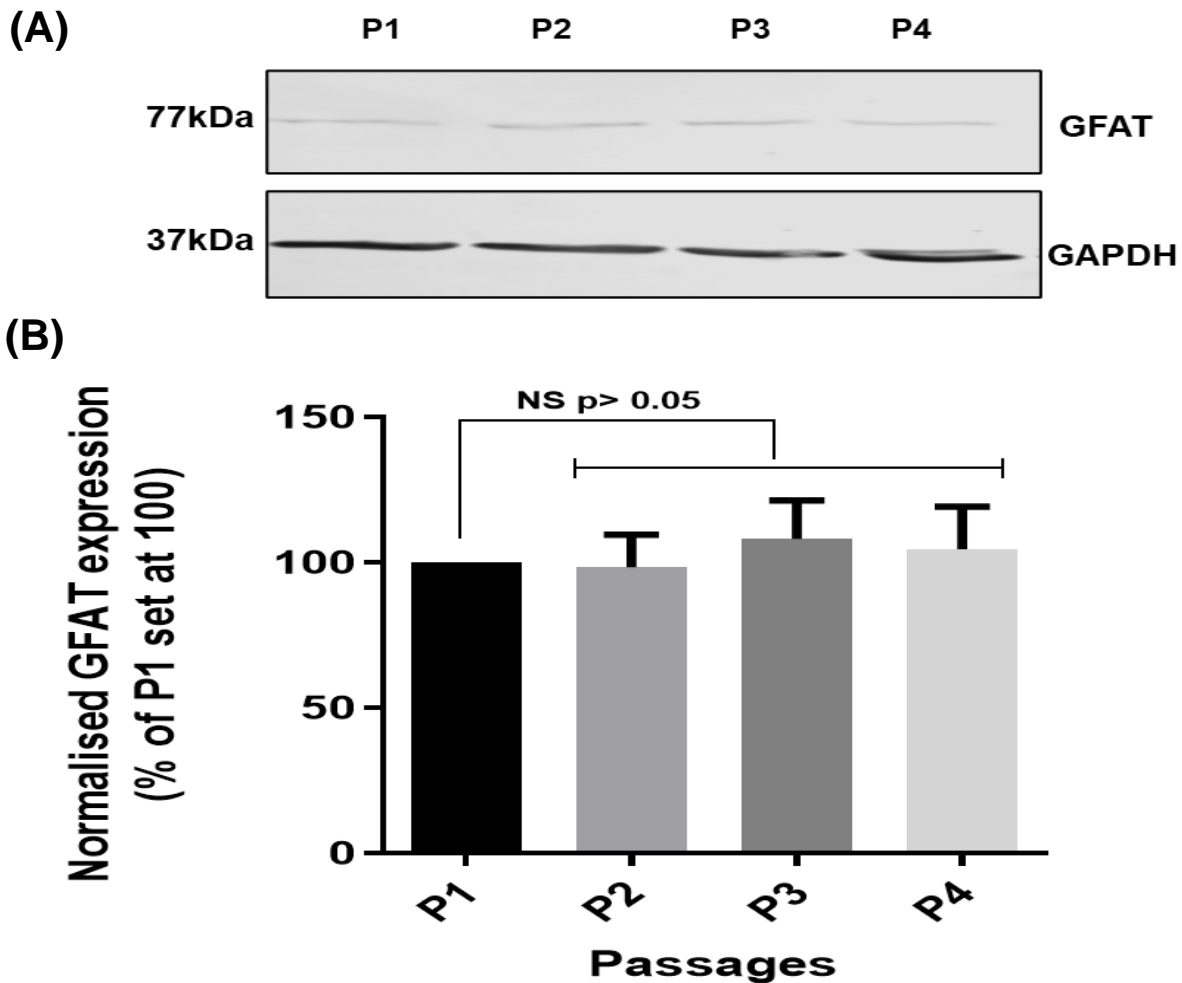


Figure 3.7: Expression of GFAT across passages (1-4) of HSVSMC samples from non-diabetic patients.

(A) Upper panel: representative western blot for GFAT (77kDa) in serially passaged HSVSMC (p1-p4) from non-diabetic patients.

Lower panel: GAPDH expression (37kDa).

(B) Densitometric analysis of GFAT, normalised to GAPDH and expressed as a percentage of HSVSMC P1 (100%). Normalised data are expressed as mean \pm SEM from n=4 biological replicates using samples from different patients. Data from P2-4 were compared to P1 for statistical difference at $p < 0.05$; NS: not significant.

GFAT: Glutamine fructose-6-phosphate amidotransferase; GAPDH: Glyceraldehyde 3-phosphate dehydrogenase; P1-4: Passage 1-4.

3.2.4 Comparison of OGA, OGT, and GFAT expression levels in HSVSMCs from T2DM versus control patients.

Our understanding of the *O*-GlcNAcylation regulating enzymes has considerably improved in recent years, in part because of advances in research tools that have aided in better characterisation (Bolanle et al., 2021). The necessity to create pharmacological tools to control the regulating enzymes of *O*-GlcNAcylation has become increasingly significant and valuable as the involvement of *O*-GlcNAcylation in disease pathologies, most notably in DM and CVDs has continued to emerge (Bolanle et al., 2021). To appreciate this significance, it is therefore important to determine if T2DM alters expression of these regulating enzymes as this can be a viable target for drug development. To achieve this, I compared the expression of these modulating enzymes of *O*-GlcNAcylation (OGA, OGT, and GFAT) in HSVSMCs from T2DM and non-diabetic patients.

Protein contents of cell lysates from passage 1 of HSVSMCs from both T2DM and non-diabetic patients were determined by BCA assay. Following this, protein contents were equalised and resolved by SDS-PAGE for immunoblotting with antibody versus OGA (Cat No: ab105217; 1:5000), OGT (Cat No: O6264; 1:1000), and GFAT (Cat No: Sc-377479; 1:500) to compare expressions of OGA, OGT, and GFAT in HSVSMCs from T2DM and non-diabetic patients. OGA and OGT expression levels were normalised to total STAT3 (Cat No: ab68153; 1:500), and GFAT was normalised to GAPDH (Cat No: ab8245; 1:15000). Detailed protocol is described in 2.2.3.

Results from these experiments as shown in figures 3.8, 3.9, and 3.10 suggest that T2DM did not significantly alter (n=6 biological replicates comparing values from T2DM and non-diabetic) the expressions of OGA, OGT, and GFAT respectively in HSVSMCs.

Figure 3.8

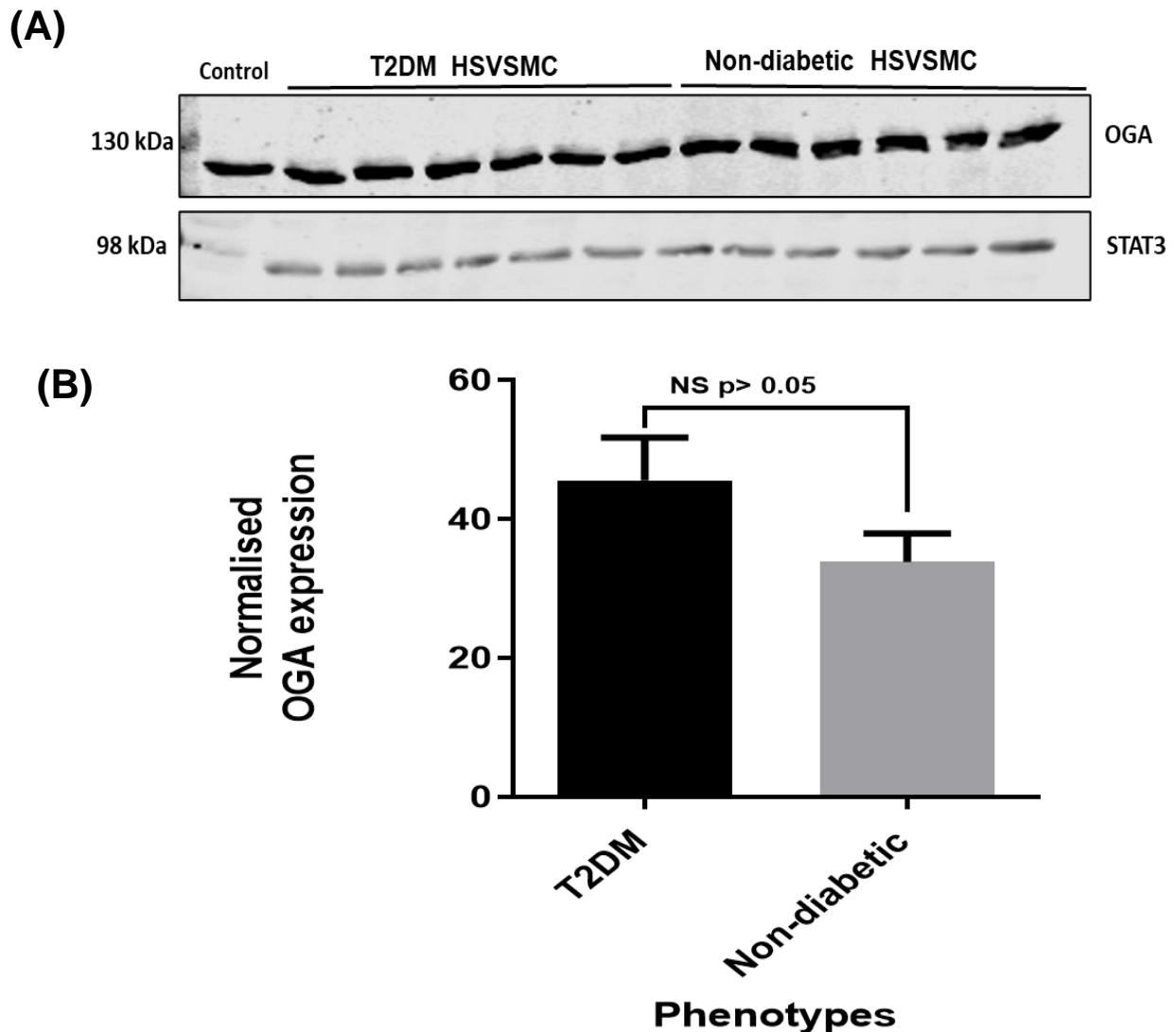


Figure 3.8: Comparison of OGA expression in HSVSMCs from T2DM and non-diabetic patients using OGA-transfected HEK 293 cells as positive control.

(A) Upper panel: representative western blot for OGA (130kDa) in HEK293 cells (positive control) and in HSVSMCs from T2DM and non-diabetic patients.

Lower panel: STAT3 expression (98kDa).

(B) Densitometric analysis of OGA normalised to STAT3. Normalised data are expressed as mean \pm SEM from $n=6$ biological replicates using samples from different patients. Data from T2DM and non-diabetic were compared for statistical difference at $p<0.05$; NS: not significant.

OGA: *O*-GlcNAcase; STAT3: Signal transducer and activator of transcription 3; T2DM: Type 2 diabetes mellitus

Figure 3.9

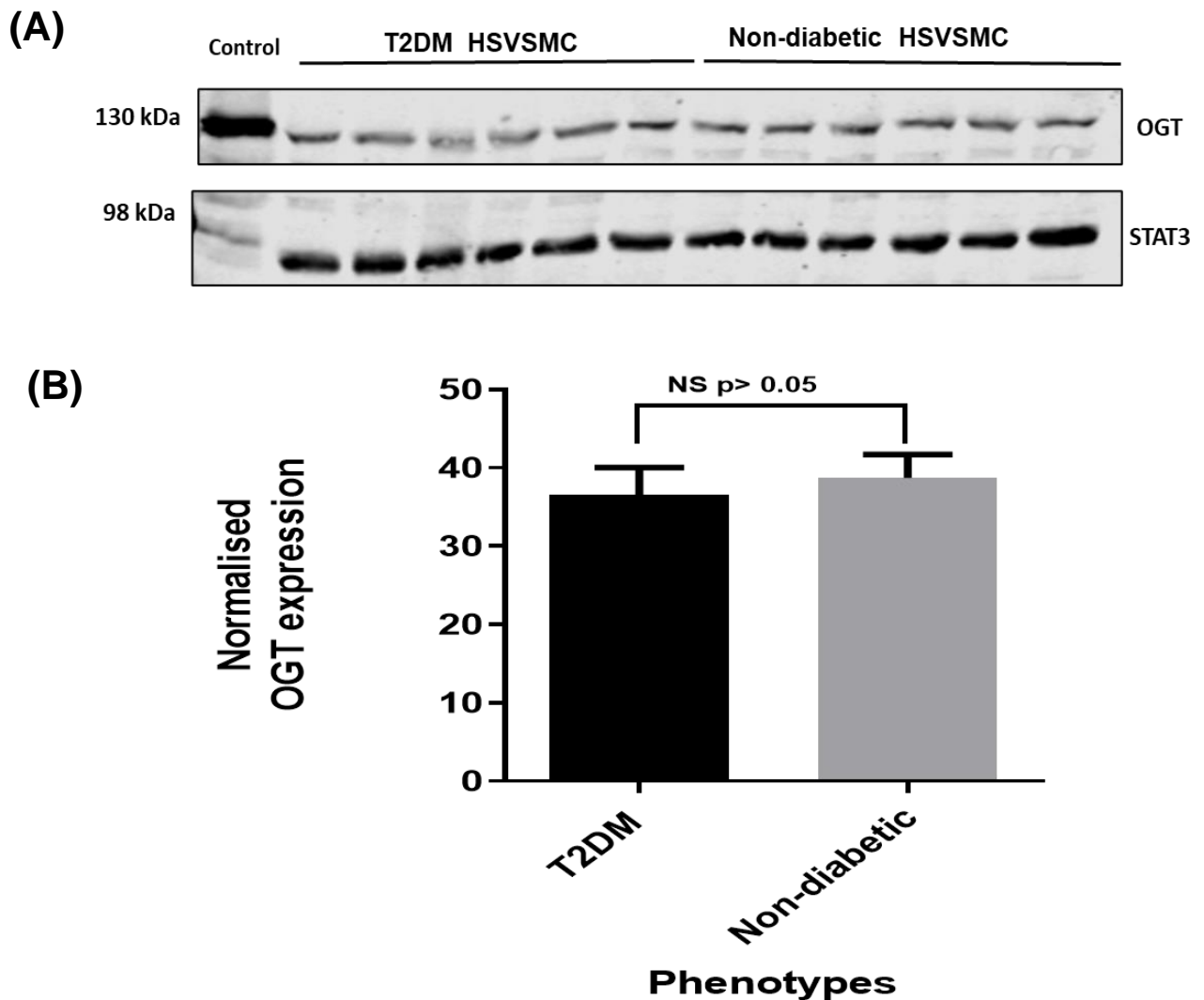


Figure 3.9: Comparison of OGT expression in HSVSMCs from T2DM and non-diabetic patients using OGT-transfected HEK 293 cells as positive control.

(A) Upper panel: representative western blot for OGT (110kDa) in HEK293 cells (positive control) and in HSVSMCs from T2DM and non-diabetic patients.

Lower panel: STAT3 expression (98kDa).

(B) Densitometric analysis of OGT normalised to STAT3. Normalised data are expressed as mean \pm SEM from n=6 biological replicates using samples from different patients. Data from T2DM and non-diabetic were compared for statistical difference at $p < 0.05$; NS: not significant.

OGT: *O*-GlcNAc transferase; STAT3: Signal transducer and activator of transcription 3; T2DM: Type 2 diabetes mellitus

Figure 3.10

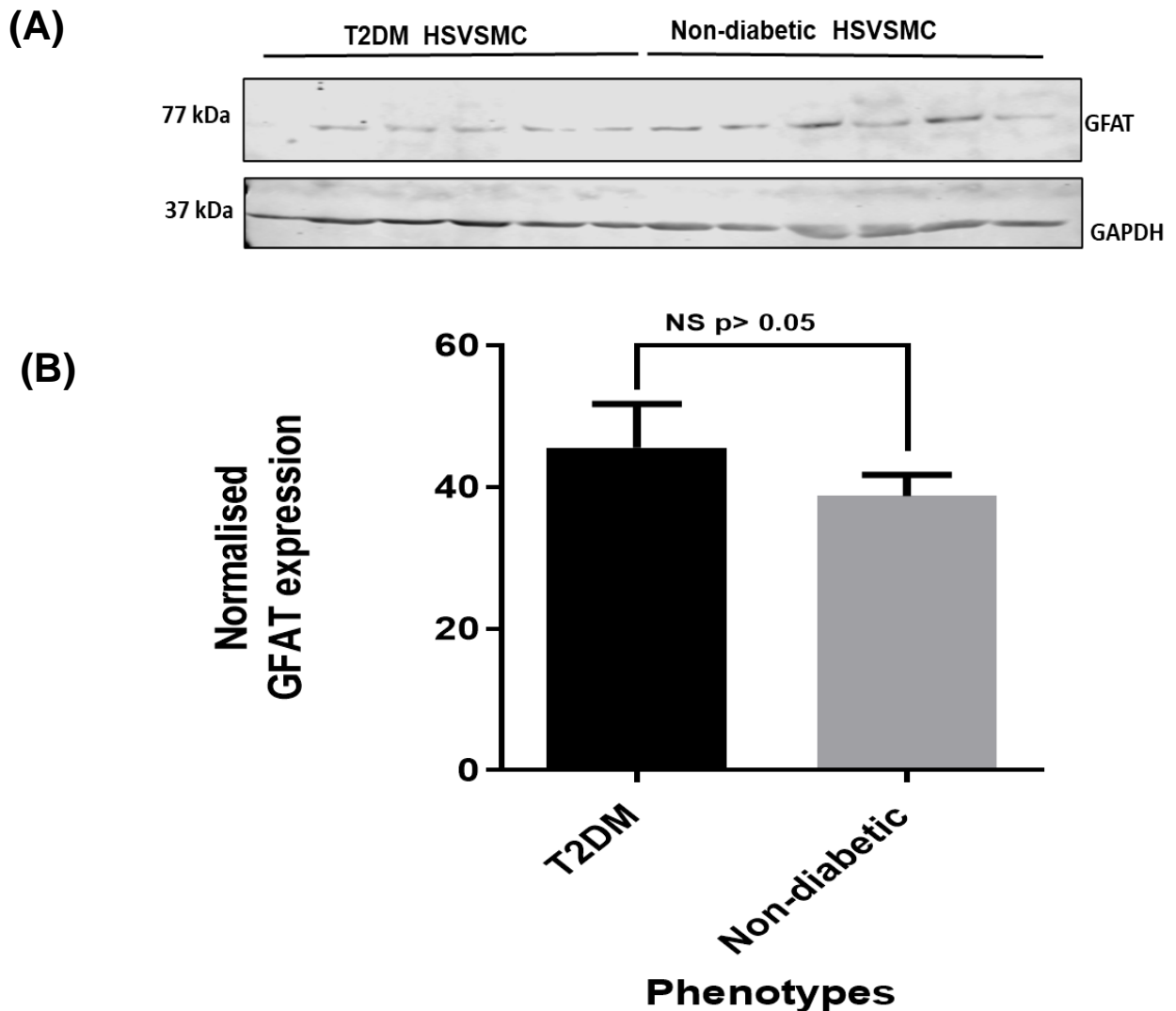


Figure 3.10: Comparison of GFAT expression in HSVSMCs from T2DM and non-diabetic patients.

(A) Upper panel: representative western blot for GFAT (77kDa) in HSVSMCs from T2DM and non-diabetic patients.

Lower panel: GAPDH expression (37kDa).

(B) Densitometric analysis of GFAT normalised to GAPDH. Normalised data are expressed as mean \pm SEM from n=6 biological replicates using samples from different patients. Data from T2DM and non-diabetic were compared for statistical difference at $p < 0.05$; NS: not significant.

GFAT: Glutamine fructose-6-phosphate amidotransferase; GAPDH: Glyceraldehyde 3-phosphate dehydrogenase; T2DM: Type 2 diabetes mellitus

3.2.5 Effect of glucose concentrations on OGT, OGA, and GFAT expression level in HSVSMCs

The connection between hyperglycaemia and *O*-GlcNAcylation is an established phenomenon (Bolanle et al., 2021, Vasconcelos-Dos-Santos et al., 2018, Bond and Hanover, 2015), as elevated glucose levels have been demonstrated to upregulate *O*-GlcNAcylation (Masaki et al., 2020, Vasconcelos-Dos-Santos et al., 2018, Bond and Hanover, 2015). Also, studies have shown that treatment of vascular cells including ECs and SMCs in vitro with high glucose concentration up to 30 mM for 48 hrs significantly elevates *O*-GlcNAcylation and miR-143/5 expression (Masaki et al., 2020; Riches et al., 2014). As at now, our understanding of the molecular mechanism(s) by which hyperglycaemia upregulates *O*-GlcNAcylation is still expanding, and it is not known if a high glucose alters the expression of these enzymes (OGA, OGT, and GFAT) that regulate cellular *O*-GlcNAcylation. Therefore, to assess this, expressions of these enzymes were determined after treating HSVSMCs with normal (5 mM) and high (10 mM, and 25 mM) glucose concentrations for 48 hours as described by (Masaki et al., 2020; Riches et al., 2014).

HSVSMCs from non-diabetic patients were cultured till they were 70-80% confluent and were treated with SMC growth medium with normal (5 mM) glucose concentration and high (10 mM and 25 mM) glucose concentrations 48 hrs before harvest. Then, cells were lysed, and protein contents of cell lysates were determined by BCA assay. Following this, protein contents were equalised and resolved by SDS-PAGE for immunoblotting with antibody versus OGA (Cat No: ab105217; 1:5000), OGT (Cat No: O6264; 1:1000), and GFAT (Cat No: Sc-377479; 1:500) to determine the effect of normal (5 mM) glucose concentration and high (10 mM and 25 mM) glucose concentrations expression levels of OGA, OGT, and GFAT in HSVSMCs from non-diabetic patients. OGA and OGT expression levels were normalised to total STAT3 (Cat No: ab68153; 1:500), and GFAT was normalised to GAPDH (Cat No: ab8245; 1:15000). Detailed protocol is described in 2.2.3.

From my findings as shown in figures 3.11, 3.12, and 3.13, expressions of OGA, OGT, and GFAT respectively in HSVSMCs were unaltered by high (10 mM and 25 mM) glucose concentrations (versus normal glucose treated cells, n=4 biological replicates).

Figure 3.11

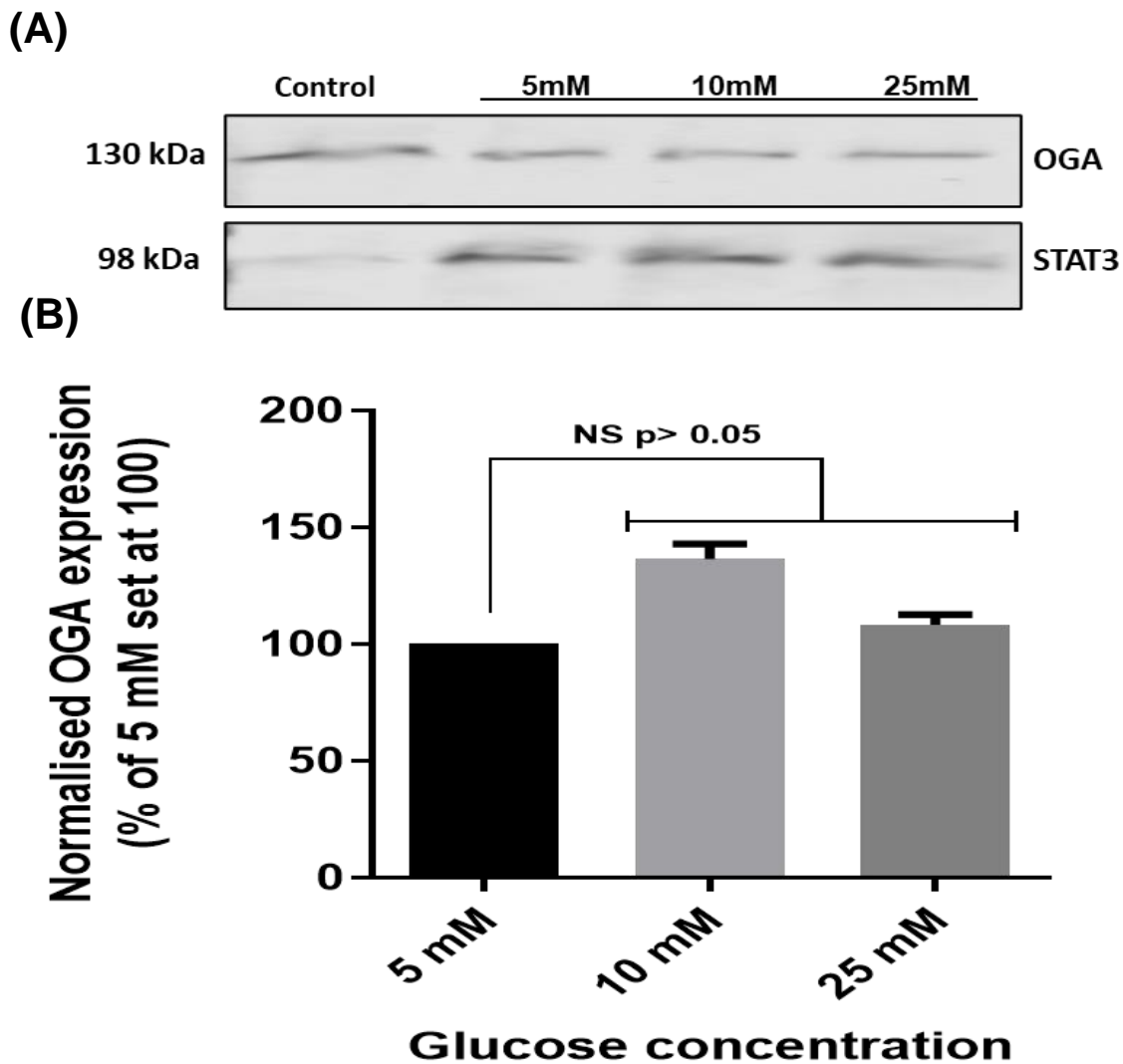


Figure 3.11: Expression of OGA by HSVSMCs from non-diabetic patients treated with normal (5 mM) and high (10 mM and 25 mM) glucose concentrations using OGA-transfected HEK 293 cells as positive control.

(A) Upper panel: representative western blot for OGA (130kDa) in HEK293 cells (positive control) and in HSVSMCs from non-diabetic patients.

Lower panel: STAT3 expression (98kDa).

(B) Densitometric analysis of OGA normalised to STAT3. Normalised data are expressed as mean \pm SEM from n=4 biological replicates using samples from different patients. Data from cells treated with high (10 mM and 25 mM) glucose concentrations were compared to cells treated with normal (5 mM) glucose concentration for statistical difference at $p < 0.05$; NS: not significant.

Figure 3.12

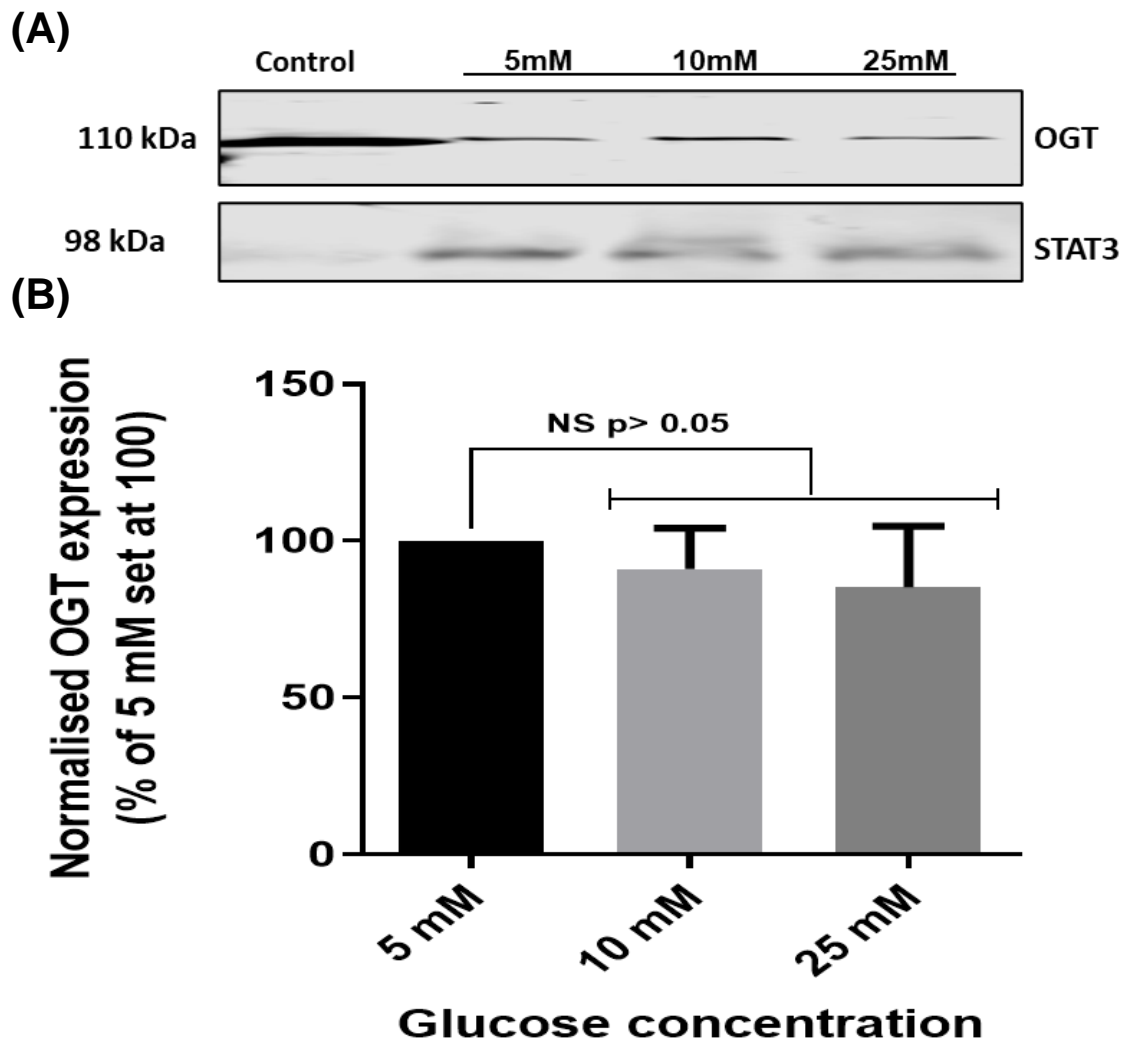


Figure 3.12: Expression of OGT by HSVSMCs from non-diabetic patients treated with normal (5 mM) and high (10 mM and 25 mM) glucose concentrations using OGT-transfected HEK 293 cells as control.

(A) Upper panel: representative western blot for OGT (110kDa) in HEK293 cells (positive control) and in HSVSMCs from non-diabetic patients.

Lower panel: STAT3 expression (98kDa).

(B) Densitometric analysis of OGT normalised to STAT3. Normalised data are expressed as mean \pm SEM from n=4 biological replicates using samples from different patients. Data from cells treated with high (10 mM and 25 mM) glucose concentrations were compared to cells treated with normal (5 mM) glucose concentration for statistical difference at $p < 0.05$; NS: not significant.

OGT: *O*-GlcNAc transferase; STAT3: Signal transducer and activator of transcription.

Figure 3.13

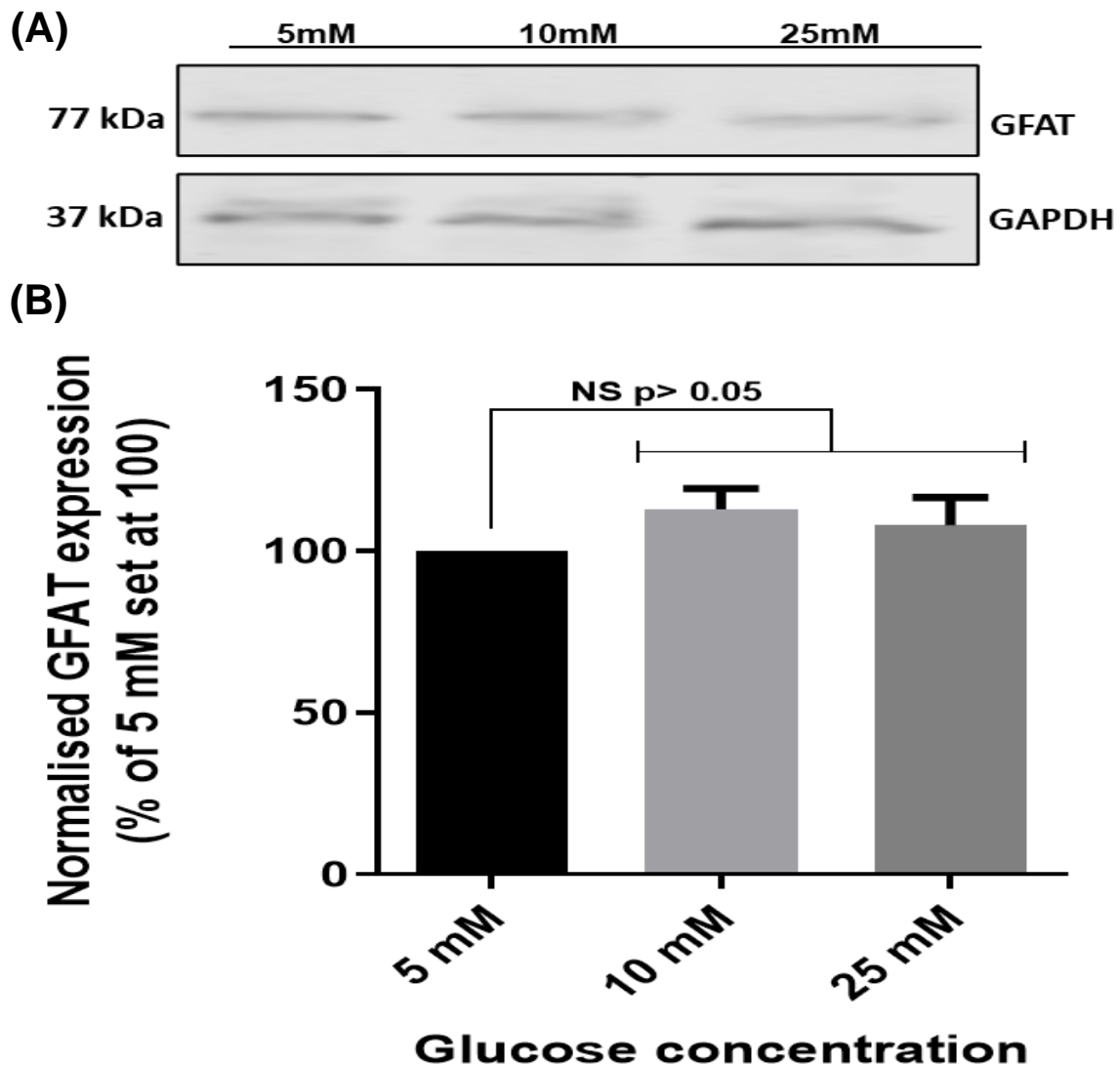


Figure 3.13: Expression of GFAT by HSVSMCs from non-diabetic patients treated with normal (5 mM) and high (10 mM and 25 mM) glucose concentrations.

(A) Upper panel: representative western blot for GFAT (77kDa) in HSVSMCs from non-diabetic patients.

Lower panel: GAPDH expression (37kDa).

(B) Densitometric analysis of GFAT normalised to GAPDH. Normalised data are expressed as mean \pm SEM from n=4 biological replicates using samples from different patients. Data from cells treated with high (10 mM and 25 mM) glucose concentrations were compared to cells treated with normal (5 mM) glucose concentration for statistical difference at $p < 0.05$; NS: not significant.

GFAT: Glutamine fructose-6-phosphate amidotransferase; GAPDH: Glyceraldehyde 3-phosphate dehydrogenase.

3.2.6 Validation of synthesised *O*-GlcNAc trap for affinity capture of *O*-GlcNAcylated proteins in HSVSMCs

A major challenge in identifying *O*-GlcNAcylated proteins is the fact that *O*-GlcNAc moiety is labile and lost during typical collision induced dissociation peptide backbone fragmentation during mass spectrometric analysis (Ma and Hart, 2014). Furthermore, *O*-GlcNAc is sub-stoichiometric, therefore enriched concentration of modified proteins is necessary before they can be detected by mass spectrometry (Ma and Hart, 2014). Usefully, it has been demonstrated that the detection of *O*-GlcNAc proteins may be accomplished using an inactive mutant of this enzyme (CpOGAD298N), which nonetheless has affinity for *O*-GlcNAcylated peptides in the nM range (Mariappa et al., 2015). Recently, (Selvan et al., 2017) utilised CpOGAD298N as a tool for enriching *O*-GlcNAcylated proteins from *Drosophila* embryos. With the aid of mass spectrometry, (Selvan et al., 2017) identified the first *O*-GlcNAc proteome linked to embryonic development in this specie. Considering the successful application of this tool by (Selvan et al., 2017), binding (CpOGAD298N) and non-binding (CpOGAWT) mutants were synthesised as described in 2.2.4.1 for catalytic enrichment of *O*-GlcNAcylated proteins in HSVSMCs. While CpOGAD298N is the binding mutant that traps these *O*-GlcNAcylated proteins, on the other hand, CpOGAWT is the non-binding mutant which serves as control. Following their synthesis, their integrity was validated by Coomassie stain on a 13 % acrylamide gel and immunoblotting versus HaloTag antibody (Cat No: G9211, 1:1000).

Figure 3.14a shows the expression of intact CpOGAWT and CpOGAD298N (size-130 kDa) on a Coomassie stained 13% acrylamide gel. Also, figure 3.14b shows a positive immunoblotting reaction versus the HaloTag antibody (Cat No: G9211, 1:1000) which further suggest that the synthesised mutants are intact. Figure 3.14c is a schematic showing how the Magne HaloTag bead is used to pull down *O*-GlcNAcylated proteins from sample lysates. Briefly, CpOGAD298 binds *O*-GlcNAcylated proteins and once coupled with the beads attaches to the halo ligand domain of the Magne HaloTag bead, pulling the attached *O*-GlcNAcylated proteins. Then, from the beads, *O*-GlcNAcylated proteins can be eluted as fully described in 2.2.4.2. On the other hand, figure 3.15 shows expression of *O*-GlcNAcylated proteins in HSVSMC lysates before and after catalytic enrichment and small-scale protein pulldown (n=2) as described in 2.2.4.2. This was done to optimise *O*-GlcNAcylated protein recovery.

Figure 3.14

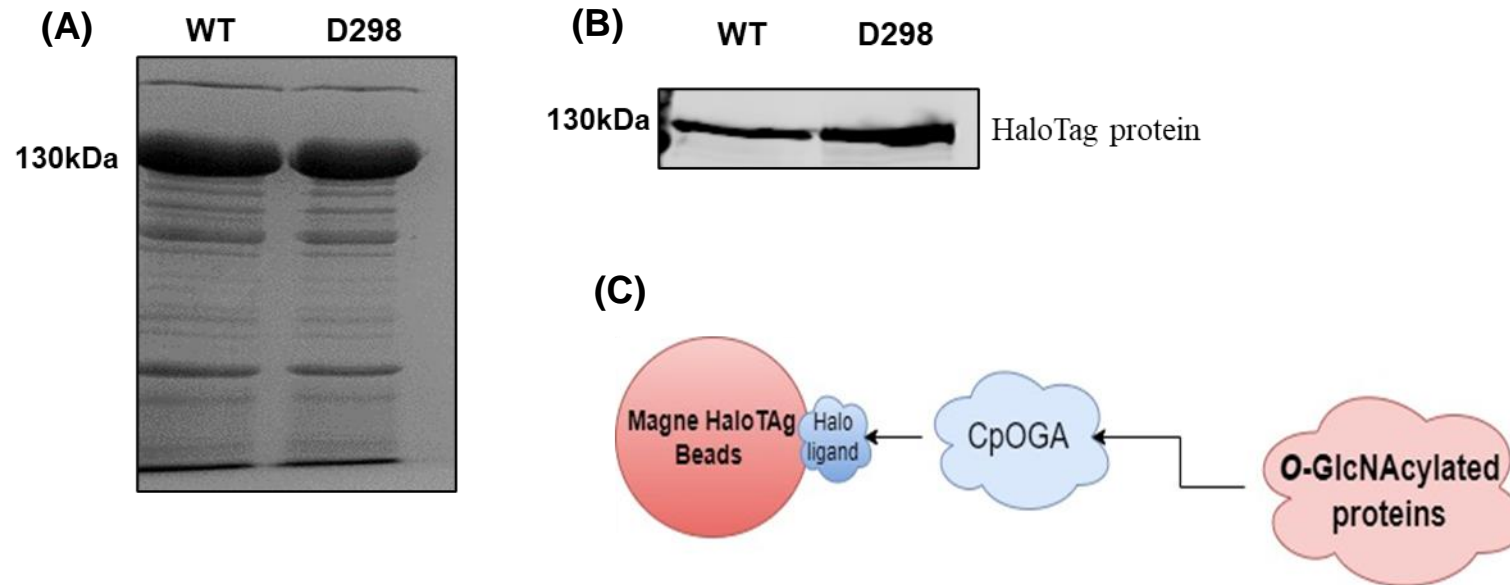


Figure 3.14: Validation of the integrity of synthesised *O*-GlcNAc trap.

(A) Resolved lysates from BL21 competent E. Coli expressing the *O*-GlcNAc affinity trap, CpOGAD298N (130kDa) and non-binding control CpOGAWT (130kDa) on a 13 % acrylamide gel stained with the Coomassie dye.

(B) Representative western blot for HaloTag reactive proteins (130kDa).

(C) A schematic showing how the Magne HaloTag bead is used to pull down *O*-GlcNAcylated proteins from sample lysates.

WT: CpOGAWT; D298: CpOGAD298N

3.3 Discussion

VSM is the main muscular and contractile component of blood vessels and regulator of numerous blood vessel functions in the circulatory system (Holt and Tulis., 2015). This is especially crucial because CVD, the leading non-communicable cause of death globally (WHO, 2016), has vascular origins in most cases. It is, therefore, highly desired to identify targets that might prevent CVDs. This, along with its importance in controlling vascular physiology, have made VSM a possible target for treating many aspects of CVD (Holt and Tulis., 2015), given that a large body of evidence points to the role of VSMCs in the pathogenesis of CV disorders such as NIH and venous graft stenosis (Wang et al. 2018). HSV wall thickening is caused by the VSMCs shifting from a differentiated to a dedifferentiated phenotype, which results in uncontrollable VSMC migration and proliferation that have now been implicated in VGF (de Vries et al. 2016). Additionally, emerging molecular mechanisms such protein *O*-GlcNAcylation have been demonstrated to promote VSMC differentiation, proliferation, and migration (Bolanle et al. 2021). Due to these factors, VSMCs have drawn a lot of attention as a possible target to reduce cardiac pathologies such as venous stenosis (Ortiz-Munoz et al. 2009; Xiang et al. 2013; Xiang et al. 2014; Wang et al. 2018).

Explant method as described in 2.2.2.1 was used to isolate VSMCs from HSV in this project. However, other cell types, such fibroblasts, and ECs, are present in the vascular wall and must be excluded. Hence, the ability to isolate uncontaminated VSMCs from HSV tissue using the explant approach is critical in this project (Cox et al. 1991). As shown in Figure 3.1-2, I have demonstrated that the isolated cells are SMCs because they co-expressed two distinct SMC markers, namely α -SMA and SMMHC. While α -SMA lacks specificity as a SMC marker, SMMHC was also employed as SMCs express it from early in development through to maturation (Miano et al. 1994). In order to rule out EC contamination in the isolated HSVSMCs, the adhesion protein PECAM-1, which is present in ECs from various origins, including venous ECs, was used as a marker (Figure 3.3). PECAM-1 is a known indicator of ECs, and its expression is primarily concentrated at junctions between adjacent cells (Woodfin et al., 2007). My results, therefore, demonstrate consistent isolation of a pure population of SMCs using an explant technique (Madi et al. 2009; Riches et al. 2014b).

When VSMCs are isolated and cultured, a phenomenon known as phenotypic modulation occurs that causes the cellular phenotype to change from being contractile to synthetic (Lin et al., 2004; Chamley-Campbell et al., 1981; Owens, 1995). This phenotypic modulation is

accompanied by accelerated cellular growth and changes in gene expression, which typically include decreased expression of contractile proteins like calponin, vimentin, and actin (Lin et al., 2004; Chamley-Campbell et al., 1981; Owens, 1995). More importantly, as passages increase, it has been suggested that these changes mimic injury-induced changes in blood vessels (Lin et al., 2004; Lincoln et al., 2001), as VSMCs in the media of uninjured blood vessels are more contractile and less proliferative than those in the neointima of injured blood vessels.

Also, cells evolve as they are continuously expanded over a large number of passages, which is a significant difficulty for tissue culture (Mouriaux et al., 2016). In addition, studies support the fact that early passages retain expression of key molecular features of the originate cell, however, cells show diminished or altered key functions, and frequently no longer serve as accurate replicas of their original source material after several passages in culture. This is probably because low-passage primary cultures nevertheless maintain a culture population made up of many cell subtypes that are genetically unique from one another (Mouriaux et al., 2016). Since continuous cell passaging have their limitations, hence it is preferred to work with short-term passages. Early passages (1-4) were used in this project to eliminate the inconsistency caused by a high passage number, and the results showed that there were no significant differences in the expression of the regulatory enzymes (OGA, OGT, and GFAT) of cellular *O*-GlcNAcylation (Figure 3.4). This suggests that employing early passage numbers could essentially guarantee that the features in these passages are identical to those in the primary cell.

Multiple studies have described the link between *O*-GlcNAcylation and T2DM (Bolanle et al., 2021; Yang and Qian, 2017; Lazarus et al., 2006, Liu et al., 2022; Masaki et al., 2020; Ma and Hart, 2013). However, the direct impact of T2DM on the regulatory enzymes of *O*-GlcNAcylation is pretty much obscure. A clear understanding of how T2DM alters the homeostasis of these enzymes could be vital in the development of therapeutic tools that can help modulate this dynamic post-translational modification and the HBP by extension. This is vital because limiting OGT results in downregulation of *O*-GlcNAcylation whose consequences are far ranging (Yang and Qian, 2017). While it might be predominantly beneficial in cardiac pathologies (Bolanle et al., 2021; Yang and Qian, 2017, Umapathi et al., 2021, Chatham et al., 2021), other studies suggest that downregulating *O*-GlcNAcylation could be detrimental in cardiac pathologies (Chatham et al., 2021, Jensen et al., 2019).

Additionally, increasing *O*-GlcNAcylation has been investigated as a potential treatment for neurological diseases (Wani et al., 2016), ranging from Alzheimer's (Park et al., 2020; Wani et al., 2016, Gong et al., 2006, Deng et al., 2009; Liu et al., 2009) to Parkinson's disease (Marotta et al., 2015, Alfaro et al., 2012). On the other hand, modulating OGA, the enzyme that reverses the *O*-GlcNAcylation is also critical as more progress has been made in the creation of therapeutic drugs that are used in clinics to raise *O*-GlcNAcylation levels (Bolanle et al., 2021). Furthermore, While the rationale for using GFAT inhibitors as prospective medicines for the treatment of CVDs is still being clarified, UDP-GlcNAc acts as a universal precursor for all amino sugars needed to create glycoproteins, glycolipids, and proteoglycans. So many important cellular processes would be hampered by GFAT suppression. OGT inhibitor development may therefore be a more practical choice (Bolanle et al., 2021).

Results from this project showed that neither T2DM nor high glucose concentration had any effect on the expressions of *O*-GlcNAcylation regulating enzymes (OGA, OGT, and GFAT) as there was no statistically significant difference in target protein expression level between HSVSMCs from T2DM patients and non-diabetic controls (Figures 3.6 and 3.7). Given that T2DM has been shown to upregulate *O*-GlcNAcylation (Bolanle et al., 2021; Yang and Qian, 2017; Lazarus et al., 2006, Liu et al., 2022; Masaki et al., 2020; Ma and Hart, 2013; Park et al., 2010), it is unclear as to why T2DM has not affected the expression of these enzymes. One reason can be because of specific technical limitations related to the experiment design of this study. For instance, a patient's medical history and whether they are presently receiving or have in the past received anti-diabetic medication was used to determine whether the patient is diabetic or not. Meanwhile, continuous diabetes process may exist even though a patient is not currently using an anti-diabetic medication or manifesting diabetes symptoms. Therefore, more accurate diagnostic methods like determination of glycated haemoglobin (HbA1C) and measurement of glucose intolerance level could have helped improve the classification method used (Maitra, 2012). But we were unable to use these more reliable techniques due to time constraints, the COVID-19 pandemic, and ethical considerations. Without a doubt, this is one of the study's limitations.

Also, there could be cell type-specific differences in how OGT, OGA, and GFAT are regulated. However, the finding of (Akimoto et al., 2007) suggests otherwise, as they showed that OGT protein levels are increased in the pancreatic islets of diabetic rats. Furthermore, (McClain et al., 2002) have shown that overexpression of OGT in the muscle and fat of transgenic male mice contributed to the development of insulin resistance and T2DM, however,

it is unknown if this connection can work in the reverse. Also, overexpression of OGT in liver, muscle, and fat tissues of diabetic mice causes insulin resistance (Yang et al., 2008). On the other hand, OGA is overexpressed in pancreatic β cells of transgenic mice which results in reduced glucose tolerance and decreased insulin secretion (Soesant et al., 2011). Conversely, overexpression of OGA in the liver of diabetic mice has been shown to increase glucose tolerance (Dentin et al., 2011). Furthermore, (Yki-Jarvinen et al., 1998) have demonstrated that insulin resistance and T2DM are caused by the overexpression of GFAT in transgenic mice. In addition, (McClain et al., 2002) demonstrated that muscles and adipocytes cells develop insulin resistance when bathed with high glucose chronically, however, treatment with DON, a potent inhibitor of GFAT ameliorated this. Also, a prior study (Robinson et al. 1995) demonstrated that there was no significant difference in the expression of GFAT between T2DM patients and non-diabetic controls in the liver and muscle of rats, a finding that is in tandem with the finding of this project. Interestingly, this same study (Robinson et al. 1995) found that GFAT activity was about 40% lower ($P < 0.05$) in the muscle and liver of diabetic rats compared to the controls, indicating that expression and activity are not necessarily causally connected.

Furthermore, the integrity of *O*-GlcNAc trap, both *Cp*OGAD298N (binding) and *Cp*OGAWT (non-binding) mutants was validated to be intact Figure 3.14. We utilised these mutants of *Clostridium perfringens* NagJ (*Cp*OGA), a bacterial orthologue of the eukaryotic OGAs, as the native enrichment of *O*-GlcNAcylated proteins because it shares 51% sequence similarity with human OGA (hOGA) and possesses high catalytic activity on human *O*-GlcNAcylated proteins (Rao et al., 2006). Although, there are other methods that would have been useful but are faced with some drawbacks (Selvan et al., 2017). For instance, β -elimination followed by Michael addition of DTT (BEMAD), which entail using chemoenzymatic labelling techniques and derivatization of modified substrates, has been previously utilised to sitemap and enrich *O*-GlcNAcylated protein (Ma and Hart, 2014). Also, capturing of native *O*-GlcNAcylated proteins, such as lectin has been achieved with immunoprecipitation with the anti-*O*-GlcNAc antibody CTD110.6 (Zachara et al., 2011), and the use of wheat germ agglutinin (WGA) weak affinity chromatography (Alfaro et al., 2012; Trinidad et al., 2012).

However, major drawbacks limiting these other methods include for instance, the millimolar affinity for GlcNAc by WGA affinity chromatography limits its application for use when the GlcNAc target is much smaller (Ma and Hart, 2014; Alfaro et al., 2012; Trinidad et al., 2012). Also, having a considerably enhanced affinity for *O*-GlcNAc, the anti-*O*-GlcNAc antibody CTD 110.6, has been found to identify other terminal GlcNAc residues in other glycans

(Reeves et al., 2014, Ogawa et al., 2013). It is also likely that CTD 110.6 does not recognise all *O*-GlcNAc sites given that it is raised against a particular immunogen from the C-terminal region of RNA pol II27 (Selvan et al., 2017). Putting these together and considering the success recorded with the utilisation of *Cp*OGA by (Selvan et al., 2017), we have therefore utilised this approach in this study.

Following several optimisations using lysates from several HSVSMC samples from different patients, not so appreciable success was recorded with the small-scale protein pulldown. Also, several attempts to optimise *O*-GlcNAcylated protein recovery from pulverised and solubilised HSV tissues did not seem to yield any appreciable success. A significant constraint of this project is due to these limitations; the Covid-19 pandemic, and the delay in receiving large-scale preps of these fusion proteins from University of York because we lack the facility to produce them here at University of Hull. However, future plans and proposed experiments for this project are well highlighted in Chapter 8.

3.4 Summary and conclusion

In this chapter, the integrity of the HSVSMCs obtained from HSV was validated by confocal immunofluorescence studies using the SMC markers SMMHC and α -SMA. Also, I have gone on to use PECAM-1 commonly known as CD31, to rule out EC contamination. Furthermore, the success of the procedure to isolate SMCs from HSV has been further supported by these validations. Additionally, I have shown that early passaging, T2DM, and high glucose concentrations have no effect on the expression of the main *O*-GlcNAcylation regulating enzymes (OGA, OGT, and GFAT). Also, I have validated the integrity of the synthesised mutants of *Cp*OGA, aimed to be used to enrich and trap *O*-GlcNAcylated proteins in HSVSMCs. These findings make valuable additions to the corpus of knowledge that will help researchers better understand *O*-GlcNAc homeostasis in HSVSMCs. This understanding is essential because vascular dysfunction, which results from altered SMC function, has continued to emerge as a factor in many diseases and so represents a viable target for therapeutic development.

Chapter 4: JAK/STAT-mediated modulation of the metabolic homeostasis of HSVSMC

4.1 Introduction

Haematopoiesis, immunity, tissue repair, and adipogenesis are a few examples of the diverse physiological processes controlled by the JAK/STAT signalling pathway (Owen et al., 2019). Consequently, numerous human disorders are correlated with the JAK/STAT pathway dysfunction (Owen et al., 2019). In brief, JAKs mediate tyrosine phosphorylation of receptors, recruit one or more STAT proteins, and are noncovalently linked with cytokine receptors (Hu et al., 2021). Tyrosine-phosphorylated STATs form dimers, which are then transported into the nucleus to bind target promoters and regulate gene transcription (Figure 4.1a). Even though multiple STATs can be triggered by cytokines that partially overlap, they each have unique biological consequences (Aittomäki and Pesu., 2014). The impact of the JAK/STAT signalling system and its involvement in the modulation of metabolic homeostasis of vascular cells is not fully understood. It is significant to note that metabolic reprogramming is now recognised as a crucial process by which malignant cancer cells are able to maintain high proliferation rates in hostile conditions with limited oxygen and nutritional availability (Boroughs and DeBerardinis., 2015). Additionally, recent research has revealed that changes in EC metabolism are responsible for the increased proliferation of pulmonary arterial SMCs observed in PAH (Fang et al., 2012; Caruso et al., 2017). However, it is unknown how stimuli that promote HSVSMC migration and proliferation events which are responsible for vascular re-modelling will affect metabolism. To prevent VGF, it may, therefore, be possible to find novel therapeutic targets by identifying characteristic metabolic modifications. Hence, in this chapter, I assessed two JAK-STAT-activating stimuli that are established mediators of HSVSMC dysfunction (IL-6/sIL-6R α and PDGF-BB) on glucose consumption, oxygen consumption, and glycolytic rate (Aibibula et al., 2018).

Both OCR and ECAR are well established validated indicators of metabolic capacity with OCR cited as the "best indicator of metabolic capacity" (Leese et al. 2016). Since oxidative phosphorylation measured by OCR accounts for most of the increase in cellular ATP demand during implantation development, the activity of this pathway is a superior indicator of metabolic function (Brinster, 1973; Sturmeijer et al., 2003). It is significant that measurement of OCR in the presence of certain inhibitors can offer valuable information on mitochondrial bioenergetic profiles. The components of oxygen consumption that are linked to ATP production can be determined by inhibitors that target the various complexes in the ETC. These

components include the so-called coupled OCR, the amount lost through passive or active proton leakage across the inner mitochondrial membrane, the difference between maximal oxygen consumption and basal (spare capacity), and non-mitochondrial oxygen consumption. Together, these tests offer a clear picture of mitochondrial function "(Leese et al. 2016).

On the other hand, ECAR measures lactic acid, which is generated when glucose is converted to lactate during glycolysis (Yetkin-Arik et al., 2019). The flow through catabolic pathways used to produce ATP is connected to a cell's OCR and ECAR. The OCR and ECAR are related to ATP turnover because, at steady state, the rate of ATP synthesis is balanced out by the rate of ATP consumption. It may be demonstrated that variations in extracellular fluxes exhibit a concordance with changes in ATP turnover rates even though quantitative estimations of ATP turnover are technically challenging (Ferrick et al., 2008).

Putting these together, the specific aim of this chapter is to determine the effects of pro-inflammatory and mitogenic stimuli, IL-6/sIL-6R α and PDGF-BB respectively, on the metabolic profile of HSVSMCs from control and T2DM patients. To achieve this, HSVSMCs from T2DM and non-diabetic control were seeded in seahorse XFp 8 well plates at a density of 10,000 cells per well and were allowed to grow over 24 hrs. Following this, cells were pre-treated with 0.1 μ M ruxolitinib for 90 min followed by treatment with or without IL-6 (5 ng/ml) and sIL-6R α (25 ng/ml) (IL-6/sIL-6R α) or 10 ng/ μ L PDGF-BB for 24 hrs. Following this, the OCR and ECAR of the pre-treated cells were determined using the seahorse analyzer as described in 2.2.6. After assay, treated cells were lysed and the protein concentrations were determined using BCA assay as described in 2.2.3.2. Determined OCR or ECAR were then normalised to the protein concentrations, and the resulting data presented as mean \pm SEM were used to generate the graphs presented in this Chapter.

In summary, the objectives of this Chapter were to:-

1. Evaluate the effects of pro-inflammatory cytokine IL-6/sIL-6R α on the mitochondrial OCR and ECAR of HSVSMC from T2DM patients and non-diabetic controls.
2. Evaluate the effects of the mitogenic growth factor PDGF-BB on the mitochondrial OCR and ECAR of HSVSMC from T2DM patients and non-diabetic controls.

4.2. Results

4.2.1 Downstream inhibition of IL-6/sIL-6R α -stimulated activation of STAT3 with ruxolitinib

Evaluating how proinflammatory cytokines and mitogens affect the metabolic homeostasis of HSVSMCs from T2DM and non-diabetic phenotypes is one of this chapter's objectives. Thus, it is essential to characterise any potential proinflammatory and mitogen-induced modifications along the JAK/STAT downstream signalling pathway (Figure 4.1A). To achieve this, IL-6/sIL-6R α trans-signalling complex was used to activate downstream signalling in HSVSMCs, as determined by quantitative immunoblotting of STAT3 phosphorylation on Tyr705 (p-STAT3), which is required for STAT3 activation. Furthermore, JAK 1/2 inhibitor (ruxolitinib) was used to inhibit the JAK/STAT signalling pathway. Ruxolitinib, a pyrrolo[2,3-d] pyrimidine derivative that inhibits JAK1 and JAK2, was used in this instance because it is already an approved drug clinically used in the management of myelofibrosis (Verstovsek et al., 2012; Haq and Adnan, 2022).

To determine an optimal concentration of ruxolitinib that significantly inhibited IL-6/sIL-6R α -induced activation of STAT3, confluent HSVSMCs from non-diabetic patients in 10 cm dishes were serum starved for 90 minutes and treated with varied concentrations (10 nM, 0.1 μ M, 1 μ M, and 10 μ M) ruxolitinib for 90 minutes before treatment with IL-6 (5 ng/ml) and sIL-6R α (25 ng/ml) (IL-6/sIL-6R α) or PBS (control) for 30 minutes. Following this, cell lysates were obtained as described in 2.2.3.1, and the protein concentrations were determined using BCA assay as described in 2.2.3.2. Cell lysates were then equalised for protein content and resolved by SDS-PAGE for immunoblotting with antibodies versus Tyr705-phosphorylated (p-STAT3, Cat No:9131; 1:500) and total STAT3 (1:500, Cat No: ab68153; 1:500).

These experiments showed that significant inhibition ($p < 0.0001$ versus cells not pre-treated with ruxolitinib, $n=4$) of IL-6/sIL-6R α -induced activation of STAT3 in HSVSMCs from non-diabetic patients was achieved at 0.1 μ M ruxolitinib (Fig 4.1C). This concentration was, therefore, used in subsequent experiments in this project.

Figure 4.1

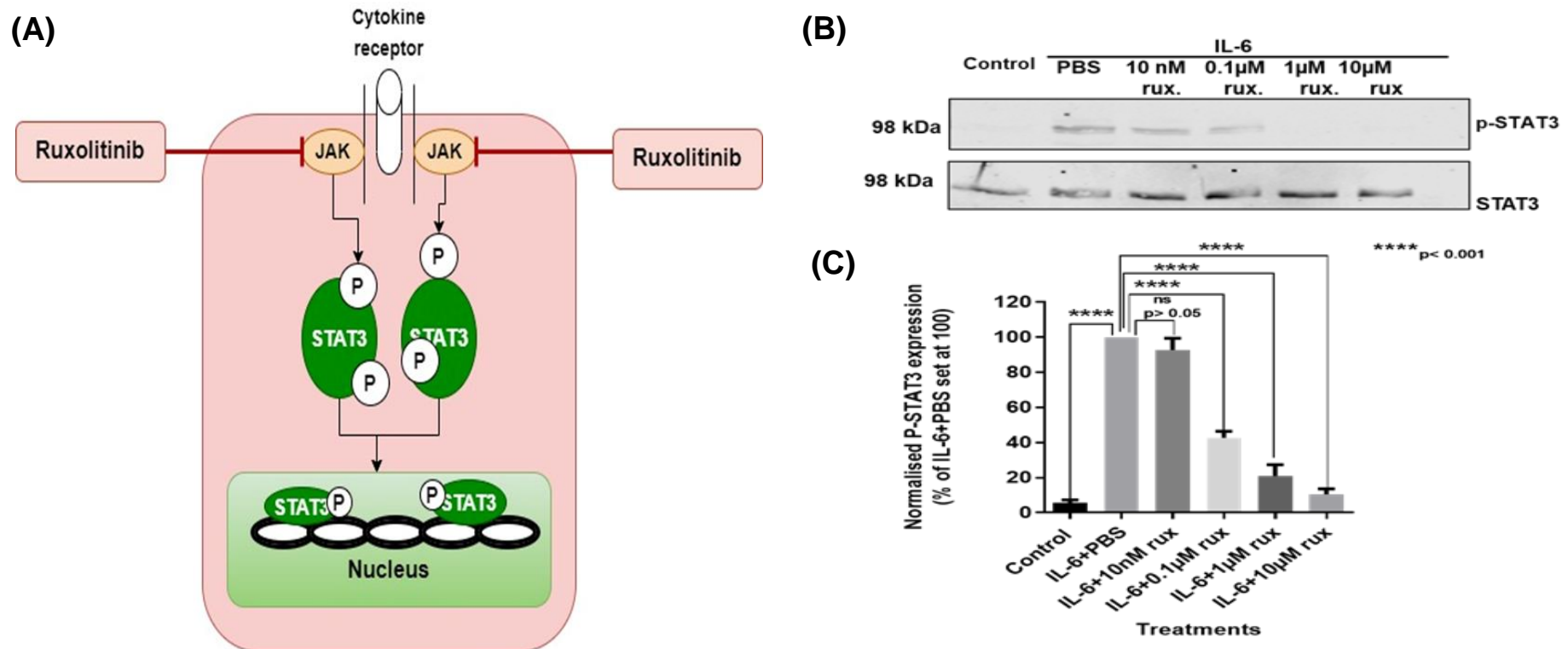


Figure 4.1: Downstream activation and inhibition of the JAK/STAT signalling pathway. (A) Schematic of downstream activation and inhibition of the JAK/STAT signalling pathway. The JAK/STAT pathway transmits information from chemical signals outside of a cell to the cell nucleus where it activates genes through transcription. This is mediated by activation of receptors such as IL-6R and proteins, Janus kinases (JAKs), and signal transducer and activator of transcription (STAT). Ruxolitinib (JAK 1 and 2 inhibitor) blocks this JAK/STAT signalling pathway.

(B) Upper panel: representative western blot of downstream inhibition of IL-6/sIL-6R α -stimulated phosphorylation of STAT3(98kDa) on Tyr705 by ruxolitinib. Lower panel: expression of total STAT3 (98kDa) (C) Densitometric analysis of p-STAT3 normalised to total STAT3. Data are four (n=4) biological replicates and are expressed as mean \pm SEM. IL-6: IL-6/sIL-6R α ; PBS: Phosphate buffered saline; rux: Ruxolitinib.

4.2.1.1 Effect of JAK inhibition on IL-6/sIL-6R α -mediated changes in OCR and ECAR in HSVSMCs from T2DM and non-diabetic patients.

4.2.1.1.1 Effect of ruxolitinib on IL-6/sIL-6R α -mediated changes in OCR in HSVSMCs from T2DM and non-diabetic patients.

Levels of pleiotropic cytokines such as IL-6 have been reported to be upregulated extramycelluarly in T2DM and this can have far-reaching effects including mitochondrial derangements (Abid et al., 2020; Johnson et al., 2013). Although the precise relationship between elevated cytokines like IL-6 and mitochondrial function is not fully understood, it has been proposed that T2DM patients exhibit altered mitochondrial dynamics that may be triggered by cytokines (Abid et al., 2020). One of the most reliable and useful metrics for defining mitochondrial function is the determination of OCR (Sturmev and Leese, 2003). Therefore, one way to evaluate how IL-6 impacts the mitochondrial function of HSVSMCs is to measure the mitochondrial OCR. The result from this evaluation will be significant because IL-6 has pleotropic qualities, which means that it can have both pro- and anti-inflammatory effects (Bolanle et al., 2021; Abid et al., 2020); it is also significant since it is the first time that this has been studied in HSVSMCs. Furthermore, ruxolitinib was used to attenuate the effect of IL-6/sIL-6R α by inhibiting the JAK/STAT downstream signaling pathway in HSVSMCs from both T2DM and non-diabetic.

As shown in Figure 4.2B, IL-6/sIL-6R α was found to significantly increase ($p < 0.05$ versus unstimulated cells, $n=4$) OCR in HSVSMCs from T2DM patients at maximal respiration, but not in those from non-diabetic phenotype (Figure 4.3B). The IL-6/sIL-6R α -stimulated increase in OCR found in HSVSMCs from T2DM patients was abolished by pre-treatment with 0.1 μM ruxolitinib (Figure 4.2B, $n=4$). Furthermore, ruxolitinib significantly decreased ($p < 0.05$ versus unstimulated cells, $n=4$) OCR in HSVSMCs from non-diabetic patients at basal and maximal respiration with or without IL-6/sIL-6R α stimulation (Figure 4.3B). Also, there are no appreciable differences between HSVSMCs from T2DM and non-diabetic when OCR was directly compared (Figure 4.4).

Figure 4.2

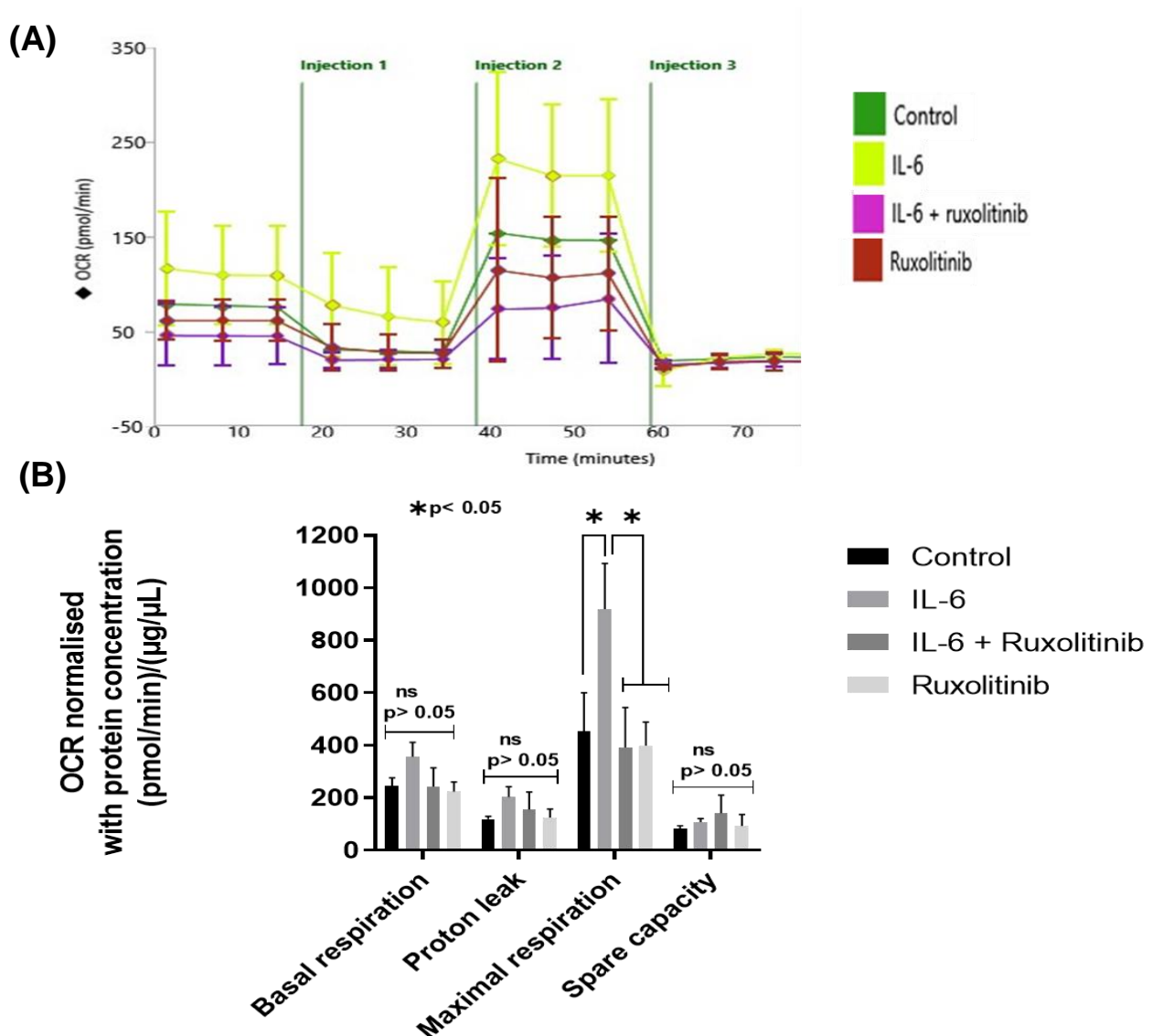


Figure 4.2: Mitochondria stress analysis to determine the OCR of HSVSMCs from T2DM patients after stimulation with IL-6/sIL-6Rα +/- ruxolitinib.

(A) representative time course curve of mitochondrial OCR of HSVSMCs from T2DM patients treated with IL-6/sIL-6Rα +/- ruxolitinib and untreated control.

Injection 1: 20 µl oligomycin (1.5 µM); Injection 2: 22 µl carbonyl cyanide p-(trifluoromethoxy) phenylhydrazone (FCCP) (5 µM); Injection 3: 25 µl rotenone (5 µM) and antimycin A (5 µM) complex.

(B) comparative analysis of normalised peak OCR between treatment groups and untreated control at basal respiration, and after addition of inhibitors of mitochondrial respiration and the uncoupler. Normalised data are presented as mean ± SEM from n=4 biological replicates using HSVSMC samples from different T2DM patients. IL-6: IL-6/sIL-6Rα; OCR: oxygen consumption rate.

Figure 4.3

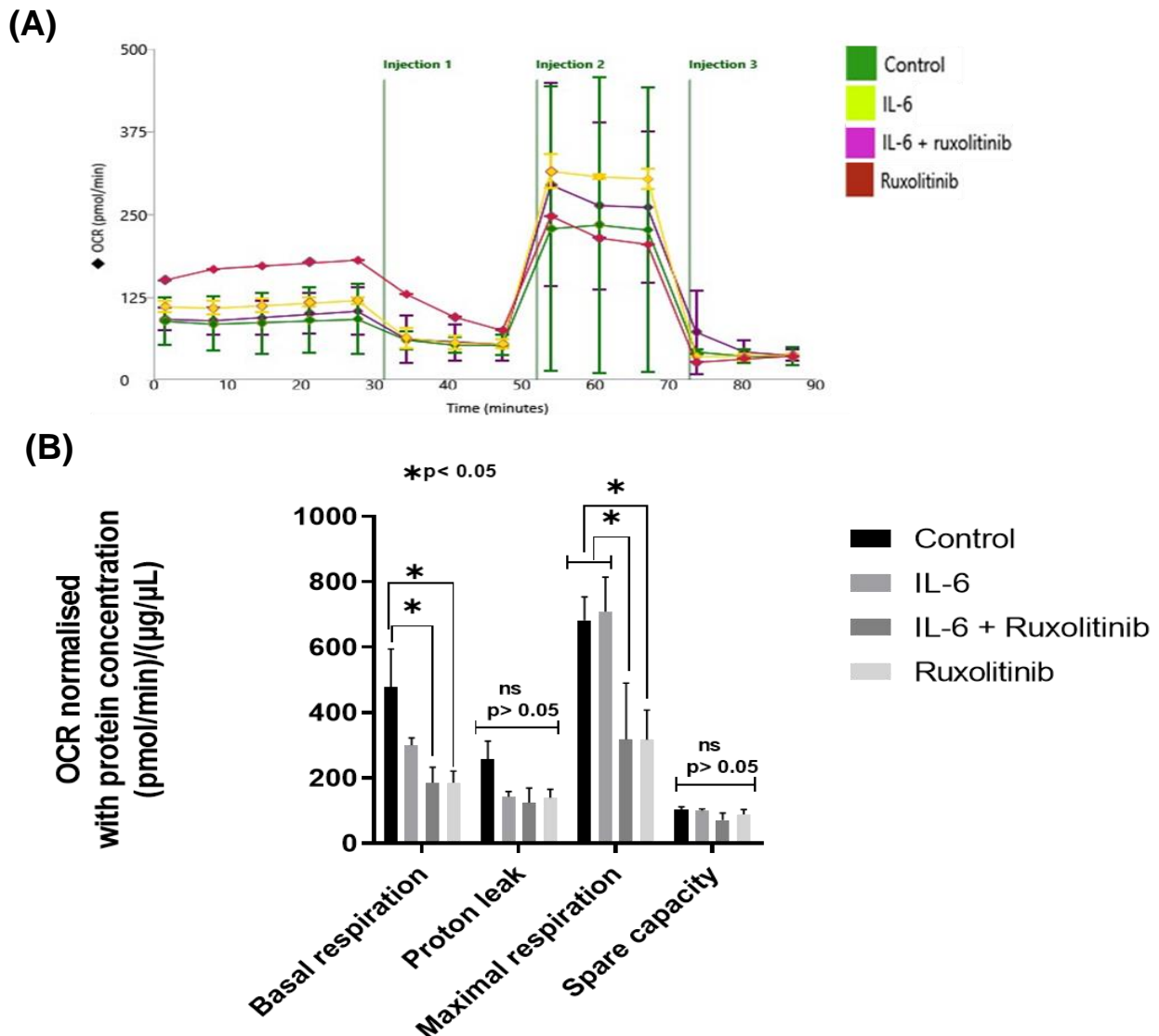


Figure 4.3: Mitochondria stress analysis to determine the OCR of HSVSMCs from non-diabetic patients after stimulation with IL-6/sIL-6Rα +/- ruxolitinib.

(A) representative time course curve of mitochondrial OCR of HSVSMCs from non-diabetic patients treated with IL-6/sIL-6Rα +/- ruxolitinib and untreated control.

Injection 1: 20 µl oligomycin (1.5 µM); Injection 2: 22 µl carbonyl cyanide p-(trifluoromethoxy) phenylhydrazone (FCCP) (5 µM); Injection 3: 25 µl rotenone (5 µM) and antimycin A (5 µM) complex.

(B) comparative analysis of normalised peak OCR between treatment groups and untreated control at basal respiration, and after addition of inhibitors of mitochondrial respiration and the uncoupler. Normalised data are presented as mean ± SEM from n=4 biological replicates using HSVSMC samples from different non-diabetic patients. IL-6: IL-6/sIL-6Rα; OCR: oxygen consumption rate.

Figure 4.4

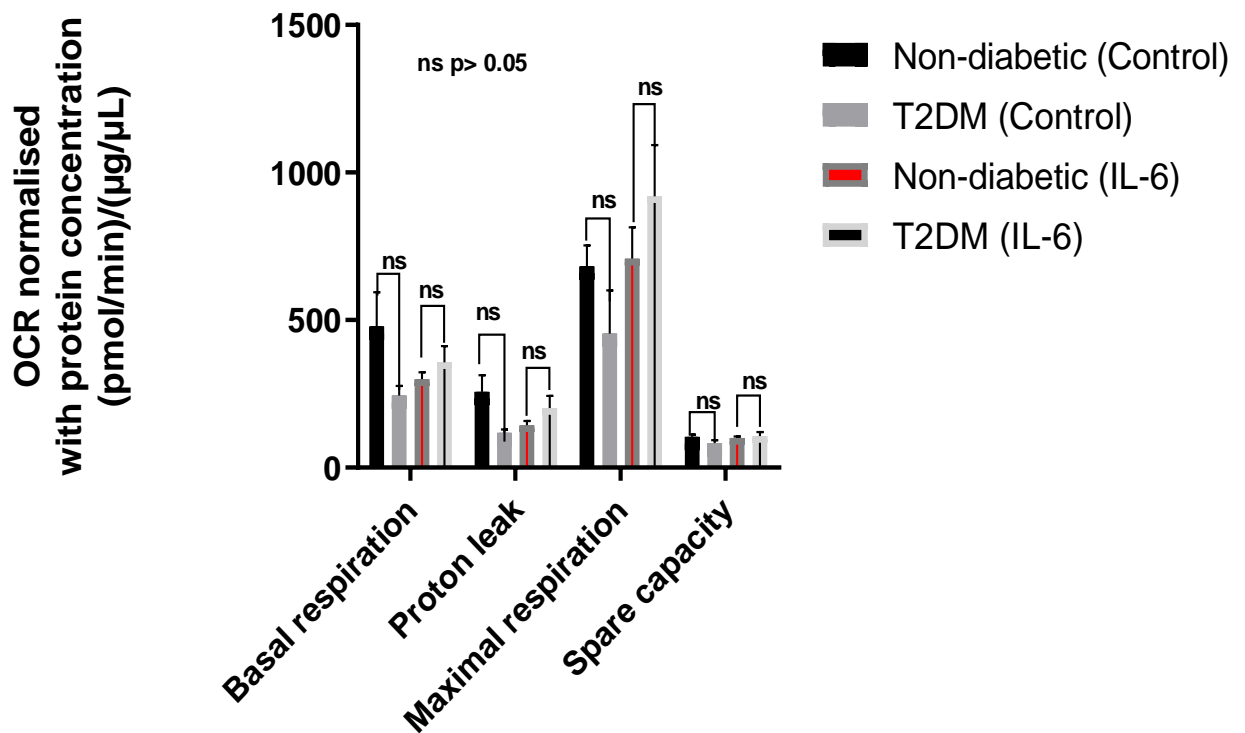


Figure 4.4: Comparison of the OCR of HSVSMCs from T2DM and non-diabetic patients after stimulation with IL-6/sIL-6R α +/- ruxolitinib.

Comparison of normalised peak OCR of unstimulated and IL-6/sIL-6R α -stimulated HSVSMCs from T2DM patients versus non-diabetic control. Normalised data are presented as mean \pm SEM from n=4 biological replicates using HSVSMC samples from different patients. IL-6: IL-6/sIL-6R α ; OCR: oxygen consumption rate.

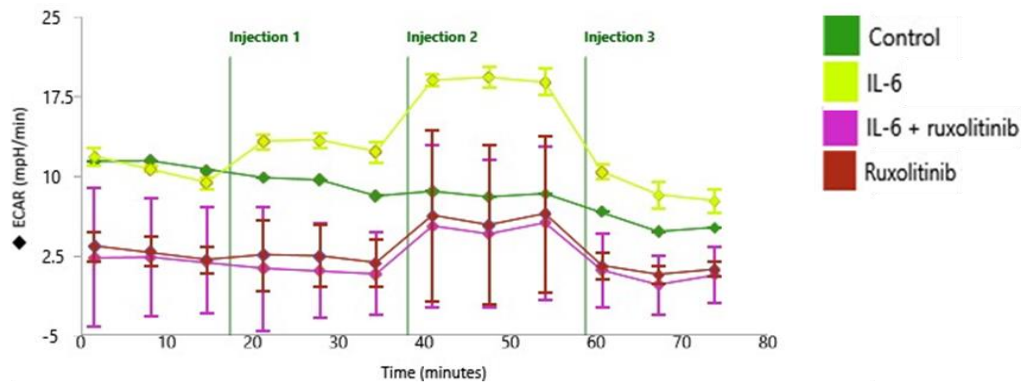
4.2.1.1.2 Effect of JAK inhibition on IL-6/sIL-6R α -mediated change in ECAR of HSVSMCs from T2DM and non-diabetic patients.

Monitoring the ECAR is a straightforward and effective way to assess rates of glycolysis and cellular respiration (Mookerjee and Brand, 2015; Brand and Nicholls, 2015). The lactate and CO₂ produced by anaerobic glycolysis and Krebs cycle during respiration, respectively, result in the release of protons into the extracellular medium (Mookerjee and Brand, 2015; Brand and Nicholls, 2015). While the source of glycolytic acidification is the conversion of glucose to lactate⁻ + H⁺ and its subsequent export, on the other hand, respiratory acidification is caused by the export of CO₂, hydration to H₂CO₃, and dissociation to HCO₃⁻ + H⁺. The ratios of glycolytic and respiratory acidification can range from nearly 100% glycolytic acidification to nearly 100% respiratory acidification, depending on the experimental conditions, including cell type and substrate(s) (Mookerjee et al., 2015; Mookerjee and Brand, 2015). However, the relationship between pro-inflammatory cytokines such as IL-6 and ECAR is currently unclear. Hence, ECAR of HSVSMCs from T2DM and non-diabetic patients were determined after treatment with IL-6/sIL-6R α following pre-treatment with or without ruxolitinib. ECAR allows for direct quantification of glycolysis (Plitzko and Loesgen, 2018), and was measured at basal conditions and following sequential addition of the mitochondria respiration inhibitors oligomycin (1.5 μ M), FCCP (5 μ M), rotenone (5 μ M) and antimycin A (5 μ M). ECAR values were then normalised to protein content of the lysed HSVSMCs.

The findings showed that IL-6/sIL-6R α did not cause any significant change in the ECAR of HSVSMCs from either T2DM or non-diabetic (Figures 4.5B and 4.6B). However, ruxolitinib without IL-6/sIL-6R α stimulation significantly decreased ($p < 0.05$ versus unstimulated cells, $n = 4$) ECAR in T2DM at glycolytic capacity, maximal glycolysis, and glycolytic reserve (Figure 4.5B). Also, ruxolitinib with or without IL-6/sIL-6R α stimulation significantly decreased ($p < 0.05$ versus unstimulated cells, $n = 4$) at basal and maximal glycolysis, and ($p < 0.01$ versus unstimulated cells, $n = 4$) at glycolytic reserve in HSVSMCs of non-diabetic patients (Figure 4.6B). Direct comparison of the ECAR of HSVSMCs from T2DM and non-diabetic patients after stimulation with IL-6/sIL-6R did not reveal any significant difference (Figure 4.7, $n = 4$).

Figure 4.5

(A)



(B)

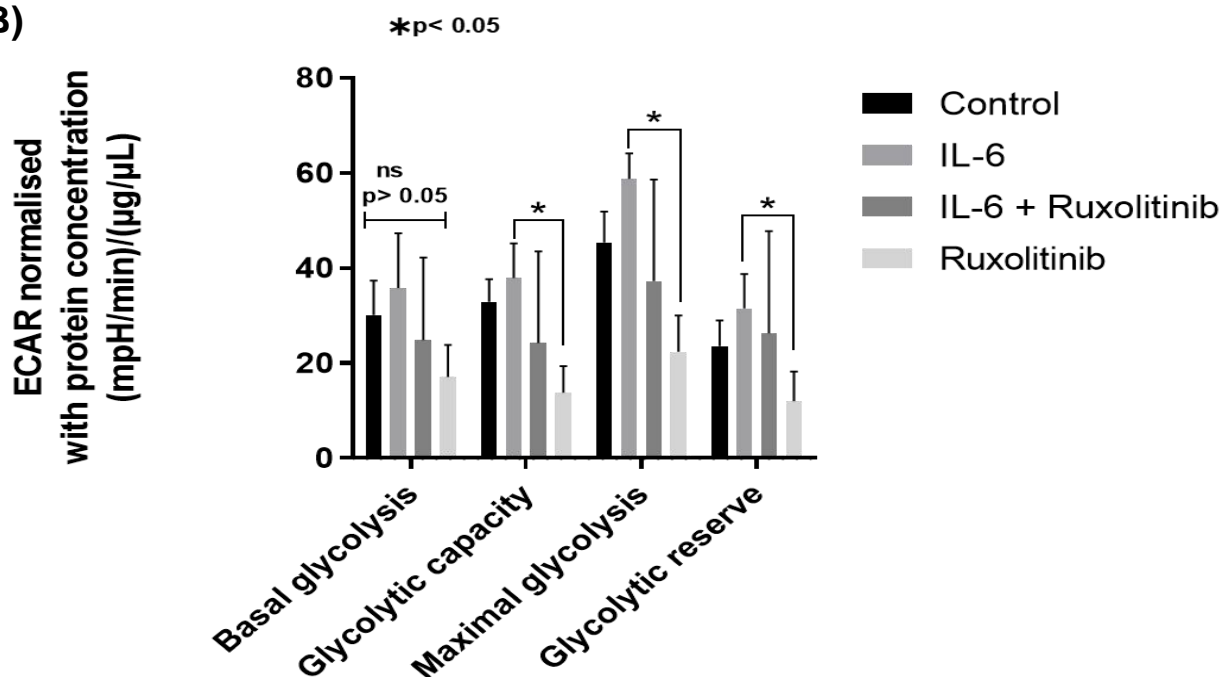


Figure 4.5: Mitochondria stress analysis to determine the ECAR of HSVSMCs from T2DM patients after stimulation with IL-6/sIL-6R α +/- ruxolitinib.

(A) representative time course curve of ECAR of HSVSMCs from T2DM patients treated with IL-6/sIL-6R α +/- ruxolitinib and untreated control.

Injection 1: 20 μ l oligomycin (1.5 μ M); Injection 2: 22 μ l carbonyl cyanide p-(trifluoromethoxy) phenylhydrazone (FCCP) (5 μ M); Injection 3: 25 μ l rotenone (5 μ M) and antimycin A (5 μ M) complex.

(B) comparative analysis of normalised peak ECAR between treatment groups and untreated control at basal glycolysis, and after addition of inhibitors of mitochondrial respiration and the uncoupler. Normalised data are presented as mean \pm SEM from n=4 biological replicates using HSVSMC samples from different T2DM patients. IL-6: IL-6/sIL-6R α ; ECAR: extracellular acidification rate.

Figure 4.6

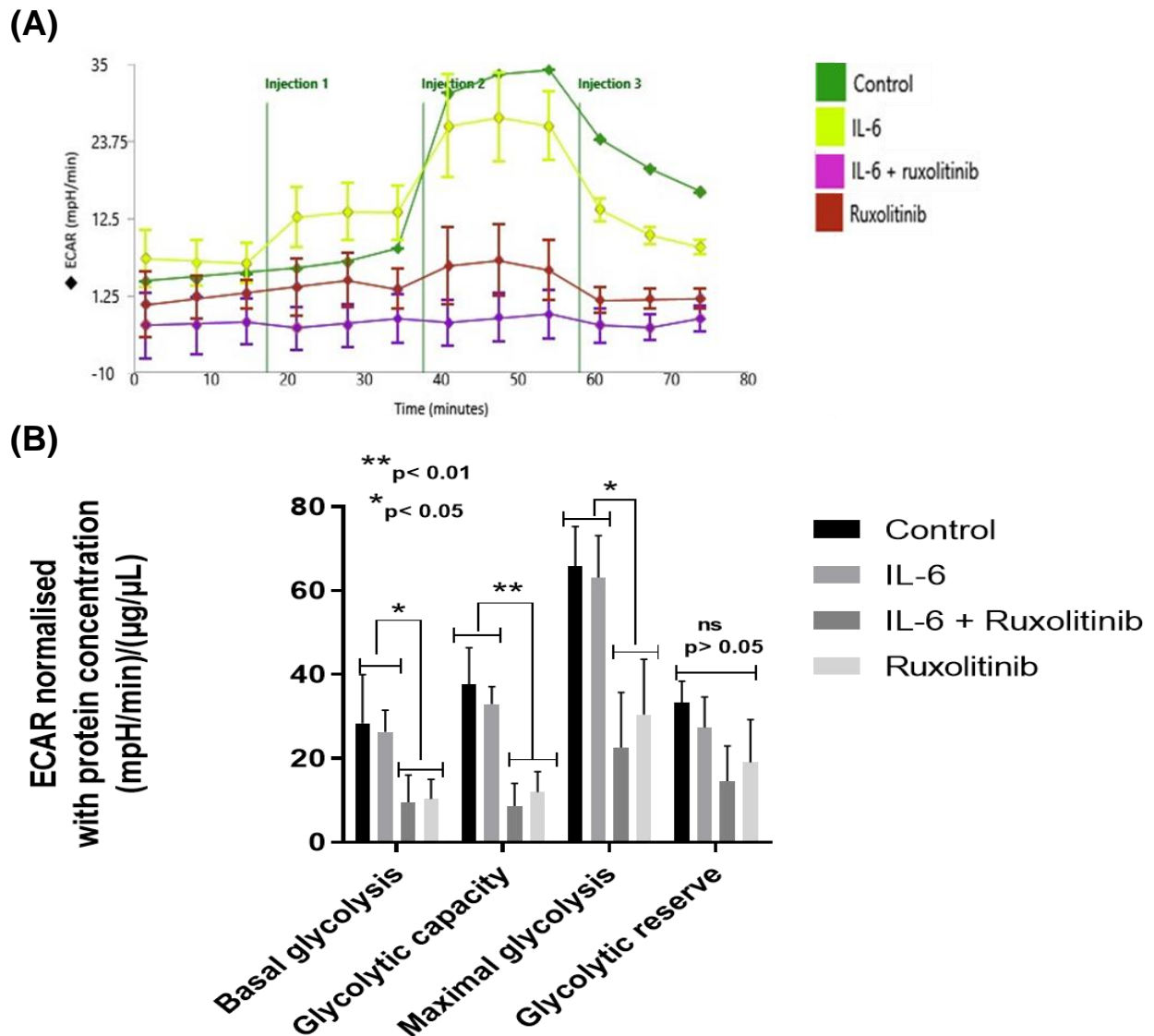


Figure 4.6: Mitochondria stress analysis to determine the ECAR of HSVSMCs from non-diabetic patients after stimulation with IL-6/sIL-6R α +/- ruxolitinib.

(A) representative time course curve of ECAR of HSVSMCs from non-diabetic patients treated with IL-6/sIL-6R α +/- ruxolitinib and untreated control.

Injection 1: 20 μ l oligomycin (1.5 μ M); Injection 2: 22 μ l carbonyl cyanide p-(trifluoromethoxy) phenylhydrazone (FCCP) (5 μ M); Injection 3: 25 μ l rotenone (5 μ M) and antimycin A (5 μ M) complex.

(B) comparative analysis of normalised peak ECAR between treatment groups and untreated control at basal glycolysis, and after addition of inhibitors of mitochondrial respiration and the uncoupler. Normalised data are presented as mean \pm SEM from n=4 biological replicates using HSVSMC samples from different non-diabetic patients. IL-6: IL-6/sIL-6R α ; ECAR: extracellular acidification rate.

Figure 4.7

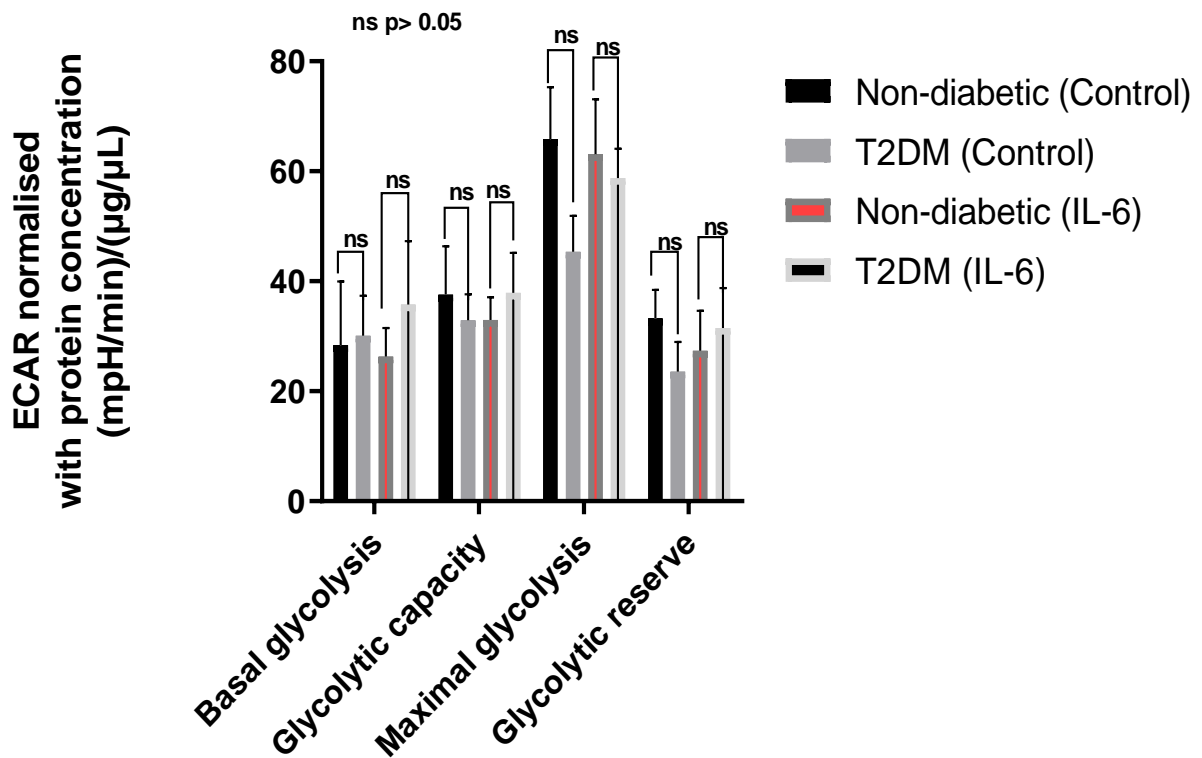


Figure 4.7: Comparison of the ECAR of HSVSMCs from T2DM and non-diabetic patients after stimulation with IL-6/sIL-6R α +/- ruxolitinib.

Comparison of normalised peak ECAR of unstimulated and IL-6/sIL-6R α -stimulated HSVSMCs from T2DM patients versus non-diabetic control. Normalised data are presented as mean \pm SEM from n=4 biological replicates using HSVSMC samples from different patients. IL-6: IL-6/sIL-6R α ; ECAR: extracellular acidification rate.

4.2.1.2 Effect of JAK inhibition on PDGF-BB-mediated changes in OCR and ECAR of HSV-SMCs from T2DM and non-diabetic patients.

4.2.1.2.1 Effect of JAK inhibition on PDGF-BB-mediated changes in OCR of HSVSMCs from T2DM and non-diabetic patients.

PDGF-BB enhances the production of pro-inflammatory cytokines like IL-6 and encourages VSMC proliferation and differentiation (Zhou et al., 2021; Masamune et al., 2005). PDGF-BB binds to its receptor (PDGFR), which triggers intercellular signalling and endogenous tyrosine phosphorylating activity (Masamune et al., 2005). It has been demonstrated that VSMCs exposed to PDGF-BB displayed mitochondrial fragmentation and a 20% reduction in glucose oxidation, followed by an increase in fatty acid oxidation and conversion towards a synthetic phenotype, suggesting that changes in mitochondrial structure can regulate VSMC metabolism and proliferation (Salabei and Hill, 2013).

However, mechanisms by which growth factors like PDGF alter cellular metabolic balance in HSVSMCs are unknown. To investigate this, the OCRs of HSVSMCs from T2DM patients and non-diabetic controls were assessed after treatment with PDGF-BB in the presence or absence of ruxolitinib (Plitzko and Loesgen, 2018). The OCR is proportional to mitochondrial respiration and was measured at basal conditions and after sequential addition of the mitochondria modulators oligomycin (1.5 μ M), FCCP (5 μ M), rotenone (5 μ M) and antimycin A (5 μ M). OCR values were then normalised to the protein content of the lysed HSVSMCs.

As shown in Figure 4.8B, PDGF-BB significantly increased OCR in HSVSMCs from T2DM patients at basal respiration, proton leak, and spare capacity ($p < 0.05$ versus unstimulated cells, $n = 4$) and maximum respiration ($p < 0.01$ versus unstimulated cells, $n = 4$) (Figure 4.8B), but not in HSVSMCs from non-diabetic phenotype (Figure 4.9B). This increase in OCR in T2DM patient HSVSMCs was abolished by pre-treatment with ruxolitinib (Figure 4.8B). On the other hand, ruxolitinib significantly reduced OCR at maximum respiration ($p < 0.05$ versus unstimulated cells and $p < 0.01$ versus PDGF-BB stimulated cells, $n = 4$) of HSVSMCs from T2DM patients (Figure 4.8B). Also, ruxolitinib reduced OCR at maximal respiration ($p < 0.05$ versus unstimulated and PDGF-BB stimulated, $n = 4$) of HSVSMCs from non-diabetic control (Figures 4.9B). When OCRs are directly compared between HSVSMCs from T2DM and non-diabetic, there are no significant differences (Figure 4.10).

Figure 4.8

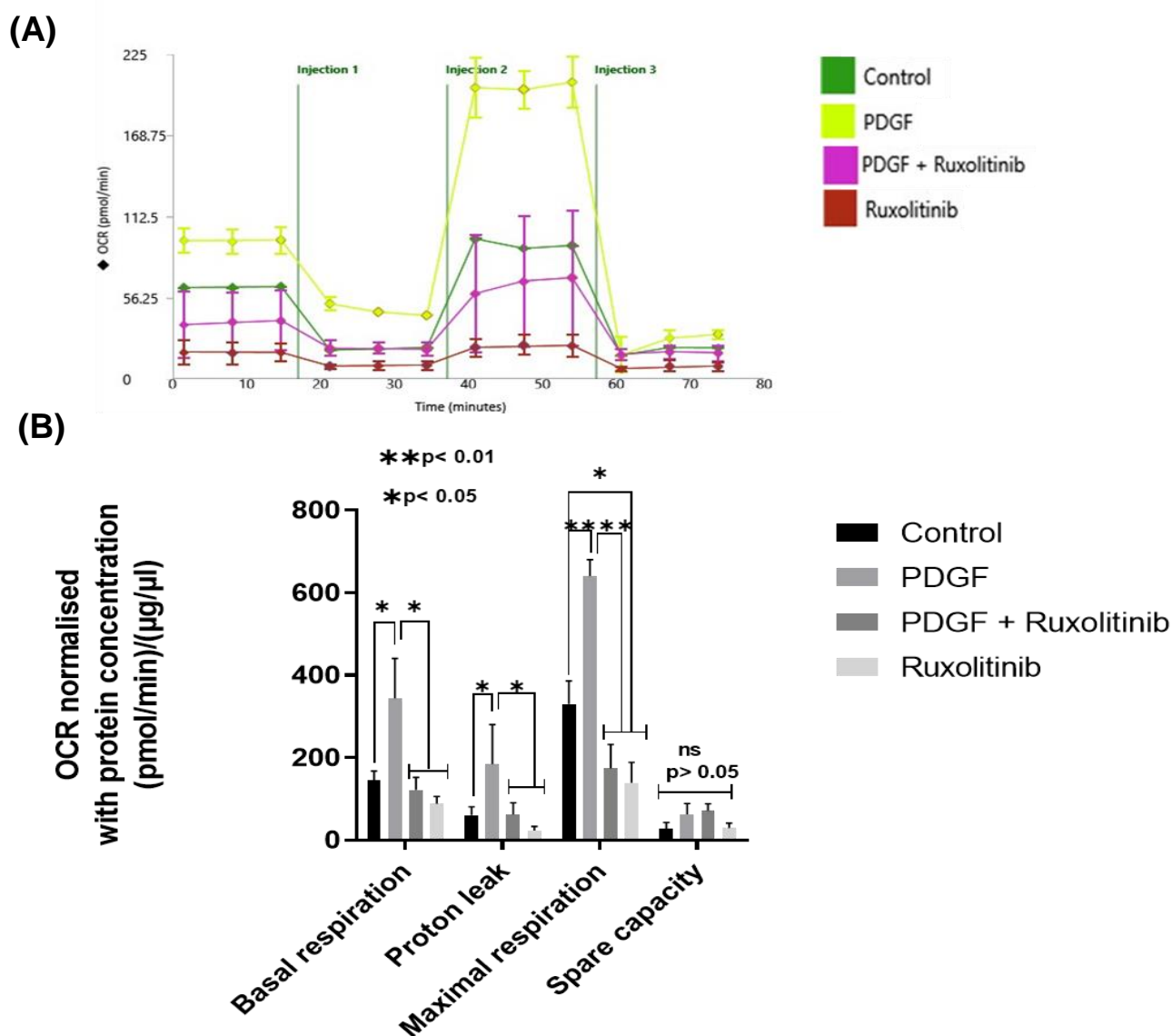


Figure 4.8: Mitochondria stress analysis to determine the OCR of HSVSMCs from T2DM patients after stimulation with PDGF-BB +/- ruxolitinib.

(A) representative time course curve of mitochondrial OCR of HSVSMCs from T2DM patients treated with PDGF-BB +/- ruxolitinib and untreated control.

Injection 1: 20 µl oligomycin (1.5 µM); Injection 2: 22 µl carbonyl cyanide p-(trifluoromethoxy) phenylhydrazine (FCCP) (5 µM); Injection 3: 25 µl rotenone (5 µM) and antimycin A (5 µM) complex.

(B) comparative analysis of normalised peak OCR between treatment groups and untreated control at basal respiration, and after addition of inhibitors of mitochondrial respiration and the uncoupler. Normalised data are presented as mean ± SEM from n=4 biological replicates using HSVSMC samples from different T2DM patients. PDGF: PDGF-BB; OCR: oxygen consumption rate.

Figure 4.9

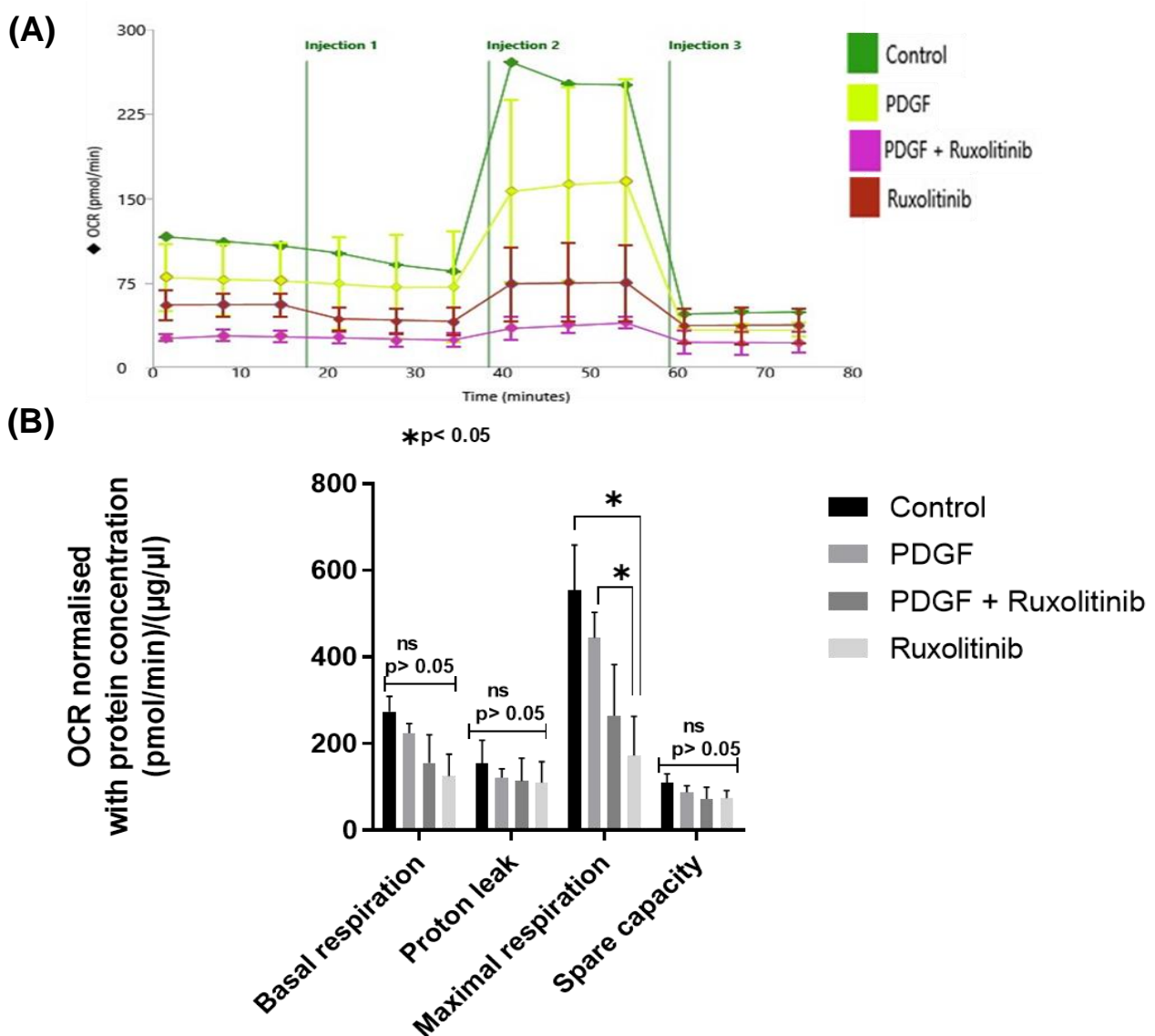


Figure 4.9: Mitochondria stress analysis to determine the OCR of HSVSMCs from non-diabetic patients after stimulation with PDGF-BB +/- ruxolitinib.

(A) representative time course curve of mitochondrial OCR of HSVSMCs from non-diabetic patients treated with PDGF-BB +/- ruxolitinib and untreated control.

Injection 1: 20 µl oligomycin (1.5 µM); Injection 2: 22 µl carbonyl cyanide p-(trifluoromethoxy) phenylhydrazone (FCCP) (5 µM); Injection 3: 25 µl rotenone (5 µM) and antimycin A (5 µM) complex.

(B) comparative analysis of normalised peak OCR between treatment groups and untreated control at basal respiration, and after addition of inhibitors of mitochondrial respiration and the uncoupler. Normalised data are presented as mean ± SEM from n=4 biological replicates using HSVSMC samples from different non-diabetic patients. PDGF: PDGF-BB; OCR: oxygen consumption rate.

Figure 4.10

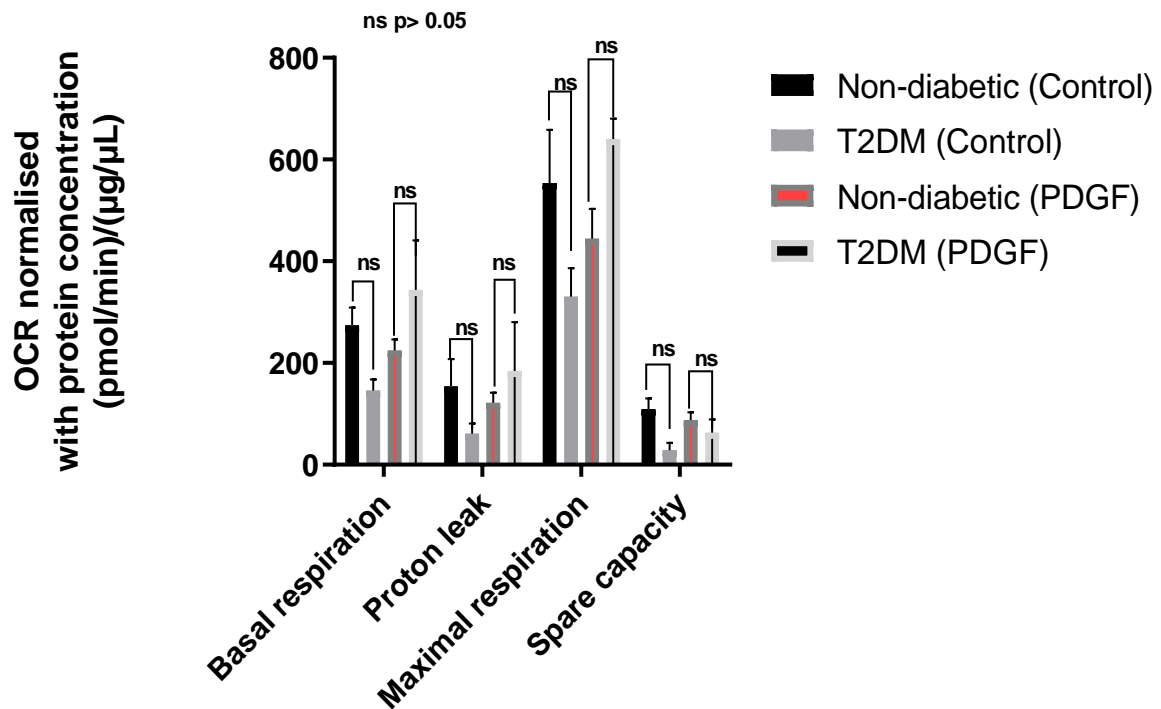


Figure 4.10: Comparison of the OCR of HSVSMCs from T2DM and non-diabetic patients after stimulating with PDGF-BB +/- ruxolitinib.

Comparison of normalised peak OCR of unstimulated and PDGF-BB-stimulated HSVSMCs from T2DM patients versus non-diabetic control. Normalised data are presented as mean \pm SEM from n=4 biological replicates using HSVSMC samples from different patients. PDGF: PDGF-BB; OCR: oxygen consumption rate.

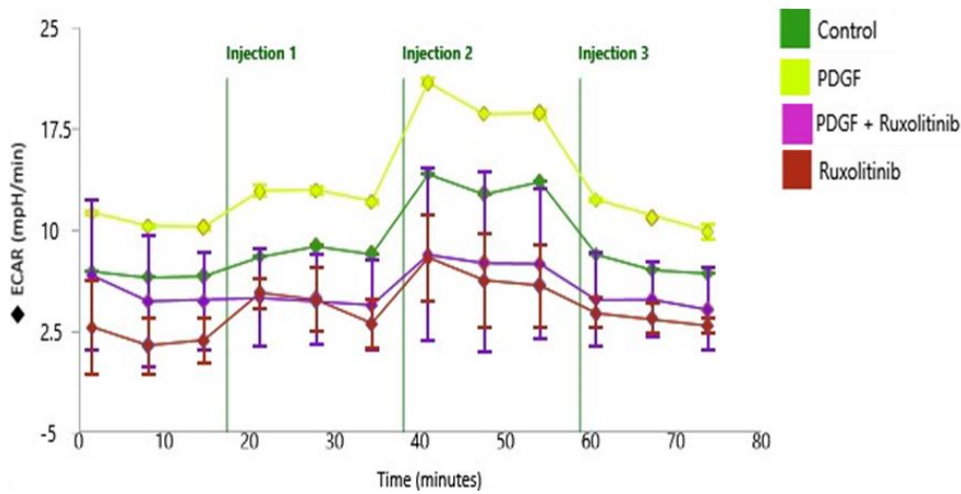
4.2.1.2.2 Effect of JAK inhibition on PDGF-BB-mediated changes in ECAR of HSVSMCs from T2DM and non-diabetic patients.

While it is unclear if PDGF-BB affects ECAR homeostasis in VCs, it has been shown that PDGF-DD, not PDGF-BB, induces extracellular acidification in prostate cancer (Najy et al., 2016), which is associated with elevated matriptase activation. The extracellular medium is widely used to gauge the rate of glycolysis under the presumption that the conversion of uncharged glucose or glycogen to lactate (-) +H (+) is a major source of acidity (Plitzko and Loesgen, 2018). In this experiment, to directly quantify glycolysis, ECAR of HSVSMCs from T2DM and non-diabetic control treated with or without PDGF-BB following pre-treatment with or without ruxolitinib was measured. This was done after sequential injections of mitochondrial modulators as previously described in 2.2.6. ECAR values were then normalised to the protein content of lysed HSVSMCs.

As shown in Figure 4.11B, PDGF-BB significantly ($p < 0.05$ versus unstimulated cells, $n=4$) increased ECAR at basal glycolysis, glycolytic capacity, maximal glycolysis, and glycolytic reserve in HSVSMCs from T2DM but not in non-diabetic (Figure 4.12B). On the other hand, ruxolitinib significantly ($p < 0.05$ versus unstimulated and PDGF-BB-stimulated cells, $n=4$) decreased ECAR at basal glycolysis, glycolytic capacity, maximal glycolysis, and glycolytic reserve in HSVSMCs from non-diabetic patients (Figure 4.12B). Also, direct comparison of the ECAR of HSVSMCs from T2DM and non-diabetic patients revealed a significantly ($p < 0.05$, $n=4$) higher ECAR in HSVSMCs from T2DM compared with non-diabetic control (Figure 4.13).

Figure 4.11

(A)



(B)

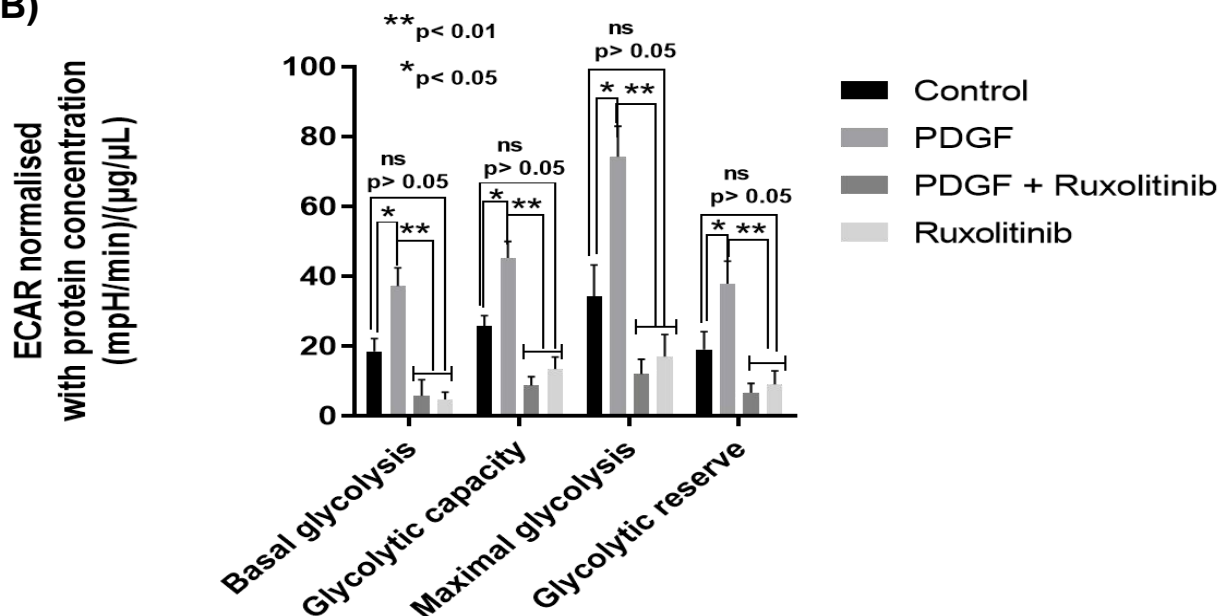


Figure 4.11: Mitochondria stress analysis to determine the ECAR of HSVSMCs from T2DM patients after stimulating with PDGF-BB +/- ruxolitinib.

(A) representative time course curve of ECAR of HSVSMCs from T2DM patients treated with PDGF-BB +/- ruxolitinib and untreated control.

Injection 1: 20 µl oligomycin (1.5 µM); Injection 2: 22 µl carbonyl cyanide p-(trifluoromethoxy) phenylhydrazone (FCCP) (5 µM); Injection 3: 25 µl rotenone (5 µM) and antimycin A (5 µM) complex.

(B) comparative analysis of normalised peak ECAR between treatment groups and untreated control at basal glycolysis, and after addition of inhibitors of mitochondrial respiration and the uncoupler. Normalised data are presented as mean ± SEM from n=4 biological replicates using HSVSMC samples from different T2DM patients. PDGF: PDGF-BB; ECAR: extracellular acidification rate.

Figure 4.11

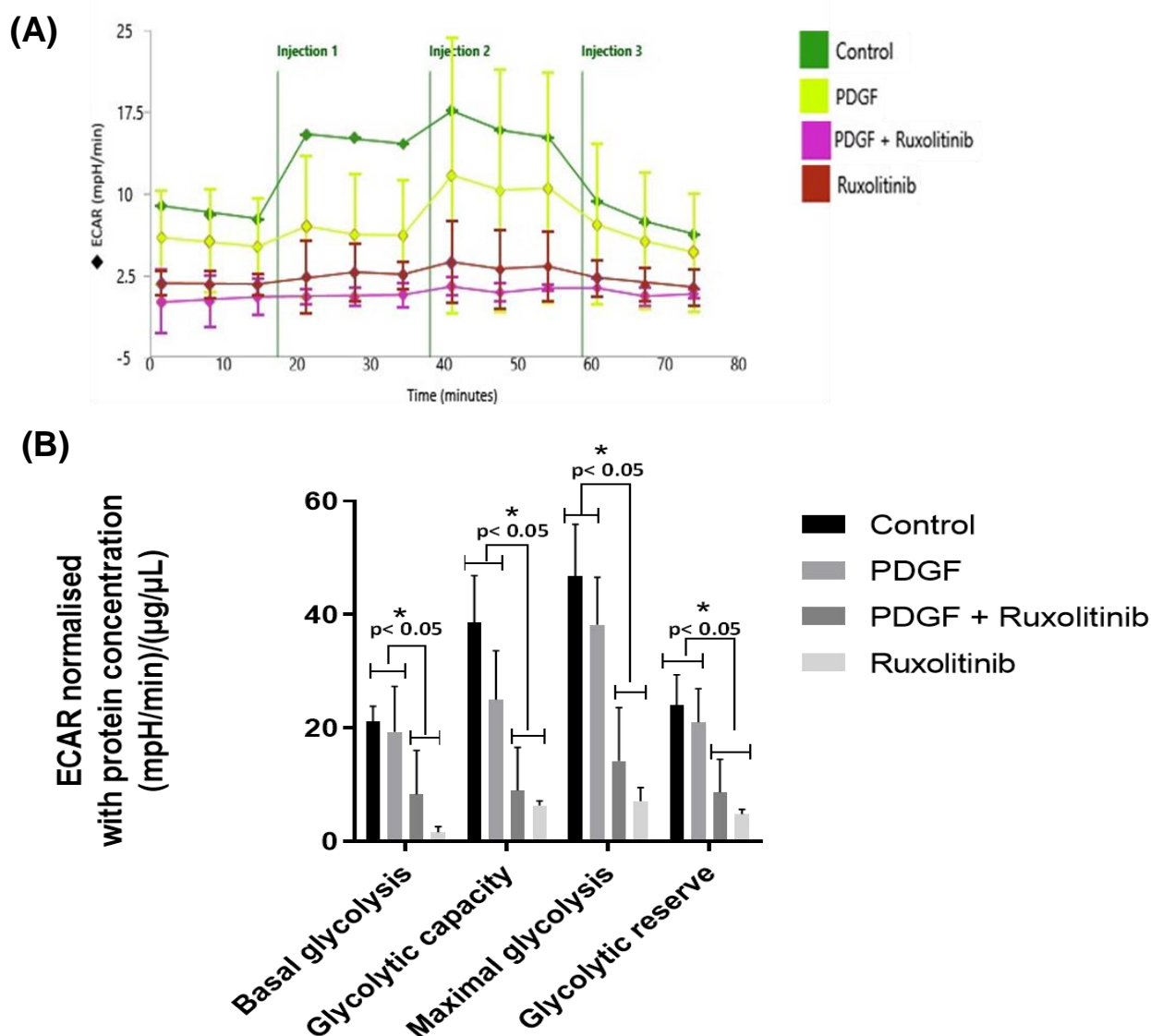


Figure 4.12: Mitochondria stress analysis to determine the ECAR of HSVSMCs from non-diabetic patients using PDGF-BB +/- ruxolitinib.

(A) representative time course curve of ECAR of HSVSMCs from non-diabetic patients treated with PDGF-BB +/- ruxolitinib and untreated control.

Injection 1: 20 µl oligomycin (1.5 µM); Injection 2: 22 µl carbonyl cyanide p-(trifluoromethoxy) phenylhydrazone (FCCP) (5 µM); Injection 3: 25 µl rotenone (5 µM) and antimycin A (5 µM) complex.

(B) comparative analysis of normalised peak ECAR between treatment groups and untreated control at basal glycolysis, and after addition of inhibitors of mitochondrial respiration and the uncoupler. Normalised data are presented as mean ± SEM from n=4 biological replicates using HSVSMC samples from different non-diabetic patients. PDGF: PDGF-BB; ECAR: extracellular acidification rate.

Figure 4.13

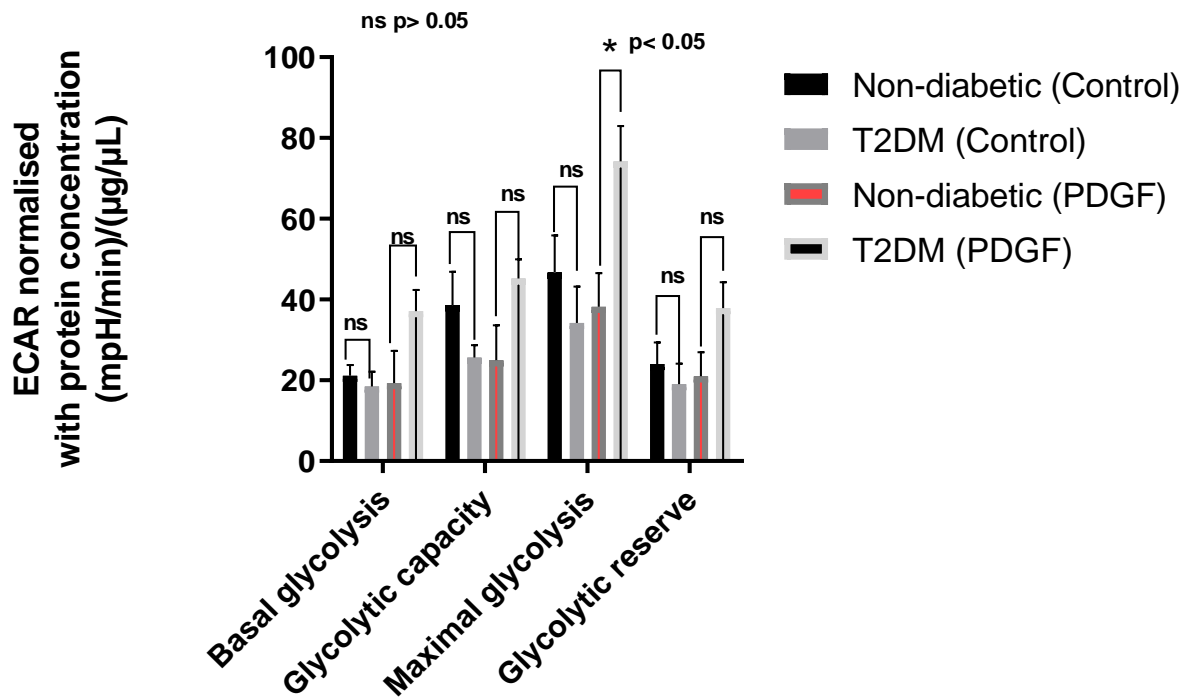


Figure 4.13: Comparison of the ECAR of HSVSMCs from T2DM and non-diabetic patients after stimulating with PDGF-BB +/- ruxolitinib.

Comparison of normalised peak ECAR of unstimulated and PDGF-BB-stimulated HSVSMCs from T2DM patients versus non-diabetic control. Normalised data are presented as mean \pm SEM from n=4 biological replicates using HSVSMC samples from different patients. PDGF: PDGF-BB; ECAR: extracellular acidification rate.

4.2.3 Alterations in metabolic homeostasis are not associated with any significant levels of IL-6/sIL-6R α and PDGF-BB -induced phosphorylation STAT3.

According to the findings from this chapter, IL-6/sIL-6R α and PDGF-BB both raised the OCR of HSVSMCs from T2DM patients, but not from non-diabetic controls. Also, PDGF-BB increased ECAR in HSVSMCs from T2DM. Considering these, it begs the research question of what might be responsible for these alterations. Therefore, one of the questions that must be addressed is whether the response of HSVSMCs from T2DM to these agonists (IL-6/sIL-6R α and PDGF-BB) is intrinsic. Although it has been previously established that HSVSMCs from T2DM patients are inherently more proliferative and mobile than those from non-diabetic controls (Madi et al. 2009), however, it is unclear whether HSVSMCs from T2DM utilise more oxygen to produce ATP than those from non-diabetic controls. To validate whether these observed alterations were caused by the agonists, the phosphorylation of STAT3 on Tyr705 (p-STAT3) in HSVSMCs from T2DM and non-diabetic patients was measured and compared. Results revealed that the alterations in the OCR and ECAR are not associated with any significant difference in levels of IL-6/sIL-6R α - and PDGF-BB-stimulated JAK-mediated STAT3 phosphorylation (Figures 4.14 and 4.15 respectively).

Figure 4.14

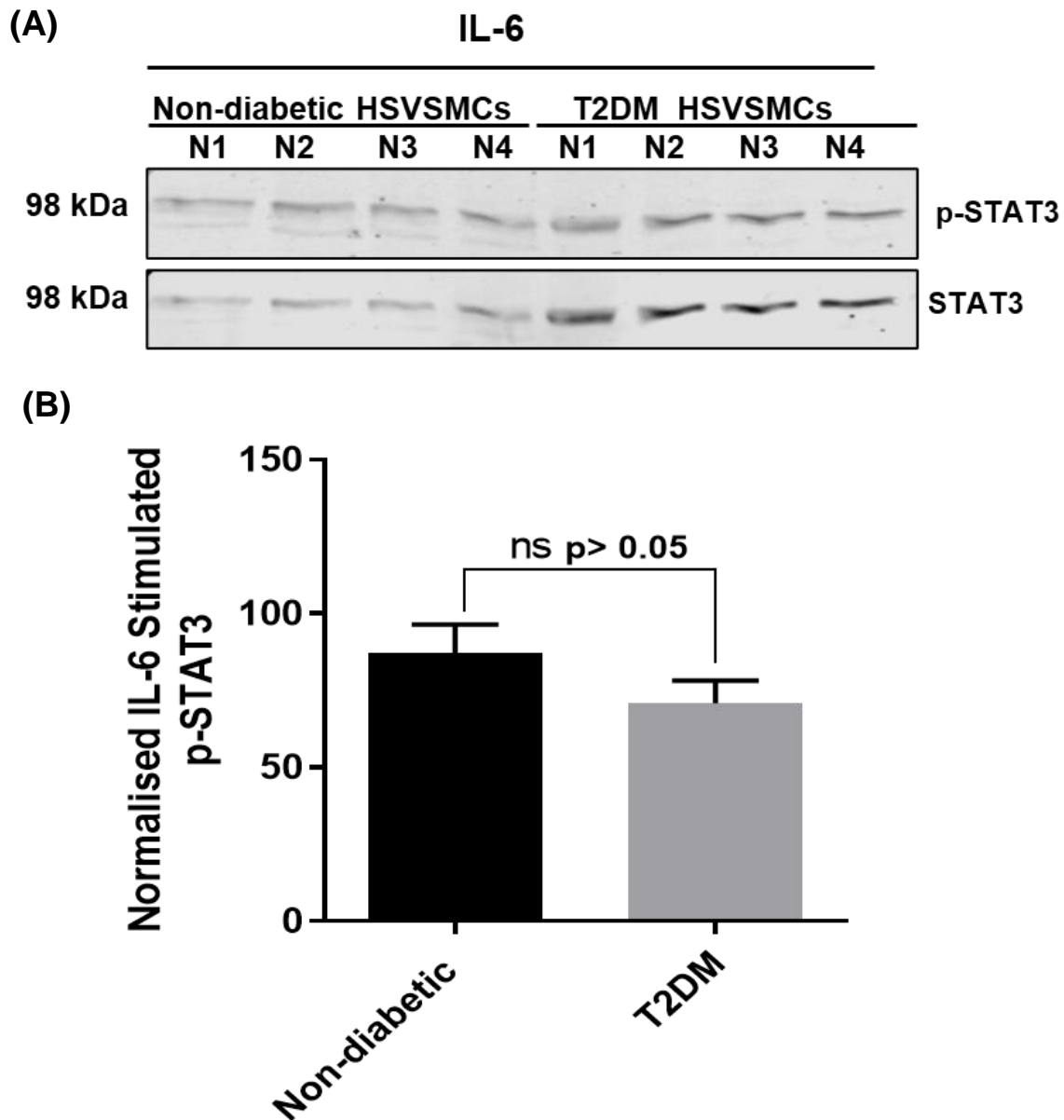


Figure 4.14: IL-6/sIL-6R α -stimulated phosphorylation of STAT3 on Tyr705 in HSVSMCs from T2DM and non-diabetic patients.

(A) **Upper panel:** representative western blot of IL-6/sIL-6R α -stimulated phosphorylation of STAT3 (98kDa) on Tyr705 in HSVSMCs from T2DM and non-diabetic patients.

Lower panel: expression of total STAT3 (98kDa)

(B) Densitometric analysis of IL-6/sIL-6R α -stimulated p-STAT3 in HSVSMCs from T2DM and non-diabetic patients. Data are normalised to total STAT3 and are four (n=4) biological replicates expressed as mean \pm SEM. IL-6: IL-6; IL-6/sIL-6R α .

Figure 4.15

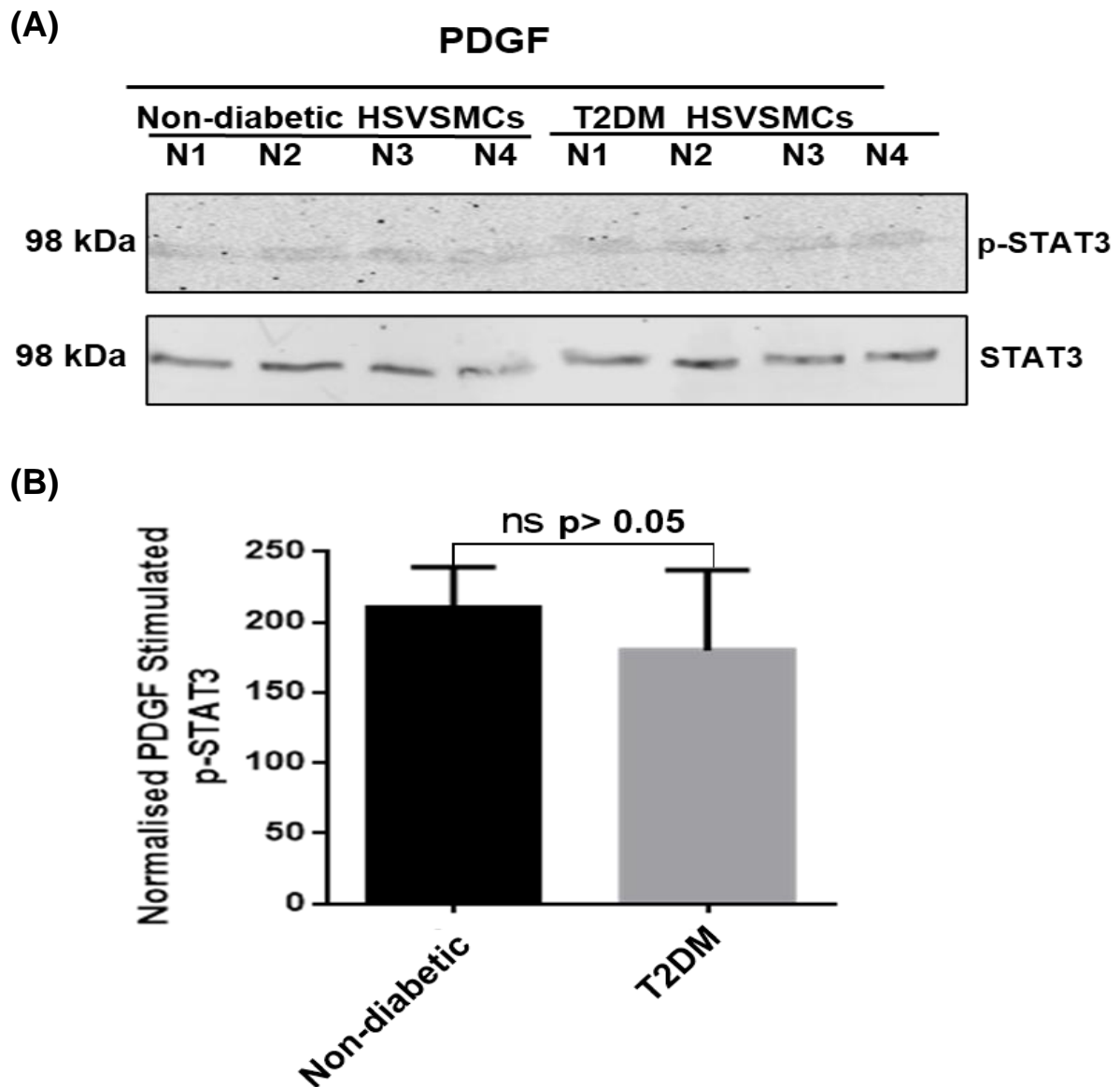


Figure 4.15: PDGF-BB-stimulated phosphorylation of STAT3 on Tyr705 in HSVSMCs from T2DM and non-diabetic patients.

(A) **Upper panel:** representative western blot of IL-6/sIL-6R α -stimulated phosphorylation of STAT3 (98kDa) on Tyr705 in HSVSMCs from T2DM and non-diabetic patients.

Lower panel: expression of total STAT3 (98kDa)

(B) Densitometric analysis of IL-6/sIL-6R α -stimulated p-STAT3 in HSVSMCs from T2DM and non-diabetic patients. Data are normalised to total STAT3 and are four (n=4) biological replicates expressed as mean \pm -SEM. PDGF: PDGF-BB.

4.2.4. mtDNA copy number in HSVSMCs from T2DM and non-diabetic patients after treatments with IL-6/sIL-6R α and PDGF-BB +/-ruxolitinib

Considering that JAK/STAT activators IL-6/sIL-6R α and PDGF-BB caused a significant increase in the OCR of HSVSMCs from T2DM and not from non-diabetic (Figures 4.2 and 4.8). It was therefore necessary to ascertain whether this increase was associated with a parallel increase in mtDNA copy number. Therefore, qPCR was used to determine mtDNA copy number of mitochondrially-encoded gene COI under different treatment conditions as described in 2.2.5.6. COI was chosen as the mtDNA marker because it is a standardised single molecular marker for the classification of animal species and is very effective at differentiating between vertebrate and invertebrate species (Hebert et al., 2003; Rodrigues et al., 2017).

As shown in Figure 4.16A, there is no significant difference in the mtDNA copy number in HSVSMCs from T2DM patients after treatments with IL-6/sIL-6R α +/-ruxolitinib compared with untreated control. Data were normalised to 18S and B-actin. Also, in the HSVSMCs from non-diabetic patients, there is no significant difference in the mtDNA copy number after treatment with IL-6/sIL-6R α +/-ruxolitinib compared with untreated control. Data were also normalised to 18S and B-actin (Figure 4.16B).

Furthermore, as shown in Figure 4.17A, there is no significant difference in the mtDNA copy number in HSVSMCs from T2DM patients after treatments with PDGF-BB+/- ruxolitinib compared with untreated control. Data were normalised to 18S and B-actin. Also, there is no significant difference in the mtDNA copy number in HSVSMCs from non-diabetic patients after treatment with PDGF-BB +/- ruxolitinib compared with untreated control. The mtDNA copy numbers were normalised to 18S and B-actin (Figure 4.17B).

Figure 4.16

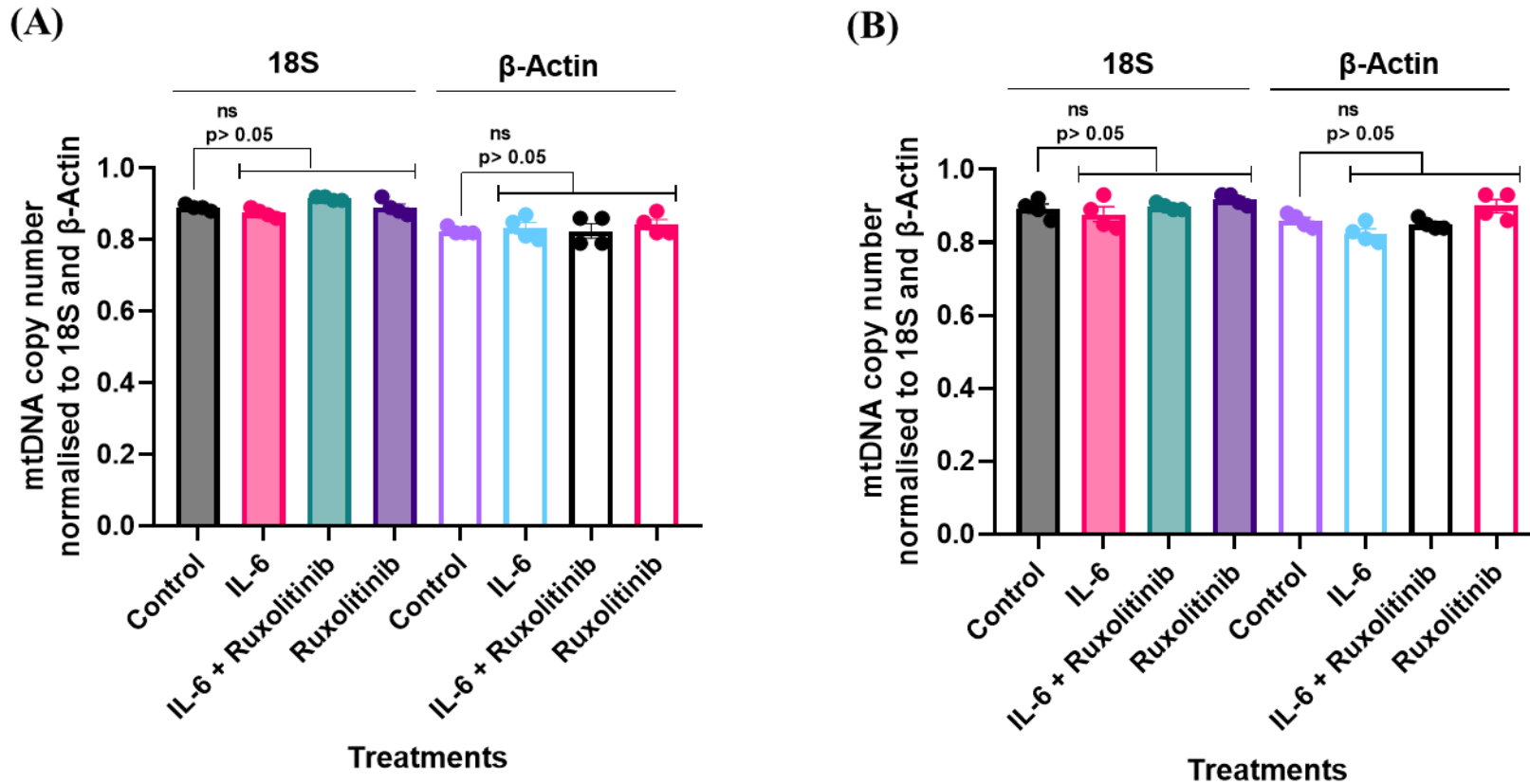


Figure 4.16: mtDNA copy number of HSVSMCs from T2DM and non-diabetic patients after treatment with IL-6/sIL-6R α +/- ruxolitinib. mtDNA copy number of mitochondrially encoded gene COI as a marker of mtDNA copy number in (A) T2DM, and (B) non-diabetic patients, normalised to 18S and β -Actin. Normalised data from different treatment conditions were compared with data from normalised untreated control for statistical difference. Data are presented as mean \pm SEM from n=4 experiments using HSVSMC from different patients. IL-6: IL-6/sIL-6R α .

Figure 4.17

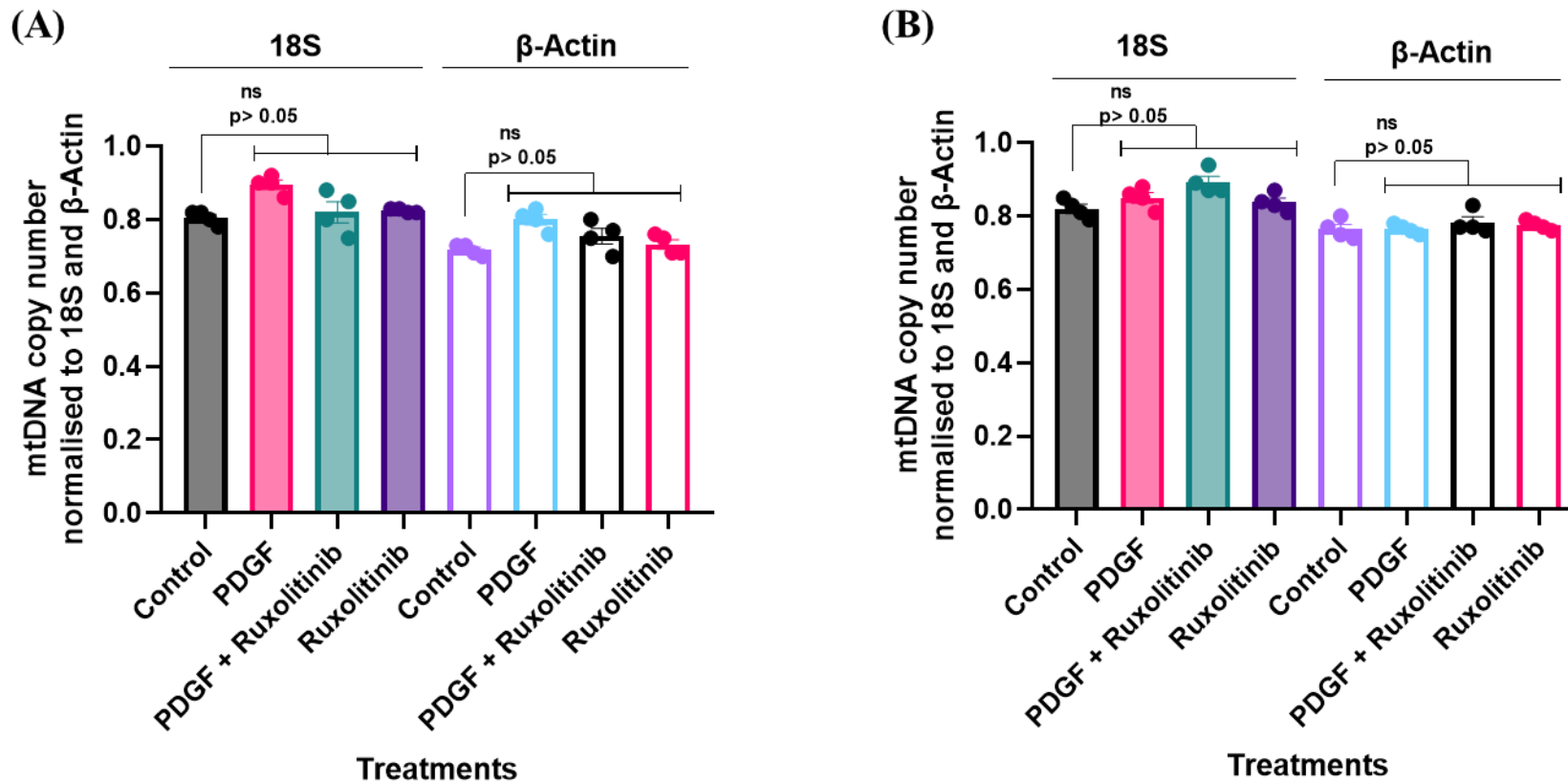


Figure 4.17: mtDNA copy number of HSVSMCs from T2DM and non-diabetic patients after treatment with PDGF-BB+/- ruxolitinib. mtDNA copy number of mitochondrially encoded gene COI as a marker of mtDNA copy number in (A) T2DM, and (B) non-diabetic patients, normalised to 18S and β -Actin. Normalised data from different treatment conditions were compared with data from normalised untreated control for statistical difference. Data are presented as mean \pm SEM from n=4 experiments using HSVSMC from different patients. PDGF: PDGF-BB.

4.3 Discussion

In this chapter, I investigated how two known JAK/STAT signalling pathway activators (IL-6/sIL-6R α and PDGF-BB) linked to vascular dysfunction that results in VGF affected the metabolic profiles of HSVSMCs from T2DM and non-diabetic controls (Aibibula et al., 2018). To assess this, I measured mitochondrial OCR and ECAR of HSVSMCs from T2DM and non-diabetic controls and evaluated the effect of JAK inhibition by ruxolitinib.

Firstly, I determined that 0.1 μ M was the practically safe concentration of ruxolitinib that caused significant and reproducible inhibition of IL-6/sIL-6R α -mediated JAK/STAT signalling activation in HSVSMCs as determined by measurement of JAK-mediated phosphorylation of STAT3 on Tyr705 (Figures 4.1B and C). While generating this data, HSVSMCs from non-diabetic patients were serum starved for 90 minutes and stimulated with IL-6/sIL-6R α for 30 minutes. This is an optimised protocol by a PhD student who worked before me in our lab on the same cell type. This PhD candidate did an extensive optimisation and a time course treatment to determine the effective condition for stimulating HSVSMCs with IL-6/sIL-6R α . Although, data from this PhD candidate's project are not yet published and I acknowledge that this is different from the protocol adopted by published studies (Jia et al., 2011; Turner et al., 2007) where HSVSMCs were serum starved for 24-72 hours. However, my results just as the result of the PhD student suggest that the experiment was successful as JAK-mediated IL-6/sIL-6R α -induced activation of STAT3 in HSVSMCs was achieved and a dose dependent inhibition of p-STAT3 by ruxolitinib was observed (Figures 4.1B and C). Various cell types require different effective concentrations of ruxolitinib to significantly block the JAK/STAT downstream signalling cascade (Casado-Garca et al., 2022). For example, while Patel et al. (2019) demonstrated downstream inhibition of JAK/STAT signalling pathway at 0.25 μ M ruxolitinib in non-small-cell lung cancer cells, Delen et al. (2020) showed significant inhibition of JAK/STAT signalling in a glioma cell line was inhibited at 50 nM concentration of ruxolitinib. Although higher concentrations (1 μ M and 10 μ M) of ruxolitinib produced greater reduction in STAT3 phosphorylation but I used 0.1 μ M ruxolitinib in this project despite that it only reduced STAT3 phosphorylation by ~50% (Figure 4.1B) because my preliminary seahorse mito stress analysis suggest that higher concentrations (1 μ M and 10 μ M) of ruxolitinib caused significant cell death. More so, subsequent results in this Chapter demonstrate that 0.1 μ M ruxolitinib was able to significantly and reproducibly inhibit the OCR

and ECAR in HSVSMCs, indicating that utilising higher concentrations would not have had an impact on the importance of the data generated.

While it is well established that activities of proinflammatory cytokines such as IL-6 are increased in T2DM (Akbari and Hassan-Zadeh, 2018), the exact impact on mitochondrial OCR, a measure of the metabolic profile, in VSMCs and specifically HSVSMCs is unclear. My finding (Figures 4.2) suggests that the IL-6/sIL-6R α possibly increases mitochondria respiration through the JAK/STAT pathway. The JAK/STAT pathway is an emerging target in inflammation which contributes centrally to cardiovascular diseases, hence, anti-inflammatory drugs are becoming popular in the management of cardiovascular events including those resulting from vascular dysfunction (Baldini et al., 2021). For instance, the current available treatments for pulmonary hypertension, which is caused by remodeling of the pulmonary arteries marked by endothelial dysfunction and proliferation of smooth muscle cells, are vasodilatory drugs, which often do not stop the disease progression (Roger et al., 2021). Therefore, targeting the molecular and cellular pathways implicated in vascular dysfunction to prevent pulmonary artery remodeling may be a viable option for drug development. Recent data suggests that the JAK/STAT pathway is overactivated in the pulmonary arteries of individuals with various forms of pulmonary hypertension (Roger et al., 2021). In addition, more research has shown that chronic inflammation contributes to pulmonary artery remodeling and pulmonary hypertension, among other vascular illnesses, and that in these circumstances, inflammatory mediators including IL-6/sIL-6R α and PDGF activate the JAK/STAT pathway (Roger et al., 2021).

Furthermore, the exact mechanisms underlying the increased risk of vascular disease in T2DM are still unknown, however, hyperglycaemia, insulin resistance, and hyperinsulinaemia have been shown to contribute to microvascular damage (Moshapa et al., 2019). Conversely, clinical trials have found that intensive glycaemic control has only a limited impact on the treatment of macrovascular complications (Hemmingsen et al., 2011). This suggests that the macrovascular complications seen in T2DM may be caused by mechanisms other than glucose intake (Hemmingsen et al., 2011; Gerstein et al., 2008; Duckworth et al., 2009). For instance, NIH is caused by dysfunctional ECs, and unchecked migration and proliferation of VSMCs. More so, IL-6 is one of the proinflammatory cytokines that are generated by the activated ECs and VSMCs (Johnson et al., 2001). It has been previously described that VSMCs from T2DM patients are less proliferative than the non-diabetic phenotype (Riches et al., 2014). This can

be detrimental to graft remodeling soon after vein graft placement because of a failure to adapt to arterial conditions. Furthermore, previous findings have suggested that VSMCs from T2DM mice and patients migrate more compared to the non-diabetic phenotype (Panchatcharam et al., 2010; Casella et al., 2015), hence, they may require more oxygen utilization for ATP production to drive cellular activities. While this is unclear, however could be a reason for increased oxygen consumption by HSVSMCs from T2DM patients (Figure 4.2). More so, there was no significant increase in OCR observed in non-diabetic patients (Figure 4.3). Additionally, a direct comparison of the OCR of HSVSMCs from T2DM and non-diabetic patients showed no discernible change (Figure 4.7).

Furthermore, ruxolitinib reduced ECAR in HSVSMCs from both T2DM and non-diabetic (Figures 4.5 and 4.6). While this observed reduction was seen at the determination of the glycolytic capacity of the HSVSMCs from T2DM (Figure 4.5), however, in HSVSMCs from non-diabetic patients, this reduction was observed in both glycolytic capacity and maximal glycolysis (Figure 4.6). Contrary to the initial finding, which showed that IL-6/sIL-6R α caused an increase in the OCR of HSVSMCs from T2DM patients (Figure 4.2), in this case, stimulation of the cells with IL-6/sIL-6R α cells did not significantly modify the ECAR of the cells (Figure 4.5). The reason for this is still unclear, however, (Berthiaume et al., 2003) did show that IL-6/sIL-6R α shifted the control for ATP synthesis towards processes that generate the mitochondrial membrane potential, indicating that IL-6/sIL-6R α induces a metabolic state where cellular functions are constrained by the mitochondrial energy supply, limiting conversion of glucose to lactate which is used to determine ECAR. Also, a direct comparison of the ECAR of HSVSMCs from patients with and without T2DM showed no significant change (Figure 4.7).

On the other hand, PDGF-BB caused a significant increase in OCR of HSVSMCs from T2DM at basal and maximal respiration (Figure 4.8). However, similar to IL-6/sIL-6R α , the increased OCR was abolished by ruxolitinib which also suggest that PDGF-BB mediated this modulation of mitochondria respiration through the JAK/STAT signalling pathway. Conversely, there was no appreciable increase in the OCR of HSVSMCs from non-diabetic subjects (Figure 4.9). Also, in both HSVSMCs from T2DM and non-diabetic patients, ruxolitinib caused a significant reduction in the OCR (Figure 4.8 and Figure 4.9). Meanwhile, direct comparison between the OCR of HSVSMCs from T2DM and non-diabetic with or without PDGF-BB stimulation showed no significant difference (Figure 4.10). The importance of mitochondrial metabolism as a key regulator of cell growth and proliferation is becoming increasingly appreciated

(Moncada et al., 2012). Increased glycolysis and glutamine usage are seen in rapidly dividing cells, which contribute to the production of energy, reducing equivalents, and the carbon and nitrogen building blocks necessary for daughter cell synthesis (Moncada et al., 2012). Growth factors like PDGF have been found to boost glycolysis and mitochondrial activity in VSMCs (Perez et al., 2010).

Additionally, it has recently been demonstrated that VSMCs have greater rates of glycolysis and take on a fragmented morphology in the context of pulmonary artery hypertension (Marsboom et al., 2012; Bonnet et al., 2006). However, little is known about how mitochondrial structure controls the phenotypic and metabolic properties of VSMCs. It has been demonstrated that such changes in mitochondrial shape have a direct impact on cell differentiation and proliferation (Mitra, 2013). Furthermore, despite numerous studies that have linked PDGF to vascular dysfunction (Hayashi et al., 1998; Hayashi et al., 2004; Martin et al., 2007; Wang et al., 2003; Radhakrishnan et al., 2010), to date, the function of PDGF on the mitochondria respiration and its metabolic components has not been investigated in HSVSMCs. The significance of the findings in this chapter is highlighted by the revelation that PDGF-BB can control mitochondrial respiration via the JAK/STAT pathway, which is less well-known for PDGF's downstream activity than other pathways such as ERK1,2 and Akt (Zhao et al., 2011).

In addition, early atherogenesis is marked by the vessel wall producing and releasing a variety of cytokines and growth factors such as PDGF that alter VSMC phenotype via autocrine and paracrine pathways (Dzau and Gibbons, 1987). More so, a significant factor in the pathophysiology of atherosclerosis and restenosis following angioplasty is PDGF, a powerful mitogen for VSMCs (Bornfeldt et al., 1994; Heldin and Westermark, 1999; Owens et al., 2004; Weissberg and Bennett, 1999). Acute vascular damage, in particular, encourages enhanced PDGF production and release from a variety of vascular cells, such as endothelial cells, VSMCs, activated monocytes, and monocyte-derived macrophages (Heldin and Westermark, 1999; Rubin et al., 1988). After angioplasty, increased PDGF and PDGF receptor expression has also been seen in human coronary arteries (Tanizawa et al., 1996; Ueda et al., 1996). Importantly, PDGF has been shown to be able to cause VSMCs to flip from the contractile state to the proliferative state, and this has been linked to the phenotypic plasticity of VSMCs (Owens et al., 2004).

Furthermore, restenosis during percutaneous coronary intervention, which eventually thickens the arterial wall as a result of neointima formation, seriously jeopardises the outcome of this surgical technique. Numerous vascular proliferative disorders, including atherosclerosis and aortic restenosis, have aberrant vascular smooth muscle cell migration and proliferation according to (Dzau et al., 2002). PDGF, which is produced by T cells, macrophages, endothelial cells, and VSMCs within the lesion, is one of many cytokines that can draw in and activate leukocytes, induce VSMC proliferation, encourage endothelial cell dysfunction, and stimulate the production of extracellular matrix components (Doran et al., 2008). One crucial mechanism in the pathophysiology of aberrant responses in VSMCs is PDGF signalling, which encourages the migration of these cells from the media to the intima (Heldin et al., 1999). Therefore, one of the main therapy focuses for vascular proliferative disorders has been thought to be the inhibition of PDGF-induced VSMCs proliferation and migration. Ruxolitinib may therefore represent a viable therapeutic approach for PDGF-induced vascular dysfunction because of its capacity to attenuate PDGF-BB JAK/STAT mediated increase in OCR of HSVSMCs from T2DM patients.

Also, PDGF caused an increase of ECAR of HSVSMCs from T2DM patients (Fig 4.11) but not in non-diabetic control (Figure 4.12). Conversely, ruxolitinib attenuated the PDGF-BB-induced increase ECAR seen in T2DM patients (Figure 4.11). Consistent with earlier findings in this Chapter, ruxolitinib caused a significant reduction of ECAR of HSVSMCs from non-diabetic patients. Additionally, a direct comparison between HSVSMCs from T2DM and non-diabetic showed that the ECAR of HSVSMCs from T2DM was higher at maximal glycolysis after stimulation with PDGF-BB (Fig 4.13). The mechanism(s) through which PDGF-BB caused a significant increase in ECAR of HSVSMCs of T2DM patients is unclear, more so that IL-6/sIL-6R α , another activator of the JAK/STAT pathway did not cause any significant change in the ECAR of HSVSMCs from T2DM. However, (Salebei and Hill, 2013) showed that PDGF-induced VSMC conversion to the synthetic phenotype was followed with mitochondrial fragmentation, a drop in apparent glucose oxidation, and a concurrent increase in fatty acid oxidation which contributes to an increase in ECAR.

It is unclear whether the observable alterations in the OCR and ECAR of HSVSMCs from T2DM patients is due in part or wholly to T2DM, hence, one research question that needs answer is whether the response of HSVSMCs from T2DM to these agonists (sIL6R α /IL-6 and PDGF-BB) is intrinsic. As revealed in (Figures 4.14 & 4.15), the observable alterations in the OCR and ECAR of HSVSMCs from T2DM patients are not associated with any significant

difference in levels of IL-6/sIL-6R α - and PDGF-BB-stimulated JAK-mediated STAT3 phosphorylation when compared with non-diabetic controls. Although this set of data is limited with that fact that unstimulated controls were not used which I admit is a flaw. However, some T2DM-induced molecular mechanisms which at the moment are unclear might be responsible for these alterations. Therefore, more investigations linking these alterations to T2DM are required to further substantiate these findings. One of such investigations includes assessing the response of HSVSMCs from both T2DM and non-diabetic control as relating to generation of reactive oxygen species which could aid the understanding of oxygen utilization in response to these activators. The findings from these investigations are documented in Chapter 6 of this thesis.

Furthermore, it has long been recognised that mitochondrial dysfunction contributes significantly to the underlying pathogenesis of a number of age-related diseases, including cancer, CVD, and neurodegenerative diseases (Longchamps et al., 2020; Gómez-Serrano et al., 2018). Hence, mtDNA copy number is increasingly used to evaluate the role of mitochondria in diseases as its measurement is a straightforward proxy for mitochondrial function (Longchamps et al., 2020). Higher levels of mtDNA copy number have been linked to lower incidence of several cancers, including breast, kidney, liver, and colorectal cancer (Ashar et al., 2017; Chen et al., 2014); neurodegenerative diseases like Parkinson's and Alzheimer's (Pyle et al., 2016; Wei et al., 2017); and CVDs like CAD and stroke (Reznik et al., 2016; Hertweck et al., 2017; Thyagarajan et al., 2012). Furthermore, it has regularly been demonstrated that the number of mitochondrial copies in peripheral blood is higher in women, decreases with age, and has a negative correlation with the WBC count (Knez et al., 2016; Tin et al., 2016). All of the above findings give a justification for the use of mtDNA copy number as a dependable tool to assess genetic characteristics. Hence, in this study, COI, a marker of mtDNA was used to assess possible changes in the mtDNA copy number after different treatments (Hebert et al., 2003; Rodrigues et al., 2017).

mtDNA copy number provides an opportunity to determine changes not only in disease conditions but as a genetic marker. In this experiment, I used the mtDNA copy number to investigate if the observed increase in OCR and ECAR detected in HSVSMCs from T2DM after the activation of the JAK/STAT signalling pathways was caused by an increase in mtDNA copy number or by other factors that are unknown but may be related to T2DM. However, from my results (Figures 4.16 and 4.17), there were no significant changes in the mtDNA copy number after treatment with the different treatment conditions as described in Chapter 2.8.1.

Therefore, while it is not entirely clear, the observed increase in OCR and ECAR in HSVSMCs from T2DM and not from non-diabetic control could be due to the T2DM status.

4.4 Summary and conclusion

In this chapter, I examined how two recognised JAK/STAT signalling pathway activators (IL-6/sIL-6R α and PDGF-BB) affected the metabolic profiles (OCR and ECAR) of HSVSMCs from T2DM patients and non-diabetic controls. These activators have been linked to vascular dysfunction responsible for a wide array of cardiovascular events including VGF (Aibibula et al., 2018). I used ruxolitinib, a JAK 1&2 inhibitor, to inhibit the downstream activation of the JAK/STAT pathway by these activators in order to investigate the potential for the development of novel treatment. The findings from my experiments documented in this Chapter suggest that T2DM alters HSVSMCs metabolic responses to proinflammatory stimulus IL-6/sIL-6R α and PDGF-BB, a known mitogen. The findings also revealed that these alterations seen in T2DM patients are not associated with any significant difference in levels of IL-6/sIL-6R α - and PDGF-BB-stimulated JAK-mediated STAT3 phosphorylation when compared with non-diabetic controls, however, this finding is flawed as there was no unstimulated control. Also, as determined by qPCR analysis, there is no difference in mtDNA copy number of both HSVSMCs from T2DM patients and non-diabetic controls after treatments with or without agonist stimulation, suggesting that these alterations are not related to a treatment-induced increase in mtDNA copy. Furthermore, these alterations were abolished by ruxolitinib which suggests a JAK-mediated modulation of mitochondrial function of HSVSMCs.

Chapter 5: MAPK/ERK-mediated modulation of metabolic homeostasis of HSVSMC

5.1 Introduction

Through a cell-mediated signalling pathway, the MAPK superfamily connects impulses to the cell initiating modifications to gene expression that affect the cellular phenotype (Albert-Gascó et al., 2020). The important molecule that controls the transmission of information that results in changes in metabolic pathways and the regulation of gene expression patterns is ERK, one of the kinases via which the MAPK signalling pathway exerts its function (Albert-Gascó et al., 2020). Changes in ERK-related pathways are linked to a variety of disease consequences, including those involving the cardiovascular and metabolic systems. More specifically, it has been demonstrated that activation of the MAPK/ERK downstream signalling pathway is associated with vascular remodelling, a key driver of VGF (Chen et al., 2009; Yoshizumi et al., 2019). Furthermore, cellular insulin response is modified by elements of the MAPK/ERK pathway (Zhang et al., 2011), and it has been shown that inhibition of MAPK/ERK pathway resulted in insulin resistance that was caused by a downregulation of the insulin-like receptor gene (Zhang et al., 2011). More so, MAPK/ERK pathway via the ETS-1 transcription factor enables physiological modulation of insulin sensitivity and thereafter maintains optimum levels of blood glucose (Zhang et al., 2011). As our knowledge in this field continues to grow, it is unclear how activators of the MAPK/ERK alter metabolic homeostasis of VSMCs, hence, in this Chapter, I examined the effect of Ang II and thrombin, two known activators of the MAPK/ERK signalling pathway, on the metabolic homeostasis of HSVSMCs.

The major effector peptide of the RAAS, Ang II, is involved in a number of cardiovascular conditions such as hypertension, atherosclerosis, and myocardial infarction which are linked to VSMC migration and proliferation (Berk et al., 2000). By inducing AT₁ receptor contraction in arterial VSMC, Ang II produces a sharp increase in blood pressure and the gradual onset of hypertension; this has also been linked to Ang II induced cardiac and vascular remodelling (Touyz and Schiffrin, 2000). A recent study (Friederich-Persson and Persson, 2020) demonstrated that Ang II decreased mitochondrial respiration via AT₂ receptor-mediated nitric oxide release in both control and diabetic rats. Furthermore, (Friederich-Persson and Persson, 2020) demonstrated that Ang II via AT₁ receptors increase mitochondria leak respiration in diabetic animals. Despite this contribution to knowledge by (Friederich-Persson and Persson, 2020), the exact impact of downstream activation of the MAPK/ERK by Ang II and the effect on the mitochondria function of HSVSMCs is unclear.

On the other hand, thrombin the second activator of the MAPK/ERK downstream signalling pathway evaluated in this Chapter has been demonstrated to promote migration of VSMCs by a number of signalling mechanisms (Tian et al., 2021; Shapiro et al., 1996) including thrombin-stimulated MAPK activation (Shapiro et al., 1996). Also, thrombin promotes an increase in OCR in intact mouse platelets (Li et al., 2020). However, the mechanism through which it does this is still obscure (Li et al., 2020). More importantly, it is unknown exactly how thrombin's downstream activation of the MAPK/ERK will affect the metabolic homeostasis of HSVSMCs.

Therefore, to investigate the involvement of the MAPK/ERK downstream signalling pathway in the modulation of the metabolic homeostasis of HSVSMC, HSVSMCs from T2DM and non-diabetic control were seeded in Seahorse XFp 8 well plates at a density of 10,000 cells per well and were allowed to grow over 24 hrs. Following this, cells were pre-treated with 10 nM trametinib for 90 min followed by treatment with or without 100 nM Ang II or 1 U/mL thrombin for 24 hrs. Following this, the OCR of the pre-treated cells was determined using the Seahorse analyzer as described in 2.2.6. After assay, treated cells were lysed and the protein concentrations were determined using BCA assay as described in 2.2.3.2. Determined OCR or ECAR were normalised to protein concentrations, and the resulting data presented as mean \pm SEM were used to generate the graphs presented in this Chapter.

In summary, the objectives of this Chapter were to:-

1. Assess how Ang II \pm trametinib affects the mitochondrial OCR and ECAR of HSVSMC from T2DM patients and non-diabetic controls via the MAPK/ERK signalling mechanism.
2. Examine the effects of thrombin \pm trametinib on the mitochondrial OCR and ECAR of HSVSMC from T2DM patients and non-diabetic controls via the MAPK/ERK signalling mechanism.

5.2 Results

5.2.1 Downstream inhibition of MAPK/ERK activation with trametinib

MAPK/ERK signalling controls a number of biological processes, including cell proliferation, division, and differentiation (Molina and Adjei, 2006). Even more so, this pathway's activators Ang II and thrombin have been linked to the initiation of vascular remodelling (Aibibula et al., 2018). In order to assess how these activators affect the metabolic homeostasis of HSVSMCs, it is necessary to investigate the downstream activation and inhibition of this pathway. Trametinib, a MEK 1&2 inhibitor, was used to achieve downstream inhibition of this pathway in order to understand this link (Figure 5.1A). It is crucial to establish the concentration of trametinib that significantly inhibited the downstream activation of ERK because this varies depending on the kind of cell (Awasthi et al., 2017).

To determine an optimal concentration of trametinib that significantly inhibited activation of ERK1/2, confluent HSVSMCs from non-diabetic patients were seeded in 10 cm dishes and allowed to be 90 % confluent. On the day of harvest, cells were serum starved for 90 minutes and treated with varied concentrations (0.1 nM, 1 nM, 10 nM, and 100 nM) of trametinib for 90 min. Then, cells were lysed as described in 2.2.3.1, and the protein concentrations were determined using BCA assay as described in 2.2.3.2. Cell lysates were then equalised for protein content and resolved by SDS-PAGE for immunoblotting with antibodies versus Thr202/Tyr204-phosphorylated p-ERK1/2 (Cat No:9106L; 1:500) and total ERK (Cat No: 9102L; 1:500) to determine the concentration of trametinib that significantly inhibited phosphorylation of ERK.

Results (Figure 5.1C) revealed that activation of ERK in HSVSMCs from non-diabetic patients was significantly ($p < 0.05$ versus untreated cells, $n=4$) inhibited by 10 nM trametinib, hence, this concentration was used in subsequent experiments in this chapter to attain downstream inhibition of the MEK/ERK pathway.

Figure 5.1

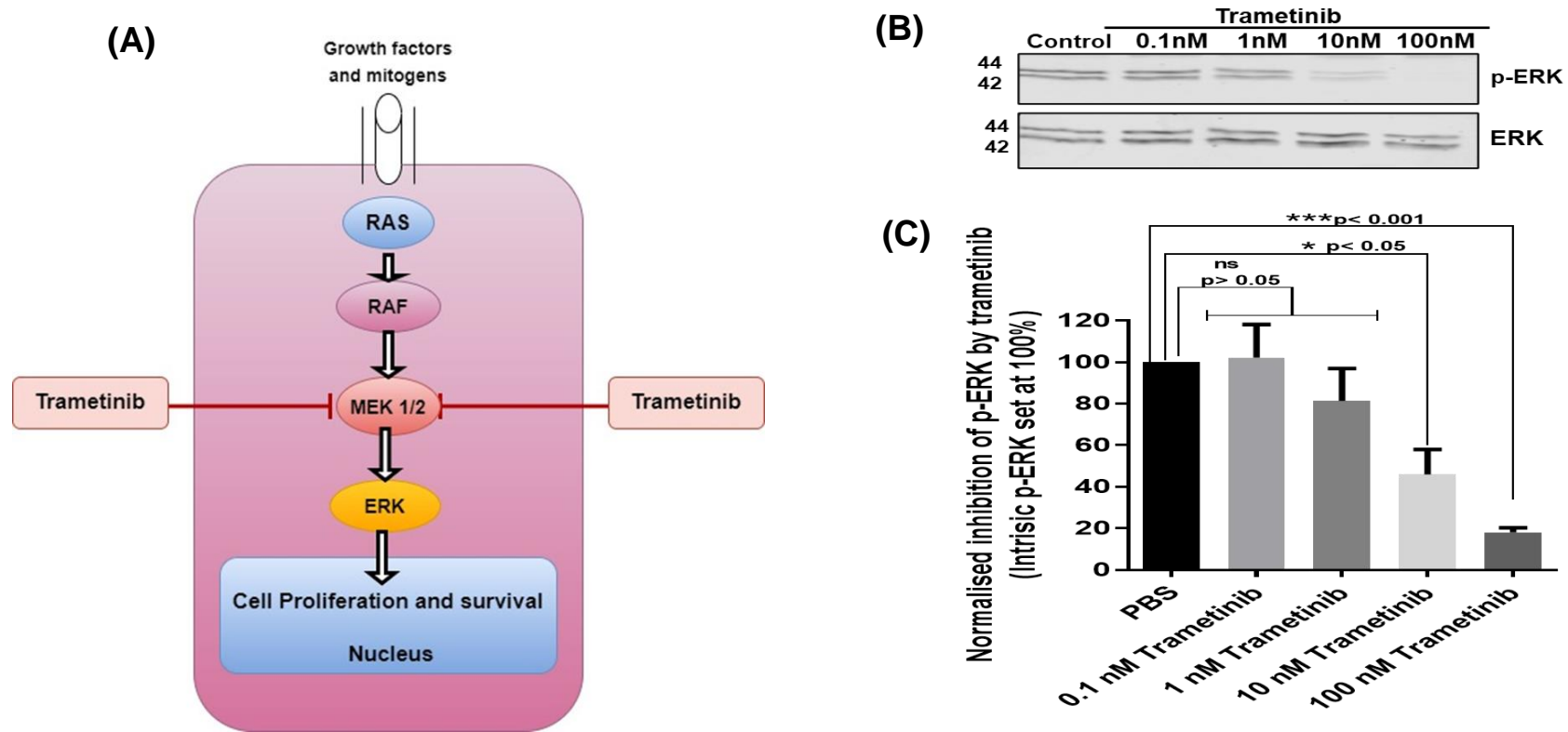


Figure 5.1: Downstream activation and inhibition of the MAPK/ERK signalling pathway. (A) Schematic of downstream activation and inhibition of the MEK/ERK signalling pathway. A mitogen activates a cell surface receptor causing the Ras protein, a small GTPase, to switch the pathway on. Ras activates Raf which activates MEK 1/2, which in turn stimulates ERK. ERK further activates a transcription factor that promotes cell proliferation and differentiation in the nucleus. (B) Upper panel: representative western blot of downstream inhibition of the MEK 1/2 by trametinib. Lower panel: expression of total ERK (44/42kDa). (C) Densitometric analysis of p-ERK at both 44/42kDa normalised to total ERK at both 44/42kDa. Data are expressed as mean \pm SEM and n=4. PBS: Phosphate buffered saline.

5.2.2. Effect of Ang II +/- MEK inhibitor on OCR and ECAR of HSVSMCs from T2DM and non-diabetic patients.

5.2.2.1. Effect of Ang II +/- trametinib on OCR of HSVSMCs from T2DM and non-diabetic patients.

VSMC hypertrophy, hyperplasia, and inflammation are induced by Ang II, the primary physiologically active component of the RAAS, which promotes the development of hypertension, atherosclerosis, heart failure, and restenosis after vascular damage (Yaghini et al., 2010; Gibbons et al., 1992; Suzuki et al., 2003; Weiss et al., 2001; Rakugi et al., 1994; Feng et al., 2001). Furthermore, findings by (Yaghini et al., 2010) suggest that Ang II facilitates VSMC migration and proliferation via activating the MAP/ERK pathway. However, it is not totally clear how Ang II modulates these processes mechanistically (Ohtsu et al., 2006). As a result, it is thought that the increased cell proliferation and migration brought on by Ang II may necessitate higher ATP synthesis, which would increase oxygen consumption, as previously discussed in Chapter 4 of this thesis. Therefore, this series of experiments assesses and contrasts the impact of Ang II +/- trametinib on the OCR of HSVSMCs from patients with and without T2DM.

As shown in Figure 5.2B, Ang II did not cause any significant alteration in the OCR of HSVSMCs from T2DM patients. However, trametinib with or without Ang II stimulation significantly reduced OCRs at basal respiration ($p < 0.01$ versus unstimulated and Ang II-stimulated cells, $n=4$) and maximal respiration ($p < 0.05$ versus unstimulated and Ang II-stimulated cells, $n=4$) in HSVSMCs from T2DM. Similarly, in HSVSMC from non-diabetic, there was no significant alteration to OCR after stimulation with Ang II. On the other hand, trametinib caused a significant reduction in the OCRs at basal respiration ($p < 0.01$ with Ang II stimulation and $p < 0.001$ without Ang II stimulation, both versus unstimulated and Ang II-stimulated cells, $n=4$) and maximal respiration ($p < 0.05$ with or without Ang II stimulation versus unstimulated and Ang II-stimulated cells, $n=4$) in HSVSMCs from non-diabetic patients (Figure 5.3B). Also, direct comparison of OCRs after treatment with Ang II revealed significant increase ($p < 0.05$ versus HSVSMCs from non-diabetic patients, $n=4$) in OCR of HSVSMCs from T2DM at maximal respiration (Figure 5.4).

Figure 5.2

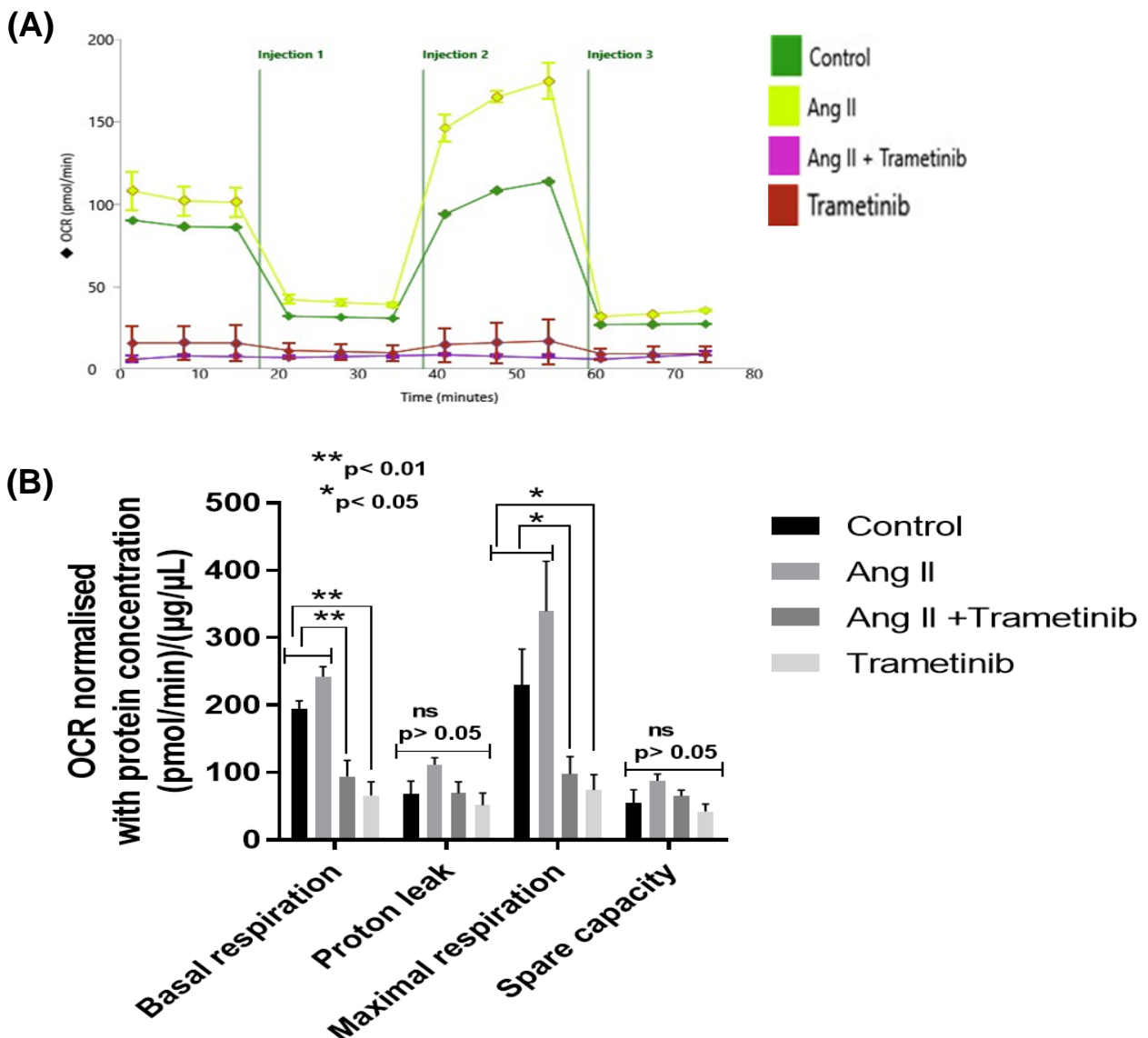


Figure 5.2: Mitochondria stress analysis to determine the OCR of HSVSMCs from T2DM patients after stimulation with Ang II +/- trametinib.

(A) representative time course curve of mitochondrial OCR of HSVSMCs from T2DM patients treated with Ang II +/- trametinib and untreated control.

Injection 1: 20 µl oligomycin (1.5 µM); Injection 2: 22 µl carbonyl cyanide p-(trifluoromethoxy) phenylhydrazone (FCCP) (5 µM); Injection 3: 25 µl rotenone (5 µM) and antimycin A (5 µM) complex.

(B) comparative analysis of normalised peak OCR between treatment groups and untreated control at basal respiration, and after addition of inhibitors of mitochondrial respiration and the uncoupler. Normalised data are presented as mean ± SEM from n=4 biological replicates using HSVSMC samples from different T2DM patients. Ang II: Angiotensin II; OCR: oxygen consumption rate.

Figure 5.3

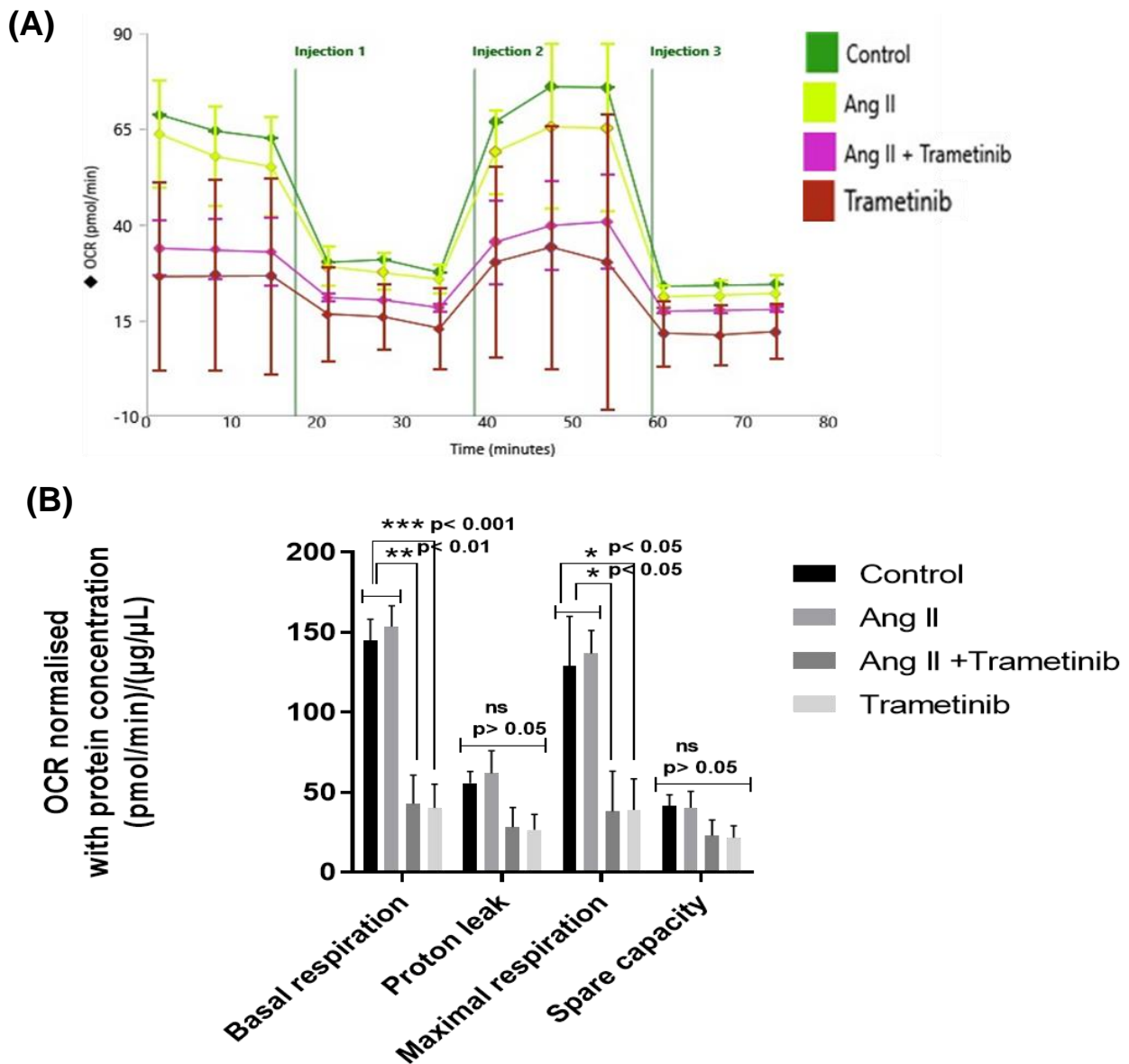


Figure 5.3: Mitochondria stress analysis to determine the OCR of HSVSMCs from non-diabetic patients after stimulation with Ang II +/- trametinib.

(A) representative time course curve of mitochondrial OCR of HSVSMCs from non-diabetic patients treated with Ang II +/- trametinib and untreated control.

Injection 1: 20 µl oligomycin (1.5 µM); Injection 2: 22 µl carbonyl cyanide p-(trifluoromethoxy) phenylhydrazine (FCCP) (5 µM); Injection 3: 25 µl rotenone (5 µM) and antimycin A (5 µM) complex.

(B) comparative analysis of normalised peak OCR between treatment groups and untreated control at basal respiration, and after addition of inhibitors of mitochondrial respiration and the uncoupler. Normalised data are presented as mean ± SEM from n=4 biological replicates using HSVSMC samples from different non-diabetic patients. Ang II: Angiotensin II; OCR: oxygen consumption rate.

Figure 5.4

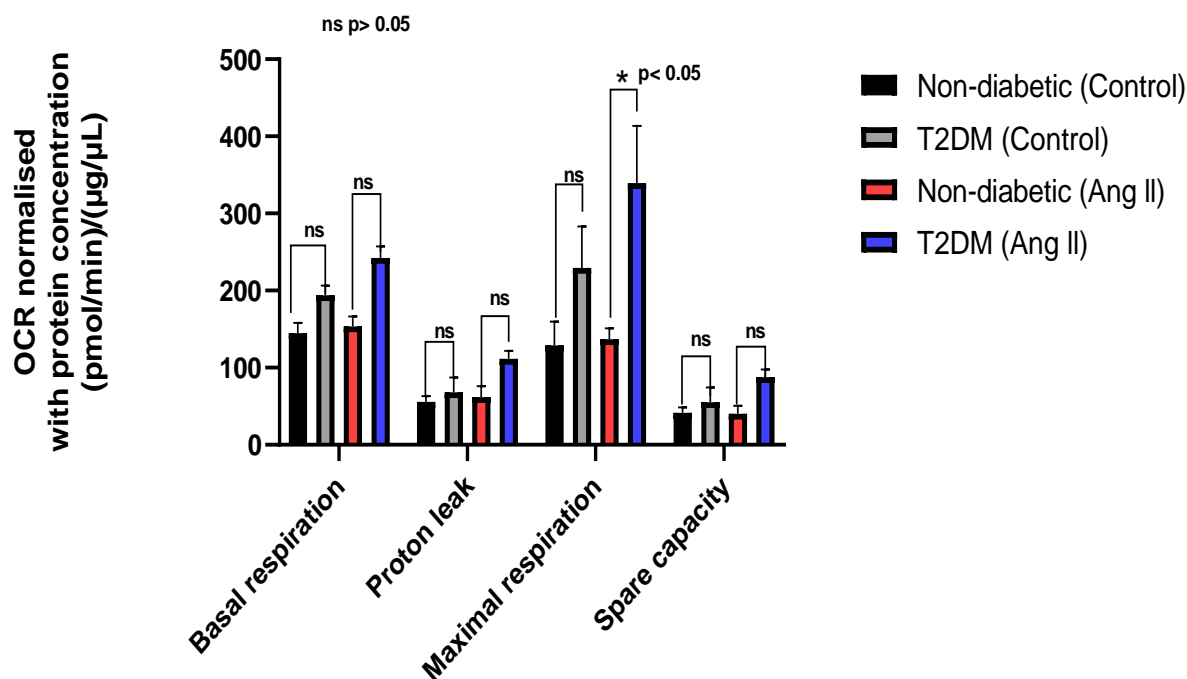


Figure 5.4: Comparison of the OCR of HSVSMCs from T2DM and non-diabetic patients after stimulation with Ang II +/- trametinib.

Comparison of normalised peak OCR of unstimulated and Ang II-stimulated HSVSMCs from T2DM versus non-diabetic control. Normalised data are presented as mean \pm SEM from n=4 biological replicates using HSVSMC samples from different patients. Ang II: Angiotensin II; OCR: oxygen consumption rate.

5.2.2.2 Effect of Ang II +/- trametinib on ECAR of HSVSMCs from T2DM and non-diabetic patients.

The effect of the activation of MAPK/ERK downstream signalling pathway by Ang II and its subsequent inhibition on the ECAR of HSVSMCs is unclear (Doughan et al., 2008). However, (Dikalov and Nazarewicz, 2013) have demonstrated that the inhibition of Ang II improves mitochondrial function. Additionally, there is evidence that Ang II may cause mitochondrial oxidative damage, which could reduce NO bioavailability and increase vascular oxidative stress (Doughan et al., 2008). While these findings emphasise Ang II's role in controlling metabolic homeostasis in VSMCs, its precise effect on ECAR of HSVSMCs has never been documented. In view of this, I have demonstrated in this series of experiments the effects of Ang II +/- trametinib on ECAR of HSVSMCs from T2DM and non-diabetic control.

As shown in Figure 5.5B, Ang II did not cause any significant alteration in the ECAR of HSVSMCs from T2DM patients. However, trametinib significantly reduced ECARs at basal glycolysis ($p < 0.05$ with Ang II stimulation and $p < 0.01$ without Ang II stimulation), glycolytic capacity ($p < 0.05$ with Ang II stimulation and $p < 0.01$ without Ang II stimulation), maximal glycolysis ($p < 0.05$ with Ang II stimulation and $p < 0.01$ without Ang II stimulation), and glycolytic reserve ($p < 0.05$ with Ang II stimulation and $p < 0.01$ without Ang II stimulation) all versus unstimulated and Ang II-stimulated cells, $n=4$) in HSVSMCs from T2DM. Similarly, in HSVSMC from non-diabetic patients, there was no significant alteration to ECAR after stimulation with Ang II. On the other hand, trametinib caused a significant reduction in the ECARs at (basal glycolysis ($p < 0.01$ with or without Ang II stimulation), glycolytic capacity ($p < 0.01$ with or without Ang II stimulation), maximal glycolysis ($p < 0.05$ with or without Ang II stimulation), and glycolytic reserve ($p < 0.05$ with or without Ang II stimulation) all versus unstimulated and Ang II-stimulated cells, $n=4$) in HSVSMCs from non-diabetic patients (Figure 5.6B). However, there was no difference in the ECARs between Ang II-stimulated HSVSMCs from T2DM and non-diabetic when directly compared (Fig 5.7).

Figure 5.5

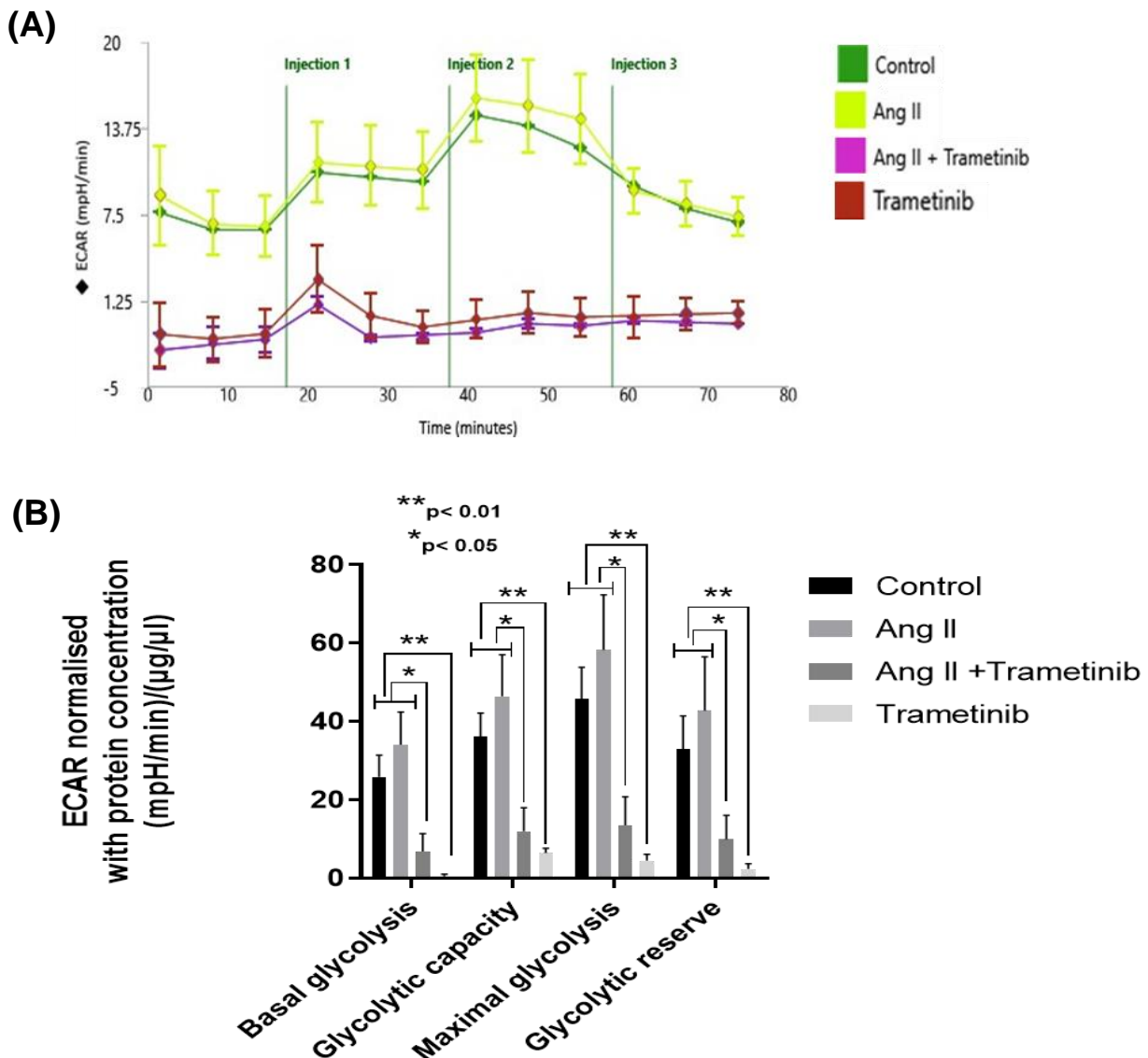


Figure 5.5: Mitochondria stress analysis to determine the ECAR of HSVSMCs from T2DM patients after stimulation with Ang II +/- trametinib.

(A) representative time course curve of ECAR of HSVSMCs from T2DM patients treated with Ang II +/- trametinib and untreated control.

Injection 1: 20 µl oligomycin (1.5 µM); Injection 2: 22 µl carbonyl cyanide p-(trifluoromethoxy) phenylhydrazine (FCCP) (5 µM); Injection 3: 25 µl rotenone (5 µM) and antimycin A (5 µM) complex.

(B) comparative analysis of normalised peak ECAR between treatment groups and untreated control at basal glycolysis, and after addition of inhibitors of mitochondrial respiration and the uncoupler. Normalised data are presented as mean ± SEM from n=4 biological replicates using HSVSMC samples from different T2DM patients. Ang II: Angiotensin II; ECAR: extracellular acidification rate.

Figure 5.6

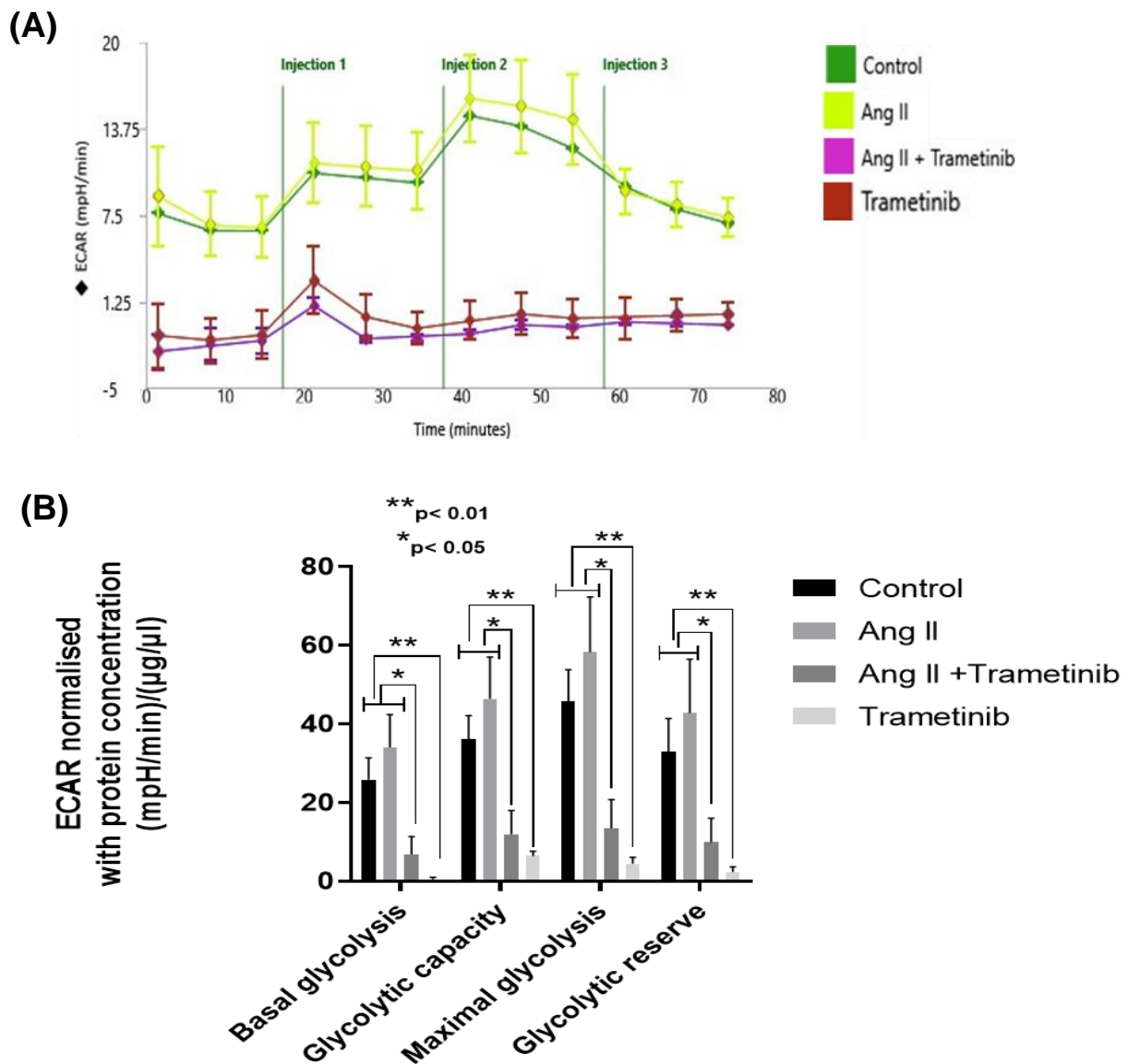


Figure 5.6: Mitochondria stress analysis to determine the ECAR of HSVSMCs from non-diabetic patients after stimulation with Ang II +/- trametinib.

(A) representative time course curve of ECAR of HSVSMCs from non-diabetic patients treated with Ang II +/- trametinib and untreated control.

Injection 1: 20 µl oligomycin (1.5 µM); Injection 2: 22 µl carbonyl cyanide p-(trifluoromethoxy) phenylhydrazone (FCCP) (5 µM); Injection 3: 25 µl rotenone (5 µM) and antimycin A (5 µM) complex.

(B) comparative analysis of normalised peak ECAR between treatment groups and untreated control at basal glycolysis, and after addition of inhibitors of mitochondrial respiration and the uncoupler. Normalised data are presented as mean ± SEM from n=4 biological replicates using HSVSMC samples from different non-diabetic patients. Ang II: Angiotensin II; ECAR: extracellular acidification rate.

Figure 5.7

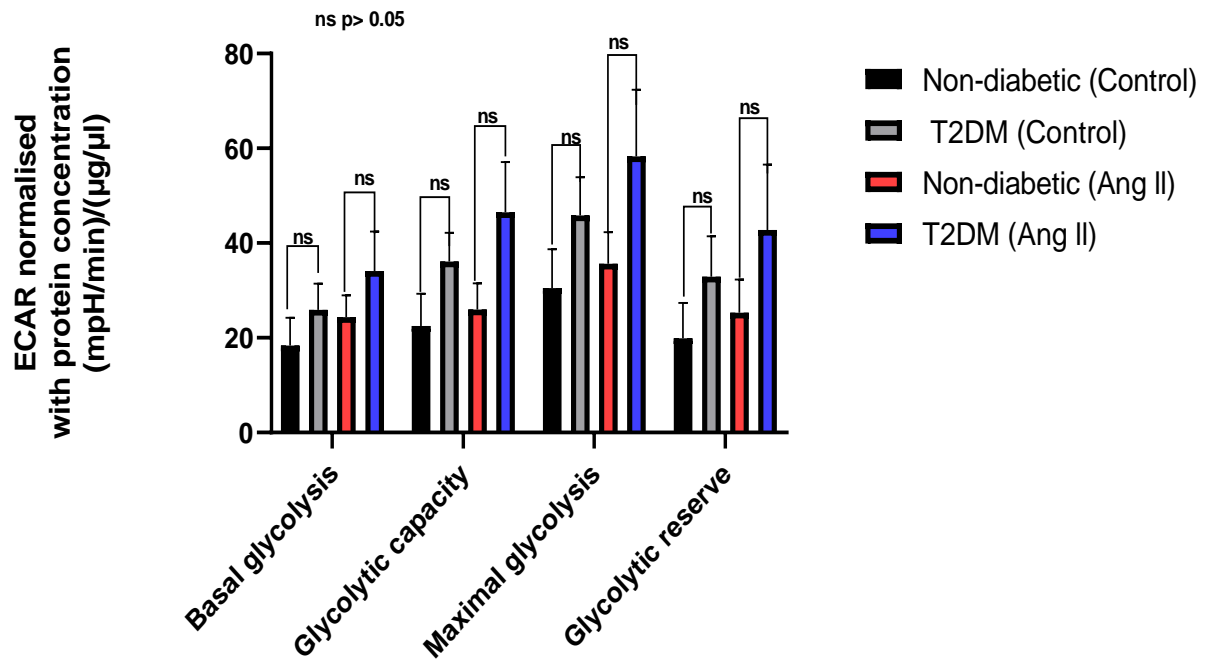


Figure 5.7: Comparison of the ECAR of HSVSMCs from T2DM and non-diabetic patients after stimulation with Ang II +/- trametinib.

Comparison of normalised peak ECAR of unstimulated and Ang II-stimulated HSVSMCs from T2DM versus non-diabetic control. Normalised data are presented as mean \pm SEM from n=4 biological replicates using HSVSMC samples from different patients. Ang II: Angiotensin II; ECAR: extracellular acidification rate.

5.2.2.2 Effect of thrombin +/- MEK inhibitor on OCR and ECAR of HSVSMCs from T2DM and non-diabetic patients.

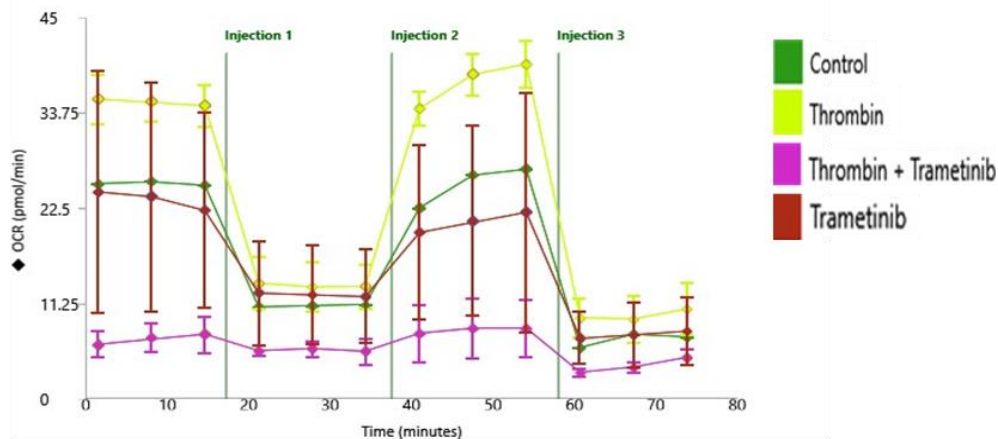
5.2.2.2.1 Effect of thrombin +/- trametinib on OCR of HSVSMCs from T2DM and non-diabetic patients.

Despite the fact that thrombin has been associated with vascular remodelling and a number of potential mechanisms, including activation of the MAPK/ERK downstream signalling pathway (Shapiro et al., 1996; Wang et al., 2004), have been put forth, it is still unknown how thrombin affects mitochondria respiration, a crucial assessor of metabolic function of VSMCs. Considering that the knowledge of the metabolic homeostasis of VSMCs is crucial for targeting vascular remodeling, therefore, I assessed the impact of thrombin +/- trametinib on the OCR of HSVSMCs from T2DM and non-diabetic control in this set of tests.

As shown in Figure 5.8B, thrombin caused a significant increase ($p < 0.05$ versus unstimulated cells, $n=4$) in OCR of HSVSMCs from T2DM patients at maximal respiration. This effect was abolished by trametinib. On the other hand, trametinib significantly reduced ($p < 0.05$ with or without thrombin stimulation versus unstimulated cells, $n=4$) OCR at basal respiration in the cells. Furthermore, in HSVSMCs from non-diabetic, thrombin did not cause any significant alteration in OCR. However, trametinib significantly reduced ($p < 0.05$ with or without thrombin stimulation versus unstimulated cells, $n=4$) at both basal and maximal respiration (Figure 5.9B). Meanwhile, direct comparison of the OCRs of thrombin-treated HSVSMCs from T2DM and non-diabetic patients revealed there was significant increase in OCR at (basal respiration ($p < 0.05$), proton leak ($p < 0.05$), maximal respiration ($p < 0.01$), and spare capacity ($p < 0.05$), $n=4$) (Figure 5.10).

Figure 5.8

(A)



(B)

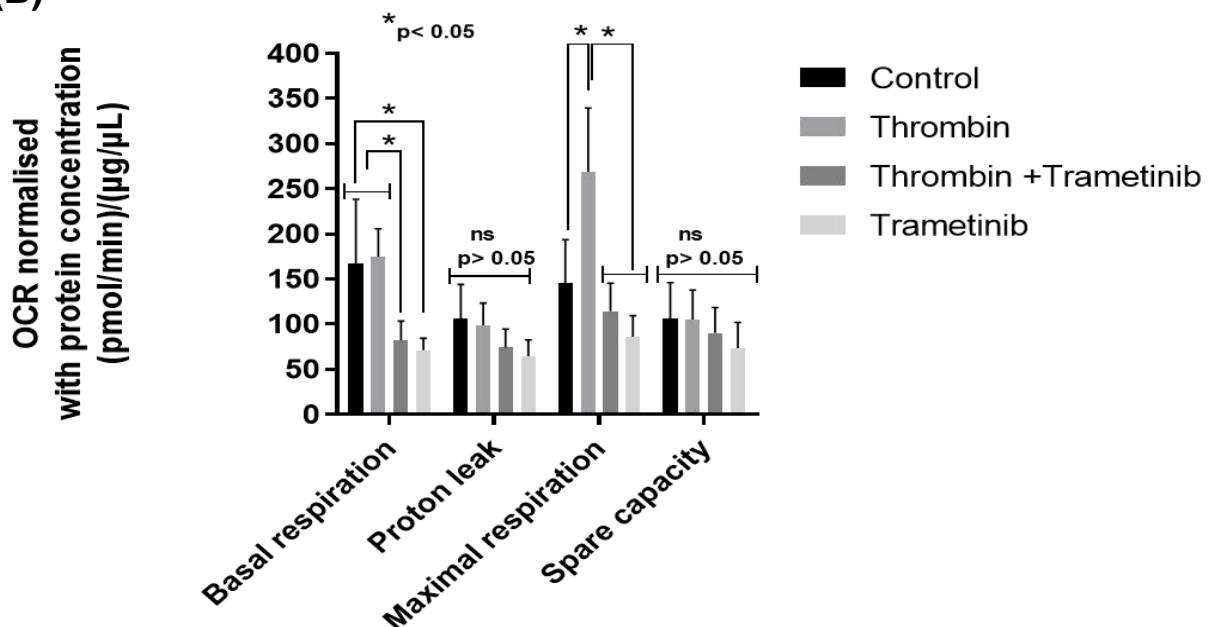


Figure 5.8: Mitochondria stress analysis to determine the OCR of HSVSMCs from T2DM patients after stimulation with thrombin +/- trametinib.

(A) representative time course curve of mitochondrial OCR of HSVSMCs from T2DM patients treated with thrombin +/- trametinib and untreated control.

Injection 1: 20 μ l oligomycin (1.5 μ M); Injection 2: 22 μ l carbonyl cyanide p-(trifluoromethoxy) phenylhydrazine (FCCP) (5 μ M); Injection 3: 25 μ l rotenone (5 μ M) and antimycin A (5 μ M) complex.

(B) comparative analysis of normalised peak OCR between treatment groups and untreated control at basal respiration, and after addition of inhibitors of mitochondrial respiration and the uncoupler. Normalised data are presented as mean \pm SEM from n=4 biological replicates using HSVSMC samples from different T2DM patients. OCR: oxygen consumption rate.

Figure 5.9

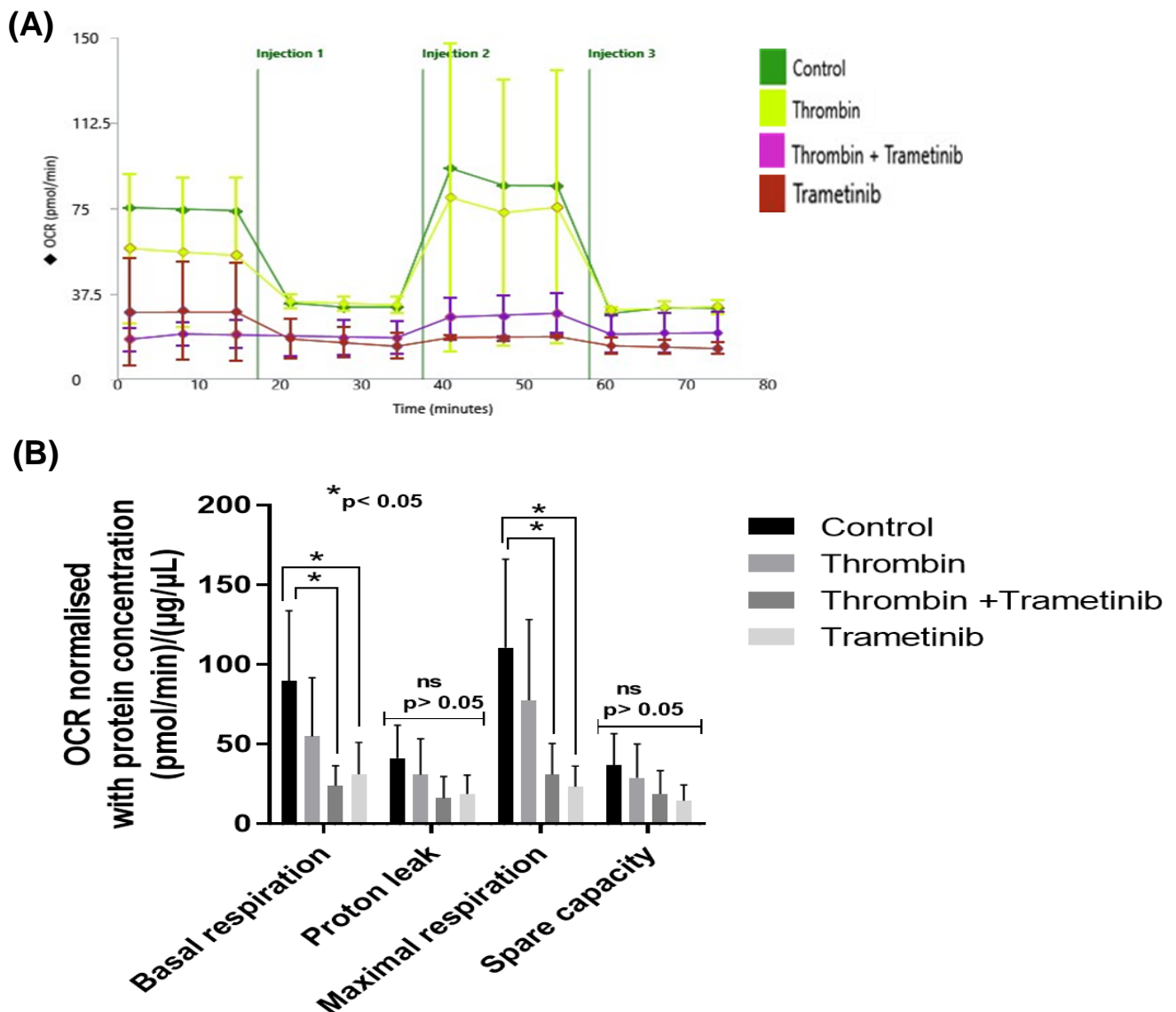


Figure 5.9: Mitochondria stress analysis to determine the OCR of HSVSMCs from non-diabetic patients after stimulation with thrombin +/- trametinib.

(A) representative time course curve of mitochondrial OCR of HSVSMCs from non-diabetic patients treated with thrombin +/- trametinib and untreated control.

Injection 1: 20 μ l oligomycin (1.5 μ M); Injection 2: 22 μ l carbonyl cyanide p-(trifluoromethoxy) phenylhydrazone (FCCP) (5 μ M); Injection 3: 25 μ l rotenone (5 μ M) and antimycin A (5 μ M) complex.

(B) comparative analysis of normalised peak OCR between treatment groups and untreated control at basal respiration, and after addition of inhibitors of mitochondrial respiration and the uncoupler. Normalised data are presented as mean \pm SEM from n=4 biological replicates using HSVSMC samples from different non-diabetic patients. OCR: oxygen consumption rate.

Figure 5.10

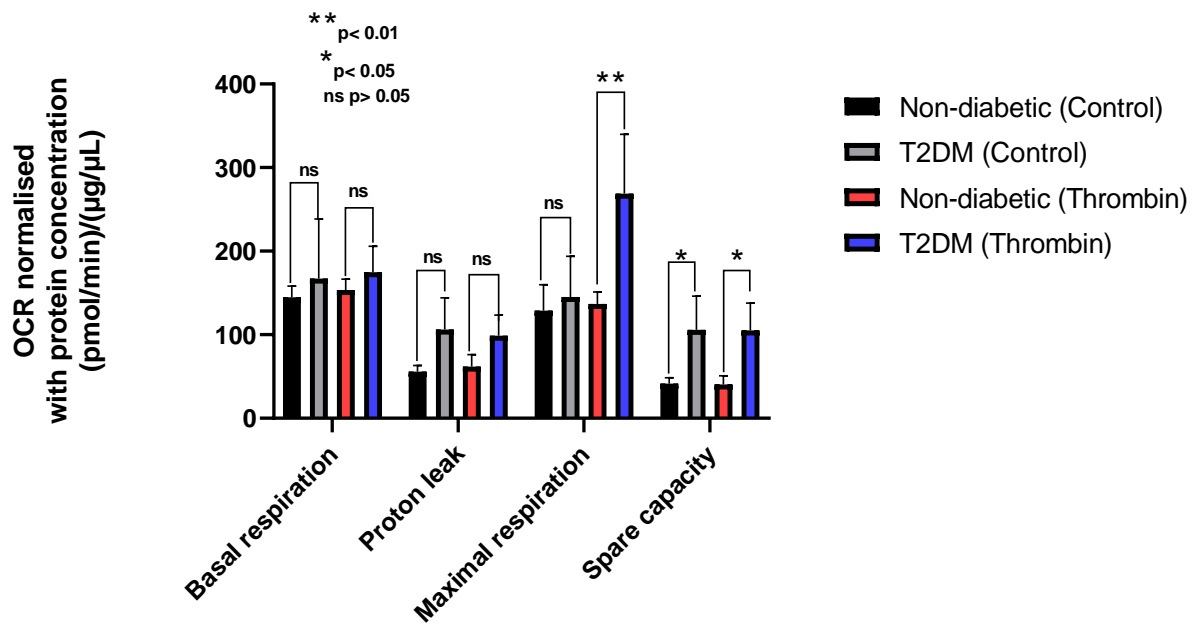


Figure 5.10: Comparison of the OCR of HSVSMCs from T2DM and non-diabetic patients after stimulation with thrombin +/- trametinib.

Comparison of normalised peak OCR of unstimulated and Ang II -stimulated HSVSMCs from T2DM versus non-diabetic control. Normalised data are presented as mean \pm SEM from n=4 biological replicates using HSVSMC samples from different patients. OCR: oxygen consumption rate.

5.2.2.2.2 Effect of thrombin +/- trametinib on ECAR of HSVSMCs from T2DM and non-diabetic patients.

Currently, there are no documented research findings highlighting the effects of the activation vis-à-vis inhibition of the MAPK/ERK pathway on ECAR of VSMCs despite the significance of ECAR as a tool for measuring glycolytic flux in cells (Mookerjee et al., 2015). In this set of studies, HSVSMCs from T2DM and non-diabetic controls were treated with thrombin +/- trametinib, and ECAR, which enables direct quantification of glycolysis, was measured at baseline and following sequential injections of the modulators of mitochondrial respiration: oligomycin (1.5 M), FCCP (5 M), rotenone (5 M), and antimycin A (5 M) complex. Following the experiment, the ECAR values were calculated and normalised using the lysed HSVSMCs' protein concentration.

As shown in Figure 5.11B, thrombin did not cause any significant alteration in the ECAR of HSVSMCs from T2DM patients. However, trametinib significantly reduced ECARs at basal glycolysis ($p < 0.01$ with or without thrombin stimulation), glycolytic capacity ($p < 0.05$ with or without thrombin stimulation), maximal glycolysis ($p < 0.05$ with or without thrombin stimulation), and glycolytic reserve ($p < 0.05$ with or without thrombin stimulation) all versus unstimulated and thrombin-stimulated cells, $n=4$) in HSVSMCs from T2DM. Similarly, in HSVSMCs from non-diabetic patients, there was no significant alteration in ECAR after stimulation with thrombin. On the other hand, trametinib caused a significant reduction in the OCRs at (basal glycolysis ($p < 0.01$ with or without thrombin stimulation), maximal glycolysis ($p < 0.05$ with or without thrombin stimulation), and glycolytic reserve ($p < 0.05$ with thrombin stimulation) all versus unstimulated and thrombin-stimulated cells, $n=4$) in HSVSMCs from non-diabetic patients (Figure 5.12B). Also, after stimulation with thrombin, ECAR in HSVSMCs from T2DM was significant higher at maximal glycolysis ($p < 0.05$, $n=4$) when compared with those from non-diabetic patients (Figure 5.13).

Figure 5.11

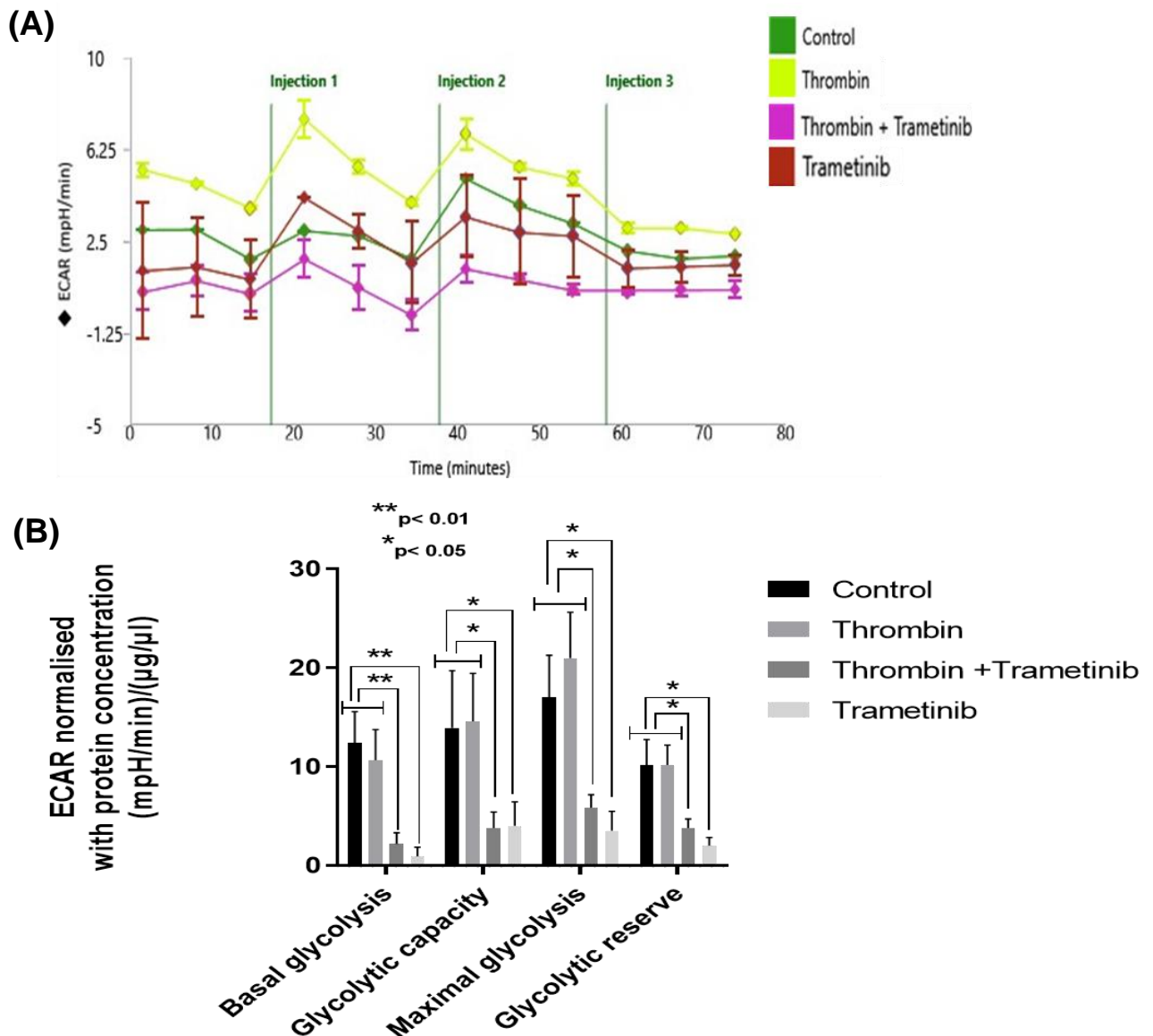


Figure 5.11: Mitochondria stress analysis to determine the ECAR of HSVSMCs from T2DM patients after stimulation with thrombin +/- trametinib.

(A) representative time course curve of ECAR of HSVSMCs from T2DM patients treated with thrombin +/- trametinib and untreated control.

Injection 1: 20 µl oligomycin (1.5 µM); Injection 2: 22 µl carbonyl cyanide p-(trifluoromethoxy) phenylhydrazone (FCCP) (5 µM); Injection 3: 25 µl rotenone (5 µM) and antimycin A (5 µM) complex.

(B) comparative analysis of normalised peak ECAR between treatment groups and untreated control at basal glycolysis, and after addition of inhibitors of mitochondrial respiration and the uncoupler. Normalised data are presented as mean ± SEM from n=4 biological replicates using HSVSMC samples from different T2DM patients. ECAR: extracellular acidification rate.

Figure 5.12

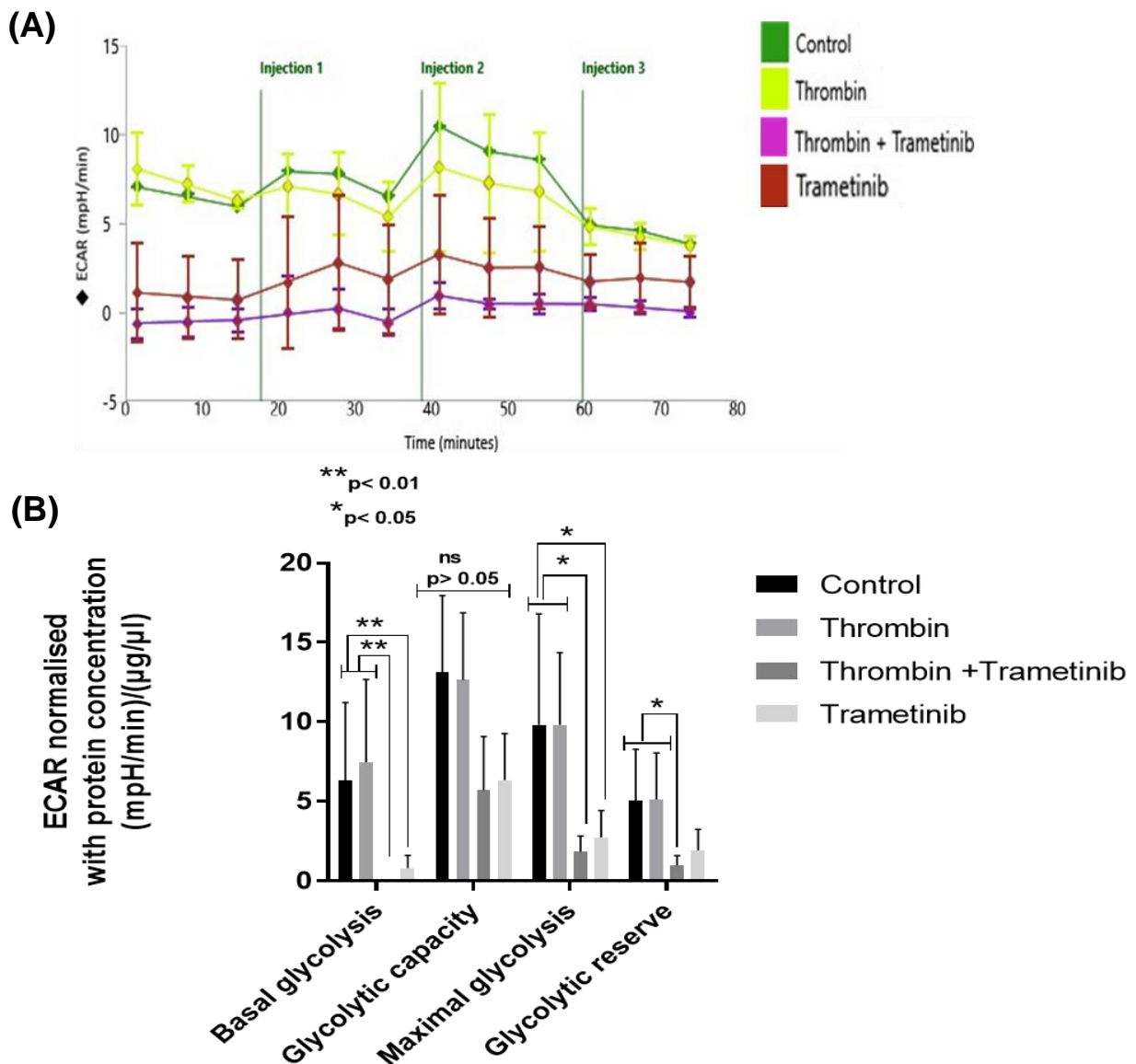


Figure 5.12: Mitochondria stress analysis to determine the ECAR of HSVSMCs from non-diabetic patients after stimulation with thrombin +/- trametinib.

(A) representative time course curve of ECAR of HSVSMCs from non-diabetic patients treated with thrombin +/- trametinib and untreated control.

Injection 1: 20 µl oligomycin (1.5 µM); Injection 2: 22 µl carbonyl cyanide p-(trifluoromethoxy) phenylhydrazone (FCCP) (5 µM); Injection 3: 25 µl rotenone (5 µM) and antimycin A (5 µM) complex.

(B) comparative analysis of normalised peak ECAR between treatment groups and untreated control at basal glycolysis, and after addition of inhibitors of mitochondrial respiration and the uncoupler. Normalised data are presented as mean ± SEM from n=4 biological replicates using HSVSMC samples from different non-diabetic patients. ECAR: extracellular acidification rate.

Figure 5.13

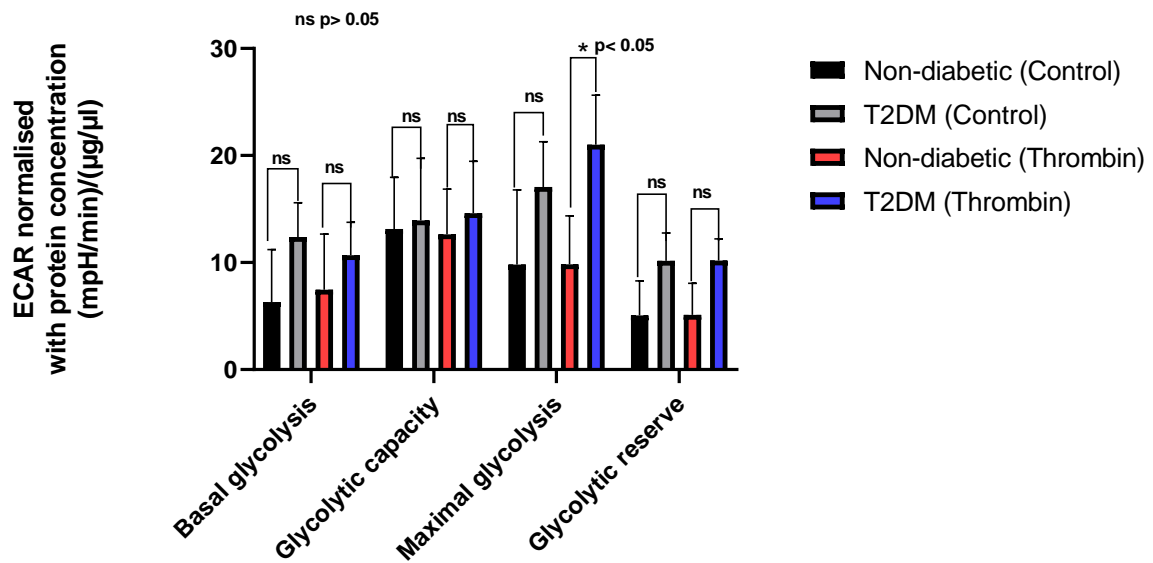


Figure 5.13: Comparison of the ECAR of HSVSMCs from T2DM and non-diabetic patients after stimulation with thrombin +/- trametinib.

Comparison of normalised peak ECAR of unstimulated and thrombin-stimulated HSVSMCs from T2DM versus non-diabetic control. Normalised data are presented as mean \pm SEM from n=4 biological replicates using HSVSMC samples from different patients. Ang II: Angiotensin II; ECAR: extracellular acidification rate.

5.2.3 Alterations in metabolic homeostasis are not associated with any significant levels of agonists' induced phosphorylation of ERK

5.2.3.2 Ang II- and thrombin- induced phosphorylation of ERK of HSVSMCs from T2DM versus non-diabetic patients

Thrombin but not Ang II increased the OCR of HSVSMCs from T2DM patients, but not from non-diabetic controls, according to the findings from this chapter. This raises the intriguing scientific question of what might be causing these changes. Therefore, one of the issues that needs to be resolved is whether the HSVSMCs from T2DM respond intrinsically to these agonists (Ang II and thrombin). It has been demonstrated that HSVSMCs from T2DM patients are fundamentally more proliferative and migratory than those from non-diabetic controls (Madi et al. 2009). However, whether HSVSMCs from T2DM utilise more oxygen to generate ATP than those from non-diabetic controls is not quite apparent. ERK was activated in HSVSMCs from T2DM and non-diabetic control using both Ang II and thrombin to evaluate whether this alteration is intrinsic. The phosphorylation of ERK (p-ERK) in HSVSMCs from patients with T2DM and non-diabetic was then assessed and compared. Results showed that the levels of Ang II- and thrombin-stimulated MEK-mediated ERK phosphorylation are not significantly different in response to altered changes (Figures 5.14 and 5.15 respectively).

Figure 5.14

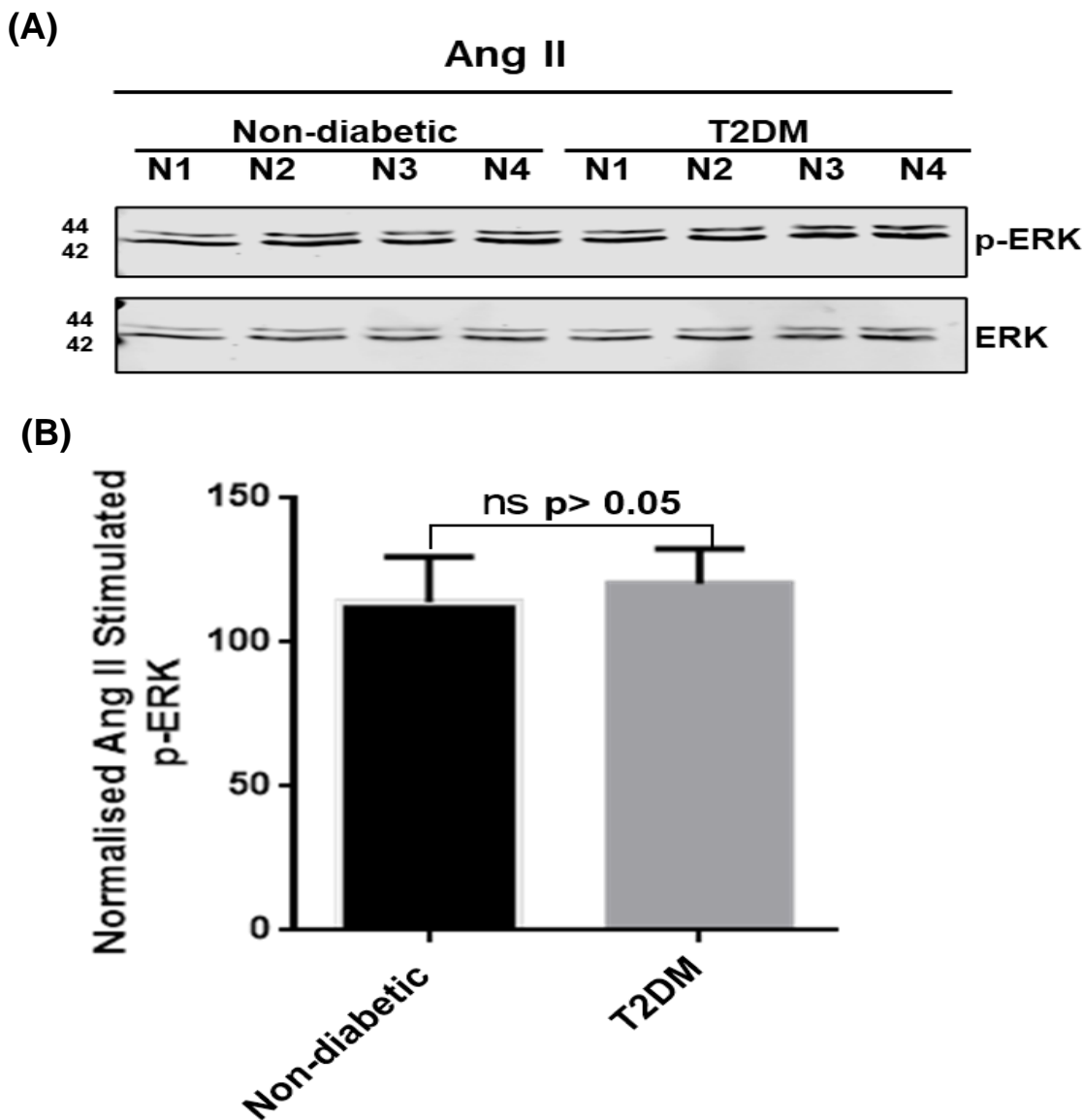


Figure 5.14: Ang II-stimulated phosphorylation of ERK in HSVSMCs from T2DM and non-diabetic patients.

(A) Upper panel: representative western blot of Ang II-stimulated phosphorylation of ERK (44/42kDa) in HSVSMCs from T2DM and non-diabetic patients.

Lower panel: expression of total ERK (44/42kDa)

(B) Densitometric analysis of Ang II-stimulated p-ERK at both 44/42kDa in HSVSMCs from T2DM and non-diabetic normalised to total ERK at both 44/42kDa. Data are four (n=4) biological replicates and are expressed as mean \pm SEM. Ang II: Angiotensin II.

Figure 5.15

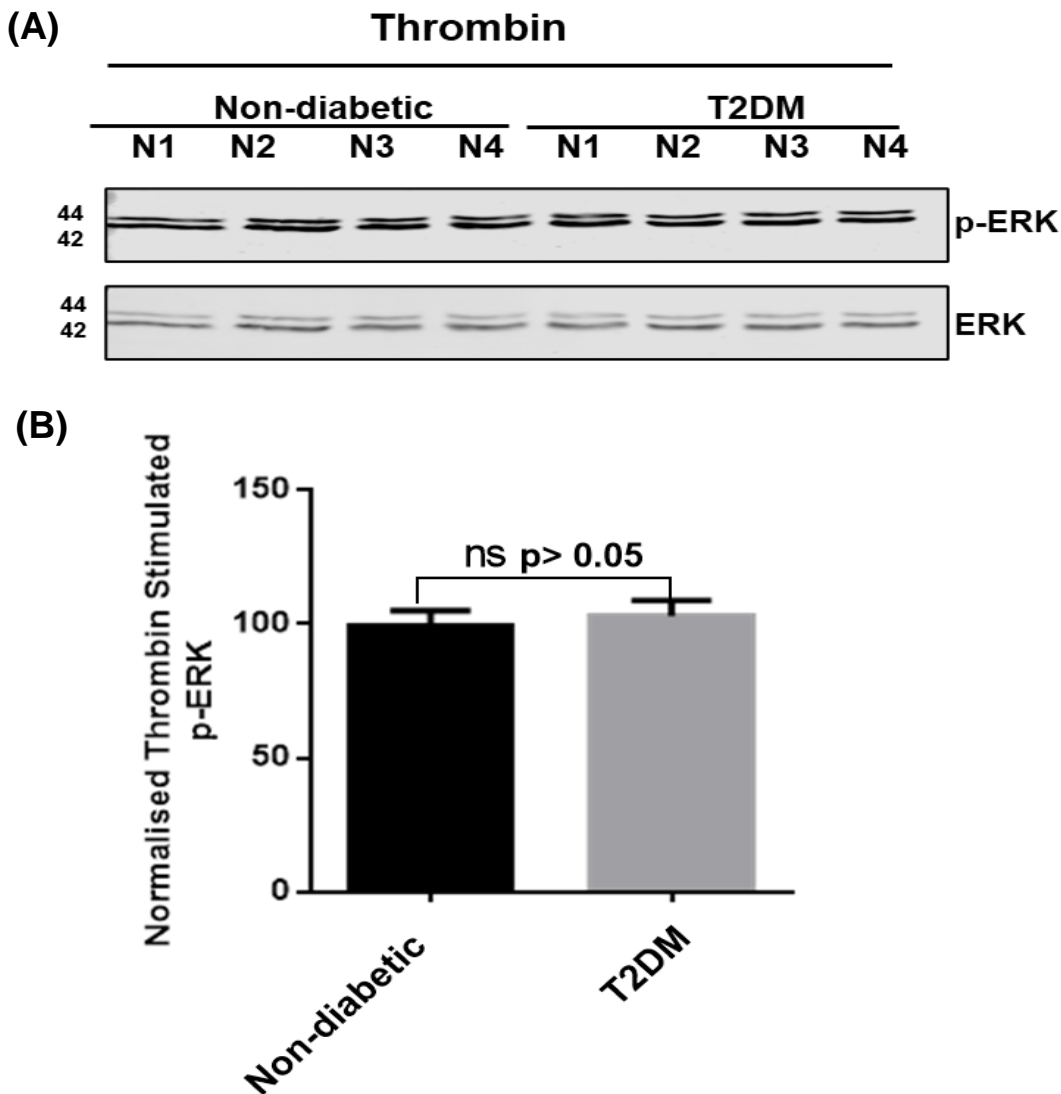


Figure 5.15: Thrombin-stimulated phosphorylation of ERK in HSVSMCs from T2DM and non-diabetic patients.

(A) **Upper panel:** representative western blot of Ang II-stimulated phosphorylation of ERK (44/42kDa) in HSVSMCs from T2DM and non-diabetic patients.

Lower panel: expression of total ERK (44/42kDa)

(B) Densitometric analysis of Ang II-stimulated p-ERK at both 44/42kDa in HSVSMCs from T2DM and non-diabetic normalised to total ERK at both 44/42kDa. Data are four (n=4) biological replicates and are expressed as mean \pm SEM. Ang II: Angiotensin II.

5.2.4. mtDNA copy number in HSVSMCs from T2DM and non-diabetic patients after treatments with Ang II and thrombin +/-trametinib

The OCR of HSVSMCs from T2DM, but not from non-diabetic, was significantly increased by thrombin via a MEK/ERK-dependent mechanisms (Figures 5.2 and 5.8). Just as in Chapter 4, it is important to determine whether this rise is connected to the HSVSMCs' mtDNA copy number increasing in response to these activators. Therefore, the copy number of the mitochondrially-encoded gene COI under various treatment conditions was determined using qPCR as detailed in 2.2.5.6. As already highlighted in 4.2.4, COI was used as mtDNA marker because it is a standardised single molecular marker for the classification of animal species and is excellent at distinguishing between vertebrate and invertebrate species (Hebert et al., 2003; Rodrigues et al., 2017).

As shown in Figure 5.16A, there is no significant difference in the mtDNA copy number in HSVSMCs from T2DM patients after treatments with Ang II +/-trametinib compared with untreated control. Data were normalised to 18S and B-actin. Also, in the HSVSMCs from non-diabetic patients, there is no significant difference in the mtDNA copy number after treatment with Ang II +/-trametinib compared with untreated control. Data were also normalised to 18S and B-actin (Figure 5.16B).

Furthermore, as shown in Figure 5.17A, there is no significant difference in the mtDNA copy number in HSVSMCs from T2DM patients after treatments with thrombin +/-trametinib compared with untreated control. Data were normalised to 18S and B-actin. On the other hand, there is no significant difference in the mtDNA copy number in HSVSMCs from non-diabetic patients after treatment with thrombin +/-trametinib compared with untreated control. The mtDNA copy numbers were normalised to 18S and B-actin (Figure 5.17B).

Figure 5.16

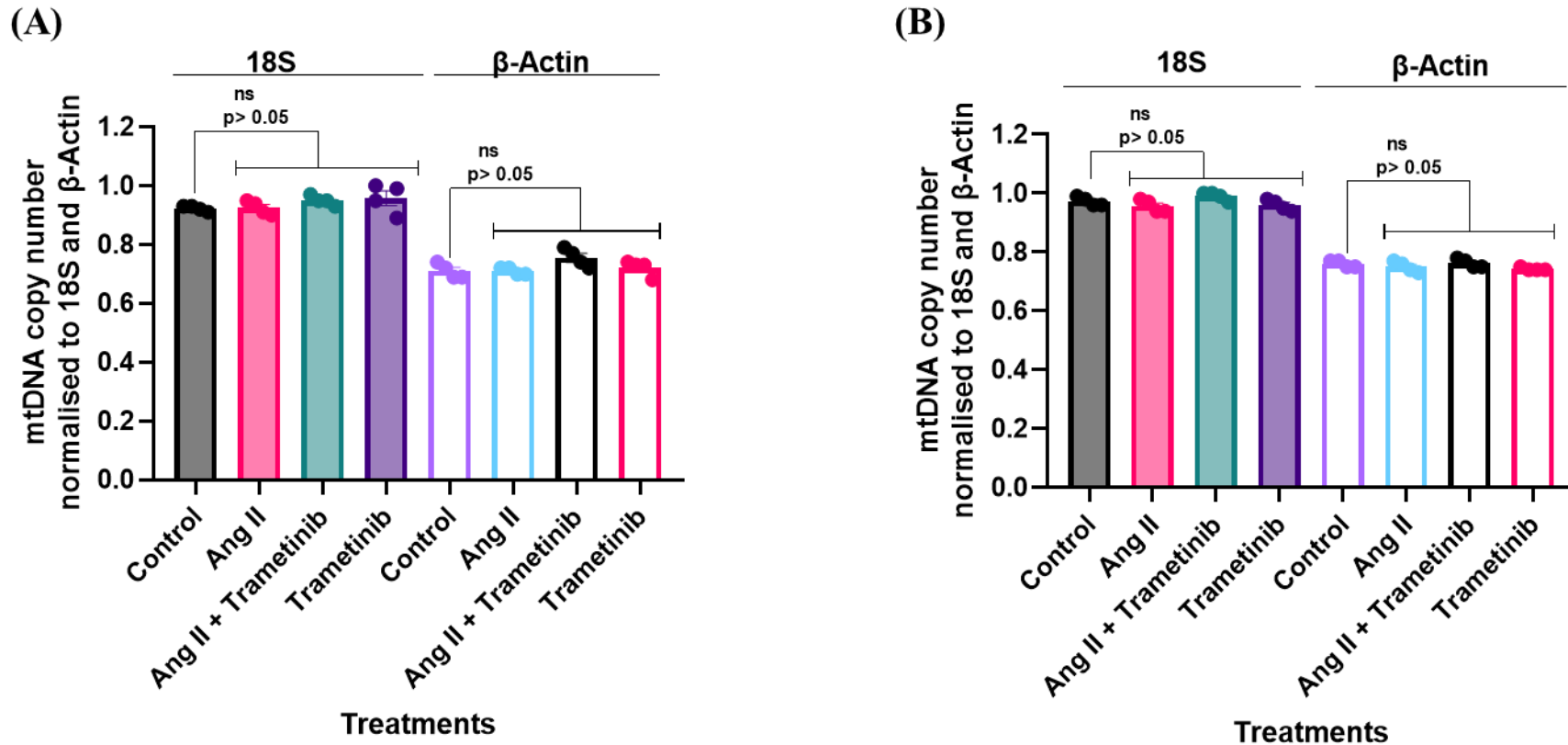


Figure 5.16: mtDNA copy number of HSVSMCs from T2DM patients after treatment with Ang II +/- trametinib. mtDNA copy number of mitochondrially encoded gene COI as a marker of mtDNA copy number in (A) T2DM, and (B) non-diabetic patients, normalised to 18S and β -Actin. Normalised data from different treatment conditions were compared with data from normalised untreated control for statistical difference. Data are presented as mean \pm SEM from n=4 experiments using HSVSMC from different patients. Ang II: Angiotensin II

Figure 5.17

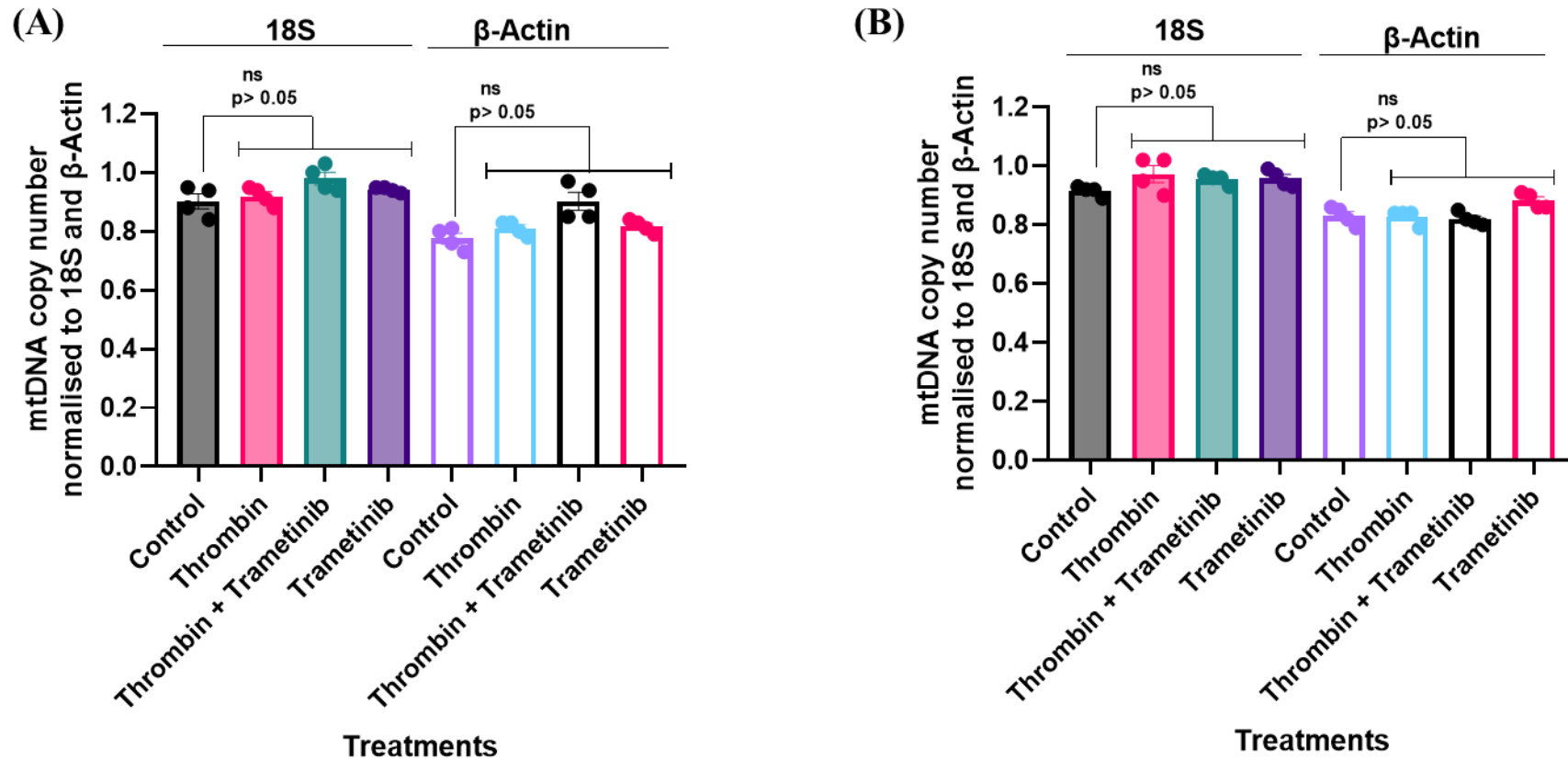


Figure 5.18: mtDNA copy number in HSVSMCs from T2DM patients after treatment with thrombin +/- trametinib. mtDNA copy number of mitochondrially encoded gene COI as a marker of mtDNA copy number in (A) T2DM, and (B) non-diabetic patients, normalised to 18S and β -Actin. Normalised data from different treatment conditions were compared with data from normalised untreated control for statistical difference. Data are presented as mean \pm SEM from n=4 experiments using HSVSMC from different patients.

5.3 Discussion

Similar to Chapter 4, in this chapter, I assessed how two activators of the MAPK/ERK signalling pathway (Ang II and thrombin) modify the metabolic profile (OCR and ECAR) of HSVSMCs from T2DM patients and non-diabetic controls. These activators have also been connected to vascular dysfunction, a characteristic of VGF (Aibibula et al., 2018; Chen et al., 2009; Yoshizumi et al., 2019). To achieve my objectives, I assessed the mitochondrial OCR and ECAR of HSVSMCs from T2DM and non-diabetic controls with or without treatment with these activators. Following this, I compared these results to determine if there was any obvious change in order to evaluate the impact of these activators on the metabolic balance. I also employed trametinib to inhibit the downstream activation of MAPK/ERK pathways by these agonists in order to further understand this characterisation and offer possible insights for therapeutic development (Fig 5.1A).

To determine the right concentration of trametinib to utilize for downstream inhibition of the MAPK/ERK in the series of experiments contained in this Chapter, intrinsic activation of ERK was inhibited by varied concentrations (0.1 nM, 1 nM, 10 nM, and 100 nM) of trametinib. Unlike in the previous Chapter where IL-6 was used to induce phosphorylation of STAT3, here, no agonist was used to induce phosphorylation of ERK. This is so because ERK proteins are capable of autophosphorylation activity, which is directed primarily toward the Tyr residue, although this does not stabilize the active conformation to induce efficient catalysis (Seeger *et al.*, 1991; Emrick *et al.*, 2001; Levin-Salomon *et al.*, 2008). As shown above (Figures 5.1A and B), 10 nM was determined as the concentration of trametinib that caused significant inhibition of the activation of ERK in HSVSMCs. However, the concentration of trametinib that induced this considerable inhibition varied for different cell types. It had been previously demonstrated that trametinib caused significant inhibition of MAPK/ERK pathway at 100 nM in *EGFR^{mut}* cells (Brägelmann et al., 2021). Meanwhile, (Leung et al., 2014) demonstrated that trametinib inhibited MAPK/ERK in MCF-7 and MDA-MB-231 breast cancer cell lines at 5 μ M and 50 μ M respectively after 24 hr treatment. Therefore, my understanding is that this is the first instance of this been described in HSVSMC.

From my findings, Ang II did not cause any noticeable alteration in OCR of HSVSMCs from both T2DM (Figure 5.2) and non-diabetic (Figure 5.3) patients. However, trametinib reduced OCR at basal and maximal respiration of HSVSMCs from both T2DM (Figure 5.2) and non-diabetic (Figure 5.3) patients. This is suggestive that mitochondrial respiration is modulated through the MAPK/ERK downstream signalling pathway. Furthermore, OCR of HSVSMCs from T2DM and non-diabetic patients with or without Ang II stimulation do not significantly differ from each other (Fig 5.4). While this is the first time this study will be described in HSVSMCs, (Chang et al., 2018) have previously demonstrated that Ang II caused a reduction in the OCR of HUVECs. In this study, (Chang et al., 2018) demonstrated that Ang II reduced OCR at basal and maximal respiration compared with the control group. However, from my findings, Ang II did not cause any significant alteration in HSVSMCs unlike the findings of (Chang et al., 2018). While the exact reason for this difference is unclear, however, the obvious is that my experiment and that of (Chang et al., 2018) were described in two different cell types.

In addition, MAPK/ERK pathway can indirectly modulate cellular metabolic homeostasis through tumor-suppressor liver kinase B1-induced activation of AMPK, a crucial regulator of energy homeostasis, under low-energy situations in most cellular contexts (Hardie et al., 2016). When activated, AMPK blocks nearly all of the biosynthetic pathways required for cell growth, reducing the amount of ATP used, and activates catabolic pathways that produce ATP, enabling cells to regain energy equilibrium (Hardie et al., 2016). Conversely, activated AMPK has been proven to increase glycolysis and glucose absorption in specific situations (Wu et al., 2013). Furthermore, (Friederich-Persson and Persson, 2020) showed that Ang II decreased mitochondrial OCR of the kidney cortex from both normal and type 1 diabetic rats via AT2 receptor-mediated nitric oxide release. (Friederich-Persson and Persson, 2020) further demonstrated that whereas Ang II via AT1 receptors increases OCR at mitochondria leak respiration in diabetic animals, AT1 receptors do not influence mitochondria function in control rats. These findings (Friederich-Persson and Persson, 2020; Hardie et al., 2016; Wu et al., 2013) suggest that Ang II could elicit its activity through several signalling pathways which yield a multi-faceted result, however, in the current study detailed in this Chapter, I have looked at the effect of Ang II as a known activator of the MAPK/ERK signalling pathways where it seemed not to have caused any significant alteration in the OCR of HSVSMCs from both T2DM and non-diabetic patients.

Also, while there were no significant alterations in ECAR of HSVSMCs from both T2DM (Fig 5.5) and non-diabetic patients (Fig 5.6) after stimulation with Ang II, however, trametinib

caused a significant reduction in ECAR in HSVSMCs from both T2DM and non-diabetic patients (Figure 5.5 & Figure 5.6). In the HSVSMCs from both T2DM and non-diabetic patients, this trametinib-induced decrease in ECAR was consistent throughout the four points of regulation of mitochondrial respiration (basal glycolysis, glycolytic capacity, maximal glycolysis, and glycolysis reserve). A direct comparison of the ECAR of HSVSMCs from T2DM and non-diabetic patients also revealed no difference with or without Ang II stimulation (Fig 5.7).

On the other hand, thrombin, the second activator of the MAPK/ERK pathways investigated in this Chapter caused a significant increase in OCR of HSVSMCs from T2DM patients; this increase was attenuated by trametinib (Figure 5.8). Conversely, there was no noticeable increase in the OCR of HSVSMCs from non-diabetic (Figure 5.9). Meanwhile, trametinib reduced the OCR of HSVSMCs from both T2DM (Figure 5.8) and non-diabetic (Figure 5.8) patients. Direct comparison of the OCR of HSVSMCs from T2DM and non-diabetic patients revealed that thrombin significantly increased the OCR of HSVSMCs from T2DM patients compared to non-diabetic control subjects at maximal glycolysis and spare capacity (Figure 5.10).

Prior study (Ravi et al., 2015) has revealed that thrombin triggered a 25% rise in OCR in platelets. Furthermore, (Sowton et al., 2018) also showed that after stimulation of platelets with thrombin, OCR significantly increased when compared with unstimulated platelets. While these two studies (Ravi et al., 2015; Sowton et al., 2018) used platelets from healthy donors, similar studies using unstimulated platelets from T2DM patients showed a decrease in OCR when compared with unstimulated platelets from healthy donors (Avila et al., 2012). Comparing these with the findings from my experiments that showed an increase in the OCR of HSVSMCs from T2DM following stimulation with thrombin, meanwhile, there was no discernible rise in the OCR of HSVSMCs from non-diabetic patients. The fact that trametinib attenuated this increase in OCR suggests that thrombin elicited its effect through the MAPK/ERK pathway. Although the underlying mechanism is not entirely clear, however, this suggests that activation of the MAPK/ERK could increase cellular OCR.

Trametinib, the MEK1/2 inhibitor employed in this series of experiments not only abolished the thrombin-induced increase in OCR of HSVSMCs from T2DM (Figure 5.8), but also reduced the OCR of HSVSMCs from both T2DM and non-diabetic patients (Figures 5.8 and 5.9). Trametinib binds to unphosphorylated MEK1/2 preferentially, blocking Raf-dependent

phosphorylation and activation of MEK (Gentry et al., 2013). While it might be premature to assume that the ability of trametinib to abolish the MAPK/ERK mediated increase in OCR in HSVSMCs from T2DM patients would be of any clinical benefit, however, trametinib used alone or in combination with dabrafenib is a clinical tool used to manage different forms of melanoma (Kim et al., 2013). It inhibits the MAPK/ERK pathway to provide its anti-melanoma effects, however, this is tainted by several on-target side effects such as cardiomyopathy and acute pneumonitis due to non-specific suppression of the MAP/ERK signalling (Chapman et al., 2014).

Furthermore, thrombin did not cause any significant alteration in the ECAR of HSVSMCs from both T2DM and non-diabetic patients (Figure 5.11 & Figure 5.12). Trametinib, however, caused a decrease in ECAR in HSVSMCs from both T2DM and non-diabetic patients (Figure 5.11 and Figure 5.12). This trametinib-induced reduction in ECAR was constant at all four modulating points (basal glycolysis, glycolytic capacity, maximal glycolysis, and glycolysis reserve) of mitochondrial respiration in the HSVSMCs of both T2DM and non-diabetic patients. There was a noticeable increase in the ECAR of HSVSMCs from T2DM patients when compared with non-diabetic controls when they were both stimulated with thrombin (Figure 5.13).

In addition to its role in controlling cell proliferation and survival, the MAPK/ERK pathway can regulate glucose metabolism (Papa et al., 2019; Cairns et al., 2011; Pavlova and Thompson, 2016). When activated, the MAPK/ERK signalling pathway has been shown to promote Warburg effect (Yang et al., 2012). The Warburg-like metabolic phenotype, characterised by a high rate of glucose uptake and conversion to lactate under aerobic conditions, is known to be present in high-proliferating and migrating cells (Hsu and Sabatini, 2008; Lunt and Vander Heiden, 2011; Senyilmaz and Teleman, 2015) which are characteristics of VSMCs from T2DM patients (Casella et al., 2015; Choi et al., 2021, Reddy et al., 2016). The fact that aerobic glycolysis is an inefficient metabolic pathway that produces less ATP per glucose molecule than OXPHOS and, obviously, cannot meet the high cellular demand for energy required during rapid cell proliferation is one of the most significant debates surrounding this metabolic phenotype (Papa et al., 2019). Thus, it would seem that the quick synthesis of ATP makes up for the hypothetically inefficient energy production of glycolysis (Locasale and Cantley, 2011; Lunt and Vander Heiden, 2011). Furthermore, it is thought that proliferating cells with a high need for reducing equivalents (like NADPH) and cellular macromolecules will benefit from an increase in glycolysis (Locasale, 2016). Given that HSVSMCs from T2DM patients had an

ECAR that was significantly ($p < 0.05$) greater than HSVSMCs from non-diabetic controls, the Warburg effect may thus be responsible for the enhanced ECAR observed after activating the MAPK/ERK pathway with thrombin.

Additionally, it must be determined whether these alterations in OCR and ECAR observed in HSVSMCs from T2DM patients in response to these agonists (Ang II and thrombin) are intrinsic. This is because it is unclear whether the observable variations in the OCR and ECAR of HSVSMCs from T2DM patients are attributable entirely or in part to T2DM. According to (Figures 5.14 and 5.15), when compared to non-diabetic controls, the visible changes in the OCR and ECAR of HSVSMCs from T2DM patients are not related with any appreciable difference in levels of Ang II- and thrombin-stimulated MEK-mediated ERK phosphorylation. However, as previously stated in Chapter 4, this set of data is limited because there was no unstimulated control. Therefore, to further support these findings, additional functional studies relating these modifications to T2DM, as described in Chapter 6, are needed.

One of the drawbacks of the research covered in this chapter is the possibility that Ang II activates additional pathways that could offset its effects on the metabolic homeostasis of HSVSMCs via activation of the MAPK/ERK signalling pathway. For instance, even if the activation of MAPK/ERK pathway could boost OCR, its AT₂ receptor-mediated production of nitric oxide effect, which lowers mitochondria OCR, could make up for this (Friederich-Persson and Persson, 2020). Since it was not an objective in this Chapter, we are unable to determine the magnitude of how the AT receptor mediated function of Ang II impacts its action through MAPK/ERK pathway. Furthermore, it is not known how T2DM might modify the MAPK/ERK signalling pathway inherently. The fact that this system does not function linearly is made apparent by the fact that, for instance, B-Raf causes muscle precursor cell migration without ERK activation (Shin et al., 2016). Also, deregulated cells may potentially become resistant to specific Raf/MEK inhibitors, as is known from cancer therapy, showing a decreased susceptibility as a result of reprogramming of this signalling cascade (Karoulia et al., 2017; Wu and Park, 2015). Additionally, alterations to the activation or inhibition sites in the master gatekeepers MEK1/2 may not always follow expected phosphorylation patterns, pointing to a much more intricate control of this extensively researched pathway (Delaney et al., 2002; Kubin et al., 2017).

Furthermore, as it has long been recognised that mitochondrial dysfunction contributes significantly to the underlying pathogenesis of a number of age-related diseases, including

cancer, CVD, and neurodegenerative diseases (Longchamps et al., 2020; Gómez-Serrano et al., 2018). Hence, mtDNA copy number is increasingly used to evaluate the role of mitochondria in disease as its measurement is a straightforward proxy for mitochondrial function (Longchamps et al., 2020). Higher levels of mtDNA copy number have been linked to lower incidence of several cancers, including breast, kidney, liver, and colorectal cancer (Ashar et al., 2017; Chen et al., 2014); neurodegenerative diseases like Parkinson's and Alzheimer's (Pyle et al., 2016; Wei et al., 2017); and CVDs like CAD and stroke (Renik et al., 2016; Hertweck et al., 2017; Thyagarajan et al., 2012). Furthermore, it has regularly been demonstrated that the number of mitochondrial copies in peripheral blood is higher in women, decreases with age, and has a negative correlation with the WBC count (Knez et al., 2016; Tin et al., 2016). All of the above findings give a justification for the use of mtDNA copy number as a dependable tool to assess genetic characteristics.

mtDNA copy number, therefore, provides an opportunity to determine changes not only in disease conditions but as a genetic marker. In this experiment, I used the mtDNA copy number to investigate if the observed increase in OCR and ECAR detected in HSVSMCs from T2DM after the activation of the MAPK/ERK signalling pathways was caused by an increase in mtDNA copy number or by other factors that are unknown but may be related to T2DM. From my results, there were no significant changes in the mitochondrial DNA copy number after treatment with the different treatment conditions as described in 2.8.1. Therefore, while it is not entirely clear, the observed increase in OCR and ECAR in HSVSMCs from T2DM and not from non-diabetic control could be due to the T2DM status.

Like Chapter 4, I performed a qPCR study utilising COI as the mtDNA marker to further determine if the observed changes in OCR and ECAR of HSVSMCs from T2DM or non-diabetic patients following stimulation with Ang II and thrombin +/- trametinib are connected with a potential treatment-induced increase in mtDNA copy number. However, according to my findings (Figures 5.16 and 5.17), the various treatment conditions as described in 2.8.1 did not result in any significant changes in the mtDNA copy number when compared with untreated cell control. Therefore, further studies could help assess if these alterations are entirely or partly due to T2DM.

5.4 Summary and conclusion

In this chapter, I examined Ang II- and thrombin- MAPK/ERK mediated modulation of metabolic profile (OCR and ECAR) of HSVSMCs from T2DM and non-diabetic patients. These activators (Ang II and thrombin) of the MAPK/ERK signalling pathway have been linked to vascular remodelling that is responsible for multiple cardiovascular events (Chen et al., 2009; Yoshizumi et al., 2019). To further appreciate the impact of this downstream signalling pathway on the OCR and ECAR, being indices used to evaluate mitochondria function in this project, I used trametinib a known MEK1/2 inhibitor to inhibit the pathway. Results from my experiments which are detailed in this Chapter showed that thrombin, at maximum respiration, caused a significant increase in the OCR of HSVSMCs from T2DM patients but not in those from non-diabetic controls. However, this noticeable increase was attenuated by trametinib. Trametinib also reduced OCR and ECAR in HSVSMCs from both T2DM and non-diabetic patients. Furthermore, my findings suggest that HSVSMCs from T2DM utilised more oxygen than those from non-diabetic controls when stimulated with Ang II and thrombin. My findings also suggest that these alterations seen in T2DM patients are not associated with any significant difference in levels of Ang II- and thrombin-stimulated MEK-mediated Erk phosphorylation when compared with non-diabetic controls which is suggestive of a T2DM-dependent alteration. However, this data is limited because unstimulated control was not used which is an experimental flaw. Additionally, as shown by qPCR analysis, there is no difference in the number of mtDNA copies in the HSVSMCs from T2DM patients and non-diabetic controls following drug treatments when compared to untreated cells, demonstrating that these alterations are not connected to a treatment-induced increase in mtDNA copies. Putting these together, these findings suggest a MAPK/ERK mediated modulation of mitochondrial function (OCR and ECAR), more so that trametinib abolished these alterations. Thus, it can be explored as a possible target for the development of drugs to treat T2DM-dependent vascular dysfunction.

Chapter 6: JAK/STAT- and MAPK/ERK- mediated production of mROS in HSVSMCs.

6.1 Introduction

Cardiometabolic disorders such as T2DM, atherosclerosis, and vascular restenosis have been linked to oxidative stress, which is an imbalance between ROS production and antioxidant buffering capacity (Akhigbe and Ajayi, 2021). At physiological levels, ROS act as a signalling mediator and controls many physiological processes, including the growth, proliferation, and migration of ECs and VSMCs, the formation and growth of new blood vessels, vascular tone, host defence, and genomic stability (Akhigbe and Ajayi, 2021). However, at pathophysiological levels, it alters cellular redox status and contributes to the onset of cardiometabolic disorders (Akhigbe and Ajayi, 2021). More so, the increase in the generation of free radicals in the heart is caused by several mechanisms which include decreased antioxidant capacity and cardiac metabolic memory, increased fatty acid oxidation, increased NOX activity, and mitochondrial malfunction and uncoupling (Akhigbe and Ajayi, 2021; Abete et al., 1999).

ROS have at least one oxygen atom in every molecule but are more reactive than molecular oxygen, and they include free radicals like superoxide, hydroxyl radicals, and singlet oxygen as well as non-radical species like hydrogen peroxide, which is created when oxygen is partially reduced (Giorgio et al., 2007; Rhee, 2006; Liochev, 2013). Most vascular cell types produce O_2^- and H_2O_2 , two of the most important ROS in the vascular wall (Gutterman et al., 2005). Several enzyme systems such as NADPH oxidases and xanthine oxidases and the mitochondria facilitate the one-electron reduction of molecular oxygen, which produces O_2^- . In the vasculature, the NADPH oxidases play a significant physiological ROS generating role. O_2^- alone may alter the signalling pathways in the vascular system, but more critically, it generates additional reactive species (Lyle and Griendling, 2006; Szocs et al., 2002). NO, a key regulator of vascular relaxation and vasodilation, is inactivated by the reaction between oxygen and NO, which results in the production of peroxynitrite, which has negative effects of its own. Hence, several disorders that involve the inactivation of NO result in vascular dysfunction (Lyle and Griendling, 2006; Szocs et al., 2002).

ROS is a major driver of cardiovascular disorders being a regulator of vascular cell proliferation and apoptosis (Akhigbe and Ajayi, 2021; Yang and Lian, 2019; Abete et al., 1999). It has been shown that ROS affect several signalling pathways such as the MAPK/ERK

and JAK/STAT pathways, but the mechanisms by which ROS interact with cell-signaling proteins, how those proteins affect the level of intracellular ROS in turn, and whether there are intricate interactions between various ROS-associated signalling pathways have not been fully understood (Zhang et al., 2016; Son et al., 2011). The suppression of ROS formation by antioxidants prevents MAPK activation after cell stimulation with cellular stimuli (Torres and Forman, 2003; McCubrey et al., 2006), demonstrating the involvement of ROS in the activation of MAPK pathways (McCubrey et al., 2006). The oxidative alteration of signalling proteins by ROS may be one of the likely mechanisms for the activation of MAPK pathways since ROS can change key amino acid residues in proteins, altering protein structure and function (Thannickal and Fanburg, 2000).

On the other hand, it has been shown that STAT3 has a cellular nongenomic function (Wang et al., 2018). To what extent STAT3 is imported into mitochondria depends on its interaction with GRIM-19, a component of the mitochondrial respiratory complex I (Lufei et al., 2003; Tamminen et al., 2013). Furthermore, selective stabilisation and expansion of mitochondrial respiratory complexes by STAT3 mitochondrial import may enable mitochondria to coordinate responses to specific stimuli (Lee et al., 2007; Wegrzyn et al., 2009). More so, it has been proposed by (Lee et al. 2007) that STAT1 promotes ROS production and apoptosis since mitochondrial respiratory complexes I and III are assumed to be the primary source for ROS generation (Chen et al., 2003; Batandier et al., 2006). On the other hand, STAT activation appears to be dependent on ROS signalling (Kim et al., 2008; Liu et al., 2004). For instance, within 5 minutes of H₂O₂ stimulation, fibroblasts and A431 carcinoma cells activate STAT1 and STAT3. ROS is, therefore, considered to be a second messenger to control STAT activation (Simon et al., 1998). These findings strongly suggest that STAT and ROS create a positive STAT-ROS feedback loop, however, little is known about its specifics.

Hence, the aim in this Chapter is to investigate the relationship between the activation and inhibition of the JAK/STAT and MAPK/ERK signalling pathways with the generation of ROS. To achieve this, I used MitoSOX dye to stain live HSVSMCs from T2DM and non-diabetic patients to assess mitochondrial-derived ROS (mROS) (O₂⁻) production as described in 2.2.7.1. Superoxide generation in HSVSMCs from T2DM and non-diabetic patients was quantified by flow cytometry as described in 2.2.7.2. %PE-A, which measures the percentage of the viable cells that responded to MitoSOX stain was used as a marker for mROS production.

In summary, the specific objectives of this Chapter were to:-

1. Evaluate the effects of the activation and inhibition of JAK/STAT pathway on the generation of mROS by HSVSMC from T2DM patients and non-diabetic controls.
2. Evaluate the effects of the activation and inhibition of MAPK/ERK pathway on the generation of mROS by HSVSMC from T2DM patients and non-diabetic controls.

6.2 Results

6.2.1 Effects of JAK inhibition on mROS production in HSVSMCs from T2DM and non-diabetic patients

How the JAK/STAT pathway impacts ROS production in VSMCs is still not fully understood. ROS production in cardiac mitochondria is increased by the activation of STAT3 by cytokines like IL-6 and growth factors like PDGF (Krylatov et al., 2018; Chen and Zweier, 2014). However, these activators can concurrently increase NADPH oxidase activity (Krylatov et al., 2018; Borchhi et al., 2010). In addition, numerous studies have established NADPH oxidase as the main source of ROS in human failing myocardium and cardiac remodelling, primarily through actions on redox-sensitive signal transduction pathways (Borchhi et al., 2010; Akki et al., 2009; Dworakowski et al., 2006; Murdoch et al., 2006; Nediani et al., 2007). Also, it is unclear to what extent the JAK/STAT pathway contributes to the total amount of ROS produced and of what significance this is in driving cardiac pathologies. Therefore, in this section of the thesis, I have investigated the role of the JAK/STAT pathway on the generation of ROS in HSVSMCs from both T2DM and non-diabetic patients. To determine mROS production, I stimulated the JAK/STAT downstream signalling pathway in the cells with IL-6/sIL-6R α and PDGF-BB and measured the responsiveness of the cells to MitoSOX stain, a measure of ROS production in the mitochondria. I also employed JAK1/2-selective inhibitor ruxolitinib for downstream inhibition of the JAK/STAT signalling pathway. Additionally, I assessed how HSVSMCs from T2DM differs from a non-diabetic phenotype in regard to sensitivity of mROS production to inhibition of the JAK/STAT pathway.

6.2.1.1 Effect of IL-6/sIL-6R α and ruxolitinib on production of mROS in HSVSMCs from T2DM and non-diabetic patients

As shown in Figure 6.1, IL-6/sIL-6R α stimulation did not cause any significant alteration in the proportion of cells that respond to MitoSOX stain which is used in this instance to measure mROS in HSVSMCs from T2DM. %PE-A in stained and unstimulated HSVSMCs from T2DM patients was used as the control and there was no significant difference when compared with %PE-A from IL-6/sIL-6R α -stimulated and stained cells. On the other hand, ruxolitinib, caused a significant reduction (compared with %PE of unstimulated stained cells, $p < 0.05$, $n = 6$) in %PE-A of cells, denoting significant decrease in the production of mROS.

On the other hand, IL-6/sIL-6R α did not significantly alter the generation of mROS in HSVSMCs from non-diabetic patients as the %PE-A of stained and unstimulated cells did not significantly differ from the %PE-A of IL-6/sIL-6R α stimulated cells (Figure 6.2). Like the observation in T2DM patients, ruxolitinib significantly decreased (compared with %PE-A of unstimulated stained cells, $p < 0.05$, $n = 6$) the production of mROS in HSVSMCs from non-diabetic with or without IL-6/sIL-6R α (Figure 6.2).

The production of mROS in HSVSMCs from T2DM and non-diabetic patients with or without IL-6/sIL-6R α stimulation +/- ruxolitinib was directly compared and presented in Figure 6.3. The findings showed that HSVSMCs from T2DM patients produced significantly more ($p < 0.001$, $n = 12$) mROS than those from non-diabetic patients at basal level. Also, the production of mROS in HSVSMCs from T2DM patients was consistently higher ($p < 0.01$, $n = 6$) after treatments with IL-6/sIL-6R α , IL-6/sIL-6R α + ruxolitinib, and ruxolitinib, when compared with those from non-diabetic control.

Figure 6.1

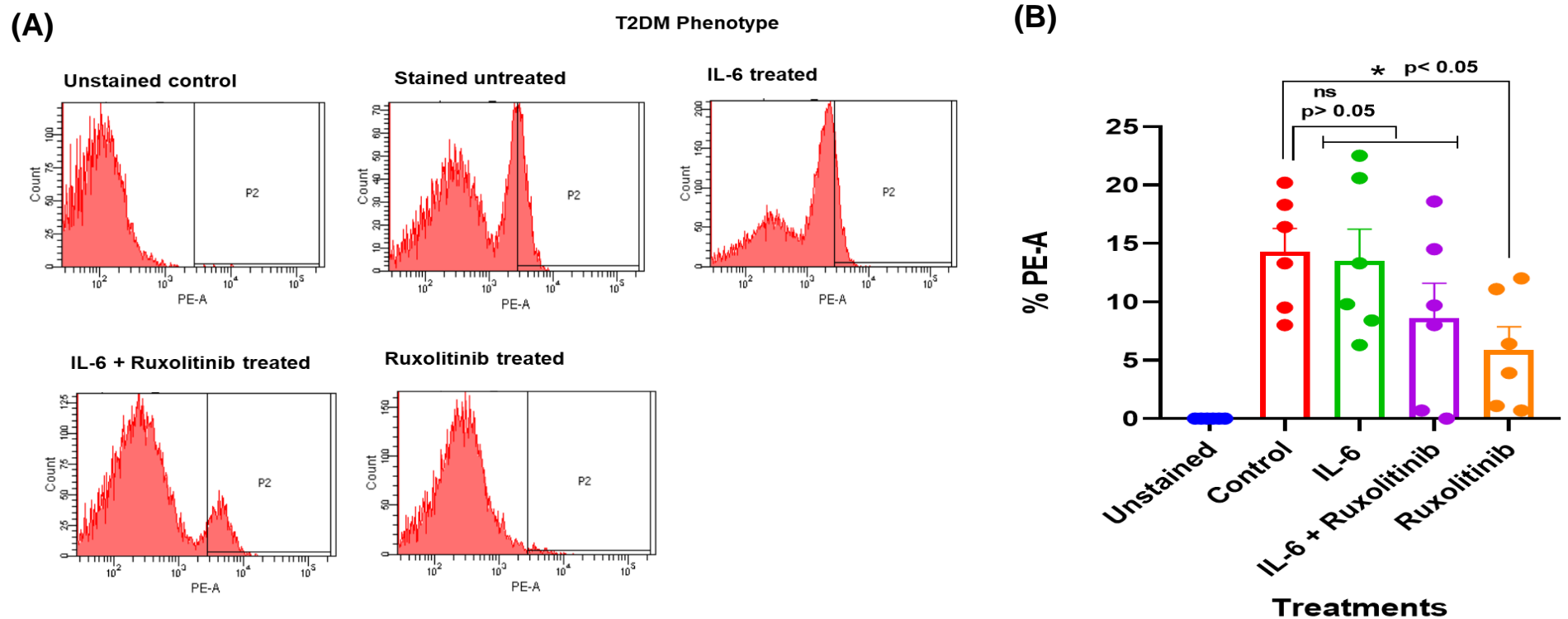


Figure 6.1: Flow cytometry analysis of mROS production in HSVSMCs from T2DM patients after treatment with IL-6/sIL-6R α +/- ruxolitinib.

(A) Flow cytometry chart showing percentage of MitoSOX-positive cells after labelled treatments. The cell population that shifts to the right represents cells that are positive to the MitoSOX stain, which correlates to the generation of mROS.

(B) Comparison of the percentage of cells that are positive to the MitoSOX staining after treatment with IL-6/sIL-6R α +/- ruxolitinib. Data are presented as mean \pm SEM from n=6 biological replicates using HSVSMC samples from different T2DM patients. All data were compared to the control (stained untreated cells) for statistical significance. IL-6: IL-6/sIL-6R α

Figure 6.2

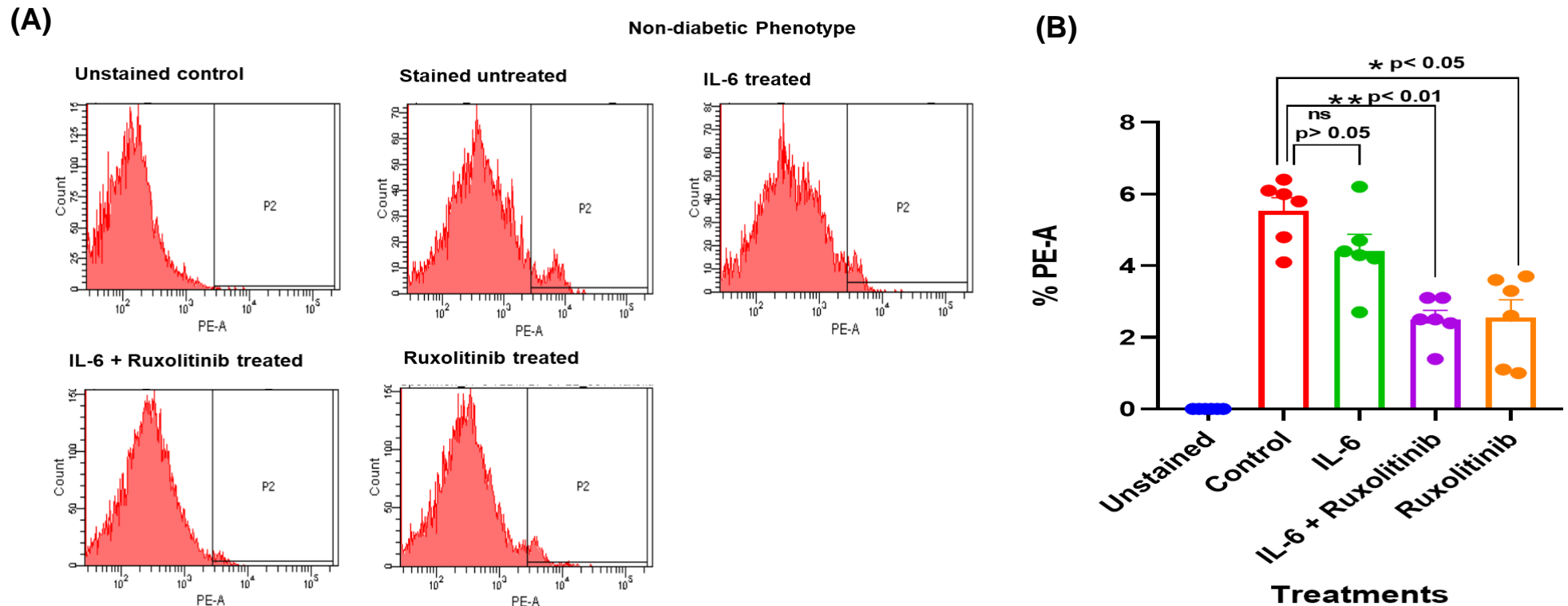


Figure 6.2: Flow cytometry analysis of mROS production in HSVSMCs from non-diabetic patients after treatment with IL-6/sIL-6R α +/- ruxolitinib.

(A) Flow cytometry chart showing percentage of MitoSOX-positive cells after labelled treatments. The cell population that shifts to the right represents cells that are positive to the MitoSOX stain, which correlates to the generation of mROS.

(B) Comparison of the percentage of cells that are positive to the MitoSOX staining after treatment with IL-6/sIL-6R α +/- ruxolitinib. Data are presented as mean \pm SEM from n=6 biological replicates using HSVSMC samples from different non-diabetic patients. All data were compared to the control (stained untreated cells) for statistical significance. IL-6: IL-6/sIL-6R α

Figure 6.3

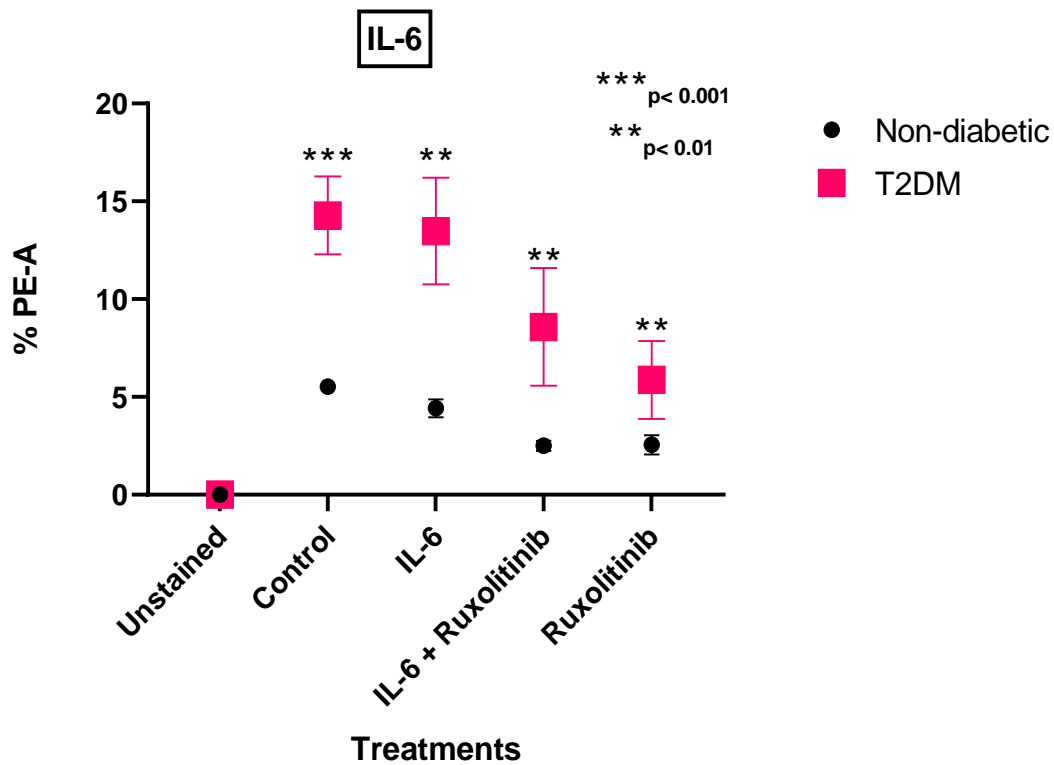


Figure 6.3: Comparison of the mROS production in HSVSMCs from T2DM and non-diabetic patients after treatment with IL-6/sIL-6R α +/- ruxolitinib.

Comparison of mROS generated by HSVSMCs from T2DM and non-diabetic patients with corresponding treatments. Data are presented as mean \pm SEM from n=12 for stained untreated samples (control) and n=6 for treated samples of biological replicates using HSVSMC samples from different patients. IL-6: IL-6/sIL-6R α .

6.2.1.2 Effect of PDGF-BB and ruxolitinib on mROS production in HSVSMCs from T2DM and non-diabetic patients

Figure 6.4 shows the production of mROS, as determined by %PE-A in HSVSMCs from T2DM patients when treated with PDGF-BB, PDGF-BB + ruxolitinib, and ruxolitinib compared with untreated cells. The control was the %PE-A in unstimulated stained HSVSMCs from T2DM patients. Results show that there was no significant alteration in mROS generated in HSVSMCs from T2DM after stimulation with PDGF-BB. Ruxolitinib however caused a significant reduction (compared with %PE-A of unstimulated stained cells, $p < 0.05$, $n=6$) in generation of mROS.

Furthermore, Figure 6.5 shows that mROS production in HSVSMCs from non-diabetic patients. As revealed, there was no significant alteration in the production of mROS after stimulation with PDGF-BB when compared with stained and untreated control. Also, there was a significant reduction (compared with %PE-A of unstimulated stained cells, $P < 0.05$, $n=6$) in mROS production in cells treated with ruxolitinib.

Figure 6.6 shows direct comparison of the mROS produced in HSVSMCs from T2DM and non-diabetic patients with or without PDGF-BB stimulation +/- ruxolitinib (Fig 6.6). The results showed that at basal level, HSVSMCs from patients with T2DM produced significantly higher ($P < 0.001$, $n=12$) mROS than those from non-diabetic patients. The formation of ROS in HSVSMCs from T2DM patients was also higher ($P < 0.01$, $n=6$) after treatment with PDGF-BB. Additionally, when comparing the mROS produced following treatment with PDGF-BB + ruxolitinib and ruxolitinib alone, the data showed that HSVSMCs from T2DM produced significantly higher amount ($P < 0.05$, $n=6$) (Figure 6.6).

Figure 6.4

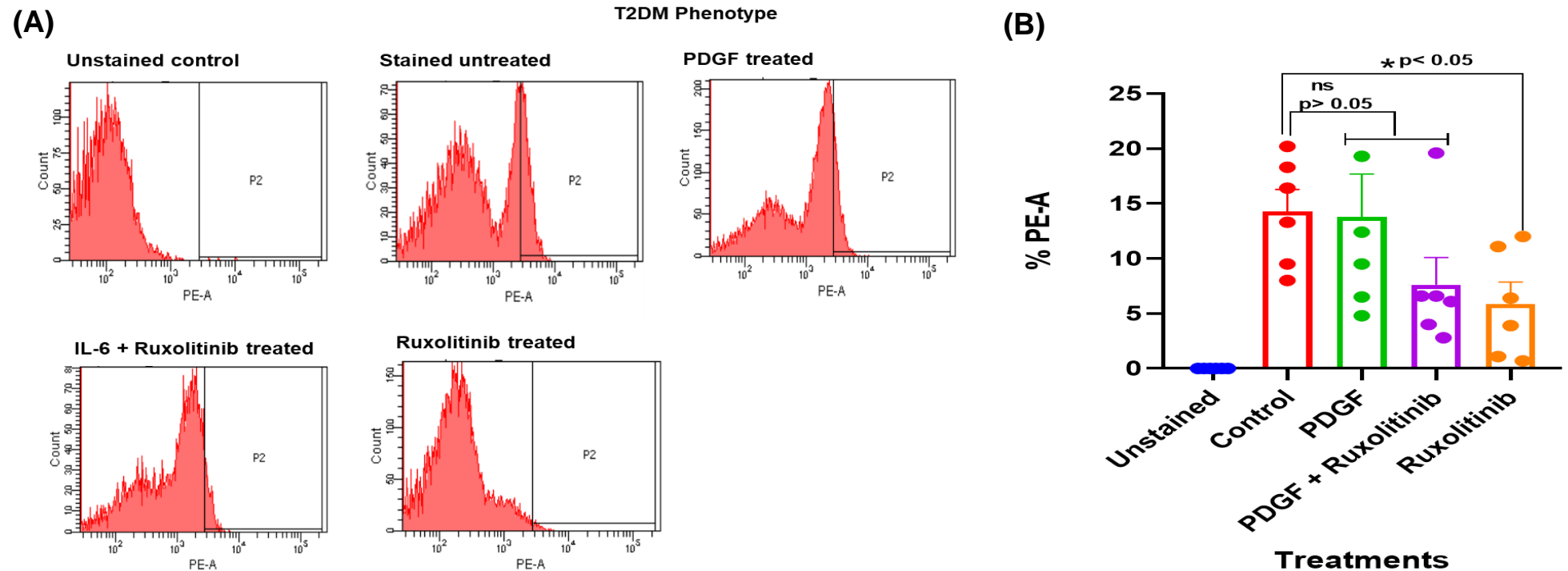


Figure 6.4: Flow cytometry analysis of mROS production in HSVSMCs from T2DM patients after treatment with PDGF-BB +/- ruxolitinib.

(A) Flow cytometry chart showing percentage of MitoSOX-positive cells after labelled treatments. The cell population that shifts to the right represents cells that are positive to the MitoSOX stain, which correlates to the generation of mROS.

(B) Comparison of the percentage of cells that are positive to the MitoSOX staining after treatment with PDGF-BB +/- ruxolitinib. Data are presented as mean \pm SEM from n=6 biological replicates using HSVSMC samples from different T2DM patients. All data were compared to the control (stained untreated cells) for statistical significance. PDGF: PDGF-BB.

Figure 6.5

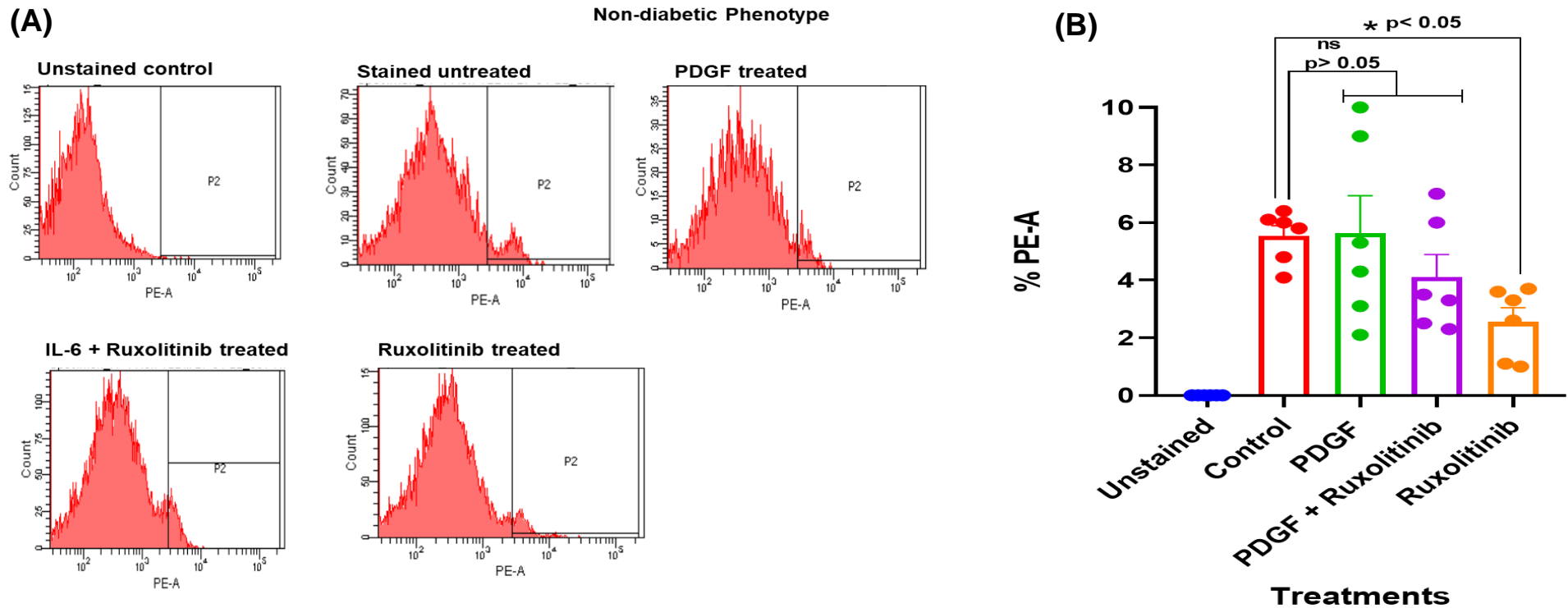


Figure 6.5: Flow cytometry analysis of mROS production in HSVSMCs from non-diabetic patients after treatment with PDGF-BB +/- ruxolitinib.

(A) Flow cytometry chart showing percentage of MitoSOX-positive cells after labelled treatments. The cell population that shifts to the right represents cells that are positive to the MitoSOX stain, which correlates to the generation of mROS.

(B) Comparison of the percentage of cells that are positive to the MitoSOX staining after treatment with PDGF-BB +/- ruxolitinib. Data are presented as mean \pm SEM from n=6 biological replicates using HSVSMC samples from different non-diabetic patients. All data were compared to the control (stained untreated cells) for statistical significance. PDGF: PDGF-BB.

Figure 6.6

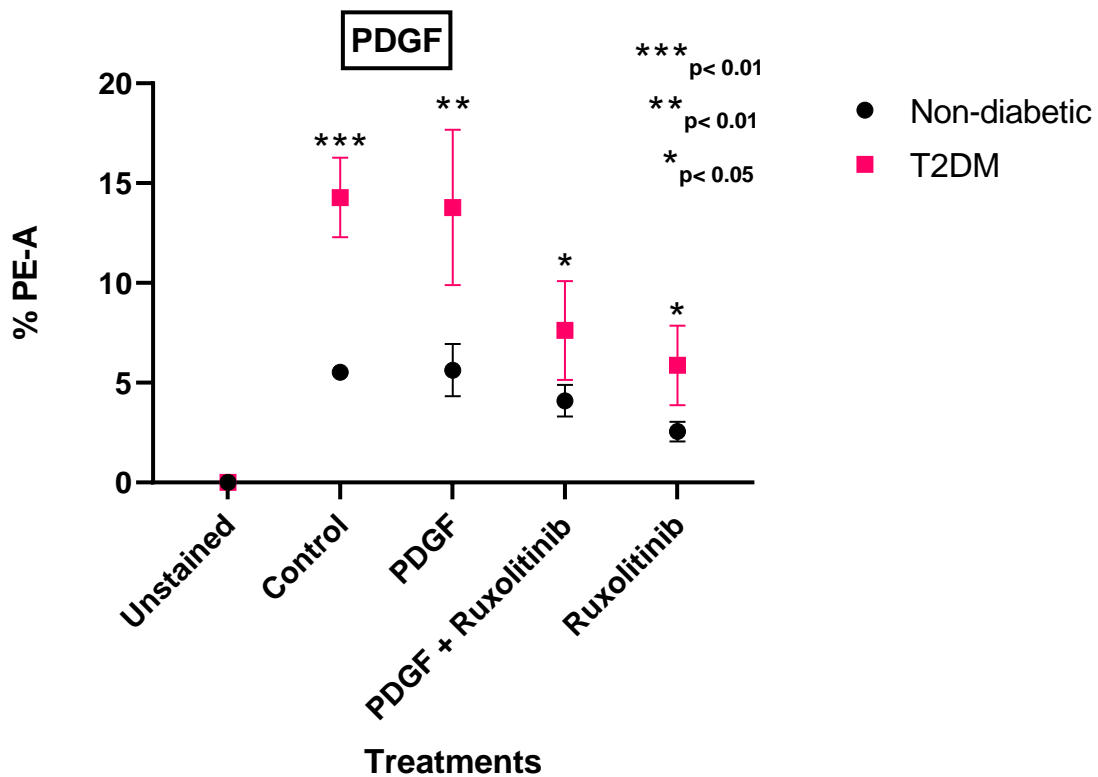


Figure 6.6: Comparison of the mROS production in HSVSMCs from T2DM and non-diabetic patients after treatment with PDGF +/- ruxolitinib.

Comparison of mROS generated by HSVSMCs from T2DM and non-diabetic patients with corresponding treatments. Data are presented as mean \pm SEM from n=12 for stained untreated samples (control) and n=6 for treated samples of biological replicates using HSVSMC samples from different patients. PDGF: PDGF-BB

6.2.2 Effects of MEK inhibition on mROS production in HSVSMCs from T2DM and non-diabetic patients

The regulation of the MAPK pathways by ROS has garnered a lot of interest as MAPK pathways mediate both mitogen- and stress-activated signals (Son et al., 2011). ROS have important functions as signalling molecules and controllers of cellular activity (Son et al., 2011). Increasing evidence suggests that ROS play a physiological role as "second messengers" in processes controlling cell growth, proliferation, migration and death (Thannickal and Fanburg, 2000). Although the exact mechanisms are still unclear, several studies have described the activation of the ERK1/2 pathway by ROS and the functional consequences in the pathogenesis of cardiovascular disorders such as ischemia, cardiac hypertrophy, cardiac remodelling after myocardial infarction, atherosclerosis and vascular restenosis (Son et al., 2011; Muslin, 2008; Torres and Forman, 2003; Thannickal and Fanburg, 2000).

Despite these advances, it is not well known the impact that the ERK1/2 pathway has on the generation ROS in SMCs. According to one study (Schattauer et al., 2019), the Gi/o protein-coupled kappa opioid receptor and D2 dopamine receptors induce ROS generation through activation of the c-Jun N-terminal kinase (JNK) pathway. Despite the contribution made by this study (Schattauer et al., 2019), the outcome of this association in HSVSMCs is still unknown. Hence, in this series of experiments, I examined the effect of MEK1/2 inhibition with trametinib on mROS generation in response to Ang II and thrombin, two stimuli which activate the ERK1/2 pathway but not the JAK-STAT pathway in HSVSMCs. To achieve this, I measured the mROS production under these treatment conditions (treatment with Ang II/thrombin alone, Ang II/thrombin + trametinib, and trametinib alone) and compared with untreated control. Furthermore, I assessed whether T2DM status impacts of ROS generation under the various treatment scenarios versus non-diabetic controls.

6.2.2.1 Effect of Ang II and trametinib on mROS production in HSVSMCs from T2DM and non-diabetic patients

Figure 6.7 shows the production of mROS in HSVSMCs from T2DM patients when treated with Ang II, Ang II + trametinib, and trametinib compared with untreated cells. There was no significant alteration in mROS generated in HSVSMCs from T2DM after stimulation with Ang II when compared with untreated cells. Trametinib however caused a significant reduction (compared with %PE-A of unstimulated stained cells, $P < 0.05$, $n=6$) in the generation of mROS with or without stimulation with Ang II.

Furthermore, Fig 6.8 shows that there was no significant alteration in the production of mROS after stimulation of HSVSMCs from non-diabetic patients with Ang II when compared with untreated stained control. On the other hand, trametinib caused a significant reduction (compared with %PE-A of untreated stained cells, $P < 0.05$, $n=6$) in ROS production in cells with or without treatment with Ang II.

Figure 6.9 shows a direct comparison of the mROS generated in HSVSMCs from T2DM and non-diabetic patients with or without Ang II stimulation +/- trametinib treatment. The results showed that untreated HSVSMCs from patients with T2DM produced significantly higher ($P < 0.05$, $n=6$) mROS than those from non-diabetic control. Meanwhile, there was no significant difference in mROS production after treatment with Ang II or trametinib. However, when comparing the mROS produced following treatment with Ang II + trametinib, there was a significant reduction ($P < 0.05$, $n=6$) in mROS generated in T2DM.

Figure 6.7

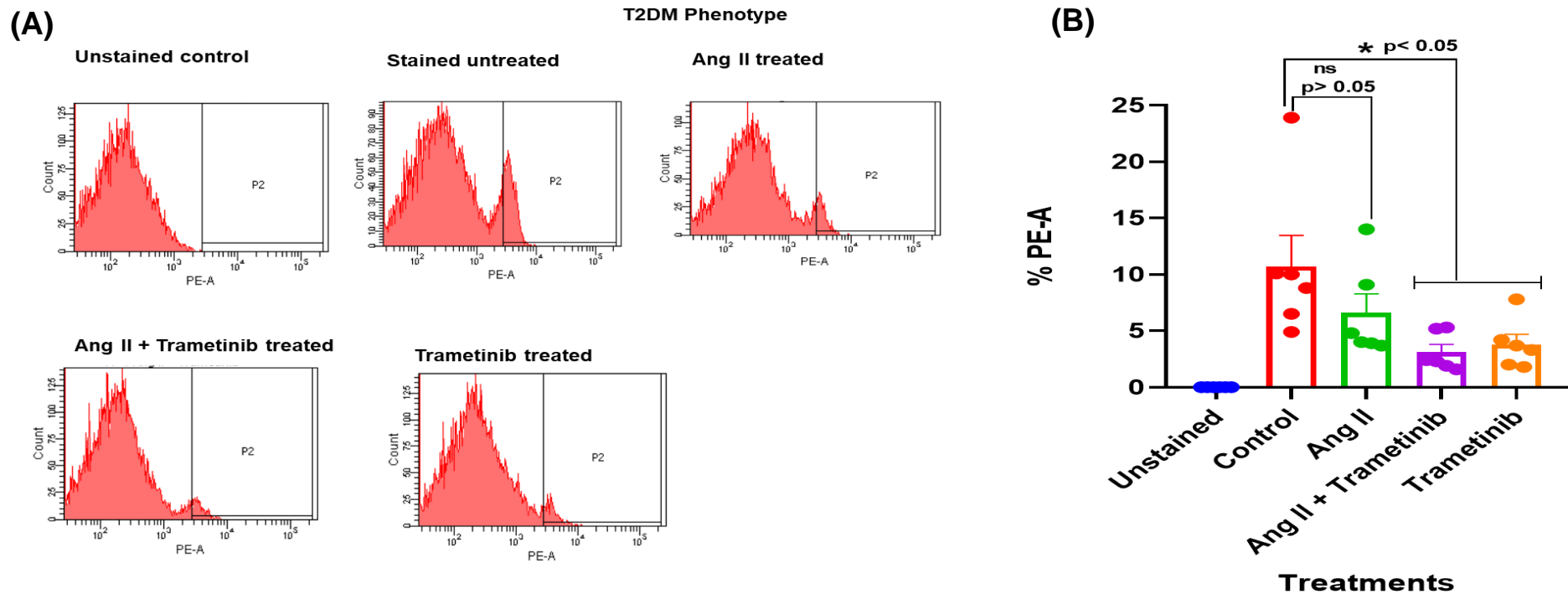


Figure 6.7: Flow cytometry analysis of mROS production in HSVSMCs from T2DM patients after treatment with Ang II +/- trametinib.

(A) Flow cytometry chart showing percentage of MitoSOX-positive cells after labelled treatments. The cell population that shifts to the right represents cells that are positive to the MitoSOX stain, which correlates to the generation of mROS.

(B) Comparison of the percentage of cells that are positive to the MitoSOX staining after treatment with Angiotensin II +/- trametinib. Data are presented as mean \pm SEM from n=6 biological replicates using HSVSMC samples from different T2DM patients. All data were compared to the control (stained untreated cells) for statistical significance. Ang II: Angiotensin II

Figure 6.8

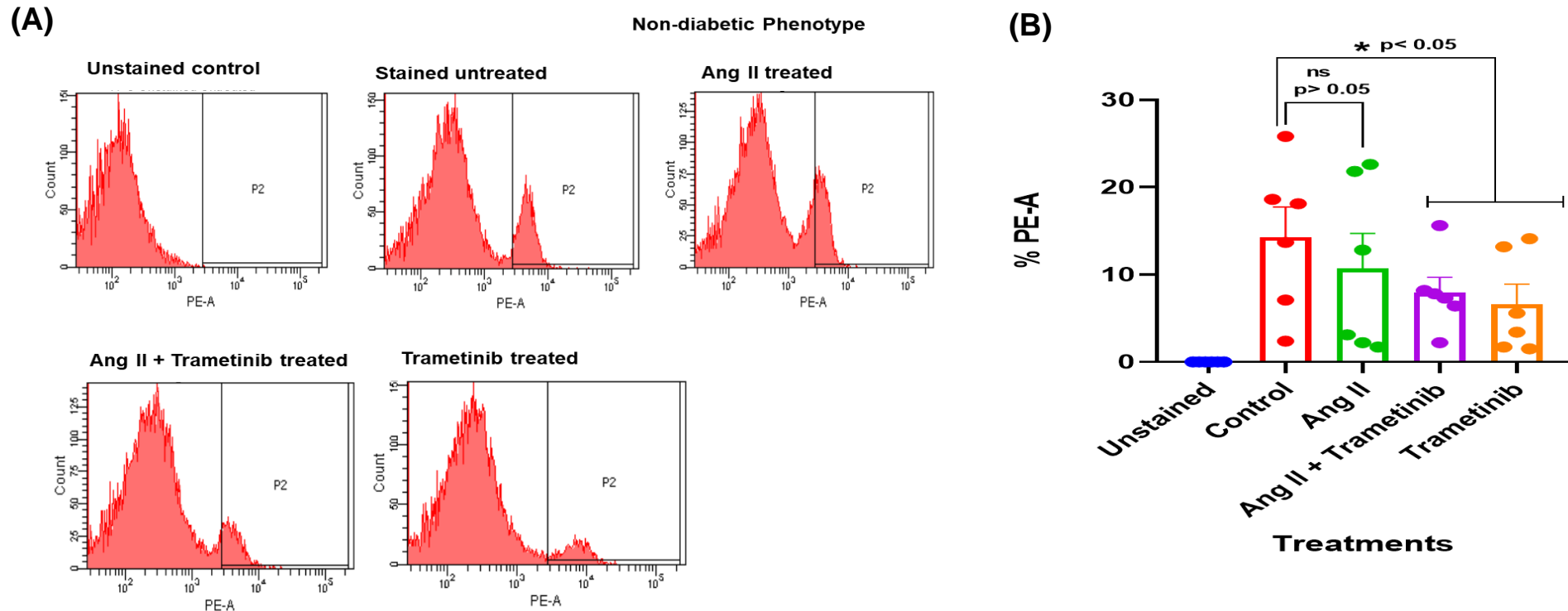


Figure 6.8: Flow cytometry analysis of mROS production in HSVSMCs from non-diabetic patients after treatment with Ang II +/- trametinib.

(A) Flow cytometry chart showing percentage of MitoSOX-positive cells after labelled treatments. The cell population that shifts to the right represents cells that are positive to the MitoSOX stain, which correlates to the generation of mROS.

(B) Comparison of the percentage of cells that are positive to the MitoSOX staining after treatment with Angiotensin II +/- trametinib. Data are presented as mean \pm SEM from $n=6$ biological replicates using HSVSMC samples from different non-diabetic patients. All data were compared to the control (stained untreated cells) for statistical significance. Ang II: Angiotensin II

Figure 6.9

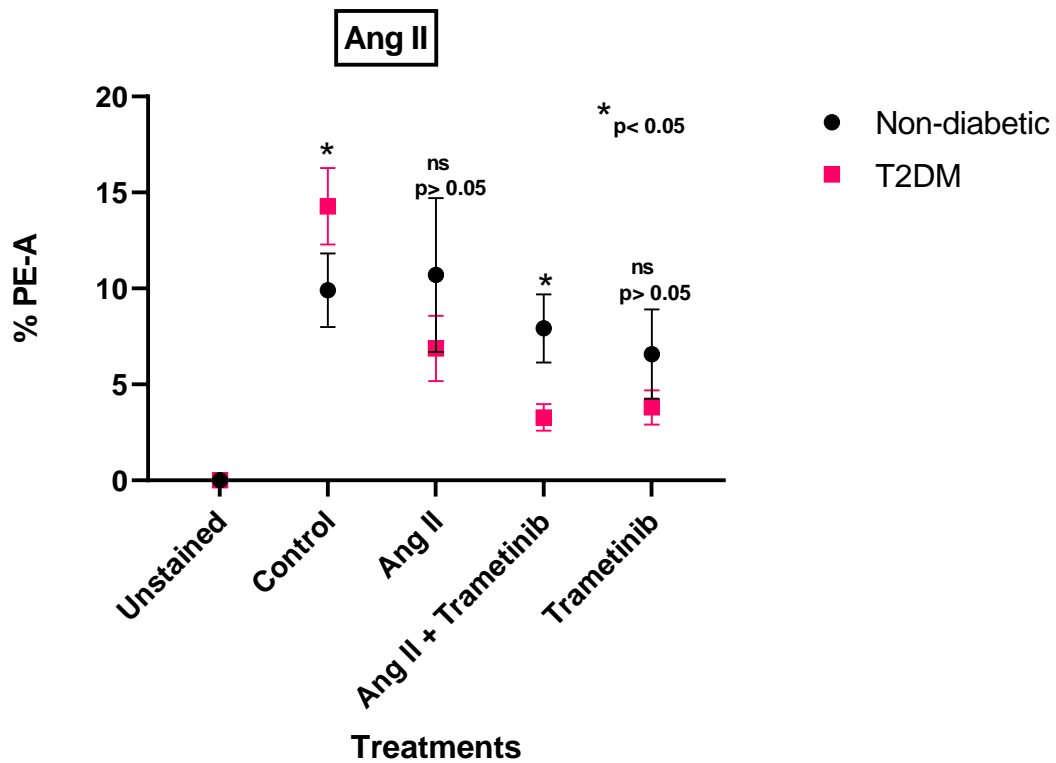


Figure 6.9: Comparison of the mROS production in HSVSMCs from T2DM and non-diabetic patients after treatment with Ang II +/- trametinib.

Comparison of mROS generated by HSVSMCs from T2DM and non-diabetic patients with corresponding treatments. Data are presented as mean \pm SEM from n=12 for stained untreated samples (control) and n=6 for treated samples of biological replicates using HSVSMC samples from different patients. Ang II: Angiotensin II

6.2.2.2 Effect of thrombin and trametinib on mROS production in HSVSMCs from T2DM and non-diabetic patients

Figure 6.10 shows the production of mROS in HSVSMCs from T2DM patients when treated with thrombin, thrombin + trametinib, and trametinib compared with untreated cells. There was no significant alteration in mROS generated in HSVSMCs from T2DM after stimulation with thrombin when compared with untreated cells. Trametinib however caused a significant reduction (compared with %PE-A of unstimulated stained cells, $p < 0.05$, $n=6$) in the generation of mROS with or without stimulation with thrombin.

Furthermore, Figure 6.11 shows that there was no significant alteration in the production of mROS after stimulation of HSVSMCs from non-diabetic patients with thrombin when compared with untreated stained control. On the other hand, trametinib caused a significant reduction (compared with %PE-A of untreated stained cells, $P < 0.05$, $n=6$) in ROS production in cells with or without treatment with thrombin.

The ROS produced in HSVSMCs from T2DM and non-diabetic patients with or without thrombin stimulation +/- trametinib treatment were directly compared in Figure 6.12. The results showed that untreated HSVSMCs from patients with T2DM produced significantly higher ($P < 0.05$, $n=6$) mROS than those from non-diabetic control. However, there was not significant difference in mROS production after treatment with thrombin, trametinib, or thrombin + trametinib.

Figure 6.10

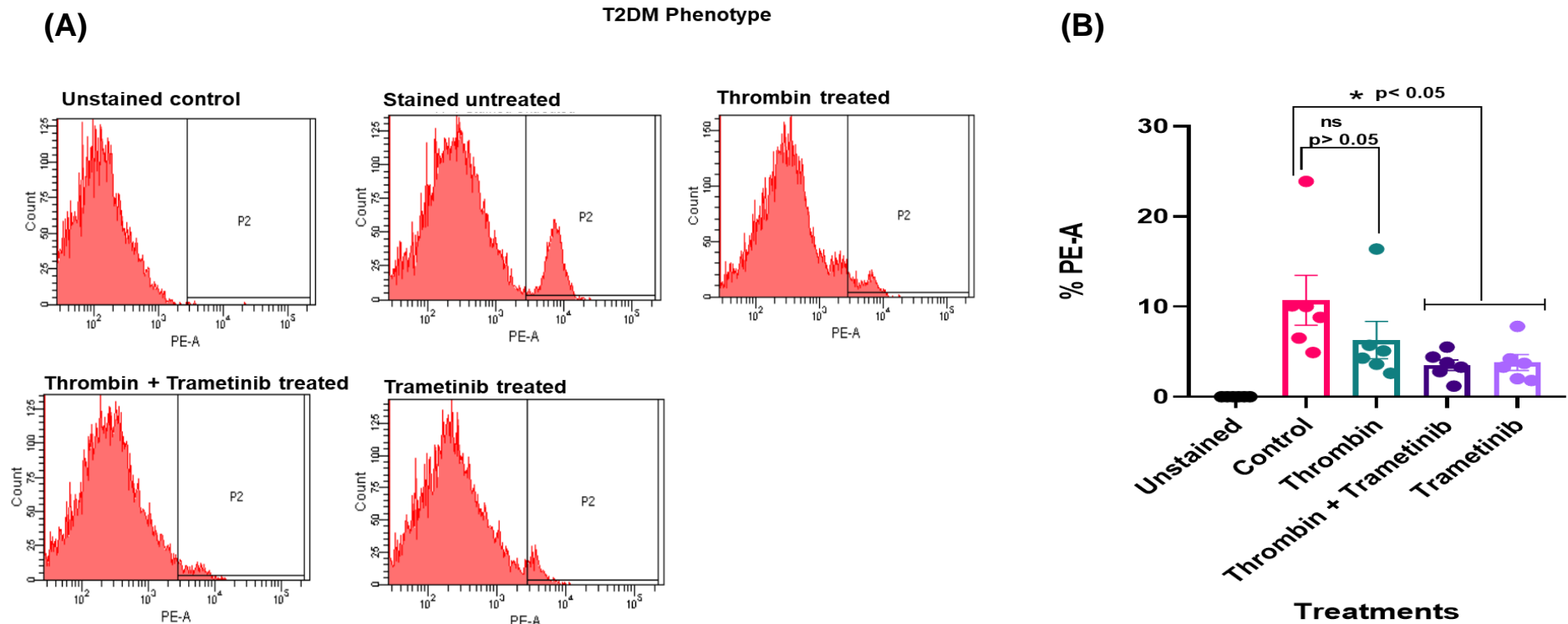


Figure 6.10: Flow cytometry analysis of mROS production in HSVSMCs from T2DM patients after treatment with thrombin +/- trametinib.

(A) Flow cytometry chart showing percentage of MitoSOX-positive cells after labelled treatments. The cell population that shifts to the right represents cells that are positive to the MitoSOX stain, which correlates to the generation of mROS.

(B) Comparison of the percentage of cells that are positive to the MitoSOX staining after treatment with thrombin +/- trametinib. Data are presented as mean \pm SEM from n=6 biological replicates using HSVSMC samples from different T2DM patients. All data were compared to the control (stained untreated cells) for statistical significance.

Figure 6.11

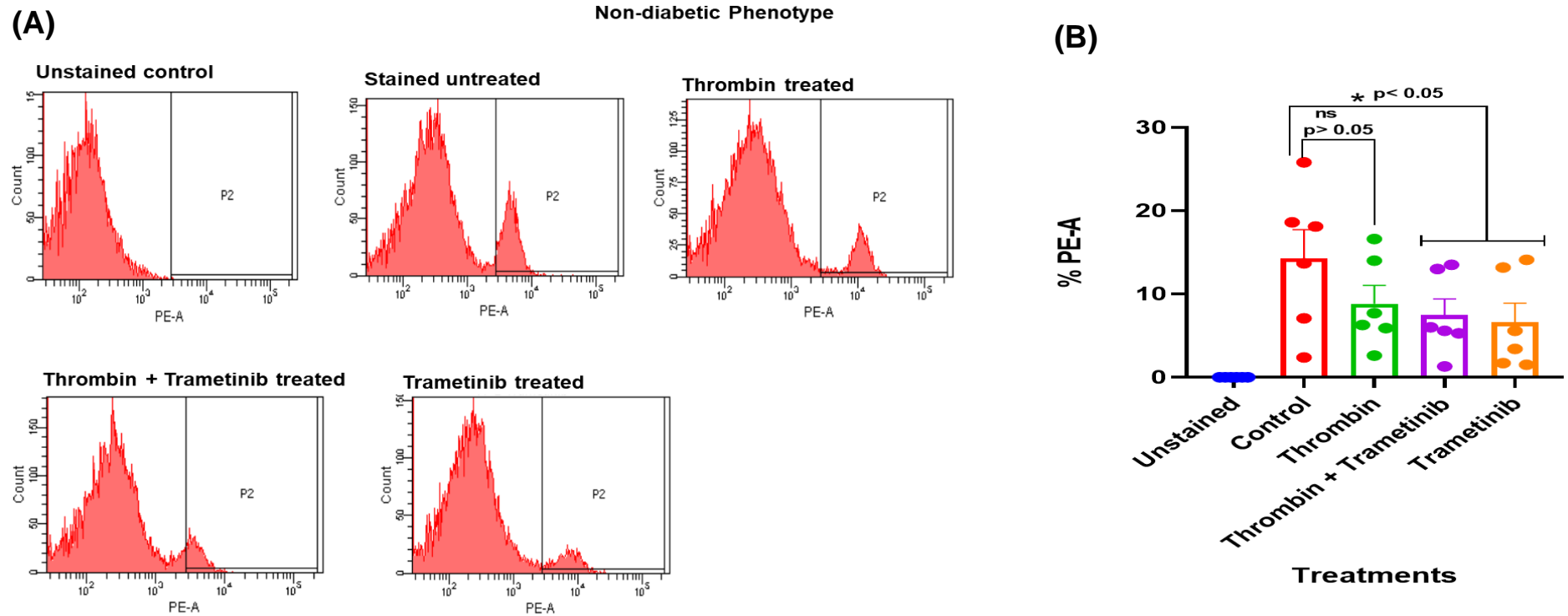


Figure 6.11: Flow cytometry analysis of mROS production in HSVSMCs from non-diabetic patients after treatment with thrombin +/- trametinib.

(A) Flow cytometry chart showing percentage of MitoSOX-positive cells after labelled treatments. The cell population that shifts to the right represents cells that are positive to the MitoSOX stain, which correlates to the generation of mROS.

(B) Comparison of the percentage of cells that are positive to the MitoSOX staining after treatment with Angiotensin II +/- trametinib. Data are presented as mean \pm SEM from n=6 biological replicates using HSVSMC samples from different non-diabetic patients. All data were compared to the control (stained untreated cells) for statistical significance.

Figure 6.12

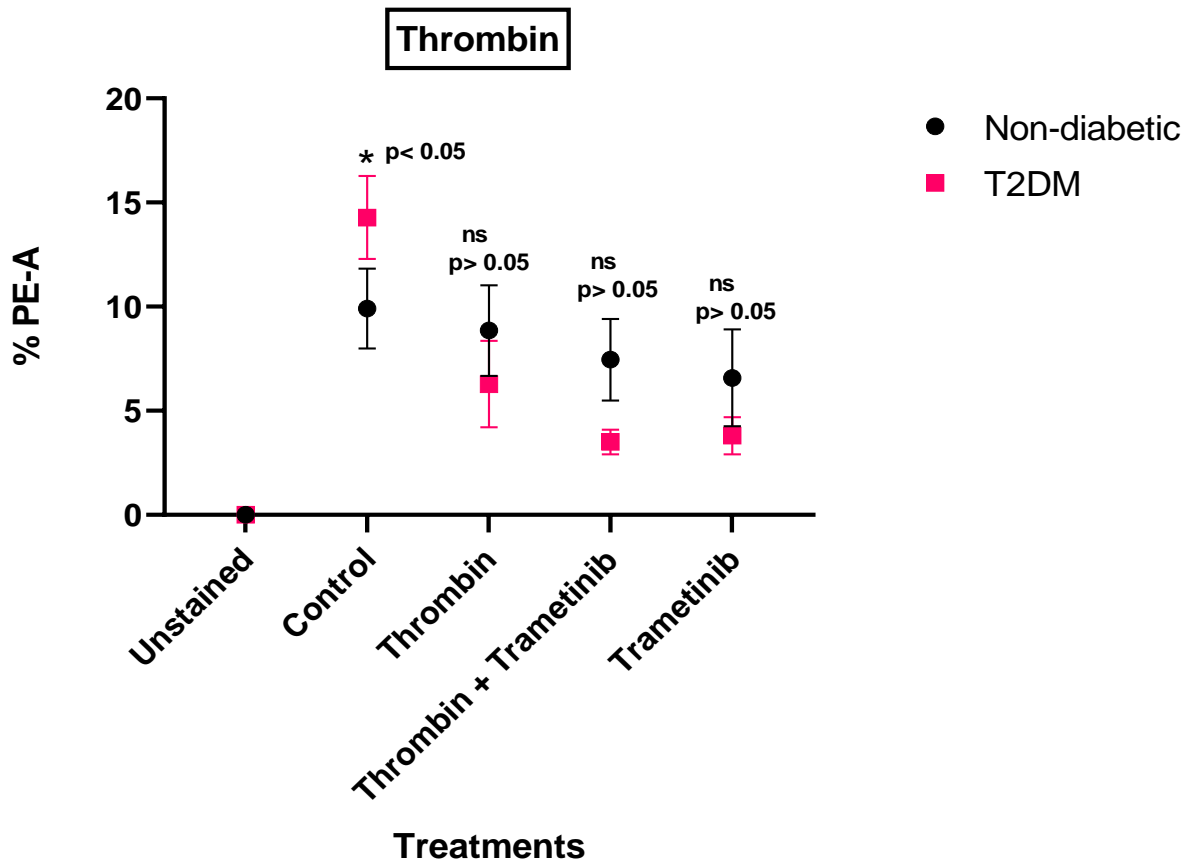


Figure 6.12: Comparison of the mROS production in HSVSMCs from T2DM and non-diabetic patients after treatment with thrombin +/- trametinib.

Comparison of mROS generated by HSVSMCs from T2DM and non-diabetic patients with corresponding treatments. Data are presented as mean \pm SEM from n=12 for stained untreated samples (control) and n=6 for treated samples of biological replicates using HSVSMC samples from different patients.

6.3 Discussion

In this chapter, I evaluated the impact of downstream JAK/STAT and MAPK/ERK signalling pathway activation and inhibition on the generation of mROS in HSVSMCs from T2DM and non-diabetic patients. In numerous cell types, including ECs, VSMCs, and platelets, which have all been linked to CVDs, activators of these signalling pathways, such as IL-6, PDGF, Ang II, and thrombin, have been shown to stimulate generation of ROS (Rosen and Freeman, 1984; Wang et al., 1997; Burtenshaw et al., 2007; Carrim et al., 2015). However, these have not yet been assessed in HSVSMC despite its significance in the aetiology of NIH and VGF. To achieve my aim, I stimulated the JAK/STAT signalling pathway with IL-6/sIL-6R α and PDGF-BB and the MAPK/ERK signalling pathway with Ang II and thrombin in HSVSMCs from T2DM and non-diabetic patients. After this, I used a flow cytometer to measure and analyze the production of mROS (superoxide) by staining cells with MitoSOX, a superoxide indicator used for live-cell imaging to measure mitochondria ROS production (Yang et al., 2021; Robinson et al., 2006; Little et al., 2020; Kauffman et al., 2016). MitoSOX penetrate live cells, target the mitochondria, and are quickly oxidised by superoxide but not by other ROS. The oxidised products are highly fluorescent (Yang et al., 2021; Robinson et al., 2006; Little et al., 2020; Kauffman et al., 2016). Additionally, I examined the effect ruxolitinib and trametinib, which block the JAK/STAT and MAPK/ERK signalling pathways respectively, on mROS generation in these cells.

Understanding the biological activities of ROS depends on detection and quantification of the rates of flux of individual ROS in intracellular compartments. In this situation, it has been determined that mitochondria are a significant generator of cellular superoxide, hence, mROS was determined (Yang et al., 2021; Kauffman et al., 2016). As described in Chapter 2.10.1, I used 5 μ M mitoSOX for cell incubation as concentrations exceeding 5 μ M have been shown to have deleterious consequences, such as changing mitochondrial shape and redistributing fluorescence to the nucleus and cytoplasm (Yang et al., 2021; Kauffman et al., 2016). It is crucial to note that an abundance of cells results in a shortage of the dye relative to each cell and poor fluorescence. Consequently, the number of cells per treatment in this set of trials was kept at 5×10^5 (Yang et al., 2021; Kauffman et al., 2016).

From my findings, IL-6/sIL-6R α did not cause any significant alteration in the production of mROS in HSVSMCs from T2DM patients via the activation of the JAK/STAT downstream signalling (Figure 6.1). Although it is unclear if IL-6/sIL-6R α enhances the generation of ROS

in T2DM subjects, however, it has been shown in a mouse model of early diabetic retinopathy that inhibiting IL-6 trans-signalling with recombinant sgp130Fc reduces oxidative stress caused by an increase in ROS production (Robinson et al., 2020). In skeletal muscle, it has been demonstrated that increased circulating IL-6 enhances the generation and accumulation of free radicals in the diaphragm muscle of adult NSE/IL-6 mice (Forcina et al., 2019). However, this study (Forcina et al., 2019) did not suggest that the increased superoxide generation was due to activation of the JAK/STAT pathway, rather, they demonstrated that this was due to enhanced expression of the protein p91phox, which functions as the catalytic subunit of the enzyme complex NOX2 that converts molecule oxygen into superoxide (Whitehead et al., 2010; Ferreira and Laitano, 2016).

Also, my findings suggest that IL-6/sIL-6R α does not alter mROS production in HSVSMCs from non-diabetic subjects by activating the JAK/STAT downstream signalling (Figure 6.2). Although, there is a substantial body of evidence connecting IL-6 to the onset, progression, and progression of cardiovascular disease through changes to vascular function, decreased NO levels, and increased vascular superoxide levels (Didion, 2017; Hooper et al., 1998; Delneste et al., 1994, Ala et al., 1992; Ali et al., 1999, Yan et al., 1995). More so, increases in vascular superoxide may play a key role in the relationship between endothelial dysfunction and the activation of inflammatory molecules and pathways such as JAK/STAT signalling in CVDs (Kofler et al., 2005; Dworakowski et al., 2008; Zhang, 2008). Emerging evidence reveals that inflammatory cytokines, such IL-6, influence the production and activity of both eNOS and NADPH oxidase, affecting the amounts of NO and superoxide which contribute to oxidative stress (Kofler et al., 2005; Dworakowski et al., 2008; Zhang, 2008; Sprague and Khalil, 2009). Like the case in T2DM, this is the first time this experiment is described in HSVSMCs from non-diabetic subjects.

While there were no alterations in the production of superoxide in HSVSMCs from both T2DM and non-diabetic patients after stimulation of the JAK/STAT pathway with IL-6/sIL-6R, however, inhibition of JAK1/2 with ruxolitinib caused a significant reduction in the production of superoxide in HSVSMCs from both T2DM and non-diabetic (Figures 6.1, 6.2, and 6.3). Chronic inflammation and the level of oxidative stress coexist in a pathological intracellular environment and are closely associated processes (Forcina et al., 2019). It is widely acknowledged that inflammatory cells serve as a source of ROS, which are, in turn, able to amplify the activation of proinflammatory pathways. However, the mechanism behind the

pathophysiologic interaction between ROS production and the inflammatory response is not well understood (Forcina et al., 2019). As a result, this finding gives insight on how JAK/STAT pathway's inhibition might be used to decrease superoxide generation. The fact that this is the first description in HSVSMCs, a crucial cell type involved in the vascular dysfunction that results in saphenous VGF seen in T2DM patients is significant. Interestingly, JAK inhibitors have been suggested as potential therapies in oxidative stress control (Charras et al., 2019; Ramos-Casals et al., 2014). For instance, the oxidative stress response is upregulated in activated salivary gland epithelial cells from patients with Primary Sjögren's syndrome (Charras et al., 2019). More so, it has been demonstrated that JAK inhibitors AG490 and ruxolitinib can both reverse ICAM-1 and PD-L1 mediated activation of salivary gland epithelial cells brought on by ROS by activating STAT3 (Charras et al., 2019).

Furthermore, from my findings, HSVSMCs from T2DM produced more mROS than those from the non-diabetic controls and the degree of ruxolitinib's inhibition of mROS with or without PDGF-BB stimulation in both phenotypes is similar (Figure 6.3). This result is consistent with several earlier studies showing increased ROS production in T2DM subjects compared to non-diabetic controls (Mizuki et al., 2021; Oguntibeju, 2019; Giacco and Brownlee, 2010). In addition, multiple experimental studies including the assessment of oxidative stress biomarkers in diabetic patients and T2DM rat models of diabetes have suggested a clear connection between oxidative stress and diabetes (Oguntibeju, 2019; Burgos-Morón et al., 2019). More so, 8-hydroxy-2'-deoxyguanosine (8-OHdG) and 8-oxo-7, 8-dihydro-2'-deoxyguanosine (8-oxo-7, 8-dihydro-2'-deoxyguanosine) are DNA damage markers that have been linked to increased oxidative stress, and their induction has also been linked to decreased antioxidant enzyme activity and hyperglycaemia (Oguntibeju, 2019). Additionally, it has been demonstrated that oxidative stress causes the insulin gene's promoter activity and mRNA expression to be inhibited in isolated pancreatic islet cells, resulting in a reduction in insulin gene expression (Kawahito et al., 2009). Chronic hyperglycaemia-induced insulin resistance is also strongly suspected to be caused by oxidative damage (Eriksson, 2007).

Furthermore, according to my findings, neither HSVSMCs from T2DM (Figure 6.4) nor those from non-diabetic patients showed significant alterations in the levels of mROS generation after treatment with PDGF-BB (Figure 6.5). However, it has been demonstrated that chicoric acid, a purified isolate from plants and vegetables, attenuated a PDGF-BB-induced VSMC, proliferation, and migration via inhibition of ROS accumulation (Lu et al., 2018). Furthermore,

numerous studies have shown that PDGF-BB induces the production of ROS in a variety of cell types, including ECs, human lens epithelial cells, renal tubular cells, and adipocytes (Kreuzer et al., 2003; Chen et al., 2007; Hannken et al., 1998; Jones et al., 1996; Krieger-Brauer and Kather, 1992), but these studies have only shown that PDGF-BB achieves this via activation of NADPH oxidases. Although some studies have suggested that PDGF-BB contributes to the production of ROS in SMCs (Kreuzer et al., 2003; Lu et al., 2017), the exact mechanisms involved are not well understood. Hence, the findings of my research give further insights as I have described this in HSVSMCs assessing the effect of stimulating JAK/STAT downstream signalling pathway with PDGF-BB.

Similar to what was observed in IL-6/sIL-6R α -treated HSVSMCs, ruxolitinib significantly reduced the generation of mROS in HSVSMCs from both T2DM and non-diabetic phenotypes even after stimulation with PDGF-BB (Figures 6.4 and 6.5). While there might be cell-specific response to activation of the JAK/STAT downstream signalling pathway and how it influences the production of mROS, however, my findings suggest that activation of the JAK/STAT downstream signalling pathway in HSVSMCs does not alter the generation of mROS. Also, mROS production was significantly higher in HSVSMCs from T2DM patients compared with those from non-diabetic controls, and this difference was observed in all treatment conditions. Also, my data suggest that the degree of ruxolitinib's inhibition of mROS with or without PDGF-BB stimulation is similar in HSVSMCs from both T2DM and non-diabetic phenotypes (Figure 6.6).

In addition, my findings showed that neither HSVSMCs from T2DM (Figure 6.7) nor those from non-diabetic patients (Figure 6.8) had any significant changes in the amounts of mROS generation following stimulation of the MAPK/ERK pathway with Ang II. Through the generation of ROS, Ang II is known to promote VSMC growth, hypertrophy and/or hyperplasia, and inflammation, and this promote the development of hypertension, atherosclerosis, heart failure, and restenosis after vascular injury (Kobori et al., 2007; Gibbons et al., 1992; Suzuki et al., 2003; Weiss et al., 2001; Feng et al., 2001; Rakugi et al., 1994, Touyz and Schiffrin, 2000; Griendling and Ushio-Fukai, 2000; Touyz, 2004). Superoxide and hydrogen peroxide are produced when Ang II activates NADPH oxidase. These two mediators may then interact with intracellular growth-related proteins and enzymes such as p38, ERK1/2 and AKT/PKB to mediate the physiological responses, such as VSMC development and proliferation (Griendling and Ushio-Fukai, 2000). Additionally, *in vivo* stimulation with Ang

II does not result in hypertension in mice lacking the cytosolic NADPH oxidase subunit p47^{phox}, a mouse model with NADPH oxidase defects (Landmesser et al., 2002). According to this study, Ang II-induced NADPH oxidase activation is responsible for the vascular ROS produced in the endothelium, adventitial, and VSMCs that are linked to hypertension (Landmesser et al., 2002).

The mechanisms by which ROS control cell-signaling proteins, and how they affect the amount of intracellular ROS in turn, and the intricate relationships between diverse ROS-linked signalling pathways are unclear and complex (Zhang et al., 2016). Studies have demonstrated how ROS influences the activation of several signalling pathways such as the NF- κ B, Keap1-Nrf2-ARE, MAPKs/ERK, and PI3K-Akt pathways (Zhang et al., 2016; Schoonbroodt et al., 2000; Katagiri et al., 2010; Kim et al., 2010; Leslie et al., 2002). However, not so much is known on how the activation of these pathways influence the generation of ROS. My findings have now given further insights with regards to activation of the MAPK/ERK pathway in HSVSMCs and the results suggest that the production of mROS, specifically superoxide is not altered.

Furthermore, my findings suggest that inhibition of the MAPK/ERK1/2 downstream signalling pathway with trametinib caused a significant reduction in the generation of mROS in HSVSMCs from both T2DM (Figure 6.7) and non-diabetic controls (Figure 6.8). Inhibiting ROS has been shown to suppress the ERK1/2 and JNK in the rat spinal cord following limb ischemia reperfusion injury (Choi et al., 2015). It was proposed that the activation of ERK1/2 and JNK in the spinal cord, which could possibly influence distant organs, was mediated by the superoxide created by hind limb ischemia reperfusion (Choi et al., 2015). This conclusion supports earlier research showing how controlling ROS generation can be used to mitigate the activation of the ERK1/2 pathway (Choi et al., 2015; Kim et al., 2010; Zhang et al., 2016). However, little is known about the reverse relationship, hence, my finding has now provided insight on how inhibiting the ERK1/2 could be explored to reduce production of mROS in HSVSMCs. Furthermore, production of mROS in HSVSMCs from T2DM was higher compared to those from non-diabetic patients (Figure 6.9). This is consistent with previously described findings (Figures 6.3 and 6.6) which showed that mROS production in HSVSMCs from T2DM was higher than those from non-diabetic phenotype. However, the degree of inhibition by trametinib in T2DM subjects tend to be significantly higher (Figure 6.9). The reason for this observation is currently not clear to me.

Furthermore, stimulation of the ERK1/2 pathway in HSVSMCs from T2DM (Figure 6.10) and non-diabetic patients (Figure 6.11) with thrombin did not alter the generation of mROS. This finding further supports the notion that activation of the ERK1/2 signalling pathway had no impact on mROS generation in HSVSMCs from both T2DM patients and non-diabetic patients, similar to the results with Ang II that were previously described. Although, thrombin has been shown to promote the generation of ROS in platelets (Wachowicz et al., 2002; Carrim et al., 2015). More so, ROS are known to play important roles in intra-platelet signalling and subsequent platelet activation. Although PAR1 and PAR4 are known as the major thrombin receptors on platelets, but thrombin can communicate with human platelets via GPIb (Coughlin, 2000). The receptors and signalling pathways involved in thrombin-induced ROS formation are still not completely understood. However, it has now been suggested that GPIb and PAR4 are both necessary for thrombin-induced ROS production in platelets, pointing to a novel functional partnership between the two proteins (Carrim et al., 2015). In addition to this vital contribution to knowledge, my finding has given further insight on this relationship as regard thrombin-induced ROS production and activation of ERK1/2 pathway in HSVSMCs.

Additionally, like the findings previously reported (Figures 6.7 and 6.8), a significant decrease in mROS production was observed after MEK1/2-selective inhibitor trametinib inhibited the MAPK/ERK signalling pathway with or without thrombin stimulation (Figures 6.10 and 6.11). This further suggests that ERK1/2 pathway can be explored in the modulation of ROS production in ROS-dependent pathologies. Also, production of mROS in HSVSMCs from T2DM patients was higher compared to those from non-diabetic control (Figure 6.12). This is also consistent with previously described findings (Figures 6.3, 6.6, and 6.9) which showed that mROS production in HSVSMCs from T2DM was higher than those from non-diabetic phenotype. However, unlike inhibition of the JAK/STAT signalling with ruxolitinib which caused a proportionate reduction in mROS in HSVSMCs from T2DM compared with those from non-diabetic control, in MAPK/ERK inhibition with trametinib, there seemed to be a higher degree in reduction of mROS production in HSVSMCs from T2DM patients compared with non-diabetic control. The reason for this is currently not clear but possibly might be cell specific or due to other compensating mechanisms.

6.4 Summary and conclusion

In this chapter, I assessed the impact of stimulation of the JAK/STAT and MAPK/ERK signalling pathways, as well as their inhibitions on the production of mROS in HSVSMCs from T2DM and non-diabetic patients. To ascertain if the T2DM status affects the production of mROS, I compared the results from T2DM with those from non-diabetic phenotype. According to my findings, activation of the JAK/STAT and MAPK/ERK signalling pathways does not significantly change the production of mROS in HSVSMCs from T2DM and non-diabetic patients. However, inhibition of both pathways, JAK/STAT and MAPK/ERK signalling pathways, with ruxolitinib and trametinib respectively, resulted in significant reduction in the generation of mROS in HSVSMCs from both T2DM and non-diabetic patients. Also, production of mROS is higher in HSVSMCs from T2DM patients compared with those from non-diabetic control. The degree of reduction in mROS production following inhibition of the JAK/STAT signalling pathway by ruxolitinib was comparable in HSVSMCs from both T2DM and non-diabetic patients. On the other hand, MAPK/ERK inhibition caused a greater degree of reduction in mROS production in T2DM patients compared to non-diabetic controls.

Chapter 7: General discussion

According to clinical data, more than 70% of T2DM patients will die from a CVD, including CAD (WHO, 2016), and the majority of these deaths are linked to the micro- and macro-vascular complications of T2DM (Powers and D'Alessio, 2010). Over time, effective pharmacological interventions have been developed that target the pathophysiology of these CVDs. Furthermore, the importance of non-pharmacological interventions such as nutrition management and lifestyle modification cannot be overstated. Nevertheless, despite the abundance of clinical and non-clinical interventions that are currently available, CVDs continue to be the world's highest non-communicable cause of death (WHO, 2016). The fact that the focus of therapies for many years has been on either reducing risk factors or modulating the pathophysiological mechanisms with little to no attention paid to the cellular or molecular mechanisms that underlie the complications associated with CVDs is one drawback in combating the increasing number of CVD-dependent mortalities (Bolanle et al., 2021).

In patients with CAD with or without T2DM, CABG using autologous saphenous vein remains the gold standard procedure for restoration of blood supply to the heart (Yusuf et al., 1994, NHS, 2020). Patients with T2DM who have CAD, however, are more susceptible to NIH, vascular remodelling, and stenosis that result in VGF (Motwani and Topol, 1998). While the underlying mechanisms responsible for this are unclear, upregulated O-GlcNAcylation that is common in T2DM has been implicated (De Vries et al., 2016). However, nothing is known about how either hyperglycaemia or T2DM regulates the expression of these regulating enzymes of O-GlcNAcylation in VSMC. Furthermore, it has been demonstrated that vascular cell proliferation and migration as well as vascular inflammation and remodelling are regulated by pro-inflammatory cytokines such as IL-6 (Aibibula et al., 2018), growth factors such as PDGF (Aibibula et al., 2018), and other vasoactive agonists such as Ang II and thrombin (Berk et al., 2000; Tian et al., 2021; Shapiro et al., 1996). In addition, exacerbated JAK/STAT and MAPK/ERK downstream signalling pathways have also been linked to development of NIH, atherosclerosis, and vascular remodelling, events that drive VGF (Ortiz-Munoz et al. 2009; Daniel et al., 2012; Xiang et al. 2013; Wu et al., 2014; Xiang et al. 2014; Chen et al., 2009; Yoshizumi et al., 2019).

Therefore, understanding the role of these pathways and their activators, and how they possibly drive T2DM-mediated vascular dysfunction could offer promising therapeutic targets to

prevent VGF. Currently, antiplatelet and lipid-lowering drugs are the only clinically viable treatments for graft stenosis following CABG, but they have no impact on NIH (Goldman et al., 1988; Mousa et al., 1999). Furthermore, drug-eluting stents and bioresorbable stent scaffolds, which are alternatives to CABG, have the potential to improve patient outcomes (Byrne et al. 2017), but they also possess the risk of impairing EC re-endothelialisation thereby promoting thrombosis (Flores-Ríos et al., 2008; Nakazawa et al., 2008; Caixeta et al., 2009). Therefore, in order to improve SVG patency, novel therapies that limit VGF without affecting VEC migration and proliferation need to be developed. Also, VSMCs have garnered attention as a possible target to treat vascular pathologies due to their role in NIH and venous graft stenosis (Ortiz-Munoz et al. 2009; Xiang et al. 2013; Xiang et al. 2014; Wang et al. 2018). More so, HSV wall thickening is caused by the HSVSMCs shifting from a differentiated to a dedifferentiated phenotype, resulting in uncontrolled cell migration and proliferation responsible for long-term VGF (de Vries et al. 2016). Hence, in this project, I have assessed HSVSMC, a key cell type involved in the vascular dysfunction that results in VGF in T2DM patients, to identify and highlight possible T2DM-dependent alterations that could be viable targets for drug development to attenuate VGF. The key findings of this project are hereby highlighted below.

7.1 T2DM or hyperglycaemia did not alter the expression of the key enzymes of cellular O-GlcNAcylation in HSVSMCs

It is now becoming clearer that protein O-GlcNAcylation (described in section 1.3) is a significant cellular modification through which T2DM initiates vascular dysfunction that has been implicated in multiple CVDs (Bolanle et al., 2021; Yang and Qian, 2017). However, it remains unexplored for possible drug development in managing vascular pathologies (Bolanle et al., 2021). Meanwhile, in cancer and neurodegenerative disorders, this dynamic PTM has gained much attention as a viable target for drug development (Yang and Qian, 2017; Ferrer et al., 2014; Lee et al., 2019; Walter et al., 2020; Sodi et al., 2015; Levine et al., 2019; Zhang et al., 2017; Yang et al., 2017; Pinho et al., 2019). The key enzymes (GFAT, OGT, and OGA) that regulate protein O-GlcNAcylation process and its reversal have now been identified and well characterised (Bolanle et al., 2021; Yang and Qian, 2017). However, how T2DM or hyperglycaemia affects the expression of these enzymes in key cell types such as HSVSMC is unknown.

My findings in this project suggest that neither T2DM nor hyperglycaemia caused any significant alteration in the expression of the regulatory enzymes of cellular O-GlcNAcylation in HSVSMC lysates from T2DM patients versus non-diabetic control. Understanding how T2DM affects the expression and functions of these enzymes could be invaluable to inform the development of therapeutic tools that can help modulate this dynamic post-translational modification in vascular diseases. This is vital because limiting OGT results in downregulation of O-GlcNAcylation whose consequences are far ranging (Yang and Qian, 2017). While it might be predominantly beneficial in cardiac pathologies (Yang and Qian, 2017, Umapathi et al., 2021, Chatham et al., 2021; Bolanle et al., 2021), other studies suggest that downregulating O-GlcNAcylation could be detrimental in cardiac pathologies (Chatham et al., 2021, Jensen et al., 2019). OGT inhibitors such as alloxan and benzoxazolinones already exist, although they have only been utilised as OGT inhibitors in experimental and in vitro investigations (Lenz and Panten, 1988; Jiang et al., 2012). Their usage in clinical applications is not advised because of their numerous toxicities and off-target effects (Ferron et al., 2019; Lenz and Panten, 1988; Jiang et al., 2012). However, Ac-5SGlcNAc, OSMI 1, OSMI 2, and L01 are recently developed OGT inhibitors that may prove more effective as prospective pharmacological treatments because of their enhanced selectivity and encouraging pharmacodynamic profiles (Gloster et al., 2011; Ortiz-Meoz et al., 2015; Martin et al., 2018; Liu et al., 2017)

On the other hand, modulating OGA, the enzyme that reverses the O-GlcNAcylation process is also critical and progress has been made in the creation of potential therapeutic drugs aimed at raising cellular O-GlcNAcylation levels (Bolanle et al., 2021). An example is PUGNAc (O-(2-acetamido-2-deoxy-d-glucopyranosylidene) amino-N-phenylcarbamate), but the drawbacks of PUGNAc include its lack of specificity and the fact that it can severely inhibit other hexosaminidases (Bolanle et al., 2021). Other OGA inhibitors that upregulate O-GlcNAcylation include Thiamet-G (5H-Pyrano[3,2-d]thiazole-6,7-diol, 2-(ethylamino)-3a,6,7,7a-tetrahydro-5-(hydroxymethyl)-(3aR,5R,6S,7R,7aR)), NButGT (1,2-dideoxy-2'-propyl- α -d-glucopyranoso-[2,1-d]- Δ 2'-thiazoline), and more recently developed GlcNAcstatin (Dorfmueller et al., 2006; Dorfmueller et al., 2009). However, while increasing O-GlcNAcylation may be a therapeutic goal in the management of conditions such as cancer (Yang and Qian, 2017; Ferrer et al., 2014; Lee et al., 2019; Walter et al., 2020; Sodi et al., 2015) and neurodegenerative disorders (Levine et al., 2019; Zhang et al., 2017; Yang et al., 2017; Pinho et al., 2019), conversely, a substantial body of evidence suggests that upregulated O-GlcNAcylation can drive pathophysiological changes that promote vascular disorders

(Bolanle et al., 2021). Hence, OGA inhibitors in this context would only be useful in further characterisation of O-GlcNAcylation process to improve our understanding of this dynamic PTM.

Furthermore, while the rationale for using GFAT inhibitors as prospective medicines for the treatment of CVDs is still being clarified, UDP-GlcNAc, the amino sugar substrate produced by GFAT, acts as a universal precursor for all amino sugars needed to create glycoproteins, glycolipids, and proteoglycans. Consequently, many important cellular processes would be impaired by GFAT suppression, thereby increasing the risk of adverse drug reactions arising from GFAT inhibitors. OGT inhibitor development may, therefore, be a more clinically viable option as a potential therapeutic target for drug development to limit VGF (Bolanle et al., 2021). Extensive studies to further investigate the hypothesis that protein O-GlcNAcylation, a glucose-dependent modification that links diabetes with protein function, alters HSVSMCs function through post-translational modification of key proteins as highlighted in 8.1-3 can be carried out.

Furthermore, while my findings have suggested that there are no significant changes in the expression of these enzymes in HSVSMCs, this does not preclude potential changes in HSVECs, another key cell type which also play an important role particularly in early VGF (Owens et al., 2015; Ehsan et al., 2002). Furthermore, this finding does not in any way suggest that activities of these enzymes and their effect on other PTMs such as phosphorylation might not be significantly altered. Given that their relationship is inversely proportional, O-GlcNAcylation and phosphorylation subcellular colocalization have been described as a potential mediator of vascular dysfunction (Bolanle et al., 2021; Fulton et al., 1999; Montagnani et al., 2001). This is because the production of nitric oxide by eNOS is compromised because eNOS phosphorylation is downregulated due to increased O-GlcNAcylation (Masaki et al., 2020; Bolanle et al., 2021; Fulton et al., 1999; Montagnani et al., 2001). Further studies to describe and assess this link in HSVSMCs and HSVECs as described in 8.5 below can be done. My findings have now provided preliminary information that will help lay a foundation into further investigations about this dynamic dysregulation in particular cell types and disease states.

7.2 Ruxolitinib attenuated JAK-mediated increase in OCR and ECAR in HSVSMCs from T2DM patients

OCR and ECAR have been described as excellent markers of cellular metabolic activity (Leese et al. 2016). More so, it is now understood that metabolic reprogramming is a crucial process by which malignant cancer cells can continue to proliferate at high rates despite adverse conditions with scarce oxygen and vital nutrients (Boroughs and DeBerardinis, 2015). Due to the unpredictable nature of cellular responses to stimuli caused by pathologic conditions, different cell types adapt to these changes in different ways. Therefore, the ability to measure these changes during cellular adaptation improves our understanding and offers viable target for drug development. From my findings, after stimulation with activators of JAK/STAT signalling pathway, IL-6/sIL-6R α and PDGF-BB, OCR and ECAR were increased in HSVSMCs from T2DM patients but not in HSVSMCs from non-diabetic patients (Figure 7.1). Activities of pro-inflammatory cytokines such as IL-6/sIL-6R α and growth factors such as PDGF-BB have been described to be upregulated in T2DM patients (Qu et al., 2014; Bowker et al., 2020; Wang et al., 2009; Shen et al., 2020). In addition, it has been shown that chronic inflammation contributes to pulmonary artery remodeling and pulmonary hypertension, among other vascular disorders, and that in these circumstances, inflammatory mediators including IL-6 and PDGF activate the JAK/STAT pathway (Roger et al., 2021). However, it is unknown how these stimuli affect metabolic profile (OCR and ECAR) of HSVSMCs, more so, that these stimuli have been implicated in VGF (Aibibula et al., 2018; Baldini et al., 2021).

Therefore, my findings suggest that ruxolitinib, a known JAK1/2 inhibitor, abolished the observed increase in OCR and ECAR in HSVSMC from T2DM and not in non-diabetic patients after stimulation with IL-6/sIL-6R α and PDGF-BB (Figure 7.1). Ruxolitinib also decreased ECAR and OCR in HSVSMC from T2DM and non-diabetic patients. These findings suggest a JAK-mediated modulation of mitochondrial function of HSVSMCs (Figure 7.1). Also, my results suggest that these alterations may not be associated with any significant difference in levels of IL-6/sIL-6R α - and PDGF-BB-stimulated JAK-mediated STAT3 phosphorylation. Although, this set of data (Figures 4.14 and 4.15) is flawed because I did not use an unstimulated control. However, earlier data (Figure 4.1 B) demonstrates IL-6/sIL-6R α -induced phosphorylation of STAT3 in HSVSMCs. Additionally, the assessment of the mitochondrial DNA copy number following various treatment conditions revealed no significant changes, suggesting that the alterations are not the result of a treatment-induced

increase in mitochondrial number (Figures 4.16 and 4.17). Putting these together, my findings suggest that other unknown factors that may or may not be T2DM-dependent are responsible for the observed increase in the OCR and ECAR of HSVSMCs from T2DM patients.

The JAK/STAT pathway is an emerging target in inflammation which contributes centrally to cardiovascular diseases, hence, anti-inflammatory drugs are becoming popular in the management of cardiovascular events including those resulting from vascular dysfunction (Baldini et al., 2021). Furthermore, emerging findings have suggested that patients with pulmonary hypertension (PH) of different types have pulmonary arteries with overactive JAK/STAT pathways (Roger et al., 2021, Milara et al., 2018). Additionally, a number of profibrotic cytokines, including IL-6, IL-13, and IL-11, as well as growth factors, including PDGF, VEGF, and TGF-1, activate the JAK/STAT pathway and cause pulmonary remodelling, which contributes to the onset of PH (Roger et al., 2021). The current available treatments for PH, marked by endothelial dysfunction and proliferation of SMC, are vasodilatory drugs, which often do not stop the disease progression (Roger et al., 2021). Therefore, targeting the cellular signalling pathways implicated in vascular dysfunction to prevent vascular remodelling may be a viable option for preventing VGF.

Furthermore, STAT3 inhibition by AxCA_{dn}STAT3, an adenoviral vector that encodes a dominant negative STAT3, has been demonstrated to limit neointimal formation by inhibiting proliferation of neointimal SMCs and also promoting their apoptosis (Shibita et al., 2003). Additionally, STAT3, according to studies, has emerged as the main angiogenesis regulator and the main node of the core prosurvival molecular signalling system (Masri et al., 2007; Roger et al., 2021). Also, it has been demonstrated that dominant-negative STAT3 prevents VEGF-induced EC migration and limits VEGF-induced tube formation on collagen gels (Yahata et al., 2003). All these facts suggest the involvement of the JAK/STAT pathway in cell proliferation and migration responsible for vascular remodelling, hence a viable therapeutic strategy to limit VGF.

Ruxolitinib assessed in this study is a clinically effective kinase inhibitor used for the treatment of polycythemia vera and myelofibrosis (Ajayi et al., 2018; Modi et al., 2019). Hence, the ability of ruxolitinib to abolish these IL-6/sIL-6R α - and PDGF-BB-induced JAK-mediated increased OCR and ECAR in HSVSMCs from T2DM patients is therefore promising. Although more functional studies are needed to link the observed alterations to T2DM moderated cellular

processes such as cell differentiation, proliferation, and migration that are implicated in VGF (Riches et al., 2014; Madi et al., 2009). Some of these studies are described in 8.6 below.

Figure 7.1

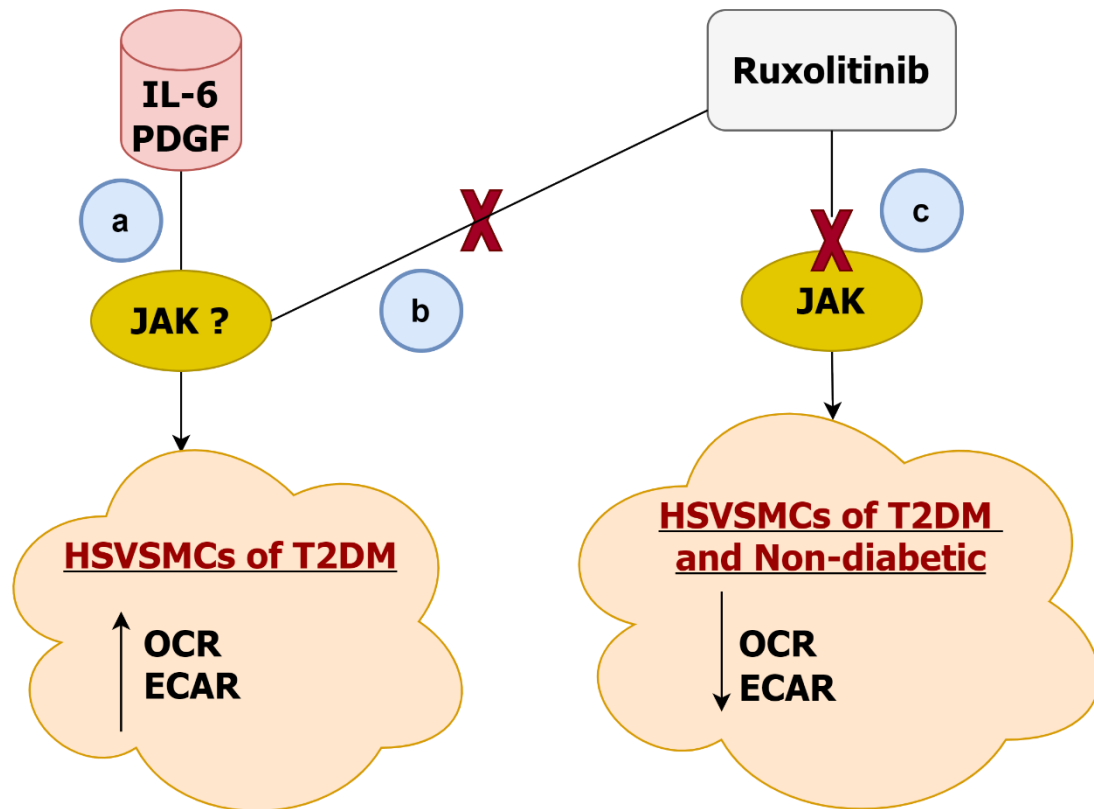


Figure 7.1: Proposed model highlighting how JAK regulates metabolic profile in HSVSMC. (a) IL-6/sIL-6R α and PDGF-BB increased OCR and ECAR in HSVSMCs from T2DM possibly through activating the JAK/STAT signalling pathways. (b) Ruxolitinib, a JAK 1/2 inhibitor, however, abolished this. (c) Ruxolitinib, on the other hand, markedly reduced OCR and ECAR in HSVSMCs from both T2DM and non-diabetic patients by inhibiting the JAK/STAT signalling pathways. IL-6: IL-6/sIL-6R α ; PDGF: PDGF-BB; JAK: Janus kinase; OCR: Oxygen consumption rate; ECAR: Extracellular acidification rate.

7.3 Trametinib attenuated MEK-mediated increase in OCR in HSVSMCs from T2DM patients

From my findings, trametinib, a MEK 1/2 inhibitor which is licenced for the management of metastatic melanoma (Zeiser et al., 2018), abolished the thrombin-induced increase in OCR in HSVSMCs from T2DM (Figure 7.2). Due to their critical role in the control of numerous cellular functions, including survival, differentiation, proliferation, angiogenesis, and migration, the MAPK/ERK pathways have remained a target for drug development and novel treatments (Zeiser et al., 2018). More so, numerous pharmacological agents targeting several points in the MAPK/ERK signalling pathways have now been licenced for treatment of several forms of cancer (Lee et al., 2020; Zeiser et al., 2018; Kim and Choi, 2010; Mahapatra et al., 2017; Faghfuri et al., 2018; Kidger et al., 2018). However, this is yet to be well explored in CVDs including CAD and associated complications such as VGF. One reason for this shortfall is that the role of individual signalling proteins in the MAPK/ERK signalling pathways and their involvement in the pathogenesis of various CVDs and vascular dysfunction is still being elucidated (Muslin, 2008).

Furthermore, it is becoming increasingly clear that the MAPK/ERK pathway is an important regulatory pathway in cardiac pathologies, making the inhibitors promising therapeutic agents (Muslin, 2008). The phenotype and calcification of valvular interstitial cells (VIC) isolated from porcine aortic valve leaflets, for instance, have been shown to be significantly regulated by the MAPK pathway as sustained activation is linked to increased VIC calcification (Gu and Masters, 2009). In this study (Gu and Masters, 2009), it was demonstrated that inhibition of the MAPK/ERK pathways by specific MEK 1/2 inhibitors, U-0126 and PD98059, caused a significant reduction in calcified area, nodule formation, and cell apoptosis. Additionally, several studies have demonstrated that in VSMC cultures, ERK activation tends to promote calcification and osteoblastic differentiation (Ding et al., 2006; Roy et al., 2001; Simmons et al., 2004). My exploration of the MAPK/ERK pathway as a potential mediator for the mitochondrial function of HSVSMCs is therefore driven by the realisation that, despite the opportunity it presents for the development of novel drugs, little is known about it.

I have now added to this body of knowledge by demonstrating that inhibiting MEK 1/2 with trametinib, not only abolished thrombin-induced increase in OCR of HSVSMCs from T2DM patients, but also reduced OCR and ECAR of HSVSMCs from both T2DM and non-diabetic patients (Figure 7.2). More studies are required to further understand how exactly OCR and

ECAR, determinants of mitochondria function, link cellular activities in HSVSMCs, the cell type that I assessed in this project. More so, it is now known that cancer cells in order to meet their metabolism requirements generate ATP through oxidative phosphorylation (measured by OCR) and anaerobic glycolysis (measured by ECAR) (Koppenol et al., 2011; Plitzko and Loesgen, 2018; Zheng, 2012, D'Souza et al., 2011). Since, VSMCs from T2DM subjects have been described to have the tendency to migrate more than those from non-diabetic controls (Riches et al., 2014; Madi et al., 2009), my understanding is that more ATP may be required to drive these cellular activities, however, this is not clear and unproven. Therefore, more studies are required to validate this hypothesis. Some of these studies such as cell proliferation and migration assays that would further improve our understanding on this link are highlighted in 8.6 below.

Figure 7.2

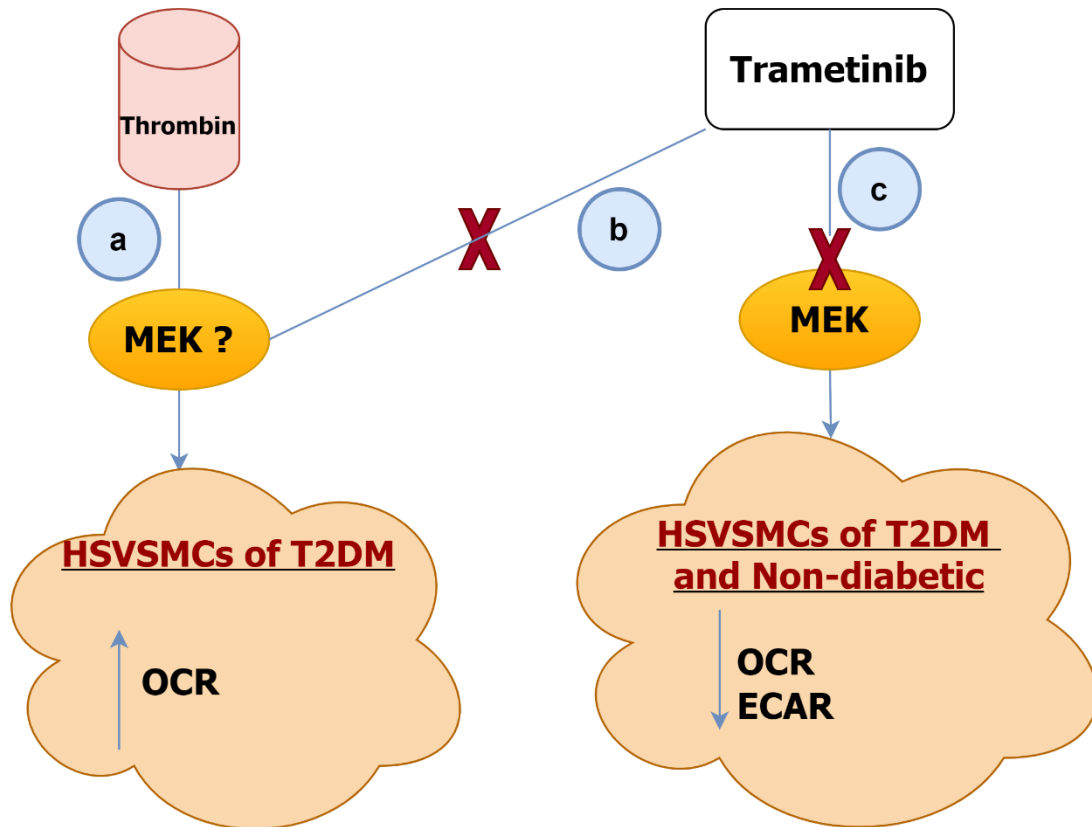


Figure 7.2: Proposed model highlighting how MEK regulates metabolic profile in HSVSMC. (a) Stimulation of HSVSMCs from T2DM with thrombin caused an increase in OCR possibly via the MAPK/ERK pathway (b) This was abolished by trametinib (MEK 1/2 inhibitor) (c) On the other hand, ruxolitinib directly caused a decrease in OCR and ECAR in HSVSMCs from both T2DM and non-diabetic patients. MEK: Mitogen-activated protein kinase kinase; OCR: Oxygen consumption rate; ECAR: Extracellular acidification rate.

7.4 ROS production is attenuated in HSVSMCs by inhibiting JAK/STAT and MAPK/ERK signalling

From my findings, inhibiting both JAK/STAT and MAPK/ERK signalling pathways in HSVSMCs from both T2DM and non-diabetic patients, caused a reduction in the production of mROS (Chapter 6). T2DM, smoking, ageing, hypercholesterolemia, and nitrate intolerance which are risk factors for CVDs, all promote the production of ROS (Panth et al., 2016). Moreover, overproduction of ROS has emerged as a critical driver of the pathogenesis of multiple chronic and degenerative disorders including cancer, cardiovascular, neurodegenerative, respiratory and inflammatory diseases (Liu et al., 2018; Wells et al., 2009; Khandrika et al., 2009; Katakwar et al., 2016; Kings et al., 2008; Masoli et al., 2004; Davila and Torres-Aleman, 2008; Madamanchi et al., 2005; Hakonen et al., 2008). Additionally, majority of CVDs have been linked to formation of atherosclerotic plaques which is promoted by ROS (Madamanchi et al., 2005). Also, inflammation and VGF, two important factors responsible for VGF, are promoted by ROS (Lo et al., 2018; Cachofeiro et al., 2008; Madamanchi et al., 2005). Considering this involvement of ROS in cardiac pathologies, lowering ROS production or effect has become an effective treatment target for several CVDs (Liu et al., 2018). For instance, increased consumption of fruits and vegetables which are sources of carotene and ascorbic acid, known antioxidants, have helped decrease cholesterol oxidation (Asplund, 2002; Zino et al., 1997).

Furthermore, it is now acknowledged that intracellular ROS generation plays a significant role in the pathophysiology of cardiovascular disorders, in part by encouraging the proliferation of VSMCs (Shimokawa, 2013). Changes in vascular redox status have also been linked to the pathophysiology of cardiac hypertrophy, atherosclerosis, aortic aneurysms, and vascular restenosis (Satoh et al., 2008; Satoh et al., 2009; Nigro et al., 2011; Satoh et al., 2011). The hallmarks of vascular damage in cardiac diseases such as hypertension and CAD include vascular remodelling, stiffness, and elevated ROS (Martinez-Revelles et al., 2017). Additionally, ROS triggers immunological activation to induce systemic inflammation (Sena et al., 2018). Activated immune cells enter the vasculature and produce a number of substances, including matrix metalloproteinases, cytokines, and chemokines that promote vascular injury and dysfunction as well as vasoconstriction and vessel remodelling that are common features in VGF (Zhou et al., 2017; Norlander et al., 2018). Therefore, limiting ROS production continues

to be a viable treatment strategy limit a variety of disease condition including CVDs and the associated vascular dysfunction.

My findings have now shown that mROS production in HSVSMCs is mediated through the JAK/STAT and MAPK/ERK signalling pathways, hence, are viable targets to limit ROS-mediated CVDs and vascular dysfunctions including atherosclerosis and VGF. Inhibiting the JAK/STAT signalling has been suggested as a promising treatment option in the management of ROS-driven Primary Sjogren's syndrome, a complex autoimmune epithelitis (Charras et al., 2019). Furthermore, inhibiting JAK/STAT-mediated ROS has been extensively described as viable target in the treatment of different forms of cancer (Venkatabalasubramanian, 2021). Additionally, inhibiting of JAK/STAT signalling significantly reduced intravitreal neovascularization in a retinopathy of prematurity ROP rat model (Byfield et al., 2009). Similarly, inhibiting MAPK/ERK pathway have been identified as treatment target in ROS-mediated cancer including leukaemia (Jasek-Gajda et al., 2020; Lee et al., 2020). These findings have further demonstrated the potential of targeting the JAK/STAT and MAPK/ERK pathways in the treatment of several ROS-driven human pathologies, but little is known about this possibility in the management of CVDs, which my findings have now demonstrated.

7.5 Strengths and limitations of this study

The strength of this study comes from the fact that it is the first to describe this set of experiments in HSVSMC, a key cell type involved in the vascular dysfunction responsible for SVGF seen in T2DM patients. Also, its strength stems from the fact that SMCs utilised in this study were explanted specifically from HSV of T2DM and non-diabetic patients undergoing CABG procedure, as opposed to using SMCs from animal or other sources. This could somehow guarantee some degree of similar molecular features *in vivo*. Additionally, adequate number of HSV samples were obtained during this study (Appendix) and this allows for frequent prepping to explant SMCs, hence only early passages (1-4) were used in this study. More so that it has been suggested that early passages are thought to retain expression of key molecular properties of the origin cell (Mouriaux et al., 2016). The use of HSVSMCs from various individuals, which allows for patient variability, is another strength of this study.

On the other hand, a major limitation of this study was the Covid-19 pandemic which disrupted the early stage of this project. Shortly before the lockdown, the fusion proteins which were supposed to be used as *O*-GlcNAc trap had just been synthesised. When the labs were re-

opened, it was now over a year since they were synthesised and the potency could no longer be guaranteed. Alternative arrangements to get large scale production of these fusion proteins from the University of York was faced with some logistic challenges. As the fusion proteins just arrived in the final months of this study, there was not much time to optimise *O*-GlcNAc capture. Also, a potential limitation of this study is the fact that isolated HSVSMCs were cultured *in vitro* precluding interactions with other VCs such as ECs. These interactions play critical roles in the pathogenesis of NIH and vascular dysfunction. Hence, it is possible that the response in cell culture where other cell types are absent and *in vivo* will differ.

Also, HSV tissues were obtained from T2DM and non-diabetic patients undergoing CABG procedure because of CAD. It is unknown, nevertheless, how much the disease condition or other molecular processes caused by the condition may have affected the cellular properties of these HSVSMCs which may not be entirely attributed to T2DM. Additionally, more detailed information such as diabetes duration and HbA1c that would have helped further characterise each patient donor was not accessible to me at the time of sample collection. Hence, patients were classified based on whether they were receiving T2DM treatment or not, and this does not preclude the fact that some of the patients classified as non-diabetic may be insulin resistant and pre-diabetic. I acknowledge that this was also a limitation and future sample collections will be done with more precise characteristic information of the patient donor.

Furthermore, in some instance such as the data from the seahorse experiments documented in Chapters 4 and 5 of this thesis, where *n* size is 4. This may be statistically insufficient to draw a conclusion as higher *n* size (≥ 6) is recommended (Razali and Wah, 2011; Ghasemi and Zahediasi, 2012). The cost of running this set of experiments is high and this was the major reason for limiting the *n* size to 4. I acknowledge that this was a limitation to this set of experiments. Another limitation was that I did not use an unstimulated control in Figures 4.14 and 4.15, as well as Figure 5.15, where I attempted to demonstrate that the observed increase in OCR of HSVSMCs from T2DM patients were not associated with IL-6/sIL-6R- and PDGF-BB-stimulated JAK-mediated STAT3 phosphorylation or thrombin-stimulated MEK-mediated Erk phosphorylation, respectively. In light of this, I would make sure that all of my future investigations are carefully controlled.

CHAPTER 8: Perspectives and future experiments

In this thesis, I have demonstrated that early passaging, T2DM, and high glucose concentrations do not alter the expressions of the key enzymes (OGA, OGT, and GFAT) that regulate cellular *O*-GlcNAcylation in HSVSMCs. Furthermore, my findings have shown that T2DM alters the metabolic responses (OCR and ECAR) of HSVSMCs to PDGF-BB and the proinflammatory stimulus IL-6/sIL-6R α . The results also showed that, when compared to non-diabetic controls, these changes are not related with any significant difference in levels of IL-6/sIL-6R α - and PDGF-stimulated JAK-mediated STAT3 phosphorylation. Also, the ability of ruxolitinib to abolish these changes as shown by my findings, points to a possible JAK-mediated modulation of HSVSMC mitochondrial activity, hence a possible therapeutic target in T2DM-induced vein graft failure. My findings also indicate that HSVSMCs stimulated with thrombin, a known activator of the MAPK/ERK pathways, utilised more oxygen than HSVSMCs from non-diabetic controls. My results also demonstrated that these alterations observed in HSVSMCs from T2DM patients are not associated with any discernible difference in levels of Ang II- and thrombin-stimulated MEK-mediated ERK phosphorylation when compared with non-diabetic controls, which is suggestive of a T2DM-dependent alteration. Additionally, these results point to a MAPK/ERK-mediated modification of mitochondrial activity, which also offers a potential therapeutic target to limit vascular dysfunction associated with T2DM.

Furthermore, my research revealed that HSVSMCs from T2DM produced more mROS than HSVSMCs from non-diabetic controls. Additionally, the production of mROS in HSVSMCs from T2DM and non-diabetic individuals is not significantly altered by the stimulation of the JAK/STAT and MAPK/ERK signalling pathways. But ruxolitinib and trametinib, which suppress the JAK/STAT and MAPK/ERK signalling pathways, respectively, significantly reduced the production of mROS in HSVSMCs from T2DM and non-diabetic patients. Considering the relevance of ROS in the pathogenesis of cardiovascular disorders including atherosclerosis, vascular remodelling, and NIH, therefore, these findings of my study have now identified the JAK/STAT and MAPK/ERK signalling pathways as possible target to limit production of mROS in HSVSMCs. Putting all these data together, my findings have therefore contributed to the body of knowledge identifying novel glucose-dependent changes that cause vascular dysfunction in T2DM patients. These findings from my project therefore offer a background and rationale for future experiments, some of which I have now highlighted below.

8.1 Optimisation and isolation of *O*-GlcNAcylated protein from HSVSMC extracts

A catalytically inactive mutant (D298N) of *Clostridium perfringens* NagJ, a bacterial orthologue of eukaryotic OGAs (CpOGAD298N), can be used to preferentially enrich *O*-GlcNAcylated proteins (Selvan et al., 2017). This allows enough *O*-GlcNAcylated protein to be affinity captured by bacterially produced and purified Halo-tagged CpOGAD298N so as to enable downstream peptide detection by mass spectrometry. To ascertain the amount of starting material necessary to achieve specific recovery of sufficient *O*-GlcNAcylated proteins, in vitro SMC cultures from explanted HSVs can be used in pilot experiments. Then, SDS/PAGE and immunoblotting of affinity purified and eluted samples using commercially available anti-*O*-GlcNAc antibody RL2 (Cat No: ab2739) can be used to determine the start-up material (Selvan et al., 2017). To further optimise *O*-GlcNAc capture, antibodies can be raised against well-characterised *O*-GlcNAcylated substrates such as the transcription factor RelA (Li et al., 2014; Ma et al., 2017) or the signalling intermediate TAB1 (Cheung et al., 2003).

8.2 Identification of *O*-GlcNAcylated target proteins in HSVSMCs from T2DM patients

HSVSMCs from poorly controlled T2DM patients (HbA1C levels >8% for >1 year who are on stable medication) can be compared to non-diabetic controls to characterise differences in the cellular *O*-GlcNAcylation machinery. To do this, RL2 antibody-based quantitative immunoblotting can be utilised to measure the total protein *O*-GlcNAcylation level. The OGA, OGT, and GFAT, *O*-GlcNAcylation regulatory enzymes' mRNA levels can be assessed using quantitative real-time PCR. Tandem mass tagging (TMT) (DeSouza and Siu, 2013) can be used to enable relative quantification of peptides in the healthy and diabetes groups following affinity purification with CpOGAD298N and trypsin digestion in order to identify proteins which are differentially *O*-GlcNAcylated in HSVSMCs from diabetic versus healthy control patients.

8.3 Validation and functional characterisation of *O*-GlcNAcylated proteins in HSV-SMC targets

After a panel of novel *O*-GlcNAcylated targets has been identified (+/- standard deviation of the mean), pathway analysis tools like DAVID, GeneTrail2, and PathVisio can be used to evaluate connections between the identified targets and disease pathophysiology and functional roles before deciding which targets to prioritise for further characterisation in HSVSMCs *in*

vitro. By affinity purification with CpOGAD298N from HSVSMC extracts obtained from healthy and T2DM patients, and then immunoblotting against the target protein, different techniques can be employed to confirm the *O*-GlcNAcylation status of selected proteins. First, the target protein's *O*-GlcNAcylation status in control HSVSMCs can be manipulated using the OGA inhibitor thiamet-G (TMG), which broadly enhances *O*-GlcNAcylation (McGreal et al., 2018), and the OGT inhibitor peracetylated 5-thio-N-acetylglucosamine (Ac4-5SGlcNAc). Short inhibitory RNA (siRNA)-mediated knockdown of OGT, OGA, and GFAT in comparison to non-targeted control siRNAs can be used to validate these observations. Before being expressed in HSVSMCs and having their *O*-GlcNAcylation status and function evaluated, altered variants of the target protein can be created in which Ser/Thr residues that have been identified as *O*-GlcNAcylation sites are changed to Ala. Furthermore, effects of *O*-GlcNAcylation-resistant target protein expression in HSVSMC function assays that are crucial for vascular re-modelling, such as modifications in proliferation and migration, can be evaluated.

8.4 Assessing these alterations in HSVECs and evaluating the effect of other post-translational modifications

The activation and denudation of the endothelium following surgical trauma and graft implantation promotes a variety of immunological, inflammatory, and cellular differentiation that leads to endothelial dysfunction, increasing NIH, and accelerated atherosclerosis that results in VGF (Ladak et al., 2022). Additionally, research has shown a connection between elevated VEC proliferation and altered EC metabolism profile in pulmonary arterial hypertension (Fang et al., 2012; Caruso et al., 2017). These findings point to ECs as a critical cell type in VGF hence, investigating these changes in HSVECs could further identify more targets in limiting VGF. Additionally, although there were no changes in the expressions of the OGT, OGA, and GFAT proteins in HSVSMCs, this does not rule out possible changes in HSVECs. Also, I did not investigate how T2DM or hyperglycaemia affect the activities of the enzymes, their subcellular localization, or any post-translational modifications like phosphorylation that may affect their activities. All of these can serve as justification/rationale for future research.

8.5 Assessing the impact of phosphorylation and *O*-GlcNAcylation crosstalk on vascular function

Since eNOS phosphorylation is essential for nitric oxide synthesis and the preservation of vascular function, the impact of augmented and decreased *O*-GlcNAcylation on eNOS phosphorylation in HSVSMCs and HSVECs can be evaluated as a measure of vascular function (Masaki et al., 2020). To do this, lysates from HSVSMCs and HSVECs of T2DM and non-diabetic controls will be equilibrated for protein content and resolved by SDS/PAGE. Following this, immunoblotting against Phospho-eNOS (Ser1177) antibody (Cat No: #9571, 1:1000) will be performed. After visualisation, membranes will be stripped and reprobed with *O*-GlcNAc antibody (Cat No: ab2739; 1:500). Then, the impact of changes in *O*-GlcNAc status on the phosphorylation of eNOS at serine 1177 in HSVSMCs and HSVECs will be examined quantitatively. This experiment will be repeated using lysates of HSVSMCs and HSVECs treated with HG (10 mM and 25 mM) concentration +/- thiamet G versus those treated with normal (5 mM) concentration +/- thiamet G.

8.6 Assessment of the relationship between altered metabolic profile of the HSVSMC and defined functional readouts of vascular dysfunction

From my findings, of the four known stimuli of HSVSMC dysfunction (IL-6/sIL-6R α , PDGF-BB, Ang II, and thrombin) assessed in this project, all but Ang II caused an increase in OCR and ECAR of HSVSMCs from T2DM. However, the connection between the HSVSMC's altered metabolic profile (OCR and ECAR) and defined functional readouts of vascular dysfunction and NIH such as proliferation and migration of VSMCs is not clear. Understanding this relationship and identifying the common changes may help identify new therapeutic targets to help limit VGF. Therefore, to help understand this connection, both proliferation and migratory assays as described by (Riches et al., 2014; Madi et al., 2009) can be done after treating HSVSMCs from T2DM and non-diabetic patients with or without the respective agonist +/- inhibitor.

9. References

- Abdul-Ghani MA, DeFronzo RA. Dapagliflozin for the treatment of type 2 diabetes. Expert opinion on pharmacotherapy. 2013 Aug 1;14(12):1695-703.
- Abdul-Ghani MA, DeFronzo RA. Pathogenesis of insulin resistance in skeletal muscle. Journal of Biomedicine and Biotechnology. 2010 Oct;2010:476279
- Abete P, Napoli C, Santoro G, Ferrara N, Tritto I, Chiariello M, Rengo F, and Ambrosio G. Age-related decrease in cardiac tolerance to oxidative stress. J Mol Cell Cardiol. 1999;31:227-36.
- Abid H, Ryan ZC, Delmotte P, Sieck GC, Lanza IR. Extramyocellular interleukin-6 influences skeletal muscle mitochondrial physiology through canonical JAK/STAT signaling pathways. The FASEB Journal. 2020 Nov;34(11):14458-72.
- Ahmad M, Wolberg A, Kahwaji CI. Biochemistry, Electron Transport Chain. [Updated 2022 Sep 5]. In: StatPearls [Internet]. Treasure Island (FL): StatPearls Publishing; 2022 Jan.
- Aibibula M, Naseem KM, Sturmey RG. Glucose metabolism and metabolic flexibility in blood platelets. Journal of Thrombosis and Haemostasis. 2018 Nov;16(11):2300-14.
- Aittomäki S, Pesu M. Therapeutic targeting of the Jak/STAT pathway. Basic & clinical pharmacology & toxicology. 2014 Jan;114(1):18-23.
- Ajayi S, Becker H, Reinhardt H, Engelhardt M, Zeiser R, Bubnoff NV, Wäsch R. Ruxolitinib. In: Small molecules in Hematology 2018 (pp. 119-132). Springer, Cham.
- Akbari M, Hassan-Zadeh V. IL-6 signalling pathways and the development of type 2 diabetes. Inflammopharmacology. 2018 Jun;26(3):685-98.
- Akhigbe R, Ajayi A. The impact of reactive oxygen species in the development of cardiometabolic disorders: a review. Lipids in Health and Disease. 2021 Dec;20(1):1-8.
- Akimoto Y, Hart GW, Wells L, Vosseller K, Yamamoto K, Munetomo E, Ohara-Imaizumi M, Nishiwaki C, Nagamatsu S, Hirano H, Kawakami H. Elevation of the post-translational modification of proteins by O-linked N-acetylglucosamine leads to deterioration of the glucose-stimulated insulin secretion in the pancreas of diabetic Goto-Kakizaki rats. Glycobiology. 2007 Feb 1;17(2):127-40.
- Akki A, Zhang M, Murdoch C, Brewer A, Shah AM. NADPH oxidase signaling and cardiac myocyte function. Journal of molecular and cellular cardiology. 2009 Jul 1;47(1):15-22.
- Akram M. Citric acid cycle and role of its intermediates in metabolism. Cell biochemistry and biophysics. 2014 Apr;68(3):475-8.
- Ala Y, Palluy O, Favero J, Bonne C, Modat G, Dornand J. Hypoxia/reoxygenation stimulates endothelial cells to promote interleukin-1 and interleukin-6 production. Effects of free radical scavengers. Agents and actions. 1992 Sep;37(1):134-9.
- Albert-Gascó H, Ros-Bernal F, Castillo-Gómez E, Olucha-Bordonau FE. MAP/ERK signaling in developing cognitive and emotional function and its effect on pathological and neurodegenerative processes. International Journal of Molecular Sciences. 2020 Jun 23;21(12):4471.

- Al-Delaimy WK, Manson JE, Solomon CG, Kawachi I, Stampfer MJ, Willett WC, Hu FB. Smoking and risk of coronary heart disease among women with type 2 diabetes mellitus. *Archives of internal medicine*. 2002 Feb 11;162(3):273-9.
- Alexander JH, Hafley G, Harrington RA, Peterson ED, Ferguson Jr TB, Lorenz TJ, Goyal A, Gibson M, Mack MJ, Gennevois D, Califf RM. PREVENT IV Investigators: Efficacy and safety of edifoligide, an E2F transcription factor decoy, for prevention of vein graft failure following coronary artery bypass graft surgery: PREVENT IV: a randomized controlled trial. *JAMA*. 2005;294(19):2446-54.
- Alfaro JF, Gong CX, Monroe ME, Aldrich JT, Clauss TR, Purvine SO, Wang Z, Camp DG, Shabanowitz J, Stanley P, Hart GW. Tandem mass spectrometry identifies many mouse brain O-GlcNAcylated proteins including EGF domain-specific O-GlcNAc transferase targets. *Proceedings of the National Academy of Sciences*. 2012 May 8;109(19):7280-5.
- Ali MH, Schlidt SA, Chandel NS, Hynes KL, Schumacker PT, Gewertz BL. Endothelial permeability and IL-6 production during hypoxia: role of ROS in signal transduction. *American Journal of Physiology-Lung Cellular and Molecular Physiology*. 1999 Nov 1;277(5):L1057-65.
- Al-Mehdi AB, Pastukh VM, Swiger BM, Reed DJ, Patel MR, Bardwell GC, Pastukh VV, Alexeyev MF, Gillespie MN. Perinuclear mitochondrial clustering creates an oxidant-rich nuclear domain required for hypoxia-induced transcription. *Science signaling*. 2012 Jul 3;5(231):ra47-.
- Al-Shabrawey M, Bartoli M, El-Remessy AB, Platt DH, Matragoon S, Behzadian MA, Caldwell RW, Caldwell RB. Inhibition of NAD (P) H oxidase activity blocks vascular endothelial growth factor overexpression and neovascularization during ischemic retinopathy. *The American journal of pathology*. 2005 Aug 1;167(2):599-607.
- Andersen JK. Oxidative stress in neurodegeneration: cause or consequence?. *Nature medicine*. 2004 Jul;10(7):S18-25.
- Arnold P, Boll I, Rothaug M, Schumacher N, Schmidt F, Wichert R, Schneppenheim J, Lokau J, Pickhinke U, Koudelka T, Tholey A. Meprin metalloproteases generate biologically active soluble interleukin-6 receptor to induce trans-signaling. *Scientific reports*. 2017 Mar 9;7(1):1-1.
- Ashar FN, Zhang Y, Longchamps RJ, Lane J, Moes A, Grove ML, Mychaleckyj JC, Taylor KD, Coresh J, Rotter JJ, Boerwinkle E. Association of mitochondrial DNA copy number with cardiovascular disease. *JAMA cardiology*. 2017 Nov 1;2(11):1247-55.
- Asplund K. Antioxidant vitamins in the prevention of cardiovascular disease: a systematic review. *Journal of internal medicine*. 2002 May;251(5):372-92.
- Avila C, Huang RJ, Stevens MV, Aponte AM, Tripodi D, Kim KY, Sack MN. Platelet mitochondrial dysfunction is evident in type 2 diabetes in association with modifications of mitochondrial anti-oxidant stress proteins. *Experimental and clinical endocrinology & diabetes*. 2012 Apr;120(04):248-51.
- Awasthi N, Monahan S, Stefaniak A, Schwarz MA, Schwarz RE. Inhibition of the MEK/ERK pathway augments nab-paclitaxel-based chemotherapy effects in preclinical models of pancreatic cancer. *Oncotarget*. 2018 Jan 1;9(4):5274.

- Badimon L, Padró T, Vilahur G. *European Heart Journal: Acute Cardiovascular. European Heart Journal: Acute Cardiovascular Care.* 2012;1(1):60-74.
- Bailey CJ. Biguanides and NIDDM. *Diabetes care.* 1992 Jun 1;15(6):755-72.
- Bakker W, Eringa EC, Sipkema P, van Hinsbergh VW. Endothelial dysfunction and diabetes: roles of hyperglycemia, impaired insulin signaling and obesity. *Cell and tissue research.* 2009 Jan;335(1):165-89.
- Baldini C, Moriconi FR, Galimberti S, Libby P, De Caterina R. The JAK–STAT pathway: an emerging target for cardiovascular disease in rheumatoid arthritis and myeloproliferative neoplasms. *European Heart Journal.* 2021 Nov 7;42(42):4389-400.
- Baliunas DO, Taylor BJ, Irving H, Roerecke M, Patra J, Mohapatra S, Rehm J. Alcohol as a risk factor for type 2 diabetes: a systematic review and meta-analysis. *Diabetes care.* 2009 Nov 1;32(11):2123-32.
- Ball LE, Berkaw MN, Buse MG. Identification of the major site of O-linked β -N-acetylglucosamine modification in the C terminus of insulin receptor substrate-1. *Molecular & Cellular Proteomics.* 2006 Feb 1;5(2):313-23.
- Banerjee S, Biehl A, Gadina M, Hasni S, Schwartz DM. JAK–STAT signaling as a target for inflammatory and autoimmune diseases: current and future prospects. *Drugs.* 2017 Apr;77(5):521-46.
- Banning AP, Westaby S, Morice MC, Kappetein AP, Mohr FW, Berti S, Glauber M, Kellett MA, Kramer RS, Leadley K, Dawkins KD. Diabetic and nondiabetic patients with left main and/or 3-vessel coronary artery disease: comparison of outcomes with cardiac surgery and paclitaxel-eluting stents. *Journal of the American College of Cardiology.* 2010 Mar 16;55(11):1067-75.
- Baran P, Nitz R, Grötzinger J, Scheller J, Garbers C. Minimal interleukin 6 (IL-6) receptor stalk composition for IL-6 receptor shedding and IL-6 classic signaling. *Journal of Biological Chemistry.* 2013 May 24;288(21):14756-68.
- Barbato E, Toth GG, De Bruyne B. Coronary-Artery Bypass Grafting. *The New England Journal of Medicine.* 2016 Sep 1;375(10):e22-.
- Bastaki S. Diabetes mellitus and its treatment. *Dubai Diabetes and Endocrinology Journal.* 2005;13:111-34.
- Batandier C, Guigas B, Detaille D, El-Mir M, Fontaine E, Rigoulet M, Leverve XM. The ROS production induced by a reverse-electron flux at respiratory-chain complex 1 is hampered by metformin. *Journal of bioenergetics and biomembranes.* 2006 Feb;38(1):33-42.
- Bays HE, Toth PP, Kris-Etherton PM, Abate N, Aronne LJ, Brown WV, Gonzalez-Campoy JM, Jones SR, Kumar R, La Forge R, Samuel VT. Obesity, adiposity, and dyslipidemia: a consensus statement from the National Lipid Association. *Journal of clinical lipidology.* 2013 Jul 1;7(4):304-83.
- Bazan JF. Structural design and molecular evolution of a cytokine receptor superfamily. *Proceedings of the National Academy of Sciences.* 1990 Sep;87(18):6934-8.
- Beckman JA, Creager MA, Libby P. Diabetes and atherosclerosis: epidemiology, pathophysiology, and management. *Jama.* 2002 May 15;287(19):2570-81.

- Bedard K, Krause KH. The NOX family of ROS-generating NADPH oxidases: physiology and pathophysiology. *Physiological reviews*. 2007 Jan;87(1):245-313.
- Behring JB, van der Post S, Mooradian AD, Egan MJ, Zimmerman MI, Clements JL, Bowman GR, Held JM. Spatial and temporal alterations in protein structure by EGF regulate cryptic cysteine oxidation. *Science signaling*. 2020 Jan 21;13(615):eaay7315.
- Benigni A, Cassis P, Remuzzi G. Angiotensin II revisited: new roles in inflammation, immunology and aging. *EMBO molecular medicine*. 2010 Jul;2(7):247-57.
- Berg J.M., Tymoczko J.L., & Stryer L. (2002). *Biochemistry*, 5th edition. New York: W H Freeman.
- Berk BC, Haendeler J, Sottile J. Angiotensin II, atherosclerosis, and aortic aneurysms. *The Journal of clinical investigation*. 2000 Jun 1;105(11):1525-6.
- Blanchetot C, Tertoolen LG, den Hertog J. Regulation of receptor protein-tyrosine phosphatase α by oxidative stress. *The EMBO journal*. 2002 Feb 15;21(4):493-503.
- Bogatcheva NV, Garcia JG, Verin AD. Molecular mechanisms of thrombin-induced endothelial cell permeability. *Biochemistry (Moscow)*. 2002 Jan;67(1):75-84.
- Bokoch GM, Diebold BA. Current molecular models for NADPH oxidase regulation by Rac GTPase. *Blood, The Journal of the American Society of Hematology*. 2002 Oct 15;100(8):2692-5.
- Boland BB, Rhodes CJ, Grimsby JS. The dynamic plasticity of insulin production in β -cells. *Molecular metabolism*. 2017 Sep 1;6(9):958-73.
- Bolanle IO, Omogbai EK, Bafor EE. Effects of amlodipine and valsartan on glibenclamide-treated streptozotocin-induced diabetic rats. *Biomedicine & Pharmacotherapy*. 2018 Oct 1;106:566-74.
- Bolanle IO, Riches-Suman K, Loubani M, Williamson R, Palmer TM. Revascularisation of type 2 diabetics with coronary artery disease: Insights and therapeutic targeting of O-GlcNAcylation. *Nutrition, Metabolism and Cardiovascular Diseases*. 2021 May 6;31(5):1349-56.
- Bolanle IO, Riches-Suman K, Williamson R, Palmer TM. Emerging roles of protein O-GlcNAcylation in cardiovascular diseases: Insights and novel therapeutic targets. *Pharmacological Research*. 2021 Mar 1;165:105467.
- Bond MR, Hanover JA. A little sugar goes a long way: the cell biology of O-GlcNAc. *Journal of Cell Biology*. 2015 Mar 30;208(7):869-80.
- Bond MR, Hanover JA. O-GlcNAc cycling: a link between metabolism and chronic disease. *Annual review of nutrition*. 2013 Jul 17;33:205-29.
- Bonnet S, Michelakis ED, Porter CJ, Andrade-Navarro MA, Thébaud B, Bonnet S, Haromy A, Harry G, Moudgil R, McMurtry MS, Weir EK. An abnormal mitochondrial-hypoxia inducible factor-1 α -Kv channel pathway disrupts oxygen sensing and triggers pulmonary arterial hypertension in fawn hooded rats: similarities to human pulmonary arterial hypertension. *Circulation*. 2006 Jun 6;113(22):2630-41.
- Borchi E, Bargelli V, Stillitano F, Giordano C, Sebastiani M, Nassi PA, d'Amati G, Cerbai E, Nediani C. Enhanced ROS production by NADPH oxidase is correlated to changes in antioxidant enzyme activity in human heart failure. *Biochim Biophys Acta*. 2010 Mar;1802(3):331-8.

- Bornfeldt KE, Raines EW, Nakano T, Graves LM, Krebs EG, Ross R. Insulin-like growth factor-I and platelet-derived growth factor-BB induce directed migration of human arterial smooth muscle cells via signaling pathways that are distinct from those of proliferation. *The Journal of clinical investigation*. 1994 Mar 1;93(3):1266-74.
- Bornfeldt KE, Tabas I. Insulin resistance, hyperglycemia, and atherosclerosis. *Cell metabolism*. 2011 Nov 2;14(5):575-85.
- Boroughs LK, DeBerardinis RJ. Metabolic pathways promoting cancer cell survival and growth. *Nature cell biology*. 2015 Apr;17(4):351-9.
- Boulay JL, O'Shea JJ, Paul WE. Molecular phylogeny within type I cytokines and their cognate receptors. *Immunity*. 2003 Aug 1;19(2):159-63.
- Bourassa MG, Fisher LD, Campeau L, Gillespie MJ, McConney M, Lesperance J. Long-term fate of bypass grafts: the Coronary Artery Surgery Study (CASS) and Montreal Heart Institute experiences. *Circulation*. 1985 Dec 1;72(6 Pt 2):V71-8.
- Bowker N, Shah RL, Sharp SJ, Stewart ID, Wheeler E, Ferreira MA, Baras A, Wareham NJ, Langenberg C, Lotta LA. Meta-analysis investigating the role of interleukin-6 mediated inflammation in type 2 diabetes. *EBioMedicine*. 2020 Nov 1;61:103062.
- BR W. Colledge NR, Ralston SH, Penman ID. Oncology in: *Davidson's Principles and Practice of Medicine*. 22nd edition, Churchill Livingstone.2014- pp 797-836
- Brägelmann J, Lorenz C, Borchmann S, Nishii K, Wegner J, Meder L, Ostendorp J, Ast DF, Heimsoeth A, Nakasuka T, Hirabae A. MAPK-pathway inhibition mediates inflammatory reprogramming and sensitizes tumors to targeted activation of innate immunity sensor RIG-I. *Nature communications*. 2021 Sep 17;12(1):1-5.
- Bragg F, Holmes MV, Iona A, Guo Y, Du H, Chen Y, Bian Z, Yang L, Herrington W, Bennett D, Turnbull I. Association between diabetes and cause-specific mortality in rural and urban areas of China. *Jama*. 2017 Jan 17;317(3):280-9.
- Brand MD, Nicholls DG. Assessing mitochondrial dysfunction in cells. *Biochemical Journal*. 2011 Apr 15;435(2):297-312.
- Brass LF, Molino M. Protease-activated G protein-coupled receptors on human platelets and endothelial cells. *Thrombosis and haemostasis*. 1997;78(07):234-41.
- Bravo J, Heath JK. Receptor recognition by gp130 cytokines. *The EMBO journal*. 2000 Jun 1;19(11):2399-411.
- Brennan JP, Bardswell SC, Burgoyne JR, Fuller W, Schroder E, Wait R, Begum S, Kentish JC, Eaton P. Oxidant-induced activation of type I protein kinase A is mediated by RI subunit interprotein disulfide bond formation. *Journal of biological chemistry*. 2006 Aug 4;281(31):21827-36.
- Brinster RL. Nutrition and metabolism of the ovum, zygote and blastocyst. *Handbook of physiology*. 1973;11:165-85.
- British Heart Foundation (2019). <https://www.bhf.org.uk/what-we-do/our-research/heart-statistics/heart-statistics-publications/cardiovascular-disease-statistics>. Accessed 02-05-2020

- British heart foundation (2020). Coronary heart disease fact sheet. <https://www.bhf.org.uk/informationsupport/conditions/coronary-heart-disease>. Accessed 15:04:2020
- Brown GC, Murphy MP, Scott I, Youle RJ. Mitochondrial fission and fusion. *Essays in biochemistry*. 2010 Jun 14;47:85-98.
- Burge MR, Zeise TM, Sobhy TA, Rassam AG, Schade DS. Low-dose ethanol predisposes elderly fasted patients with type 2 diabetes to sulfonylurea-induced low blood glucose. *Diabetes Care*. 1999 Dec 1;22(12):2037-43.
- Burgos-Morón E, Abad-Jiménez Z, Martínez de Marañón A, Iannantuoni F, Escribano-López I, López-Domènech S, Salom C, Jover A, Mora V, Roldan I, Solá E. Relationship between oxidative stress, ER stress, and inflammation in type 2 diabetes: the battle continues. *Journal of clinical medicine*. 2019 Sep 4;8(9):1385.
- Burgoyne JR, Madhani M, Cuello F, Charles RL, Brennan JP, Schröder E, Browning DD, Eaton P. Cysteine redox sensor in PKGI α enables oxidant-induced activation. *Science*. 2007 Sep 7;317(5843):1393-7.
- Burtenshaw D, Hakimjavadi R, Redmond EM, Cahill PA. Nox, reactive oxygen species and regulation of vascular cell fate. *Antioxidants*. 2017 Nov 14;6(4):90.
- Byfield G, Budd S, Hartnett ME. The role of supplemental oxygen and JAK/STAT signaling in intravitreal neovascularization in a ROP rat model. *Investigative ophthalmology & visual science*. 2009 Jul 1;50(7):3360-5.
- Cacalano NA, Sanden D, Johnston JA. Tyrosine-phosphorylated SOCS-3 inhibits STAT activation but binds to p120 RasGAP and activates Ras. *Nature cell biology*. 2001 May;3(5):460-5.
- Cachofeiro V, Goicochea M, De Vinuesa SG, Oubiña P, Lahera V, Luño J. Oxidative stress and inflammation, a link between chronic kidney disease and cardiovascular disease: New strategies to prevent cardiovascular risk in chronic kidney disease. *Kidney International*. 2008 Dec 1;74:S4-9.
- Cahill PA, Redmond EM. Vascular endothelium—gatekeeper of vessel health. *Atherosclerosis*. 2016 May 1;248:97-109.
- Cairns RA, Harris IS, Mak TW. Regulation of cancer cell metabolism. *Nature Reviews Cancer*. 2011 Feb;11(2):85-95.
- Caixeta A, Leon MB, Lansky AJ, Nikolsky E, Aoki J, Moses JW, Schofer J, Morice MC, Schampaert E, Kirtane AJ, Popma JJ. 5-Year clinical outcomes after sirolimus-eluting stent implantation: insights from a patient-level pooled analysis of 4 randomized trials comparing sirolimus-eluting stents with bare-metal stents. *Journal of the American College of Cardiology*. 2009 Sep 1;54(10):894-902.
- Calhoun MW, Thomas JW, Gennis RB. The cytochrome oxidase superfamily of redox-driven proton pumps. *Trends in biochemical sciences*. 1994 Aug 1;19(8):325-30.
- Campbell DJ, Lawrence AC, Towrie A, Kladis A, Valentijn AJ. Differential regulation of angiotensin peptide levels in plasma and kidney of the rat. *Hypertension*. 1991 Dec;18(6):763-73.

- Campbell IW, Howlett HC. Worldwide experience of metformin as an effective glucose-lowering agent: a meta-analysis. *Diabetes/metabolism reviews*. 1995 Sep;11(S1):S57-62.
- Campeau LJ, Lesperance J, Hermann J, Corbara F, Grondin CM, Bourassa MG. Loss of the improvement of angina between 1 and 7 years after aortocoronary bypass surgery: correlations with changes in vein grafts and in coronary arteries. *Circulation*. 1979 Aug;60(2):1-5.
- Candler TP, Mahmoud O, Lynn RM, Majbar AA, Barrett TG, Shield JP. Continuing rise of type 2 diabetes incidence in children and young people in the UK. *Diabetic Medicine*. 2018 Jun;35(6):737-44.
- Carrim N, Arthur JF, Hamilton JR, Gardiner EE, Andrews RK, Moran N, Berndt MC, Metharom P. Thrombin-induced reactive oxygen species generation in platelets: A novel role for protease-activated receptor 4 and GPIIb/IIIa. *Redox biology*. 2015 Dec 1;6:640-7.
- Caruso P, Dunmore BJ, Schlosser K, Schoors S, Dos Santos C, Perez-Iratxeta C, Lavoie JR, Zhang H, Long L, Flockton AR, Frid MG. Identification of microRNA-124 as a major regulator of enhanced endothelial cell glycolysis in pulmonary arterial hypertension via PTBPI (polypyrimidine tract binding protein) and pyruvate kinase M2. *Circulation*. 2017 Dec 19;136(25):2451-67.
- Casella S, Bielli A, Mauriello A, Orlandi A. Molecular pathways regulating macrovascular pathology and vascular smooth muscle cells phenotype in type 2 diabetes. *International journal of molecular sciences*. 2015 Oct 14;16(10):24353-68.
- Chait A, Brazg RL, Tribble DL, Krauss RM. Susceptibility of small, dense, low-density lipoproteins to oxidative modification in subjects with the atherogenic lipoprotein phenotype, pattern B. *The American journal of medicine*. 1993 Apr 1;94(4):350-6.
- Chalaris A, Garbers C, Rabe B, Rose-John S, Scheller J. The soluble Interleukin 6 receptor: generation and role in inflammation and cancer. *European journal of cell biology*. 2011 Jun 1;90(6-7):484-94.
- Chalaris A, Rabe B, Paliga K, Lange H, Laskay T, Fielding CA, Jones SA, Rose-John S, Scheller J. Apoptosis is a natural stimulus of IL6R shedding and contributes to the proinflammatory trans-signaling function of neutrophils. *Blood, The Journal of the American Society of Hematology*. 2007 Sep 15;110(6):1748-55.
- Chamley-Campbell JH, Campbell GR, Ross R. Phenotype-dependent response of cultured aortic smooth muscle to serum mitogens. *The Journal of cell biology*. 1981 May;89(2):379-83.
- Chang YH, Weng CL, Lin KI. O-GlcNAcylation and its role in the immune system. *Journal of Biomedical Science*. 2020 Dec;27(1):1-5.
- Chapman PB, Solit DB, Rosen N. Combination of RAF and MEK inhibition for the treatment of BRAF-mutated melanoma: feedback is not encouraged. *Cancer cell*. 2014 Nov 10;26(5):603-4.
- Charras A, Arvaniti P, Le Dantec C, Dalekos GN, Zachou K, Bordron A, Renaudineau Y. JAK inhibitors and oxidative stress control. *Frontiers in Immunology*. 2019 Dec 6;10:2814.
- Chatham JC, Zhang J, Wende AR. Role of O-linked N-acetylglucosamine protein modification in cellular (patho) physiology. *Physiological Reviews*. 2021 Apr 1;101(2):427-93.

- Chaudhry R., & Varacallo, M. (2018). *Biochemistry, Glycolysis*. Treasure Island (FL): StatPearls Publishing.
- Chava KR, Karpurapu M, Wang D, Bhanoori M, Kundumani-Sridharan V, Zhang Q, Ichiki T, Glasgow WC, Rao GN. CREB-mediated IL-6 expression is required for 15 (S)-hydroxyeicosatetraenoic acid-induced vascular smooth muscle cell migration. *Arteriosclerosis, thrombosis, and vascular biology*. 2009 Jun 1;29(6):809-15.
- Chen H, Chen G, Zheng X, Guo Y. Contribution of specific diseases and injuries to changes in health adjusted life expectancy in 187 countries from 1990 to 2013: retrospective observational study. *bmj*. 2019 Mar 27;364.
- Chen KC, Zhou Y, Zhang W, Lou MF. Control of PDGF-induced reactive oxygen species (ROS) generation and signal transduction in human lens epithelial cells. *Molecular vision*. 2007;13:374.
- Chen Q, Vazquez EJ, Moghaddas S, Hoppel CL, Lesnefsky EJ. Production of reactive oxygen species by mitochondria: central role of complex III. *Journal of Biological Chemistry*. 2003 Sep 19;278(38):36027-31.
- Chen QW, Edvinsson L, Xu CB. Role of ERK/MAPK in endothelin receptor signaling in human aortic smooth muscle cells. *BMC cell biology*. 2009 Dec;10(1):1-3.
- Chen S, Xie X, Wang Y, Gao Y, Xie X, Yang J, Ye J. Association between leukocyte mitochondrial DNA content and risk of coronary heart disease: a case-control study. *Atherosclerosis*. 2014 Nov 1;237(1):220-6.
- Chen YR, Zweier JL. Cardiac mitochondria and reactive oxygen species generation. *Circulation research*. 2014 Jan 31;114(3):524-37.
- Cheng V, Kashyap SR. Weight considerations in pharmacotherapy for type 2 diabetes. *Journal of obesity*. 2011 Jan 1;2011.
- Cherrington AD, Moore MC, Sindelar DK, Edgerton DS. Insulin action on the liver in vivo. *Biochemical Society Transactions*. 2007 Nov 1;35(5):1171-4.
- Cheung BM, Li C. Diabetes and hypertension: is there a common metabolic pathway?. *Current atherosclerosis reports*. 2012 Apr;14(2):160-6.
- Cheung PC, Campbell DG, Nebreda AR, Cohen P. Feedback control of the protein kinase TAK1 by SAPK2a/p38 α . *The EMBO journal*. 2003 Nov 3;22(21):5793-805.
- Chinnery PF, Hudson G. *British Medical Bulletin* 2013, 106 (1), 135-159. *British Medical Bulletin*. 2013;106(1):135-59.
- Choi EK, Yeo JS, Park CY, in Na H, a Lim J, Lee JE, Hong SW, Park SS, Lim DG, Kwak KH. Inhibition of reactive oxygen species downregulates the MAPK pathway in rat spinal cord after limb ischemia reperfusion injury. *International Journal of Surgery*. 2015 Oct 1;22:74-8.
- Choi T, Lee JW, Kim SK, Yoo KH. Diabetes Mellitus Promotes Smooth Muscle Cell Proliferation in Mouse Ureteral Tissue through the P-ERK/P-JNK/VEGF/PKC Signaling Pathway. *Medicina*. 2021 Jun 1;57(6):560.

- Choi TG, Lee J, Ha J, Kim SS. Apoptosis signal-regulating kinase 1 is an intracellular inducer of p38 MAPK-mediated myogenic signalling in cardiac myoblasts. *Biochimica et Biophysica Acta (BBA)-Molecular Cell Research*. 2011 Aug 1;1813(8):1412-21.
- Christensen AA, Gannon M. The beta cell in type 2 diabetes. *Current diabetes reports*. 2019 Sep;19(9):1-8.
- Chung S, Sawyer JK, Gebre AK, Maeda N, Parks JS. Adipose tissue ATP binding cassette transporter A1 contributes to high-density lipoprotein biogenesis in vivo. *Circulation*. 2011 Oct 11;124(15):1663-72.
- Cirri P, Chiarugi P, Marra F, Raugei G, Camici G, Manao G, Ramponi G. c-Src activates both STAT1 and STAT3 in PDGF-stimulated NIH3T3 cells. *Biochemical and biophysical research communications*. 1997 Oct 20;239(2):493-7.
- Clackson T, Wells JA. A hot spot of binding energy in a hormone-receptor interface. *Science*. 1995 Jan 20;267(5196):383-6.
- Coelho M, Oliveira T, Fernandes R. Biochemistry of adipose tissue: an endocrine organ. *Arch Med Sci*. 2013; 9: 191–200.
- Cooper GM, Hausman RO. A molecular approach. *The Cell*. 2nd ed. Sunderland, MA: Sinauer Associates. 2000.
- Coughlin SR. Thrombin signalling and protease-activated receptors. *Nature*. 2000 Sep;407(6801):258-64.
- Coutelle O, Hornig-Do HT, Witt A, Andree M, Schiffmann LM, Piekarek M, Brinkmann K, Seeger JM, Liwschitz M, Miwa S, Hallek M. Embelin inhibits endothelial mitochondrial respiration and impairs neoangiogenesis during tumor growth and wound healing. *EMBO molecular medicine*. 2014 May;6(5):624-39.
- Cox JL, Chiasson DA, Gotlieb AI. Stranger in a strange land: the pathogenesis of saphenous vein graft stenosis with emphasis on structural and functional differences between veins and arteries. *Progress in cardiovascular diseases*. 1991 Jul 1;34(1):45-68.
- Cuññas A, García-Morales V, Viña D, Gil-Longo J, Campos-Toimil M. Activation of PKA and Epac proteins by cyclic AMP depletes intracellular calcium stores and reduces calcium availability for vasoconstriction. *Life sciences*. 2016 Jun 15;155:102-9.
- Cusi K, Maezono K, Osman A, Pendergrass M, Patti ME, Pratipanawatr T, DeFronzo RA, Kahn CR, Mandarino LJ. Insulin resistance differentially affects the PI 3-kinase–and MAP kinase–mediated signaling in human muscle. *The Journal of clinical investigation*. 2000 Feb 1;105(3):311-20.
- Czech MP. Insulin action and resistance in obesity and type 2 diabetes. *Nature medicine*. 2017 Jul;23(7):804-14.
- Czech MP. Mechanisms of insulin resistance related to white, beige, and brown adipocytes. *Molecular metabolism*. 2020 Apr 1;34:27-42.
- da Costa RM, Fais RS, Dechandt CR, Louzada-Junior P, Alberici LC, Lobato NS, Tostes RC. Increased mitochondrial ROS generation mediates the loss of the anti-contractile effects of perivascular adipose tissue in high-fat diet obese mice. *British Journal of Pharmacology*. 2017 Oct;174(20):3527-41.

- Da Costa RM, Silva JF, Alves JV, Dias TB, Rassi DM, Garcia LV, Lobato ND, Tostes RC. Increased O-GlcNAcylation of endothelial nitric oxide synthase compromises the anti-contractile properties of perivascular adipose tissue in metabolic syndrome. *Frontiers in physiology*. 2018 Apr 6;9:341.
- Dagnell M, Cheng Q, Rizvi SH, Pace PE, Boivin B, Winterbourn CC, Arnér ES. Bicarbonate is essential for protein-tyrosine phosphatase 1B (PTP1B) oxidation and cellular signaling through EGF-triggered phosphorylation cascades. *Journal of Biological Chemistry*. 2019 Aug 16;294(33):12330-8.
- D'Alessandris C, Andreozzi F, Federici M, Cardellini M, Brunetti A, Ranalli M, Del Guerra S, Lauro D, Del Prato S, Marchetti P, Lauro R. Increased O-glycosylation of insulin signaling proteins results in their impaired activation and enhanced susceptibility to apoptosis in pancreatic β -cells. *The FASEB journal*. 2004 Jun;18(9):959-61.
- Daniel JM, Dutzmann J, Bielenberg W, Widmer-Teske R, Gündüz D, Hamm CW, Sedding DG. Inhibition of STAT3 signaling prevents vascular smooth muscle cell proliferation and neointima formation. *Basic research in cardiology*. 2012 May;107:1-2.
- Darnell Jr JE. STATs and gene regulation. *Science*. 1997 Sep 12;277(5332):1630-5.
- Davidson JA, Parkin CG. Is hyperglycemia a causal factor in cardiovascular disease? Does proving this relationship really matter? Yes. *Diabetes care*. 2009 Nov 1;32(suppl_2):S331-3.
- Davidson SM, Duchon MR. Endothelial mitochondria: contributing to vascular function and disease. *Circulation research*. 2007 Apr 27;100(8):1128-41.
- Davies MG, Klyachkin ML, Dalen H, Massey MF, Svendsen E, Hagen PO. The integrity of experimental vein graft endothelium—implications on the etiology of early graft failure. *European Journal of Vascular Surgery*. 1993 Mar 1;7(2):156-65.
- Dávila D, Torres-Aleman I. Neuronal death by oxidative stress involves activation of FOXO3 through a two-arm pathway that activates stress kinases and attenuates insulin-like growth factor I signaling. *Molecular biology of the cell*. 2008 May;19(5):2014-25.
- De Gasparo M, Catt KJ, Inagami T, Wright JW, Unger TH. International union of pharmacology. XXIII. The angiotensin II receptors. *Pharmacological reviews*. 2000 Sep 1;52(3):415-72.
- de Lannoy LM, Danser AJ, Bouhuizen AM, Saxena PR, Schalekamp MA. Localization and production of angiotensin II in the isolated perfused rat heart. *Hypertension*. 1998 May;31(5):1111-7.
- De Vries MR, Simons KH, Jukema JW, Braun J, Quax PH. Vein graft failure: from pathophysiology to clinical outcomes. *Nature Reviews Cardiology*. 2016 Aug;13(8):451-70.
- Degn KB, Brock B, Juhl CB, Djurhuus CB, Grubert J, Kim D, Han J, Taylor K, Fineman M, Schmitz O. Effect of intravenous infusion of exenatide (synthetic exendin-4) on glucose-dependent insulin secretion and counterregulation during hypoglycemia. *Diabetes*. 2004 Sep 1;53(9):2397-403.
- Delaney AM, Printen JA, Chen H, Fauman EB, Dudley DT. Identification of a novel mitogen-activated protein kinase kinase activation domain recognized by the inhibitor PD 184352. *Molecular and cellular biology*. 2002 Nov 1;22(21):7593-602.

- Delen E, Doğanlar O. The dose dependent effects of ruxolitinib on the invasion and tumorigenesis in gliomas cells via inhibition of interferon gamma-dependent JAK/STAT signaling pathway. *Journal of Korean Neurosurgical Society*. 2020 Jun 4;63(4):444-54.
- Delneste Y, Lassalle P, Jeannin P, Joseph M, Tonnel AB, Gosset P. Histamine induces IL-6 production by human endothelial cells. *Clinical & Experimental Immunology*. 1994 Nov;98(2):344-9.
- Deng D, Yan N. GLUT, SGLT, and SWEET: Structural and mechanistic investigations of the glucose transporters. *Protein Science*. 2016 Mar;25(3):546-58.
- Deng Y, Li B, Liu Y, Iqbal K, Grundke-Iqbal I, Gong CX. Dysregulation of insulin signaling, glucose transporters, O-GlcNAcylation, and phosphorylation of tau and neurofilaments in the brain: Implication for Alzheimer's disease. *The American journal of pathology*. 2009 Nov 1;175(5):2089-98.
- Dentin R, Hedrick S, Xie J, Yates III J, Montminy M. Hepatic glucose sensing via the CREB coactivator CRTC2. *Science*. 2008 Mar 7;319(5868):1402-5.
- Denu JM, Tanner KG. Specific and reversible inactivation of protein tyrosine phosphatases by hydrogen peroxide: evidence for a sulfenic acid intermediate and implications for redox regulation. *Biochemistry*. 1998 Apr 21;37(16):5633-42.
- DeSouza LV, Siu KM. Mass spectrometry-based quantification. *Clinical biochemistry*. 2013 Apr 1;46(6):421-31.
- Detter C, Deuse T, Christ F, Boehm DH, Reichenspurner H, Reichart B. Comparison of two stabilizer concepts for off-pump coronary artery bypass grafting. *The Annals of thoracic surgery*. 2002 Aug 1;74(2):497-501.
- Devenish SO, Johnston GA, Chebib M, Hanrahan JR. Optimising the transient expression of GABA (A) receptors in adherent HEK293 cells. *Protein expression and purification*. 2019 Feb 1;154:7-15.
- Diabetes UK (2019). Diabetes Mellitus. Fact Sheet. <https://www.diabetes.co.uk/diabetes-prevalence>. Accessed 12th November, 2022.
- Didion SP. Cellular and oxidative mechanisms associated with interleukin-6 signaling in the vasculature. *International journal of molecular sciences*. 2017 Nov 29;18(12):2563.
- Dikalov SI, Nazarewicz RR. Angiotensin II-induced production of mitochondrial reactive oxygen species: potential mechanisms and relevance for cardiovascular disease. *Antioxidants & redox signaling*. 2013 Oct 1;19(10):1085-94.
- Ding HT, Wang CG, Zhang TL, Wang K. Fibronectin enhances in vitro vascular calcification by promoting osteoblastic differentiation of vascular smooth muscle cells via ERK pathway. *Journal of cellular biochemistry*. 2006 Dec 1;99(5):1343-52.
- Divers J, Mayer-Davis EJ, Lawrence JM, Isom S, Dabelea D, Dolan L, Imperatore G, Marcovina S, Pettitt DJ, Pihoker C, Hamman RF. Trends in incidence of type 1 and type 2 diabetes among youths—selected counties and Indian reservations, United States, 2002–2015. *Morbidity and Mortality Weekly Report*. 2020 Feb 14;69(6):161.

- Dong DL, Hart GW. Purification and characterization of an O-GlcNAc selective N-acetyl-beta-D-glucosaminidase from rat spleen cytosol. *Journal of Biological Chemistry*. 1994 Jul 29;269(30):19321-30.
- Doran AC, Meller N, McNamara CA. Role of smooth muscle cells in the initiation and early progression of atherosclerosis. *Arteriosclerosis, thrombosis, and vascular biology*. 2008 May 1;28(5):812-9.
- Dorfmueller HC, Borodkin VS, Schimpl M, Shepherd SM, Shpiro NA, van Aalten DM. GlcNAcstatin: a picomolar, selective O-GlcNAcase inhibitor that modulates intracellular O-glcNAcylation levels. *Journal of the American Chemical Society*. 2006 Dec 27;128(51):16484-5.
- Dorfmueller HC, Borodkin VS, Schimpl M, van Aalten DM. GlcNAcstatins are nanomolar inhibitors of human O-GlcNAcase inducing cellular hyper-O-GlcNAcylation. *Biochemical Journal*. 2009 Jun 1;420(2):221-7.
- Doughan AK, Harrison DG, Dikalov SI. Molecular mechanisms of angiotensin II-mediated mitochondrial dysfunction: linking mitochondrial oxidative damage and vascular endothelial dysfunction. *Circulation research*. 2008 Feb 29;102(4):488-96.
- Dranka BP, Hill BG, Darley-Usmar VM. Mitochondrial reserve capacity in endothelial cells: The impact of nitric oxide and reactive oxygen species. *Free Radical Biology and Medicine*. 2010 Apr 1;48(7):905-14.
- Dronadula N, Liu Z, Wang C, Cao H, Rao GN. STAT-3-dependent cytosolic phospholipase A2 expression is required for thrombin-induced vascular smooth muscle cell motility. *Journal of Biological Chemistry*. 2005 Jan 28;280(4):3112-20.
- Drucker DJ. Glucagon-like peptides: regulators of cell proliferation, differentiation, and apoptosis. *Molecular endocrinology*. 2003 Feb 1;17(2):161-71.
- D'Souza GG, Wagle MA, Saxena V, Shah A. Approaches for targeting mitochondria in cancer therapy. *Biochimica et Biophysica Acta (BBA)-Bioenergetics*. 2011 Jun 1;1807(6):689-96.
- Du XL, Edelstein D, Dimmeler S, Ju Q, Sui C, Brownlee M. Hyperglycemia inhibits endothelial nitric oxide synthase activity by posttranslational modification at the Akt site. *The Journal of clinical investigation*. 2001 Nov 1;108(9):1341-8.
- Duckworth W, Abaira C, Moritz T, Reda D, Emanuele N, Reaven PD, Zieve FJ, Marks J, Davis SN, Hayward R, Warren SR. Glucose control and vascular complications in veterans with type 2 diabetes. *New England journal of medicine*. 2009 Jan 8;360(2):129-39.
- Dunn JD, Alvarez LA, Zhang X, Soldati T. Reactive oxygen species and mitochondria: A nexus of cellular homeostasis. *Redox biology*. 2015 Dec 1;6:472-85.
- Dustin CM, Heppner DE, Lin MC, van der Vliet A. Redox regulation of tyrosine kinase signalling: more than meets the eye. *The Journal of Biochemistry*. 2020 Feb 1;167(2):151-63.
- Dworakowski R, Alom-Ruiz SP, Shah AM. NADPH oxidase-derived reactive oxygen species in the regulation of endothelial phenotype. *Pharmacological Reports*. 2008 Jan 1;60(1):21.
- Dworakowski R, Anilkumar N, Zhang M, Shah AM. Redox signalling involving NADPH oxidase-derived reactive oxygen species. *Biochemical Society Transaction*. 2006 Oct 26; 34: 960-964

- Dzau VJ, Braun-Dullaeus RC, Sedding DG. Vascular proliferation and atherosclerosis: new perspectives and therapeutic strategies. *Nature medicine*. 2002 Nov;8(11):1249-56.
- Dzau VJ, Gibbons GH. Autocrine-paracrine mechanisms of vascular myocytes in systemic hypertension. *The American journal of cardiology*. 1987 Dec 14;60(17):99-103.
- Edgerton DS, Lautz M, Scott M, Everett CA, Stettler KM, Neal DW, Chu CA, Cherrington AD. Insulin's direct effects on the liver dominate the control of hepatic glucose production. *The Journal of clinical investigation*. 2006 Feb 1;116(2):521-7.
- Ehsan A, Mann MJ, Dell'Acqua G, Tamura K, Braun-Dullaeus R, Dzau VJ. Endothelial healing in vein grafts: proliferative burst unimpaired by genetic therapy of neointimal disease. *Circulation*. 2002 Apr 9;105(14):1686-92.
- Emrick MA, Hoofnagle AN, Miller AS, Ten Eyck LF, Ahn NG. Constitutive activation of extracellular signal-regulated kinase 2 by synergistic point mutations. *Journal of Biological Chemistry*. 2001 Dec 7;276(49):46469-79.
- Eriksson JW. Metabolic stress in insulin's target cells leads to ROS accumulation—a hypothetical common pathway causing insulin resistance. *FEBS letters*. 2007 Jul 31;581(19):3734-42.
- Ernst M, Jenkins BJ. Acquiring signalling specificity from the cytokine receptor gp130. *Trends in Genetics*. 2004 Jan 1;20(1):23-32.
- Ernster L, Schatz G. Mitochondria: a historical review. *The Journal of cell biology*. 1981 Dec;91(3):227s-55s.
- Esper RJ, Nordaby RA, Vilariño JO, Paragano A, Cacharrón JL, Machado RA. Endothelial dysfunction: a comprehensive appraisal. *Cardiovascular diabetology*. 2006 Dec;5(1):1-8.
- Faghfuri E, Nikfar S, Niaz K, Faramarzi MA, Abdollahi M. Mitogen-activated protein kinase (MEK) inhibitors to treat melanoma alone or in combination with other kinase inhibitors. *Expert Opinion on Drug Metabolism & Toxicology*. 2018 Mar 4;14(3):317-30.
- Fang YH, Piao L, Hong Z, Toth PT, Marsboom G, Bache-Wiig P, Rehman J, Archer SL. Therapeutic inhibition of fatty acid oxidation in right ventricular hypertrophy: exploiting Randle's cycle. *Journal of molecular medicine*. 2012 Jan;90(1):31-43.
- Farbstein D, Levy AP. HDL dysfunction in diabetes: causes and possible treatments. *Expert review of cardiovascular therapy*. 2012 Mar 1;10(3):353-61.
- Faulkner SL, Fisher RD, Conkle D, Page DL, Bender Jr HW. Effect of blood flow rate on subendothelial proliferation in venous autografts used as arterial substitutes. *Circulation*. 1975 Aug 1;52(2 Suppl):I163-72.
- Favetta LA, Robert C, King WA, Betts DH. Expression profiles of p53 and p66shc during oxidative stress-induced senescence in fetal bovine fibroblasts. *Experimental cell research*. 2004 Sep 10;299(1):36-48.
- Federici M, Menghini R, Mauriello A, Hribal ML, Ferrelli F, Lauro D, Sbraccia P, Spagnoli LG, Sesti G, Lauro R. Insulin-dependent activation of endothelial nitric oxide synthase is impaired by O-linked glycosylation modification of signaling proteins in human coronary endothelial cells. *Circulation*. 2002 Jul 23;106(4):466-72.

- Feng TC, Ying WY, Hua RJ, Ji YY, de Gasparo M. Effect of valsartan and captopril in rabbit carotid injury. Possible involvement of bradykinin in the antiproliferative action of the renin-angiotensin blockade. *Journal of the Renin-Angiotensin-Aldosterone System*. 2001 Mar;2(1):19-24.
- Ference BA, Ginsberg HN, Graham I, Ray KK, Packard CJ, Bruckert E, Hegele RA, Krauss RM, Raal FJ, Schunkert H, Watts GF. Low-density lipoproteins cause atherosclerotic cardiovascular disease. 1. Evidence from genetic, epidemiologic, and clinical studies. A consensus statement from the European Atherosclerosis Society Consensus Panel. *European heart journal*. 2017 Aug 21;38(32):2459-72.
- Fernández-Alfonso MS, Gil-Ortega M, García-Prieto CF, Aranguez I, Ruiz-Gayo M, Somoza B. Mechanisms of perivascular adipose tissue dysfunction in obesity. *International journal of endocrinology*. 2013 Oct;2013.
- Ferrer CM, Lynch TP, Sodi VL, Falcone JN, Schwab LP, Peacock DL, Vocadlo DJ, Seagroves TN, Reginato MJ. O-GlcNAcylation regulates cancer metabolism and survival stress signaling via regulation of the HIF-1 pathway. *Molecular cell*. 2014 Jun 5;54(5):820-31.
- Ferrick DA, Neilson A, Beeson C. Advances in measuring cellular bioenergetics using extracellular flux. *Drug discovery today*. 2008 Mar 1;13(5-6):268-74.
- Ferron M, Denis M, Persello A, Rathagirishnan R, Lauzier B. Protein O-GlcNAcylation in cardiac pathologies: past, present, future. *Frontiers in endocrinology*. 2019 Jan 15;9:819.
- Fitzgibbon GM, Kafka HP, Leach AJ, Keon WJ, Hooper GD, Burton JR. Coronary bypass graft fate and patient outcome: angiographic follow-up of 5,065 grafts related to survival and reoperation in 1,388 patients during 25 years. *Journal of the American College of Cardiology*. 1996 Sep 1;28(3):616-26.
- Flemma RJ, Johnson WD, Lepley D. Triple aorto-coronary vein bypass as treatment for coronary insufficiency. *Archives of Surgery*. 1971 Jul 1;103(1):82-3.
- Flores-Ríos X, Marzoa-Rivas R, Abugattás-de Torres JP, Piñón-Esteban P, Aldama-López G, Salgado-Fernández J, Calviño-Santos R, Vázquez-Rodríguez JM, Vázquez-González N, Castro-Beiras A. Late thrombosis of paclitaxel-eluting stents: long-term incidence, clinical consequences, and risk factors in a cohort of 604 patients. *American heart journal*. 2008 Apr 1;155(4):648-53.
- Fontanesi F. Mitochondria: structure and role in respiration. *eLS*. 2015:1-3.
- Forcina L, Miano C, Scicchitano BM, Rizzuto E, Berardinelli MG, De Benedetti F, Pelosi L, Musarò A. Increased circulating levels of interleukin-6 affect the redox balance in skeletal muscle. *Oxidative medicine and cellular longevity*. 2019 Nov 16;2019.
- Forrester SJ, Booz GW, Sigmund CD, Coffman TM, Kawai T, Rizzo V, Scalia R, Eguchi S. Angiotensin II signal transduction: an update on mechanisms of physiology and pathophysiology. *Physiological reviews*. 2018 Jul 1;98(3):1627-738.
- Frederick, R.L., & Shaw, J.M. (2007). Moving mitochondria: establishing distribution of an essential organelle. *Traffic*, 8 12, 1668-1675.
- Fredriksson L, Li H, Eriksson U. The PDGF family: four gene products form five dimeric isoforms. *Cytokine & growth factor reviews*. 2004 Aug 1;15(4):197-204.

- Frid MG, Shekhonin BV, Koteliansky VE, Glukhova MA. Phenotypic changes of human smooth muscle cells during development: late expression of heavy caldesmon and calponin. *Developmental biology*. 1992 Oct 1;153(2):185-93.
- Friederich-Persson M, Persson P. Mitochondrial angiotensin II receptors regulate oxygen consumption in kidney mitochondria from healthy and type 1 diabetic rats. *American Journal of Physiology-Renal Physiology*. 2020 Mar 1;318(3):F683-8.
- Frizzell N, Stillway LW. 10 The Tricarboxylic Acid Cycle. *Medical Biochemistry E-Book*. 2018 Jan 3:124.
- Fu Z, R Gilbert E, Liu D. Regulation of insulin synthesis and secretion and pancreatic Beta-cell dysfunction in diabetes. *Current diabetes reviews*. 2013 Jan 1;9(1):25-53.
- Fujino G, Noguchi T, Matsuzawa A, Yamauchi S, Saitoh M, Takeda K, Ichijo H. Thioredoxin and TRAF family proteins regulate reactive oxygen species-dependent activation of ASK1 through reciprocal modulation of the N-terminal homophilic interaction of ASK1. *Molecular and cellular biology*. 2007 Dec 1;27(23):8152-63.
- Fukui T, Takanashi S, Hosoda Y, Suehiro S. Total arterial myocardial revascularization using composite and sequential grafting with the off-pump technique. *The Annals of thoracic surgery*. 2005 Aug 1;80(2):579-85.
- Fülöp N, Marchase RB, Chatham JC. Role of protein O-linked N-acetyl-glucosamine in mediating cell function and survival in the cardiovascular system. *Cardiovascular research*. 2007 Jan 15;73(2):288-97.
- Fulton D, Gratton JP, McCabe TJ, Fontana J, Fujio Y, Walsh K, Franke TF, Papapetropoulos A, Sessa WC. Regulation of endothelium-derived nitric oxide production by the protein kinase Akt. *Nature*. 1999 Jun;399(6736):597-601.
- Gadsby R. Efficacy and safety of sitagliptin in the treatment of type 2 diabetes. *Clinical Medicine. Therapeutics*. 2009 Jan;1:CMT-S2313.
- Galicia-Garcia U, Benito-Vicente A, Jebari S, Larrea-Sebal A, Siddiqi H, Uribe KB, Ostolaza H, Martín C. Pathophysiology of Type 2 Diabetes Mellitus. *Int J Mol Sci*. 2020 Aug 30;21(17):6275.
- García-Olivas R, Vilaró S, Reina M, Castel S. PDGF-stimulated cell proliferation and migration of human arterial smooth muscle cells: Colocalization of PDGF isoforms with glycosaminoglycans. *The international journal of biochemistry & cell biology*. 2007 Jan 1;39(10):1915-29.
- Gastaldelli A, Gaggini M, DeFronzo RA. Role of adipose tissue insulin resistance in the natural history of type 2 diabetes: results from the San Antonio Metabolism Study. *Diabetes*. 2017 Apr 1;66(4):815-22.
- GBD RFC. Global Burden of 87 Risk Factors in 204 Countries and Territories, 1990-2019: A Systematic Analysis for the Global Burden of Disease Study 2019. *Lancet (London England)* 2020- 396:1223–49.
- Geisen P, Peterson LJ, Martiniuk D, Uppal A, Saito Y, Hartnett ME. Neutralizing antibody to VEGF reduces intravitreal neovascularization and may not interfere with ongoing intraretinal vascularization in a rat model of retinopathy of prematurity. *Molecular Vision*. 2008;14:345.

- Gélinas DS, Bernatchez PN, Rollin S, Bazan NG, Sirois MG. Immediate and delayed VEGF-mediated NO synthesis in endothelial cells: role of PI3K, PKC and PLC pathways. *British journal of pharmacology*. 2002 Dec;137(7):1021-30.
- Gentry L, Samatar AA, Der CJ. Inhibitors of the ERK mitogen-activated protein kinase cascade for targeting RAS mutant cancers. *The Enzymes*. 2013 Jan 1;34:67-106.
- Gerstein HC. Action to Control Cardiovascular Risk in Diabetes Study Group: Effects of intensive glucose lowering in type 2 diabetes. *N Engl j Med*. 2008;358:2545-59.
- Gertz M, Fischer F, Wolters D, Steegborn C. Activation of the lifespan regulator p66Shc through reversible disulfide bond formation. *Proceedings of the National Academy of Sciences*. 2008 Apr 15;105(15):5705-9.
- Gertz M, Steegborn C. The Lifespan-regulator p66Shc in mitochondria: redox enzyme or redox sensor?. *Antioxidants & redox signaling*. 2010 Nov 1;13(9):1417-28.
- Ghasemi A, Zahediasl S. Normality tests for statistical analysis: a guide for non-statisticians. *International journal of endocrinology and metabolism*. 2012;10(2):486.
- Gheorghe A, Griffiths U, Murphy A, Legido-Quigley H, Lamptey P, Perel P. The economic burden of cardiovascular disease and hypertension in low-and middle-income countries: a systematic review. *BMC public health*. 2018 Dec;18(1):1-1.
- Giacco F, Brownlee M. Oxidative stress and diabetic complications. *Circulation research*. 2010 Oct 29;107(9):1058-70.
- Giannini C, Mohn A, Chiarelli F, Kelnar CJ. Macrovascular angiopathy in children and adolescents with type 1 diabetes. *Diabetes/Metabolism Research and Reviews*. 2011 Jul;27(5):436-60.
- Gibbons GH, Pratt R, Dzau VJ. Vascular smooth muscle cell hypertrophy vs. hyperplasia. Autocrine transforming growth factor-beta 1 expression determines growth response to angiotensin II. *The Journal of clinical investigation*. 1992 Aug 1;90(2):456-61.
- Gimbrone Jr MA, García-Cardena G. Vascular endothelium, hemodynamics, and the pathobiology of atherosclerosis. *Cardiovascular Pathology*. 2013 Jan 1;22(1):9-15.
- Gimona M, Herzog M, Vandekerckhove J, Small JV. Smooth muscle specific expression of calponin. *FEBS letters*. 1990 Nov 12;274(1-2):159-62.
- Ginsberg HN. Lipoprotein physiology in nondiabetic and diabetic states: relationship to atherogenesis. *Diabetes care*. 1991 Sep 1;14(9):839-55.
- Giorgio M, Migliaccio E, Orsini F, Paolucci D, Moroni M, Contursi C, Pelliccia G, Luzi L, Minucci S, Marcaccio M, Pinton P. Electron transfer between cytochrome c and p66Shc generates reactive oxygen species that trigger mitochondrial apoptosis. *Cell*. 2005 Jul 29;122(2):221-33.
- Giorgio M, Trinei M, Migliaccio E, Pelicci PG. Hydrogen peroxide: a metabolic by-product or a common mediator of ageing signals?. *Nature reviews Molecular cell biology*. 2007 Sep;8(9):722-8.
- Gloster TM, Zandberg WF, Heinonen JE, Shen DL, Deng L, Vocadlo DJ. Hijacking a biosynthetic pathway yields a glycosyltransferase inhibitor within cells. *Nature chemical biology*. 2011 Mar;7(3):174-81.

- Go YM, Chandler JD, Jones DP. The cysteine proteome. *Free Radical Biology and Medicine*. 2015 Jul 1;84:227-45.
- Go YM, Jones DP. The redox proteome. *Journal of Biological Chemistry*. 2013 Sep 13;288(37):26512-20.
- Goldman L. Analyzing the decline in the CAD death rate. *Hospital Practice*. 1988 Feb 15;23(2):109-17.
- Goldman S, Zadina K, Moritz T, Ovitt T, Sethi G, Copeland JG, Thottapurathu L, Krasnicka B, Ellis N, Anderson RJ, Henderson W. Long-term patency of saphenous vein and left internal mammary artery grafts after coronary artery bypass surgery: results from a Department of Veterans Affairs Cooperative Study. *Journal of the American College of Cardiology*. 2004 Dec 7;44(11):2149-56.
- Goldsack NR, Chambers RC, Dabbagh K, Laurent GJ. Molecules in focus Thrombin. *The International Journal of Biochemistry & Cell Biology*. 1998 Jun 12;30(6):641-6.
- Gómez-Serrano M, Camafeita E, Loureiro M, Peral B. Mitoproteomics: Tackling Mitochondrial Dysfunction in Human Disease. *Oxid Med Cell Longev*. 2018 Nov 8;2018:1435934.
- Gómez-Serrano M, Camafeita E, Loureiro M, Peral B. Mitoproteomics: tackling mitochondrial dysfunction in human disease. *Oxidative medicine and cellular longevity*. 2018 Oct;2018.
- Gong CX, Liu F, Grundke-Iqbal I, Iqbal K. Impaired brain glucose metabolism leads to Alzheimer neurofibrillary degeneration through a decrease in tau O-GlcNAcylation. *Journal of Alzheimer's disease*. 2006 Jan 1;9(1):1-2.
- Graf K, Xi XP, Yang D, Fleck E, Hsueh WA, Law RE. Mitogen-activated protein kinase activation is involved in platelet-derived growth factor-directed migration by vascular smooth muscle cells. *Hypertension*. 1997 Jan 1;29(1):334-9.
- Grarup N, Sandholt CH, Hansen T, Pedersen O. Genetic susceptibility to type 2 diabetes and obesity: from genome-wide association studies to rare variants and beyond. *Diabetologia*. 2014 Aug;57(8):1528-41.
- Gray MW. Mitochondrial evolution. *Cold Spring Harbor perspectives in biology*. 2012 Sep 1;4(9):a011403.
- Gress TW, Nieto FJ, Shahar E, Wofford MR, Brancati FL. Hypertension and antihypertensive therapy as risk factors for type 2 diabetes mellitus. *New England Journal of Medicine*. 2000 Mar 30;342(13):905-12.
- Griendling KK, Ushio-Fukai M. Reactive oxygen species as mediators of angiotensin II signaling. *Regulatory peptides*. 2000 Jul 28;91(1-3):21-7.
- Grondin CM, Limet R. Sequential anastomoses in coronary artery grafting: technical aspects and early and late angiographic results. *The Annals of Thoracic Surgery*. 1977 Jan 1;23(1):1-8.
- Gu X, Masters KS. Role of the MAPK/ERK pathway in valvular interstitial cell calcification. *American Journal of Physiology-Heart and Circulatory Physiology*. 2009 Jun;296(6):H1748-57.

- Guerra G, Martínez F, Pardo JP. On the $H^+/2e^-$ stoichiometry of the respiratory chain. *Biochemistry and Molecular Biology Education*. 2002 Nov;30(6):363-7.
- Gutterman DD, Miura H, Liu Y. Redox modulation of vascular tone: focus of potassium channel mechanisms of dilation. *Arteriosclerosis, thrombosis, and vascular biology*. 2005 Apr 1;25(4):671-8.
- Haffner SM, Lehto S, Rönnemaa T, Pyörälä K, Laakso M. Mortality from coronary heart disease in subjects with type 2 diabetes and in nondiabetic subjects with and without prior myocardial infarction. *New England journal of medicine*. 1998 Jul 23;339(4):229-34.
- Haigis MC, Yankner BA. The aging stress response. *Molecular cell*. 2010 Oct 22;40(2):333-44.
- Hakonen AH, Goffart S, Marjavaara S, Paetau A, Cooper H, Mattila K, Lampinen M, Sajantila A, Lönnqvist T, Spelbrink JN, Suomalainen A. Infantile-onset spinocerebellar ataxia and mitochondrial recessive ataxia syndrome are associated with neuronal complex I defect and mtDNA depletion. *Human molecular genetics*. 2008 Dec 1;17(23):3822-35.
- Halban PA, Polonsky KS, Bowden DW, Hawkins MA, Ling C, Mather KJ, Powers AC, Rhodes CJ, Sussel L, Weir GC. β -cell failure in type 2 diabetes: postulated mechanisms and prospects for prevention and treatment. *The Journal of Clinical Endocrinology & Metabolism*. 2014 Jun 1;99(6):1983-92.
- Halban PA. Proinsulin processing in the regulated and the constitutive secretory pathway. *Diabetologia*. 1994 Sep;37(2):S65-72.
- Hannken T, Schroeder R, Stahl RA, Wolf G. Angiotensin II-mediated expression of p27Kip1 and induction of cellular hypertrophy in renal tubular cells depend on the generation of oxygen radicals. *Kidney international*. 1998 Jan 1;54(6):1923-33.
- Haq M, Adnan G. Ruxolitinib. [Updated 2022 Sep 27]. In: StatPearls [Internet]. Treasure Island (FL): StatPearls Publishing; 2022 Jan.
- Hardie DG, Schaffer BE, Brunet A. AMPK: an energy-sensing pathway with multiple inputs and outputs. *Trends in cell biology*. 2016 Mar 1;26(3):190-201.
- Harnett EM, Alderman J, Wood T. The surface energy of various biomaterials coated with adhesion molecules used in cell culture. *Colloids and surfaces B: Biointerfaces*. 2007 Mar 15;55(1):90-7.
- Harris RA, Harper ET. Glycolytic pathway. *eLS*. 2015:1-8.
- Hart GW, Haltiwanger RS, Holt GD, Kelly WG. Glycosylation in the nucleus and cytoplasm. *Annual review of biochemistry*. 1989 Jul;58(1):841-74.
- Hart GW, Housley MP, Slawson C. Cycling of O-linked β -N-acetylglucosamine on nucleocytoplasmic proteins. *Nature*. 2007 Apr;446(7139):1017-22.
- Hattler B, Messenger JC, Shroyer AL, Collins JF, Haugen SJ, Garcia JA, Baltz JH, Cleveland Jr JC, Novitzky D, Grover FL. Off-Pump coronary artery bypass surgery is associated with worse arterial and saphenous vein graft patency and less effective revascularization: Results from the Veterans Affairs Randomized On/Off Bypass (ROOBY) trial. *Circulation*. 2012 Jun 12;125(23):2827-35.

- Hayashi KI, Saga H, Chimori Y, Kimura K, Yamanaka Y, Sobue K. Differentiated phenotype of smooth muscle cells depends on signaling pathways through insulin-like growth factors and phosphatidylinositol 3-kinase. *Journal of Biological Chemistry*. 1998 Nov 30;273(44):28860-7.
- Hayashi KI, Shibata K, Morita T, Iwasaki K, Watanabe M, Sobue K. Insulin receptor substrate-1/SHP-2 interaction, a phenotype-dependent switching machinery of insulin-like growth factor-I signaling in vascular smooth muscle cells. *Journal of Biological Chemistry*. 2004 Sep 24;279(39):40807-18.
- Hebert PD, Cywinska A, Ball SL, DeWaard JR. Biological identifications through DNA barcodes. *Proceedings of the Royal Society of London. Series B: Biological Sciences*. 2003 Feb 7;270(1512):313-21.
- Heinrich PC, Behrmann I, Haan S, Hermanns HM, Müller-Newen G, Schaper F. Principles of interleukin (IL)-6-type cytokine signalling and its regulation. *Biochemical journal*. 2003 Aug 15;374(1):1-20.
- Heinrich PC, Behrmann I, Müller-Newen G, Schaper F, Graeve L. Interleukin-6-type cytokine signalling through the gp130/Jak/STAT pathway. *Biochemical journal*. 1998 Sep 1;334(2):297-314.
- Heldin CH, Westermark B. Mechanism of action and in vivo role of platelet-derived growth factor. *Physiological reviews*. 1999 Jan 10.
- Heldin CH, Westermark B. Mechanism of action and in vivo role of platelet-derived growth factor. *Physiological reviews*. 1999 Oct;79(4):1283-316.
- Helmrich SP, Ragland DR, Leung RW, Paffenbarger Jr RS. Physical activity and reduced occurrence of non-insulin-dependent diabetes mellitus. *New England journal of medicine*. 1991 Jul 18;325(3):147-52.
- Hemmingsen B, Lund SS, Gluud C, Vaag A, Almdal T, Hemmingsen C, Wetterslev J. Intensive glycaemic control for patients with type 2 diabetes: systematic review with meta-analysis and trial sequential analysis of randomised clinical trials. *Bmj*. 2011 Nov 24;343.
- Heppner DE, Dustin CM, Liao C, Hristova M, Veith C, Little AC, Ahlers BA, White SL, Deng B, Lam YW, Li J. Direct cysteine sulfenylation drives activation of the Src kinase. *Nature communications*. 2018 Oct 30;9(1):1-1.
- Herman GA, Bergman A, Liu F, Stevens C, Wang AQ, Zeng W, Chen L, Snyder K, Hilliard D, Tanen M, Tanaka W. Pharmacokinetics and pharmacodynamic effects of the oral DPP-4 inhibitor sitagliptin in middle-aged obese subjects. *The Journal of Clinical Pharmacology*. 2006 Aug;46(8):876-86.
- Hertweck KL, Dasgupta S. The landscape of mtDNA modifications in cancer: a tale of two cities. *Frontiers in oncology*. 2017:262.
- Higdon A, Diers AR, Oh JY, Landar A, Darley-Usmar VM. Cell signalling by reactive lipid species: new concepts and molecular mechanisms. *Biochemical Journal*. 2012 Mar 15;442(3):453-64.
- Hillis LD, Smith PK, Anderson JL, Bittl JA, Bridges CR, Byrne JG, Cigarroa JE, Disesa VJ, Hiratzka LF, Hutter AM, Jessen ME, Keeley EC, Lahey SJ, Lange RA, London MJ, Mack MJ, Patel MR, Puskas JD, Sabik JF, Selnes O, Shahian DM, Trost JC, Winniford MD. 2011 ACCF/AHA Guideline for Coronary Artery Bypass Graft Surgery: a report of the American

College of Cardiology Foundation/American Heart Association Task Force on Practice Guidelines. *Circulation*. 2011 Dec 06;124(23):e652-735.

- Hirata Y, Taga T, Hibi M, Nakano N, Hirano T, Kishimoto T. Characterization of IL-6 receptor expression by monoclonal and polyclonal antibodies. *The Journal of Immunology*. 1989 Nov 1;143(9):2900-6.
- Hirst J. Energy transduction by respiratory complex I—an evaluation of current knowledge. *Biochemical Society Transactions*. 2005 Jun 1;33(3):525-9.
- Hirst J. Towards the molecular mechanism of respiratory complex I. *Biochemical Journal*. 2010 Jan 15;425(2):327-39.
- Hoang Do O, Thorn P. Insulin secretion from beta cells within intact islets: location matters. *Clinical and Experimental Pharmacology and Physiology*. 2015 Apr;42(4):406-14.
- Hoffner B, Benchich K. Trametinib: a targeted therapy in metastatic melanoma. *Journal of the advanced practitioner in oncology*. 2018 Nov;9(7):741.
- Hofmann F, Feil R, Kleppisch T, Schlossmann J. Function of cGMP-dependent protein kinases as revealed by gene deletion. *Physiological reviews*. 2006 Jan;86(1):1-23.
- Holt AW, Tulis DA. Vascular smooth muscle as a therapeutic target in disease pathology. *Muscle Cell and Tissue*. 2015 Sep 2:3-26.
- Holt GD, Hart GW. The subcellular distribution of terminal N-acetylglucosamine moieties. Localization of a novel protein-saccharide linkage, O-linked GlcNAc. *J Biol Chem*. 1986;261:8049-57.
- Holub MC, Szalai C, Polgár A, Tóth S, Falus A. Generation of ‘truncated’ interleukin-6 receptor (IL-6R) mRNA by alternative splicing; a possible source of soluble IL-6R. *Immunology letters*. 1999 May 3;68(1):121-4.
- Hoogeveen RC, Gaubatz JW, Sun W, Dodge RC, Crosby JR, Jiang J, Couper D, Virani SS, Kathiresan S, Boerwinkle E, Ballantyne CM. Small dense low-density lipoprotein-cholesterol concentrations predict risk for coronary heart disease: the Atherosclerosis Risk In Communities (ARIC) study. *Arteriosclerosis, thrombosis, and vascular biology*. 2014 May;34(5):1069-77.
- Hooper WC, Phillips DJ, Renshaw MA, Evatt BL, Benson JM. The up-regulation of IL-6 and IL-8 in human endothelial cells by activated protein C. *The Journal of Immunology*. 1998 Sep 1;161(5):2567-73.
- Horsefield R, Iwata S, Byrne B. Complex II from a structural perspective. *Current Protein and Peptide Science*. 2004 Apr 1;5(2):107-18.
- Hotamisligil GS. Inflammation and metabolic disorders. *Nature*. 2006 Dec;444(7121):860-7.
- Hsu PP, Sabatini DM. Cancer cell metabolism: Warburg and beyond. *Cell*. 2008 Sep 5;134(5):703-7.
- Hu FB. Globalization of diabetes: the role of diet, lifestyle, and genes. *Diabetes care*. 2011 Jun 1;34(6):1249-57.
- Hu X, Fu M, Zhao X, Wang W. The JAK/STAT signaling pathway: From bench to clinic. *Signal Transduction and Targeted Therapy*. 2021 Nov 26;6(1):1-33.

- Ichijo H, Nishida E, Irie K, Dijke PT, Saitoh M, Moriguchi T, Takagi M, Matsumoto K, Miyazono K, Gotoh Y. Induction of apoptosis by ASK1, a mammalian MAPKKK that activates SAPK/JNK and p38 signaling pathways. *Science*. 1997 Jan 3;275(5296):90-4.
- Inoguchi T, Sonta T, Tsubouchi H, Etoh T, Kakimoto M, Sonoda N, Sato N, Sekiguchi N, Kobayashi K, Sumimoto H, Utsumi H. Protein kinase C–dependent increase in reactive oxygen species (ROS) production in vascular tissues of diabetes: role of vascular NAD (P) H oxidase. *Journal of the American Society of Nephrology*. 2003 Aug 1;14(suppl_3):S227-32.
- International Diabetes Federation (2022). *Diabetes Mellitus. Fact Sheet*. (<https://diabetesatlas.org/atlas/tenth-edition/>). Accessed 22nd November, 2022.
- Ioannidis I, Laurini JA. Use of smooth muscle myosin heavy chain as an effective marker of follicular dendritic cells. *Applied immunohistochemistry & molecular morphology*. 2019 Jan 1;27(1):48-53.
- Islam MS. The ryanodine receptor calcium channel of β -cells: molecular regulation and physiological significance. *Diabetes*. 2002 May 1;51(5):1299-309.
- Ivashkiv LB, Donlin LT. Regulation of type I interferon responses. *Nature Reviews Immunology*. 2014 Jan;14(1):36-49.
- Iwata S, Lee JW, Okada K, Lee JK, Iwata M, Rasmussen B, Link TA, Ramaswamy S, Jap BK. Complete structure of the 11-subunit bovine mitochondrial cytochrome bc₁ complex. *Science*. 1998 Jul 3;281(5373):64-71.
- Jasek-Gajda E, Jurkowska H, Jasińska M, Lis GJ. Targeting the MAPK/ERK and PI3K/AKT signaling pathways affects NRF2, Trx and GSH antioxidant systems in leukemia cells. *Antioxidants*. 2020 Jul 17;9(7):633.
- Jensen RV, Andreadou I, Hausenloy DJ, Bøtker HE. The role of O-GlcNAcylation for protection against ischemia-reperfusion injury. *International Journal of Molecular Sciences*. 2019 Jan 18;20(2):404.
- Jia G, Aggarwal A, Yohannes A, Gangahar DM, Agrawal DK. Cross-talk between angiotensin II and IGF-1-induced connexin 43 expression in human saphenous vein smooth muscle cells. *Journal of cellular and molecular medicine*. 2011 Aug;15(8):1695-702.
- Jiang J, Lazarus MB, Pasquina L, Sliz P, Walker S. A neutral diphosphate mimic crosslinks the active site of human O-GlcNAc transferase. *Nature chemical biology*. 2012 Jan;8(1):72-7.
- Johnson AR, Justin Milner J, Makowski L. The inflammation highway: metabolism accelerates inflammatory traffic in obesity. *Immunological reviews*. 2012 Sep;249(1):218-38.
- Johnson C, Galis ZS. Matrix metalloproteinase-2 and– 9 differentially regulate smooth muscle cell migration and cell-mediated collagen organization. *Arteriosclerosis, thrombosis, and vascular biology*. 2004 Jan 1;24(1):54-60.
- Johnson JL, van Eys GJ, Angelini GD, George SJ. Injury induces dedifferentiation of smooth muscle cells and increased matrix-degrading metalloproteinase activity in human saphenous vein. *Arteriosclerosis, thrombosis, and vascular biology*. 2001 Jul;21(7):1146-51.

- Johnson ML, Robinson MM, Nair KS. Skeletal muscle aging and the mitochondrion. *Trends in endocrinology & metabolism*. 2013 May 1;24(5):247-56.
- Jones SA, O'Donnell VB, Wood JD, Broughton JP, Hughes EJ, Jones OT. Expression of phagocyte NADPH oxidase components in human endothelial cells. *American Journal of Physiology-Heart and Circulatory Physiology*. 1996 Oct 1;271(4):H1626-34.
- Jones SA, Richards PJ, Scheller J, Rose-John S. IL-6 transsignaling: the in vivo consequences. *Journal of Interferon and Cytokine Research*. 2005 May 1;25(5):241-53.
- Juhn SK, Jung MK, Hoffman MD, Drew BR, Preciado DA, Sausen NJ, Jung TT, Kim BH, Park SY, Lin J, Ondrey FG. The role of inflammatory mediators in the pathogenesis of otitis media and sequelae. *Clinical and experimental otorhinolaryngology*. 2008 Sep 30;1(3):117-38.
- Junge W, Nelson N. ATP synthase. *Annu Rev Biochem*. 2015 Mar 23;84(1):631-57.
- Kabir NN, Kazi JU. Comparative analysis of human and bovine protein kinases reveals unique relationship and functional diversity. *Genetics and molecular biology*. 2011;34:587-91.
- Kahn CR, Rosenthal AS. Immunologic reactions to insulin: insulin allergy, insulin resistance, and the autoimmune insulin syndrome. *Diabetes care*. 1979 May 1;2(3):283-95.
- Kamata H, Honda SI, Maeda S, Chang L, Hirata H, Karin M. Reactive oxygen species promote TNF α -induced death and sustained JNK activation by inhibiting MAP kinase phosphatases. *Cell*. 2005 Mar 11;120(5):649-61.
- Kaneto H, Katakami N, Matsuhisa M, Matsuoka TA. Role of reactive oxygen species in the progression of type 2 diabetes and atherosclerosis. *Mediators of inflammation*. 2010 Oct;2010.
- Karoulia Z, Gavathiotis E, Poulidakos PI. New perspectives for targeting RAF kinase in human cancer. *Nature Reviews Cancer*. 2017 Nov;17(11):676-91.
- Katagiri K, Matsuzawa A, Ichijo H. Regulation of apoptosis signal-regulating kinase 1 in redox signaling. In *Methods in enzymology* 2010 Jan 1 (Vol. 474, pp. 277-288). Academic Press.
- Katakwar P, Metgud R, Naik S, Mittal R. Oxidative stress marker in oral cancer: a review. *Journal of cancer research and therapeutics*. 2016 Apr 1;12(2):438.
- Kauffman ME, Kauffman MK, Traore K, Zhu H, Trush MA, Jia Z, Li YR. MitoSOX-based flow cytometry for detecting mitochondrial ROS. *Reactive oxygen species (Apex, NC)*. 2016;2(5):361.
- Kawahito S, Kitahata H, Oshita S. Problems associated with glucose toxicity: role of hyperglycemia-induced oxidative stress. *World journal of gastroenterology: WJG*. 2009 Sep 9;15(33):4137.
- Kay AM, Simpson CL, Stewart JA. The role of AGE/RAGE signaling in diabetes-mediated vascular calcification. *Journal of diabetes research*. 2016 Oct;2016.
- Khan MA, Hashim MJ, King JK, Govender RD, Mustafa H, Al Kaabi J. Epidemiology of type 2 diabetes—global burden of disease and forecasted trends. *Journal of epidemiology and global health*. 2020 Mar;10(1):107.
- Khan MA, Hashim MJ, Mustafa H, Baniyas MY, Al Suwaidi SK, AlKatheeri R, Alblooshi FM, Almatrooshi ME, Alzaabi ME, Al Darmaki RS, Lootah SN. Global epidemiology of ischemic heart disease: results from the global burden of disease study. *Cureus*. 2020 Jul 23;12(7).

- Khan S, Ullah MW, Siddique R, Nabi G, Manan S, Yousaf M, Hou H. Role of recombinant DNA technology to improve life. *International journal of genomics*. 2016 Oct;2016.
- Khanday FA, Yamamori T, Mattagajasingh I, Zhang Z, Bugayenko A, Naqvi A, Santhanam L, Nabi N, Kasuno K, Day BW, Irani K. Rac1 leads to phosphorylation-dependent increase in stability of the p66shc adaptor protein: role in Rac1-induced oxidative stress. *Molecular biology of the cell*. 2006 Jan;17(1):122-9.
- Khandrika L, Kumar B, Koul S, Maroni P, Koul HK. Oxidative stress in prostate cancer. *Cancer letters*. 2009 Sep 18;282(2):125-36.
- Kidger AM, Siphthorp J, Cook SJ. ERK1/2 inhibitors: New weapons to inhibit the RAS-regulated RAF-MEK1/2-ERK1/2 pathway. *Pharmacology & therapeutics*. 2018 Jul 1;187:45-60.
- Kim EK, Choi EJ. Pathological roles of MAPK signaling pathways in human diseases. *Biochimica et Biophysica Acta (BBA)-Molecular Basis of Disease*. 2010 Apr 1;1802(4):396-405.
- Kim HS, Cho IH, Kim JE, Shin YJ, Jeon JH, Kim Y, Yang YM, Lee KH, Lee JW, Lee WJ, Ye SK. Ethyl pyruvate has an anti-inflammatory effect by inhibiting ROS-dependent STAT signaling in activated microglia. *Free radical biology & medicine*. 2008 Jun 16;45(7):950-63.
- Kim KB, Kefford R, Pavlick AC, Infante JR, Ribas A, Sosman JA, Fecher LA, Millward M, McArthur GA, Hwu P, Gonzalez R. Phase II study of the MEK1/MEK2 inhibitor Trametinib in patients with metastatic BRAF-mutant cutaneous melanoma previously treated with or without a BRAF inhibitor. *Journal of Clinical Oncology*. 2013 Feb 1;31(4):482.
- Kim KC, Kang KA, Zhang R, Piao MJ, Kim GY, Kang MY, Lee SJ, Lee NH, Surh YJ, Hyun JW. Up-regulation of Nrf2-mediated heme oxygenase-1 expression by eckol, a phlorotannin compound, through activation of Erk and PI3K/Akt. *The international journal of biochemistry & cell biology*. 2010 Feb 1;42(2):297-305.
- Kim S, Tokuyama M, Hosoi M, Yamamoto K. Adrenal and circulating renin-angiotensin system in stroke-prone hypertensive rats. *Hypertension*. 1992 Sep;20(3):280-91.
- King DA, Cordova F, Scharf SM. Nutritional aspects of chronic obstructive pulmonary disease. *Proceedings of the American Thoracic Society*. 2008 May 1;5(4):519-23.
- Knez J, Winkelmanns E, Plusquin M, Thijs L, Cauwenberghs N, Gu Y, Staessen JA, Nawrot TS, Kuznetsova T. Correlates of peripheral blood mitochondrial DNA content in a general population. *American journal of epidemiology*. 2016 Jan 15;183(2):138-46.
- Knez J, Winkelmanns E, Plusquin M, Thijs L, Cauwenberghs N, Gu Y, Staessen JA, Nawrot TS, Kuznetsova T. Correlates of peripheral blood mitochondrial DNA content in a general population. *American journal of epidemiology*. 2016 Jan 15;183(2):138-46.
- Knock GA. NADPH oxidase in the vasculature: Expression, regulation and signalling pathways; role in normal cardiovascular physiology and its dysregulation in hypertension. *Free Radical Biology and Medicine*. 2019 Dec 1;145:385-427.
- Kobori H, Nangaku M, Navar LG, Nishiyama A. The intrarenal renin-angiotensin system: from physiology to the pathobiology of hypertension and kidney disease. *Pharmacological reviews*. 2007 Sep 1;59(3):251-87.

- Koenen TB, Stienstra R, Van Tits LJ, De Graaf J, Stalenhoef AF, Joosten LA, Tack CJ, Netea MG. Hyperglycemia activates caspase-1 and TXNIP-mediated IL-1 β transcription in human adipose tissue. *Diabetes*. 2011 Feb 1;60(2):517-24.
- Kofler S, Nickel T, Weis M. Role of cytokines in cardiovascular diseases: a focus on endothelial responses to inflammation. *Clinical science*. 2005 Mar 1;108(3):205-13.
- Koppenol WH, Bounds PL, Dang CV. Otto Warburg's contributions to current concepts of cancer metabolism. *Nature Reviews Cancer*. 2011 May;11(5):325-37.
- Koppes LL, Dekker JM, Hendriks HF, Bouter LM, Heine RJ. Moderate alcohol consumption lowers the risk of type 2 diabetes: a meta-analysis of prospective observational studies. *Diabetes care*. 2005 Mar 1;28(3):719-25.
- Kreuzer J, Viedt C, Brandes RP, Seeger F, Rosenkranz AS, Sauer H, Babich A, Nürnberg B, Kather H, Krieger-Brauer HI. Platelet-derived growth factor activates production of reactive oxygen species by NAD (P) H-oxidase in smooth muscle cells through Gi1, 2. *The FASEB Journal*. 2003 Jan;17(1):38-40.
- Krieger-Brauer HI, Kather H. Human fat cells possess a plasma membrane-bound H₂O₂-generating system that is activated by insulin via a mechanism bypassing the receptor kinase. *The Journal of clinical investigation*. 1992 Mar 1;89(3):1006-13.
- Kruszynska YT, Olefsky JM. Cellular and molecular mechanisms of non-insulin dependent diabetes mellitus. *Journal of investigative medicine: the official publication of the American Federation for Clinical Research*. 1996 Oct 1;44(8):413-28.
- Krylatov AV, Maslov LN, Voronkov NS, Boshchenko AA, Popov SV, Gomez L, Wang H, Jaggi AS, Downey JM. Reactive oxygen species as intracellular signaling molecules in the cardiovascular system. *Current cardiology reviews*. 2018 Oct 1;14(4):290-300.
- Kubin T, Cetinkaya A, Schönburg M, Beiras-Fernandez A, Walther T, Richter M. The MEK1 inhibitors UO126 and PD98059 block PDGF-AB induced phosphorylation of threonine 292 in porcine smooth muscle cells. *Cytokine*. 2017 Jul 1;95:51-4.
- Kurozumi A, Nakano K, Yamagata K, Okada Y, Nakayamada S, Tanaka Y. IL-6 and sIL-6R induces STAT3-dependent differentiation of human VSMCs into osteoblast-like cells through JMJD2B-mediated histone demethylation of RUNX2. *Bone*. 2019 Jul 1;124:53-61.
- Laakso M, Kuusisto J. Insulin resistance and hyperglycaemia in cardiovascular disease development. *Nature Reviews Endocrinology*. 2014 May;10(5):293-302.
- Ladak SS, McQueen LW, Layton GR, Aujla H, Adebayo A, Zakkar M. The Role of Endothelial Cells in the Onset, Development and Modulation of Vein Graft Disease. *Cells*. 2022 Sep 29;11(19):3066.
- LaMack JA, Himburg HA, Zhang J, Friedman MH. Endothelial gene expression in regions of defined shear exposure in the porcine iliac arteries. *Annals of biomedical engineering*. 2010 Jul;38(7):2252-62.
- Landgraf R. Meglitinide analogues in the treatment of type 2 diabetes mellitus. *Drugs & aging*. 2000 Nov;17(5):411-25.

- Landmesser U, Cai H, Dikalov S, McCann L, Hwang J, Jo H, Holland SM, Harrison DG. Role of p47 phox in vascular oxidative stress and hypertension caused by angiotensin II. *Hypertension*. 2002 Oct 1;40(4):511-5.
- Landsberg L, Molitch M. Diabetes and hypertension: pathogenesis, prevention and treatment. *Clinical and experimental hypertension*. 2004 Jan 1;26(7-8):621-8.
- Lathief S, Inzucchi SE. Approach to diabetes management in patients with CVD. *Trends in cardiovascular medicine*. 2016 Feb 1;26(2):165-79.
- Lazarus BD, Love DC, Hanover JA. Recombinant O-GlcNAc transferase isoforms: identification of O-GlcNAcase, yes tyrosine kinase, and tau as isoform-specific substrates. *Glycobiology*. 2006 May 1;16(5):415-21.
- Lazarus MB, Nam Y, Jiang J, Sliz P, Walker S. Structure of human O-GlcNAc transferase and its complex with a peptide substrate. *Nature*. 2011 Jan;469(7331):564-7.
- Leclercq IA, Morais AD, Schroyen B, Van Hul N, Geerts A. Insulin resistance in hepatocytes and sinusoidal liver cells: mechanisms and consequences. *Journal of hepatology*. 2007 Jul 1;47(1):142-56.
- Lecube A, Pachón G, Petriz J, Hernández C, Simó R. Phagocytic activity is impaired in type 2 diabetes mellitus and increases after metabolic improvement. *PloS one*. 2011 Aug 18;6(8):e23366.
- Lee H, Oh Y, Jeon YJ, Lee SY, Kim H, Lee HJ, Jung YK. DR4-Ser424 O-GlcNAcylation Promotes Sensitization of TRAIL-Tolerant Persisters and TRAIL-Resistant Cancer Cells to Death DR4 O-GlcNAcylation and TRAIL Sensitivity in Cancer. *Cancer Research*. 2019 Jun 1;79(11):2839-52.
- Lee HJ, Oh YK, Rhee M, Lim JY, Hwang JY, Park YS, Kwon Y, Choi KH, Jo I, Park SI, Gao B. The role of STAT1/IRF-1 on synergistic ROS production and loss of mitochondrial transmembrane potential during hepatic cell death induced by LPS/d-GalN. *Journal of molecular biology*. 2007 Jun 15;369(4):967-84.
- Lee HM, Kim JJ, Kim HJ, Shong M, Ku BJ, Jo EK. Upregulated NLRP3 inflammasome activation in patients with type 2 diabetes. *Diabetes*. 2013 Jan 1;62(1):194-204.
- Lee JH, Yang SH, Oh JM, Lee MG. Pharmacokinetics of drugs in rats with diabetes mellitus induced by alloxan or streptozocin: comparison with those in patients with type I diabetes mellitus. *Journal of Pharmacy and Pharmacology*. 2010 Jan;62(1):1-23.
- Lee K, Esselman WJ. Inhibition of PTPs by H₂O₂ regulates the activation of distinct MAPK pathways. *Free Radical Biology and Medicine*. 2002 Oct 15;33(8):1121-32.
- Lee S, Rauch J, Kolch W. Targeting MAPK signaling in cancer: mechanisms of drug resistance and sensitivity. *International journal of molecular sciences*. 2020 Feb 7;21(3):1102.
- Lee SR, Kwon KS, Kim SR, Rhee SG. Reversible inactivation of protein-tyrosine phosphatase 1B in A431 cells stimulated with epidermal growth factor. *Journal of Biological Chemistry*. 1998 Jun 19;273(25):15366-72.
- Leese HJ, Guerif F, Allgar V, Brison DR, Lundin K, Sturmeay RG. Biological optimization, the Goldilocks principle, and how much is lagom in the preimplantation embryo. *Molecular reproduction and development*. 2016 Sep;83(9):748-54.

- Lemmon MA, Schlessinger J. Cell signaling by receptor tyrosine kinases. *Cell*. 2010 Jun 25;141(7):1117-34.
- Lencina AM, Franza T, Sullivan MJ, Ulett GC, Ipe DS, Gaudu P, Gennis RB, Schurig-Briccio LA. Type 2 NADH dehydrogenase is the only point of entry for electrons into the *Streptococcus agalactiae* respiratory chain and is a potential drug target. *MBio*. 2018 Jul 3;9(4):e01034-18.
- Lenzen S, Panten U. Alloxan: history and mechanism of action. *Diabetologia*. 1988 Jun;31:337-42.
- Leslie NR, Downes CP. PTEN: The down side of PI 3-kinase signalling. *Cellular signalling*. 2002 Apr 1;14(4):285-95.
- Levine PM, Galesic A, Balana AT, Mahul-Mellier AL, Navarro MX, De Leon CA, Lashuel HA, Pratt MR. α -Synuclein O-GlcNAcylation alters aggregation and toxicity, revealing certain residues as potential inhibitors of Parkinson's disease. *Proceedings of the National Academy of Sciences*. 2019 Jan 29;116(5):1511-9.
- Levine ZG, Walker S. The biochemistry of O-GlcNAc transferase: which functions make it essential in mammalian cells?. *Annual review of biochemistry*. 2016 Jun 2;85:631-57.
- Levin-Salomon V, Kogan K, Ahn NG, Livnah O, Engelberg D. Isolation of Intrinsically Active (MEK-independent) Variants of the ERK Family of Mitogen-activated Protein (MAP) Kinases* \blacklozenge . *Journal of Biological Chemistry*. 2008 Dec 12;283(50):34500-10.
- Li L, Blumenthal DK, Terry CM, He Y, Carlson ML, Cheung AK. PDGF-induced proliferation in human arterial and venous smooth muscle cells: molecular basis for differential effects of PDGF isoforms. *Journal of cellular biochemistry*. 2011 Jan;112(1):289-98.
- Li W. Constitutive laws with damage effect for the human great saphenous vein. *Journal of the Mechanical Behavior of Biomedical Materials*. 2018 May 1;81:202-13.
- Li Y, Li R, Feng Z, Wan Q, Wu J. Linagliptin regulates the mitochondrial respiratory reserve to alter platelet activation and arterial thrombosis. *Frontiers in Pharmacology*. 2020 Nov 30;11:585612.
- Li Y, Liu H, Xu QS, Du YG, Xu J. Chitosan oligosaccharides block LPS-induced O-GlcNAcylation of NF- κ B and endothelial inflammatory response. *Carbohydrate polymers*. 2014 Jan 2;99:568-78.
- Li Z, Zhang G, Feil R, Han J, Du X. Sequential activation of p38 and ERK pathways by cGMP-dependent protein kinase leading to activation of the platelet integrin α IIb β 3. *Blood*. 2006 Feb 1;107(3):965-72.
- Libby P, Ridker PM, Maseri A. Inflammation and atherosclerosis. *Circulation*. 2002 Mar 5;105(9):1135-43.
- Lim RZ, Li L, Yong EL, Chew N. STAT-3 regulation of CXCR4 is necessary for the prenylflavonoid Icaritin to enhance mesenchymal stem cell proliferation, migration and osteogenic differentiation. *Biochimica et Biophysica Acta (BBA)-General Subjects*. 2018 Jul 1;1862(7):1680-92.
- Lima VV, Rigsby CS, Hardy DM, Webb RC, Tostes RC. O-GlcNAcylation: a novel post-translational mechanism to alter vascular cellular signaling in health and disease: focus on hypertension. *Journal of the American Society of Hypertension*. 2009 Nov 1;3(6):374-87.

- Lin G, Chow S, Lin J, Wang G, Lue TF, Lin CS. Effect of cell passage and density on protein kinase G expression and activation in vascular smooth muscle cells. *Journal of cellular biochemistry*. 2004 May 1;92(1):104-12.
- Lin X, Xu Y, Pan X, Xu J, Ding Y, Sun X, Song X, Ren Y, Shan PF. Global, regional, and national burden and trend of diabetes in 195 countries and territories: an analysis from 1990 to 2025. *Sci Rep*. 2020 Sep 8;10(1):14790.
- Lincoln TM, Dey N, Sellak H. Invited review: cGMP-dependent protein kinase signaling mechanisms in smooth muscle: from the regulation of tone to gene expression. *Journal of applied physiology*. 2001 Sep 1;91(3):1421-30.
- Linge C, Green MR, Brooks RF. A method for removal of fibroblasts from human tissue culture systems. *Experimental cell research*. 1989 Dec 1;185(2):519-28.
- Linton MF, Yancey PG, Davies SS, Jerome WG, Linton EF, Song WL, Doran AC, Vickers KC. The role of lipids and lipoproteins in atherosclerosis. *Endotext* [Internet]. 2019 Jan 3.
- Liochev SI. Reactive oxygen species and the free radical theory of aging. *Free Radical Biology and Medicine*. 2013 Jul 1;60:1-4.
- Little AC, Kovalenko I, Goo LE, Hong HS, Kerk SA, Yates JA, Purohit V, Lombard DB, Merajver SD, Lyssiotis CA. High-content fluorescence imaging with the metabolic flux assay reveals insights into mitochondrial properties and functions. *Communications biology*. 2020 May 29;3(1):1-0.
- Liu C, Dong W, Li J, Kong Y, Ren X. O-GlcNAc Modification and Its Role in Diabetic Retinopathy. *Metabolites*. 2022 Aug 5;12(8):725.
- Liu H, Nishitoh H, Ichijo H, Kyriakis JM. Activation of apoptosis signal-regulating kinase 1 (ASK1) by tumor necrosis factor receptor-associated factor 2 requires prior dissociation of the ASK1 inhibitor thioredoxin. *Molecular and cellular biology*. 2000 Mar 15;20(6):2198-208.
- Liu M., Weiss M.A., Arunagiri A., Yong J., Rege N., Sun J., Haataja L., Kaufman R.J., Arvan P. Biosynthesis, structure, and folding of the insulin precursor protein. *Diabetes Obes. Metab*. 2018;20(Suppl. 2):28–50.
- Liu Q, Zhou Y, Li Z. PDGF BB promotes the differentiation and proliferation of MC3T3 E1 cells through the Src/JAK2 signaling pathway. *Molecular Medicine Reports*. 2018 Oct 1;18(4):3719-26.
- Liu RM, Choi J, Wu JH, Pravia KA, Lewis KM, Brand JD, Mochel NR, Krzywanski DM, Lambeth JD, Hagood JS, Forman HJ. Oxidative modification of nuclear mitogen-activated protein kinase phosphatase 1 is involved in transforming growth factor β 1-induced expression of plasminogen activator inhibitor 1 in fibroblasts. *Journal of Biological Chemistry*. 2010 May 21;285(21):16239-47.
- Liu T, Castro S, Brasier AR, Jamaluddin M, Garofalo RP, Casola A. Reactive oxygen species mediate virus-induced STAT activation: role of tyrosine phosphatases. *Journal of Biological Chemistry*. 2004 Jan 23;279(4):2461-9.
- Liu Y, Liu F, Grundke-Iqbal I, Iqbal K, Gong CX. Brain glucose transporters, O-GlcNAcylation and phosphorylation of tau in diabetes and Alzheimer's disease. *Journal of neurochemistry*. 2009 Oct;111(1):242-9.

- Liu Y, Ren Y, Cao Y, Huang H, Wu Q, Li W, Wu S, Zhang J. Discovery of a low toxicity O-GlcNAc transferase (OGT) inhibitor by structure-based virtual screening of natural products. *Scientific reports*. 2017 Sep 26;7(1):12334.
- Liu Z, Ren Z, Zhang J, Chuang CC, Kandaswamy E, Zhou T, Zuo L. Role of ROS and nutritional antioxidants in human diseases. *Frontiers in physiology*. 2018 May 17;9:477.
- Lo WY, Yang WK, Peng CT, Pai WY, Wang HJ. Corrigendum: MicroRNA-200a/200b Modulate High Glucose-Induced Endothelial Inflammation by Targeting O-linked N-Acetylglucosamine Transferase Expression. *Frontiers in Physiology*. 2018 Jun 19;9:786.
- Lo WY, Yang WK, Peng CT, Pai WY, Wang HJ. MicroRNA-200a/200b modulate high glucose-induced endothelial inflammation by targeting O-linked N-acetylglucosamine transferase expression. *Frontiers in physiology*. 2018 Apr 18;9:355.
- Locasale JW, Cantley LC. Metabolic flux and the regulation of mammalian cell growth. *Cell metabolism*. 2011 Oct 5;14(4):443-51.
- LoGerfo FW, Corson JD, Mannick JA. Improved results with femoropopliteal vein grafts for limb salvage. *Archives of Surgery*. 1977 May 1;112(5):567-70.
- Londhe AD, Bergeron A, Curley SM, Zhang F, Rivera KD, Kannan A, Coulis G, Rizvi SH, Kim SJ, Pappin DJ, Tonks NK. Regulation of PTP1B activation through disruption of redox-complex formation. *Nature chemical biology*. 2020 Feb;16(2):122-5.
- Longchamps RJ, Castellani CA, Yang SY, Newcomb CE, Sumpter JA, Lane J, Grove ML, Guallar E, Pankratz N, Taylor KD, Rotter JI. Evaluation of mitochondrial DNA copy number estimation techniques. *PloS one*. 2020 Jan 31;15(1):e0228166.
- Lovero D, Giordano L, Marsano RM, Sanchez-Martinez A, Boukhatmi H, Drechsler M, Oliva M, Whitworth AJ, Porcelli D, Caggese C. Characterization of Drosophila ATPsynC mutants as a new model of mitochondrial ATP synthase disorders. *PLoS One*. 2018 Aug 10;13(8):e0201811.
- Lu QB, Wan MY, Wang PY, Zhang CX, Xu DY, Liao X, Sun HJ. Chicoric acid prevents PDGF-BB-induced VSMC dedifferentiation, proliferation and migration by suppressing ROS/NFκB/mTOR/P70S6K signaling cascade. *Redox biology*. 2018 Apr 1;14:656-68.
- Lufei C, Ma J, Huang G, Zhang T, Novotny-Diermayr V, Ong CT, Cao X. GRIM-19, a death-regulatory gene product, suppresses Stat3 activity via functional interaction. *The EMBO journal*. 2003 Mar 17;22(6):1325-35.
- Lunt SY, Vander Heiden MG. Aerobic glycolysis: meeting the metabolic requirements of cell proliferation. *Annual Review of Cell Developmental Biology*. 2011 Nov; 27 (1):441–64.
- Luo S, Valencia CA, Zhang J, Lee NC, Slone J, Gui B, Wang X, Li Z, Dell S, Brown J, Chen SM. Biparental inheritance of mitochondrial DNA in humans. *Proceedings of the National Academy of Sciences*. 2018 Dec 18;115(51):13039-44.
- Lust JA, Donovan KA, Kline MP, Greipp PR, Kyle RA, Maihle NJ. Isolation of an mRNA encoding a soluble form of the human interleukin-6 receptor. *Cytokine*. 1992 Mar 1;4(2):96-100.
- Lustig KD, Shiau AK, Brake AJ, Julius D. Expression cloning of an ATP receptor from mouse neuroblastoma cells. *Proceedings of the National Academy of Sciences*. 1993 Jun 1;90(11):5113-7.

- Lyle AN, Griendling KK. Modulation of vascular smooth muscle signaling by reactive oxygen species. *Physiology*. 2006 Aug;21(4):269-80.
- Ma J, Hart GW. O-GlcNAc profiling: from proteins to proteomes. *Clinical proteomics*. 2014 Dec;11(1):1-6.
- Ma J, Hart GW. Protein O-GlcNAcylation in diabetes and diabetic complications. *Expert review of proteomics*. 2013 Aug 1;10(4):365-80.
- Ma L, Ma S, He H, Yang D, Chen X, Luo Z, Liu D, Zhu Z. Perivascular fat-mediated vascular dysfunction and remodeling through the AMPK/mTOR pathway in high-fat diet-induced obese rats. *Hypertension Research*. 2010 May;33(5):446-53.
- Ma Z, Chalkley RJ, Vosseller K. Hyper-O-GlcNAcylation activates nuclear factor κ -light-chain-enhancer of activated B cells (NF- κ B) signaling through interplay with phosphorylation and acetylation. *Journal of Biological Chemistry*. 2017 Jun 2;292(22):9150-63.
- Macaulay MS, He Y, Gloster TM, Stubbs KA, Davies GJ, Vocadlo DJ. Inhibition of O-GlcNAcase using a potent and cell-permeable inhibitor does not induce insulin resistance in 3T3-L1 adipocytes. *Chemistry & biology*. 2010 Sep 24;17(9):937-48.
- Madamanchi NR, Li S, Patterson C, Runge MS. Thrombin regulates vascular smooth muscle cell growth and heat shock proteins via the JAK-STAT pathway. *Journal of Biological Chemistry*. 2001 Jun 1;276(22):18915-24.
- Madamanchi NR, Vendrov A, Runge MS. Oxidative stress and vascular disease. *Arteriosclerosis, thrombosis, and vascular biology*. 2005 Jan 1;25(1):29-38.
- Madi HA, Riches K, Warburton P, O'Regan DJ, Turner NA, Porter KE. Inherent differences in morphology, proliferation, and migration in saphenous vein smooth muscle cells cultured from nondiabetic and Type 2 diabetic patients. *American Journal of Physiology-Cell Physiology*. 2009 Nov;297(5):C1307-17.
- Magenta A, Cencioni C, Fasanaro P, Zaccagnini G, Greco S, Sarra-Ferraris G, Antonini A, Martelli F, Capogrossi MC. miR-200c is upregulated by oxidative stress and induces endothelial cell apoptosis and senescence via ZEB1 inhibition. *Cell Death & Differentiation*. 2011 Oct;18(10):1628-39.
- Mahapatra DK, Asati V, Bharti SK. MEK inhibitors in oncology: A patent review (2015-Present). *Expert Opinion on Therapeutic Patents*. 2017 Aug 3;27(8):887-906.
- Maitra A. The Endocrine System. In Kumar, V., Abbas, A.A., Fausto, N., Aster, J.C. (eds). *Robins and Cotran Pathologic Basis of Disease 9th Edition*. 2012-Elsevier. pp1131.
- Maki KC, Kelley KM, Lawless AL, Hubacher RL, Schild AL, Dicklin MR, Rains TM. Validation of insulin sensitivity and secretion indices derived from the liquid meal tolerance test. *Diabetes technology & therapeutics*. 2011 Jun 1;13(6):661-6.
- Mannacio VA, Di Tommaso L, Antignan A, De Amicis V, Vosa C. Aspirin plus clopidogrel for optimal platelet inhibition following off-pump coronary artery bypass surgery: results from the CRYSSA (prevention of Coronary arteRY bypaSS occlusion After off-pump procedures) randomised study. *Heart*. 2012 Dec 1;98(23):1710-5.
- Manning G, Whyte DB, Martinez R, Hunter T, Sudarsanam S. The protein kinase complement of the human genome. *Science*. 2002 Dec 6;298(5600):1912-34.

- Manson JE, Nathan DM, Krolewski AS, Stampfer MJ, Willett WC, Hennekens CH. A prospective study of exercise and incidence of diabetes among US male physicians. *Jama*. 1992 Jul 1;268(1):63-7.
- Mariappa D, Selvan N, Borodkin VS, Alonso J, Ferenbach AT, Shepherd C, Navratilova IH, Van Aalten DM. A mutant O-GlcNAcase as a probe to reveal global dynamics of protein O-GlcNAcylation during *Drosophila* embryonic development. *Biochemical Journal*. 2015 Sep 1;470(2):255-62.
- Marin T, Gongol B, Chen Z, Woo B, Subramaniam S, Chien S, Shyy JY. Mechanosensitive microRNAs—role in endothelial responses to shear stress and redox state. *Free Radical Biology and Medicine*. 2013 Sep 9;64:61-8.
- Marinho HS, Real C, Cyrne L, Soares H, Antunes F. Hydrogen peroxide sensing, signaling and regulation of transcription factors. *Redox biology*. 2014 Jan 1;2:535-62.
- Marotta NP, Lin YH, Lewis YE, Ambroso MR, Zaro BW, Roth MT, Arnold DB, Langen R, Pratt MR. O-GlcNAc modification blocks the aggregation and toxicity of the protein α -synuclein associated with Parkinson's disease. *Nature chemistry*. 2015 Nov;7(11):913-20.
- Marsboom G, Toth PT, Ryan JJ, Hong Z, Wu X, Fang YH, Thenappan T, Piao L, Zhang HJ, Pogoriler J, Chen Y. Dynamin-related protein 1-mediated mitochondrial mitotic fission permits hyperproliferation of vascular smooth muscle cells and offers a novel therapeutic target in pulmonary hypertension. *Circulation research*. 2012 May 25;110(11):1484-97.
- Marshall CJ. Ras effectors. *Current opinion in cell biology*. 1996 Apr 1;8(2):197-204.
- Martin KA, Merenick BL, Ding M, Fetalvero KM, Rzucidlo EM, Kozul CD, Brown DJ, Chiu HY, Shyu M, Drapeau BL, Wagner RJ. Rapamycin promotes vascular smooth muscle cell differentiation through insulin receptor substrate-1/phosphatidylinositol 3-kinase/Akt2 feedback signaling. *Journal of Biological Chemistry*. 2007 Dec 7;282(49):36112-20.
- Martin SE, Tan ZW, Itkonen HM, Duveau DY, Paulo JA, Janetzko J, Boutz PL, Törk L, Moss FA, Thomas CJ, Gygi SP. Structure-based evolution of low nanomolar O-GlcNAc transferase inhibitors. *Journal of the American Chemical Society*. 2018 Oct 4;140(42):13542-5.
- Martínez-Revelles S, García-Redondo AB, Avendaño MS, Varona S, Palao T, Orriols M, Roque FR, Fortuño A, Touyz RM, Martínez-González J, Salaices M. Lysyl oxidase induces vascular oxidative stress and contributes to arterial stiffness and abnormal elastin structure in hypertension: role of p38MAPK. *Antioxidants & redox signaling*. 2017 Sep 1;27(7):379-97.
- Martín-Timón I, Sevillano-Collantes C, Segura-Galindo A, del Cañizo-Gómez FJ. Type 2 diabetes and cardiovascular disease: have all risk factors the same strength?. *World journal of diabetes*. 2014 Aug 8;5(4):444.
- Masaki N, Feng B, Bretón-Romero R, Inagaki E, Weisbrod RM, Fetterman JL, Hamburg NM. O-GlcNAcylation Mediates Glucose-Induced Alterations in Endothelial Cell Phenotype in Human Diabetes Mellitus. *Journal of the American Heart Association*. 2020 Jun 16;9(12):e014046.
- Masamune A, Satoh M, Kikuta K, Suzuki N, Shimosegawa T. Activation of JAK-STAT pathway is required for platelet-derived growth factor-induced proliferation of pancreatic stellate cells. *World journal of gastroenterology: WJG*. 2005 Jun 14;11(22):3385.

- Masoli M, Fabian D, Holt S, Beasley R, Global Initiative for Asthma (GINA) Program. The global burden of asthma: executive summary of the GINA Dissemination Committee report. *Allergy*. 2004 May;59(5):469-78.
- Masri FA, Xu W, Comhair SA, Asosingh K, Koo M, VasANJI A, Drazba J, Anand-Apte B, Erzurum SC. Hyperproliferative apoptosis-resistant endothelial cells in idiopathic pulmonary arterial hypertension. *American Journal of Physiology-Lung Cellular and Molecular Physiology*. 2007 Sep;293(3):L548-54.
- Maston LD, Jones DT, Giermakowska W, Resta TC, Ramiro-Diaz J, Howard TA, Jernigan NL, Herbert L, Maurice AA, Gonzalez Bosc LV. Interleukin-6 trans-signaling contributes to chronic hypoxia-induced pulmonary hypertension. *Pulmonary Circulation*. 2018 Jul;8(3):2045894018780734.
- McClain DA, Lubas WA, Cooksey RC, Hazel M, Parker GJ, Love DC, Hanover JA. Altered glycan-dependent signaling induces insulin resistance and hyperleptinemia. *Proceedings of the National Academy of Sciences*. 2002 Aug 6;99(16):10695-9.
- McCubrey JA, LaHair MM, Franklin RA. Reactive oxygen species-induced activation of the MAP kinase signaling pathways. *Antioxidants & redox signaling*. 2006 Sep 1;8(9-10):1775-89.
- McGillicuddy FC, Reilly MP, Rader DJ. Adipose modulation of high-density lipoprotein cholesterol: implications for obesity, high-density lipoprotein metabolism, and cardiovascular disease. *Circulation*. 2011 Oct 11;124(15):1602-5.
- McGreal SR, Bhushan B, Walesky C, McGill MR, Lebofsky M, Kandel SE, Winefield RD, Jaeschke H, Zachara NE, Zhang Z, Tan EP. Modulation of O-GlcNAc levels in the liver impacts acetaminophen-induced liver injury by affecting protein adduct formation and glutathione synthesis. *Toxicological Sciences*. 2018 Apr 1;162(2):599-610.
- McKavanagh P, Yanagawa B, Zawadowski G, Cheema A. Management and prevention of saphenous vein graft failure: a review. *Cardiology and therapy*. 2017 Dec;6(2):203-23.
- McMillan-Price J, Brand-Miller J. Low-glycaemic index diets and body weight regulation. *International journal of obesity*. 2006 Dec;30(3):S40-6.
- Mehta RH, Ferguson TB, Lopes RD, Hafley GE, Mack MJ, Kouchoukos NT, Gibson CM, Harrington RA, Califf RM, Peterson ED, Alexander JH. Saphenous vein grafts with multiple versus single distal targets in patients undergoing coronary artery bypass surgery: one-year graft failure and five-year outcomes from the Project of Ex-Vivo Vein Graft Engineering via Transfection (PREVENT) IV trial. *Circulation*. 2011 Jul 19;124(3):280-8.
- Meloni AR, DeYoung MB, Lowe C, Parkes DG. GLP-1 receptor activated insulin secretion from pancreatic β -cells: mechanism and glucose dependence. *Diabetes, Obesity and Metabolism*. 2013 Jan;15(1):15-27.
- Menegazzo L, Ciciliot S, Poncina N, Mazzucato M, Persano M, Bonora B, Albiero M, Vigili de Kreutzenberg S, Avogaro A, Fadini GP. NETosis is induced by high glucose and associated with type 2 diabetes. *Acta diabetologica*. 2015 Jun;52(3):497-503.
- Meng TC, Fukada T, Tonks NK. Reversible oxidation and inactivation of protein tyrosine phosphatases in vivo. *Molecular cell*. 2002 Feb 1;9(2):387-99.

- Meng XF, Wang XL, Tian XJ, Yang ZH, Chu GP, Zhang J, Li M, Shi J, Zhang C. Nod-like receptor protein 1 inflammasome mediates neuron injury under high glucose. *Molecular neurobiology*. 2014 Apr;49(2):673-84.
- Meshkani R, Adeli K. Mechanisms linking the metabolic syndrome and cardiovascular disease: role of hepatic insulin resistance. *The Journal of Tehran University Heart Center*. 2009;4(2):77-84.
- Metallo CM, Vander Heiden MG. Understanding metabolic regulation and its influence on cell physiology. *Molecular cell*. 2013 Feb 7;49(3):388-98.
- Miano JM, Cserjesi P, Ligon KL, Periasamy M, Olson EN. Smooth muscle myosin heavy chain exclusively marks the smooth muscle lineage during mouse embryogenesis. *Circulation research*. 1994 Nov;75(5):803-12.
- Michell BJ, Griffiths JE, Mitchelhill KI, Rodriguez-Crespo I, Tiganis T, Bozinovski S, de Montellano PO, Kemp BE, Pearson RB. The Akt kinase signals directly to endothelial nitric oxide synthase. *Current biology*. 1999 Aug 12;9(15):845-S1.
- Migliaccio E, Giorgio M, Pelicci PG. Apoptosis and aging: role of p66Shc redox protein. *Antioxidants & redox signaling*. 2006 Mar 1;8(3-4):600-8.
- Milara J, Ballester B, Morell A, Ortiz JL, Escrivá J, Fernández E, Perez-Vizcaino F, Cogolludo A, Pastor E, Artigues E, Morcillo E. JAK2 mediates lung fibrosis, pulmonary vascular remodelling and hypertension in idiopathic pulmonary fibrosis: an experimental study. *Thorax*. 2018 Jun 1;73(6):519-29.
- Mitra AK, Gangahar DM, Agrawal DK. Cellular, molecular and immunological mechanisms in the pathophysiology of vein graft intimal hyperplasia. *Immunology and cell biology*. 2006 Apr;84(2):115-24.
- Mitra K. Mitochondrial fission-fusion as an emerging key regulator of cell proliferation and differentiation. *Bioessays*. 2013 Nov;35(11):955-64.
- Miyazaki Y, Cersosimo E, Triplitt C, DeFronzo RA. Rosiglitazone decreases albuminuria in type 2 diabetic patients. *Kidney international*. 2007 Dec 1;72(11):1367-73.
- Mizuki Y, Sakamoto S, Okahisa Y, Yada Y, Hashimoto N, Takaki M, Yamada N. Mechanisms underlying the comorbidity of schizophrenia and type 2 diabetes mellitus. *International Journal of Neuropsychopharmacology*. 2021 May;24(5):367-82.
- Modi B, Hernandez-Henderson M, Yang D, Klein J, Dadwal S, Kopp E, Huelsman K, Mokhtari S, Ali H, Al Malki MM, Spielberger R. Ruxolitinib as salvage therapy for chronic graft-versus-host disease. *Biology of Blood and Marrow Transplantation*. 2019 Feb 1;25(2):265-9.
- Molina JR, Adjei AA. The ras/raf/mapk pathway. *Journal of Thoracic Oncology*. 2006 Jan 1;1(1):7-9.
- Molloy CJ, Pawlowski JE, Taylor DS, Turner CE, Weber H, Peluso M. Thrombin receptor activation elicits rapid protein tyrosine phosphorylation and stimulation of the raf-1/MAP kinase pathway preceding delayed mitogenesis in cultured rat aortic smooth muscle cells: evidence for an obligate autocrine mechanism promoting cell proliferation induced by G-protein-coupled receptor agonist. *The Journal of clinical investigation*. 1996 Mar 1;97(5):1173-83.

- Moncada S, Higgs EA, Colombo SL. Fulfilling the metabolic requirements for cell proliferation. *Biochemical Journal*. 2012 Aug 15;446(1):1-7.
- Montagnani M, Chen H, Barr VA, Quon MJ. Insulin-stimulated activation of eNOS is independent of Ca²⁺ but requires phosphorylation by Akt at Ser1179. *Journal of Biological Chemistry*. 2001 Aug 10;276(32):30392-8.
- Montal E, Dewi R, Bhalla K, Ou L, Hwang B, Ropell A, Gordon C, Liu WJ, DeBerardinis R, Sudderth J, Twaddel W. PEPCCK coordinates the regulation of central carbon metabolism to promote cancer cell growth. *Molecular cell*. 2015 Nov 19;60(4):571-83.
- Moodley L, Franz T, Human P, Wolf MF, Bezuidenhout D, Scherman J, Zilla P. Protective constriction of coronary vein grafts with knitted nitinol. *European Journal of Cardio-Thoracic Surgery*. 2013 Jul 1;44(1):64-71.
- Mookerjee SA, Brand MD. Measurement and analysis of extracellular acid production to determine glycolytic rate. *JoVE (Journal of Visualized Experiments)*. 2015 Dec 12(106):e53464.
- Mookerjee SA, Goncalves RL, Gerencser AA, Nicholls DG, Brand MD. The contributions of respiration and glycolysis to extracellular acid production. *Biochimica et Biophysica Acta (BBA)-Bioenergetics*. 2015 Feb 1;1847(2):171-81.
- Mooradian AD, Haas MJ, Wong NC. Transcriptional control of apolipoprotein AI gene expression in diabetes. *Diabetes*. 2004 Mar 1;53(3):513-20.
- Moremen KW, Tiemeyer M, Nairn AV. Vertebrate protein glycosylation: diversity, synthesis and function. *Nature reviews Molecular cell biology*. 2012 Jul;13(7):448-62.
- Morita KI, Saitoh M, Tobiume K, Matsuura H, Enomoto S, Nishitoh H, Ichijo H. Negative feedback regulation of ASK1 by protein phosphatase 5 (PP5) in response to oxidative stress. *The EMBO journal*. 2001 Nov 1;20(21):6028-36.
- Moshapa FT, Riches-Suman K, Palmer TM. Therapeutic targeting of the proinflammatory IL-6-JAK/STAT signalling pathways responsible for vascular restenosis in type 2 diabetes mellitus. *Cardiology research and practice*. 2019 Jan 2;2019.
- Motwani JG, Topol EJ. Aortocoronary saphenous vein graft disease: pathogenesis, predisposition, and prevention. *Circulation*. 1998 Mar 10;97(9):916-31.
- Mouriaux F, Zaniolo K, Bergeron MA, Weidmann C, De La Fouchardiere A, Fournier F, Droit A, Morcos MW, Landreville S, Guérin SL. Effects of long-term serial passaging on the characteristics and properties of cell lines derived from uveal melanoma primary tumors. *Investigative Ophthalmology & Visual Science*. 2016 Oct 1;57(13):5288-301.
- Mousa SA, Kapil R, Mu DX. Intravenous and oral antithrombotic efficacy of the novel platelet GPIIb/IIIa antagonist roxifiban (DMP754) and its free acid form, XV459. *Arteriosclerosis, thrombosis, and vascular biology*. 1999 Oct;19(10):2535-41.
- Mukai E, Fujimoto S, Inagaki N. Role of Reactive Oxygen Species in Glucose Metabolism Disorder in Diabetic Pancreatic β -Cells. *Biomolecules*. 2022 Sep 2;12(9):1228.
- Mülberg J, Schooltink H, Stoyan T, Günther M, Graeve L, Buse G, Mackiewicz A, Heinrich PC, Rose-John S. The soluble interleukin-6 receptor is generated by shedding. *European journal of immunology*. 1993 Feb;23(2):473-80.

- Murakami M, Hibi M, Nakagawa N, Nakagawa T, Yasukawa K, Yamanishi K, Taga T, Kishimoto T. IL-6-induced homodimerization of gp130 and associated activation of a tyrosine kinase. *Science*. 1993 Jun 18;260(5115):1808-10.
- Murdoch CE, Zhang M, Cave AC, Shah AM. NADPH oxidase-dependent redox signalling in cardiac hypertrophy, remodelling and failure. *Cardiovascular research*. 2006 Jul 15;71(2):208-15.
- Murphy MP. How mitochondria produce reactive oxygen species. *Biochemical journal*. 2009 Jan 1;417(1):1-3.
- Muslin AJ. MAPK signalling in cardiovascular health and disease: molecular mechanisms and therapeutic targets. *Clinical science*. 2008 Oct 1;115(7):203-18.
- Nakazawa G, Ladich E, Finn AV, Virmani R. Pathophysiology of vascular healing and stent mediated arterial injury. *EuroIntervention: journal of EuroPCR in collaboration with the Working Group on Interventional Cardiology of the European Society of Cardiology*. 2008 Aug 1;4:C7-10.
- Narayanan S. Multifunctional roles of thrombin. *Annals of Clinical & Laboratory Science*. 1999 Oct 1;29(4):275-80.
- National Health Service (NHS) inform (2020). Coronary heart bypass graft. <https://www.nhsinform.scot/tests-and-treatments/surgical-procedures/coronary-artery-bypass-graft>. Accessed 14-06-2020
- Nediani C, Borch E, Giordano C, Baruzzo S, Ponziani V, Sebastiani M, Nassi P, Mugelli A, d'Amati G, Cerbai E. NADPH oxidase-dependent redox signaling in human heart failure: relationship between the left and right ventricle. *Journal of molecular and cellular cardiology*. 2007 Apr 1;42(4):826-34.
- Nelson PR, Yamamura S, Mureebe L, Itoh H, Kent KC. Smooth muscle cell migration and proliferation are mediated by distinct phases of activation of the intracellular messenger mitogen-activated protein kinase. *Journal of vascular surgery*. 1998 Jan 1;27(1):117-25.
- Nesto RW. Correlation between cardiovascular disease and diabetes mellitus: current concepts. *The American journal of medicine*. 2004 Mar 8;116(5):11-22.
- Neumann E, Riepl B, Knedla A, Lefèvre S, Tarner IH, Grifka J, Steinmeyer J, Schölmerich J, Gay S, Müller-Ladner U. Cell culture and passaging alters gene expression pattern and proliferation rate in rheumatoid arthritis synovial fibroblasts. *Arthritis research & therapy*. 2010 Jun;12(3):1-0.
- Niedzwiecki MM, Walker DI, Vermeulen R, Chadeau-Hyam M, Jones DP, Miller GW. The exposome: molecules to populations. *Annual review of pharmacology and toxicology*. 2019 Jan 6;59:107-27.
- Nigro P, Satoh K, O'Dell MR, Soe NN, Cui Z, Mohan A, Abe JI, Alexis JD, Sparks JD, Berk BC. Cyclophilin A is an inflammatory mediator that promotes atherosclerosis in apolipoprotein E-deficient mice. *Journal of Experimental Medicine*. 2011 Jan 17;208(1):53-66.
- Norlander AE, Madhur MS, Harrison DG. The immunology of hypertension. *Journal of Experimental Medicine*. 2018 Jan 2;215(1):21-33.
- Nussey S., Whitehead S. *Endocrinology: An Integrated Approach*. BIOS Scientific Publishers; Oxford, UK: 2001.

- Ogawa M, Nakamura N, Nakayama Y, Kurosaka A, Many H, Kanagawa M, Endo T, Furukawa K, Okajima T. GTDC2 modifies O-mannosylated α -dystroglycan in the endoplasmic reticulum to generate N-acetyl glucosamine epitopes reactive with CTD110. 6 antibody. *Biochemical and biophysical research communications*. 2013 Oct 11;440(1):88-93.
- Ogbera AO, Ekpebegh C. Diabetes mellitus in Nigeria: The past, present and future. *World journal of diabetes*. 2014 Dec 12;5(6):905.
- Oguntibeju OO. Type 2 diabetes mellitus, oxidative stress and inflammation: examining the links. *International journal of physiology, pathophysiology and pharmacology*. 2019;11(3):45.
- Oh KJ, Han HS, Kim MJ, Koo SH. CREB and FoxO1: two transcription factors for the regulation of hepatic gluconeogenesis. *BMB reports*. 2013 Dec;46(12):567.
- Ohtsu H, Suzuki H, Nakashima H, Dhobale S, Frank GD, Motley ED, Eguchi S. Angiotensin II signal transduction through small GTP-binding proteins: mechanism and significance in vascular smooth muscle cells. *Hypertension*. 2006 Oct 1;48(4):534-40.
- Okuno D, Iino R, Noji H. Rotation and structure of F_oF₁-ATP synthase. *The Journal of Biochemistry*. 2011 Jun 1;149(6):655-64.
- Olson AK, Bouchard B, Zhu WZ, Chatham JC, Des Rosiers C. First characterization of glucose flux through the hexosamine biosynthesis pathway (HBP) in ex vivo mouse heart. *Journal of Biological Chemistry*. 2020 Feb 14;295(7):2018-33.
- Ooi A, Wong A, Esau L, Lemtiri-Chlieh F, Gehring C. A guide to transient expression of membrane proteins in HEK-293 cells for functional characterization. *Frontiers in physiology*. 2016 Jul 19;7:300.
- Ortiz-Meoz RF, Jiang J, Lazarus MB, Orman M, Janetzko J, Fan C, Duveau DY, Tan ZW, Thomas CJ, Walker S. A small molecule that inhibits OGT activity in cells. *ACS chemical biology*. 2015 Jun 19;10(6):1392-7.
- Ortiz-Munoz G, Martin-Ventura JL, Hernandez-Vargas P, Mallavia B, Lopez-Parra V, Lopez-Franco O, Munoz-Garcia B, Fernandez-Vizarra P, Ortega L, Egido J, Gomez-Guerrero C. Suppressors of cytokine signaling modulate JAK/STAT-mediated cell responses during atherosclerosis. *Arteriosclerosis, thrombosis, and vascular biology*. 2009 Apr 1;29(4):525-31.
- O'Shea JJ, Schwartz DM, Villarino AV, Gadina M, McInnes IB, Laurence A. The JAK-STAT pathway: impact on human disease and therapeutic intervention. *Annual review of medicine*. 2015 Jan 14;66:311-28.
- Owen KL, Brockwell NK, Parker BS. JAK-STAT signaling: a double-edged sword of immune regulation and cancer progression. *Cancers*. 2019 Dec 12;11(12):2002.
- Owens CD, Gasper WJ, Rahman AS, Conte MS. Vein graft failure. *Journal of vascular surgery*. 2015 Jan 1;61(1):203-16.
- Owens GK, Kumar MS, Wamhoff BR. Molecular regulation of vascular smooth muscle cell differentiation in development and disease. *Physiological reviews*. 2004 Jul;84(3):767-801.
- Owens GK. Regulation of differentiation of vascular smooth muscle cells. *Physiological reviews*. 1995 Jul 1;75(3):487-517.

- Oz BS, Iyem H, Akay HT, Bolcal C, Yokusoglu M, Kuralay E, Demirkilic U, Tatar H. Mid-Term Angiographic Comparison of Sequential and Individual Anastomosis Techniques for Diagonal Artery. *Journal of cardiac surgery*. 2006 Sep;21(5):471-4.
- Pacini S, Pellegrini M, Migliaccio E, Patrussi L, Ulivieri C, Ventura A, Carraro F, Naldini A, Lanfrancone L, Pelicci P, Baldari CT. p66SHC promotes apoptosis and antagonizes mitogenic signaling in T cells. *Molecular and Cellular Biology*. 2004 Feb 15;24(4):1747-57.
- Paice BJ, Paterson KR, Lawson DH. Undesired effects of the sulphonylurea drugs. Adverse drug reactions and acute poisoning reviews. 1985;4(1):23-36.
- Panchatcharam M, Miriyala S, Yang F, Leitges M, Chrzanowska-Wodnicka M, Quilliam LA, Anaya P, Morris AJ, Smyth SS. Enhanced proliferation and migration of vascular smooth muscle cells in response to vascular injury under hyperglycemic conditions is controlled by β 3 integrin signaling. *The international journal of biochemistry & cell biology*. 2010 Jun 1;42(6):965-74.
- Panth N, Paudel KR, Parajuli K. Reactive oxygen species: a key hallmark of cardiovascular disease. *Advances in medicine*. 2016 Oct;2016.
- Paonessa G, Graziani R, De Serio A, Savino R, Ciapponi L, Lahm A, Salvati AL, Toniatti C, Ciliberto G. Two distinct and independent sites on IL-6 trigger gp 130 dimer formation and signalling. *The EMBO journal*. 1995 May;14(9):1942-51.
- Papa S, Choy PM, Bubici C. The ERK and JNK pathways in the regulation of metabolic reprogramming. *Oncogene*. 2019 Mar;38(13):2223-40.
- Papoushek C. The “glitazones”: rosiglitazone and pioglitazone. *Journal of Obstetrics and Gynaecology Canada*. 2003 Oct 1;25(10):853-7.
- Parascandolo A, Laukkanen MO. Carcinogenesis and reactive oxygen species signaling: Interaction of the NADPH oxidase NOX1–5 and superoxide dismutase 1–3 signal transduction pathways. *Antioxidants & redox signaling*. 2019 Jan 1;30(3):443-86.
- Park J, Lai MK, Arumugam TV, Jo DG. O-GlcNAcylation as a therapeutic target for Alzheimer’s disease. *Neuromolecular medicine*. 2020 Jun;22(2):171-93.
- Park K, Saudek CD, Hart GW. Increased expression of β -N-acetylglucosaminidase in erythrocytes from individuals with pre-diabetes and diabetes. *Diabetes*. 2010 Jul 1;59(7):1845-50.
- Patti ME, Virkamäki A, Landaker EJ, Kahn CR, Yki-Järvinen H. Activation of the hexosamine pathway by glucosamine in vivo induces insulin resistance of early postreceptor insulin signaling events in skeletal muscle. *Diabetes*. 1999 Aug 1;48(8):1562-71.
- Pavlova NN, Thompson CB. The emerging hallmarks of cancer metabolism. *Cell metabolism*. 2016 Jan 12;23(1):27-47.
- Payushina OV, Butorina NN, Sheveleva ON, Kozhevnikova MN, Starostin VI. Cell composition of the primary culture of fetal liver. *Bulletin of experimental biology and medicine*. 2013 Feb;154(4):566-73.
- Pearson T, Wattis JA, King JR, MacDonald IA, Mazzatti DJ. The effects of insulin resistance on individual tissues: an application of a mathematical model of metabolism in humans. *Bulletin of mathematical biology*. 2016 Jun;78(6):1189-217.

- Pechanova O, Varga ZV, Cebova M, Giricz Z, Pacher P, Ferdinandy P. Cardiac NO signalling in the metabolic syndrome. *British Journal of Pharmacology*. 2015 Mar;172(6):1415-33.
- Pelicci G, Lanfrancone L, Grignani F, McGlade J, Cavallo F, Forni G, Nicoletti I, Grignani F, Pawson T, Pelicci PG. A novel transforming protein (SHC) with an SH2 domain is implicated in mitogenic signal transduction. *Cell*. 1992 Jul 10;70(1):93-104.
- Perez J, Hill BG, Benavides GA, Dranka BP, Darley-Usmar VM. Role of cellular bioenergetics in smooth muscle cell proliferation induced by platelet-derived growth factor. *Biochemical Journal*. 2010 Jun 1;428(2):255-67.
- Perriello G, Misericordia P, Volpi E, Santucci A, Santucci C, Ferrannini E, Ventura MM, Santeusano F, Brunetti P, Bolli GB. Acute antihyperglycemic mechanisms of metformin in NIDDM: evidence for suppression of lipid oxidation and hepatic glucose production. *Diabetes*. 1994 Jul 1;43(7):920-8.
- Persson C, Sjöblom T, Groen A, Kappert K, Engström U, Hellman U, Heldin CH, den Hertog J, Östman A. Preferential oxidation of the second phosphatase domain of receptor-like PTP- α revealed by an antibody against oxidized protein tyrosine phosphatases. *Proceedings of the National Academy of Sciences*. 2004 Feb 17;101(7):1886-91.
- Peters SC, Reis A, Noll T. Preparation of endothelial cells from microand macrovascular origin. In *Practical methods in cardiovascular research 2005* (pp. 610-629). Springer, Berlin, Heidelberg.
- Petersen KF, Shulman GI. Etiology of insulin resistance. *Am J Med*. 2006;119:S10-6.
- Pinho TS, Correia SC, Perry G, Ambrósio AF, Moreira PI. Diminished O-GlcNAcylation in Alzheimer's disease is strongly correlated with mitochondrial anomalies. *Biochimica et Biophysica Acta (BBA)-Molecular Basis of Disease*. 2019 Aug 1;1865(8):2048-59.
- Pinton P, Rimessi A, Marchi S, Orsini F, Migliaccio E, Giorgio M, Contursi C, Minucci S, Mantovani F, Wieckowski MR, Del Sal G. Protein kinase C β and prolyl isomerase 1 regulate mitochondrial effects of the life-span determinant p66Shc. *Science*. 2007 Feb 2;315(5812):659-63.
- Plitzko B, Loesgen S. Measurement of oxygen consumption rate (OCR) and extracellular acidification rate (ECAR) in culture cells for assessment of the energy metabolism. *Bio-protocol*. 2018 May 20;8(10):e2850.
- Policardo L, Seghieri G, Anichini R, De Bellis A, Franconi F, Francesconi P, Del Prato S, Mannucci E. Effect of diabetes on hospitalization for ischemic stroke and related in-hospital mortality: a study in Tuscany, Italy, over years 2004–2011. *Diabetes/metabolism research and reviews*. 2015 Mar;31(3):280-6.
- Powers AC, D'Alessio D. Endocrine pancreas and pharmacotherapy of diabetes mellitus and hypoglycemia. *Goodman and Gilman's, The Pharmacological Basis of Therapeutics*. 12th Ed. New York: McGraw-Hill. 2011:1237-271.
- Prendergast FG, Mann KG. Chemical and physical properties of aequorin and the green fluorescent protein isolated from *Aequorea forskalea*. *Biochemistry*. 1978 Aug 1;17(17):3448-53.
- Pyle A, Anugrha H, Kurzawa-Akanbi M, Yarnall A, Burn D, Hudson G. Reduced mitochondrial DNA copy number is a biomarker of Parkinson's disease. *Neurobiology of aging*. 2016 Feb 1;38:216-e7.

- Pyle A. et al. Reduced mitochondrial DNA copy number is a biomarker of Parkinson's disease. *Neurobiol. Aging* 38, 216.e7–216.e10 (2016).
- Pyörälä K, Pedersen TR, Kjekshus J, Faergeman O, Olsson AG, Thorgeirsson G, Scandinavian Simvastatin Survival Study (4S) Group. Cholesterol lowering with simvastatin improves prognosis of diabetic patients with coronary heart disease: a subgroup analysis of the Scandinavian Simvastatin Survival Study (4S). *Diabetes care*. 1997 Apr 1;20(4):614-20.
- Qu D, Liu J, Lau CW, Huang Y. IL-6 in diabetes and cardiovascular complications. *British journal of pharmacology*. 2014 Aug;171(15):3595-603.
- Radhakrishnan Y, Busby WH, Shen X, Maile LA, Clemmons DR. Insulin-like growth factor-I-stimulated insulin receptor substrate-1 negatively regulates Src homology 2 domain-containing protein-tyrosine phosphatase substrate-1 function in vascular smooth muscle cells. *Journal of Biological Chemistry*. 2010 May 21;285(21):15682-95.
- Rakugi H, Wang DS, Dzau VJ, Pratt RE. Potential importance of tissue angiotensin-converting enzyme inhibition in preventing neointima formation. *Circulation*. 1994 Jul;90(1):449-55.
- Ramji DP, Davies TS. Cytokines in atherosclerosis: Key players in all stages of disease and promising therapeutic targets. *Cytokine & growth factor reviews*. 2015 Dec 1;26(6):673-85.
- Ramos-Casals M, Brito-Zeron P, Siso-Almirall A, Bosch X. PRACTICE POINTER: Primary Sjögren syndrome. *BMJ: British Medical Journal*. 2012 Sep 1;345(7872):36-40.
- Ravi S, Chacko B, Sawada H, Kramer PA, Johnson MS, Benavides GA, O'Donnell V, Marques MB, Darley-Usmar VM. Metabolic plasticity in resting and thrombin activated platelets. *PloS one*. 2015 Apr 13;10(4):e0123597.
- Ravi V, Jain A, Taneja A, Chatterjee K, Sundaresan NR. Isolation and culture of neonatal murine primary Cardiomyocytes. *Current Protocols*. 2021 Jul;1(7):e196.
- Ray PD, Huang BW, Tsuji Y. Reactive oxygen species (ROS) homeostasis and redox regulation in cellular signaling. *Cellular signalling*. 2012 May 1;24(5):981-90.
- Razali NM, Wah YB. Power comparisons of shapiro-wilk, kolmogorov-smirnov, lilliefors and anderson-darling tests. *Journal of statistical modeling and analytics*. 2011 Jan 1;2(1):21-33.
- Reaven G. Insulin resistance and coronary heart disease in nondiabetic individuals. *Arteriosclerosis, thrombosis, and vascular biology*. 2012 Aug;32(8):1754-9.
- Reddy MA, Das S, Zhuo C, Jin W, Wang M, Lanting L, Natarajan R. Regulation of vascular smooth muscle cell dysfunction under diabetic conditions by miR-504. *Arteriosclerosis, thrombosis, and vascular biology*. 2016 May;36(5):864-73.
- Reeves RA, Lee A, Henry R, Zachara NE. Characterization of the specificity of O-GlcNAc reactive antibodies under conditions of starvation and stress. *Analytical biochemistry*. 2014 Jul 15;457:8-18.
- Reyna SM, Tantiwong P, Cersosimo E, DeFronzo RA, Sriwijitkamol A, Musi N. Short-term exercise training improves insulin sensitivity but does not inhibit inflammatory pathways in immune cells from insulin-resistant subjects. *Journal of diabetes research*. 2013 Oct;2013.

- Reznik E, Miller ML, Şenbabaoğlu Y, Riaz N, Sarungbam J, Tickoo SK, Al-Ahmadie HA, Lee W, Seshan VE, Hakimi AA, Sander C. Mitochondrial DNA copy number variation across human cancers. *elife*. 2016;5.
- Rhee SG. H₂O₂, a necessary evil for cell signaling. *Science*. 2006 Jun 30;312(5782):1882-3.
- Riches K, Alshanwani AR, Warburton P, O'Regan DJ, Ball SG, Wood IC, Turner NA, Porter KE. Elevated expression levels of miR-143/5 in saphenous vein smooth muscle cells from patients with Type 2 diabetes drive persistent changes in phenotype and function. *Journal of molecular and cellular cardiology*. 2014 Sep 1;74:240-50.
- Riches K, Morley ME, Turner NA, O'Regan DJ, Ball SG, Peers C, Porter KE. Chronic hypoxia inhibits MMP-2 activation and cellular invasion in human cardiac myofibroblasts. *Journal of molecular and cellular cardiology*. 2009 Sep 1;47(3):391-9.
- Riches K, Warburton P, O'Regan DJ, Turner NA, Porter KE. Type 2 diabetes impairs venous, but not arterial smooth muscle cell function: possible role of differential RhoA activity. *Cardiovascular Revascularization Medicine*. 2014 Apr 1;15(3):141-8.
- Riches-Suman K, Hussain A. Identifying and targeting the molecular signature of smooth muscle cells undergoing early vascular ageing. *Biochimica et Biophysica Acta (BBA)-Molecular Basis of Disease*. 2022 Jul 1;1868(7):166403.
- Riethmueller S, Ehlers JC, Lokau J, Düsterhöft S, Knittler K, Dombrowsky G, Grötzinger J, Rabe B, Rose-John S, Garbers C. Cleavage site localization differentially controls interleukin-6 receptor proteolysis by ADAM10 and ADAM17. *Scientific reports*. 2016 May 6;6(1):1-4.
- Rizzuto R, De Stefani D, Raffaello A, Mammucari C. Mitochondria as sensors and regulators of calcium signalling. *Nature reviews Molecular cell biology*. 2012 Sep;13(9):566-78.
- Robinson KA, Stewart CA, Pye QN, Nguyen X, Kenney L, Salzman S, Floyd RA, Hensley K. Redox-sensitive protein phosphatase activity regulates the phosphorylation state of p38 protein kinase in primary astrocyte culture. *Journal of neuroscience research*. 1999 Mar 15;55(6):724-32.
- Robinson KA, Weinstein ML, Lindenmayer GE, Buse MG. Effects of diabetes and hyperglycemia on the hexosamine synthesis pathway in rat muscle and liver. *Diabetes*. 1995 Dec 1;44(12):1438-46.
- Robinson R, Srinivasan M, Shanmugam A, Ward A, Ganapathy V, Bloom J, Sharma A, Sharma S. Interleukin-6 trans-signaling inhibition prevents oxidative stress in a mouse model of early diabetic retinopathy. *Redox Biology*. 2020 Jul 1;34:101574.
- Roden M, Shulman GI. The integrative biology of type 2 diabetes. *Nature*. 2019 Dec;576(7785):51-60.
- Rodrigues MS, Morelli KA, Jansen AM. Cytochrome c oxidase subunit 1 gene as a DNA barcode for discriminating *Trypanosoma cruzi* DTUs and closely related species. *Parasites & vectors*. 2017 Dec;10(1):1-8.
- Roger I, Milara J, Montero P, Cortijo J. The role of JAK/STAT molecular pathway in vascular remodeling associated with pulmonary hypertension. *International Journal of Molecular Sciences*. 2021 May 7;22(9):4980.

- Rojkind M, Novikoff PM, Greenwel P, Rubin J, Rojas-Valencia L, de Carvalho AC, Stockert R, Spray D, Hertzberg EL, Wolkoff AW. Characterization and functional studies on rat liver fat-storing cell line and freshly isolated hepatocyte coculture system. *The American journal of pathology*. 1995 Jun;146(6):1508.
- Romano M, Sironi M, Toniatti C, Polentarutti N, Fruscella P, Ghezzi P, Faggioni R, Luini W, Van Hinsbergh V, Sozzani S, Bussolino F. Role of IL-6 and its soluble receptor in induction of chemokines and leukocyte recruitment. *Immunity*. 1997 Mar 1;6(3):315-25.
- Rorsman P, Ashcroft FM. Pancreatic β -cell electrical activity and insulin secretion: of mice and men. *Physiological reviews*. 2018 Jan 1;98(1):117-214.
- Rose-John S. IL-6 trans-signaling via the soluble IL-6 receptor: importance for the pro-inflammatory activities of IL-6. *International journal of biological sciences*. 2012 Oct 24;8(9):1237-47.
- Rosen ED, Spiegelman. Adipocytes as regulators of energy balance and glucose homeostasis. *Nature*. 2006;444(7121):847-53.
- Rosen GM, Freeman BA. Detection of superoxide generated by endothelial cells. *Proceedings of the National Academy of Sciences*. 1984 Dec;81(23):7269-73.
- Ross R, Dagnone D, Jones PJ, Smith H, Paddags A, Hudson R, Janssen I. Reduction in obesity and related comorbid conditions after diet-induced weight loss or exercise-induced weight loss in men: a randomized, controlled trial. *Annals of internal medicine*. 2000 Jul 18;133(2):92-103.
- Roy J, Kazi M, Hedin U, Thyberg J. Phenotypic modulation of arterial smooth muscle cells is associated with prolonged activation of ERK1/2. *Differentiation*. 2001 Feb 1;67(1-2):50-8.
- Ruan HB, Singh JP, Li MD, Wu J, Yang X. Cracking the O-GlcNAc code in metabolism. *Trends in Endocrinology & Metabolism*. 2013 Jun 1;24(6):301-9.
- Rubin K, Hansson G, Rönstrand L, Claesson-Welsh L, Fellström B, Tingström A, Larsson E, Klareskog L, Heldin CH, Terracio L. Induction of B-type receptors for platelet-derived growth factor in vascular inflammation: possible implications for development of vascular proliferative lesions. *The Lancet*. 1988 Jun 18;331(8599):1353-6.
- Sabik JF, Blackstone EH. Coronary artery bypass graft patency and competitive flow. *Journal of the American College of Cardiology*. 2008 Jan 15;51(2):126-8.
- Saito Y, Geisen P, Uppal A, Hartnett ME. Inhibition of NAD (P) H oxidase reduces apoptosis and avascular retina in an animal model of retinopathy of prematurity. *Molecular vision*. 2007;13:840.
- Saitoh M, Nishitoh H, Fujii M, Takeda K, Tobiume K, Sawada Y, Kawabata M, Miyazono K, Ichijo H. Mammalian thioredoxin is a direct inhibitor of apoptosis signal-regulating kinase (ASK) 1. *The EMBO journal*. 1998 May 1;17(9):2596-606.
- Salabei JK, Hill BG. Mitochondrial fission induced by platelet-derived growth factor regulates vascular smooth muscle cell bioenergetics and cell proliferation. *Redox biology*. 2013 Jan 1;1(1):542-51.
- Satoh K, Matoba T, Suzuki J, O'Dell MR, Nigro P, Cui Z, Mohan A, Pan S, Li L, Jin ZG, Yan C. Cyclophilin A mediates vascular remodeling by promoting inflammation and vascular smooth muscle cell proliferation. *Circulation*. 2008 Jun 17;117(24):3088-98.

- Satoh K, Nigro P, Matoba T, O'dell MR, Cui Z, Shi X, Mohan A, Yan C, Abe JI, Illig KA, Berk BC. Cyclophilin A enhances vascular oxidative stress and the development of angiotensin II–induced aortic aneurysms. *Nature medicine*. 2009 Jun;15(6):649-56.
- Satoh K, Nigro P, Zeidan A, Soe NN, Jaffré F, Oikawa M, O'Dell MR, Cui Z, Menon P, Lu Y, Mohan A. Cyclophilin A Promotes Cardiac Hypertrophy in Apolipoprotein E–Deficient Mice. *Arteriosclerosis, thrombosis, and vascular biology*. 2011 May;31(5):1116-23.
- Satoh T. Molecular mechanisms for the regulation of insulin-stimulated glucose uptake by small guanosine triphosphatases in skeletal muscle and adipocytes. *International journal of molecular sciences*. 2014 Oct 16;15(10):18677-92.
- Savino R, Lahm A, Giorgio M, Cabibbo A, Tramontano A, Ciliberto G. Saturation mutagenesis of the human interleukin 6 receptor-binding site: implications for its three-dimensional structure. *Proceedings of the National Academy of Sciences*. 1993 May 1;90(9):4067-71.
- Sazanov LA, Hinchliffe P. Structure of the hydrophilic domain of respiratory complex I from *Thermus thermophilus*. *science*. 2006 Mar 10;311(5766):1430-6.
- Schäfer G. Biguanides. A review of history, pharmacodynamics and therapy. *Diabete & metabolisme*. 1983 May 1;9(2):148-63.
- Schaper F, Rose-John S. Interleukin-6: Biology, signaling and strategies of blockade. *Cytokine & growth factor reviews*. 2015 Oct 1;26(5):475-87.
- Schattauer SS, Bedini A, Summers F, Reilly-Treat A, Andrews MM, Land BB, Chavkin C. Reactive oxygen species (ROS) generation is stimulated by κ opioid receptor activation through phosphorylated c-Jun N-terminal kinase and inhibited by p38 mitogen-activated protein kinase (MAPK) activation. *J Biol Chem*. 2019 Nov 8;294(45):16884-16896.
- Scheller J, Chalaris A, Schmidt-Arras D, Rose-John S. The pro-and anti-inflammatory properties of the cytokine interleukin-6. *Biochimica et Biophysica Acta (BBA)-Molecular Cell Research*. 2011 May 1;1813(5):878-88.
- Scherer PE. The many secret lives of adipocytes: implications for diabetes. *Diabetologia*. 2019 Feb;62(2):223-32.
- Schmidt-Rohr K. Oxygen is the high-energy molecule powering complex multicellular life: Fundamental corrections to traditional bioenergetics. *ACS omega*. 2020 Jan 28;5(5):2221-33.
- Schoonbroodt S, Ferreira V, Best-Belpomme M, Boelaert JR, Legrand-Poels S, Korner M, Piette J. Crucial role of the amino-terminal tyrosine residue 42 and the carboxyl-terminal PEST domain of I κ B α in NF- κ B activation by an oxidative stress. *The Journal of immunology*. 2000 Apr 15;164(8):4292-300.
- Schuett H, Oestreich R, Waetzig GH, Annema W, Luchtefeld M, Hillmer A, Bavendiek U, von Felden J, Divchev D, Kempf T, Wollert KC. Transsignaling of interleukin-6 crucially contributes to atherosclerosis in mice. *Arteriosclerosis, thrombosis, and vascular biology*. 2012 Feb;32(2):281-90.
- Schumacher N, Meyer D, Mauermann A, von der Heyde J, Wolf J, Schwarz J, Knittler K, Murphy G, Michalek M, Garbers C, Bartsch JW. Shedding of endogenous interleukin-6 receptor (IL-6R) is governed by a disintegrin and metalloproteinase (ADAM) proteases while a full-length IL-6R isoform localizes to circulating microvesicles. *Journal of Biological Chemistry*. 2015 Oct 23;290(43):26059-71.

- Seasholtz TM, Majumdar M, Kaplan DD, Brown JH. Rho and Rho kinase mediate thrombin-stimulated vascular smooth muscle cell DNA synthesis and migration. *Circulation Research*. 1999 May 28;84(10):1186-93.
- Seger R, Ahn NG, Boulton TG, Yancopoulos GD, Panayotatos N, Radziejewska E, Ericsson L, Bratlien RL, Cobb MH, Krebs EG. Microtubule-associated protein 2 kinases, ERK1 and ERK2, undergo autophosphorylation on both tyrosine and threonine residues: implications for their mechanism of activation. *Proceedings of the National Academy of Sciences*. 1991 Jul 15;88(14):6142-6.
- Seif F, Khoshmirsafa M, Aazami H, Mohsenzadegan M, Sedighi G, Bahar M. The role of JAK-STAT signaling pathway and its regulators in the fate of T helper cells. *Cell communication and signaling*. 2017 Dec;15(1):1-3.
- Seino S, Shibasaki T, Minami K. Dynamics of insulin secretion and the clinical implications for obesity and diabetes. *The Journal of clinical investigation*. 2011 Jun 1;121(6):2118-25.
- Seki Y, Kai H, Shibata R, Nagata T, Yasukawa H, Yoshimura A, Imaizumi T. Role of the JAK/STAT pathway in rat carotid artery remodeling after vascular injury. *Circulation research*. 2000 Jul 7;87(1):12-8.
- Selvan N, Williamson R, Mariappa D, Campbell DG, Gourlay R, Ferenbach AT, Aristotelous T, Hopkins-Navratilova I, Trost M, van Aalten DM. A mutant O-GlcNAcase enriches *Drosophila* developmental regulators. *Nature chemical biology*. 2017 Aug;13(8):882-7.
- Sena CM, Leandro A, Azul L, Seça R, Perry G. Vascular oxidative stress: impact and therapeutic approaches. *Frontiers in physiology*. 2018 Dec 4;9:1668.
- Senyilmaz D, Teleman AA. Chicken or the egg: Warburg effect and mitochondrial dysfunction. *F1000prime reports*. 2015;7.
- Seo AY, Joseph AM, Dutta D, Hwang JC, Aris JP, Leeuwenburgh C. New insights into the role of mitochondria in aging: mitochondrial dynamics and more. *Journal of cell science*. 2010 Aug 1;123(15):2533-42.
- Sesti G, Federici M, Hribal ML, Lauro D, Sbraccia P, Lauro R. Defects of the insulin receptor substrate (IRS) system in human metabolic disorders. *The FASEB Journal*. 2001 Oct;15(12):2099-111.
- Sewell WH, Sewell KV. Technique for the coronary snake graft operation. *The Annals of Thoracic Surgery*. 1976 Jul 1;22(1):58-65.
- Shapiro PS, Evans JN, Davis RJ, Posada JA. The Seven-transmembrane-spanning Receptors for Endothelin and Thrombin Cause Proliferation of Airway Smooth Muscle Cells and Activation of the Extracellular Regulated Kinase and c-Jun NH2-terminal Kinase Groups of Mitogen-activated Protein Kinases (*). *Journal of Biological Chemistry*. 1996 Mar 8;271(10):5750-4.
- Shekar PS. On-pump and off-pump coronary artery bypass grafting. *Circulation*. 2006 Jan 31;113(4):e51-2.
- Shen S, Wang F, Fernandez A, Hu W. Role of platelet-derived growth factor in type II diabetes mellitus and its complications. *Diabetes and Vascular Disease Research*. 2020 Aug;17(4):1479164120942119.

- Shibata R, Kai H, Seki Y, Kato S, Wada Y, Hanakawa Y, Hashimoto K, Yoshimura A, Imaizumi T. Inhibition of STAT3 prevents neointima formation by inhibiting proliferation and promoting apoptosis of neointimal smooth muscle cells. *Human gene therapy*. 2003 May 1;14(7):601-10.
- Shimokawa H. Reactive oxygen species promote vascular smooth muscle cell proliferation. *Circulation research*. 2013 Oct 12;113(9):1040-2.
- Shin J, Watanabe S, Hoelper S, Krüger M, Kostin S, Pöling J, Kubin T, Braun T. BRAF activates PAX3 to control muscle precursor cell migration during forelimb muscle development. *Elife*. 2016;5.
- Shukla N, Jeremy JY. Pathophysiology of saphenous vein graft failure: a brief overview of interventions. *Current opinion in pharmacology*. 2012 Apr 1;12(2):114-20.
- Sies H, Jones DP. Reactive oxygen species (ROS) as pleiotropic physiological signalling agents. *Nature reviews Molecular cell biology*. 2020 Jul;21(7):363-83.
- Simmons CA, Nikolovski J, Thornton AJ, Matlis S, Mooney DJ. Mechanical stimulation and mitogen-activated protein kinase signaling independently regulate osteogenic differentiation and mineralization by calcifying vascular cells. *Journal of biomechanics*. 2004 Oct 1;37(10):1531-41.
- Simon AR, Rai U, Fanburg BL, Cochran BH. Activation of the JAK-STAT pathway by reactive oxygen species. *American Journal of Physiology-Cell Physiology*. 1998 Dec 1;275(6):C1640-52.
- Simon J, Webb TE, King BF, Burnstock G, Barnard EA. Characterisation of a recombinant P2Y purinoceptor. *European Journal of Pharmacology: Molecular Pharmacology*. 1995 Nov 30;291(3):281-9.
- Slawson C, Hart GW. O-GlcNAc signalling: implications for cancer cell biology. *Nature Reviews Cancer*. 2011 Sep;11(9):678-84.
- Sodi VL, Khaku S, Krutilina R, Schwab LP, Vocadlo DJ, Seagroves TN, Reginato MJ. mTOR/MYC Axis Regulates O-GlcNAc Transferase Expression and O-GlcNAcylation in Breast Cancer- MYC Regulates OGT Expression in Cancer Cells. *Molecular Cancer Research*. 2015 May 1;13(5):923-33.
- Soesanto Y, Luo B, Parker G, Jones D, Cooksey RC, McClain DA. Pleiotropic and age-dependent effects of decreased protein modification by O-linked N-acetylglucosamine on pancreatic β -cell function and vascularization. *Journal of Biological Chemistry*. 2011 Jul 22;286(29):26118-26.
- Somers W, Stahl M, Sehra JS. 1.9 Å crystal structure of interleukin 6: implications for a novel mode of receptor dimerization and signaling. *The EMBO journal*. 1997 Mar 1;16(5):989-97.
- Son Y, Cheong YK, Kim NH, Chung HT, Kang DG, Pae HO. Mitogen-activated protein kinases and reactive oxygen species: how can ROS activate MAPK pathways?. *Journal of signal transduction*. 2011;2011.
- Song B, Jin H, Yu X, Zhang Z, Yu H, Ye J, Xu Y, Zhou T, Oudit GY, Ye JY, Chen C. Angiotensin-converting enzyme 2 attenuates oxidative stress and VSMC proliferation via the

- JAK2/STAT3/SOCS3 and profilin-1/MAPK signaling pathways. *Regulatory peptides*. 2013 Aug 10;185:44-51.
- Southerland KW, Frazier SB, Bowles DE, Milano CA, Kontos CD. Gene therapy for the prevention of vein graft disease. *Translational Research*. 2013 Apr 1;161(4):321-38.
- Souza DS, Johansson B, Bojö L, Karlsson R, Geijer H, Filbey D, Bodin L, Arbeus M, Dashwood MR. Harvesting the saphenous vein with surrounding tissue for CABG provides long-term graft patency comparable to the left internal thoracic artery: results of a randomized longitudinal trial. *The Journal of thoracic and cardiovascular surgery*. 2006 Aug 1;132(2):373-8.
- Sowton AP, Millington-Burgess SL, Murray AJ, Harper MT. Rapid kinetics of changes in oxygen consumption rate in thrombin-stimulated platelets measured by high-resolution respirometry. *Biochemical and biophysical research communications*. 2018 Sep 18;503(4):2721-7.
- Sprague AH, Khalil RA. Inflammatory cytokines in vascular dysfunction and vascular disease. *Biochemical pharmacology*. 2009 Sep 15;78(6):539-52.
- Staffers DA, Ferrer J, Clarke WL, Habener JF. Early-onset type-II diabetes mellitus (MODY4) linked to IPF1. *Nature genetics*. 1997 Oct 1;17(2):138-9.
- Sturmeijer RG, Leese HJ. Energy metabolism in pig oocytes and early embryos. *Reproduction-Cambridge*. 2003 Aug 1;126(2):197-204.
- Sukovich DA, Kauser K, Shirley FD, DelVecchio V, Halks-Miller M, Rubanyi GM. Expression of interleukin-6 in atherosclerotic lesions of male ApoE-knockout mice: inhibition by 17 β -estradiol. *Arteriosclerosis, thrombosis, and vascular biology*. 1998 Sep;18(9):1498-505.
- Sun C, Benlekber S, Venkatakrisnan P, Wang Y, Hong S, Hosler J, Tajkhorshid E, Rubinstein JL, Gennis RB. Structure of the alternative complex III in a supercomplex with cytochrome oxidase. *Nature*. 2018 May;557(7703):123-6.
- Sundaresan M, Yu ZX, Ferrans VJ, Irani K, Finkel T. Requirement for generation of H₂O₂ for platelet-derived growth factor signal transduction. *Science*. 1995 Oct 13;270(5234):296-9.
- Suzuki T, Ishiwata S, Hasegawa K, Yamamoto K, Yamazaki T. Raised interleukin 6 concentrations as a predictor of postangioplasty restenosis. *Heart*. 2000 May 1;83(5):578-.
- Suzuki Y, Ruiz-Ortega M, Lorenzo O, Ruperez M, Esteban V, Egido J. Inflammation and angiotensin II. *The international journal of biochemistry & cell biology*. 2003 Jun 1;35(6):881-900.
- Swamy M, Pathak S, Grzes KM, Damerow S, Sinclair LV, van Aalten DM, Cantrell DA. Glucose and glutamine fuel protein O-GlcNAcylation to control T cell self-renewal and malignancy. *Nature immunology*. 2016 Jun;17(6):712-20.
- Szöcs K, Lassègue B, Sorescu D, Hilenski LL, Valppu L, Couse TL, Wilcox JN, Quinn MT, Lambeth JD, Griendling KK. Upregulation of Nox-based NAD (P) H oxidases in restenosis after carotid injury. *Arteriosclerosis, thrombosis, and vascular biology*. 2002 Jan 1;22(1):21-7.
- Taanman JW. The mitochondrial genome: structure, transcription, translation and replication. *Biochimica et Biophysica Acta (BBA)-Bioenergetics*. 1999 Feb 9;1410(2):103-23.
- Tait SW, Green DR. Mitochondria and cell signalling. *Journal of cell science*. 2012 Feb 15;125(4):807-15.

- Takagi H, Matsui M, Umemoto T. Lower graft patency after off-pump than on-pump coronary artery bypass grafting: an updated meta-analysis of randomized trials. *The Journal of Thoracic and Cardiovascular Surgery*. 2010 Sep 1;140(3):e45-7.
- Takeda K, Shimozono R, Noguchi T, Umeda T, Morimoto Y, Naguro I, Tobiume K, Saitoh M, Matsuzawa A, Ichijo H. Apoptosis signal-regulating kinase (ASK) 2 functions as a mitogen-activated protein kinase kinase kinase in a heteromeric complex with ASK1. *Journal of Biological Chemistry*. 2007 Mar 9;282(10):7522-31.
- Tammineni P, Anugula C, Mohammed F, Anjaneyulu M, Larner AC, Sepuri NB. The import of the transcription factor STAT3 into mitochondria depends on GRIM-19, a component of the electron transport chain. *Journal of Biological Chemistry*. 2013 Feb 1;288(7):4723-32.
- Tamura Y, Phan C, Tu L, Le Hiress M, Thuillet R, Jutant EM, Fadel E, Savale L, Huertas A, Humbert M, Guignabert C. Ectopic upregulation of membrane-bound IL6R drives vascular remodeling in pulmonary arterial hypertension. *The Journal of clinical investigation*. 2018 May 1;128(5):1956-70.
- Tanizawa S, Ueda M, van der Loos CM, van der Wal AC, Becker AE. Expression of platelet derived growth factor B chain and beta receptor in human coronary arteries after percutaneous transluminal coronary angioplasty: an immunohistochemical study. *Heart*. 1996 Jun 1;75(6):549-56.
- Taylor RP, Geisler TS, Chambers JH, McClain DA. Up-regulation of O-GlcNAc transferase with glucose deprivation in HepG2 cells is mediated by decreased hexosamine pathway flux. *Journal of Biological Chemistry*. 2009 Feb 6;284(6):3425-32.
- Teo CF, Wollaston-Hayden EE, Wells L. Hexosamine flux, the O-GlcNAc modification, and the development of insulin resistance in adipocytes. *Molecular and cellular endocrinology*. 2010 Apr 29;318(1-2):44-53.
- Thannickal VJ, Fanburg BL. Reactive oxygen species in cell signaling. *American Journal of Physiology-Lung Cellular and Molecular Physiology*. 2000 Dec 1;279(6):L1005-28.
- Thyagarajan B, Wang R, Barcelo H, Koh WP, Yuan JM. Mitochondrial Copy Number is Associated with Colorectal Cancer Risk Mitochondria and Colorectal Cancer. *Cancer epidemiology, biomarkers & prevention*. 2012 Sep 1;21(9):1574-81.
- Tian L, Huang CK, Ding F, Zhang R. Galectin-3 Mediates Thrombin-Induced Vascular Smooth Muscle Cell Migration. *Frontiers in Cardiovascular Medicine*. 2021;8.
- Tin A, Grams ME, Ashar FN, Lane JA, Rosenberg AZ, Grove ML, Boerwinkle E, Selvin E, Coresh J, Pankratz N, Arking DE. Association between mitochondrial DNA copy number in peripheral blood and incident CKD in the atherosclerosis risk in communities study. *Journal of the American Society of Nephrology: JASN*. 2016 Aug;27(8):2467.
- Titchenell PM, Lazar MA, Birnbaum MJ. Unraveling the regulation of hepatic metabolism by insulin. *Trends in Endocrinology & Metabolism*. 2017 Jul 1;28(7):497-505.
- Tobiume K, Matsuzawa A, Takahashi T, Nishitoh H, Morita KI, Takeda K, Minowa O, Miyazono K, Noda T, Ichijo H. ASK1 is required for sustained activations of JNK/p38 MAP kinases and apoptosis. *EMBO reports*. 2001 Mar 1;2(3):222-8.

- Tojo T, Ushio-Fukai M, Yamaoka-Tojo M, Ikeda S, Patrushev N, Alexander RW. Role of gp91phox (Nox2)-containing NAD (P) H oxidase in angiogenesis in response to hindlimb ischemia. *Circulation*. 2005 May 10;111(18):2347-55.
- Tonks NK. *Nat Rev Mol Cell Biol*, Protein tyrosine phosphatases: From genes, to function, to disease., 2006, 7, 833-846.
- Torres M, Forman HJ. Redox signaling and the MAP kinase pathways. *Biofactors*. 2003 Jan 1;17(1-4):287-96.
- Touyz RM, Schiffrin EL. Signal transduction mechanisms mediating the physiological and pathophysiological actions of angiotensin II in vascular smooth muscle cells. *Pharmacological reviews*. 2000 Dec 1;52(4):639-72.
- Touyz RM. Reactive oxygen species, vascular oxidative stress, and redox signaling in hypertension: what is the clinical significance?. *Hypertension*. 2004 Sep 1;44(3):248-52.
- Trachootham D, Alexandre J, Huang P. Targeting cancer cells by ROS-mediated mechanisms: a radical therapeutic approach?. *Nature reviews Drug discovery*. 2009 Jul;8(7):579-91.
- Trinidad JC, Barkan DT, Gullledge BF, Thalhammer A, Sali A, Schoepfer R, Burlingame AL. Global identification and characterization of both O-GlcNAcylation and phosphorylation at the murine synapse. *Molecular & Cellular Proteomics*. 2012 Aug 1;11(8):215-29.
- Triplitt, CL., Reasner, CA. Diabetes Mellitus. In: Joseph T. Dipro, *Pharmacotherapy-A pathophysiological approach*, 8th ed. MC Graw Hill; 2011:p. 1255-302.
- Trumpower BL. The protonmotive Q cycle: energy transduction by coupling of proton translocation to electron transfer by the cytochrome bc1 complex. *The Journal of biological chemistry (Print)*. 1990;265(20):11409-12.
- Truong TH, Carroll KS. Redox regulation of protein kinases. *Critical reviews in biochemistry and molecular biology*. 2013 Jul 1;48(4):332-56.
- Truong TH, Ung PM, Palde PB, Paulsen CE, Schlessinger A, Carroll KS. Molecular basis for redox activation of epidermal growth factor receptor kinase. *Cell chemical biology*. 2016 Jul 21;23(7):837-48.
- Truzzi DR, Coelho FR, Paviani V, Alves SV, Netto LE, Augusto O. The bicarbonate/carbon dioxide pair increases hydrogen peroxide-mediated hyperoxidation of human peroxiredoxin 1. *Journal of Biological Chemistry*. 2019 Sep 20;294(38):14055-67.
- Turner NA, Ho S, Warburton P, O'Regan DJ, Porter KE. Smooth muscle cells cultured from human saphenous vein exhibit increased proliferation, invasion, and mitogen-activated protein kinase activation in vitro compared with paired internal mammary artery cells. *Journal of Vascular Surgery*. 2007 May 1;45(5):1022-8.
- Ueda M, Becker AE, Kasayuki N, Kojima A, Morita Y, Tanaka S. In situ detection of platelet-derived growth factor-A and-B chain mRNA in human coronary arteries after percutaneous transluminal coronary angioplasty. *The American journal of pathology*. 1996 Sep;149(3):831.

- Umapathi P, Mesubi OO, Banerjee PS, Abrol N, Wang Q, Luczak ED, Wu Y, Granger JM, Wei AC, Reyes Gaido OE, Florea L. Excessive O-GlcNAcylation causes heart failure and sudden death. *Circulation*. 2021 Apr 27;143(17):1687-703.
- Unger T, Chung O, Csikos T, Culman J, Gallinat S, Gohlke P, Höhle S, Meffert S, Stoll M, Stroth U, Zhu YZ. Angiotensin receptors. *Journal of hypertension. Supplement: official journal of the International Society of Hypertension*. 1996 Dec 1;14(5):S95-103.
- Ushio-Fukai M, Tang Y, Fukai T, Dikalov SI, Ma Y, Fujimoto M, Quinn MT, Pagano PJ, Johnson C, Alexander RW. Novel role of gp91phox-containing NAD (P) H oxidase in vascular endothelial growth factor-induced signaling and angiogenesis.
- Uzui H, Lee JD, Shimizu H, Tsutani H, Ueda T. The role of protein-tyrosine phosphorylation and gelatinase production in the migration and proliferation of smooth muscle cells. *Atherosclerosis*. 2000 Mar 1;149(1):51-9.
- Valera S, Hussy N, Evans RI, Adami N, North A, Surprenant A, Buell G: A new class of ligand-gated ion channel defined by P₂U₁ receptor for extracellular ATP. *Nature*. 1994;371:516.
- Valgeirsdóttir S, Paukku K, Silvennoinen O, Heldin CH, Claesson-Welsh L. Activation of Stat5 by platelet-derived growth factor (PDGF) is dependent on phosphorylation sites in PDGF β -receptor juxtamembrane and kinase insert domains. *Oncogene*. 1998 Jan;16(4):505-15.
- Van Schaftingen E, Gerin I. The glucose-6-phosphatase system. *Biochemical Journal*. 2002 Mar 15;362(3):513-32.
- Vargas E, Carrillo Sepulveda MA. Biochemistry, Insulin Metabolic Effects. [Updated 2019 Apr 21]. In: StatPearls [Internet]. Treasure Island (FL): StatPearls Publishing; 2019 Jan-. Available from: <https://www.ncbi.nlm.nih.gov/books/NBK525983/>
- Vasconcelos-dos-Santos A, de Queiroz RM, da Costa Rodrigues B, Todeschini AR, Dias WB. Hyperglycemia and aberrant O-GlcNAcylation: contributions to tumor progression. *Journal of Bioenergetics and Biomembranes*. 2018 Jun;50(3):175-87.
- Veith FJ, Gupta SK, Ascer E, White-Flores S, Samson RH, Scher LA, Towne JB, Bernhard VM, Bonier P, Flinn WR, Astelford P. Six-year prospective multicenter randomized comparison of autologous saphenous vein and expanded polytetrafluoroethylene grafts in infrainguinal arterial reconstructions. *Journal of vascular surgery*. 1986 Jan 1;3(1):104-14.
- Venkatabalasubramanian S. The Complex Interplay Between JAK-STAT Pathway and ROS in Regulating Stem Cells During Inflammation and Cancer. In *Handbook of Oxidative Stress in Cancer: Therapeutic Aspects* 2021 Dec 14 (pp. 1-12). Singapore: Springer Singapore.
- Venkatasamy VV, Pericherla S, Manthuruthil S, Mishra S, Hanno R. Effect of physical activity on insulin resistance, inflammation and oxidative stress in diabetes mellitus. *Journal of Clinical & Diagnostic Research*. 2013 Aug 1;7(8).
- Vergès B. Pathophysiology of diabetic dyslipidaemia: where are we?. *Diabetologia*. 2015 May;58(5):886-99.
- Verma S, Lovren F, Pan Y, Yanagawa B, Deb S, Karkhanis R, Quan A, Teoh H, Feder-Elituv R, Moussa F, Souza DS. Pedicled no-touch saphenous vein graft harvest limits vascular smooth muscle cell activation: the PATENT saphenous vein graft study. *European Journal of Cardio-Thoracic Surgery*. 2014 Apr 1;45(4):717-25.

- Verstovsek S, Mesa RA, Gotlib J, Levy RS, Gupta V, DiPersio JF, Catalano JV, Deininger M, Miller C, Silver RT, Talpaz M. A double-blind, placebo-controlled trial of ruxolitinib for myelofibrosis. *New England Journal of Medicine*. 2012 Mar 1;366(9):799-807.
- Villarino AV, Kanno Y, O'Shea JJ. Mechanisms and consequences of Jak–STAT signaling in the immune system. *Nature immunology*. 2017 Apr;18(4):374-84.
- Vogel SM, Gao X, Mehta D, Ye RD, John TA, Andrade-Gordon PA, Tirupathi C, Malik AB. Abrogation of thrombin-induced increase in pulmonary microvascular permeability in PAR-1 knockout mice. *Physiological genomics*. 2000 Dec 18;4(2):137-45.
- Vosseller K, Wells L, Lane MD, Hart GW. Elevated nucleocytoplasmic glycosylation by O-GlcNAc results in insulin resistance associated with defects in Akt activation in 3T3-L1 adipocytes. *Proceedings of the National Academy of Sciences*. 2002 Apr 16;99(8):5313-8.
- Vu TK, Hung DT, Wheaton VI, Coughlin SR. Molecular cloning of a functional thrombin receptor reveals a novel proteolytic mechanism of receptor activation. *Cell*. 1991 Mar 22;64(6):1057-68.
- Wachowicz B, Olas B, Zbikowska HM, Buczyński A. Generation of reactive oxygen species in blood platelets. *Platelets*. 2002 Jan 1;13(3):175-82.
- Walter LA, Lin YH, Halbrook CJ, Chuh KN, He L, Pedowitz NJ, Batt AR, Brennan CK, Stiles BL, Lyssiotis CA, Pratt MR. Inhibiting the hexosamine biosynthetic pathway lowers O-GlcNAcylation levels and sensitizes cancer to environmental stress. *Biochemistry*. 2019 Oct 18;59(34):3169-79.
- Wang C, Youle RJ. The role of mitochondria in apoptosis. *Annual review of genetics*. 2009;43:95.
- Wang CC, Gurevich I, Draznin B. Insulin affects vascular smooth muscle cell phenotype and migration via distinct signaling pathways. *Diabetes*. 2003 Oct 1;52(10):2562-9.
- Wang D, Uhrin P, Mocan A, Waltenberger B, Breuss JM, Tewari D, Mihaly-Bison J, Huminiecki Ł, Starzyński RR, Tzvetkov NT, Horbańczuk J. Vascular smooth muscle cell proliferation as a therapeutic target. Part 1: molecular targets and pathways. *Biotechnology Advances*. 2018 Nov 1;36(6):1586-607.
- Wang JH, Redmond HP, Watson RW, Bouchier-Hayes D. Induction of human endothelial cell apoptosis requires both heat shock and oxidative stress responses. *American Journal of Physiology-Cell Physiology*. 1997 May 1;272(5):C1543-51.
- Wang QY, Guan QH, Chen FQ. The changes of platelet-derived growth factor-BB (PDGF-BB) in T2DM and its clinical significance for early diagnosis of diabetic nephropathy. *Diabetes research and clinical practice*. 2009 Aug 1;85(2):166-70.
- Wang Y, Fuller GM. Phosphorylation and internalization of gp130 occur after IL-6 activation of Jak2 kinase in hepatocytes. *Molecular biology of the cell*. 1994 Jul;5(7):819-28.
- Wang Y, Yu X, Song H, Feng D, Jiang Y, Wu S, Geng J. The STAT-ROS cycle extends IFN induced cancer cell apoptosis. *International journal of oncology*. 2018 Jan 1;52(1):305-13.
- Wang Z, Castresana MR, Newman WH. Reactive oxygen species-sensitive p38 MAPK controls thrombin-induced migration of vascular smooth muscle cells. *Journal of molecular and cellular cardiology*. 2004 Jan 1;36(1):49-56.

- Wani WY, Chatham JC, Darley-Usmar V, McMahon LL, Zhang J. O-GlcNAcylation and neurodegeneration. *Brain research bulletin*. 2017 Jul 1;133:80-7.
- Way KL, Hackett DA, Baker MK, Johnson NA. The effect of regular exercise on insulin sensitivity in type 2 diabetes mellitus: a systematic review and meta-analysis. *Diabetes & metabolism journal*. 2016 Aug 2;40(4):253-71.
- Wegrzyn J, Potla R, Chwae YJ, Sepuri NB, Zhang Q, Koeck T, Derecka M, Szczepanek K, Szelag M, Gornicka A, Moh A. Function of mitochondrial Stat3 in cellular respiration. *Science*. 2009 Feb 6;323(5915):793-7.
- Wei W, Keogh MJ, Wilson I, Coxhead J, Ryan S, Rollinson S, Griffin H, Kurzawa-Akanbi M, Santibanez-Koref M, Talbot K, Turner MR. Mitochondrial DNA point mutations and relative copy number in 1363 disease and control human brains. *Acta neuropathologica communications*. 2017 Dec;5(1):1-8.
- Weigert C, Klopfer K, Kausch C, Brodbeck K, Stumvoll M, Häring HU, Schleicher ED. Palmitate-induced activation of the hexosamine pathway in human myotubes: increased expression of glutamine: fructose-6-phosphate aminotransferase. *Diabetes*. 2003 Mar 1;52(3):650-6.
- Weiss D, Kools JJ, Taylor WR. Angiotensin II-induced hypertension accelerates the development of atherosclerosis in apoE-deficient mice. *Circulation*. 2001;103:448-54.
- Weissberg PL, Bennett MR. Atherosclerosis--an inflammatory disease. *The New England journal of medicine*. 1999 Jun 17;340(24):1928-9.
- Wellen KE, Lu C, Mancuso A, Lemons JM, Ryczko M, Dennis JW, Rabinowitz JD, Collier HA, Thompson CB. The hexosamine biosynthetic pathway couples growth factor-induced glutamine uptake to glucose metabolism. *Genes & development*. 2010 Dec 15;24(24):2784-99.
- Wells L, Vosseller K, Hart GW. Glycosylation of nucleocytoplasmic proteins: signal transduction and O-GlcNAc. *Science*. 2001 Mar 23;291(5512):2376-8.
- Wells PG, McCallum GP, Chen CS, Henderson JT, Lee CJ, Perstin J, Preston TJ, Wiley MJ, Wong AW. Oxidative stress in developmental origins of disease: teratogenesis, neurodevelopmental deficits, and cancer. *Toxicological sciences*. 2009 Mar 1;108(1):4-18.
- Wentworth CC, Alam A, Jones RM, Nusrat A, Neish AS. Enteric commensal bacteria induce ERK pathway signaling via formyl peptide receptor (FPR)-dependent redox modulation of Dual specific phosphatase 3 (DUSP3). *J Biol Chem*. 2011;286(44):38448-55.
- Werdich XQ, Penn JS. Specific involvement of SRC family kinase activation in the pathogenesis of retinal neovascularization. *Investigative ophthalmology & visual science*. 2006 Nov 1;47(11):5047-56.
- Whelan SA, Dias WB, Thiruneelakantapillai L, Lane MD, Hart GW. Regulation of insulin receptor substrate 1 (IRS-1)/AKT kinase-mediated insulin signaling by O-linked β -N-acetylglucosamine in 3T3-L1 adipocytes. *Journal of biological chemistry*. 2010 Feb 19;285(8):5204-11.
- Whitehead NP, Yeung EW, Froehner SC, Allen DG. Skeletal muscle NADPH oxidase is increased and triggers stretch-induced damage in the mdx mouse. *PloS one*. 2010 Dec 20;5(12):e15354.
- Wilcox G. Insulin and insulin resistance. *Clinical biochemist reviews*. 2005 May;26(2):19.

- Wild S, Roglic G, Green A, Sicree R, King H. Global prevalence of diabetes: estimates for the year 2000 and projections for 2030. *Diabetes care*. 2004 May 1;27(5):1047-53.
- Wilding J. The importance of weight management in type 2 diabetes mellitus. *International journal of clinical practice*. 2014 Jun;68(6):682-91.
- Witztum JL, Mahoney EM, Branks MJ, Fisher M, Elam R, Steinberg D. Nonenzymatic glycosylation of low-density lipoprotein alters its biologic activity. *Diabetes*. 1982 Apr 1;31(4):283-91.
- Wong HS, Benoit B, Brand MD. Mitochondrial and cytosolic sources of hydrogen peroxide in resting C2C12 myoblasts. *Free Radical Biology and Medicine*. 2019 Jan 1;130:140-50.
- Wong ND, Zhao Y, Patel R, Patao C, Malik S, Bertoni AG, Correa A, Folsom AR, Kachroo S, Mukherjee J, Taylor H. Cardiovascular risk factor targets and cardiovascular disease event risk in diabetes: a pooling project of the Atherosclerosis Risk in Communities Study, Multi-Ethnic Study of Atherosclerosis, and Jackson Heart Study. *Diabetes care*. 2016 May 1;39(5):668-76.
- Woodfin A, Voisin MB, Nourshargh S. PECAM-1: a multi-functional molecule in inflammation and vascular biology. *Arteriosclerosis, thrombosis, and vascular biology*. 2007 Dec 1;27(12):2514-23.
- World Health Organization (2016). Diabetes Mellitus. Fact Sheet. <https://www.who.int/news-room/fact-sheets/detail/diabetes>. Accessed 5th June, 2020.
- World Health Organization (2016). Diabetes Mellitus. Fact Sheet. <https://www.who.int/news-room/fact-sheets/detail/diabetes>. Accessed 5th June, 2020.
- Wu H, Ballantyne CM. Skeletal muscle inflammation and insulin resistance in obesity. *The Journal of clinical investigation*. 2017 Jan 3;127(1):43-54.
- Wu N, Zheng B, Shaywitz A, Dagon Y, Tower C, Bellinger G, Shen CH, Wen J, Asara J, McGraw TE, Kahn BB. AMPK-dependent degradation of TXNIP upon energy stress leads to enhanced glucose uptake via GLUT1. *Molecular cell*. 2013 Mar 28;49(6):1167-75.
- Wu PK, Park JI. MEK1/2 inhibitors: molecular activity and resistance mechanisms. In *Seminars in oncology* 2015 Dec 1 (Vol. 42, No. 6, pp. 849-862). WB Saunders.
- Wu WY, Kim H, Zhang CL, Meng XL, Wu ZS. Loss of suppressors of cytokine signaling 3 promotes aggressiveness in hepatocellular carcinoma. *Journal of Investigative Surgery*. 2014 Aug 1;27(4):197-204.
- Xia N, Li H. The role of perivascular adipose tissue in obesity-induced vascular dysfunction. *British journal of pharmacology*. 2017 Oct;174(20):3425-42.
- Xiang S, Dong NG, Liu JP, Wang Y, Shi JW, Wei ZJ, Hu XJ, Gong L. Inhibitory effects of suppressor of cytokine signaling 3 on inflammatory cytokine expression and migration and proliferation of IL-6/IFN- γ -induced vascular smooth muscle cells. *Journal of Huazhong University of Science and Technology [Medical Sciences]*. 2013 Oct;33(5):615-22.
- Xiang S, Liu J, Dong N, Shi J, Xiao Y, Wang Y, Hu X, Gong L, Wang W. Suppressor of cytokine signaling 3 is a negative regulator for neointimal hyperplasia of vein graft stenosis. *Journal of Vascular Research*. 2014;51(2):132-43.

- Xing D, Feng W, Not LG, Miller AP, Zhang Y, Chen YF, Majid-Hassan E, Chatham JC, Oparil S. Increased protein O-GlcNAc modification inhibits inflammatory and neointimal responses to acute endoluminal arterial injury. *American Journal of Physiology-Heart and Circulatory Physiology*. 2008 Jul;295(1):H335-42.
- Yaghini FA, Song CY, Lavrentyev EN, Ghafoor HU, Fang XR, Estes AM, Campbell WB, Malik KU. Angiotensin II-induced vascular smooth muscle cell migration and growth are mediated by cytochrome P450 1B1-dependent superoxide generation. *Hypertension*. 2010 Jun 1;55(6):1461-7.
- Yahata Y, Shirakata Y, Tokumaru S, Yamasaki K, Sayama K, Hanakawa Y, Detmar M, Hashimoto K. Nuclear translocation of phosphorylated STAT3 is essential for vascular endothelial growth factor-induced human dermal microvascular endothelial cell migration and tube formation. *Journal of Biological Chemistry*. 2003 Oct 10;278(41):40026-31.
- Yamamoto H, Crow M, Cheng L, Lakatta E, Kinsella J. PDGF receptor-to-nucleus signaling of p91 (STAT1 α) transcription factor in rat smooth muscle cells. *Experimental cell research*. 1996 Jan 10;222(1):125-30.
- Yamamoto WR, Bone RN, Sohn P, Syed F, Reissaus CA, Mosley AL, Wijeratne AB, True JD, Tong X, Kono T, Evans-Molina C. Endoplasmic reticulum stress alters ryanodine receptor function in the murine pancreatic β cell. *Journal of Biological Chemistry*. 2019 Jan 1;294(1):168-81.
- Yan I, Schwarz J, Lücke K, Schumacher N, Schumacher V, Schmidt S, Rabe B, Saftig P, Donners M, Rose-John S, Mittrücker HW. ADAM17 controls IL-6 signaling by cleavage of the murine IL-6R α from the cell surface of leukocytes during inflammatory responses. *Journal of leukocyte biology*. 2016 May;99(5):749-60.
- Yan JF, Huang WJ, Zhao JF, Fu HY, Zhang GY, Huang XJ, Lv BD. The platelet-derived growth factor receptor/STAT3 signaling pathway regulates the phenotypic transition of corpus cavernosum smooth muscle in rats. *PLoS One*. 2017 Feb 28;12(2):e0172191.
- Yan SF, Tritto I, Pinsky D, Liao H, Huang J, Fuller G, Brett J, May L, Stern D. Induction of interleukin 6 (IL-6) by hypoxia in vascular cells: central role of the binding site for nuclear factor-IL-6. *Journal of Biological Chemistry*. 1995 May 12;270(19):11463-71.
- Yanagawa B, Algarni KD, Singh SK, Deb S, Vincent J, Elituv R, Desai ND, Rajamani K, McManus BM, Liu PP, Cohen EA. Clinical, biochemical, and genetic predictors of coronary artery bypass graft failure. *The Journal of thoracic and cardiovascular surgery*. 2014 Aug 1;148(2):515-20.
- Yang W, Zheng Y, Xia Y, Ji H, Chen X, Guo F, Lyssiotis CA, Aldape K, Cantley LC, Lu Z. ERK1/2-dependent phosphorylation and nuclear translocation of PKM2 promotes the Warburg effect. *Nature cell biology*. 2012 Dec;14(12):1295-304.
- Yang X, Ongusaha PP, Miles PD, Havstad JC, Zhang F, So WV, Kudlow JE, Michell RH, Olefsky JM, Field SJ, Evans RM. Phosphoinositide signalling links O-GlcNAc transferase to insulin resistance. *Nature*. 2008 Feb;451(7181):964-9.
- Yang X, Qian K. Protein O-GlcNAcylation: emerging mechanisms and functions. *Nature reviews Molecular cell biology*. 2017 Jul;18(7):452-65.
- Yang Y, Zhang G, Yang T, Gan J, Xu L, Yang H. A flow-cytometry-based protocol for detection of mitochondrial ROS production under hypoxia. *STAR protocols*. 2021 Jun 18;2(2):100466.

- Yang YR, Song S, Hwang H, Jung JH, Kim SJ, Yoon S, Hur JH, Park JI, Lee C, Nam D, Seo YK. Memory and synaptic plasticity are impaired by dysregulated hippocampal O-GlcNAcylation. *Scientific reports*. 2017 Apr 3;7(1):1-9.
- Yankovskaya V, Horsefield R, Tornroth S, Luna-Chavez C, Miyoshi H, Léger C, Byrne B, Cecchini G, Iwata S. Architecture of succinate dehydrogenase and reactive oxygen species generation. *Science*. 2003 Jan 31;299(5607):700-4.
- Yawata H, Yasukawa K, Natsuka S, Murakami M, Yamasaki K, Hibi M, Taga T, Kishimoto T. Structure-function analysis of human IL-6 receptor: dissociation of amino acid residues required for IL-6-binding and for IL-6 signal transduction through gp130. *The EMBO journal*. 1993 Apr;12(4):1705-12.
- Yetkin-Arik B, Vogels I, Nowak-Sliwinska P, Weiss A, Houtkooper RH, Van Noorden CJ, Klaassen I, Schlingemann RO. The role of glycolysis and mitochondrial respiration in the formation and functioning of endothelial tip cells during angiogenesis. *Scientific reports*. 2019 Aug 30;9(1):1-4.
- Yi W, Clark PM, Mason DE, Keenan MC, Hill C, Goddard III WA, Peters EC, Driggers EM, Hsieh-Wilson LC. Phosphofructokinase 1 glycosylation regulates cell growth and metabolism. *Science*. 2012 Aug 24;337(6097):975-80.
- Yki-Järvinen H, Virkamäki A, Daniels MC, McClain D, Gottschalk WK. Insulin and glucosamine infusions increase O-linked N-acetyl-glucosamine in skeletal muscle proteins in vivo. *Metabolism*. 1998 Apr 1;47(4):449-55.
- Yoshizumi M, Kyotani Y, Zhao J, Nakahira K. Targeting the mitogen-activated protein kinase-mediated vascular smooth muscle cell remodeling by angiotensin II. *Annals of Translational Medicine*. 2020 Mar;8(5).
- Yuzwa SA, Shan X, Macauley MS, Clark T, Skorobogatko Y, Vosseller K, Vocadlo DJ. Increasing O-GlcNAc slows neurodegeneration and stabilizes tau against aggregation. *Nature chemical biology*. 2012 Apr;8(4):393-9.
- Zachara NE, Hart GW. Cell signaling, the essential role of O-GlcNAc!. *Biochimica et Biophysica Acta (BBA)-Molecular and Cell Biology of Lipids*. 2006 May 1;1761(5-6):599-617.
- Zachara NE, Molina H, Wong KY, Pandey A, Hart GW. The dynamic stress-induced “O-GlcNAcome” highlights functions for O-GlcNAc in regulating DNA damage/repair and other cellular pathways. *Amino acids*. 2011 Mar;40(3):793-808.
- Zachara NE. Detecting the “O-GlcNAcome”; detection, purification, and analysis of O-GlcNAc modified proteins. *Glycomics*. 2009:250-79.
- Zain MA, Jamil RT, Siddiqui WJ. Neointimal Hyperplasia. 2022 Oct 25. In: *StatPearls* [Internet]. Treasure Island (FL): StatPearls Publishing; 2022 Jan-. PMID: 29763068.
- Zeadin MG, Petlura CI, Werstuck GH. Molecular mechanisms linking diabetes to the accelerated development of atherosclerosis. *Canadian journal of diabetes*. 2013 Oct 1;37(5):345-50.
- Zegeye MM, Lindkvist M, Fälker K, Kumawat AK, Paramel G, Grenegård M, Sirsjö A, Ljungberg LU. Activation of the JAK/STAT3 and PI3K/AKT pathways are crucial for IL-6 trans-signaling-mediated pro-inflammatory response in human vascular endothelial cells. *Cell Communication and Signaling*. 2018 Dec;16(1):1-0.

- Zeiser R, Andrlová H, Meiss F. Trametinib (GSK1120212). *Small Molecules in Oncology*. 2018:91-100.
- Zhang C. The role of inflammatory cytokines in endothelial dysfunction. *Basic research in cardiology*. 2008 Sep;103(5):398-406.
- Zhang J, Lei H, Chen Y, Ma YT, Jiang F, Tan J, Zhang Y, Li JD. Enzymatic O-GlcNAcylation of α -synuclein reduces aggregation and increases SDS-resistant soluble oligomers. *Neuroscience Letters*. 2017 Aug 10;655:90-4.
- Zhang J, Wang X, Vikash V, Ye Q, Wu D, Liu Y, Dong W. ROS and ROS-mediated cellular signaling. *Oxidative medicine and cellular longevity*. 2016 Oct;2016.
- Zhang J, Wang X, Vikash V, Ye Q, Wu D, Liu Y, Dong W. ROS and ROS-mediated cellular signaling. *Oxidative Med Cell Longev* 2016: 4350965.
- Zhang QJ, McMillin SL, Tanner JM, Palionyte M, Abel ED, Symons JD. Endothelial nitric oxide synthase phosphorylation in treadmill-running mice: role of vascular signalling kinases. *The Journal of physiology*. 2009 Aug 1;587(15):3911-20.
- Zhang W, Thompson BJ, Hietakangas V, Cohen SM. MAPK/ERK signaling regulates insulin sensitivity to control glucose metabolism in *Drosophila*. *PLoS genetics*. 2011 Dec 29;7(12):e1002429.
- Zhang Y, McGillicuddy FC, Hinkle CC, O'Neill S, Glick JM, Rothblat GH, Reilly MP. Adipocyte modulation of high-density lipoprotein cholesterol. *Circulation*. 2010 Mar 23;121(11):1347-55.
- Zhao Y, Biswas SK, McNulty PH, Kozak M, Jun JY, Segar L. PDGF-induced vascular smooth muscle cell proliferation is associated with dysregulation of insulin receptor substrates. *American Journal of Physiology-Cell Physiology*. 2011 Jun;300(6):C1375-85.
- Zheng JI. Energy metabolism of cancer: Glycolysis versus oxidative phosphorylation. *Oncology letters*. 2012 Dec 1;4(6):1151-7.
- Zhong JC, Ye JY, Jin HY, Yu X, Yu HM, Zhu DL, Gao PJ, Huang DY, Shuster M, Loibner H, Guo JM. Telmisartan attenuates aortic hypertrophy in hypertensive rats by the modulation of ACE2 and profilin-1 expression. *Regulatory peptides*. 2011 Jan 17;166(1-3):90-7.
- Zhou J, Shao L, Yu J, Huang J, Feng Q. PDGF-BB promotes vascular smooth muscle cell migration by enhancing Pim-1 expression via inhibiting miR-214. *Annals of Translational Medicine*. 2021 Dec;9(23).
- Zhou N, Lee JJ, Stoll S, Ma B, Costa KD, Qiu H. Rho kinase regulates aortic vascular smooth muscle cell stiffness via actin/SRF/myocardin in hypertension. *Cellular Physiology and Biochemistry*. 2017;44(2):701-15.
- Zhu Y, Hart GW. Targeting O-GlcNAcylation to develop novel therapeutics. *Molecular Aspects of Medicine*. 2021 Jun 1;79:100885.
- Zhu Y, Shan X, Yuzwa SA, Vocadlo DJ. The emerging link between O-GlcNAc and Alzheimer disease. *Journal of Biological Chemistry*. 2014 Dec 12;289(50):34472-81.

- Zhuang PY, Wang JD, Tang ZH, Zhou XP, Quan ZW, Liu YB, Shen J. Higher proliferation of peritumoral endothelial cells to IL-6/sIL-6R than tumoral endothelial cells in hepatocellular carcinoma. *BMC cancer*. 2015 Dec;15(1):1-9.
- Zimmer M. Green fluorescent protein (GFP): applications, structure, and related photophysical behavior. *Chemical reviews*. 2002 Mar 13;102(3):759-82.
- Zino S, Skeaff M, Williams S, Mann J. Randomised controlled trial of effect of fruit and vegetable consumption on plasma concentrations of lipids and antioxidants. *Bmj*. 1997 Jun 21;314(7097):1787

10. Appendix

10.1 Patients' characteristics with medication history and sample ID number

Patient ID	Age	Sex	Ethnic origin	Reason for surgery	Medical History	T2DM	Medication history
TP- HSV001	69	Male	British White	Coronary artery disease	T2DM, hypertension, hypercholesterolaemia	Yes	Metformin, atorvastatin, bisoprolol
TP- HSV002	70	Male	British White	Coronary artery disease	Hypertension, hypercholesterolaemia.	No	Aspirin, metformin, ramipril, ISMN, rosuvastatin, omeprazole, dapagliflozin
TP- HSV003	84	Male	British White	Coronary artery disease	Hypertension, hypercholesterolaemia	No	Aspirin, amlodipine, atorvastatin, bisoprolol
TP- HSV004	73	Male	British White	Coronary artery disease, aortic valve stenosis	Heart attack, peripheral vascular disease, rectal cancer	No	Allopurinol, clopidogrel, latanoprost, ramipril
TP- HSV005	58	Male	British	Coronary artery disease, recent MI: Jan 2020	Heart attack, hypertensive, asthmatic	No	Aspirin, ticagrelor, isosorbide dinitrate, bisoprolol, ramipril, atorvastatin, spiromax.
TP- HSV006	77	Male	British	Coronary artery disease	T2DM, MI (2000), Basal cell carcinoma (removed), IHD, epilepsy	Yes	Carbamazepine, verapamil, rosuvastatin, clopidogrel
TP- HSV007	66	Male	British	Coronary artery disease	MI (2000), hypothyroidism, myeloid dysplasia disorder	No	Amlodipine, nicorandil, perindopril
TP- HSV008	61	Male	White	Triple vessel disease	High cholesterol	No	Aspirin, bisoprolol, isosorbide mononitrate, atorvastatin, amlodipine, sertraline

TP- HSV009	69	Male	Caucasian	Coronary artery disease	Heart attacks (2003), BPH, Cholesterol +HTL	No	Aspirin, bisoprolol, colecalciferol, eplerenone, ESMN, ramipril atorvastatin, ranitidine, tamsulosin
TP- HSV010	68	Male	White British	Coronary artery disease	T2DM, hypertension, hypercholesterolaemia	Yes	Metformin, atorvastatin, bisoprolol
TP- HSV011	69	Male	White	Coronary artery disease	T2DM, heart attack, hypercholesterolaemia	Yes	Bisoprolol, atorvastatin, amlodipine, omeprazole, metformin and aspirin
TP- HSV012	73	Male	White	Coronary artery disease	High cholesterol	No	Isorsorbide(stopped due to surgery), bisoprolol, aspirin, allopurinol, tamsulosin, simvastatin and ramipril
TP- HSV013	48	Male	White	Coronary artery disease	Heart attack (August 2020), Kidney failure, Asthma, hypercholesterolaemia and recent sepsis	No	Carvedilol, furosemide, salbutamol, doxazosin, atovastatin, lansoprazole and ISMN
TP- HSV014	69	Male	White	Worsening angina	Not Known		Isorsorbide mononitrate, bisoprolol, aspirin, atovastatin and ramipril
TP- HSV015	54	Male	White	Coronary artery disease	Heart attack	No	Ramipril,atorvastatin, lansoprazole, aspirin, apixaban and lercanidipine
TP- HSV016	80	Male	White	Coronary artery disease	T2DM, Prostate CA, HTN, Carotid Artery disease	Yes	Clopidogrel, bisoprolol, amlodipine, ISMN atorvastatin, Lansoprazole, Ranolazine, tamsulosin

TP- HSV017	73	Male	White British	Coronary artery disease	Hypertension	No	Isorsorbide mononitrate, atenolol, amlodipine, atorvastatin, clopidogrel and nitrolingual pump spray
TP- HSV018	63	Male	White British	Coronary artery disease	T2DM, hypercholesterolaemia	Yes	Empagliflozin, Humilin mix, aspirin, losartan, amlodipine, atorvastatin and Sukkarto SR
TP- HSV019	63	Male	White British	Double Coronary vessel disease	Heart attack, Carpal tunnel syndrome, Osteoarthritis, Hypertension, Varicose vein	No	Empagliflozin, Carvedilol, Omeprazole, Glyceryl trinitrate, Cocodamol, Lactulose, Aspirin, Ramipril, Ezetimibe, Tildem Retard, Furosemide and Fenbid Firta (10% Gel)
TP- HSV020	68	Male	White	Coronary artery disease	Heart attack, left knee replacement, Osteoarthritis	No	Amlodipine, Gabapentin, Aspirin, Bisoprolol, Atorvastatin and Omeprazole
TP- HSV021	74	Male	White	Coronary artery disease	Heart attack, Perivascular disease, Rheumatoid and Osteoarthritis	No	Amlodipine, Lansoprazole, Citalopram, Paracetamol, Aspirin, Loperamide, Ramipril, Atorvastatin and Isorsorbide mononitrate
TP- HSV022	68	Male	White British	Coronary artery disease	Hypertension, Hypercholesterolemia	No	Aspirin, Bisoprolol, Atorvastatin and Omeprazole
TP- HSV023	72	Male	White	Coronary artery disease	T2DM, Gout, GORD, Hypertension, Hypercholesterolemia and BPH	Yes	Amlodipine, Lansoprazole, Clopidogrel, Doxazosin, Spironolactone, Atorvastatin, Finasteride, Allopurinol and Lercanidipine

TP- HSV024	63	Male	White British	Coronary artery disease	T2DM and heart attack	Yes	Aspirin, Bisoprolol, Atorvastatin, Lanzoprazole and Ramipril.
TP- HSV025	73	Male	White British	Coronary artery disease	Heart attack and hypertension	No	Ticagrelor, Amlodipine, Lanzoprazole, Deltapapin, Pantoprazole, Aspirin, Ramipril, Atorvastatin and Bisoprolol.
TP- HSV026	70	Male	White	Triple vessel disease	Covid 19 +ve, now -ve	No	Aspirin, Bisoprolol, Bimatropost and Ramipril
TP- HSV027	76	Male	White British	Coronary artery disease- recent myocardial infarction	Heart attack, Hypercholesterolemia and Gout	No	Throxin, atorvastatin, calcisine and lansoprazol
TP- HSV028	52	Male	White	Coronary artery disease	Heart attack and Hypercholesterolemia	No	Isosorbide mononitrate. Aspirin, Ramipril and Atorvastatin
TP- HSV029	75	Male	White British	Coronary artery disease	T2DM, Hypertension, Parkinson and Dyslipidaemia	Yes	Lansoprazole, metformin, aspirin, bisoprolol, co-caveldopa, furosemid, gliclizide, irbesatan, simvastatin and sitagliptin.
TP- HSV030	59	Male	White British	Coronary artery disease	Heart attack (2018)	No	Omeprazole, Losartan, Paracetamol, Aspirin, Oxycodone, Atorvastatin, isorsorbide mononitrate, and Bisoprolol.
TP- HSV031	72	Male	White British	Coronary artery disease	Sleep apnea, Gout, Diverticulosis, Bilateral osteoarthritis, shoulder replacement.	No	Allopurinol, Bisoprolol, Amiodarone, Furosemide, Lanzoprazole, Atorvastatin, isosorbide mononitrate, and Malirogol.

TP- HSV032	55	Male	White British	Coronary artery disease	Heart attack	No	Bisoprolol, Ramipril, Aspirin, Ticagrelor, Atorvastatin, isosorbide mononitrate and Vitamin D3
TP- HSV033	57	Male	White British	Coronary artery disease	Heart attack, Hypertension and Hypercholesterolemia	No	Aspirin, Amlodipine, Atorvastatin, Ramipril and Bisoprolol
TP- HSV034	82	Male	White British	Coronary artery disease	Cancer	No	Aspirin, Atorvastatin, isosorbide mononitrate, omeprazole, lactulose and paracetamol
TP- HSV035	53	Male	White British	Coronary artery disease	Heart attack, kidney failure.	No	Aspirin, Atorvastatin, isosorbide dinitrate, Budesonide, Clopidogrel, Lansoprazole, Losartan, metoprolol, and venlafaxine
TP- HSV037	65	Male	White British	Coronary artery disease	Hypertension and hypercholesterolaemia	No	Amlodipine, atorvastatin, bisoprolol, ISMN and losartan.
TP- HSV038	63	Male	White British	Coronary artery disease	T2DM, Heart attack, Recent infection and Osteoarthritis	Yes	Lansoprazole, bisoprolol, amlodipine, candesartan, metformin, rosuvastatin, liraglutide, empagliflozin, ranolazine, aspirin. ISMN, glycerol trinitrate and paracetamol.
TP- HSV039	47	Male	White British	Coronary artery disease	Heart attack, recent infection-MSA.	No	Aspirin, Atorvastatin, Bisoprolol, Omeprazole, Ramipril, isosorbide mononitrate and paracetamol
TP- HSV040	65	Male	White British	Coronary artery disease	Aortic valve stenosis, Asthma	No	Bisoprolol, Enalapril, Simvastatin, Allupurinol, Nifedipine and Aspirin.

TP- HSV041	63	Male	White British	Coronary artery disease	T2DM, heart attack, total hip replacement	Yes	Aspirin, monomil, bisoprolol, rosuvastatin and clopidogrel
TP- HSV042	69	Male	White British	Coronary artery disease	Unstable angina, blood cancer, larynthritis, steoarthritis, hypothyroidism, hypertension, polythemia	No	Aspirin, cinnarizine, levothyroxine, solifenacin, ISMN, bisoprolol and paracetamol
TP- HSV043	69	Male	White British	Coronary artery disease	Borderline T2DM, eye peripheral vision loss due to embolus, COPD, Hypercholesterolemia	Yes	Losartan, digoxin, bisoprolol, simvastatin, elantin and Inipta
TP- HSV044	56	Male	White British	Coronary artery disease	T2DM, Heart attack, Asthma, left ventricular hypertrophy and acute coronary syndrome	Yes	Aspirin, allupurinol, bisoprolol, atorvastatin, doxozosin, indaprimed and ramipril
TP- HSV045	67	Male	White British	Coronary artery disease	Hypercholesterolaemia	No	Aspirin, atorvastatin, ramipril, tramadol, paracetamol, and oxycodone.
TP- HSV046	72	Female	White British	Coronary artery disease	Steroid-induced T2DM, Pancreatis, chronic anaemia, myasthenia gravis, diventriculitis	Yes	Bisoprolol, Ezetimibe, Fenofexadine, Folic acid, Isosorbide mononitrate, Lansoprazole, Linagliptin, Losartan, Wicoradil, Prednisolone, Methotrexate
TP- HSV047	73	Male	White British	Coronary artery disease	Hypertension, Hypercholesterolaemia	No	Aspirin, Atorvastatin, Ferrous fumerate, ISMN, Ramipril, GTN Spray, Clipidogrl, Bisoprolol, and Nirondil.

TP- HSV048	73	Male	White	Aortic valve stenosis and coronary heart disease	T2DM, Heart attack, Thrombocytopenia, Hypertension, and Gilbert's disease	Yes	Aspirin, Atovastatin, Doxazosin, Lisinopril, Metformin
TP- HSV049	73	Female	White	Coronary artery disease	Kidney failure (CKD Stage 3A), Hypercholesterolaemia	No	Aspirin, Amlodipine, Ezetimibe, Atorvastatin, cansoprazole, isorsobide mononitrate
TP- HSV050	68	Male	White	Coronary artery disease	Osteoarthritis, appendectomy, resectomy, tonsilectomy + aderoids and ex-smoker	No	Aspirin, Bisoprolol, Rosuvastatin, Lansoprazole, Citalopram, ISMN
TP- HSV051	76	Male	White	Coronary artery disease	Heart attack, Hypercholesterolaemia	No	Alfuzosin, Atorvastatin, and Oxybutynin
TP- HSV052	75	Male	White British	Coronary artery disease	T2DM	Yes	Citalopram, Metformin, Nicorandil, Pravastatin, Aspirin, ISMN, Lansoprazole, Ramdazine, Nicorandil, Azithromycin, Salbutamol and Fostail
TP- HSV053	69	Female	White British	Coronary artery disease	T2DM	Yes	Lansoprazole
TP- HSV054	57	Male	Asian	Coronary artery disease	Heart attack and hypercholesterolemia	No	Aspirin, Atorvastatin, Bisoprolol, Lansoprazole, Ramipril, Ranolazone, Codeine, Paracetamol, Resomni, and Mitazapine
TP- HSV055	73	Male	White British	Coronary artery disease	Heart attack	No	Tamsulosin, Salmeterol, Momentazone, Bulometxre

10.2 Buffers for SDS-PAGE gel electrophoresis and immunoblotting

<p>SDS Buffer 1 (0.5L)</p> <p>1.5M Tris-HCL, pH 8.8 (90.8 g/500 ml)</p> <p>0.4% SDS (20ml 10% SDS/500ml)</p> <p>0.5 L Distilled water</p>	<p>SDS Buffer 2 (0.5L)</p> <p>0.5M Tris-HCL, pH 6.8 (30.3 g/500 ml)</p> <p>0.4% SDS (20 ml 10% SDS/500 ml)</p> <p>0.5 L Distilled water</p>
<p>10x Stock Running buffer (2L)</p> <p>Glycine (288 g)</p> <p>TRIS (60 g)</p> <p>2L Distilled water</p>	<p>Running buffer</p> <p>10% RB^o stock (100 ml)</p> <p>10% SDS (10 ml)</p> <p>dH₂O (890 ml)</p>
<p>10% Resolving/Running Gel</p> <p>Distilled water (3.4 ml)</p> <p>Buffer 1 (2.5 ml)</p> <p>50% Glycerol (0.65 ml)</p> <p>Ammonium Persulphate (APS) (32 µl)</p> <p>TEMED (8 µl)</p> <p>Acrylamide (3.3 ml)</p>	<p>13% Resolving/Running Gel</p> <p>Distilled water (2.41 ml)</p> <p>Buffer 1 (2.5 ml)</p> <p>50% Glycerol (0.65 ml)</p> <p>Ammonium Persulphate (32 µl)</p> <p>TEMED (8 µl)</p> <p>Acrylamide (4.29 ml)</p>
<p>Stacking Gel</p> <p>Distilled water (3.4 ml)</p> <p>Buffer 2 (1.34 ml)</p> <p>Ammonium Persulphate (54 µl)</p> <p>TEMED (7 µl)</p> <p>Acrylamide (0.63 ml)</p>	<p>8% Resolving/Running Gel</p> <p>Distilled water (4.07 ml)</p> <p>Buffer 1 (2.5 ml)</p> <p>50% Glycerol (0.65 ml)</p> <p>Ammonium Persulphate (32 µl)</p> <p>TEMED (8 µl)</p> <p>Acrylamide (2.64 ml)</p>
<p>Stripping buffer (1L)</p> <p>0.1M glycine (7.5 g)</p> <p>0.15M NaCl (8.7 g)</p> <p>HCl dropwise at pH2.0</p> <p>1 L Distilled water</p>	<p>Transfer buffer (1.5L)</p> <p>Methanol (300 ml)</p> <p>10x Running buffer (100 ml)</p> <p>1.2 L Distilled water</p>

10.3 Lysing buffer

<p>1.28 RIPA (500ml)</p> <p>64nM HEPES, pH7.5 (7.62g)</p> <p>192nM Sodium Chloride – NaCl (5.61g)</p> <p>1.28% (v/v) Triton X-100 (32ml of 20% stock)</p> <p>0.64% (w/v) Sodium Deoxycholate (32ml of 10% freshly prepared stock)</p> <p>0.128% (w/v) SDS (6.4ml of 10% stock)</p> <p>Distilled water (500ml)</p>	<p>Ripa (-)</p> <p>1.28 RIPA (3.9ml) <i>RT</i></p> <p>0.5M Sodium Fluoride – NaF (0.1ml) <i>RT</i></p> <p>0.5M EDTA pH 8 (50µl) <i>RT</i></p> <p>0.1M Sodium Phosphate – NaPO₄ (0.5ml)</p> <p>Distilled water (0.4ml)</p> <p>Ripa (+) (lysis buffer)</p> <p>Add ¾ complete protease inhibitor to RIPA (-)</p>
--------------------------------------------------------------------------------------------------------------------------------------------------------------------------------------------------------------------------------------------------------------------------------------------------------------------------	----------------------------------------------------------------------------------------------------------------------------------------------------------------------------------------------------------------------------------------------------------------------------------------------------------------------------------------

10.4 PCR and qPCR mix

PCR	(µL)	qPCR	(µL)
RNAse free H ₂ O	14.4	RNAse free H ₂ O	7.4
Template	2	Template (1 ng/µl in H ₂ O)	1.6
Primers	1	Primer	1.0
Taq (Polymerase mix)	2.6	SYBR Green Master Mix	10

10.5 Coomassie staining and destaining

Coomassie staining solution	%	Destaining solution	%	Gel drying solution	%
Ethanol	50	Ethanol	20	Ethanol	50
Acetic acid	10	Acetic acid	7	Glycerine	5
Coomassie brilliant blue	0.25	Distilled water	73	Distilled water	45
Distilled water	40				